

An Analytic Scale-dependent Dark Matter Profile and the Baryonic Tully-Fisher Relation

V.K. Oikonomou^{1,2*}

¹⁾*Department of Physics, Aristotle University of Thessaloniki, Thessaloniki 54124, Greece*

²⁾*Center for Theoretical Physics, Khazar University,
41 Mehseti Str., Baku, AZ-1096, Azerbaijan*

In this work we use the recently introduced concept of self-interacting dark matter with scale-dependent equation of state, and we provide an analytic model of dark matter that can produce viable rotation curves even for low-surface-brightness galaxies, irregular galaxies, low-luminosity spirals and dwarf galaxies, all known to challenge the cold dark matter description. The radius dependent effective equation of state of the self-interacting dark matter model we shall introduce is assumed to be an isothermal equation of state of the form $P(r) = K(r) \left(\frac{\rho(r)}{\rho_*} \right)$, where the energy density will have the form $\rho(r) = \frac{\rho_0}{(1 + \frac{r^2}{\alpha^2})^{5/2}}$, while the entropy function $K(r)$ is $K(r) = \frac{K_0}{(1 + \frac{r^2}{\alpha^2})^{1/2}}$.

The resulting model is confronted in detail with the SPARC galaxy data and 175 galaxies are used and tested. It proves that the analytic model can successfully produce the rotation curves of 116 galaxies, most of which are small mass spirals, irregular galaxies, low-surface-brightness and low-luminosity spirals and dwarf galaxies. For some of these, especially the intermediate mass spirals, we used the rotation velocity of the other components of the galaxy, namely the gas, baryon and disk. On the other hand, 59 galaxies cannot be successfully described by our analytic model. We tested statistically the correlation between the parameter K_0 of the entropy function corresponding to the viable galaxies, and the flat rotation velocity V_{flat} and the maximum rotation velocity V_{max} of the galaxies from the SPARC data. We also examined the baryon mass M_b - K_0 relation and the luminosity L - K_0 relation. We have been able to produce the baryonic Tully-Fisher relation for the viable galaxies, directly from the correlation K_0 - M_b and K_0 - V_{flat} , with the resulting relation being $M_b \sim V_{flat}^{4.026 \pm 0.371}$, however we failed to produce the canonical Tully-Fisher relation. We thoroughly discuss this outcome, which must be a model-dependent result, since near isothermal equation-of-state scale-dependent models of the form $P(r) = K(r) \left(\frac{\rho(r)}{\rho_*} \right)^{\gamma(r)}$, succeed in providing a semi-empirical proof of both the canonical and baryonic Tully-Fisher relations.

PACS numbers: 04.50.Kd, 95.36.+x, 98.80.-k, 98.80.Cq, 11.25.-w

I. INTRODUCTION

The large scale structure of the Universe is mysterious and many questions related to it are still unanswered in a definitive way. Although there is a rather clear picture on facts like, how the quantum fluctuations of the Universe created the instabilities on which the dark matter (DM) started to built up gravitational potentials, on which sequentially, baryons have built up to create proto-galactic structure, which resulted eventually to the galaxies. Much of this complex process is still unknown since many non-linear relaxation regimes of both baryonic matter and DM are still vague to our understanding. The galactic generation process must certainly be hierarchical, and some parts of the galaxy must have been formed earlier. Most of the galaxies are speculated to contain a DM halo. This DM halo was hypothesized by Zwicky a hundred years ago, after comparing the mass-to-light ratio in the Coma cluster and compared it to the mass-to-light ratio of spirals based on the rotation curves of their visible parts. Zwicky concluded that there is 400 times dark mass in the Coma cluster. A DM halo can explain the uniformity of the behavior of the rotation curves of spirals and irregulars and even dwarfs, which either increases and remains flat in the outer skirts of the galaxies, for spirals, or behaves linearly as in irregulars and dwarfs. Especially in dwarfs, DM is expected to contribute to the dynamics of the galaxy at a percentage 90%. To date, the Λ -Cold-Dark-Matter (Λ CDM) model is the most consistent and successful model cosmologically and at galactic scales, but it faces challenges. Specifically, the problems it faces regarding galactic dynamics are the cusp-core problem, the too-big-to-fail problem and the diversity problem [30]. Self-interacting DM offers an interesting and consistent solution to these problems.

*Electronic address: voikonomou@gapps.auth.gr, v.k.oikonomou1979@gmail.com

Building up and continuing a previous work [2], in this work we shall assume that the DM is self-interacting in its nature, without assuming a specific theoretical model, but the main assumption will be on its effective equation-of-state (EoS). Specifically we assume that it is radius-dependent, we will refer to it as scale-dependent, and it is an isothermal EoS of the form, $P(r) = K(r) \left(\frac{\rho}{\rho_*} \right)$, with the energy density $\rho(r)$ and the entropy function $K(r)$ being analytic functions, of the form,

$$\rho(r) = \frac{\rho_0}{\left(1 + \frac{r^2}{\alpha^2} \right)^{\frac{5}{2}}}, \quad (1)$$

$$K(r) = \frac{K_0}{\left(1 + \frac{r^2}{\alpha^2} \right)^{\frac{1}{2}}}. \quad (2)$$

This will prove to be a two parameter model, since only ρ_0 and K_0 will be the parameters determining the dynamics of the model, and the transition radius α can be evaluated from these two. This radius-dependent isothermal EoS is an analytic solution to the hydrodynamic equilibrium equation, thus the rotation curves of galaxies having such a DM component can be evaluated fully analytically. For more general discussions on self-interacting DM and for DM with polytropic EoS, see [3–20]. Although in principle, many self-interacting DM models can accommodate such a scale-dependent EoS, we find the mirror DM perspective rather fascinating [21–68], since the mirror DM can describe such scale-dependent behaviors due to the fact that it allows pressure gradients changes. It is also important to note that the Tully-Fisher relation finds a nice explanation in the context of mirror DM [34].

In this article we shall investigate the phenomenological implications of the isothermal scale-dependent EoS, focusing on the rotation curves of the SPARC data [69]. We shall examine 175 galaxies from the SPARC data, and as we shall demonstrate, a total number of 116 galaxies can be perfectly described by our model and the rotation curves are perfectly fitted. The rest 59 galaxies are not well described by our model, regarding their rotation curves. Our two parameter model (1) seems to describe accurately dwarfs, irregular galaxies, low-surface-brightness spirals and low-luminosity spirals. The parameters that determine the dynamics are K_0 , the entropy parameter, and also ρ_0 the central density parameter. We examined the correlation of K_0 , the entropy parameter corresponding to the viable galaxies, and the V_{flat} and V_{max} of the galaxies from the SPARC data. We also examined the baryon mass M_b - K_0 relation and in addition, the luminosity L - K_0 relation. We produced the baryonic Tully-Fisher relation for the viable galaxies, directly from the correlations K_0 - M_b and the K_0 - V_{flat} , with the resulting baryonic Tully-Fisher relation being $M_b \sim V_{flat}^{4.026 \pm 0.371}$. On the other hand we failed to produce the canonical Tully-Fisher relation from the relations $L - K_0$ and $K_0 - V_{max}$. We discuss this outcome in some detail, since near isothermal equation-of-state scale-dependent models of the form $P(r) = K(r) \left(\frac{\rho(r)}{\rho_*} \right)^{\gamma(r)}$, succeed in providing a semi-empirical proof of both the canonical and baryonic Tully-Fisher relations, as was demonstrated in Ref. [2].

Regarding the presentation of the galactic rotation curves, we chose a rather small number of 10 viable and non-viable galaxies from the total of 175 galaxies of the SPARC data. We include the complete study of the rest 165 galaxies in the Appendix of the arXiv version of this article and not the journal version of this article.

II. AN ANALYTIC ISOTHERMAL SCALE-DEPENDENT DM PROFILE

As we mentioned in the introduction, in this work we shall assume that DM is self interacting and also that it has a scale-dependent (radius dependent) EoS of the form $P(r) = K(r) \left(\frac{\rho}{\rho_*} \right)$, with the energy density $\rho(r)$ and the entropy function $K(r)$ being analytic functions of the form,

$$\rho(r) = \frac{\rho_0}{\left(1 + \frac{r^2}{\alpha^2} \right)^{\frac{5}{2}}}, \quad (3)$$

$$K(r) = \frac{K_0}{\left(1 + \frac{r^2}{\alpha^2} \right)^{\frac{1}{2}}}, \quad (4)$$

and we shall assume that $\rho_* = 1 M_\odot \text{Kpc}^{-3}$ for simplicity. Note that the model is essentially two parameter, because only K_0 and ρ_0 are free parameters, and the parameter α can be obtained by the relation,

$$K_0 = \frac{2\pi\alpha^2 G \rho_0}{9\rho_*}. \quad (5)$$

The hydrostatic equilibrium in a spherical symmetry setting reads,

$$\frac{dP}{dr} = -\frac{G M(r) \rho(r)}{r^2}, \quad (6)$$

and the enclosed mass is,

$$M(r) = \int_0^r 4\pi r'^2 \rho(r') dr'. \quad (7)$$

The corresponding differential equation obeyed by the total mass is the standard relation,

$$\frac{dM}{dr} = 4\pi r^2 \rho(r). \quad (8)$$

Therefore, the complete set of differential equations governing the hydrodynamic equilibrium is the following,

$$\frac{dP}{dr} = -\rho(r) \frac{GM(r)}{r^2}, \quad (9)$$

$$P(r) = K(r) \left(\frac{\rho(r)}{\rho_*} \right)^{\gamma(r)}, \quad (10)$$

$$\frac{dM}{dr} = 4\pi r^2 \rho(r). \quad (11)$$

The functions $\rho(r)$ and $K(r)$ from Eq. (3) with an isothermal relation between them $P(r) = K(r) \left(\frac{\rho}{\rho_*} \right)$, analytically satisfy the set of differential equations (9). For these functions, we shall derive the rotation curves and fit 175 galaxies from the SPARC data. When necessary we shall invoke the other galactic parts that contribute to the rotation curves, namely, the gas, the bulge and disk components. In this case, the total rotation curve velocity will be,

$$V_{\text{total}}^2(r) = V_{\text{disk}}^2(r) + V_{\text{bulge}}^2(r) + V_{\text{gas}}^2(r) + V_{\text{DM}}^2(r).$$

Regarding the physical units, the pressure has units,

$$[P] = [\rho][v^2] = M_\odot \text{Kpc}^{-3} (\text{km/s})^2, \quad (12)$$

and also,

$$P(r) = K(r) \frac{\rho(r)}{\rho_*},$$

thus,

$$[K(r)] = [P] = M_\odot \text{Kpc}^{-3} (\text{km/s})^2. \quad (13)$$

III. SIMULATIONS OF THE ANALYTIC MODEL OF SCALE-DEPENDENT EOS DM WITH SPARC GALAXIES

In this section we shall present simulations of the rotation curves for some characteristic galaxies, using the model of Eq. (3). The model is essentially a two parameter model, with only K_0 and ρ_0 varying. We shall run some optimization codes for the model, trying to find the optimal values of K_0 and ρ_0 which provide perfect fits for the rotation curves of the 175 galaxies from the SPARC data [69]. For some galaxies, the model (3) suffices to provide a perfect fit for the rotation curves, but for some other galaxies we shall include the other components of the galaxy, namely the disk, bulge and gas, and then the desirable result is obtained. From the 175 galaxies, 116 are found to be viable, meaning that the model can mimic their rotation curves optimally, using simply the model or the combination of the model in the presence of gas, bulge and disk components. On the other hand, 59 galaxies are found to be non-viable. Specifically, the following galaxies are found to be viable, **CamB**, **D512-2**, **D564-8**, **D631-7**, **DDO064**, **DDO154**, **DDO161**, **ESO079-G014**, **ESO116-G012**, **F565-V2**, **F568-3**, **F568-V1**, **F571-8**, **F571-V1**, **F574-1**, **F583-1**, **F583-4**, **KK98-251**, **NGC0055**, **NGC0100**, **NGC0300**, **NGC0801**, **NGC0891**, **NGC1003**, **NGC1090**, **NGC2403**, **NGC2683**, **NGC2841**,

NGC2903, NGC2915, NGC2955, NGC2976, NGC2998, NGC3109, NGC3198, NGC3521, NGC3726, NGC3741, NGC3769, NGC3877, NGC3893, NGC3917, NGC3949, NGC3953, NGC3972, NGC3992, NGC4010, NGC4013, NGC4051, NGC4068, NGC4085, NGC4088, NGC4100, NGC4138, NGC4157, NGC4183, NGC4217, NGC4559, NGC5005, NGC5033, NGC5055, NGC5371, NGC5585, NGC5907, NGC5985, NGC6015, NGC6195, NGC6503, NGC6674, NGC6789, NGC6946, NGC7331, NGC7793, NGC7814, UGC00128, UGC00191, UGC00634, UGC00731, UGC00891, UGC01281, UGC02259, UGC02487, UGC02885, UGC02916, UGC02953, UGC03205, UGC03546, UGC03580, UGC04278, UGC04325, UGC04483, UGC04499, UGC05005, UGC05253, UGC05414, UGC05716, UGC05721, UGC05750, UGC05764, UGC05829, UGC05918, UGC05986, UGC06399, UGC06446, UGC06614, UGC06667, UGC06786, UGC06787, UGC06818, UGC06917, UGC06923, UGC06930, UGC06983, UGC07089, UGC07125, UGC07151, UGC07232, UGC07261, UGC07323, UGC07399, UGC07524, UGC07559, UGC07577, UGC07603, UGC07690, UGC07866, UGC08286, UGC08490, UGC08550, UGC08699, UGC08837, UGC09037, UGC09133, UGC09992, UGC10310, UGC11455, UGC11557, UGC11820, UGC11914, UGC12506, UGC12632, UGC12732, UGCA442, UGCA444, F561-1, F563-1, F563-V1, F563-V2, F567-2, F568-1, F574-2, F579-V1, NGC1705, NGC2366, NGC4214, NGC4389, NGC6946, PGC51017, UGC01230, UGC02023, UGC04305, UGC05999, UGC06628, UGC06973, UGC07608, UGCA281.

On the other hand the non-viable galaxies are, DDO168, DDO170, ESO079-G014, ESO116-G012, ESO444-G084, ESO563-G021, F565-V2, F568-3, F568-V1, F571-8, F571-V1, F574-1, F583-1, F583-4, IC2574, IC4202, KK98-251, NGC0024, NGC0055, NGC0100, NGC0247, NGC0289, NGC0300, NGC0801, NGC0891, NGC1003, NGC1090, NGC2403, NGC2683, NGC2841, NGC2903, NGC2915, NGC2955, NGC2976, NGC2998, NGC3109, NGC3198, NGC3521, NGC3726, NGC3741, NGC3769, NGC3877, NGC3893, NGC3917, NGC3949, NGC3953, NGC3972, NGC3992, NGC4010, NGC4013, NGC4051, NGC4068, NGC4085, NGC4088, NGC4100, NGC4138, NGC4157, NGC4183, NGC4217, NGC4559, NGC5005, NGC5033, NGC5055, NGC5371, NGC5585, NGC5907, NGC5985, NGC6015, NGC6195, NGC6503, NGC6674, NGC6789, NGC6946, NGC7331, NGC7793, NGC7814, UGC00128, UGC00191, UGC00634, UGC00731, UGC00891, UGC01281, UGC02259, UGC02487, UGC02885, UGC02916, UGC02953, UGC03205, UGC03546, UGC03580, UGC04278, UGC04325, UGC04483, UGC04499, UGC05005, UGC05253, UGC05414, UGC05716, UGC05721, UGC05750, UGC05764, UGC05829, UGC05918, UGC05986, UGC06399, UGC06446, UGC06614, UGC06667, UGC06786, UGC06787, UGC06818, UGC06917, UGC06923, UGC06930, UGC06983, UGC07089, UGC07125, UGC07151, UGC07232, UGC07261, UGC07323, UGC07399, UGC07524, UGC07559, UGC07577, UGC07603, UGC07690, UGC07866, UGC08286, UGC08490, UGC08550, UGC08699, UGC08837, UGC09037, UGC09133, UGC09992, UGC10310, UGC11455, UGC11557, UGC11820, UGC11914, UGC12506, UGC12632, UGC12732, UGCA442, UGCA444, F561-1, F563-1, F563-V1, F563-V2, F567-2, F568-1, F574-2, F579-V1, NGC1705, NGC2366, NGC4214, NGC4389, NGC6946, PGC51017, UGC01230, UGC02023, UGC04305, UGC05999, UGC06628, UGC06973.

In the following subsections we present five viable and five non-viable examples from the total of the 175 galaxies. The rest of the study is presented in the Appendix of the arXiv version of this article.

A. Sample of Viable Galaxies

1. The Galaxy CamB

For this galaxy, the optimization method we used, ensures maximum compatibility of the analytic SIDM model of Eq. (3) with the SPARC data, if we choose $\rho_0 = 1.20484 \times 10^7 M_\odot/\text{Kpc}^3$ and $K_0 = 206.963 M_\odot \text{Kpc}^{-3} (\text{km/s})^2$, in which case the reduced χ^2_{red} value is $\chi^2_{red} = 0.493168$. Also the parameter α in this case is $\alpha = 2.51 \text{Kpc}$.

In Table I we present the optimized values of K_0 and ρ_0 for the analytic SIDM model of Eq. (3) for which the maximum compatibility with the SPARC data is achieved. In Figs. 1, 2 we present the density of the analytic SIDM model, the predicted rotation curves for the SIDM model (3), versus the SPARC observational data and the sound speed, as a function of the radius respectively. As it can be seen, for this galaxy, the SIDM model produces viable rotation curves which are compatible with the SPARC data.

TABLE I: SIDM Optimization Values for the galaxy CamB

Parameter	Optimization Values
$\rho_0 (M_\odot/\text{Kpc}^3)$	1.20484×10^7
$K_0 (M_\odot \text{ Kpc}^{-3} (\text{km/s})^2)$	206.963

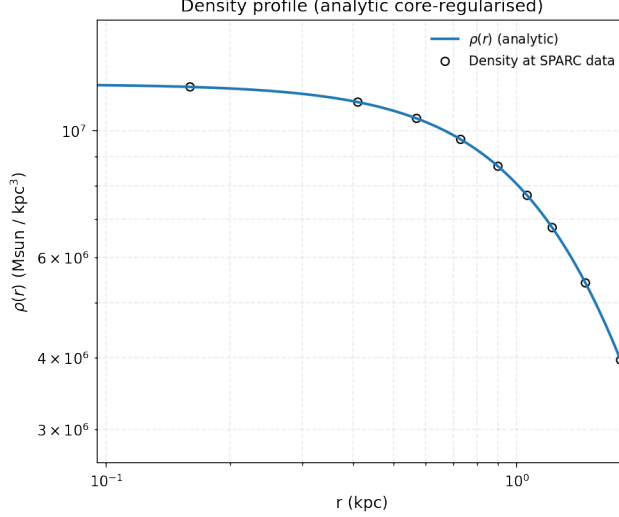


FIG. 1: The density of the SIDM model of Eq. (3) for the galaxy CamB, versus the radius.

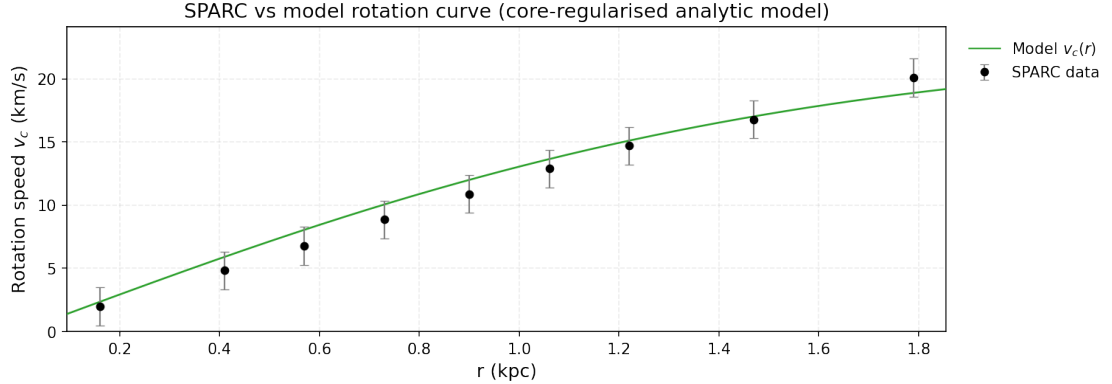


FIG. 2: The predicted rotation curves for the optimized SIDM model of Eq. (3), versus the SPARC observational data for the galaxy CamB.

2. The Galaxy D512-2

For this galaxy, the optimization method we used, ensures maximum compatibility of the analytic SIDM model of Eq. (3) with the SPARC data, if we choose $\rho_0 = 4.00327 \times 10^7 M_\odot/\text{Kpc}^3$ and $K_0 = 552.819 M_\odot \text{ Kpc}^{-3} (\text{km/s})^2$, in which case the reduced χ^2_{red} value is $\chi^2_{\text{red}} = 0.0925236$. Also the parameter α in this case is $\alpha = 2.14454 \text{ Kpc}$.

In Table II we present the optimized values of K_0 and ρ_0 for the analytic SIDM model of Eq. (3) for which the maximum compatibility with the SPARC data is achieved. In Figs. 3, 4 we present the

TABLE II: SIDM Optimization Values for the galaxy D512-2

Parameter	Optimization Values
$\rho_0 (M_\odot/\text{Kpc}^3)$	4.00327×10^7
$K_0 (M_\odot \text{ Kpc}^{-3} (\text{km/s})^2)$	552.819

density of the analytic SIDM model, the predicted rotation curves for the SIDM model (3), versus the SPARC observational data and the sound speed, as a function of the radius respectively. As it can be seen, for this galaxy, the SIDM model produces viable rotation curves which are compatible with the SPARC data.

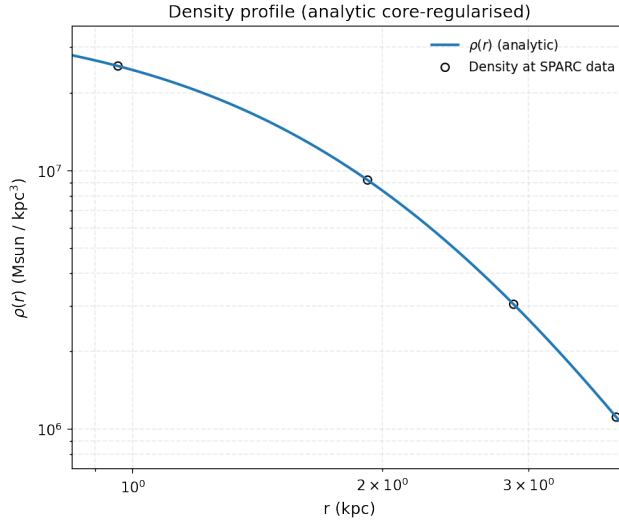


FIG. 3: The density of the SIDM model of Eq. (3) for the galaxy D512-2, versus the radius.

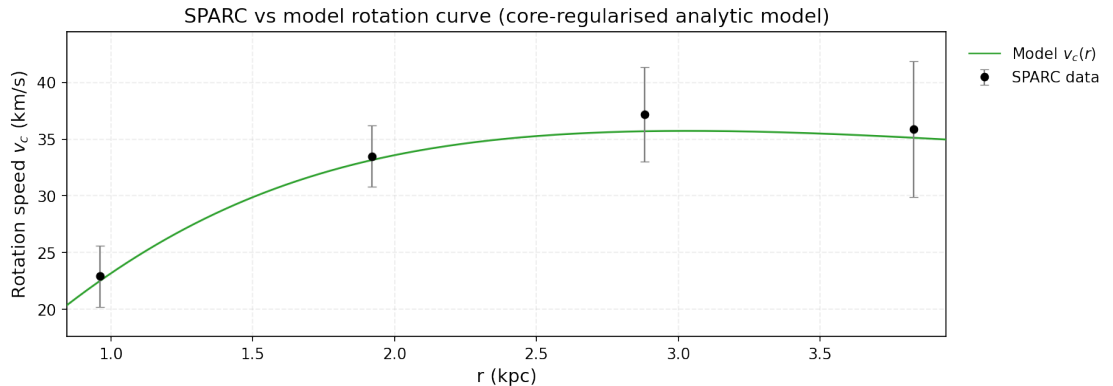


FIG. 4: The predicted rotation curves for the optimized SIDM model of Eq. (3), versus the SPARC observational data for the galaxy D512-2.

3. The Galaxy D564-8

For this galaxy, the optimization method we used, ensures maximum compatibility of the analytic SIDM model of Eq. (3) with the SPARC data, if we choose $\rho_0 = 1.46575 \times 10^7 M_\odot / \text{Kpc}^3$ and $K_0 = 242.656 M_\odot \text{ Kpc}^{-3} (\text{km/s})^2$, in which case the reduced χ^2_{red} value is $\chi^2_{\text{red}} = 0.277623$. Also the parameter α in this case is $\alpha = 2.3481 \text{ Kpc}$.

In Table III we present the optimized values of K_0 and ρ_0 for the analytic SIDM model of Eq. (3) for which the maximum compatibility with the SPARC data is achieved. In Figs. 5, 6 we present the

TABLE III: SIDM Optimization Values for the galaxy D564-8

Parameter	Optimization Values
$\rho_0 (M_\odot / \text{Kpc}^3)$	1.46575×10^7
$K_0 (M_\odot \text{ Kpc}^{-3} (\text{km/s})^2)$	242.656

density of the analytic SIDM model, the predicted rotation curves for the SIDM model (3), versus the SPARC observational data and the sound speed, as a function of the radius respectively. As it can be seen, for this galaxy, the SIDM model produces viable rotation curves which are compatible with the SPARC data.

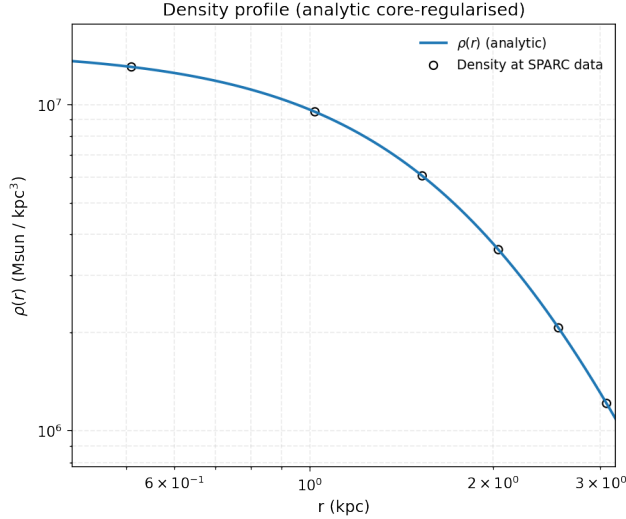


FIG. 5: The density of the SIDM model of Eq. (3) for the galaxy D564-8, versus the radius.

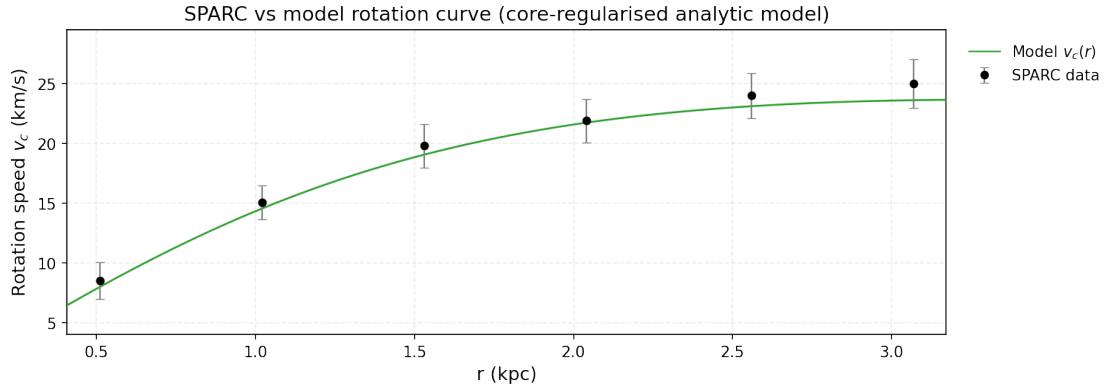


FIG. 6: The predicted rotation curves for the optimized SIDM model of Eq. (3), versus the SPARC observational data for the galaxy D564-8.

4. The Galaxy DDO154, Marginally Viable, Extended Viable by One Miss

For this galaxy, the optimization method we used, ensures maximum compatibility of the analytic SIDM model of Eq. (3) with the SPARC data, if we choose $\rho_0 = 2.566 \times 10^7 M_\odot / \text{Kpc}^3$ and $K_0 = 965.604 M_\odot \text{ Kpc}^{-3} (\text{km/s})^2$, in which case the reduced χ^2_{red} value is $\chi^2_{\text{red}} = 4.31061$. Also the parameter α in this case is $\alpha = 3.54015 \text{ Kpc}$.

In Table IV we present the optimized values of K_0 and ρ_0 for the analytic SIDM model of Eq. (3) for which the maximum compatibility with the SPARC data is achieved. In Figs. 7, 8 we present the

TABLE IV: SIDM Optimization Values for the galaxy DDO154

Parameter	Optimization Values
$\rho_0 (M_\odot / \text{Kpc}^3)$	2.566×10^7
$K_0 (M_\odot \text{ Kpc}^{-3} (\text{km/s})^2)$	965.604

density of the analytic SIDM model, the predicted rotation curves for the SIDM model (3), versus the SPARC observational data and the sound speed, as a function of the radius respectively. As it can be seen, for this galaxy, the SIDM model produces marginally viable rotation curves which are marginally compatible with the SPARC data.

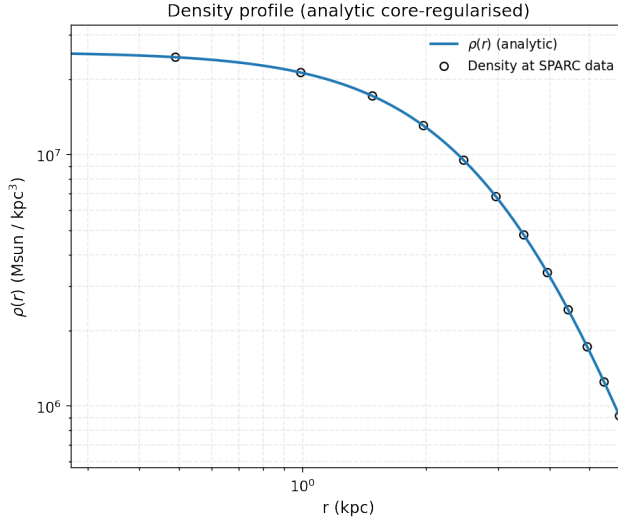


FIG. 7: The density of the SIDM model of Eq. (3) for the galaxy DDO154, versus the radius.

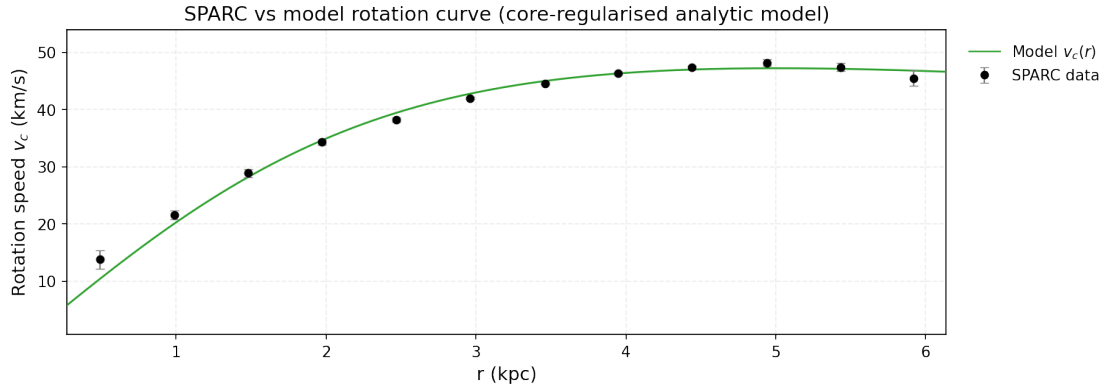


FIG. 8: The predicted rotation curves for the optimized SIDM model of Eq. (3), versus the SPARC observational data for the galaxy DDO154.

Now we shall include contributions to the rotation velocity from the other components of the galaxy, namely the disk, the gas, and the bulge if present. In Fig. 9 we present the combined rotation curves including all the components of the galaxy along with the SIDM. As it can be seen, the extended collisional DM model is almost viable (missed one point). Also in Table V we present the optimized values of the free parameters of the SIDM model for which we achieve the maximum compatibility with the SPARC data, for the galaxy DDO154, and also the resulting reduced χ^2_{red} value.

TABLE V: Optimized Parameter Values of the Extended SIDM model for the Galaxy DDO154.

Parameter	Value
$\rho_0 (M_\odot / \text{Kpc}^3)$	1.73089×10^7
$K_0 (M_\odot \text{ Kpc}^{-3} (\text{km/s})^2)$	852.337
ml_{disk}	0.8442
ml_{bulge}	0.9721
$\alpha (\text{Kpc})$	4.04919
χ^2_{red}	0.765527

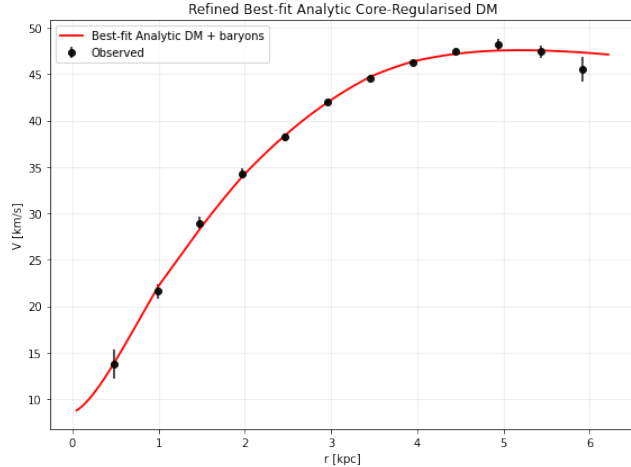


FIG. 9: The predicted rotation curves after using an optimization for the SIDM model (3), and the extended SPARC data for the galaxy DDO154. We included the rotation curves of the gas, the disk velocities, the bulge (where present) along with the SIDM model.

5. The Galaxy UGC00634

For this galaxy, the optimization method we used, ensures maximum compatibility of the analytic SIDM model of Eq. (3) with the SPARC data, if we choose $\rho_0 = 1.51522 \times 10^7 M_\odot/\text{Kpc}^3$ and $K_0 = 5162.06 M_\odot \text{Kpc}^{-3} (\text{km/s})^2$, in which case the reduced χ^2_{red} value is $\chi^2_{\text{red}} = 1.24441$. Also the parameter α in this case is $\alpha = 10.6518 \text{Kpc}$.

In Table VI we present the optimized values of K_0 and ρ_0 for the analytic SIDM model of Eq. (3) for which the maximum compatibility with the SPARC data is achieved. In Figs. 10, 11 we present the

TABLE VI: SIDM Optimization Values for the galaxy UGC00634

Parameter	Optimization Values
$\rho_0 (M_\odot/\text{Kpc}^3)$	1.51522×10^7
$K_0 (M_\odot \text{Kpc}^{-3} (\text{km/s})^2)$	5162.06

density of the analytic SIDM model, the predicted rotation curves for the SIDM model (3), versus the SPARC observational data and the sound speed, as a function of the radius respectively. As it can be seen, for this galaxy, the SIDM model produces viable rotation curves which are compatible with the SPARC data.

B. Sample of Non-Viable Galaxies

1. The Galaxy ESO444-G084, Non-viable

For this galaxy, the optimization method we used, ensures maximum compatibility of the analytic SIDM model of Eq. (3) with the SPARC data, if we choose $\rho_0 = 1.16532 \times 10^8 M_\odot/\text{Kpc}^3$ and $K_0 = 1660.95 M_\odot \text{Kpc}^{-3} (\text{km/s})^2$, in which case the reduced χ^2_{red} value is $\chi^2_{\text{red}} = 4.40899$. Also the parameter α in this case is $\alpha = 2.17875 \text{Kpc}$.

In Table VII we present the optimized values of K_0 and ρ_0 for the analytic SIDM model of Eq. (3) for which the maximum compatibility with the SPARC data is achieved. In Figs. 12, 13 we present the

TABLE VII: SIDM Optimization Values for the galaxy ESO444-G084

Parameter	Optimization Values
$\rho_0 (M_\odot/\text{Kpc}^3)$	1.16532×10^8
$K_0 (M_\odot \text{Kpc}^{-3} (\text{km/s})^2)$	1660.95

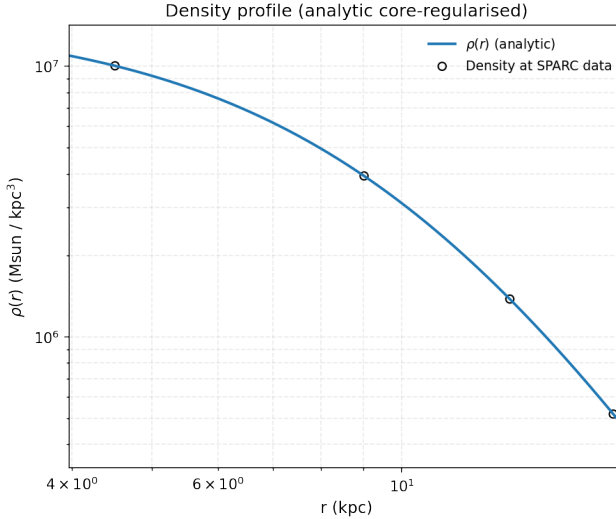


FIG. 10: The density of the SIDM model of Eq. (3) for the galaxy UGC00634, versus the radius.

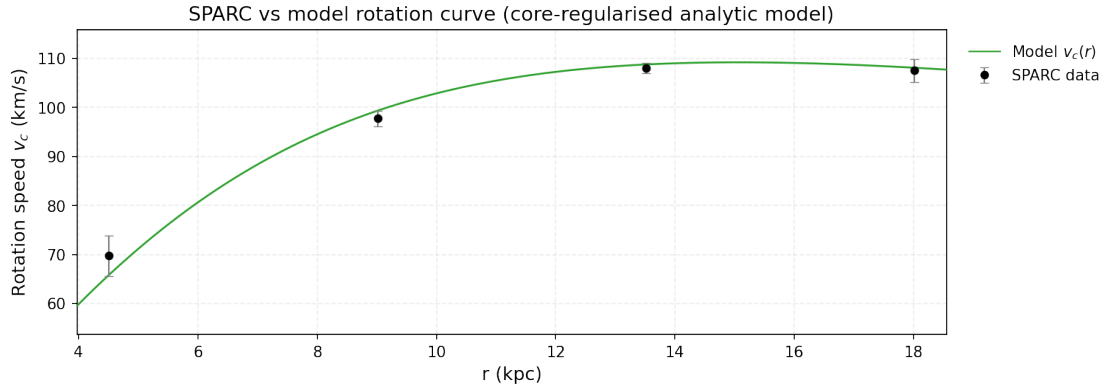


FIG. 11: The predicted rotation curves for the optimized SIDM model of Eq. (3), versus the SPARC observational data for the galaxy UGC00634.

density of the analytic SIDM model, the predicted rotation curves for the SIDM model (3), versus the SPARC observational data and the sound speed, as a function of the radius respectively. As it can be seen, for this galaxy, the SIDM model produces marginally viable rotation curves which are marginally compatible with the SPARC data.

Now we shall include contributions to the rotation velocity from the other components of the galaxy, namely the disk, the gas, and the bulge if present. In Fig. 14 we present the combined rotation curves including all the components of the galaxy along with the SIDM. As it can be seen, the extended collisional DM model is marginally viable. Also in Table VIII we present the optimized values of the free parameters of the SIDM model for which we achieve the maximum compatibility with the SPARC data, for the galaxy ESO444-G084, and also the resulting reduced χ^2_{red} value.

TABLE VIII: Optimized Parameter Values of the Extended SIDM model for the Galaxy ESO444-G084.

Parameter	Value
$\rho_0 (M_\odot / \text{Kpc}^3)$	7.0461×10^7
$K_0 (M_\odot \text{ Kpc}^{-3} (\text{km/s})^2)$	1530.99
ml_{disk}	1
ml_{bulge}	0.2225
$\alpha (\text{Kpc})$	2.68972
χ^2_{red}	3.66799

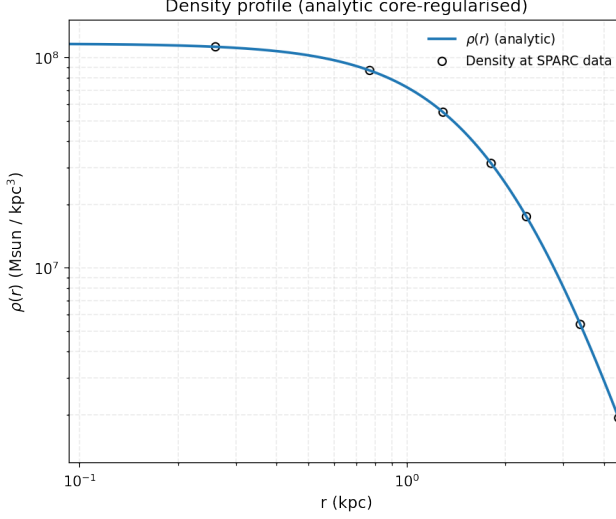


FIG. 12: The density of the SIDM model of Eq. (3) for the galaxy ESO444-G084, versus the radius.

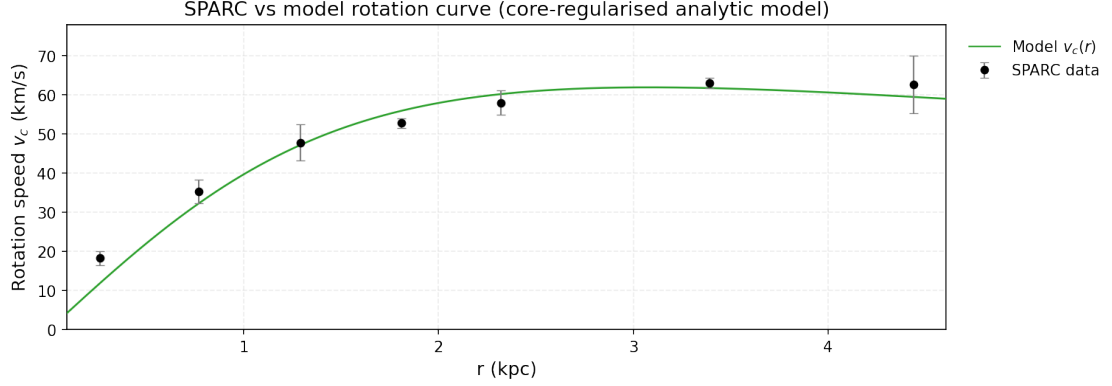


FIG. 13: The predicted rotation curves for the optimized SIDM model of Eq. (3), versus the SPARC observational data for the galaxy ESO444-G084.

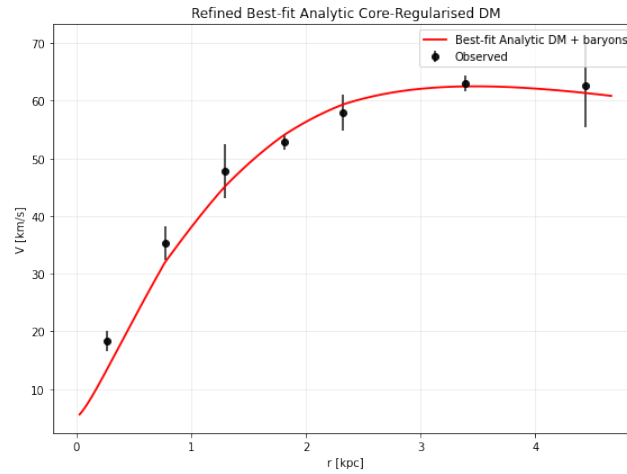


FIG. 14: The predicted rotation curves after using an optimization for the SIDM model (3), and the extended SPARC data for the galaxy ESO444-G084. We included the rotation curves of the gas, the disk velocities, the bulge (where present) along with the SIDM model.

2. The Galaxy IC4202, Non-viable

For this galaxy, the optimization method we used, ensures maximum compatibility of the analytic SIDM model of Eq. (3) with the SPARC data, if we choose $\rho_0 = 1.36561 \times 10^8 M_\odot/\text{Kpc}^3$ and $K_0 = 27737.5 M_\odot \text{Kpc}^{-3} (\text{km/s})^2$, in which case the reduced χ^2_{red} value is $\chi^2_{red} = 6.79581$. Also the parameter α in this case is $\alpha = 8.22471 \text{Kpc}$.

In Table IX we present the optimized values of K_0 and ρ_0 for the analytic SIDM model of Eq. (3) for which the maximum compatibility with the SPARC data is achieved. In Figs. 15, 16 we present the

TABLE IX: SIDM Optimization Values for the galaxy IC4202

Parameter	Optimization Values
$\rho_0 (M_\odot/\text{Kpc}^3)$	1.36561×10^8
$K_0 (M_\odot \text{Kpc}^{-3} (\text{km/s})^2)$	27737.5

density of the analytic SIDM model, the predicted rotation curves for the SIDM model (3), versus the SPARC observational data and the sound speed, as a function of the radius respectively. As it can be seen, for this galaxy, the SIDM model produces non-viable rotation curves which are incompatible with the SPARC data.

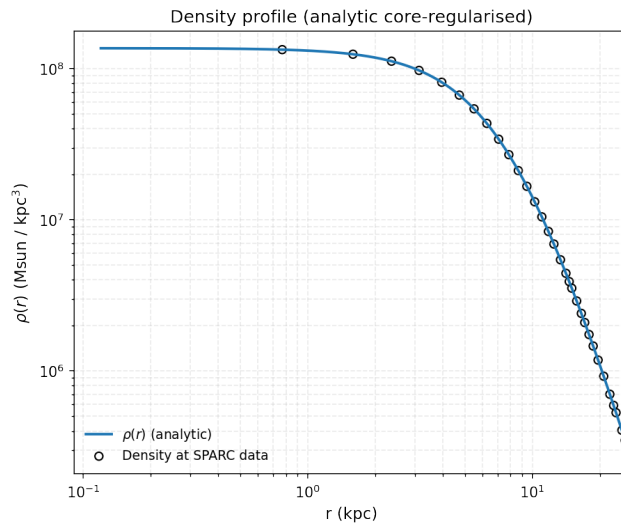


FIG. 15: The density of the SIDM model of Eq. (3) for the galaxy IC4202, versus the radius.

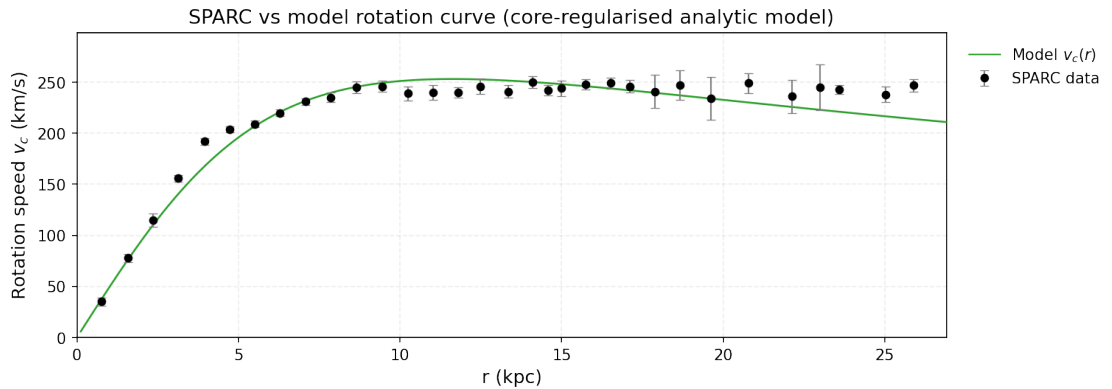


FIG. 16: The predicted rotation curves for the optimized SIDM model of Eq. (3), versus the SPARC observational data for the galaxy IC4202.

Now we shall include contributions to the rotation velocity from the other components of the galaxy, namely the disk, the gas, and the bulge if present. In Fig. 17 we present the combined rotation curves

including all the components of the galaxy along with the SIDM. As it can be seen, the extended collisional DM model is non-viable. Also in Table X we present the optimized values of the free parameters of the

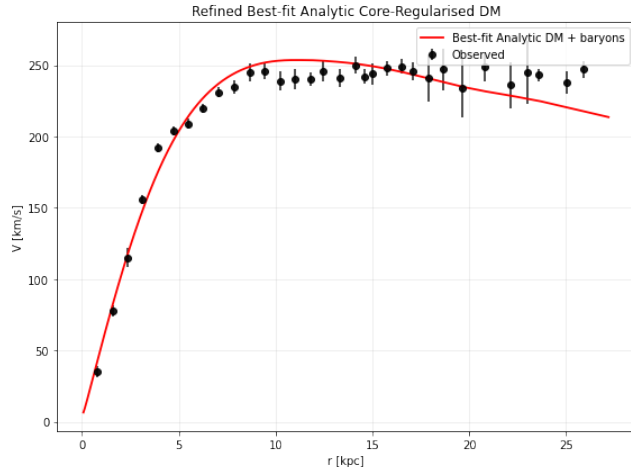


FIG. 17: The predicted rotation curves after using an optimization for the SIDM model (3), and the extended SPARC data for the galaxy IC4202. We included the rotation curves of the gas, the disk velocities, the bulge (where present) along with the SIDM model.

SIDM model for which we achieve the maximum compatibility with the SPARC data, for the galaxy IC4202, and also the resulting reduced χ^2_{red} value.

TABLE X: Optimized Parameter Values of the Extended SIDM model for the Galaxy IC4202.

Parameter	Value
ρ_0 (M_\odot/Kpc^3)	1.55781×10^8
K_0 ($M_\odot \text{ Kpc}^{-3} (\text{km/s})^2$)	27821.3
ml_{disk}	0.7
ml_{bulge}	0.0523
α (Kpc)	7.7113
χ^2_{red}	4.67298

3. The Galaxy UGC00128, Non-viable

For this galaxy, the optimization method we used, ensures maximum compatibility of the analytic SIDM model of Eq. (3) with the SPARC data, if we choose $\rho_0 = 7.17146 \times 10^6 M_\odot/\text{Kpc}^3$ and $K_0 = 7652.87 M_\odot \text{ Kpc}^{-3} (\text{km/s})^2$, in which case the reduced χ^2_{red} value is $\chi^2_{red} = 40.4415$. Also the parameter α in this case is $\alpha = 18.8521 \text{ Kpc}$.

In Table XI we present the optimized values of K_0 and ρ_0 for the analytic SIDM model of Eq. (3) for which the maximum compatibility with the SPARC data is achieved. In Figs. 18, 19 we present the

TABLE XI: SIDM Optimization Values for the galaxy UGC00128

Parameter	Optimization Values
ρ_0 (M_\odot/Kpc^3)	7.17146×10^6
K_0 ($M_\odot \text{ Kpc}^{-3} (\text{km/s})^2$)	7652.87

density of the analytic SIDM model, the predicted rotation curves for the SIDM model (3), versus the SPARC observational data and the sound speed, as a function of the radius respectively. As it can be seen, for this galaxy, the SIDM model produces non-viable rotation curves which are incompatible with the SPARC data.

Now we shall include contributions to the rotation velocity from the other components of the galaxy, namely the disk, the gas, and the bulge if present. In Fig. 20 we present the combined rotation curves including all the components of the galaxy along with the SIDM. As it can be seen, the extended collisional

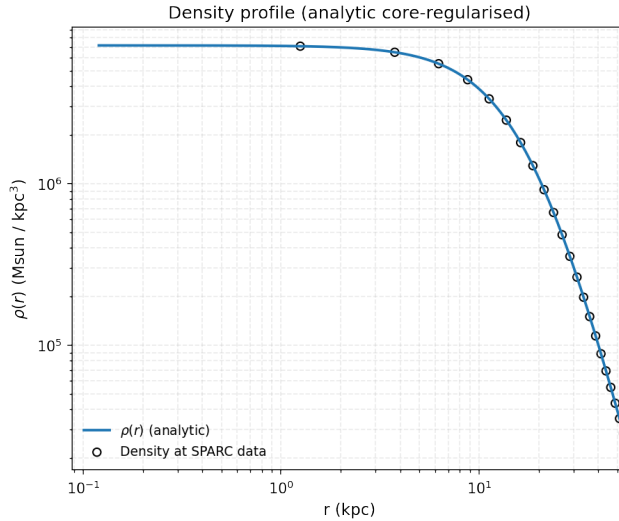


FIG. 18: The density of the SIDM model of Eq. (3) for the galaxy UGC00128, versus the radius.

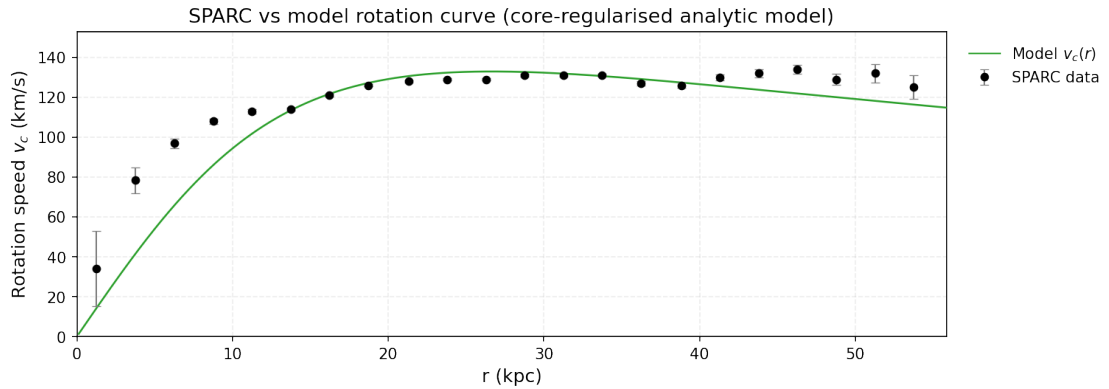


FIG. 19: The predicted rotation curves for the optimized SIDM model of Eq. (3), versus the SPARC observational data for the galaxy UGC00128.

DM model is non-viable. Also in Table XII we present the optimized values of the free parameters of

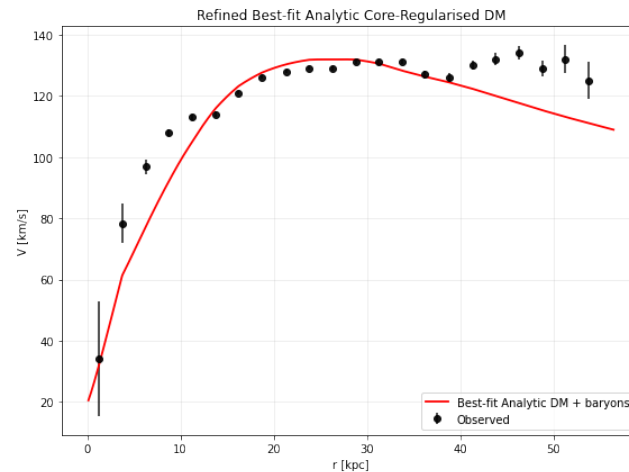


FIG. 20: The predicted rotation curves after using an optimization for the SIDM model (3), and the extended SPARC data for the galaxy UGC00128. We included the rotation curves of the gas, the disk velocities, the bulge (where present) along with the SIDM model.

the SIDM model for which we achieve the maximum compatibility with the SPARC data, for the galaxy UGC00128, and also the resulting reduced χ^2_{red} value.

TABLE XII: Optimized Parameter Values of the Extended SIDM model for the Galaxy UGC00128.

Parameter	Value
$\rho_0 (M_\odot/\text{Kpc}^3)$	5.5792×10^6
$K_0 (M_\odot \text{ Kpc}^{-3} (\text{km/s})^2)$	5775.12
m_{disk}	1
m_{bulge}	0.3491
$\alpha (\text{Kpc})$	18.5648
χ^2_{red}	30.8249

4. The Galaxy UGC00191, Non-viable

For this galaxy, the optimization method we used, ensures maximum compatibility of the analytic SIDM model of Eq. (3) with the SPARC data, if we choose $\rho_0 = 1.02285 \times 10^8 M_\odot/\text{Kpc}^3$ and $K_0 = 3293.19 M_\odot \text{ Kpc}^{-3} (\text{km/s})^2$, in which case the reduced χ^2_{red} value is $\chi^2_{red} = 26.1093$. Also the parameter α in this case is $\alpha = 3.27457 \text{ Kpc}$.

In Table XIII we present the optimized values of K_0 and ρ_0 for the analytic SIDM model of Eq. (3) for which the maximum compatibility with the SPARC data is achieved. In Figs. 21, 22 we present the

TABLE XIII: SIDM Optimization Values for the galaxy UGC00191

Parameter	Optimization Values
$\rho_0 (M_\odot/\text{Kpc}^3)$	1.02285×10^8
$K_0 (M_\odot \text{ Kpc}^{-3} (\text{km/s})^2)$	3293.19

density of the analytic SIDM model, the predicted rotation curves for the SIDM model (3), versus the SPARC observational data and the sound speed, as a function of the radius respectively. As it can be seen, for this galaxy, the SIDM model produces non-viable rotation curves which are incompatible with the SPARC data.

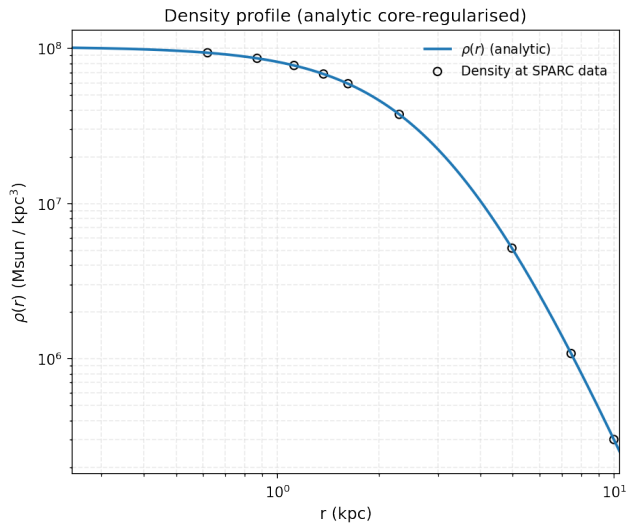


FIG. 21: The density of the SIDM model of Eq. (3) for the galaxy UGC00191, versus the radius.

Now we shall include contributions to the rotation velocity from the other components of the galaxy, namely the disk, the gas, and the bulge if present. In Fig. 23 we present the combined rotation curves including all the components of the galaxy along with the SIDM. As it can be seen, the extended collisional DM model is non-viable. Also in Table XIV we present the optimized values of the free parameters of

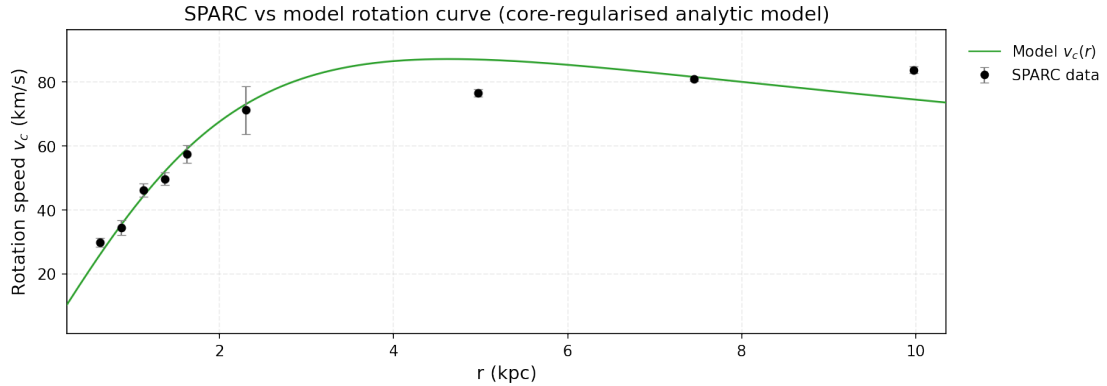


FIG. 22: The predicted rotation curves for the optimized SIDM model of Eq. (3), versus the SPARC observational data for the galaxy UGC00191.

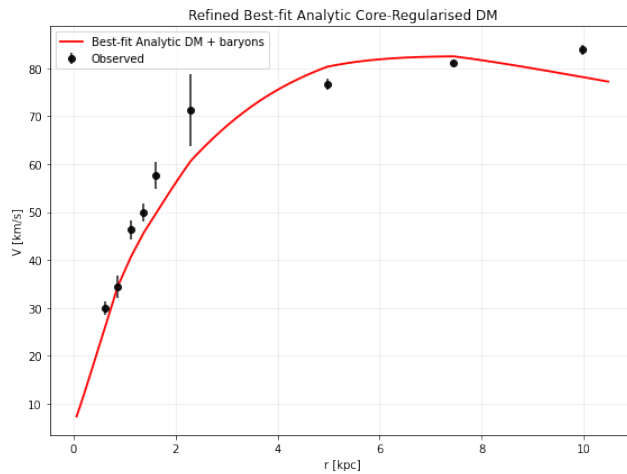


FIG. 23: The predicted rotation curves after using an optimization for the SIDM model (3), and the extended SPARC data for the galaxy UGC00191. We included the rotation curves of the gas, the disk velocities, the bulge (where present) along with the SIDM model.

the SIDM model for which we achieve the maximum compatibility with the SPARC data, for the galaxy UGC00191, and also the resulting reduced χ^2_{red} value.

TABLE XIV: Optimized Parameter Values of the Extended SIDM model for the Galaxy UGC00191.

Parameter	Value
ρ_0 (M_\odot/Kpc^3)	2.92141×10^7
K_0 ($M_\odot \text{ Kpc}^{-3} (\text{km/s})^2$)	1897.33
ml_{disk}	1
ml_{bulge}	0.2668
α (Kpc)	4.6502
χ^2_{red}	15.5091

5. The Galaxy UGC00731, Non-viable

For this galaxy, the optimization method we used, ensures maximum compatibility of the analytic SIDM model of Eq. (3) with the SPARC data, if we choose $\rho_0 = 2.29854 \times 10^7 M_\odot/\text{Kpc}^3$ and $K_0 = 2228.14 M_\odot \text{ Kpc}^{-3} (\text{km/s})^2$, in which case the reduced χ^2_{red} value is $\chi^2_{red} = 5.02761$. Also the parameter α in this case is $\alpha = 5.68194 \text{ Kpc}$.

In Table XV we present the optimized values of K_0 and ρ_0 for the analytic SIDM model of Eq. (3) for which the maximum compatibility with the SPARC data is achieved. In Figs. 24, 25 we present the

TABLE XV: SIDM Optimization Values for the galaxy UGC00731

Parameter	Optimization Values
$\rho_0 (M_\odot/\text{Kpc}^3)$	2.29854×10^7
$K_0 (M_\odot \text{ Kpc}^{-3} (\text{km/s})^2)$	2228.14

density of the analytic SIDM model, the predicted rotation curves for the SIDM model (3), versus the SPARC observational data and the sound speed, as a function of the radius respectively. As it can be seen, for this galaxy, the SIDM model produces non-viable rotation curves which are incompatible with the SPARC data.

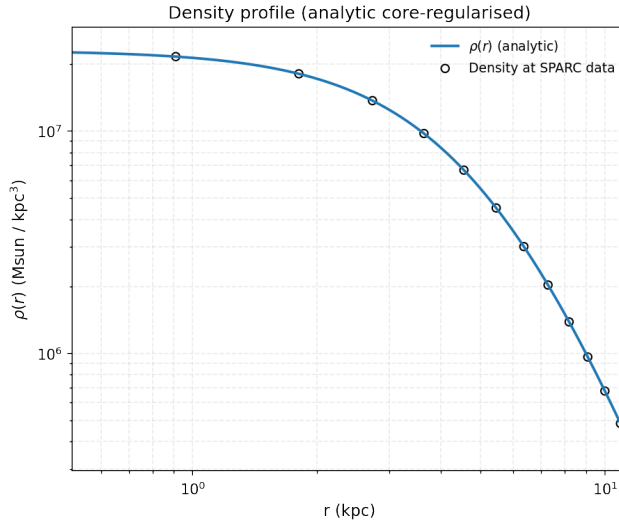


FIG. 24: The density of the SIDM model of Eq. (3) for the galaxy UGC00731, versus the radius.

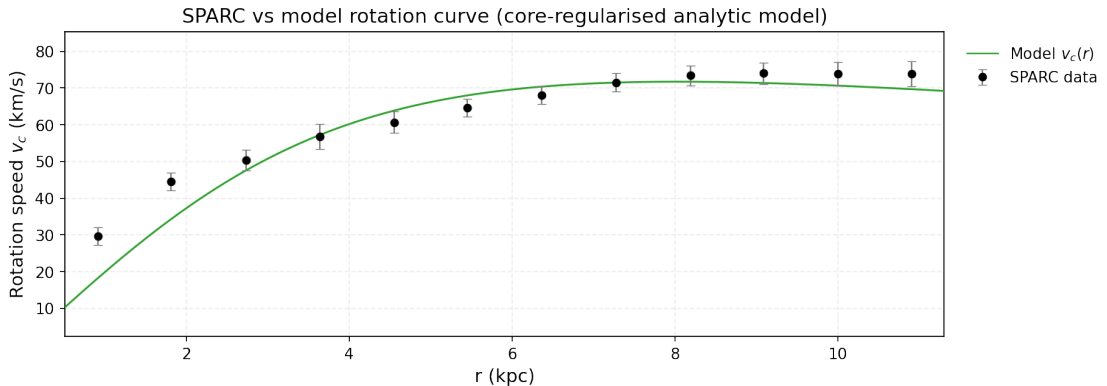


FIG. 25: The predicted rotation curves for the optimized SIDM model of Eq. (3), versus the SPARC observational data for the galaxy UGC00731.

Now we shall include contributions to the rotation velocity from the other components of the galaxy, namely the disk, the gas, and the bulge if present. In Fig. 26 we present the combined rotation curves including all the components of the galaxy along with the SIDM. As it can be seen, the extended collisional DM model is non-viable. Also in Table XVI we present the optimized values of the free parameters of the SIDM model for which we achieve the maximum compatibility with the SPARC data, for the galaxy UGC00731, and also the resulting reduced χ^2_{red} value.

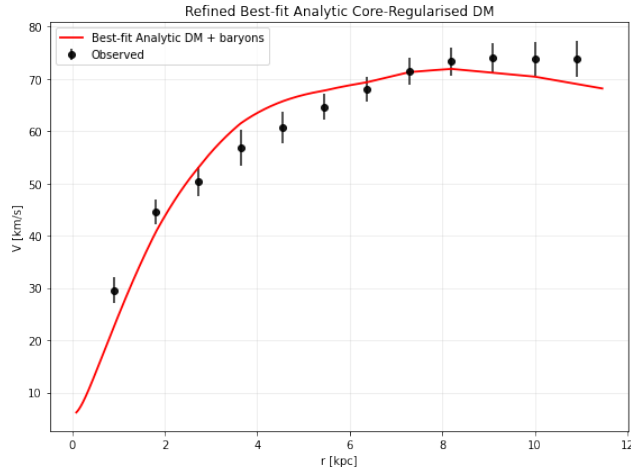


FIG. 26: The predicted rotation curves after using an optimization for the SIDM model (3), and the extended SPARC data for the galaxy UGC00731. We included the rotation curves of the gas, the disk velocities, the bulge (where present) along with the SIDM model.

TABLE XVI: Optimized Parameter Values of the Extended SIDM model for the Galaxy UGC00731.

Parameter	Value
$\rho_0 (M_\odot/\text{Kpc}^3)$	3.25951×10^7
$K_0 (M_\odot \text{ Kpc}^{-3} (\text{km/s})^2)$	1759.7
ml_{disk}	1
ml_{bulge}	0.5214
$\alpha (\text{Kpc})$	4.23974
χ^2_{red}	2.85359

C. Viable Galaxies and Their Characteristics

A central outcome of the present work is the clear distinction of the SPARC galaxy sample into two main classes: firstly systems for which our analytic isothermal-like halo model fits well the rotation curves, and systems for which the rotation curves are not fitted optimally by the analytic model. In this section we shall discuss the common properties of these two classes and we shall attempt to provide a physical interpretation of why the model succeeds in the former while fails in the latter class of galaxies.

The viable galaxies share several qualitative properties, first, viable galaxies are mostly late-type systems, typically classified in the literature as irregulars, dwarfs, or late-type (small size) spirals. These galaxies are generally bulge-less, or have only negligible bulge components. Their stellar mass distributions are therefore dynamically subdominant over the radii of the galaxies, and especially in the outer skirts of the galaxies, where the rotation curves approach a quasi-flat regime, at least for the spirals. Second, the viable galaxies tend to be gas-rich systems with extended rotation curves. Observationally, these galaxies exhibit well-defined measurements of the flat rotation velocity V_{flat} which is different from the maximum inner velocity V_{max} . Thirdly, the viable galaxies typically show smooth and slowly rising rotation curves, with a small-scale structure. This behavior is consistent with systems that are close to a hydrodynamical equilibrium and are not strongly perturbed by bar structures. In these galaxies, the assumption of a hydrostatic equilibrium for the DM halo, which is the basis of our analytic model, is physically well motivated.

In contrast, a significant fraction of the non-viable systems are early-type spirals or galaxies with prominent bulge components. In these objects, the inner gravitational potential is mostly dominated by baryons, and the rotation curve often reaches its maximum value well inside the optical radius. Non-viable galaxies also seem to show more complex rotation curve morphologies, including inner steep rises, strongly declining outer profiles, and strong features that must be associated with the complex physics of the spiral arms, the bars, or even warps. This complexity indicates distinctive departures from the hydrodynamic (and thermodynamic) equilibrium conditions assumed for our analytic DM halo model. Thus, in the case of non-viable galaxies, a single and smooth, mostly pressure-supported halo, cannot simply reproduce the observed kinematics of the galaxies. In addition, several non-viable galaxies are relatively compact systems for which the baryonic mass remains dynamically important up to very large radii. In these galaxies, the dark halo does not dominate the gravitational potential regions where the model attempts

to achieve a quasi-flat velocity plateau. Hence, the interplay between halo thermodynamics and the observed kinematics breaks down. Our model basically describes a finite-mass, isothermal dark halo, with a radius dependent pressure profile,

$$P(r) = K(r)\rho(r),$$

with the parameter K_0 , the entropy parameter, encoding the global thermodynamic state of the halo. In late-type, DM-dominated galaxies, the outer rotation curve is mainly governed by the DM halo, and thus the baryonic components sub-dominantly affect the dynamics. Under these conditions, the hydrostatic equilibrium provides a correlation between the entropy parameter K_0 and the characteristic flat circular velocity.

Thus concluding, our results indicate that the analytic isothermal, scale-dependent EoS DM halo model, is compatible with galaxies that are DM dominated and structurally simple. For these systems, the model links the halo thermodynamics to the rotation curve kinematics and the baryonic mass.

IV. THE MODEL FAILS TO PRODUCE THE CANONICAL TULLY-FISHER LAW

One of the central goals of this work is to assess whether the fully analytic, scale-dependent isothermal EoS DM model can reproduce the observed baryonic scaling relations of disk galaxies, and specifically the baryonic Tully-Fisher relation. Firstly however, let us investigate the canonical Tully-Fisher relation using an empirical, bottom-up approach. We shall investigate whether the observed luminosity-velocity scaling $L_0 \sim V_{max}^4$ can emerge naturally in our model, from the following relations, the $L_0 - K_0$ relation and the $K_0 - V_{max}$ relation. If both relations are well described by power-law behavior, then the model should in principle predict an effective Tully-Fisher relation based on the role of K_0 , without any direct coupling between the baryons and the kinematics. For our analysis, we shall restrict ourselves to the subset of viable galaxies, which are those for which the fully analytic, scale-dependent isothermal EoS DM model can optimally reproduce their rotation curves. We first fit the luminosity-halo relation $L_0 - K_0$, using a power-law ansatz of the form,

$$L_0 = A_L K_0^\alpha. \quad (14)$$

Using the SPARC data for the viable galaxies, and the values of K_0 we found, we obtained,

$$A_L = (1.63 \pm 2.91) \times 10^{-5}, \quad (15)$$

$$\alpha = 1.62 \pm 0.19. \quad (16)$$

This result indicates a moderately strong scaling between the luminosity and the thermodynamic normalization K_0 of the halo. The slope $\alpha > 1$ implies that more luminous systems reside in the halos with a substantially larger effective pressure support.

Next, we fitted the relation between the halo normalization K_0 and the maximum circular velocity V_{max} ,

$$K_0 = A_K V_{max}^\beta, \quad (17)$$

which yielded the following results,

$$A_K = 2.57 \pm 0.96, \quad (18)$$

$$\beta = 1.60 \pm 0.07. \quad (19)$$

This relation suggests that K_0 is strongly correlated to the depth of the gravitational potential, and this result may be interpreted as an effective thermodynamic characteristic of the halo mass and velocity scale. By combining the two relations we found above, the model predicts the following effective luminosity-velocity $L_0 - V_{max}$ relation,

$$L_0 \propto V_{max}^\gamma, \quad \gamma = \alpha \beta. \quad (20)$$

Using the best-fit values from our results we find that the analytic halo model predicts,

$$L_0 \propto V_{max}^{2.6}, \quad (21)$$

which is significantly shallower than the well-known canonical Tully-Fisher relation $L_0 \sim V_{max}^4$. In Fig. 27 we present the $L_0 - V_{max}$ relation for the the fully analytic, scale-dependent isothermal EoS DM

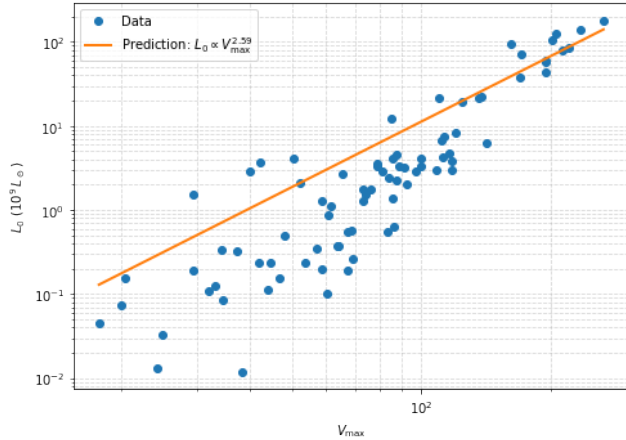


FIG. 27: The plot $L - V_{max}$ for the 116 viable galaxies we found from the SPARC data and the optimal fit of it with the orange line.

model. The discrepancy between the predicted slope $\gamma \simeq 2.6$ and the observed value near 4 clearly demonstrates that the analytic isothermal scale-dependent EoS DM halo model fails to reproduce the canonical Tully-Fisher law. This is in contrast to the nearly isothermal model we developed in Ref. [2], and it seems that the presence of a polytropic exponent, even if it is nearly isothermal, plays a role. We do not fully understand this result, since we expected that the isothermal EoS will reproduce the exact canonical Tully-Fisher relation. But it seems that this result might be model-dependent, and for the analytic model, the canonical Tully-Fisher relation is not reproduced. A correct and definitive answer to this can be obtained if the model [2] is analyzed through the prism of a purely isothermal EoS. Then a direct comparison can be made, and we aim to perform this analysis in a forthcoming article.

V. THE BARYONIC TULLY-FISHER RELATION FOR THE VIABLE GALAXIES AND ITS DERIVATION FROM $K_0 - M_b$ AND $K_0 - V_{flat}$ RELATIONS

While the failure of the luminosity-based Tully-Fisher relation highlights the limitations of the analytic scale-dependent EoS DM model, the physically more fundamental relation related to purely DM dominated galaxies, is the baryonic Tully-Fisher relation, which links the total baryonic mass M_b to the asymptotic flat rotation velocity V_{flat} . Unlike the luminosity, the baryonic mass is a conserved quantity and is not a quantity which is directly affected by the star-formation history or from stellar mass-to-light ratio variations. Consequently, the baryonic Tully-Fisher provides a more clear probe of the underlying dynamical equilibrium of galaxies. And also, since the flat velocity is used, it is more related to the strength of the DM gravitational potential.

In this section, we shall investigate whether the analytic isothermal scale-dependent EoS DM model, is capable of reproducing the baryonic Tully-Fisher relation, when the asymptotic velocity V_{flat} is used as the relevant kinematic variable and the baryonic mass is used instead of the luminosity. We proceed in direct analogy with the previous luminosity-based analysis. Firstly, let us examine the correlation between the halo thermodynamic normalization parameter K_0 and the flat rotation velocity V_{flat} , fitting a power-law relation of the form

$$K_0 = A V_{flat}^n. \quad (22)$$

The best-fit parameters we found are,

$$A = 2.62 \pm 1.21, \quad (23)$$

$$n = 1.61 \pm 0.09. \quad (24)$$

Next, we fit the baryonic mass as a function of the halo normalization parameter K_0 ,

$$M_b = A K_0^n, \quad (25)$$

and in this case we found,

$$A = 2.68 \pm 4.91, \quad (26)$$

$$n = 2.49 \pm 0.19. \quad (27)$$

Combining the two empirical relations we found above, the model predicts a baryonic Tully-Fisher relation of the form,

$$M_b \propto V_{flat}^\gamma, \quad \gamma = n_{(M_b - K_0)} \times n_{(K_0 - V_{flat})}. \quad (28)$$

Using the best-fit values, we get,

$$\gamma = 4.03 \pm 0.37, \quad (29)$$

which is fully consistent with the observed baryonic Tully-Fisher relation,

$$M_b \propto V_{flat}^4. \quad (30)$$

Also in Fig. 28 we present the resulting $M_b - V_{flat}$ relation using the intermediate relations $M_b - K_0$ and $K_0 - V_{flat}$. The orange line is the optimal fitting. Thus the analytic isothermal scale-dependent

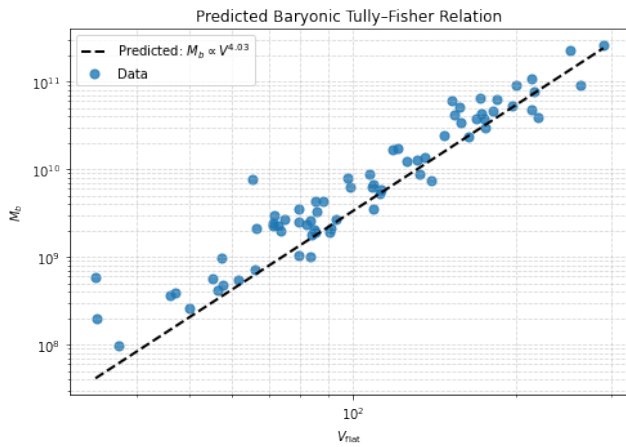


FIG. 28: The plot $K_0 - V_{flat}$ for the viable galaxies we found from the SPARC data, for which a V_{flat} is given. The orange line is the best fit.

EoS DM model is capable of producing the baryonic Tully-Fisher relation. The key distinction relative to the failed luminosity-based canonical Tully-Fisher relation lies, probably, in using of V_{flat} instead of V_{max} . The flat velocity probes directly the outer halo, which is dominated by DM, and where the galactic system reaches the hydrostatic equilibrium. There, the analytic DM density profile provides an accurate description of the DM gravitational potential. Hence, the effective pressure radial support embodied in the entropy parameter K_0 directly controls the flat circular velocity. However, in Ref. [2], both the canonical and the baryonic Tully-Fisher relation were produced in a semi-empirical and semi-theoretical way. In the present framework only the baryonic Tully-Fisher relation was derived by the $M_b - K_0$ and $K_0 - V_{flat}$ relations. The reason for this difference has to be model-dependent, and we will be certain on this, after further work is done on the model developed [2] in its purely isothermal limit.

VI. CONCLUSIONS

In this work we extended the scale-dependent EoS self-interacting DM framework developed in Ref. [2], and provided an analytic framework of scale-dependent EoS self-interacting DM with an isothermal EoS. Our model can provide perfect fit for the rotation curves of 116 galaxies taken from the SPARC data [69], however 59 galaxies cannot be fitted optimally. The rotation curves of the 116 viable galaxies are either described solely by the analytic scale-dependent EoS self-interacting DM, or by the combination of the latter with the other galaxy components such as the bulge (where present), the disk and the gas. The viable galaxies consist mostly of late-time galaxies, which are low-luminosity spirals, low-mass spirals, low surface brightness spirals, irregular galaxies and dwarfs. On the other hand, the non-viable galaxies consist of early-time objects, such as massive spirals with prominent bulge and bar structures. For the viable galaxies, we also thoroughly sought for correlations of the entropy parameter K_0 with the maximum velocity of each galaxy V_{max} , the flat velocity V_{flat} , the luminosity L_0 and the baryonic mass

M_b . In this way the correlation between $K_0 - V_{flat}$ and $M_b - K_0$ for the viable galaxies, yielded naturally the baryonic Tully-Fisher relation $M_b \sim V_{flat}^4$. However, this model failed to produce the canonical Tully-Fisher relation via the correlations $L_0 - K_0$ and $K_0 - V_{max}$. On the contrary the model used in Ref. [2] was able to reproduce both the baryonic Tully-Fisher relation and the canonical Tully-Fisher relation almost naturally. Honestly we cannot explain this feature of the present work. Intuitively, one expects that the findings of [2] would apply in the present context too, because the model [2] yields viable results for a near isothermal scale-dependent EoS. And one naturally expects the correlations $K_0 \sim V_{max}^2$ and $K_0 - V_{flat}^2$ do hold true in nearly isothermal halos. We did not find such evidence for the present model and we do not fully understand why. Perhaps it is a model dependent feature, and the only way to be certain is to take the direct isothermal limit of Ref. [2] and compare the results. If the findings of the new research directive do not yield the correlations $K_0 \sim V_{max}^2$ and $K_0 - V_{flat}^2$, this will be a clear indication

that the presence of an exponent in the radius-dependent EoS $P(r) = K(r) \left(\frac{\rho(r)}{\rho_*} \right)^{\gamma(r)}$, even if it is nearly isothermal, eventually plays a role. If the correlations $K_0 \sim V_{max}^2$ and $K_0 - V_{flat}^2$ are validated even for the isothermal version of Ref. [2], then this would imply that the correlations $K_0 \sim V_{max}^2$ and $K_0 - V_{flat}^2$ are somehow a model dependent feature. We suspect that the presence of a non-trivial exponent, even if it is nearly isothermal, stabilizes the halo and provides more concrete radial pressure support that eventually realizes the correlations $K_0 \sim V_{max}^2$ and $K_0 - V_{flat}^2$ in the halo. Work and research is planned towards this problem and we expect to report on this issue soon.

Of course, there is much work to be done even for the analytic model we introduced, this was an introductory article. Having a scale-dependent EoS self-interacting DM, this would mean that DM is dissipative, so there is always the possibility of having a dark disk [36, 70, 71]. This must be discussed also in view of the maximum disk hypothesis. The gravothermal stability in these models must also be studied, but these studies stretch far beyond the aims and scopes of this article.

In addition, an interesting class of galaxies in the Universe that might be perfectly theoretically harbored by the scale-dependent EoS self-interacting DM framework are the dark galaxies. Recent evidence from the Cloud-9 galaxy indicated that it is gas dominated and DM dominated but contains no stars [72–74]. So it is a dark galaxy, not perfectly described (if described at all) by the Λ CDM. Let us discuss this issue, because it is rather physically interesting. The Cloud-9 system, is characterized by extreme DM dominance, and also negligible stellar luminosity, and challenges directly standard galaxy formation scenarios which are implied by the Λ CDM model.

In the conventional Λ CDM models, such objects would require a combination of inefficient star formation, strong feedback, and a truly fine-tuned halo, in order to suppress the baryonic collapse and in parallel, maintaining a dynamically cold and extended halo. However, even under these assumptions, reproducing the observed smoothness and equilibrium remains problematic, as collisionless DM halos do not naturally thermalize without invoking an additional baryonic regulation.

In contrast, the analytic model we developed here, based on a radius-dependent isothermal EoS, provides a natural and self-consistent framework for the Cloud-9 galaxy. In our framework, the DM halo is an effective fluid with a pressure proportional to density, which allows the system to reach a hydrostatic equilibrium. The absence of a luminous disk is thus not a pathology but a rather expected outcome of the DM halo, without requiring baryon feedback to stabilize the galaxy. Hence, the existence of Cloud-9 types of dark galaxies, supports the notion that DM halos may possess an intrinsic, approximately isothermal structure on galactic scales, with a pressure support and the thermalization playing a central dynamical role. Λ CDM cannot easily harbor such pressure supported baryon-less galactic structures. On the other hand, DM emulator theoretical constructions, such as MOND theories, cannot describe Cloud-9 types of galaxies. Specifically, the Cloud-9 system itself by observation, imposes fundamental problems for the MOND description, precisely because its observed kinematics are not those of a rotating disk galaxy. Cloud-9 is basically a starless neutral atomic hydrogen (HI) cloud, the dynamical state of which is inferred from the narrow 21 cm line widths, and the associated spatially resolved gas morphology, and not from an extended rotation curve, like in baryon existing spirals. The observations indicate that the Cloud-9 system is dynamically cold, it lacks rotation, and it is consistent with a gas cloud embedded in a DM halo.

In the MOND theoretical construction, the gravitational dynamics are determined entirely by the total distribution of the baryonic matter, and thus MOND aims to explain the rotationally supported systems where circular velocities trace the baryonic mass distribution. For the Cloud-9, however, the baryonic content is small-if present at all. The observed HI line width cannot be straightforwardly interpreted as circular velocity, and even if it was, the baryonic mass is very small to provide dynamical support in the context of MOND without perhaps invoking unrealistically strong external field effects. Moreover, MOND lacks a natural framework to describe a pressure-supported, starless equilibrium systems. The very own existence of a long-lived, and dynamically coherent HI cloud with a negligible stellar mass

and also no rotational support, apparently contradicts the MOND central theme, that the baryons by themselves can determine galactic dynamics. In this sense, the Cloud-9 is a sound example of objects that directly contradict the core axioms of MOND, and regardless if fine-tunings are used, MOND cannot describe dark galaxies at all. The scale-dependent EoS self-interacting DM provides a natural theoretical framework that can harbor pressure supported hydrogen clouds embedded in a pressure self-regulated DM halo in hydrodynamic and thermodynamic equilibrium.

Appendix: Complete List of Galactic Rotation Curves Simulations for All the SPARC Galaxies

In this appendix we present the full analysis of the fitting of the analytic model of scale-dependent EoS DM with the SPARC galaxies .

1. The Galaxy D631-7

For this galaxy, the optimization method we used, ensures maximum compatibility of the analytic SIDM model of Eq. (3) with the SPARC data, if we choose $\rho_0 = 1.80239 \times 10^7 M_\odot/\text{Kpc}^3$ and $K_0 = 1349.32 M_\odot \text{Kpc}^{-3} (\text{km/s})^2$, in which case the reduced χ^2_{red} value is $\chi^2_{\text{red}} = 0.631699$. Also the parameter α in this case is $\alpha = 4.99326 \text{Kpc}$.

In Table XVII we present the optimized values of K_0 and ρ_0 for the analytic SIDM model of Eq. (3) for which the maximum compatibility with the SPARC data is achieved. In Figs. 29, 30 we present the

TABLE XVII: SIDM Optimization Values for the galaxy D631-7

Parameter	Optimization Values
$\rho_0 (M_\odot/\text{Kpc}^3)$	1.80239×10^7
$K_0 (M_\odot \text{Kpc}^{-3} (\text{km/s})^2)$	1349.32

density of the analytic SIDM model, the predicted rotation curves for the SIDM model (3), versus the SPARC observational data and the sound speed, as a function of the radius respectively. As it can be seen, for this galaxy, the SIDM model produces viable rotation curves which are compatible with the SPARC data.

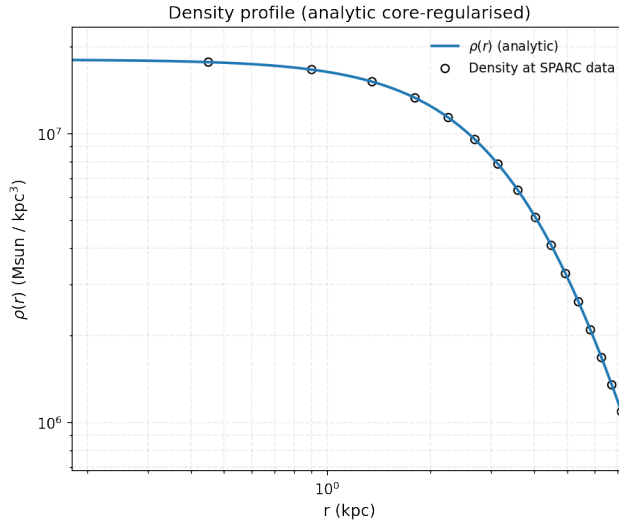


FIG. 29: The density of the SIDM model of Eq. (3) for the galaxy D631-7, versus the radius.

2. The Galaxy DDO064

For this galaxy, the optimization method we used, ensures maximum compatibility of the analytic SIDM model of Eq. (3) with the SPARC data, if we choose $\rho_0 = 5.49286 \times 10^7 M_\odot/\text{Kpc}^3$ and $K_0 =$

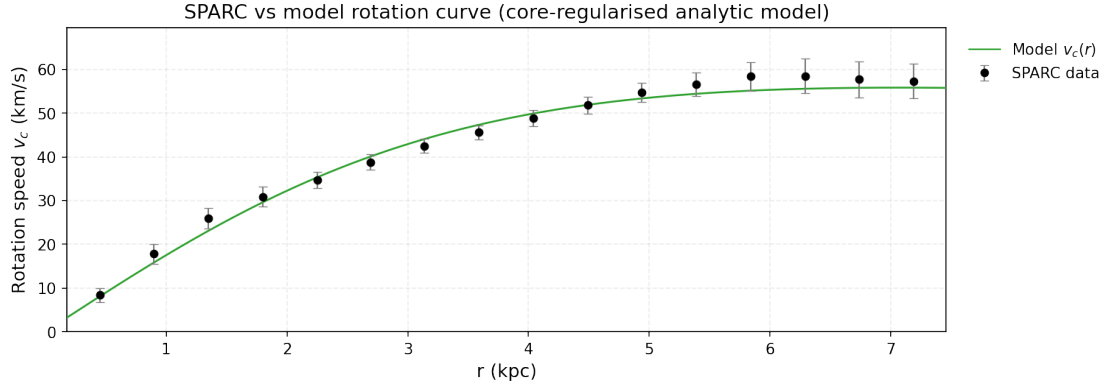


FIG. 30: The predicted rotation curves for the optimized SIDM model of Eq. (3), versus the SPARC observational data for the galaxy D631-7.

$1385.86 M_{\odot} \text{Kpc}^{-3} (\text{km/s})^2$, in which case the reduced χ^2_{red} value is $\chi^2_{red} = 0.456646$. Also the parameter α in this case is $\alpha = 2.89875 \text{Kpc}$.

In Table XVIII we present the optimized values of K_0 and ρ_0 for the analytic SIDM model of Eq. (3) for which the maximum compatibility with the SPARC data is achieved. In Figs. 31, 32 we present the

TABLE XVIII: SIDM Optimization Values for the galaxy DDO064

Parameter	Optimization Values
$\rho_0 (M_{\odot}/\text{Kpc}^3)$	5.49286×10^7
$K_0 (M_{\odot} \text{Kpc}^{-3} (\text{km/s})^2)$	1385.86

density of the analytic SIDM model, the predicted rotation curves for the SIDM model (3), versus the SPARC observational data and the sound speed, as a function of the radius respectively. As it can be seen, for this galaxy, the SIDM model produces viable rotation curves which are compatible with the SPARC data.

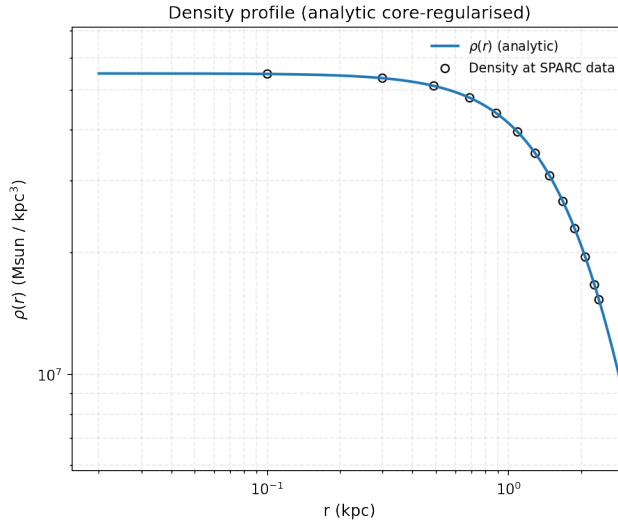


FIG. 31: The density of the SIDM model of Eq. (3) for the galaxy DDO064, versus the radius.

3. The Galaxy DDO161, Non-viable, Extended Viable

For this galaxy, the optimization method we used, ensures maximum compatibility of the analytic SIDM model of Eq. (3) with the SPARC data, if we choose $\rho_0 = 9.31455 \times 10^6 M_{\odot}/\text{Kpc}^3$ and $K_0 =$

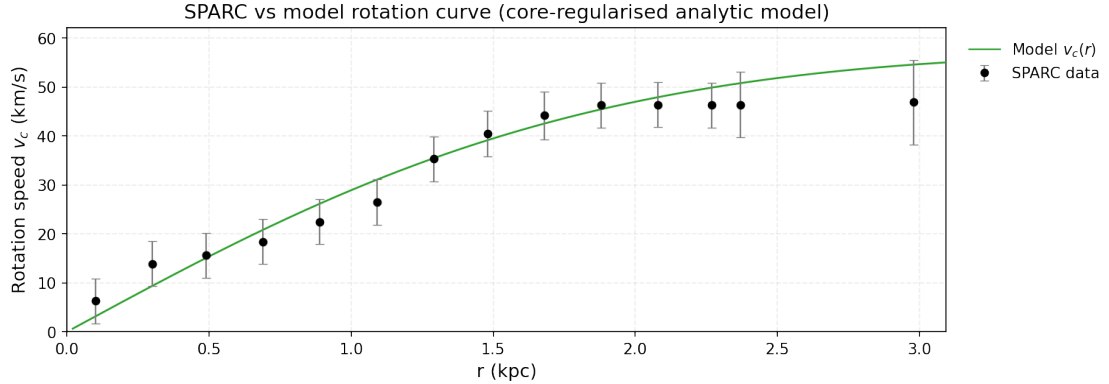


FIG. 32: The predicted rotation curves for the optimized SIDM model of Eq. (3), versus the SPARC observational data for the galaxy DDO064.

$1875.28 M_{\odot} \text{Kpc}^{-3} (\text{km/s})^2$, in which case the reduced χ^2_{red} value is $\chi^2_{red} = 2.22523$. Also the parameter α in this case is $\alpha = 8.18847 \text{Kpc}$.

In Table XIX we present the optimized values of K_0 and ρ_0 for the analytic SIDM model of Eq. (3) for which the maximum compatibility with the SPARC data is achieved. In Figs. 33, 34 we present the

TABLE XIX: SIDM Optimization Values for the galaxy DDO161

Parameter	Optimization Values
$\rho_0 (M_{\odot}/\text{Kpc}^3)$	9.31455×10^6
$K_0 (M_{\odot} \text{Kpc}^{-3} (\text{km/s})^2)$	1875.28

density of the analytic SIDM model, the predicted rotation curves for the SIDM model (3), versus the SPARC observational data and the sound speed, as a function of the radius respectively. As it can be seen, for this galaxy, the SIDM model produces non-viable rotation curves which are incompatible with the SPARC data.

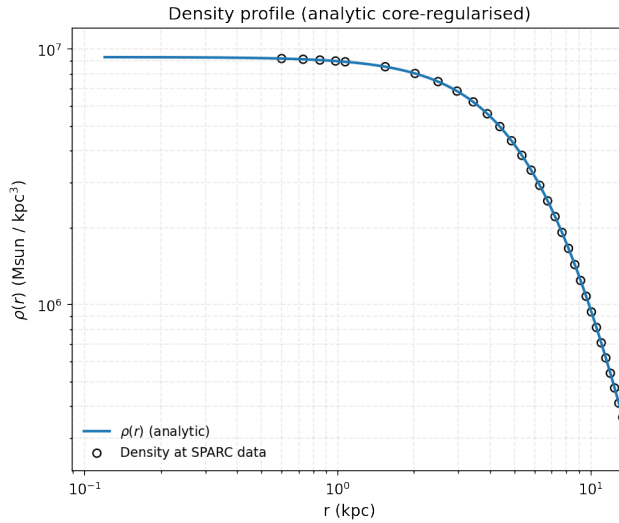


FIG. 33: The density of the SIDM model of Eq. (3) for the galaxy DDO161, versus the radius.

Now we shall include contributions to the rotation velocity from the other components of the galaxy, namely the disk, the gas, and the bulge if present. In Fig. 35 we present the combined rotation curves including all the components of the galaxy along with the SIDM. As it can be seen, the extended collisional DM model is viable. Also in Table XX we present the optimized values of the free parameters of the SIDM model for which we achieve the maximum compatibility with the SPARC data, for the galaxy DDO161, and also the resulting reduced χ^2_{red} value.

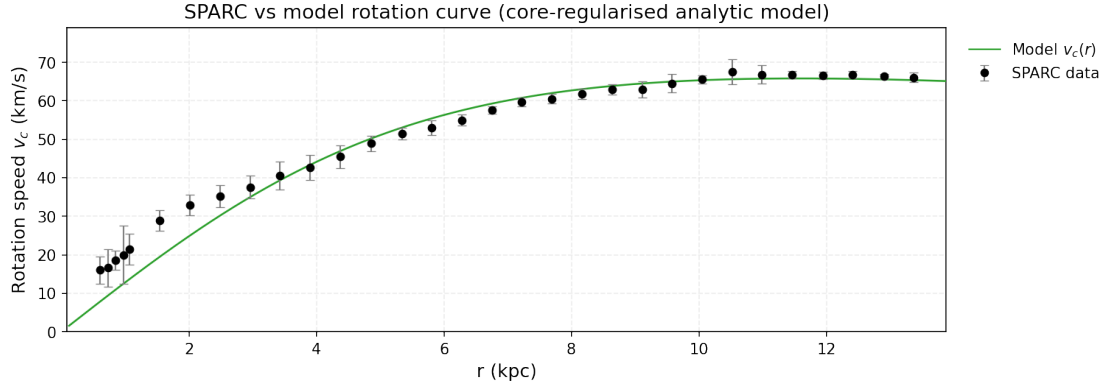


FIG. 34: The predicted rotation curves for the optimized SIDM model of Eq. (3), versus the SPARC observational data for the galaxy DDO161.

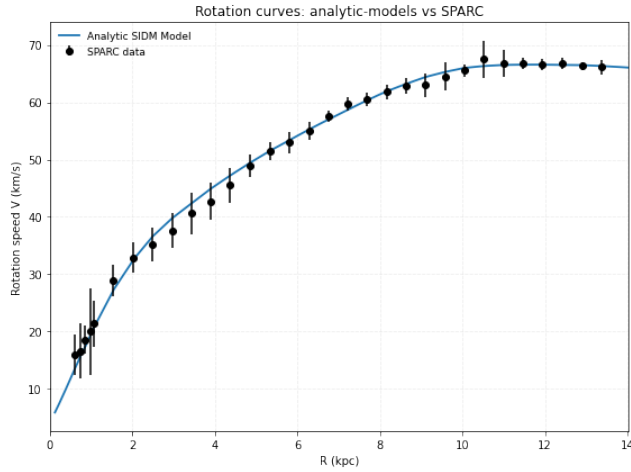


FIG. 35: The predicted rotation curves after using an optimization for the SIDM model (3), and the extended SPARC data for the galaxy DDO161. We included the rotation curves of the gas, the disk velocities, the bulge (where present) along with the SIDM model.

TABLE XX: Optimized Parameter Values of the Extended SIDM model for the Galaxy DDO161.

Parameter	Value
$\rho_0 (M_\odot/\text{Kpc}^3)$	4.03068×10^6
$K_0 (M_\odot \text{ Kpc}^{-3} (\text{km/s})^2)$	1549.15
ml_{disk}	0.8271
ml_{bulge}	0.5529
$\alpha (\text{Kpc})$	
χ^2_{red}	0.202594

4. The Galaxy DDO168, Non-viable

For this galaxy, the optimization method we used, ensures maximum compatibility of the analytic SIDM model of Eq. (3) with the SPARC data, if we choose $\rho_0 = 4.32263 \times 10^7 M_\odot/\text{Kpc}^3$ and $K_0 = 1301.75 M_\odot \text{ Kpc}^{-3} (\text{km/s})^2$, in which case the reduced χ^2_{red} value is $\chi^2_{\text{red}} = 2.5666$. Also the parameter α in this case is $\alpha = 3.16695 \text{ Kpc}$.

In Table XXI we present the optimized values of K_0 and ρ_0 for the analytic SIDM model of Eq. (3) for which the maximum compatibility with the SPARC data is achieved. In Figs. 36, 37 we present the density of the analytic SIDM model, the predicted rotation curves for the SIDM model (3), versus the SPARC observational data and the sound speed, as a function of the radius respectively. As it can be seen, for this galaxy, the SIDM model produces non-viable rotation curves which are incompatible with the SPARC data.

TABLE XXI: SIDM Optimization Values for the galaxy DDO168

Parameter	Optimization Values
$\rho_0 (M_\odot/\text{Kpc}^3)$	4.32263×10^7
$K_0 (M_\odot \text{ Kpc}^{-3} (\text{km/s})^2)$	1301.75

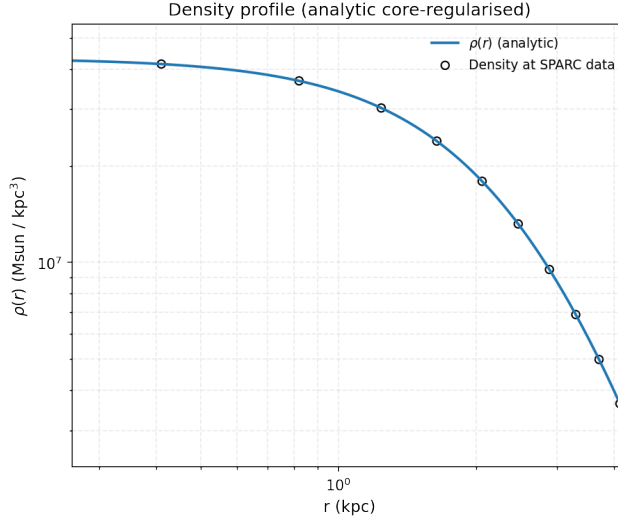


FIG. 36: The density of the SIDM model of Eq. (3) for the galaxy DDO168, versus the radius.

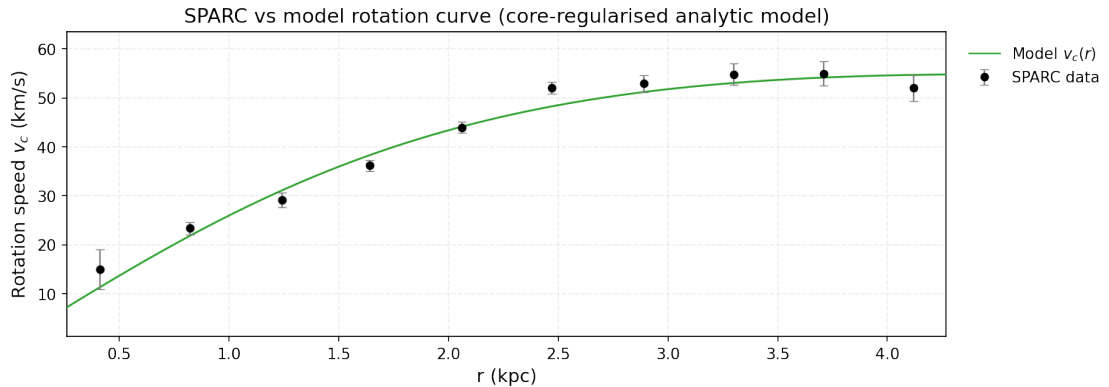


FIG. 37: The predicted rotation curves for the optimized SIDM model of Eq. (3), versus the SPARC observational data for the galaxy DDO168.

Now we shall include contributions to the rotation velocity from the other components of the galaxy, namely the disk, the gas, and the bulge if present. In Fig. 38 we present the combined rotation curves including all the components of the galaxy along with the SIDM. As it can be seen, the extended collisional DM model is non-viable. Also in Table XXII we present the optimized values of the free parameters of the SIDM model for which we achieve the maximum compatibility with the SPARC data, for the galaxy DDO168, and also the resulting reduced χ^2_{red} value.

TABLE XXII: Optimized Parameter Values of the Extended SIDM model for the Galaxy DDO168.

Parameter	Value
$\rho_0 (M_\odot/\text{Kpc}^3)$	2.59085×10^7
$K_0 (M_\odot \text{ Kpc}^{-3} (\text{km/s})^2)$	1359.19
ml_{disk}	0.0000
ml_{bulge}	0.0738
$\alpha (\text{Kpc})$	4.17941
χ^2_{red}	3.92914

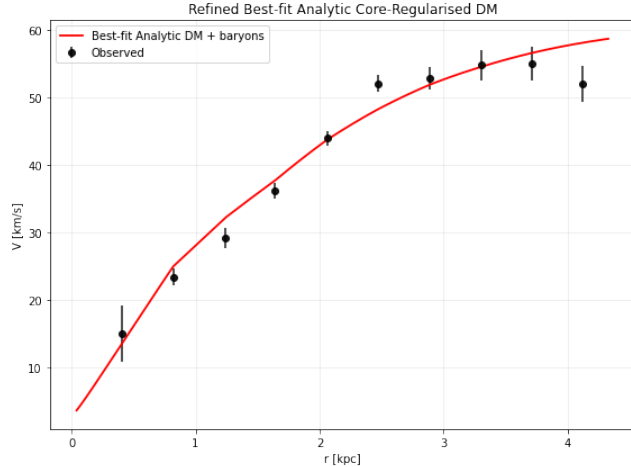


FIG. 38: The predicted rotation curves after using an optimization for the SIDM model (3), and the extended SPARC data for the galaxy DDO168. We included the rotation curves of the gas, the disk velocities, the bulge (where present) along with the SIDM model.

5. The Galaxy DDO170 Marginally

For this galaxy, the optimization method we used, ensures maximum compatibility of the analytic SIDM model of Eq. (3) with the SPARC data, if we choose $\rho_0 = 1.14592 \times 10^7 M_\odot/\text{Kpc}^3$ and $K_0 = 1569.79 M_\odot \text{Kpc}^{-3} (\text{km/s})^2$, in which case the reduced χ^2_{red} value is $\chi^2_{red} = 2.79013$. Also the parameter α in this case is $\alpha = 6.75451 \text{Kpc}$.

In Table XXIII we present the optimized values of K_0 and ρ_0 for the analytic SIDM model of Eq. (3) for which the maximum compatibility with the SPARC data is achieved. In Figs. 39, 40 we present the

TABLE XXIII: SIDM Optimization Values for the galaxy DDO170

Parameter	Optimization Values
$\rho_0 (M_\odot/\text{Kpc}^3)$	1.14592×10^7
$K_0 (M_\odot \text{Kpc}^{-3} (\text{km/s})^2)$	1569.79

density of the analytic SIDM model, the predicted rotation curves for the SIDM model (3), versus the SPARC observational data and the sound speed, as a function of the radius respectively. As it can be seen, for this galaxy, the SIDM model produces marginally viable rotation curves which are marginally compatible with the SPARC data.

Now we shall include contributions to the rotation velocity from the other components of the galaxy, namely the disk, the gas, and the bulge if present. In Fig. 41 we present the combined rotation curves including all the components of the galaxy along with the SIDM. As it can be seen, the extended collisional DM model is marginally viable. Also in Table XXIV we present the optimized values of the free parameters of the SIDM model for which we achieve the maximum compatibility with the SPARC data, for the galaxy DDO170, and also the resulting reduced χ^2_{red} value.

TABLE XXIV: Optimized Parameter Values of the Extended SIDM model for the Galaxy DDO170.

Parameter	Value
$\rho_0 (M_\odot/\text{Kpc}^3)$	6.85225×10^7
$K_0 (M_\odot \text{Kpc}^{-3} (\text{km/s})^2)$	1184.82
ml_{disk}	1
ml_{bulge}	0.8749
$\alpha (\text{Kpc})$	7.58762
χ^2_{red}	4.81285

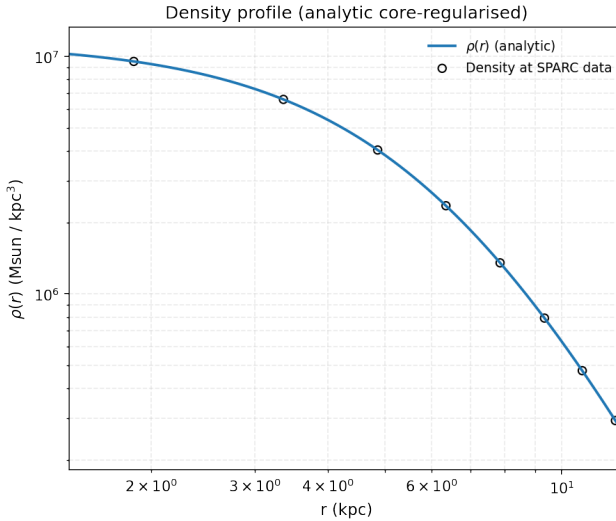


FIG. 39: The density of the SIDM model of Eq. (3) for the galaxy DDO170, versus the radius.

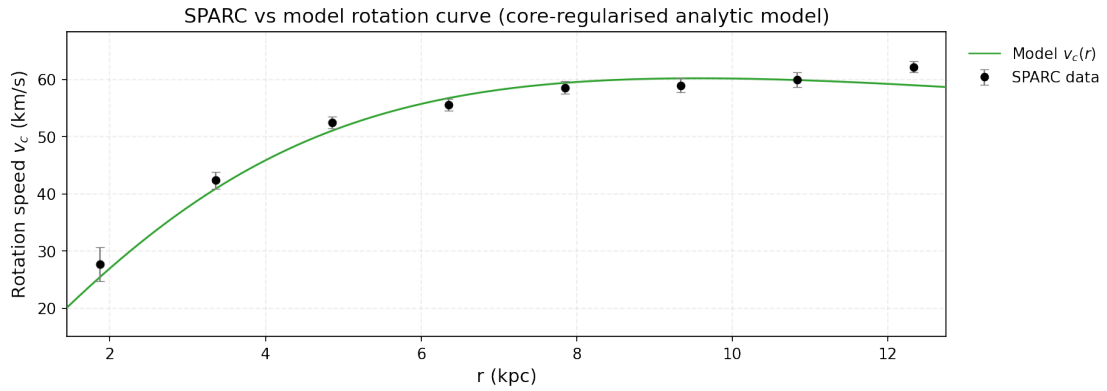


FIG. 40: The predicted rotation curves for the optimized SIDM model of Eq. (3), versus the SPARC observational data for the galaxy DDO170.

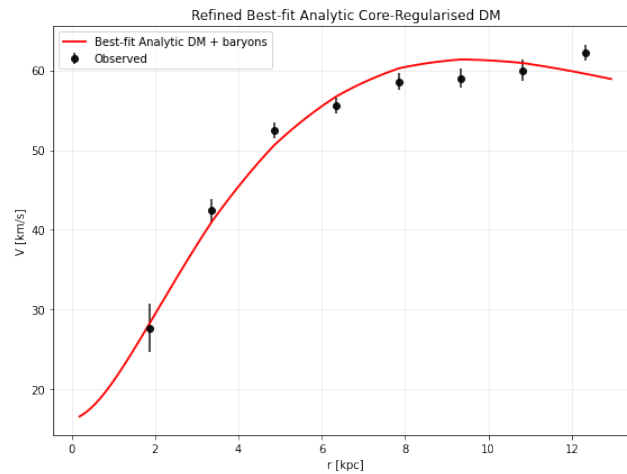


FIG. 41: The predicted rotation curves after using an optimization for the SIDM model (3), and the extended SPARC data for the galaxy DDO170. We included the rotation curves of the gas, the disk velocities, the bulge (where present) along with the SIDM model.

6. The Galaxy ESO079-G014, Marginally Viable, Extended Viable

For this galaxy, the optimization method we used, ensures maximum compatibility of the analytic SIDM model of Eq. (3) with the SPARC data, if we choose $\rho_0 = 3.70427 \times 10^7 M_\odot/\text{Kpc}^3$ and $K_0 = 13450.9 M_\odot \text{Kpc}^{-3} (\text{km/s})^2$, in which case the reduced χ^2_{red} value is $\chi^2_{red} = 2.79013$. Also the parameter α in this case is $\alpha = 10.997 \text{Kpc}$.

In Table XXV we present the optimized values of K_0 and ρ_0 for the analytic SIDM model of Eq. (3) for which the maximum compatibility with the SPARC data is achieved. In Figs. 42, 43 we present the

TABLE XXV: SIDM Optimization Values for the galaxy ESO079-G014

Parameter	Optimization Values
$\rho_0 (M_\odot/\text{Kpc}^3)$	3.70427×10^7
$K_0 (M_\odot \text{Kpc}^{-3} (\text{km/s})^2)$	13450.9

density of the analytic SIDM model, the predicted rotation curves for the SIDM model (3), versus the SPARC observational data and the sound speed, as a function of the radius respectively. As it can be seen, for this galaxy, the SIDM model produces marginally viable rotation curves which are marginally compatible with the SPARC data.

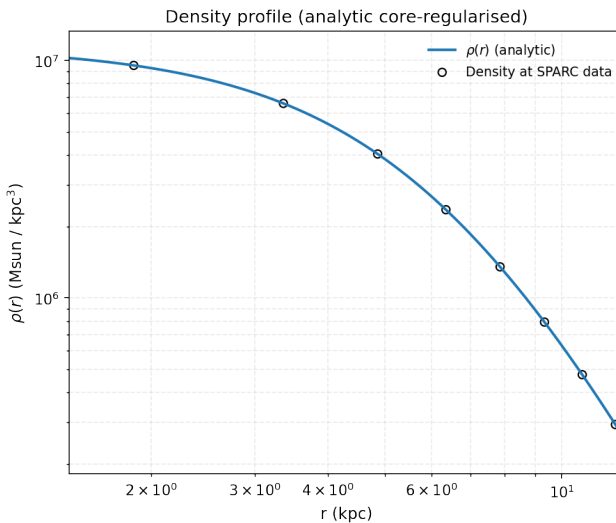


FIG. 42: The density of the SIDM model of Eq. (3) for the galaxy ESO079-G014, versus the radius.

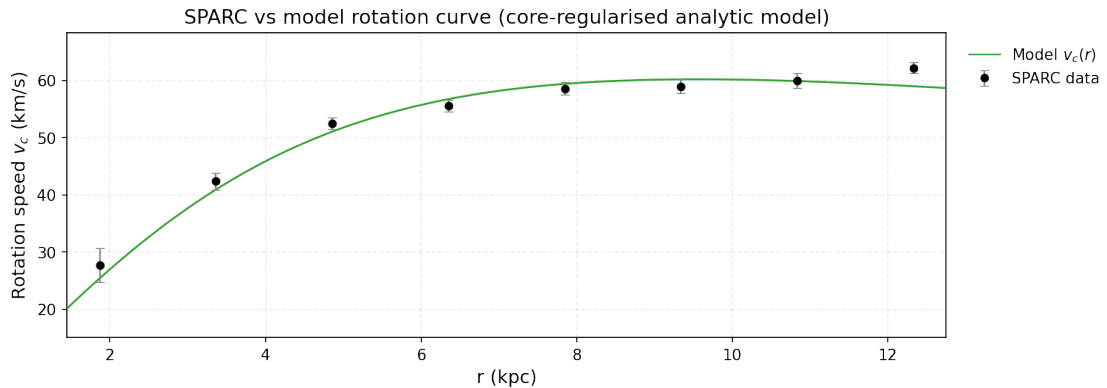


FIG. 43: The predicted rotation curves for the optimized SIDM model of Eq. (3), versus the SPARC observational data for the galaxy ESO079-G014.

Now we shall include contributions to the rotation velocity from the other components of the galaxy, namely the disk, the gas, and the bulge if present. In Fig. 44 we present the combined rotation curves

including all the components of the galaxy along with the SIDM. As it can be seen, the extended collisional DM model is marginally viable. Also in Table XXVI we present the optimized values of the

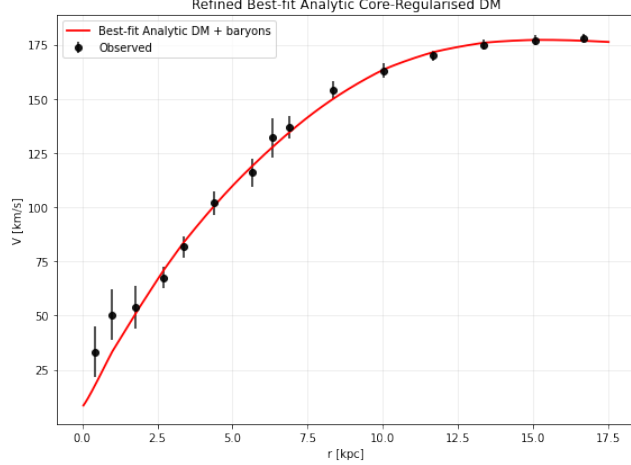


FIG. 44: The predicted rotation curves after using an optimization for the SIDM model (3), and the extended SPARC data for the galaxy ESO079-G014. We included the rotation curves of the gas, the disk velocities, the bulge (where present) along with the SIDM model.

free parameters of the SIDM model for which we achieve the maximum compatibility with the SPARC data, for the galaxy ESO079-G014, and also the resulting reduced χ^2_{red} value.

TABLE XXVI: Optimized Parameter Values of the Extended SIDM model for the Galaxy ESO079-G014.

Parameter	Value
$\rho_0 (M_\odot/\text{Kpc}^3)$	2.88609×10^7
$K_0 (M_\odot \text{ Kpc}^{-3} (\text{km/s})^2)$	11146.3
ml_{disk}	0.5030
ml_{bulge}	0.6404
$\alpha (\text{Kpc})$	11.3399
χ^2_{red}	0.649054

7. The Galaxy ESO116-G012, Non-viable, Extended Viable

For this galaxy, the optimization method we used, ensures maximum compatibility of the analytic SIDM model of Eq. (3) with the SPARC data, if we choose $\rho_0 = 7.7304 \times 10^7 M_\odot/\text{Kpc}^3$ and $K_0 = 5382.81 M_\odot \text{ Kpc}^{-3} (\text{km/s})^2$, in which case the reduced χ^2_{red} value is $\chi^2_{red} = 3.2133$. Also the parameter α in this case is $\alpha = 4.81564 \text{ Kpc}$.

In Table XXVII we present the optimized values of K_0 and ρ_0 for the analytic SIDM model of Eq. (3) for which the maximum compatibility with the SPARC data is achieved. In Figs. 45, 46 we present the

TABLE XXVII: SIDM Optimization Values for the galaxy ESO116-G012

Parameter	Optimization Values
$\rho_0 (M_\odot/\text{Kpc}^3)$	7.7304×10^7
$K_0 (M_\odot \text{ Kpc}^{-3} (\text{km/s})^2)$	5382.81

density of the analytic SIDM model, the predicted rotation curves for the SIDM model (3), versus the SPARC observational data and the sound speed, as a function of the radius respectively. As it can be seen, for this galaxy, the SIDM model produces non-viable rotation curves which are incompatible with the SPARC data.

Now we shall include contributions to the rotation velocity from the other components of the galaxy, namely the disk, the gas, and the bulge if present. In Fig. 47 we present the combined rotation curves including all the components of the galaxy along with the SIDM. As it can be seen, the extended

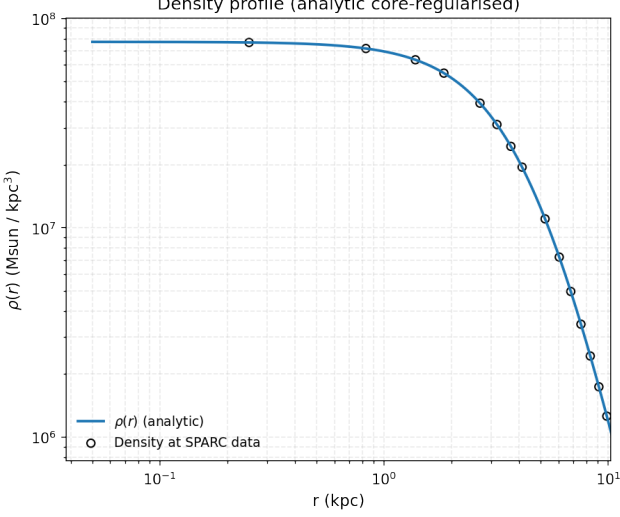


FIG. 45: The density of the SIDM model of Eq. (3) for the galaxy ESO116-G012, versus the radius.

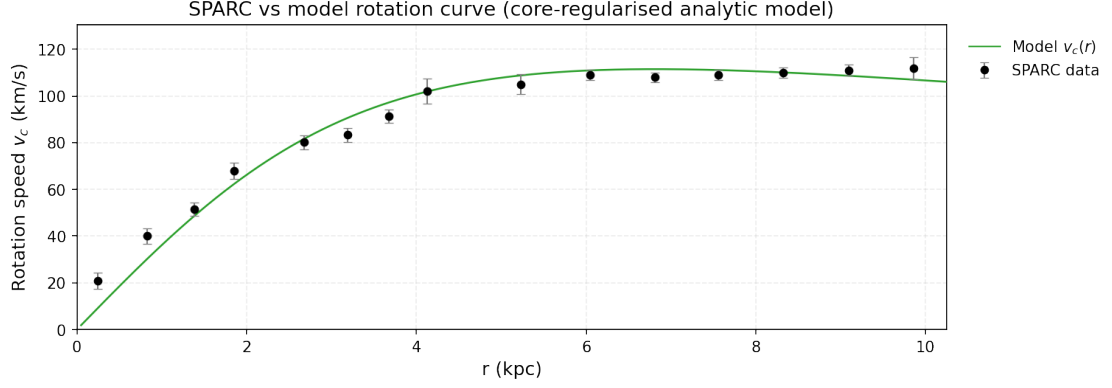


FIG. 46: The predicted rotation curves for the optimized SIDM model of Eq. (3), versus the SPARC observational data for the galaxy ESO116-G012.

collisional DM model is non-viable. Also in Table XXVIII we present the optimized values of the free

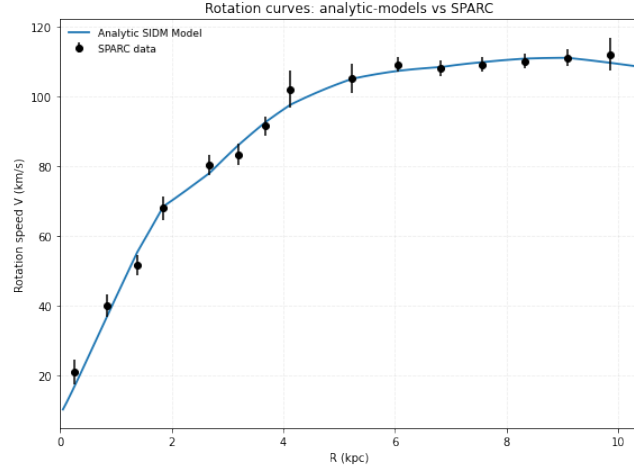


FIG. 47: The predicted rotation curves after using an optimization for the SIDM model (3), and the extended SPARC data for the galaxy ESO116-G012. We included the rotation curves of the gas, the disk velocities, the bulge (where present) along with the SIDM model.

parameters of the SIDM model for which we achieve the maximum compatibility with the SPARC data, for the galaxy ESO116-G012, and also the resulting reduced χ^2_{red} value.

TABLE XXVIII: Optimized Parameter Values of the Extended SIDM model for the Galaxy ESO116-G012.

Parameter	Value
$\rho_0 (M_\odot/\text{Kpc}^3)$	2.86227×10^7
$K_0 (M_\odot \text{ Kpc}^{-3} (\text{km/s})^2)$	3959.08
ml_{disk}	0.8969
ml_{bulge}	0.5851
$\alpha (\text{Kpc})$	6.78637
χ^2_{red}	0.700004

8. The Galaxy ESO563-G021

For this galaxy, the optimization method we used, ensures maximum compatibility of the analytic SIDM model of Eq. (3) with the SPARC data, if we choose $\rho_0 = 9.63711 \times 10^7 M_\odot/\text{Kpc}^3$ and $K_0 = 48595.1 M_\odot \text{ Kpc}^{-3} (\text{km/s})^2$, in which case the reduced χ^2_{red} value is $\chi^2_{red} = 5.60671$. Also the parameter α in this case is $\alpha = 12.9591 \text{ Kpc}$.

In Table XXIX we present the optimized values of K_0 and ρ_0 for the analytic SIDM model of Eq. (3) for which the maximum compatibility with the SPARC data is achieved. In Figs. 48, 49 we present the

TABLE XXIX: SIDM Optimization Values for the galaxy ESO563-G021

Parameter	Optimization Values
$\rho_0 (M_\odot/\text{Kpc}^3)$	9.63711×10^7
$K_0 (M_\odot \text{ Kpc}^{-3} (\text{km/s})^2)$	48595.1

density of the analytic SIDM model, the predicted rotation curves for the SIDM model (3), versus the SPARC observational data and the sound speed, as a function of the radius respectively. As it can be seen, for this galaxy, the SIDM model produces non-viable rotation curves which are incompatible with the SPARC data.

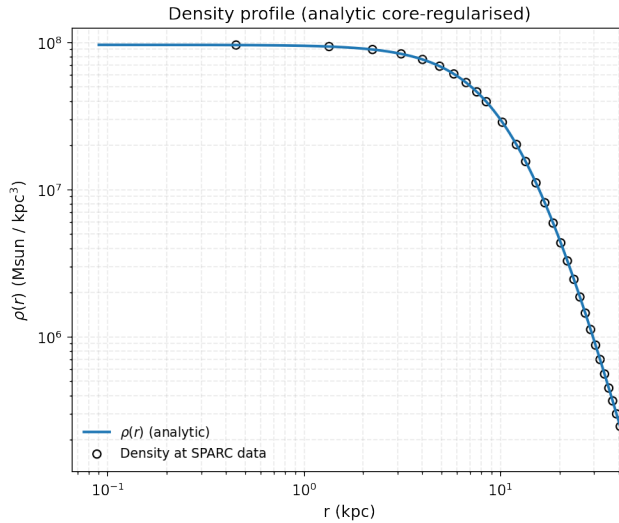


FIG. 48: The density of the SIDM model of Eq. (3) for the galaxy ESO563-G021, versus the radius.

Now we shall include contributions to the rotation velocity from the other components of the galaxy, namely the disk, the gas, and the bulge if present. In Fig. 50 we present the combined rotation curves including all the components of the galaxy along with the SIDM. As it can be seen, the extended collisional DM model is non-viable. Also in Table XXX we present the optimized values of the free

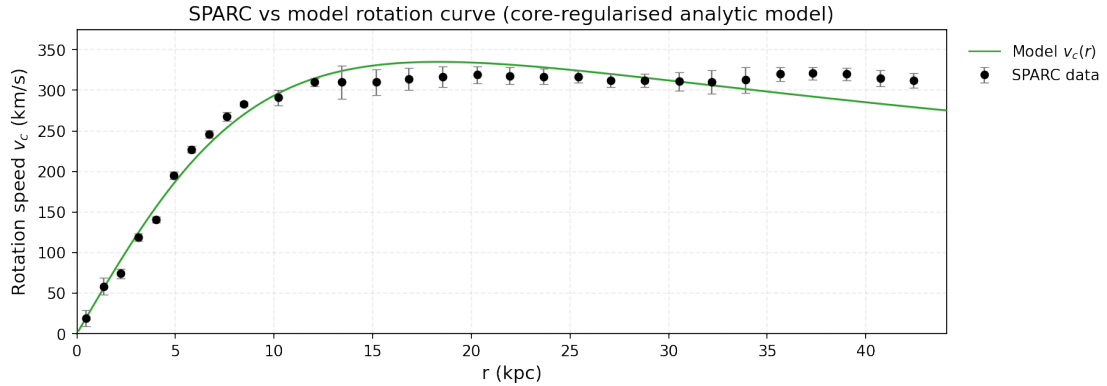


FIG. 49: The predicted rotation curves for the optimized SIDM model of Eq. (3), versus the SPARC observational data for the galaxy ESO563-G021.

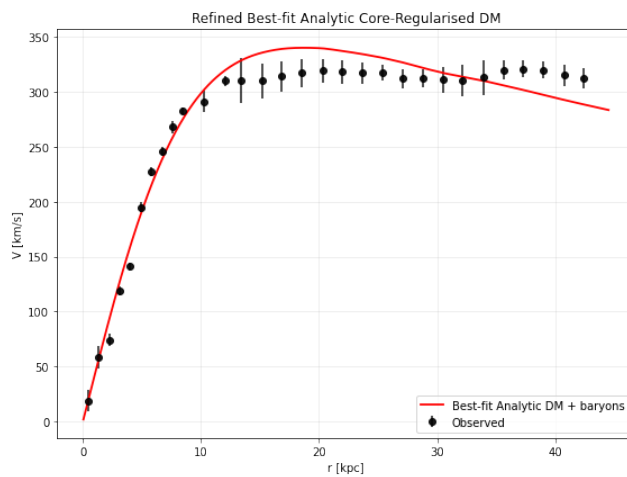


FIG. 50: The predicted rotation curves after using an optimization for the SIDM model (3), and the extended SPARC data for the galaxy ESO563-G021. We included the rotation curves of the gas, the disk velocities, the bulge (where present) along with the SIDM model.

parameters of the SIDM model for which we achieve the maximum compatibility with the SPARC data, for the galaxy ESO563-G021, and also the resulting reduced χ^2_{red} value.

TABLE XXX: Optimized Parameter Values of the Extended SIDM model for the Galaxy ESO563-G021.

Parameter	Value
ρ_0 (M_\odot/Kpc^3)	1.00755×10^7
K_0 ($M_\odot \text{ Kpc}^{-3} (\text{km/s})^2$)	49854.6
ml_{disk}	1
ml_{bulge}	0.0253
α (Kpc)	12.8356
χ^2_{red}	4.84033

9. The Galaxy F565-V2

For this galaxy, the optimization method we used, ensures maximum compatibility of the analytic SIDM model of Eq. (3) with the SPARC data, if we choose $\rho_0 = 1.64594 \times 10^7 M_\odot/\text{Kpc}^3$ and $K_0 = 2804.34 M_\odot \text{ Kpc}^{-3} (\text{km/s})^2$, in which case the reduced χ^2_{red} value is $\chi^2_{red} = 0.152429$. Also the parameter α in this case is $\alpha = 7.53286 \text{ Kpc}$.

In Table XXXI we present the optimized values of K_0 and ρ_0 for the analytic SIDM model of Eq. (3) for which the maximum compatibility with the SPARC data is achieved. In Figs. 51, 52 we present the

TABLE XXXI: SIDM Optimization Values for the galaxy F565-V2

Parameter	Optimization Values
$\rho_0 (M_\odot/\text{Kpc}^3)$	1.64594×10^7
$K_0 (M_\odot \text{ Kpc}^{-3} (\text{km/s})^2)$	2804.34

density of the analytic SIDM model, the predicted rotation curves for the SIDM model (3), versus the SPARC observational data and the sound speed, as a function of the radius respectively. As it can be seen, for this galaxy, the SIDM model produces viable rotation curves which are compatible with the SPARC data.

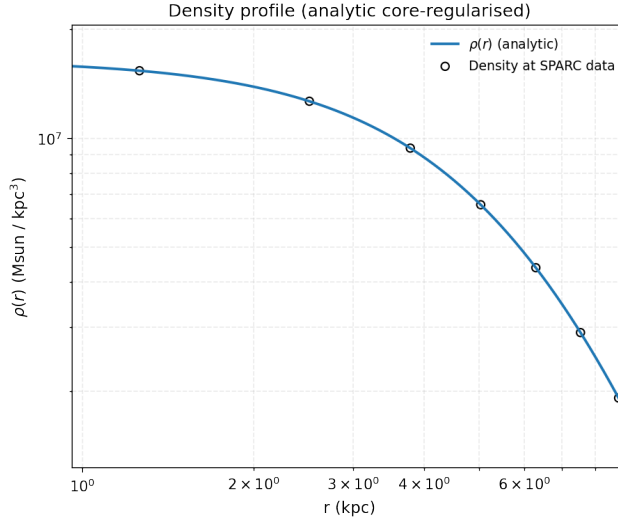


FIG. 51: The density of the SIDM model of Eq. (3) for the galaxy F565-V2, versus the radius.

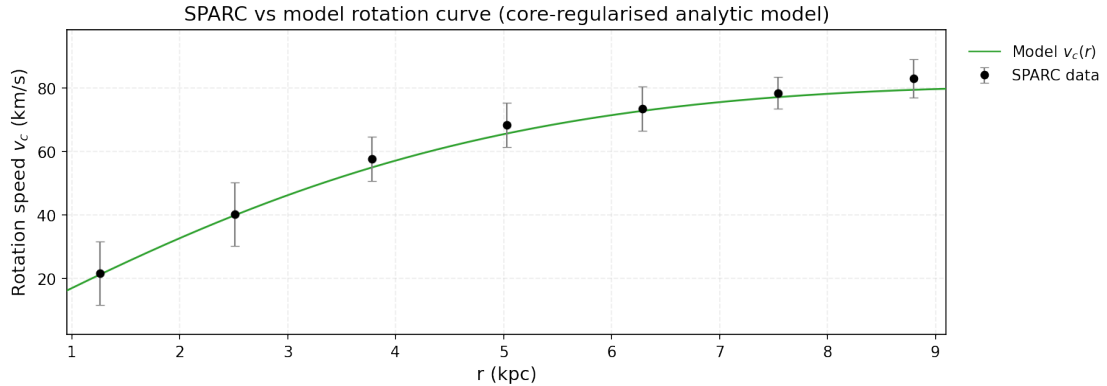


FIG. 52: The predicted rotation curves for the optimized SIDM model of Eq. (3), versus the SPARC observational data for the galaxy F565-V2.

10. The Galaxy F568-3

For this galaxy, the optimization method we used, ensures maximum compatibility of the analytic SIDM model of Eq. (3) with the SPARC data, if we choose $\rho_0 = 2.11755 \times 10^7 M_\odot/\text{Kpc}^3$ and $K_0 = 5378.52 M_\odot \text{ Kpc}^{-3} (\text{km/s})^2$, in which case the reduced χ^2_{red} value is $\chi^2_{red} = 0.680511$. Also the parameter α in this case is $\alpha = 9.1974 \text{ Kpc}$.

In Table XXXII we present the optimized values of K_0 and ρ_0 for the analytic SIDM model of Eq. (3) for which the maximum compatibility with the SPARC data is achieved. In Figs. 53, 54 we present

TABLE XXXII: SIDM Optimization Values for the galaxy F568-3

Parameter	Optimization Values
$\rho_0 (M_\odot/\text{Kpc}^3)$	2.11755×10^7
$K_0 (M_\odot \text{ Kpc}^{-3} (\text{km/s})^2)$	5378.52

the density of the analytic SIDM model, the predicted rotation curves for the SIDM model (3), versus the SPARC observational data and the sound speed, as a function of the radius respectively. As it can be seen, for this galaxy, the SIDM model produces viable rotation curves which are compatible with the SPARC data.

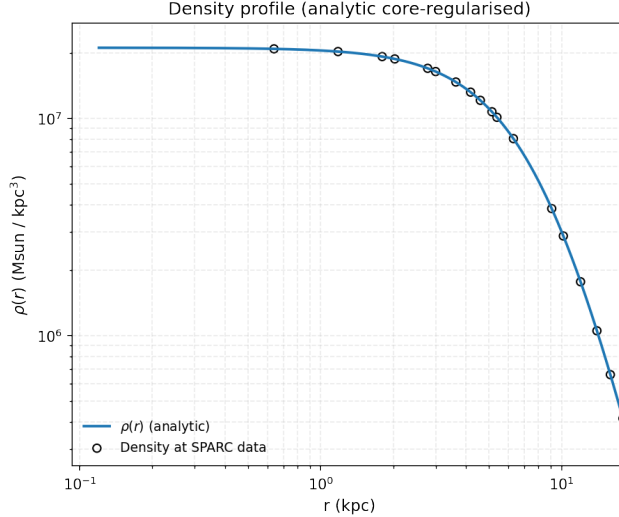


FIG. 53: The density of the SIDM model of Eq. (3) for the galaxy F568-3, versus the radius.

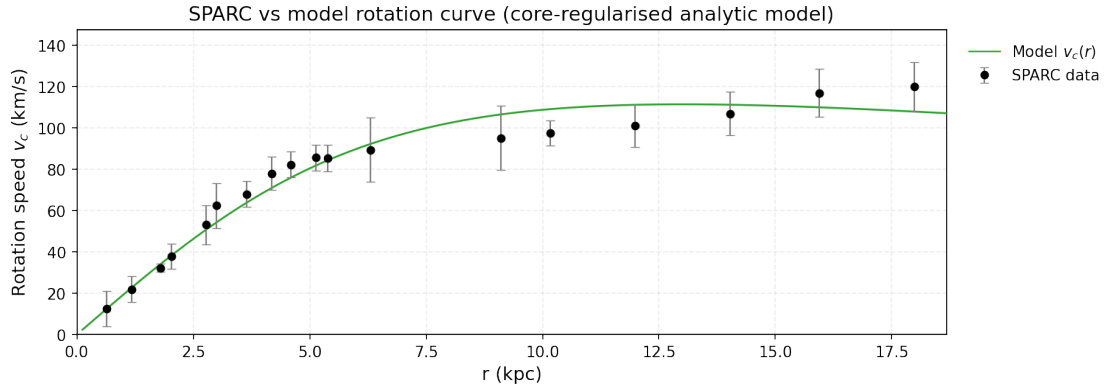


FIG. 54: The predicted rotation curves for the optimized SIDM model of Eq. (3), versus the SPARC observational data for the galaxy F568-3.

11. The Galaxy F568-V1

For this galaxy, the optimization method we used, ensures maximum compatibility of the analytic SIDM model of Eq. (3) with the SPARC data, if we choose $\rho_0 = 6.25735 \times 10^7 M_\odot/\text{Kpc}^3$ and $K_0 = 6374.56 M_\odot \text{ Kpc}^{-3} (\text{km/s})^2$, in which case the reduced χ^2_{red} value is $\chi^2_{red} = 0.3568$. Also the parameter α in this case is $\alpha = 5.82479 \text{ Kpc}$.

In Table XXXIII we present the optimized values of K_0 and ρ_0 for the analytic SIDM model of Eq. (3) for which the maximum compatibility with the SPARC data is achieved. In Figs. 55, 56 we present

TABLE XXXIII: SIDM Optimization Values for the galaxy F568-V1

Parameter	Optimization Values
$\rho_0 (M_\odot/\text{Kpc}^3)$	6.25735×10^7
$K_0 (M_\odot \text{ Kpc}^{-3} (\text{km/s})^2)$	6374.56

the density of the analytic SIDM model, the predicted rotation curves for the SIDM model (3), versus the SPARC observational data and the sound speed, as a function of the radius respectively. As it can be seen, for this galaxy, the SIDM model produces viable rotation curves which are compatible with the SPARC data.

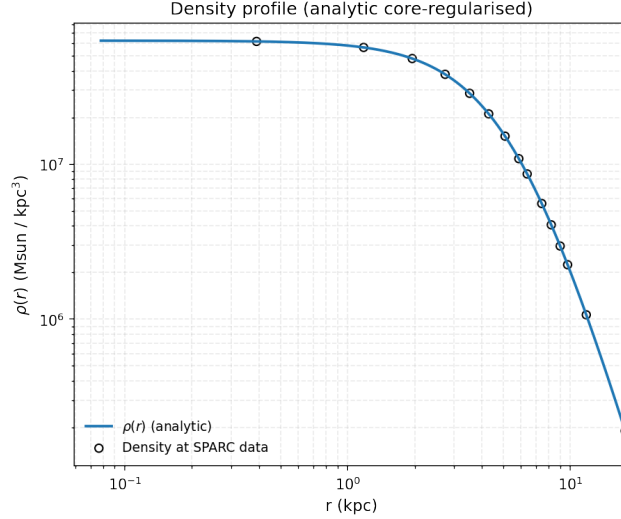


FIG. 55: The density of the SIDM model of Eq. (3) for the galaxy F568-V1, versus the radius.

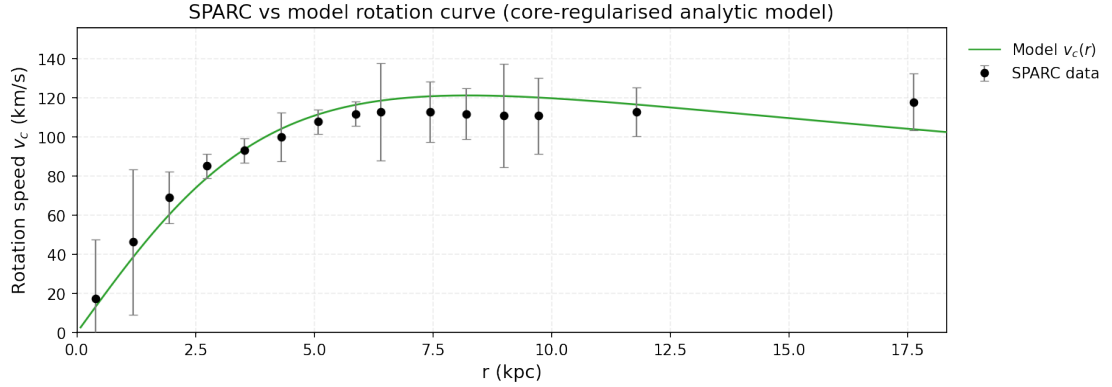


FIG. 56: The predicted rotation curves for the optimized SIDM model of Eq. (3), versus the SPARC observational data for the galaxy F568-V1.

12. The Galaxy F571-V1

For this galaxy, the optimization method we used, ensures maximum compatibility of the analytic SIDM model of Eq. (3) with the SPARC data, if we choose $\rho_0 = 1.39508 \times 10^7 M_\odot/\text{Kpc}^3$ and $K_0 = 3247.46 M_\odot \text{ Kpc}^{-3} (\text{km/s})^2$, in which case the reduced χ^2_{red} value is $\chi^2_{red} = 0.178266$. Also the parameter α in this case is $\alpha = 8.80488 \text{ Kpc}$.

In Table XXXIV we present the optimized values of K_0 and ρ_0 for the analytic SIDM model of Eq. (3) for which the maximum compatibility with the SPARC data is achieved. In Figs. 57, 58 we present

TABLE XXXIV: SIDM Optimization Values for the galaxy F571-V1

Parameter	Optimization Values
$\rho_0 (M_\odot/\text{Kpc}^3)$	1.39508×10^7
$K_0 (M_\odot \text{ Kpc}^{-3} (\text{km/s})^2)$	3247.46

the density of the analytic SIDM model, the predicted rotation curves for the SIDM model (3), versus the SPARC observational data and the sound speed, as a function of the radius respectively. As it can be seen, for this galaxy, the SIDM model produces viable rotation curves which are compatible with the SPARC data.

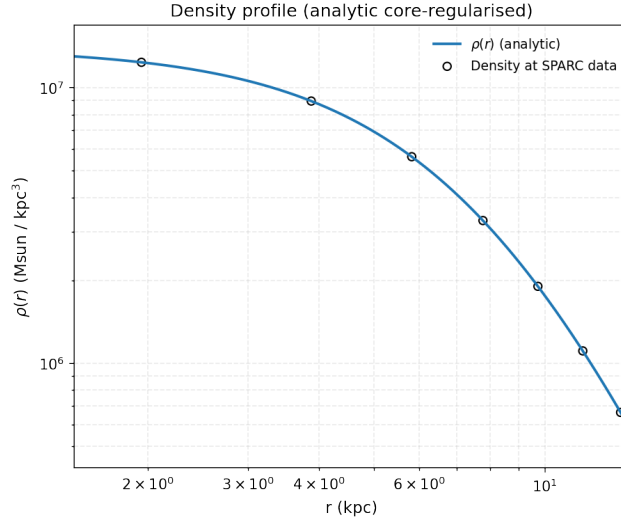


FIG. 57: The density of the SIDM model of Eq. (3) for the galaxy F571-V1, versus the radius.

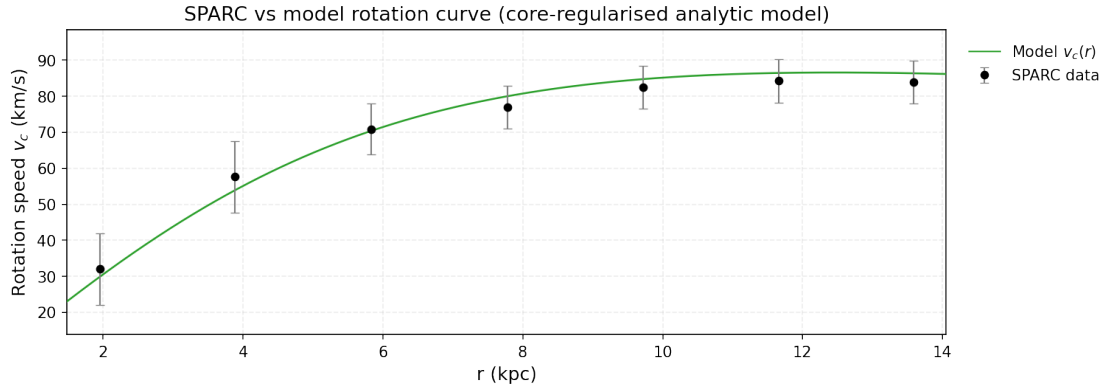


FIG. 58: The predicted rotation curves for the optimized SIDM model of Eq. (3), versus the SPARC observational data for the galaxy F571-V1.

13. The Galaxy F571-8, Non-viable, Extended Viable

For this galaxy, the optimization method we used, ensures maximum compatibility of the analytic SIDM model of Eq. (3) with the SPARC data, if we choose $\rho_0 = 3.98342 \times 10^7 M_\odot/\text{Kpc}^3$ and $K_0 = 8709.25 M_\odot \text{ Kpc}^{-3} (\text{km/s})^2$, in which case the reduced χ^2_{red} value is $\chi^2_{red} = 5.29502$. Also the parameter α in this case is $\alpha = 8.53322 \text{ Kpc}$.

In Table XXXV we present the optimized values of K_0 and ρ_0 for the analytic SIDM model of Eq. (3) for which the maximum compatibility with the SPARC data is achieved. In Figs. 59, 60 we present the

TABLE XXXV: SIDM Optimization Values for the galaxy F571-8

Parameter	Optimization Values
$\rho_0 (M_\odot/\text{Kpc}^3)$	3.98342×10^7
$K_0 (M_\odot \text{ Kpc}^{-3} (\text{km/s})^2)$	8709.25

density of the analytic SIDM model, the predicted rotation curves for the SIDM model (3), versus the SPARC observational data and the sound speed, as a function of the radius respectively. As it can be seen, for this galaxy, the SIDM model produces non-viable rotation curves which are incompatible with the SPARC data.

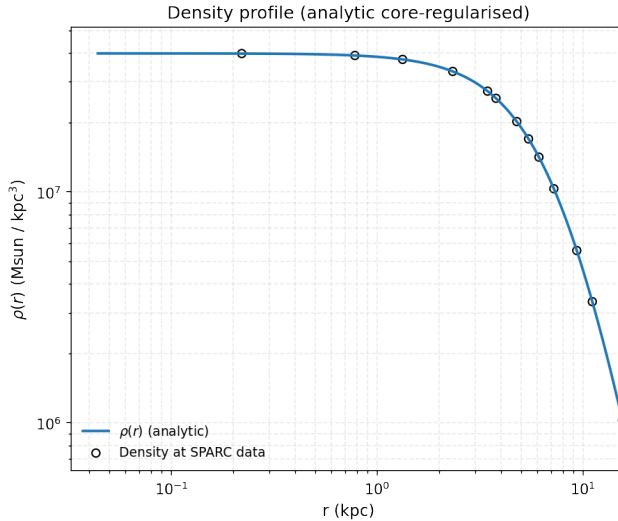


FIG. 59: The density of the SIDM model of Eq. (3) for the galaxy F571-8, versus the radius.

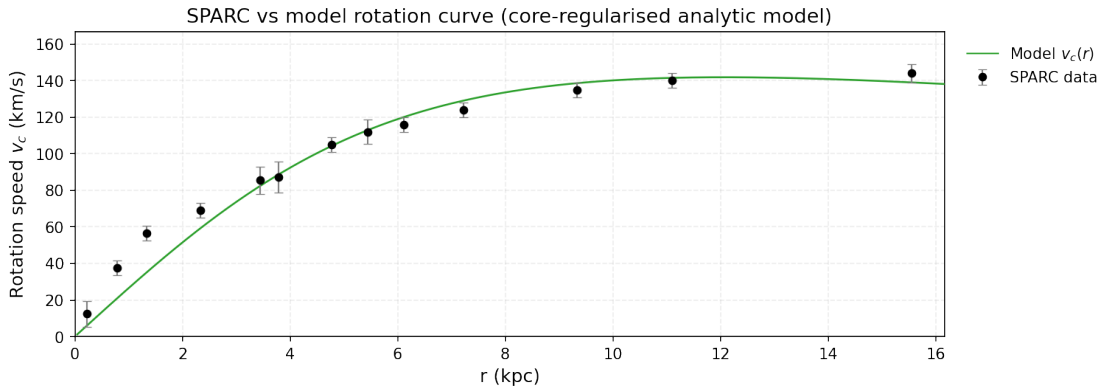


FIG. 60: The predicted rotation curves for the optimized SIDM model of Eq. (3), versus the SPARC observational data for the galaxy F571-8.

Now we shall include contributions to the rotation velocity from the other components of the galaxy, namely the disk, the gas, and the bulge if present. In Fig. 61 we present the combined rotation curves including all the components of the galaxy along with the SIDM. As it can be seen, the extended collisional DM model is viable. Also in Table XXXVI we present the optimized values of the free parameters of the SIDM model for which we achieve the maximum compatibility with the SPARC data, for the galaxy F571-8, and also the resulting reduced χ^2_{red} value.

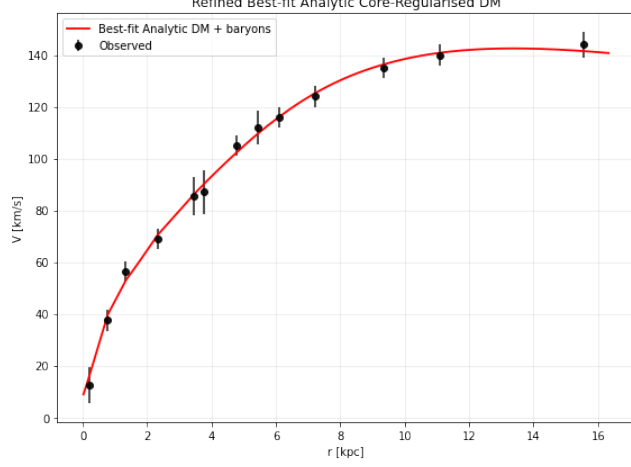


FIG. 61: The predicted rotation curves after using an optimization for the SIDM model (3), and the extended SPARC data for the galaxy F571-8. We included the rotation curves of the gas, the disk velocities, the bulge (where present) along with the SIDM model.

TABLE XXXVI: Optimized Parameter Values of the Extended SIDM model for the Galaxy F571-8.

Parameter	Value
$\rho_0 (M_\odot/\text{Kpc}^3)$	3.02249×10^7
$K_0 (M_\odot \text{ Kpc}^{-3} (\text{km/s})^2)$	8483.67
ml_{disk}	0.4126
ml_{bulge}	0.2105
$\alpha (\text{Kpc})$	9.6673
χ^2_{red}	0.326601

14. The Galaxy F574-1, Marginally viable, Extended Viable

For this galaxy, the optimization method we used, ensures maximum compatibility of the analytic SIDM model of Eq. (3) with the SPARC data, if we choose $\rho_0 = 3.96165 \times 10^7 M_\odot/\text{Kpc}^3$ and $K_0 = 4201.07 M_\odot \text{ Kpc}^{-3} (\text{km/s})^2$, in which case the reduced χ^2_{red} value is $\chi^2_{\text{red}} = 0.850431$. Also the parameter α in this case is $\alpha = 5.94282 \text{ Kpc}$.

In Table XXXVII we present the optimized values of K_0 and ρ_0 for the analytic SIDM model of Eq. (3) for which the maximum compatibility with the SPARC data is achieved. In Figs. 62, 63 we present

TABLE XXXVII: SIDM Optimization Values for the galaxy F574-1

Parameter	Optimization Values
$\rho_0 (M_\odot/\text{Kpc}^3)$	3.96165×10^7
$K_0 (M_\odot \text{ Kpc}^{-3} (\text{km/s})^2)$	4201.07

the density of the analytic SIDM model, the predicted rotation curves for the SIDM model (3), versus the SPARC observational data and the sound speed, as a function of the radius respectively. As it can be seen, for this galaxy, the SIDM model produces marginally viable rotation curves which are incompatible with the SPARC data.

Now we shall include contributions to the rotation velocity from the other components of the galaxy, namely the disk, the gas, and the bulge if present. In Fig. 64 we present the combined rotation curves including all the components of the galaxy along with the SIDM. As it can be seen, the extended collisional DM model is viable. Also in Table XXXVIII we present the optimized values of the free parameters of the SIDM model for which we achieve the maximum compatibility with the SPARC data, for the galaxy F574-1, and also the resulting reduced χ^2_{red} value.

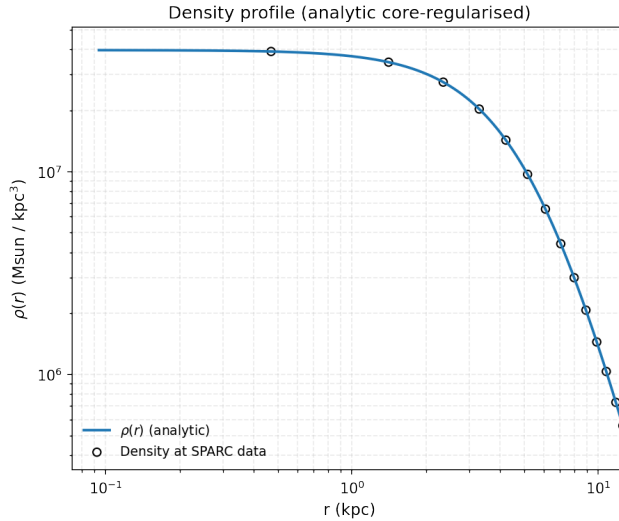


FIG. 62: The density of the SIDM model of Eq. (3) for the galaxy F574-1, versus the radius.

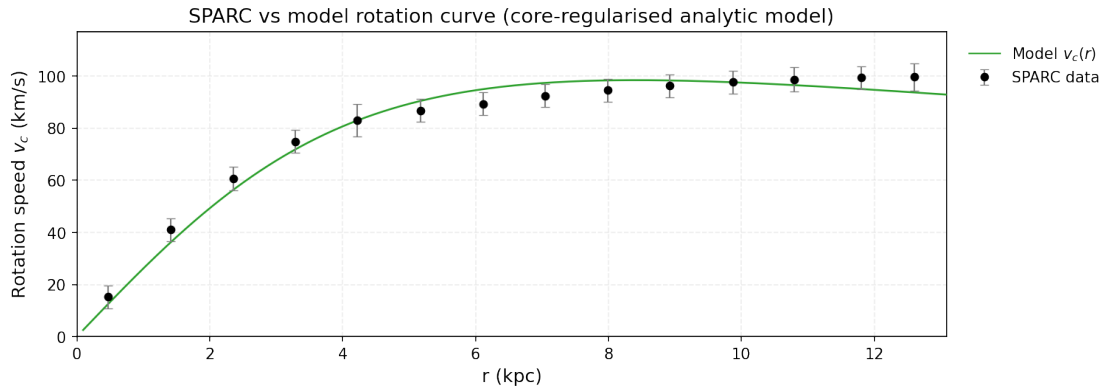


FIG. 63: The predicted rotation curves for the optimized SIDM model of Eq. (3), versus the SPARC observational data for the galaxy F574-1.

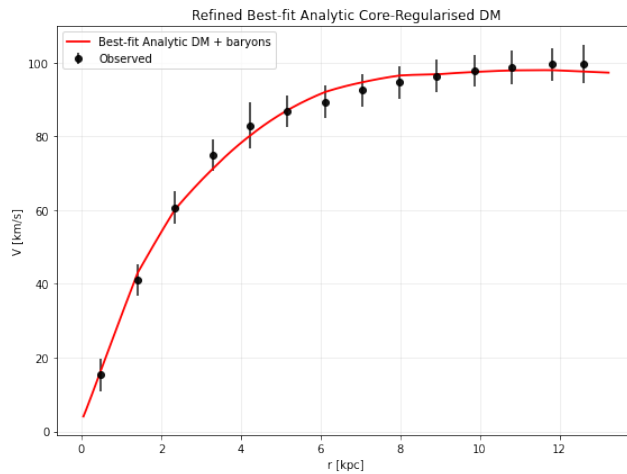


FIG. 64: The predicted rotation curves after using an optimization for the SIDM model (3), and the extended SPARC data for the galaxy F574-1. We included the rotation curves of the gas, the disk velocities, the bulge (where present) along with the SIDM model.

TABLE XXXVIII: Optimized Parameter Values of the Extended SIDM model for the Galaxy F574-1.

Parameter	Value
$\rho_0 (M_\odot/\text{Kpc}^3)$	2.46509×10^7
$K_0 (M_\odot \text{ Kpc}^{-3} (\text{km/s})^2)$	2904.38
ml_{disk}	0.9765
ml_{bulge}	0.6321
$\alpha (\text{Kpc})$	6.26334
χ^2_{red}	0.230896

15. The Galaxy F583-1

For this galaxy, the optimization method we used, ensures maximum compatibility of the analytic SIDM model of Eq. (3) with the SPARC data, if we choose $\rho_0 = 1.88326 \times 10^7 M_\odot/\text{Kpc}^3$ and $K_0 = 3160.22 M_\odot \text{ Kpc}^{-3} (\text{km/s})^2$, in which case the reduced χ^2_{red} value is $\chi^2_{\text{red}} = 0.249447$. Also the parameter α in this case is $\alpha = 7.47573 \text{ Kpc}$.

In Table XXXIX we present the optimized values of K_0 and ρ_0 for the analytic SIDM model of Eq. (3) for which the maximum compatibility with the SPARC data is achieved. In Figs. 65, 66 we present the

TABLE XXXIX: SIDM Optimization Values for the galaxy F583-1

Parameter	Optimization Values
$\rho_0 (M_\odot/\text{Kpc}^3)$	1.88326×10^7
$K_0 (M_\odot \text{ Kpc}^{-3} (\text{km/s})^2)$	3160.22

density of the analytic SIDM model, the predicted rotation curves for the SIDM model (3), versus the SPARC observational data and the sound speed, as a function of the radius respectively. As it can be seen, for this galaxy, the SIDM model produces viable rotation curves which are marginally compatible with the SPARC data.

Now we shall include contributions to the rotation velocity from the other components of the galaxy, namely the disk, the gas, and the bulge if present. In Fig. 67 we present the combined rotation curves including all the components of the galaxy along with the SIDM. As it can be seen, the extended collisional DM model is viable. Also in Table XL we present the optimized values of the free parameters of the SIDM model for which we achieve the maximum compatibility with the SPARC data, for the galaxy F583-1, and also the resulting reduced χ^2_{red} value.

TABLE XL: Optimized Parameter Values of the Extended SIDM model for the Galaxy F583-1.

Parameter	Value
$\rho_0 (M_\odot/\text{Kpc}^3)$	1.8539×10^7
$K_0 (M_\odot \text{ Kpc}^{-3} (\text{km/s})^2)$	2654.75
ml_{disk}	0.5424
ml_{bulge}	0.5184
$\alpha (\text{Kpc})$	6.90502
χ^2_{red}	0.147575

16. The Galaxy F583-4, Marginally Viable, Extended Viable

For this galaxy, the optimization method we used, ensures maximum compatibility of the analytic SIDM model of Eq. (3) with the SPARC data, if we choose $\rho_0 = 3.99539 \times 10^7 M_\odot/\text{Kpc}^3$ and $K_0 = 1735.41 M_\odot \text{ Kpc}^{-3} (\text{km/s})^2$, in which case the reduced χ^2_{red} value is $\chi^2_{\text{red}} = 1.10839$. Also the parameter α in this case is $\alpha = 3.8034 \text{ Kpc}$.

In Table XLI we present the optimized values of K_0 and ρ_0 for the analytic SIDM model of Eq. (3) for which the maximum compatibility with the SPARC data is achieved. In Figs. 68, 69 we present the density of the analytic SIDM model, the predicted rotation curves for the SIDM model (3), versus the SPARC observational data and the sound speed, as a function of the radius respectively. As it can be seen, for this galaxy, the SIDM model produces marginally viable rotation curves which are marginally compatible with the SPARC data.

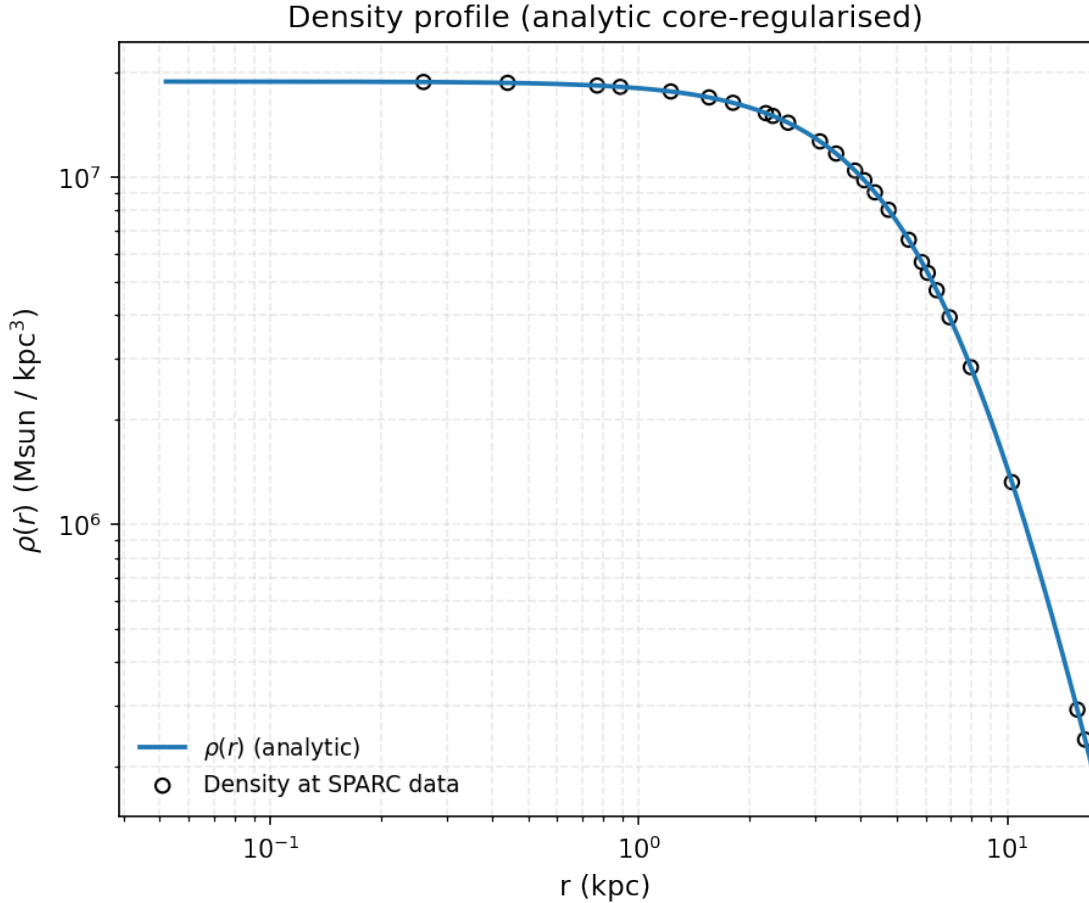


FIG. 65: The density of the SIDM model of Eq. (3) for the galaxy F583-1, versus the radius.

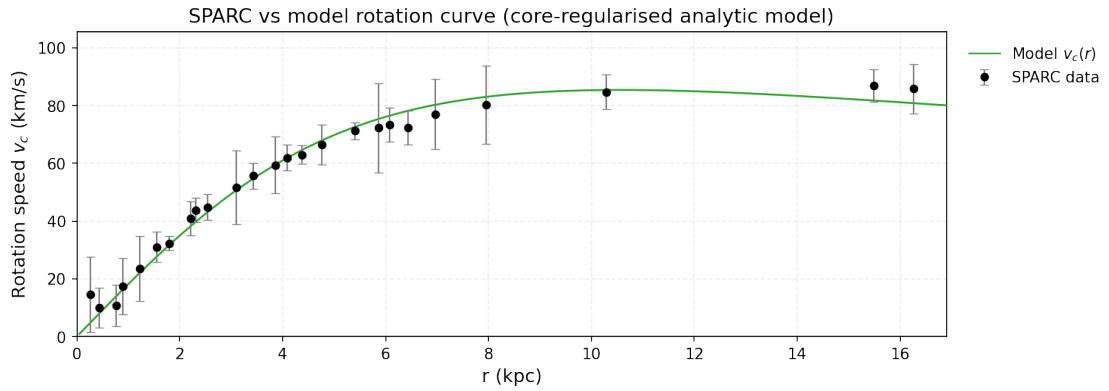


FIG. 66: The predicted rotation curves for the optimized SIDM model of Eq. (3), versus the SPARC observational data for the galaxy F583-1.

TABLE XLI: SIDM Optimization Values for the galaxy F583-4

Parameter	Optimization Values
$\rho_0 (M_\odot / \text{Kpc}^3)$	3.99539×10^7
$K_0 (M_\odot \text{ Kpc}^{-3} (\text{km/s})^2)$	1735.41

Now we shall include contributions to the rotation velocity from the other components of the galaxy, namely the disk, the gas, and the bulge if present. In Fig. 70 we present the combined rotation curves

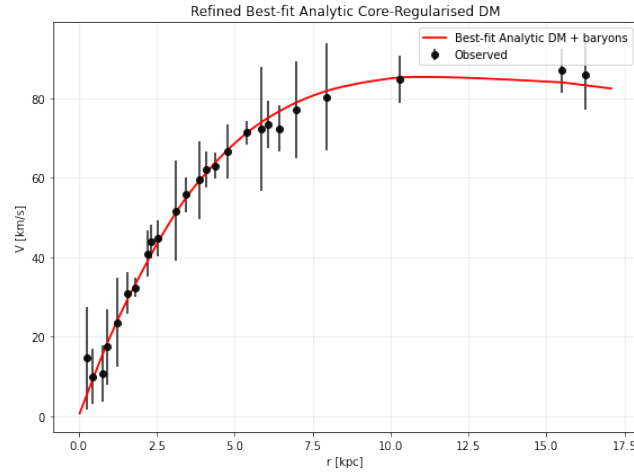


FIG. 67: The predicted rotation curves after using an optimization for the SIDM model (3), and the extended SPARC data for the galaxy F583-1. We included the rotation curves of the gas, the disk velocities, the bulge (where present) along with the SIDM model.

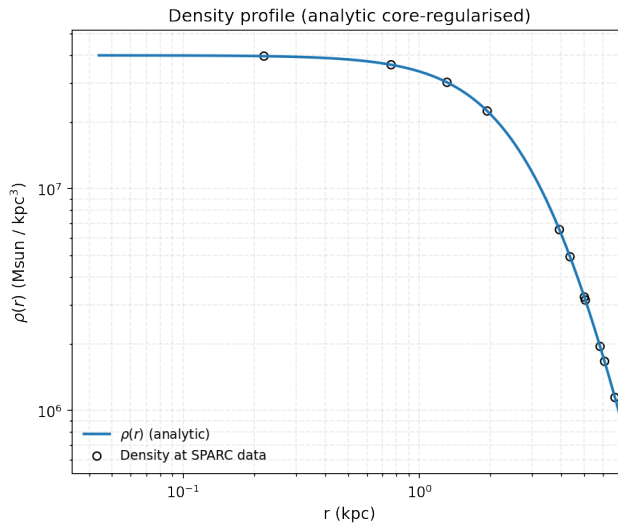


FIG. 68: The density of the SIDM model of Eq. (3) for the galaxy F583-4, versus the radius.

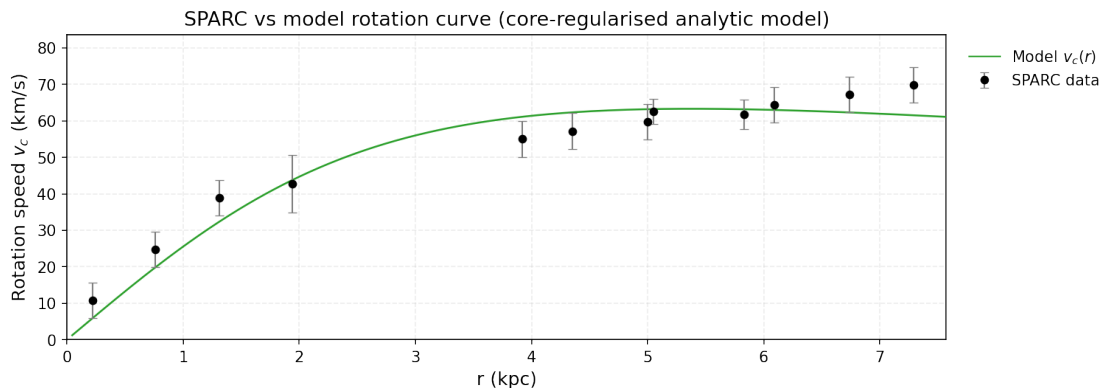


FIG. 69: The predicted rotation curves for the optimized SIDM model of Eq. (3), versus the SPARC observational data for the galaxy F583-4.

including all the components of the galaxy along with the SIDM. As it can be seen, the extended

collisional DM model is marginally viable. Also in Table XLII we present the optimized values of the

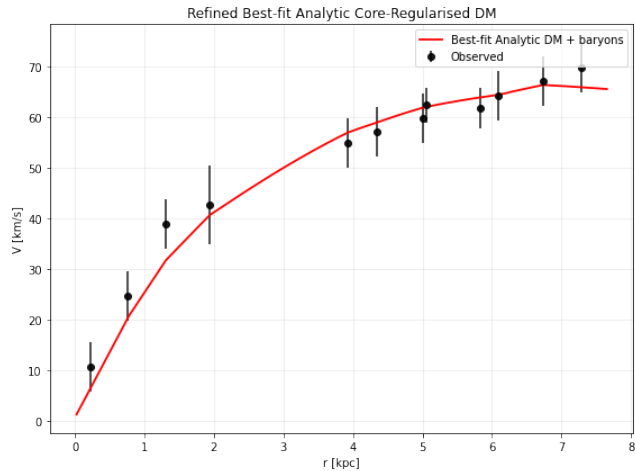


FIG. 70: The predicted rotation curves after using an optimization for the SIDM model (3), and the extended SPARC data for the galaxy F583-4. We included the rotation curves of the gas, the disk velocities, the bulge (where present) along with the SIDM model.

free parameters of the SIDM model for which we achieve the maximum compatibility with the SPARC data, for the galaxy F583-4, and also the resulting reduced χ^2_{red} value.

TABLE XLII: Optimized Parameter Values of the Extended SIDM model for the Galaxy F583-4.

Parameter	Value
$\rho_0 (M_\odot/\text{Kpc}^3)$	9.93357×10^6
$K_0 (M_\odot \text{ Kpc}^{-3} (\text{km/s})^2)$	1233.91
ml_{disk}	1
ml_{bulge}	0.3
$\alpha (\text{Kpc})$	6.43111
χ^2_{red}	0.652711

17. The Galaxy IC2574 Non-viable

For this galaxy, the optimization method we used, ensures maximum compatibility of the analytic SIDM model of Eq. (3) with the SPARC data, if we choose $\rho_0 = 5.59403 \times 10^6 M_\odot/\text{Kpc}^3$ and $K_0 = 1904.15 M_\odot \text{ Kpc}^{-3} (\text{km/s})^2$, in which case the reduced χ^2_{red} value is $\chi^2_{red} = 7.51187$. Also the parameter α in this case is $\alpha = 10.6473 \text{ Kpc}$.

In Table XLIII we present the optimized values of K_0 and ρ_0 for the analytic SIDM model of Eq. (3) for which the maximum compatibility with the SPARC data is achieved. In Figs. 71, 72 we present the

TABLE XLIII: SIDM Optimization Values for the galaxy IC2574

Parameter	Optimization Values
$\rho_0 (M_\odot/\text{Kpc}^3)$	5.59403×10^6
$K_0 (M_\odot \text{ Kpc}^{-3} (\text{km/s})^2)$	1904.15

density of the analytic SIDM model, the predicted rotation curves for the SIDM model (3), versus the SPARC observational data and the sound speed, as a function of the radius respectively. As it can be seen, for this galaxy, the SIDM model produces non-viable rotation curves which are incompatible with the SPARC data.

Now we shall include contributions to the rotation velocity from the other components of the galaxy, namely the disk, the gas, and the bulge if present. In Fig. 73 we present the combined rotation curves including all the components of the galaxy along with the SIDM. As it can be seen, the extended collisional DM model is non-viable. Also in Table XLIV we present the optimized values of the free

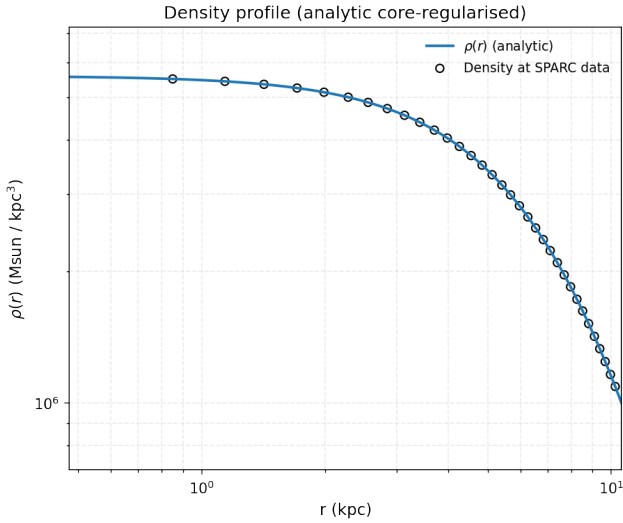


FIG. 71: The density of the SIDM model of Eq. (3) for the galaxy IC2574, versus the radius.

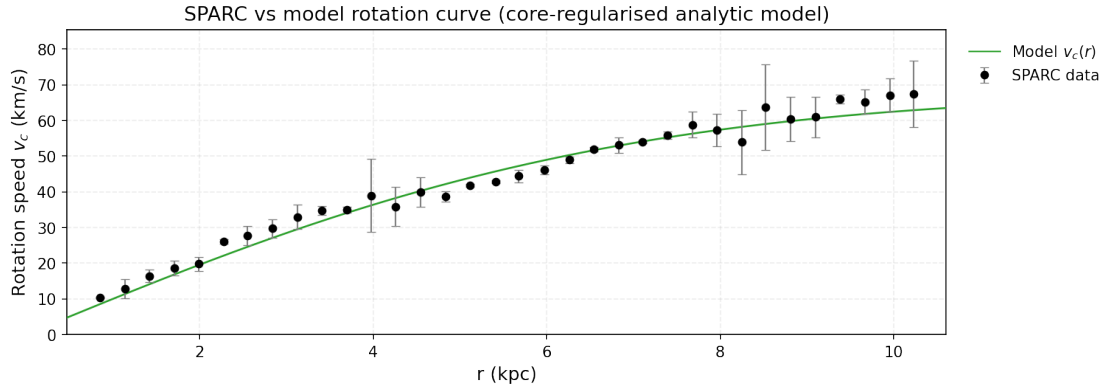


FIG. 72: The predicted rotation curves for the optimized SIDM model of Eq. (3), versus the SPARC observational data for the galaxy IC2574.

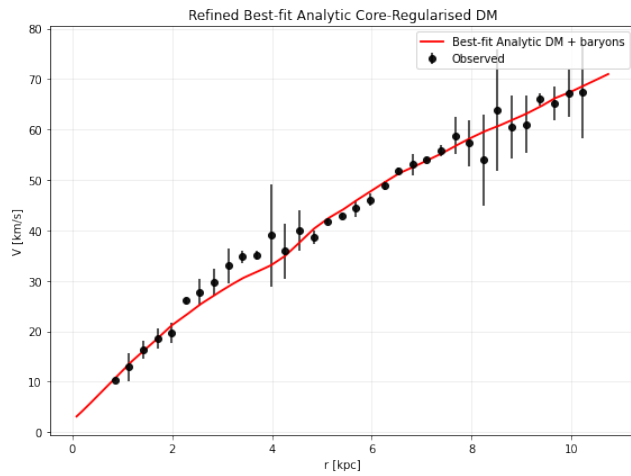


FIG. 73: The predicted rotation curves after using an optimization for the SIDM model (3), and the extended SPARC data for the galaxy IC2574. We included the rotation curves of the gas, the disk velocities, the bulge (where present) along with the SIDM model.

parameters of the SIDM model for which we achieve the maximum compatibility with the SPARC data,

for the galaxy IC2574, and also the resulting reduced χ^2_{red} value.

TABLE XLIV: Optimized Parameter Values of the Extended SIDM model for the Galaxy IC2574.

Parameter	Value
$\rho_0 (M_\odot/\text{Kpc}^3)$	2.41695×10^6
$K_0 (M_\odot \text{ Kpc}^{-3} (\text{km/s})^2)$	3730.76
ml_{disk}	0.9459
ml_{bulge}	0.1211
$\alpha (\text{Kpc})$	22.6705 **
χ^2_{red}	2.44598

18. The Galaxy KK98-251

For this galaxy, the optimization method we used, ensures maximum compatibility of the analytic SIDM model of Eq. (3) with the SPARC data, if we choose $\rho_0 = 2.10907 \times 10^7 M_\odot/\text{Kpc}^3$ and $K_0 = 616.254 M_\odot \text{ Kpc}^{-3} (\text{km/s})^2$, in which case the reduced χ^2_{red} value is $\chi^2_{red} = 0.569321$. Also the parameter α in this case is $\alpha = 3.1195 \text{ Kpc}$.

In Table XLV we present the optimized values of K_0 and ρ_0 for the analytic SIDM model of Eq. (3) for which the maximum compatibility with the SPARC data is achieved. In Figs. 74, 75 we present the

TABLE XLV: SIDM Optimization Values for the galaxy KK98-251

Parameter	Optimization Values
$\rho_0 (M_\odot/\text{Kpc}^3)$	2.10907×10^7
$K_0 (M_\odot \text{ Kpc}^{-3} (\text{km/s})^2)$	616.254

density of the analytic SIDM model, the predicted rotation curves for the SIDM model (3), versus the SPARC observational data and the sound speed, as a function of the radius respectively. As it can be seen, for this galaxy, the SIDM model produces viable rotation curves which are compatible with the SPARC data.

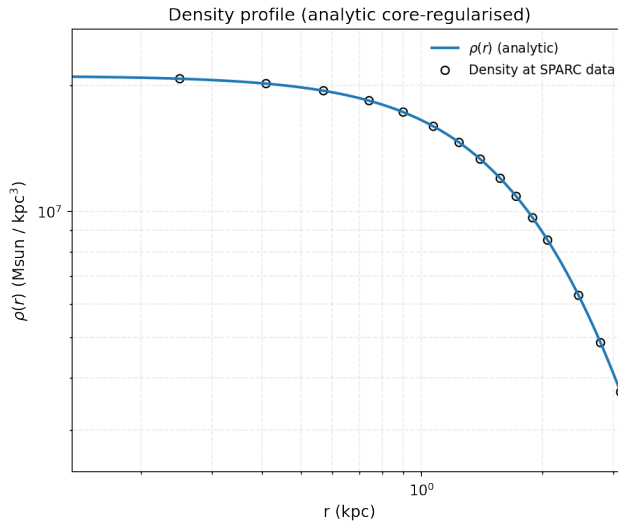


FIG. 74: The density of the SIDM model of Eq. (3) for the galaxy KK98-251, versus the radius.

19. The Galaxy NGC0024, Non-viable

For this galaxy, the optimization method we used, ensures maximum compatibility of the analytic SIDM model of Eq. (3) with the SPARC data, if we choose $\rho_0 = 3.1262 \times 10^8 M_\odot/\text{Kpc}^3$ and $K_0 =$

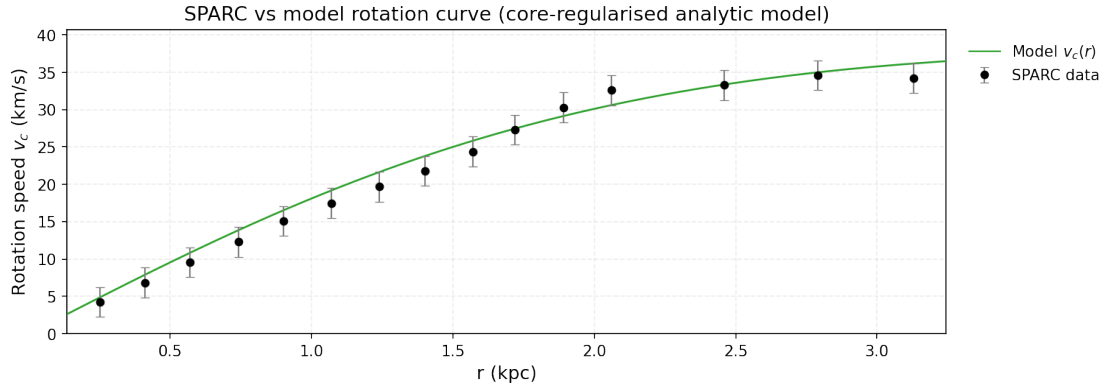


FIG. 75: The predicted rotation curves for the optimized SIDM model of Eq. (3), versus the SPARC observational data for the galaxy KK98-251.

$6437.6 M_{\odot} \text{Kpc}^{-3} (\text{km/s})^2$, in which case the reduced χ^2_{red} value is $\chi^2_{red} = 2.86598$. Also the parameter α in this case is $\alpha = 2.61881 \text{Kpc}$.

In Table XLVI we present the optimized values of K_0 and ρ_0 for the analytic SIDM model of Eq. (3) for which the maximum compatibility with the SPARC data is achieved. In Figs. 76, 77 we present the

TABLE XLVI: SIDM Optimization Values for the galaxy NGC0024

Parameter	Optimization Values
$\rho_0 (M_{\odot}/\text{Kpc}^3)$	3.1262×10^8
$K_0 (M_{\odot} \text{Kpc}^{-3} (\text{km/s})^2)$	3.1262

density of the analytic SIDM model, the predicted rotation curves for the SIDM model (3), versus the SPARC observational data and the sound speed, as a function of the radius respectively. As it can be seen, for this galaxy, the SIDM model produces non-viable rotation curves which are incompatible with the SPARC data.

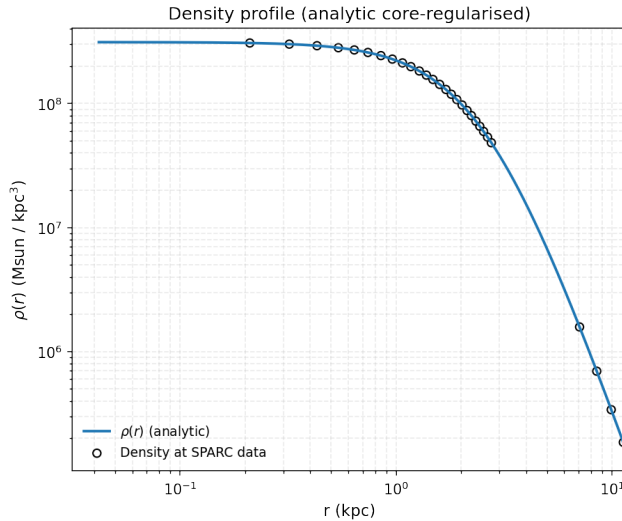


FIG. 76: The density of the SIDM model of Eq. (3) for the galaxy NGC0024, versus the radius.

Now we shall include contributions to the rotation velocity from the other components of the galaxy, namely the disk, the gas, and the bulge if present. In Fig. 78 we present the combined rotation curves including all the components of the galaxy along with the SIDM. As it can be seen, the extended collisional DM model is non-viable. Also in Table XLVII we present the optimized values of the free parameters of the SIDM model for which we achieve the maximum compatibility with the SPARC data, for the galaxy NGC0024, and also the resulting reduced χ^2_{red} value.

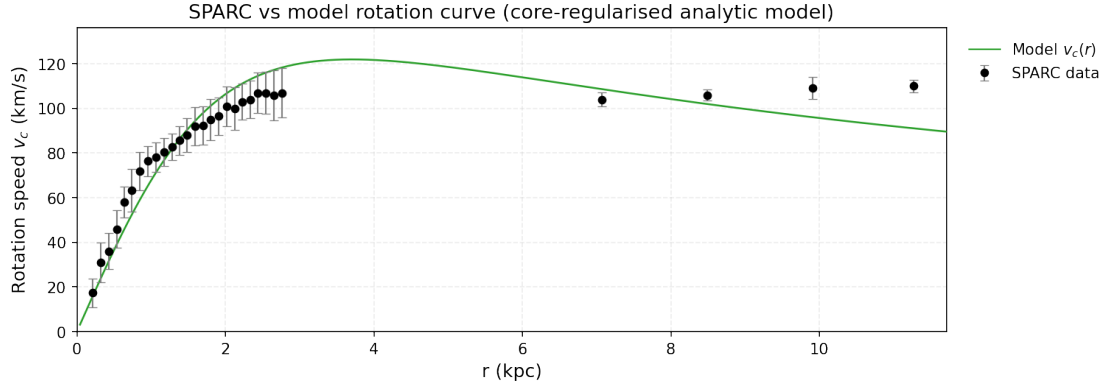


FIG. 77: The predicted rotation curves for the optimized SIDM model of Eq. (3), versus the SPARC observational data for the galaxy NGC0024.

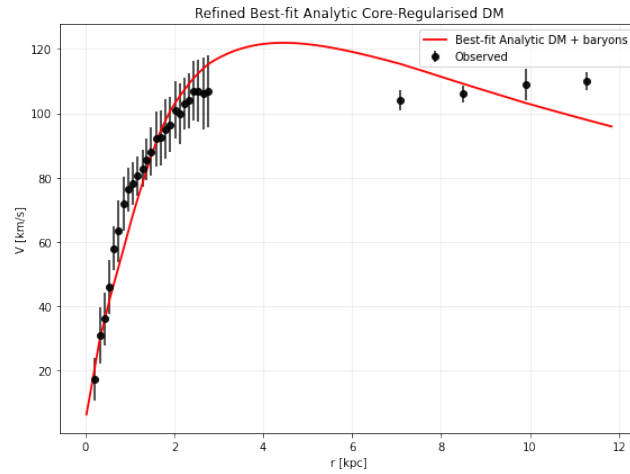


FIG. 78: The predicted rotation curves after using an optimization for the SIDM model (3), and the extended SPARC data for the galaxy NGC0024. We included the rotation curves of the gas, the disk velocities, the bulge (where present) along with the SIDM model.

TABLE XLVII: Optimized Parameter Values of the Extended SIDM model for the Galaxy NGC0024.

Parameter	Value
$\rho_0 (M_\odot/\text{Kpc}^3)$	1.18583×10^8
$K_0 (M_\odot \text{ Kpc}^{-3} (\text{km/s})^2)$	4583.52
ml_{disk}	1
ml_{bulge}	0.5
$\alpha (\text{Kpc})$	3.58743
χ^2_{red}	2.11333

20. The Galaxy NGC0055, Marginally Viable, Extended Viable

For this galaxy, the optimization method we used, ensures maximum compatibility of the analytic SIDM model of Eq. (3) with the SPARC data, if we choose $\rho_0 = 1.87465 \times 10^7 M_\odot/\text{Kpc}^3$ and $K_0 = 3194.12 M_\odot \text{ Kpc}^{-3} (\text{km/s})^2$, in which case the reduced χ^2_{red} value is $\chi^2_{\text{red}} = 0.731137$. Also the parameter α in this case is $\alpha = 7.53296 \text{ Kpc}$.

In Table XLVIII we present the optimized values of K_0 and ρ_0 for the analytic SIDM model of Eq. (3) for which the maximum compatibility with the SPARC data is achieved. In Figs. 79, 80 we present the density of the analytic SIDM model, the predicted rotation curves for the SIDM model (3), versus the SPARC observational data and the sound speed, as a function of the radius respectively. As it can be seen, for this galaxy, the SIDM model produces marginally viable rotation curves which are marginally compatible with the SPARC data.

TABLE XLVIII: SIDM Optimization Values for the galaxy NGC0055

Parameter	Optimization Values
$\rho_0 (M_\odot/\text{Kpc}^3)$	1.87465×10^7
$K_0 (M_\odot \text{ Kpc}^{-3} (\text{km/s})^2)$	3194.12

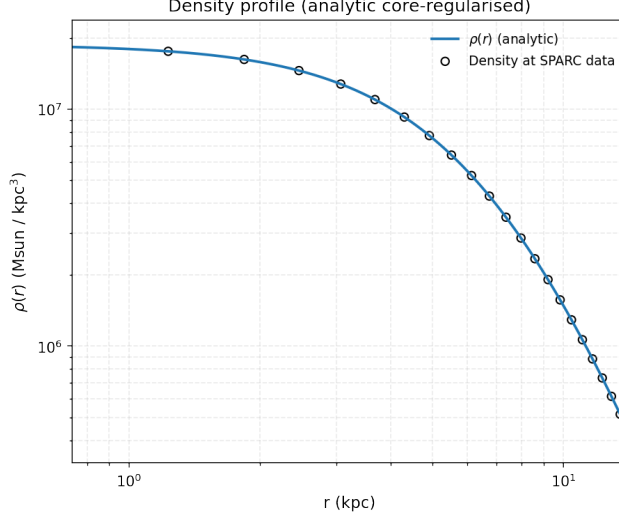


FIG. 79: The density of the SIDM model of Eq. (3) for the galaxy NGC0055, versus the radius.

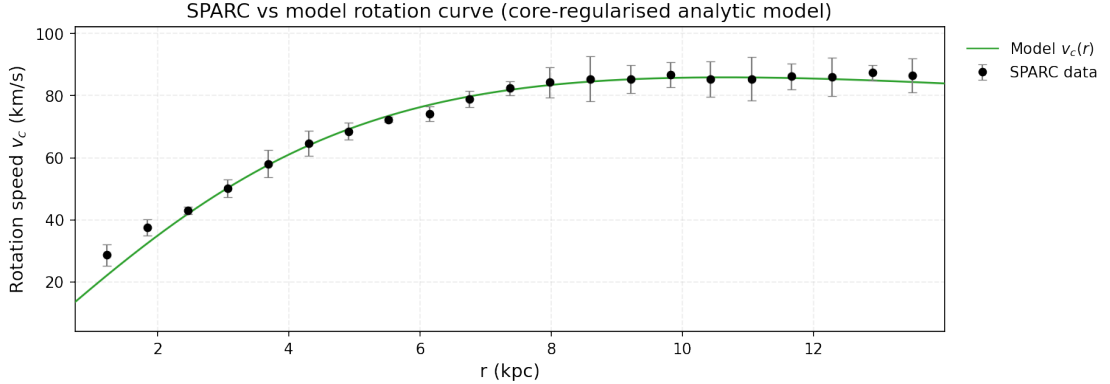


FIG. 80: The predicted rotation curves for the optimized SIDM model of Eq. (3), versus the SPARC observational data for the galaxy NGC0055.

Now we shall include contributions to the rotation velocity from the other components of the galaxy, namely the disk, the gas, and the bulge if present. In Fig. 81 we present the combined rotation curves including all the components of the galaxy along with the SIDM. As it can be seen, the extended collisional DM model is viable. Also in Table XLIX we present the optimized values of the free parameters of the SIDM model for which we achieve the maximum compatibility with the SPARC data, for the galaxy NGC0055, and also the resulting reduced χ^2_{red} value.

TABLE XLIX: Optimized Parameter Values of the Extended SIDM model for the Galaxy NGC0055.

Parameter	Value
$\rho_0 (M_\odot/\text{Kpc}^3)$	9.57524×10^6
$K_0 (M_\odot \text{ Kpc}^{-3} (\text{km/s})^2)$	2410.56
ml_{disk}	0.6115
ml_{bulge}	0.2901
$\alpha (\text{Kpc})$	9.15547
χ^2_{red}	0.131558

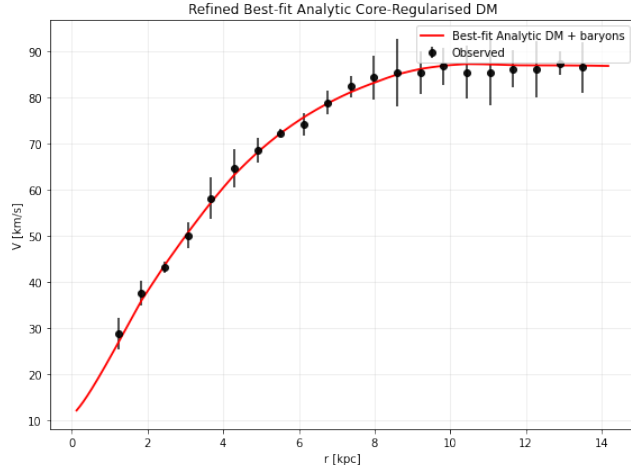


FIG. 81: The predicted rotation curves after using an optimization for the SIDM model (3), and the extended SPARC data for the galaxy NGC0055. We included the rotation curves of the gas, the disk velocities, the bulge (where present) along with the SIDM model.

21. The Galaxy NGC0100

For this galaxy, the optimization method we used, ensures maximum compatibility of the analytic SIDM model of Eq. (3) with the SPARC data, if we choose $\rho_0 = 3.77865 \times 10^7 M_\odot/\text{Kpc}^3$ and $K_0 = 3237.93 M_\odot \text{Kpc}^{-3} (\text{km/s})^2$, in which case the reduced χ^2_{red} value is $\chi^2_{\text{red}} = 0.386342$. Also the parameter α in this case is $\alpha = 5.34215 \text{Kpc}$.

In Table L we present the optimized values of K_0 and ρ_0 for the analytic SIDM model of Eq. (3) for which the maximum compatibility with the SPARC data is achieved. In Figs. 82, 83 we present the

TABLE L: SIDM Optimization Values for the galaxy NGC0100

Parameter	Optimization Values
$\rho_0 (M_\odot/\text{Kpc}^3)$	3.77865×10^7
$K_0 (M_\odot \text{Kpc}^{-3} (\text{km/s})^2)$	3237.93

density of the analytic SIDM model, the predicted rotation curves for the SIDM model (3), versus the SPARC observational data and the sound speed, as a function of the radius respectively. As it can be seen, for this galaxy, the SIDM model produces viable rotation curves which are compatible with the SPARC data.

22. The Galaxy NGC0247, Non-viable

For this galaxy, the optimization method we used, ensures maximum compatibility of the analytic SIDM model of Eq. (3) with the SPARC data, if we choose $\rho_0 = 2.1361 \times 10^7 M_\odot/\text{Kpc}^3$ and $K_0 = 4233.3 M_\odot \text{Kpc}^{-3} (\text{km/s})^2$, in which case the reduced χ^2_{red} value is $\chi^2_{\text{red}} = 38.458$. Also the parameter α in this case is $\alpha = 8.12419 \text{Kpc}$.

In Table LI we present the optimized values of K_0 and ρ_0 for the analytic SIDM model of Eq. (3) for which the maximum compatibility with the SPARC data is achieved. In Figs. 84, 85 we present the

TABLE LI: SIDM Optimization Values for the galaxy NGC0247

Parameter	Optimization Values
$\rho_0 (M_\odot/\text{Kpc}^3)$	2.1361×10^7
$K_0 (M_\odot \text{Kpc}^{-3} (\text{km/s})^2)$	4233.3

density of the analytic SIDM model, the predicted rotation curves for the SIDM model (3), versus the SPARC observational data and the sound speed, as a function of the radius respectively. As it can be

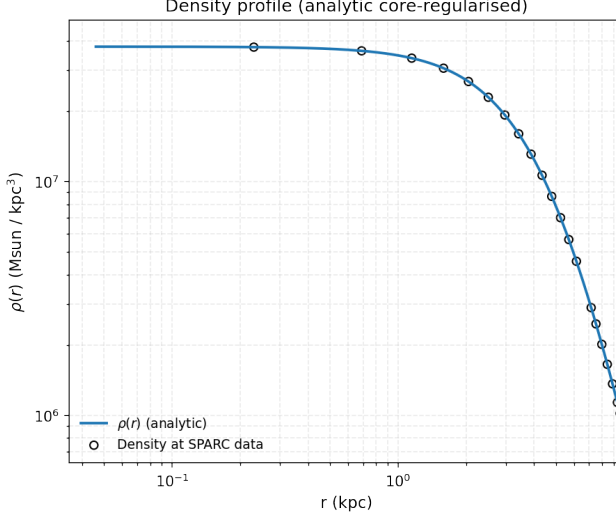


FIG. 82: The density of the SIDM model of Eq. (3) for the galaxy NGC0100, versus the radius.

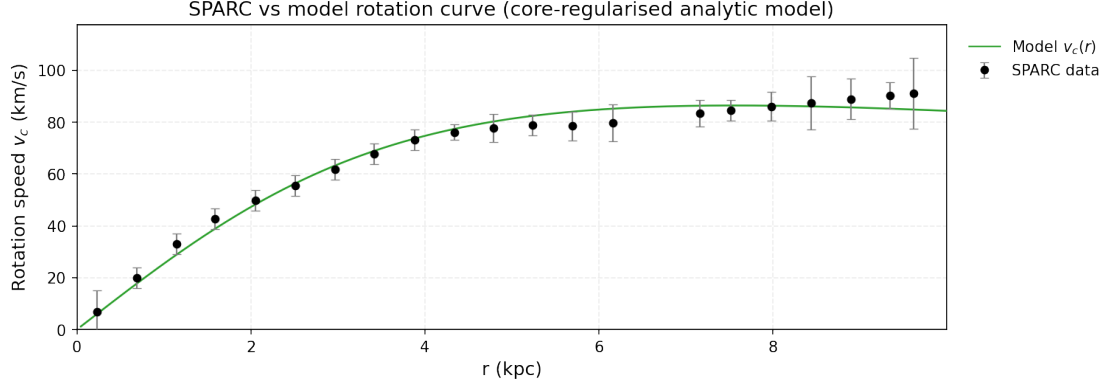


FIG. 83: The predicted rotation curves for the optimized SIDM model of Eq. (3), versus the SPARC observational data for the galaxy NGC0100.

seen, for this galaxy, the SIDM model produces non-viable rotation curves which are incompatible with the SPARC data.

Now we shall include contributions to the rotation velocity from the other components of the galaxy, namely the disk, the gas, and the bulge if present. In Fig. 86 we present the combined rotation curves including all the components of the galaxy along with the SIDM. As it can be seen, the extended collisional DM model is non-viable. Also in Table LII we present the optimized values of the free parameters of the SIDM model for which we achieve the maximum compatibility with the SPARC data, for the galaxy NGC0247, and also the resulting reduced χ^2_{red} value.

TABLE LII: Optimized Parameter Values of the Extended SIDM model for the Galaxy NGC0247.

Parameter	Value
$\rho_0 (M_\odot / \text{Kpc}^3)$	2.28958×10^7
$K_0 (M_\odot \text{ Kpc}^{-3} (\text{km/s})^2)$	1861.68
ml_{disk}	1
ml_{bulge}	0.2749
$\alpha (\text{Kpc})$	5.2032
χ^2_{red}	7.7912

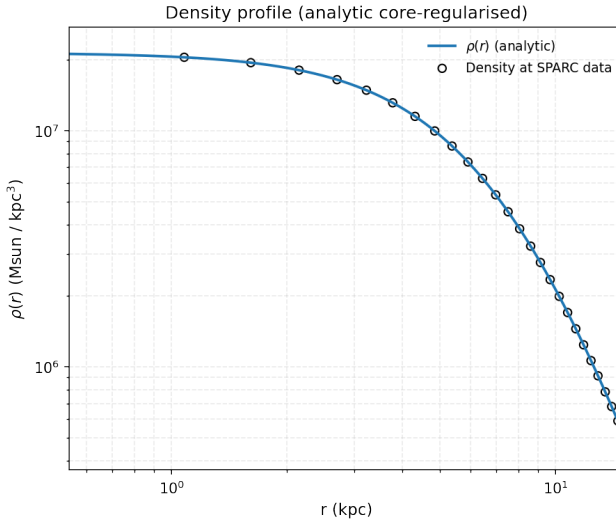


FIG. 84: The density of the SIDM model of Eq. (3) for the galaxy NGC0247, versus the radius.

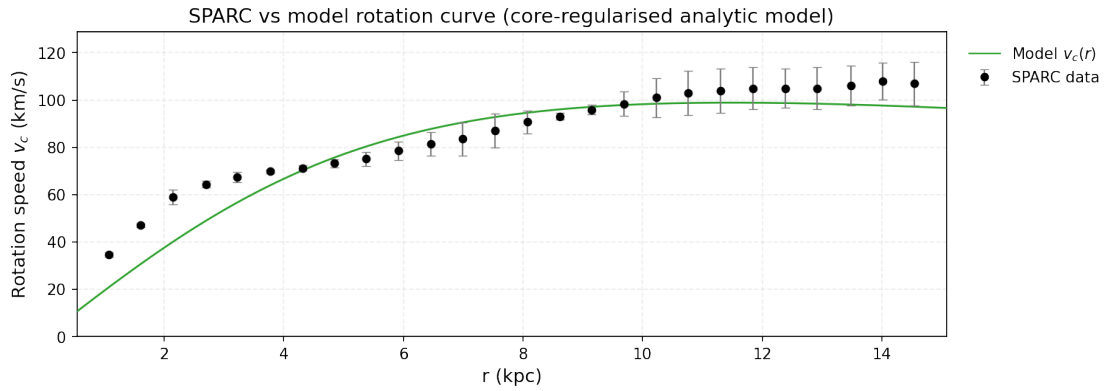


FIG. 85: The predicted rotation curves for the optimized SIDM model of Eq. (3), versus the SPARC observational data for the galaxy NGC0247.

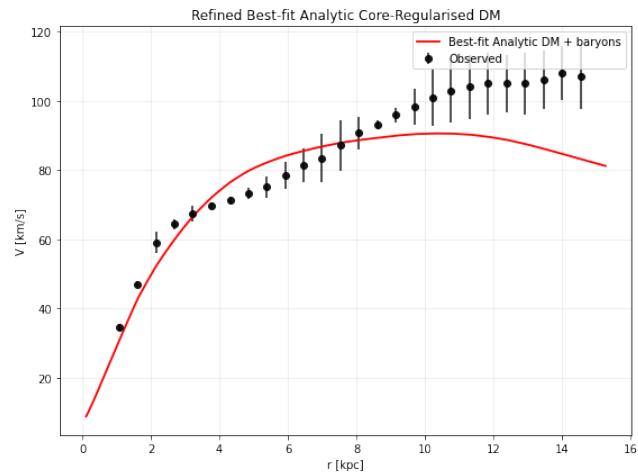


FIG. 86: The predicted rotation curves after using an optimization for the SIDM model (3), and the extended SPARC data for the galaxy NGC0247. We included the rotation curves of the gas, the disk velocities, the bulge (where present) along with the SIDM model.

23. The Galaxy NGC0289, Non-viable, Extended Marginally Viable

For this galaxy, the optimization method we used, ensures maximum compatibility of the analytic SIDM model of Eq. (3) with the SPARC data, if we choose $\rho_0 = 3.07333 \times 10^7 M_\odot/\text{Kpc}^3$ and $K_0 = 18670.3 M_\odot \text{Kpc}^{-3} (\text{km/s})^2$, in which case the reduced χ^2_{red} value is $\chi^2_{red} = 17.9695$. Also the parameter α in this case is $\alpha = 14.224 \text{Kpc}$.

In Table LIII we present the optimized values of K_0 and ρ_0 for the analytic SIDM model of Eq. (3) for which the maximum compatibility with the SPARC data is achieved. In Figs. 87, 88 we present the

TABLE LIII: SIDM Optimization Values for the galaxy NGC0289

Parameter	Optimization Values
$\rho_0 (M_\odot/\text{Kpc}^3)$	3.07333×10^7
$K_0 (M_\odot \text{Kpc}^{-3} (\text{km/s})^2)$	18670.3

density of the analytic SIDM model, the predicted rotation curves for the SIDM model (3), versus the SPARC observational data and the sound speed, as a function of the radius respectively. As it can be seen, for this galaxy, the SIDM model produces non-viable rotation curves which are incompatible with the SPARC data.

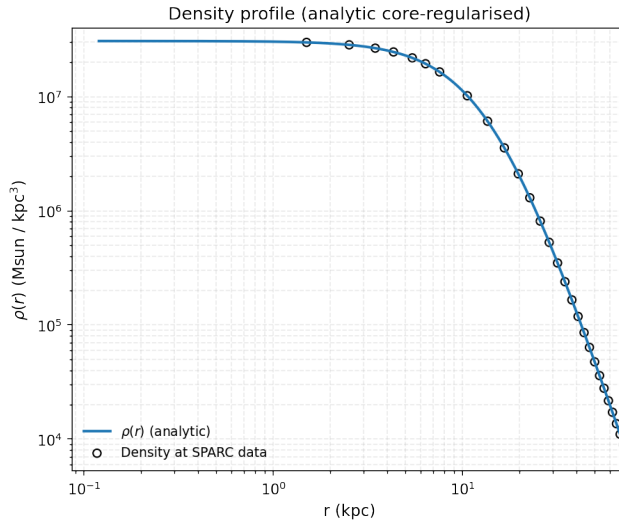


FIG. 87: The density of the SIDM model of Eq. (3) for the galaxy NGC0289, versus the radius.

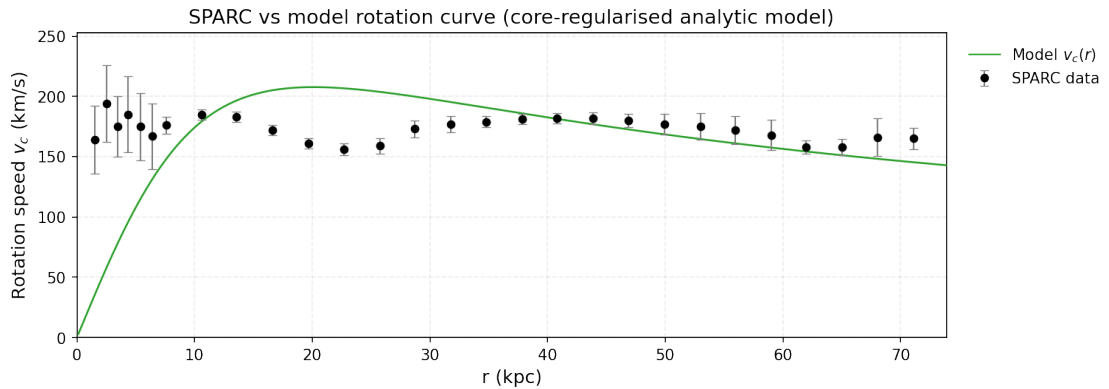


FIG. 88: The predicted rotation curves for the optimized SIDM model of Eq. (3), versus the SPARC observational data for the galaxy NGC0289.

Now we shall include contributions to the rotation velocity from the other components of the galaxy, namely the disk, the gas, and the bulge if present. In Fig. 89 we present the combined rotation curves

including all the components of the galaxy along with the SIDM. As it can be seen, the extended collisional DM model is non-viable. Also in Table LIV we present the optimized values of the free parameters of

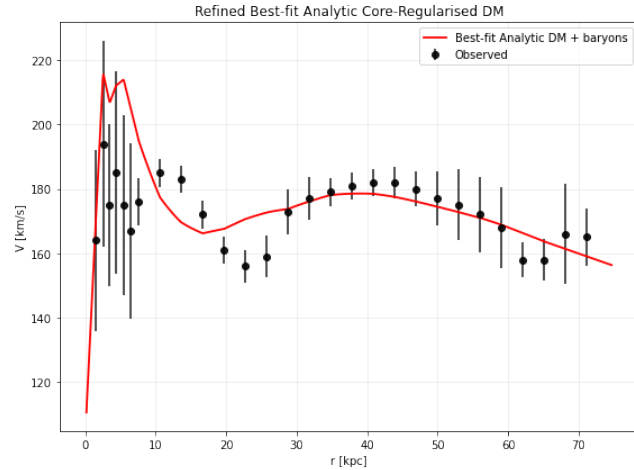


FIG. 89: The predicted rotation curves after using an optimization for the SIDM model (3), and the extended SPARC data for the galaxy NGC0289. We included the rotation curves of the gas, the disk velocities, the bulge (where present) along with the SIDM model.

the SIDM model for which we achieve the maximum compatibility with the SPARC data, for the galaxy NGC0289, and also the resulting reduced χ^2_{red} value.

TABLE LIV: Optimized Parameter Values of the Extended SIDM model for the Galaxy NGC0289.

Parameter	Value
ρ_0 (M_\odot/Kpc^3)	2.60432×10^7
K_0 ($M_\odot \text{ Kpc}^{-3} (\text{km/s})^2$)	8825.33
ml_{disk}	0.9509
ml_{bulge}	0.4
α (Kpc)	33.5903
χ^2_{red}	2.09307

24. The Galaxy NGC0300, Non-viable, Extended Viable

For this galaxy, the optimization method we used, ensures maximum compatibility of the analytic SIDM model of Eq. (3) with the SPARC data, if we choose $\rho_0 = 4.85635 \times 10^7 M_\odot/\text{Kpc}^3$ and $K_0 = 3788.38 M_\odot \text{ Kpc}^{-3} (\text{km/s})^2$, in which case the reduced χ^2_{red} value is $\chi^2_{red} = 2.38282$. Also the parameter α in this case is $\alpha = 5.09709 \text{ Kpc}$.

In Table LV we present the optimized values of K_0 and ρ_0 for the analytic SIDM model of Eq. (3) for which the maximum compatibility with the SPARC data is achieved. In Figs. 90, 91 we present the

TABLE LV: SIDM Optimization Values for the galaxy NGC0300

Parameter	Optimization Values
ρ_0 (M_\odot/Kpc^3)	4.85635×10^7
K_0 ($M_\odot \text{ Kpc}^{-3} (\text{km/s})^2$)	3788.38

density of the analytic SIDM model, the predicted rotation curves for the SIDM model (3), versus the SPARC observational data and the sound speed, as a function of the radius respectively. As it can be seen, for this galaxy, the SIDM model produces non-viable rotation curves which are incompatible with the SPARC data.

Now we shall include contributions to the rotation velocity from the other components of the galaxy, namely the disk, the gas, and the bulge if present. In Fig. 92 we present the combined rotation curves including all the components of the galaxy along with the SIDM. As it can be seen, the extended

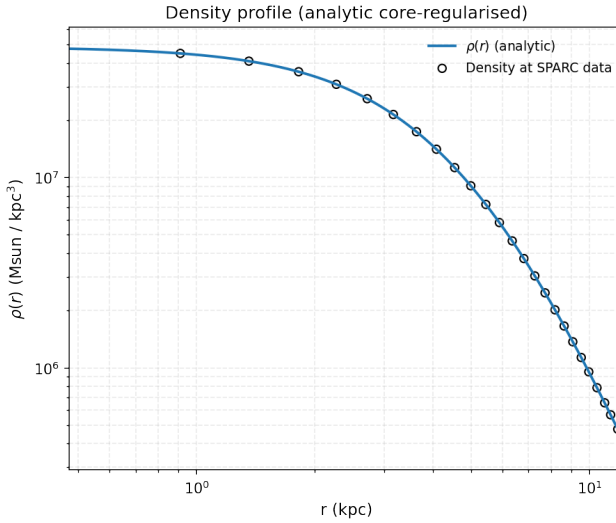


FIG. 90: The density of the SIDM model of Eq. (3) for the galaxy NGC0300, versus the radius.

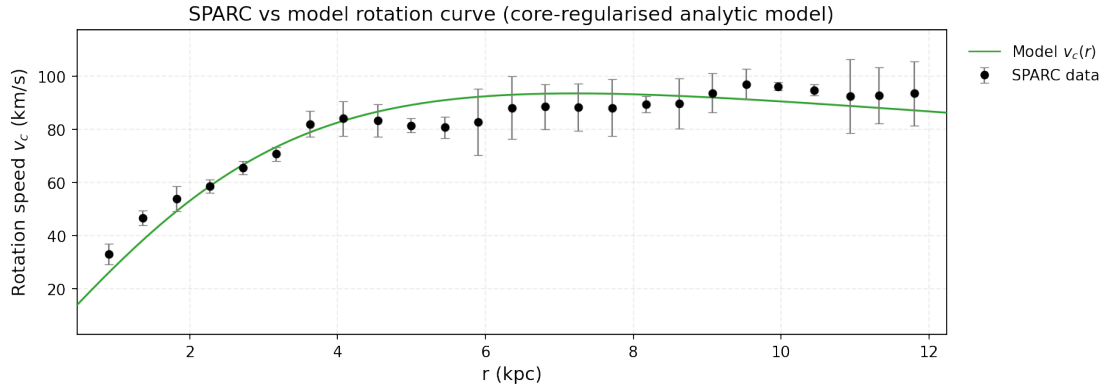


FIG. 91: The predicted rotation curves for the optimized SIDM model of Eq. (3), versus the SPARC observational data for the galaxy NGC0300.

collisional DM model is viable. Also in Table LVI we present the optimized values of the free parameters

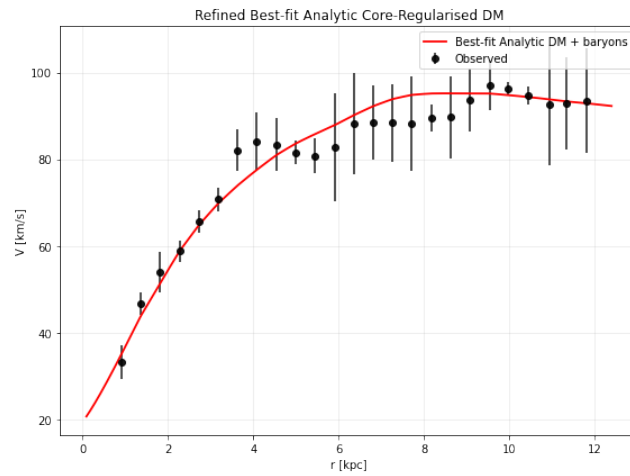


FIG. 92: The predicted rotation curves after using an optimization for the SIDM model (3), and the extended SPARC data for the galaxy NGC0300. We included the rotation curves of the gas, the disk velocities, the bulge (where present) along with the SIDM model.

of the SIDM model for which we achieve the maximum compatibility with the SPARC data, for the galaxy NGC0300, and also the resulting reduced χ^2_{red} value.

TABLE LVI: Optimized Parameter Values of the Extended SIDM model for the Galaxy NGC0300.

Parameter	Value
$\rho_0 (M_\odot/\text{Kpc}^3)$	1.59765×10^7
$K_0 (M_\odot \text{ Kpc}^{-3} (\text{km/s})^2)$	3002.46
ml_{disk}	1
ml_{bulge}	0.1373
$\alpha (\text{Kpc})$	7.91032
χ^2_{red}	0.664034

25. The Galaxy NGC0801, Non-viable, Extended Marginally Viable

For this galaxy, the optimization method we used, ensures maximum compatibility of the analytic SIDM model of Eq. (3) with the SPARC data, if we choose $\rho_0 = 6.64818 \times 10^7 M_\odot/\text{Kpc}^3$ and $K_0 = 28572.9 M_\odot \text{ Kpc}^{-3} (\text{km/s})^2$, in which case the reduced χ^2_{red} value is $\chi^2_{red} = 179.525$. Also the parameter α in this case is $\alpha = 11.964 \text{ Kpc}$.

In Table LVII we present the optimized values of K_0 and ρ_0 for the analytic SIDM model of Eq. (3) for which the maximum compatibility with the SPARC data is achieved. In Figs. 93, 94 we present the

TABLE LVII: SIDM Optimization Values for the galaxy NGC0801

Parameter	Optimization Values
$\rho_0 (M_\odot/\text{Kpc}^3)$	6.64818×10^7
$K_0 (M_\odot \text{ Kpc}^{-3} (\text{km/s})^2)$	28572.9

density of the analytic SIDM model, the predicted rotation curves for the SIDM model (3), versus the SPARC observational data and the sound speed, as a function of the radius respectively. As it can be seen, for this galaxy, the SIDM model produces non-viable rotation curves which are incompatible with the SPARC data.

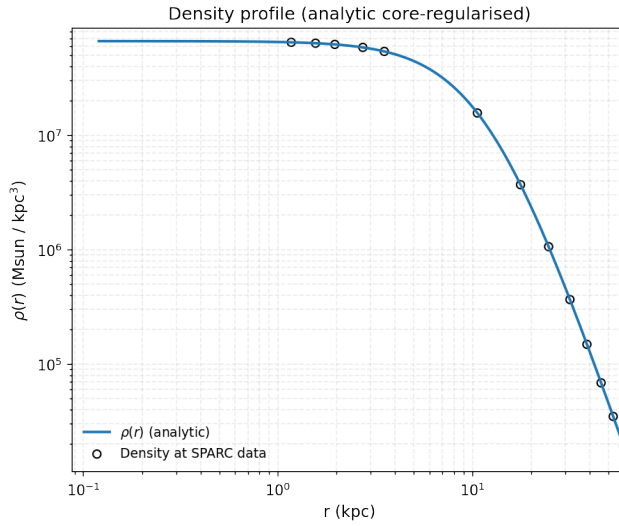


FIG. 93: The density of the SIDM model of Eq. (3) for the galaxy NGC0801, versus the radius.

Now we shall include contributions to the rotation velocity from the other components of the galaxy, namely the disk, the gas, and the bulge if present. In Fig. 95 we present the combined rotation curves including all the components of the galaxy along with the SIDM. As it can be seen, the extended collisional DM model is non-viable. Also in Table LVIII we present the optimized values of the free

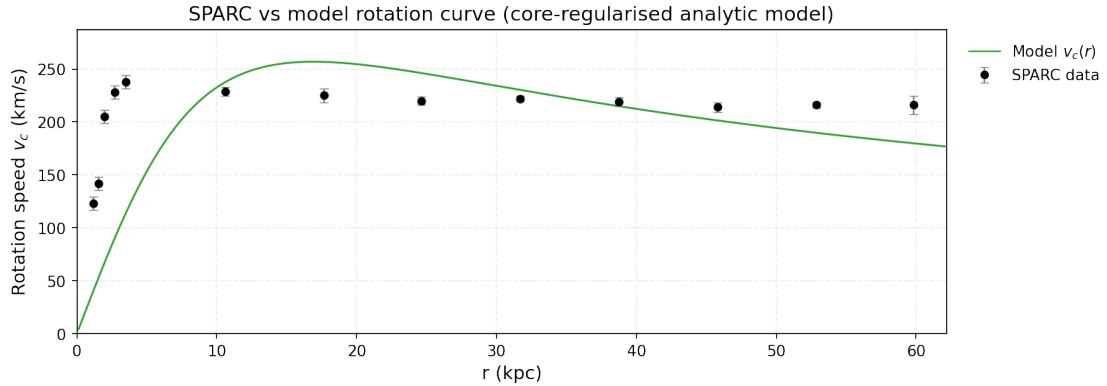


FIG. 94: The predicted rotation curves for the optimized SIDM model of Eq. (3), versus the SPARC observational data for the galaxy NGC0801.

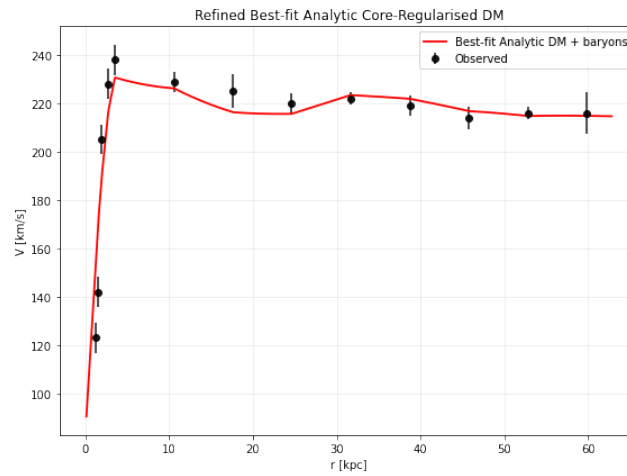


FIG. 95: The predicted rotation curves after using an optimization for the SIDM model (3), and the extended SPARC data for the galaxy NGC0801. We included the rotation curves of the gas, the disk velocities, the bulge (where present) along with the SIDM model.

parameters of the SIDM model for which we achieve the maximum compatibility with the SPARC data, for the galaxy NGC0801, and also the resulting reduced χ^2_{red} value.

TABLE LVIII: Optimized Parameter Values of the Extended SIDM model for the Galaxy NGC0801.

Parameter	Value
$\rho_0 (M_\odot/\text{Kpc}^3)$	1.18198×10^6
$K_0 (M_\odot \text{ Kpc}^{-3} (\text{km/s})^2)$	11504.5
ml_{disk}	0.8169
ml_{bulge}	0.2987
$\alpha (\text{Kpc})$	56.9279
χ^2_{red}	6.46751

26. The Galaxy NGC0891, Non-viable, Extended Viable

For this galaxy, the optimization method we used, ensures maximum compatibility of the analytic SIDM model of Eq. (3) with the SPARC data, if we choose $\rho_0 = 3.37381 \times 10^8 M_\odot/\text{Kpc}^3$ and $K_0 = 25248.6 M_\odot \text{ Kpc}^{-3} (\text{km/s})^2$, in which case the reduced χ^2_{red} value is $\chi^2_{red} = 19.8621$. Also the parameter α in this case is $\alpha = 4.9924 \text{ Kpc}$.

In Table LIX we present the optimized values of K_0 and ρ_0 for the analytic SIDM model of Eq. (3) for which the maximum compatibility with the SPARC data is achieved. In Figs. 96, 97 we present the

TABLE LIX: SIDM Optimization Values for the galaxy NGC0891

Parameter	Optimization Values
$\rho_0 (M_\odot/\text{Kpc}^3)$	3.37381×10^7
$K_0 (M_\odot \text{ Kpc}^{-3} (\text{km/s})^2)$	25248.6

density of the analytic SIDM model, the predicted rotation curves for the SIDM model (3), versus the SPARC observational data and the sound speed, as a function of the radius respectively. As it can be seen, for this galaxy, the SIDM model produces non-viable rotation curves which are incompatible with the SPARC data.

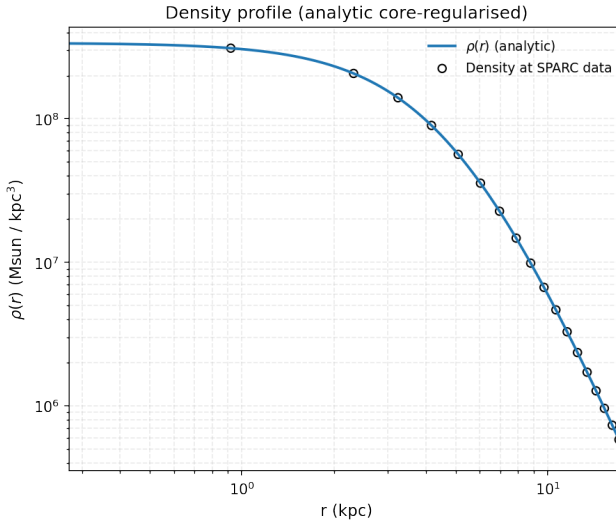


FIG. 96: The density of the SIDM model of Eq. (3) for the galaxy NGC0891, versus the radius.

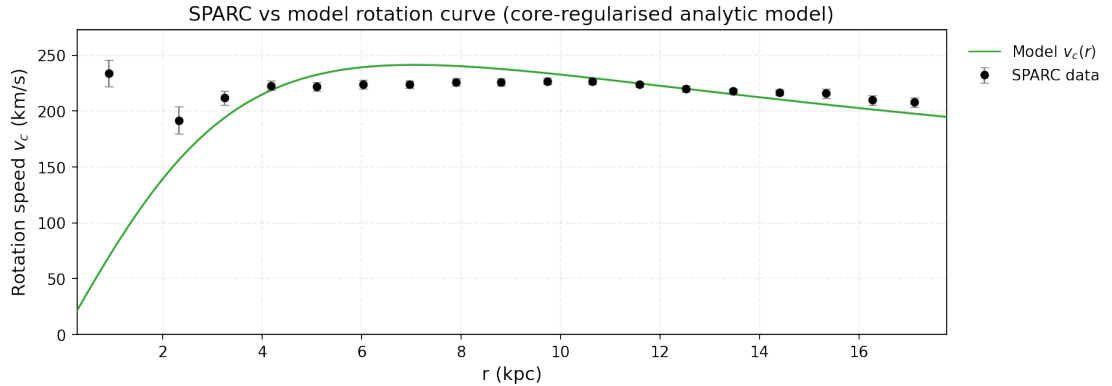


FIG. 97: The predicted rotation curves for the optimized SIDM model of Eq. (3), versus the SPARC observational data for the galaxy NGC0891.

Now we shall include contributions to the rotation velocity from the other components of the galaxy, namely the disk, the gas, and the bulge if present. In Fig. 98 we present the combined rotation curves including all the components of the galaxy along with the SIDM. As it can be seen, the extended collisional DM model is non-viable. Also in Table LX we present the optimized values of the free parameters of the SIDM model for which we achieve the maximum compatibility with the SPARC data, for the galaxy NGC0891, and also the resulting reduced χ^2_{red} value.

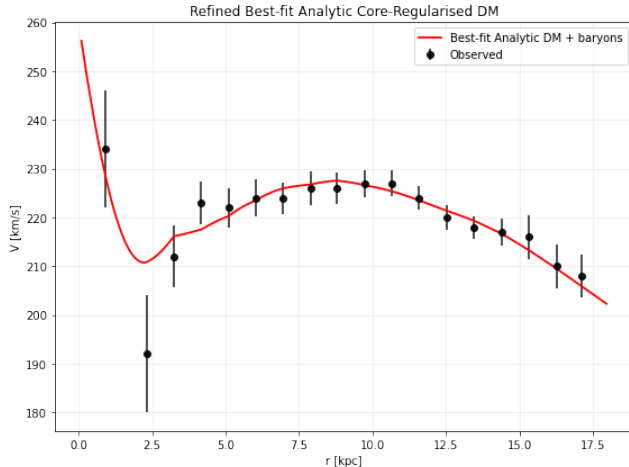


FIG. 98: The predicted rotation curves after using an optimization for the SIDM model (3), and the extended SPARC data for the galaxy NGC0891. We included the rotation curves of the gas, the disk velocities, the bulge (where present) along with the SIDM model.

TABLE LX: Optimized Parameter Values of the Extended SIDM model for the Galaxy NGC0891.

Parameter	Value
$\rho_0 (M_\odot/\text{Kpc}^3)$	9.35254×10^7
$K_0 (M_\odot \text{ Kpc}^{-3} (\text{km/s})^2)$	15975.8
ml_{disk}	0.876
ml_{bulge}	0.8656
$\alpha (\text{Kpc})$	7.54159
χ^2_{red}	0.51822

27. The Galaxy NGC1003, Non-viable

For this galaxy, the optimization method we used, ensures maximum compatibility of the analytic SIDM model of Eq. (3) with the SPARC data, if we choose $\rho_0 = 1.89193 \times 10^7 M_\odot/\text{Kpc}^3$ and $K_0 = 5656.14 M_\odot \text{ Kpc}^{-3} (\text{km/s})^2$, in which case the reduced χ^2_{red} value is $\chi^2_{\text{red}} = 33.3223$. Also the parameter α in this case is $\alpha = 9.97834 \text{ Kpc}$.

In Table LXI we present the optimized values of K_0 and ρ_0 for the analytic SIDM model of Eq. (3) for which the maximum compatibility with the SPARC data is achieved. In Figs. 99, 100 we present the

TABLE LXI: SIDM Optimization Values for the galaxy NGC1003

Parameter	Optimization Values
$\rho_0 (M_\odot/\text{Kpc}^3)$	1.89193×10^7
$K_0 (M_\odot \text{ Kpc}^{-3} (\text{km/s})^2)$	5656.14

density of the analytic SIDM model, the predicted rotation curves for the SIDM model (3), versus the SPARC observational data and the sound speed, as a function of the radius respectively. As it can be seen, for this galaxy, the SIDM model produces non-viable rotation curves which are incompatible with the SPARC data.

Now we shall include contributions to the rotation velocity from the other components of the galaxy, namely the disk, the gas, and the bulge if present. In Fig. 101 we present the combined rotation curves including all the components of the galaxy along with the SIDM. As it can be seen, the extended collisional DM model is non-viable. Also in Table LXII we present the optimized values of the free parameters of the SIDM model for which we achieve the maximum compatibility with the SPARC data, for the galaxy NGC1003, and also the resulting reduced χ^2_{red} value.

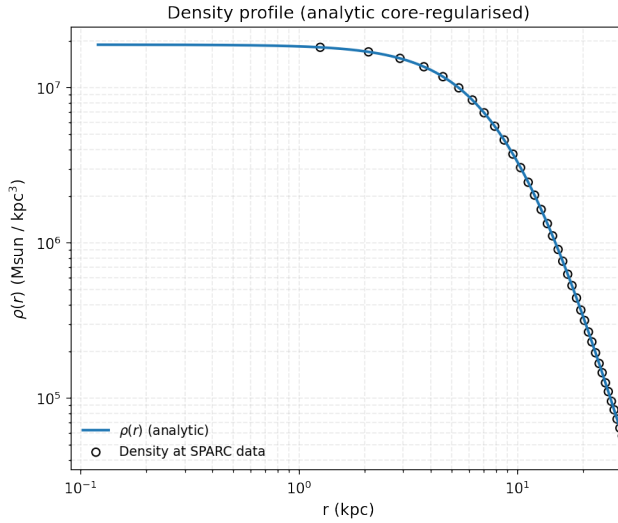


FIG. 99: The density of the SIDM model of Eq. (3) for the galaxy NGC1003, versus the radius.

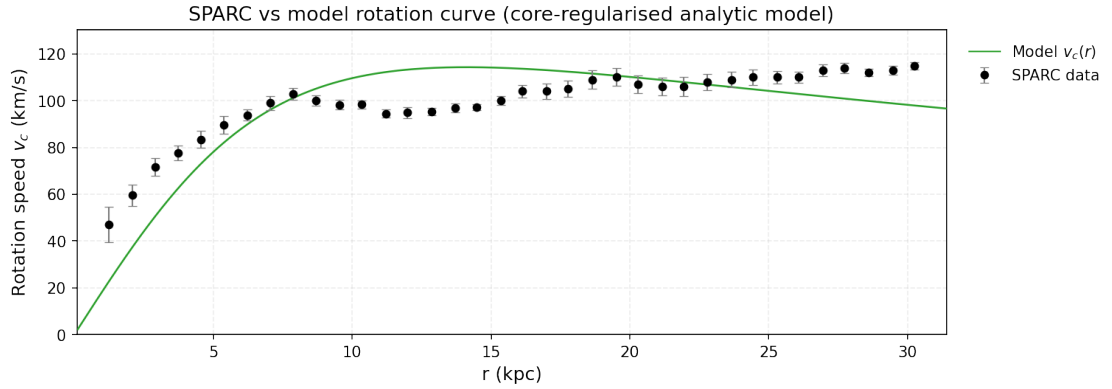


FIG. 100: The predicted rotation curves for the optimized SIDM model of Eq. (3), versus the SPARC observational data for the galaxy NGC1003.

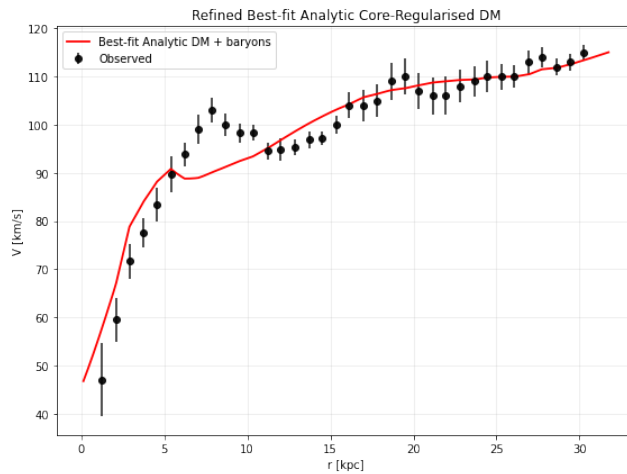


FIG. 101: The predicted rotation curves after using an optimization for the SIDM model (3), and the extended SPARC data for the galaxy NGC1003. We included the rotation curves of the gas, the disk velocities, the bulge (where present) along with the SIDM model.

TABLE LXII: Optimized Parameter Values of the Extended SIDM model for the Galaxy NGC1003.

Parameter	Value
$\rho_0 (M_\odot/\text{Kpc}^3)$	3.29588×10^6
$K_0 (M_\odot \text{ Kpc}^{-3} (\text{km/s})^2)$	4532.84
ml_{disk}	1
ml_{bulge}	0.3459
$\alpha (\text{Kpc})$	21.3991
χ^2_{red}	3.6682

28. The Galaxy NGC1090, Non-viable, Extended Marginally Viable

For this galaxy, the optimization method we used, ensures maximum compatibility of the analytic SIDM model of Eq. (3) with the SPARC data, if we choose $\rho_0 = 7.47031 \times 10^7 M_\odot/\text{Kpc}^3$ and $K_0 = 14724.3 M_\odot \text{ Kpc}^{-3} (\text{km/s})^2$, in which case the reduced χ^2_{red} value is $\chi^2_{\text{red}} = 11.4881$. Also the parameter α in this case is $\alpha = 8.10212 \text{ Kpc}$.

In Table LXIII we present the optimized values of K_0 and ρ_0 for the analytic SIDM model of Eq. (3) for which the maximum compatibility with the SPARC data is achieved. In Figs. 102, 103 we present

TABLE LXIII: SIDM Optimization Values for the galaxy NGC1090

Parameter	Optimization Values
$\rho_0 (M_\odot/\text{Kpc}^3)$	7.47031×10^7
$K_0 (M_\odot \text{ Kpc}^{-3} (\text{km/s})^2)$	14724.3

the density of the analytic SIDM model, the predicted rotation curves for the SIDM model (3), versus the SPARC observational data and the sound speed, as a function of the radius respectively. As it can be seen, for this galaxy, the SIDM model produces non-viable rotation curves which are incompatible with the SPARC data.

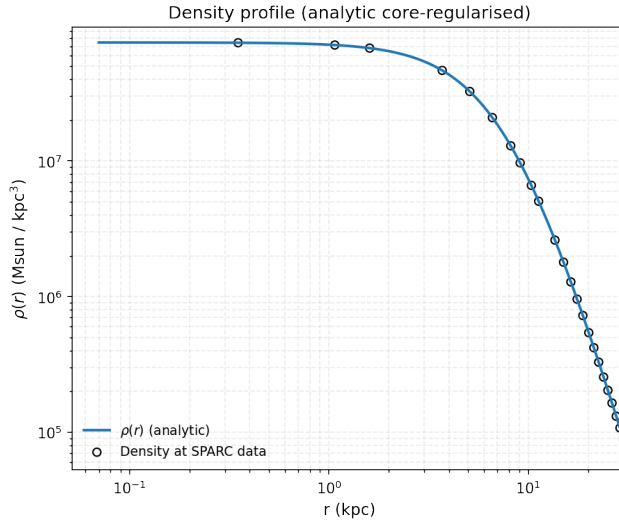


FIG. 102: The density of the SIDM model of Eq. (3) for the galaxy NGC1090, versus the radius.

Now we shall include contributions to the rotation velocity from the other components of the galaxy, namely the disk, the gas, and the bulge if present. In Fig. 104 we present the combined rotation curves including all the components of the galaxy along with the SIDM. As it can be seen, the extended collisional DM model is marginally viable. Also in Table LXIV we present the optimized values of the free parameters of the SIDM model for which we achieve the maximum compatibility with the SPARC data, for the galaxy NGC1090, and also the resulting reduced χ^2_{red} value.

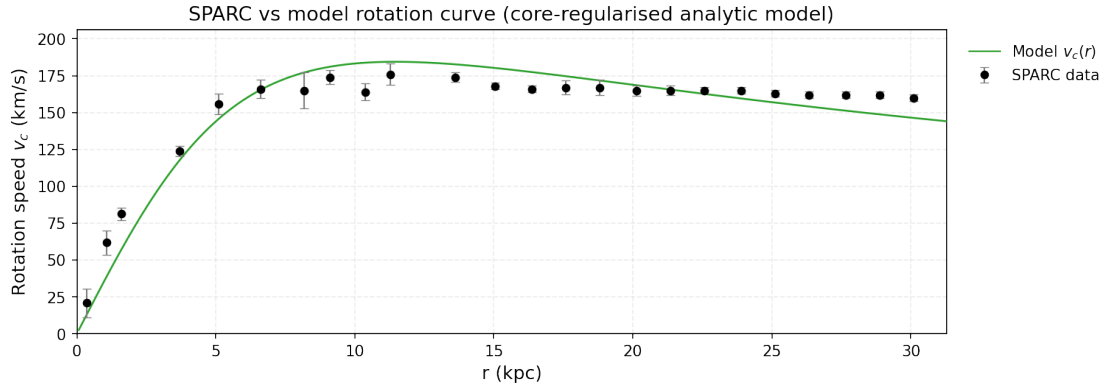


FIG. 103: The predicted rotation curves for the optimized SIDM model of Eq. (3), versus the SPARC observational data for the galaxy NGC1090.

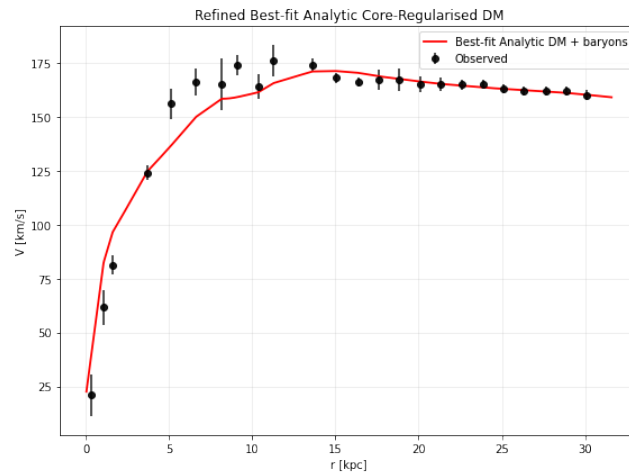


FIG. 104: The predicted rotation curves after using an optimization for the SIDM model (3), and the extended SPARC data for the galaxy NGC1090. We included the rotation curves of the gas, the disk velocities, the bulge (where present) along with the SIDM model.

TABLE LXIV: Optimized Parameter Values of the Extended SIDM model for the Galaxy NGC1090.

Parameter	Value
$\rho_0 (M_\odot/\text{Kpc}^3)$	4.58371×10^6
$K_0 (M_\odot \text{ Kpc}^{-3} (\text{km/s})^2)$	6534.69
ml_{disk}	0.8333
ml_{bulge}	0.5974
$\alpha (\text{Kpc})$	21.7871
χ^2_{red}	2.83686

29. The Galaxy NGC2403, Non-viable

For this galaxy, the optimization method we used, ensures maximum compatibility of the analytic SIDM model of Eq. (3) with the SPARC data, if we choose $\rho_0 = 9.93149 \times 10^7 M_\odot/\text{Kpc}^3$ and $K_0 = 8809.92 M_\odot \text{ Kpc}^{-3} (\text{km/s})^2$, in which case the reduced χ^2_{red} value is $\chi^2_{\text{red}} = 345.534$. Also the parameter α in this case is $\alpha = 5.43538 \text{ Kpc}$.

In Table LXV we present the optimized values of K_0 and ρ_0 for the analytic SIDM model of Eq. (3) for which the maximum compatibility with the SPARC data is achieved. In Figs. 105, 106 we present the density of the analytic SIDM model, the predicted rotation curves for the SIDM model (3), versus the SPARC observational data and the sound speed, as a function of the radius respectively. As it can be seen, for this galaxy, the SIDM model produces non-viable rotation curves which are incompatible with the SPARC data.

TABLE LXV: SIDM Optimization Values for the galaxy NGC2403

Parameter	Optimization Values
$\rho_0 (M_\odot/\text{Kpc}^3)$	9.93149×10^7
$K_0 (M_\odot \text{ Kpc}^{-3} (\text{km/s})^2)$	8809.92

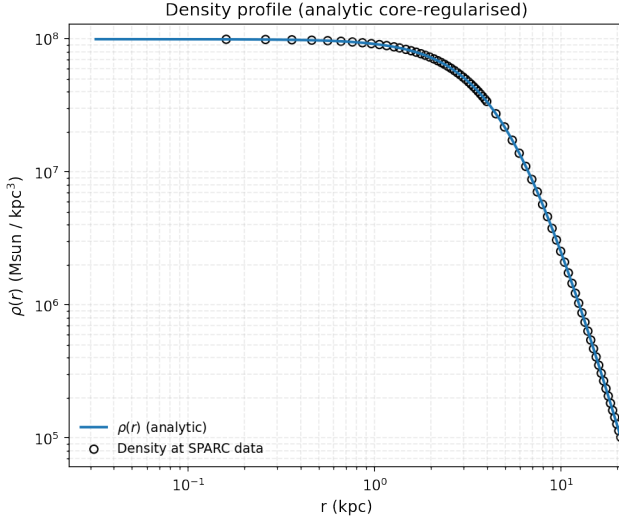


FIG. 105: The density of the SIDM model of Eq. (3) for the galaxy NGC2403, versus the radius.

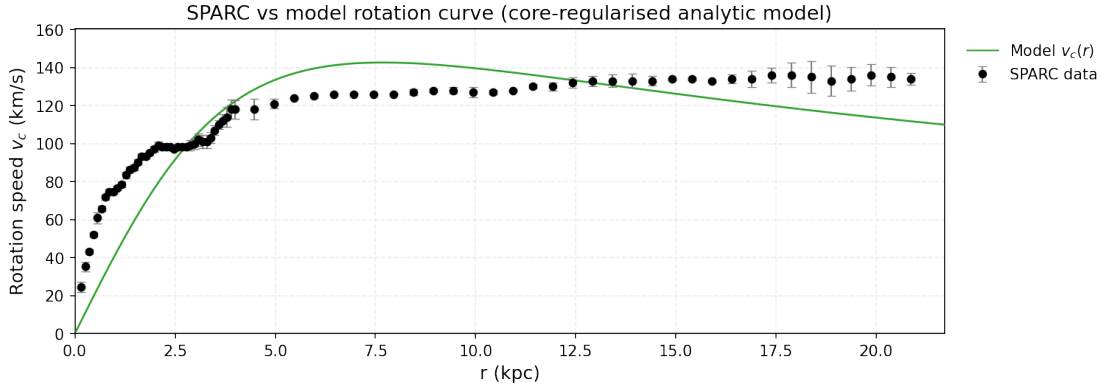


FIG. 106: The predicted rotation curves for the optimized SIDM model of Eq. (3), versus the SPARC observational data for the galaxy NGC2403.

Now we shall include contributions to the rotation velocity from the other components of the galaxy, namely the disk, the gas, and the bulge if present. In Fig. 107 we present the combined rotation curves including all the components of the galaxy along with the SIDM. As it can be seen, the extended collisional DM model is non-viable. Also in Table LXVI we present the optimized values of the free parameters of the SIDM model for which we achieve the maximum compatibility with the SPARC data, for the galaxy NGC2403, and also the resulting reduced χ^2_{red} value.

TABLE LXVI: Optimized Parameter Values of the Extended SIDM model for the Galaxy NGC2403.

Parameter	Value
$\rho_0 (M_\odot/\text{Kpc}^3)$	1.71982×10^7
$K_0 (M_\odot \text{ Kpc}^{-3} (\text{km/s})^2)$	5194.29
ml_{disk}	0.9229
ml_{bulge}	0.3255
$\alpha (\text{Kpc})$	10.0281
χ^2_{red}	15.7327

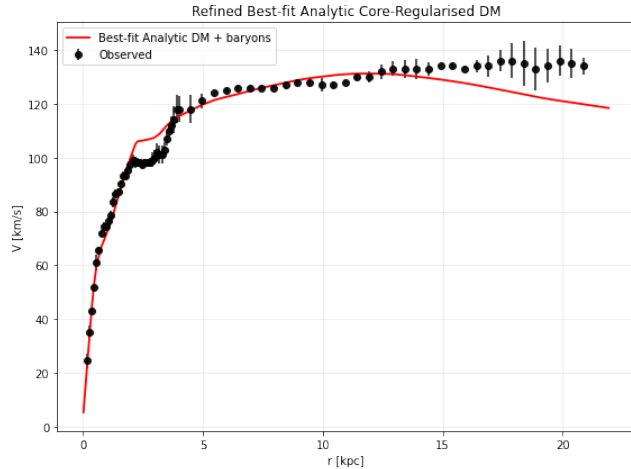


FIG. 107: The predicted rotation curves after using an optimization for the SIDM model (3), and the extended SPARC data for the galaxy NGC2403. We included the rotation curves of the gas, the disk velocities, the bulge (where present) along with the SIDM model.

30. The Galaxy NGC2683, Non-viable, Extended Viable

For this galaxy, the optimization method we used, ensures maximum compatibility of the analytic SIDM model of Eq. (3) with the SPARC data, if we choose $\rho_0 = 1.2279 \times 10^8 M_\odot/\text{Kpc}^3$ and $K_0 = 17675.6 M_\odot \text{Kpc}^{-3} (\text{km/s})^2$, in which case the reduced χ^2_{red} value is $\chi^2_{\text{red}} = 10.0865$. Also the parameter α in this case is $\alpha = 6.924 \text{Kpc}$.

In Table LXVII we present the optimized values of K_0 and ρ_0 for the analytic SIDM model of Eq. (3) for which the maximum compatibility with the SPARC data is achieved. In Figs. 108, 109 we present

TABLE LXVII: SIDM Optimization Values for the galaxy NGC2683

Parameter	Optimization Values
$\rho_0 (M_\odot/\text{Kpc}^3)$	1.2279×10^8
$K_0 (M_\odot \text{Kpc}^{-3} (\text{km/s})^2)$	17675.6

the density of the analytic SIDM model, the predicted rotation curves for the SIDM model (3), versus the SPARC observational data and the sound speed, as a function of the radius respectively. As it can be seen, for this galaxy, the SIDM model produces non-viable rotation curves which are incompatible with the SPARC data.

Now we shall include contributions to the rotation velocity from the other components of the galaxy, namely the disk, the gas, and the bulge if present. In Fig. 110 we present the combined rotation curves including all the components of the galaxy along with the SIDM. As it can be seen, the extended collisional DM model is non-viable. Also in Table LXVIII we present the optimized values of the free parameters of the SIDM model for which we achieve the maximum compatibility with the SPARC data, for the galaxy NGC2683, and also the resulting reduced χ^2_{red} value.

TABLE LXVIII: Optimized Parameter Values of the Extended SIDM model for the Galaxy NGC2683.

Parameter	Value
$\rho_0 (M_\odot/\text{Kpc}^3)$	1.5699×10^7
$K_0 (M_\odot \text{Kpc}^{-3} (\text{km/s})^2)$	7502.51
ml_{disk}	0.8237
ml_{bulge}	0.8055
$\alpha (\text{Kpc})$	12.6143
χ^2_{red}	1.11827

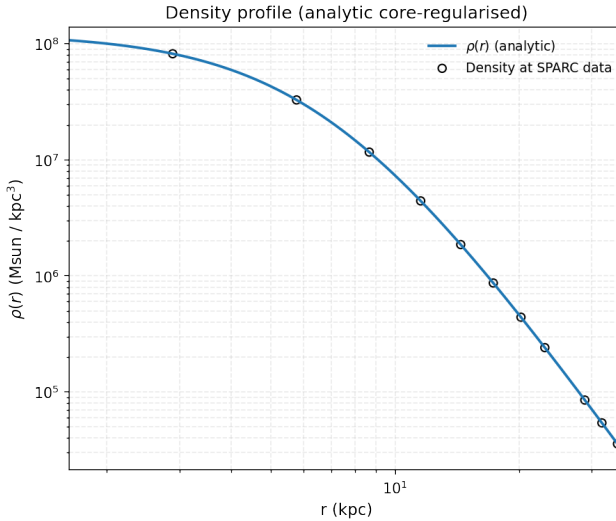


FIG. 108: The density of the SIDM model of Eq. (3) for the galaxy NGC2683, versus the radius.

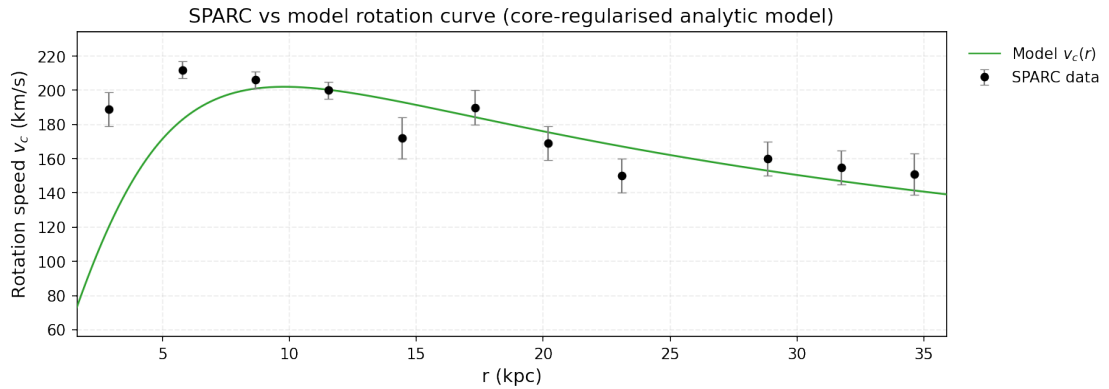


FIG. 109: The predicted rotation curves for the optimized SIDM model of Eq. (3), versus the SPARC observational data for the galaxy NGC2683.

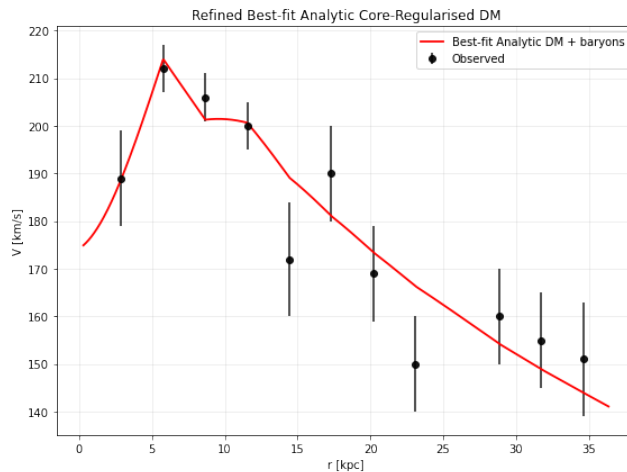


FIG. 110: The predicted rotation curves after using an optimization for the SIDM model (3), and the extended SPARC data for the galaxy NGC2683. We included the rotation curves of the gas, the disk velocities, the bulge (where present) along with the SIDM model.

31. The Galaxy NGC2841, Non-viable

For this galaxy, the optimization method we used, ensures maximum compatibility of the analytic SIDM model of Eq. (3) with the SPARC data, if we choose $\rho_0 = 1.15657 \times 10^8 M_\odot/\text{Kpc}^3$ and $K_0 = 56258.9 M_\odot \text{Kpc}^{-3} (\text{km/s})^2$, in which case the reduced χ^2_{red} value is $\chi^2_{red} = 72.7703$. Also the parameter α in this case is $\alpha = 12.728 \text{Kpc}$.

In Table LXIX we present the optimized values of K_0 and ρ_0 for the analytic SIDM model of Eq. (3) for which the maximum compatibility with the SPARC data is achieved. In Figs. 111, 112 we present

TABLE LXIX: SIDM Optimization Values for the galaxy NGC2841

Parameter	Optimization Values
$\rho_0 (M_\odot/\text{Kpc}^3)$	1.15657×10^8
$K_0 (M_\odot \text{Kpc}^{-3} (\text{km/s})^2)$	56258.9

the density of the analytic SIDM model, the predicted rotation curves for the SIDM model (3), versus the SPARC observational data and the sound speed, as a function of the radius respectively. As it can be seen, for this galaxy, the SIDM model produces non-viable rotation curves which are incompatible with the SPARC data.

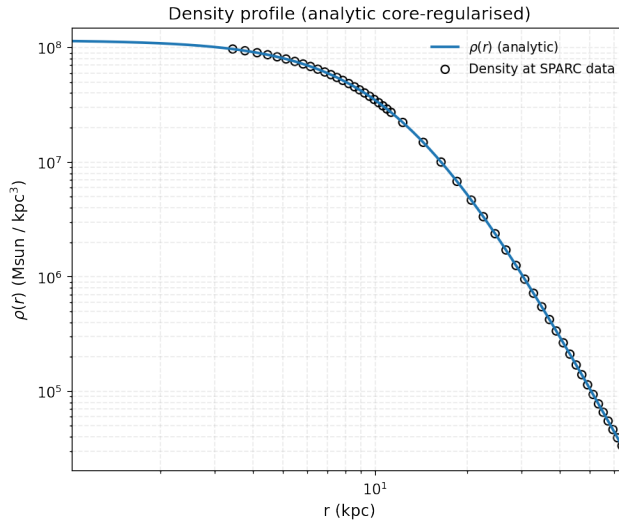


FIG. 111: The density of the SIDM model of Eq. (3) for the galaxy NGC2841, versus the radius.

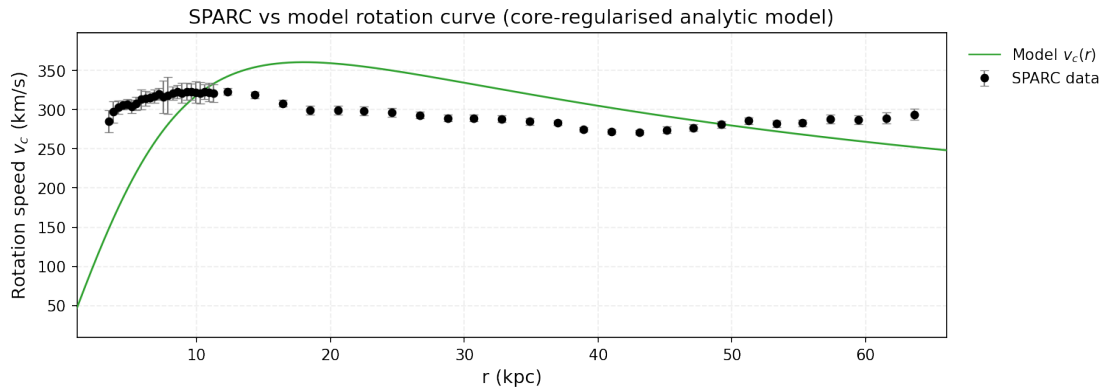


FIG. 112: The predicted rotation curves for the optimized SIDM model of Eq. (3), versus the SPARC observational data for the galaxy NGC2841.

Now we shall include contributions to the rotation velocity from the other components of the galaxy, namely the disk, the gas, and the bulge if present. In Fig. 113 we present the combined rotation

curves including all the components of the galaxy along with the SIDM. As it can be seen, the extended collisional DM model is non-viable. Also in Table LXX we present the optimized values of the free

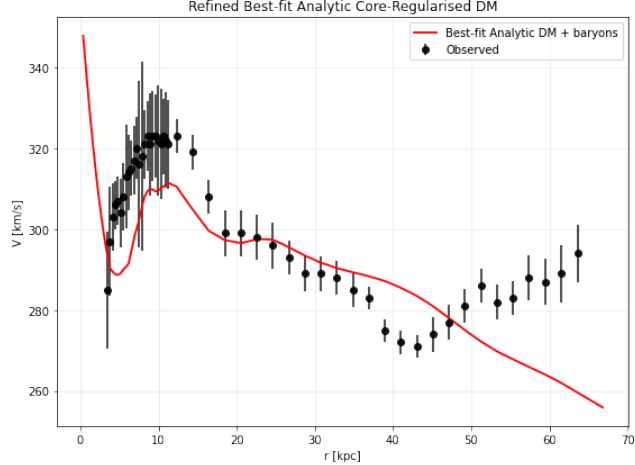


FIG. 113: The predicted rotation curves after using an optimization for the SIDM model (3), and the extended SPARC data for the galaxy NGC2841. We included the rotation curves of the gas, the disk velocities, the bulge (where present) along with the SIDM model.

parameters of the SIDM model for which we achieve the maximum compatibility with the SPARC data, for the galaxy NGC2841, and also the resulting reduced χ^2_{red} value.

TABLE LXX: Optimized Parameter Values of the Extended SIDM model for the Galaxy NGC2841.

Parameter	Value
ρ_0 (M_\odot/Kpc^3)	1.0076×10^7
K_0 ($M_\odot \text{ Kpc}^{-3} (\text{km/s})^2$)	24413.8
ml_{disk}	1
ml_{bulge}	0.9
α (Kpc)	28.4033
χ^2_{red}	5.87791

32. The Galaxy NGC2903, Non-viable, Extended Marginally

For this galaxy, the optimization method we used, ensures maximum compatibility of the analytic SIDM model of Eq. (3) with the SPARC data, if we choose $\rho_0 = 3.06984 \times 10^8 M_\odot/\text{Kpc}^3$ and $K_0 = 22970.1 M_\odot \text{ Kpc}^{-3} (\text{km/s})^2$, in which case the reduced χ^2_{red} value is $\chi^2_{red} = 111.987$. Also the parameter α in this case is $\alpha = 4.992 \text{ Kpc}$.

In Table LXXI we present the optimized values of K_0 and ρ_0 for the analytic SIDM model of Eq. (3) for which the maximum compatibility with the SPARC data is achieved. In Figs. 114, 115 we present

TABLE LXXI: SIDM Optimization Values for the galaxy NGC2903

Parameter	Optimization Values
ρ_0 (M_\odot/Kpc^3)	5×10^7
K_0 ($M_\odot \text{ Kpc}^{-3} (\text{km/s})^2$)	1250

the density of the analytic SIDM model, the predicted rotation curves for the SIDM model (3), versus the SPARC observational data and the sound speed, as a function of the radius respectively. As it can be seen, for this galaxy, the SIDM model produces non-viable rotation curves which are incompatible with the SPARC data.

Now we shall include contributions to the rotation velocity from the other components of the galaxy, namely the disk, the gas, and the bulge if present. In Fig. 116 we present the combined rotation curves including all the components of the galaxy along with the SIDM. As it can be seen, the extended

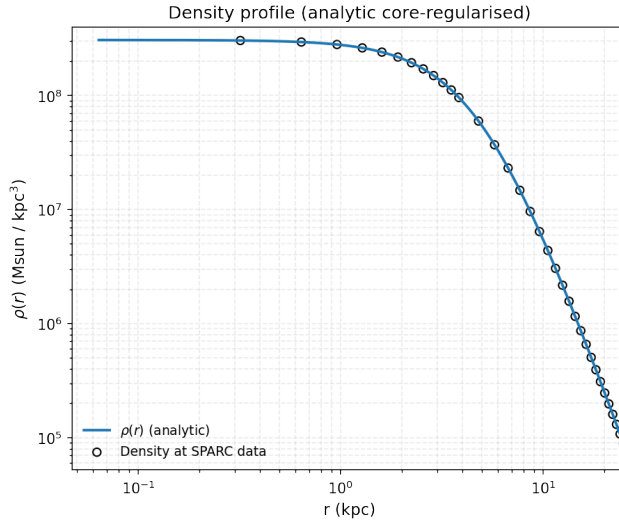


FIG. 114: The density of the SIDM model of Eq. (3) for the galaxy NGC2903, versus the radius.

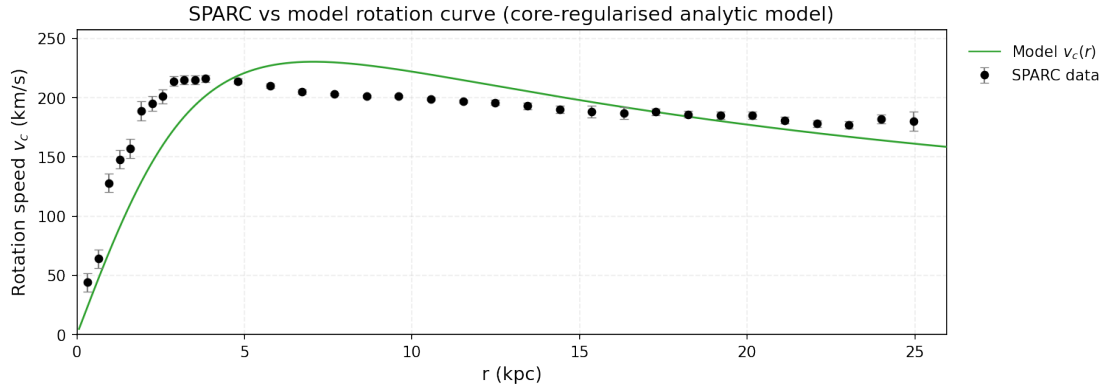


FIG. 115: The predicted rotation curves for the optimized SIDM model of Eq. (3), versus the SPARC observational data for the galaxy NGC2903.

collisional DM model is non-viable. Also in Table LXXII we present the optimized values of the free

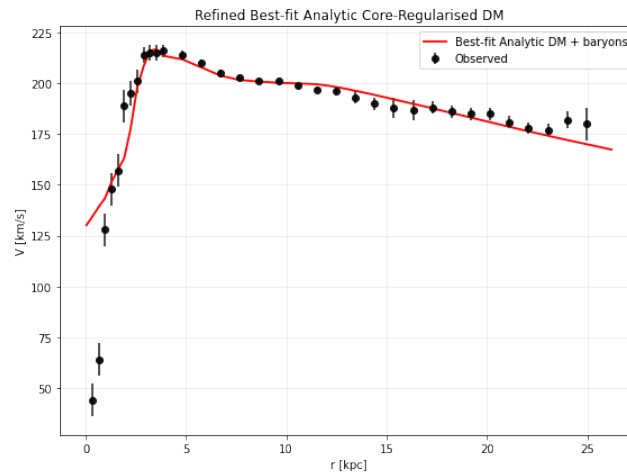


FIG. 116: The predicted rotation curves after using an optimization for the SIDM model (3), and the extended SPARC data for the galaxy NGC2903. We included the rotation curves of the gas, the disk velocities, the bulge (where present) along with the SIDM model.

parameters of the SIDM model for which we achieve the maximum compatibility with the SPARC data, for the galaxy NGC2903, and also the resulting reduced χ^2_{red} value.

TABLE LXXII: Optimized Parameter Values of the Extended SIDM model for the Galaxy NGC2903.

Parameter	Value
$\rho_0 (M_\odot/\text{Kpc}^3)$	3.04394×10^7
$K_0 (M_\odot \text{ Kpc}^{-3} (\text{km/s})^2)$	10665.8
ml_{disk}	0.6777
ml_{bulge}	0.3
$\alpha (\text{Kpc})$	10.8012
χ^2_{red}	9.03616

33. The Galaxy NGC2915

For this galaxy, the optimization method we used, ensures maximum compatibility of the analytic SIDM model of Eq. (3) with the SPARC data, if we choose $\rho_0 = 7.76155 \times 10^7 M_\odot/\text{Kpc}^3$ and $K_0 = 3353.32 M_\odot \text{ Kpc}^{-3} (\text{km/s})^2$, in which case the reduced χ^2_{red} value is $\chi^2_{red} = 0.624307$. Also the parameter α in this case is $\alpha = 3.79327 \text{ Kpc}$.

In Table LXXIII we present the optimized values of K_0 and ρ_0 for the analytic SIDM model of Eq. (3) for which the maximum compatibility with the SPARC data is achieved. In Figs. 117, 118 we present

TABLE LXXIII: SIDM Optimization Values for the galaxy NGC2915

Parameter	Optimization Values
$\rho_0 (M_\odot/\text{Kpc}^3)$	7.76155×10^7
$K_0 (M_\odot \text{ Kpc}^{-3} (\text{km/s})^2)$	3353.32

the density of the analytic SIDM model, the predicted rotation curves for the SIDM model (3), versus the SPARC observational data and the sound speed, as a function of the radius respectively. As it can be seen, for this galaxy, the SIDM model produces viable rotation curves which are compatible with the SPARC data.

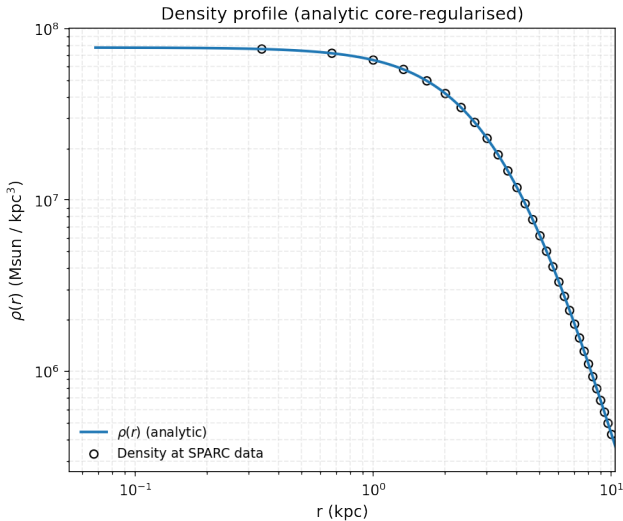


FIG. 117: The density of the SIDM model of Eq. (3) for the galaxy NGC2915, versus the radius.

34. The Galaxy NGC2955, Non-viable

For this galaxy, the optimization method we used, ensures maximum compatibility of the analytic SIDM model of Eq. (3) with the SPARC data, if we choose $\rho_0 = 2.51138 \times 10^8 M_\odot/\text{Kpc}^3$ and $K_0 =$

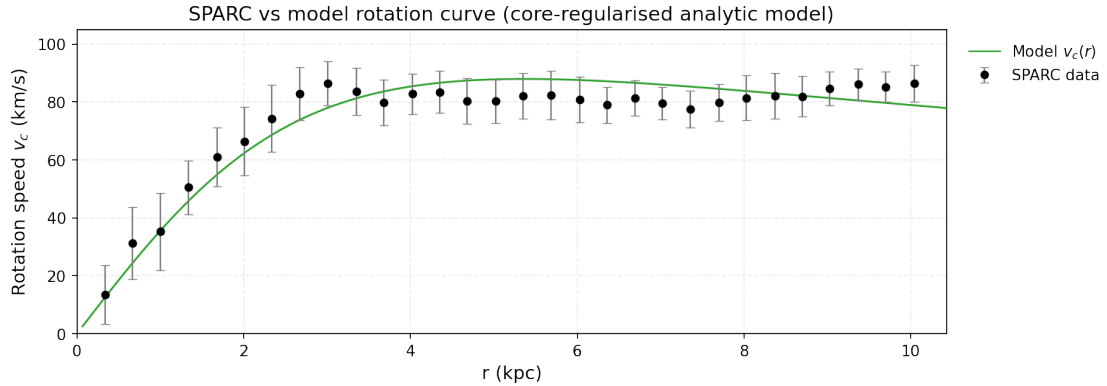


FIG. 118: The predicted rotation curves for the optimized SIDM model of Eq. (3), versus the SPARC observational data for the galaxy NGC2915.

$37862.9 M_{\odot} \text{Kpc}^{-3} (\text{km/s})^2$, in which case the reduced χ^2_{red} value is $\chi^2_{red} = 92.9359$. Also the parameter α in this case is $\alpha = 7.086 \text{Kpc}$.

In Table LXXIV we present the optimized values of K_0 and ρ_0 for the analytic SIDM model of Eq. (3) for which the maximum compatibility with the SPARC data is achieved. In Figs. 119, 120 we present

TABLE LXXIV: SIDM Optimization Values for the galaxy NGC2955

Parameter	Optimization Values
$\rho_0 (M_{\odot}/\text{Kpc}^3)$	2.51138×10^8
$K_0 (M_{\odot} \text{Kpc}^{-3} (\text{km/s})^2)$	37862.9

the density of the analytic SIDM model, the predicted rotation curves for the SIDM model (3), versus the SPARC observational data and the sound speed, as a function of the radius respectively. As it can be seen, for this galaxy, the SIDM model produces non-viable rotation curves which are incompatible with the SPARC data.

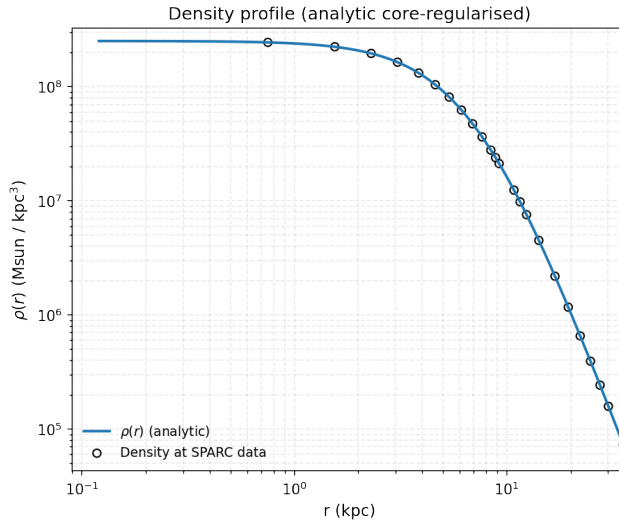


FIG. 119: The density of the SIDM model of Eq. (3) for the galaxy NGC2955, versus the radius.

Now we shall include contributions to the rotation velocity from the other components of the galaxy, namely the disk, the gas, and the bulge if present. In Fig. 121 we present the combined rotation curves including all the components of the galaxy along with the SIDM. As it can be seen, the extended collisional DM model is non-viable. Also in Table LXXV we present the optimized values of the free parameters of the SIDM model for which we achieve the maximum compatibility with the SPARC data, for the galaxy NGC2955, and also the resulting reduced χ^2_{red} value.

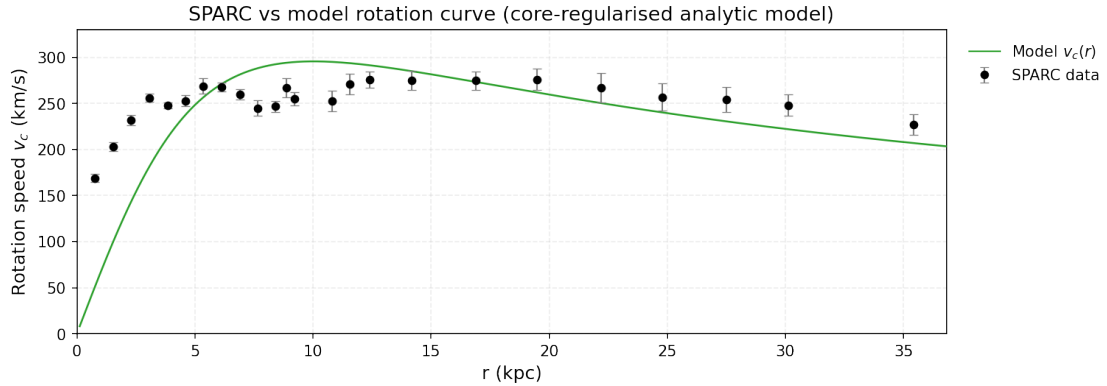


FIG. 120: The predicted rotation curves for the optimized SIDM model of Eq. (3), versus the SPARC observational data for the galaxy NGC2955.

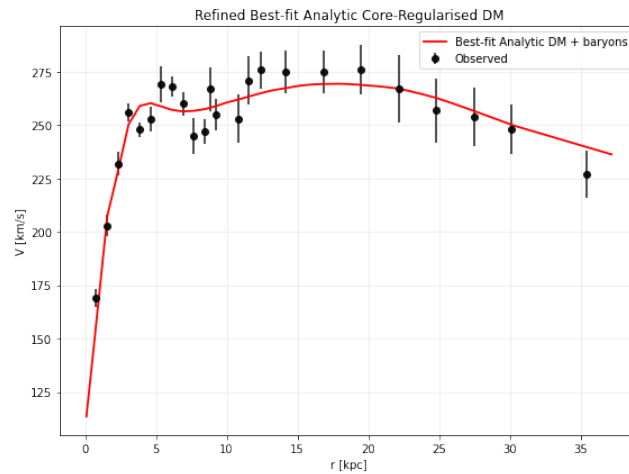


FIG. 121: The predicted rotation curves after using an optimization for the SIDM model (3), and the extended SPARC data for the galaxy NGC2955. We included the rotation curves of the gas, the disk velocities, the bulge (where present) along with the SIDM model.

TABLE LXXV: Optimized Parameter Values of the Extended SIDM model for the Galaxy NGC2955.

Parameter	Value
$\rho_0 (M_\odot/\text{Kpc}^3)$	4.13996×10^7
$K_0 (M_\odot \text{ Kpc}^{-3} (\text{km/s})^2)$	23227.9
ml_{disk}	0.8
ml_{bulge}	0.9478
$\alpha (\text{Kpc})$	13.6679
χ^2_{red}	2.14925

35. The Galaxy NGC2976 Marginally, Extended Viable

For this galaxy, the optimization method we used, ensures maximum compatibility of the analytic SIDM model of Eq. (3) with the SPARC data, if we choose $\rho_0 = 1.87478 \times 10^8 M_\odot/\text{Kpc}^3$ and $K_0 = 4469.65 M_\odot \text{ Kpc}^{-3} (\text{km/s})^2$, in which case the reduced χ^2_{red} value is $\chi^2_{\text{red}} = 0.59403$. Also the parameter α in this case is $\alpha = 2.81781 \text{ Kpc}$.

In Table LXXVI we present the optimized values of K_0 and ρ_0 for the analytic SIDM model of Eq. (3) for which the maximum compatibility with the SPARC data is achieved. In Figs. 122, 123 we present the density of the analytic SIDM model, the predicted rotation curves for the SIDM model (3), versus the SPARC observational data and the sound speed, as a function of the radius respectively. As it can be seen, for this galaxy, the SIDM model produces viable rotation curves which are marginally compatible with the SPARC data (off by two data points).

TABLE LXXVI: SIDM Optimization Values for the galaxy NGC2976

Parameter	Optimization Values
$\rho_0 (M_\odot/\text{Kpc}^3)$	1.87478×10^8
$K_0 (M_\odot \text{ Kpc}^{-3} (\text{km/s})^2)$	4469.65

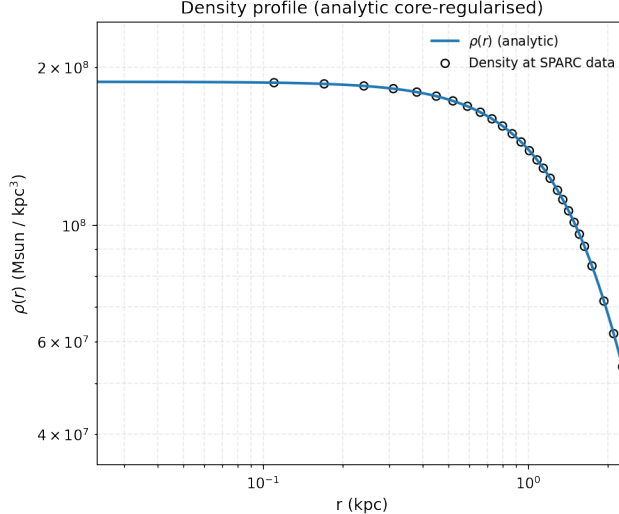


FIG. 122: The density of the SIDM model of Eq. (3) for the galaxy NGC2976, versus the radius.

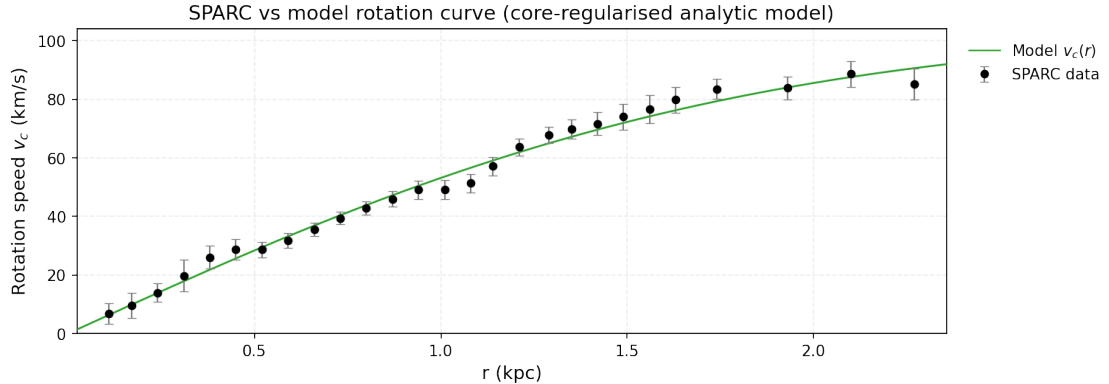


FIG. 123: The predicted rotation curves for the optimized SIDM model of Eq. (3), versus the SPARC observational data for the galaxy NGC2976.

Now we shall include contributions to the rotation velocity from the other components of the galaxy, namely the disk, the gas, and the bulge if present. In Fig. 124 we present the combined rotation curves including all the components of the galaxy along with the SIDM. As it can be seen, the extended collisional DM model is viable. Also in Table LXXVII we present the optimized values of the free parameters of the SIDM model for which we achieve the maximum compatibility with the SPARC data, for the galaxy NGC2976, and also the resulting reduced χ^2_{red} value.

TABLE LXXVII: Optimized Parameter Values of the Extended SIDM model for the Galaxy NGC2976.

Parameter	Value
$\rho_0 (M_\odot/\text{Kpc}^3)$	9.75843×10^7
$K_0 (M_\odot \text{ Kpc}^{-3} (\text{km/s})^2)$	2899.61
ml_{disk}	0.6165
ml_{bulge}	0.0917
$\alpha (\text{Kpc})$	3.1454
χ^2_{red}	0.304637

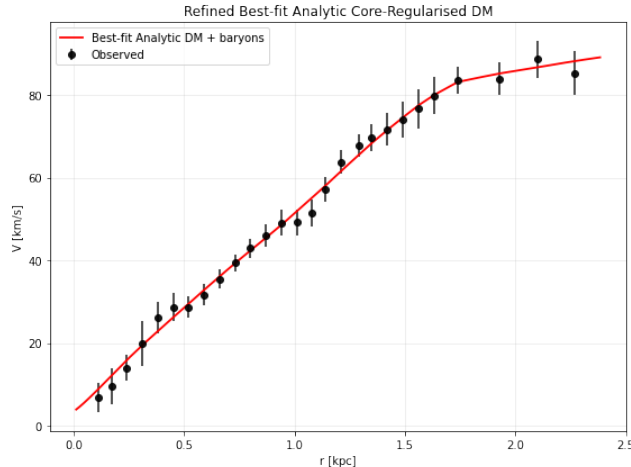


FIG. 124: The predicted rotation curves after using an optimization for the SIDM model (3), and the extended SPARC data for the galaxy NGC2976. We included the rotation curves of the gas, the disk velocities, the bulge (where present) along with the SIDM model.

36. The Galaxy NGC2998, Non-viable

For this galaxy, the optimization method we used, ensures maximum compatibility of the analytic SIDM model of Eq. (3) with the SPARC data, if we choose $\rho_0 = 1.34663 \times 10^8 M_\odot/\text{Kpc}^3$ and $K_0 = 28911.8 M_\odot \text{Kpc}^{-3} (\text{km/s})^2$, in which case the reduced χ^2_{red} value is $\chi^2_{red} = 39.3903$. Also the parameter α in this case is $\alpha = 8.456 \text{Kpc}$.

In Table LXXVIII we present the optimized values of K_0 and ρ_0 for the analytic SIDM model of Eq. (3) for which the maximum compatibility with the SPARC data is achieved. In Figs. 125, 126 we present

TABLE LXXVIII: SIDM Optimization Values for the galaxy NGC2998

Parameter	Optimization Values
$\rho_0 (M_\odot/\text{Kpc}^3)$	1.34663×10^8
$K_0 (M_\odot \text{Kpc}^{-3} (\text{km/s})^2)$	28911.8

the density of the analytic SIDM model, the predicted rotation curves for the SIDM model (3), versus the SPARC observational data and the sound speed, as a function of the radius respectively. As it can be seen, for this galaxy, the SIDM model produces non-viable rotation curves which are incompatible with the SPARC data.

Now we shall include contributions to the rotation velocity from the other components of the galaxy, namely the disk, the gas, and the bulge if present. In Fig. 127 we present the combined rotation curves including all the components of the galaxy along with the SIDM. As it can be seen, the extended collisional DM model is non-viable. Also in Table LXXIX we present the optimized values of the free parameters of the SIDM model for which we achieve the maximum compatibility with the SPARC data, for the galaxy NGC2998, and also the resulting reduced χ^2_{red} value.

TABLE LXXIX: Optimized Parameter Values of the Extended SIDM model for the Galaxy NGC2998.

Parameter	Value
$\rho_0 (M_\odot/\text{Kpc}^3)$	2.81529×10^6
$K_0 (M_\odot \text{Kpc}^{-3} (\text{km/s})^2)$	10365.5
ml_{disk}	0.9393
ml_{bulge}	0.7347
$\alpha (\text{Kpc})$	35.0131
χ^2_{red}	2.7979

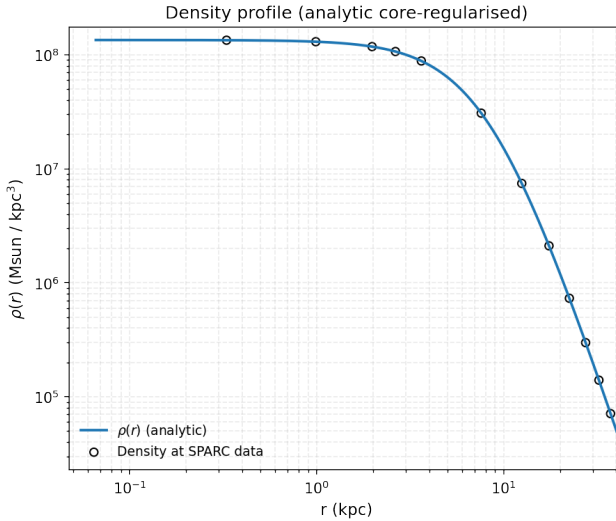


FIG. 125: The density of the SIDM model of Eq. (3) for the galaxy NGC2998, versus the radius.

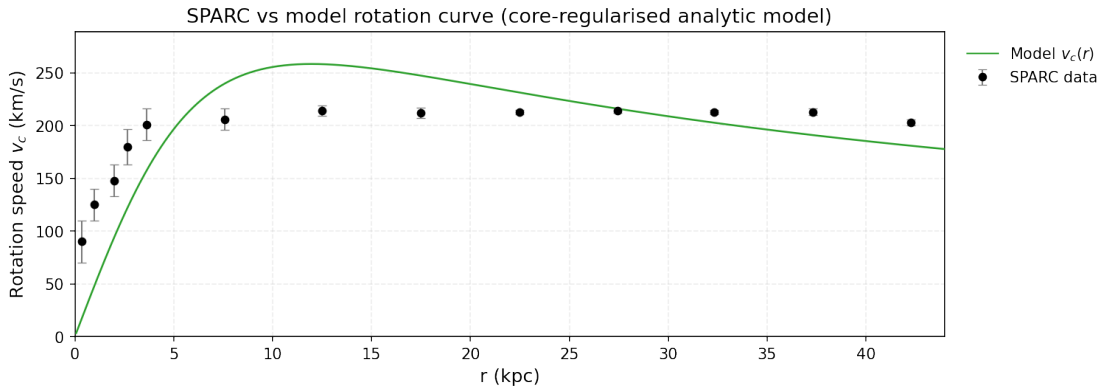


FIG. 126: The predicted rotation curves for the optimized SIDM model of Eq. (3), versus the SPARC observational data for the galaxy NGC2998.

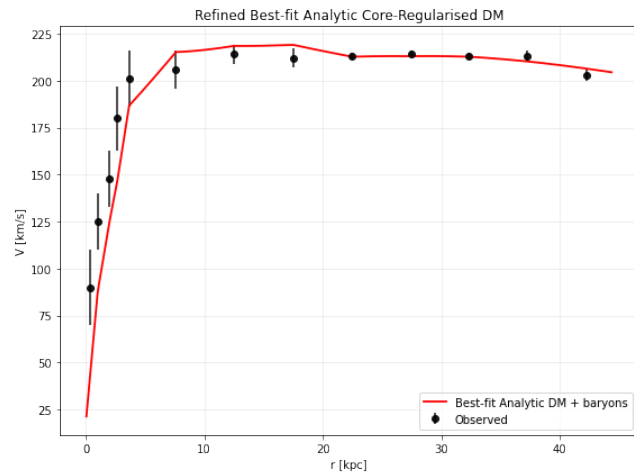


FIG. 127: The predicted rotation curves after using an optimization for the SIDM model (3), and the extended SPARC data for the galaxy NGC2998. We included the rotation curves of the gas, the disk velocities, the bulge (where present) along with the SIDM model.

37. The Galaxy NGC3109

For this galaxy, the optimization method we used, ensures maximum compatibility of the analytic SIDM model of Eq. (3) with the SPARC data, if we choose $\rho_0 = 2.31771 \times 10^7 M_\odot/\text{Kpc}^3$ and $K_0 = 1836.37 M_\odot \text{Kpc}^{-3} (\text{km/s})^2$, in which case the reduced χ^2_{red} value is $\chi^2_{red} = 0.360257$. Also the parameter α in this case is $\alpha = 5.13691 \text{Kpc}$.

In Table LXXX we present the optimized values of K_0 and ρ_0 for the analytic SIDM model of Eq. (3) for which the maximum compatibility with the SPARC data is achieved. In Figs. 128, 129 we present

TABLE LXXX: SIDM Optimization Values for the galaxy NGC3109

Parameter	Optimization Values
$\rho_0 (M_\odot/\text{Kpc}^3)$	2.31771×10^7
$K_0 (M_\odot \text{Kpc}^{-3} (\text{km/s})^2)$	1836.37

the density of the analytic SIDM model, the predicted rotation curves for the SIDM model (3), versus the SPARC observational data and the sound speed, as a function of the radius respectively. As it can be seen, for this galaxy, the SIDM model produces viable rotation curves which are compatible with the SPARC data.

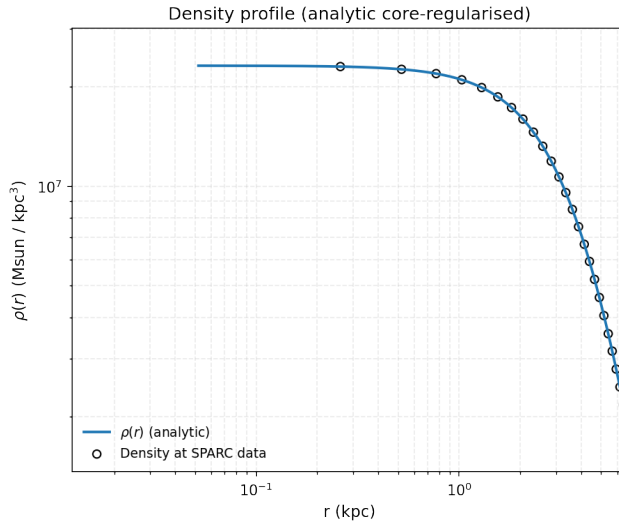


FIG. 128: The density of the SIDM model of Eq. (3) for the galaxy NGC3109, versus the radius.

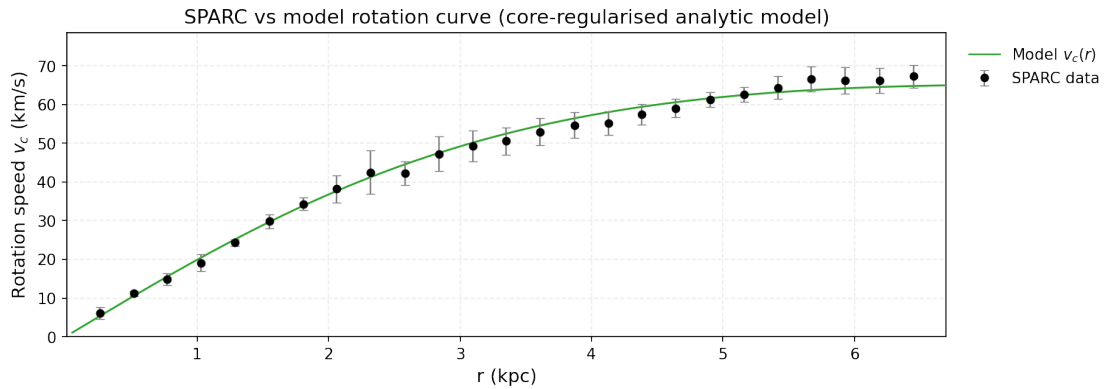


FIG. 129: The predicted rotation curves for the optimized SIDM model of Eq. (3), versus the SPARC observational data for the galaxy NGC3109.

38. The Galaxy NGC3198, Non-viable

For this galaxy, the optimization method we used, ensures maximum compatibility of the analytic SIDM model of Eq. (3) with the SPARC data, if we choose $\rho_0 = 5.29788 \times 10^7 M_\odot/\text{Kpc}^3$ and $K_0 = 12494.5 M_\odot \text{Kpc}^{-3} (\text{km/s})^2$, in which case the reduced χ^2_{red} value is $\chi^2_{red} = 25.8211$. Also the parameter α in this case is $\alpha = 8.86258 \text{Kpc}$.

In Table LXXXI we present the optimized values of K_0 and ρ_0 for the analytic SIDM model of Eq. (3) for which the maximum compatibility with the SPARC data is achieved. In Figs. 130, 131 we present

TABLE LXXXI: SIDM Optimization Values for the galaxy NGC3198

Parameter	Optimization Values
$\rho_0 (M_\odot/\text{Kpc}^3)$	5.29788×10^7
$K_0 (M_\odot \text{Kpc}^{-3} (\text{km/s})^2)$	12494.5

the density of the analytic SIDM model, the predicted rotation curves for the SIDM model (3), versus the SPARC observational data and the sound speed, as a function of the radius respectively. As it can be seen, for this galaxy, the SIDM model produces non-viable rotation curves which are incompatible with the SPARC data.

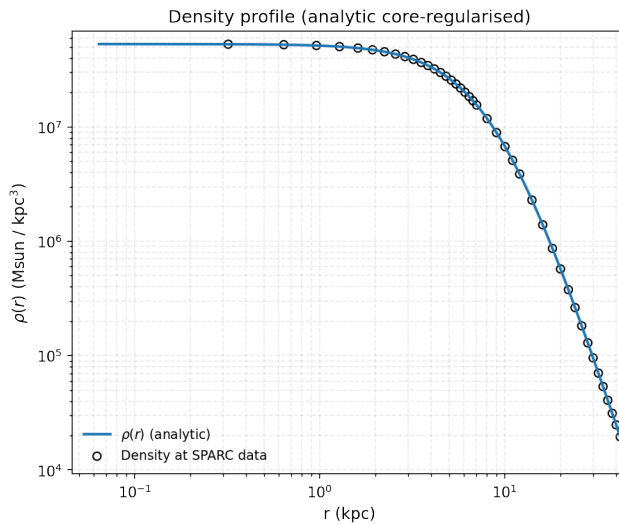


FIG. 130: The density of the SIDM model of Eq. (3) for the galaxy NGC3198, versus the radius.

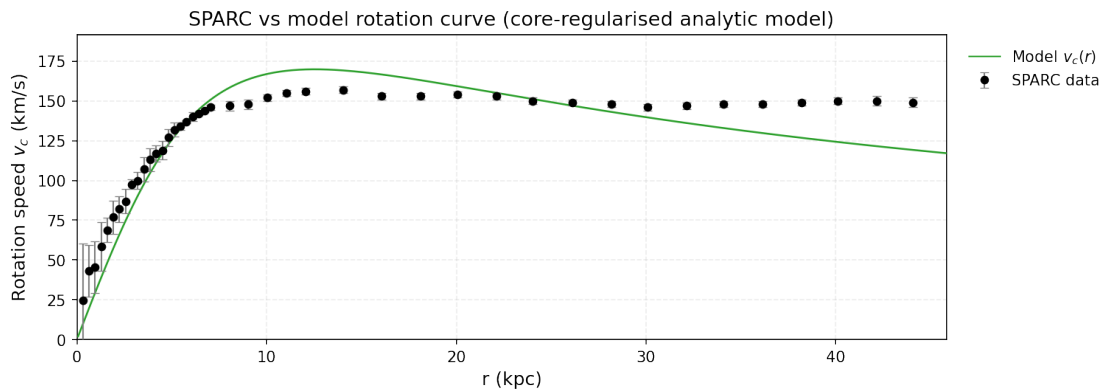


FIG. 131: The predicted rotation curves for the optimized SIDM model of Eq. (3), versus the SPARC observational data for the galaxy NGC3198.

Now we shall include contributions to the rotation velocity from the other components of the galaxy, namely the disk, the gas, and the bulge if present. In Fig. 132 we present the combined rotation

curves including all the components of the galaxy along with the SIDM. As it can be seen, the extended collisional DM model is non-viable. Also in Table LXXXII we present the optimized values of the free

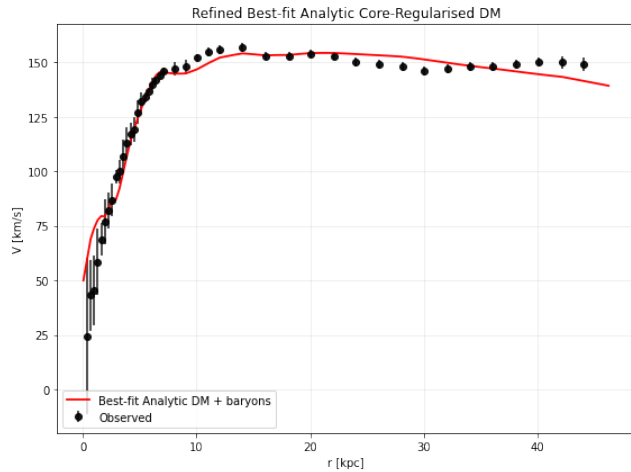


FIG. 132: The predicted rotation curves after using an optimization for the SIDM model (3), and the extended SPARC data for the galaxy NGC3198. We included the rotation curves of the gas, the disk velocities, the bulge (where present) along with the SIDM model.

parameters of the SIDM model for which we achieve the maximum compatibility with the SPARC data, for the galaxy NGC3198, and also the resulting reduced χ^2_{red} value.

TABLE LXXXII: Optimized Parameter Values of the Extended SIDM model for the Galaxy NGC3198.

Parameter	Value
$\rho_0 (M_\odot/\text{Kpc}^3)$	5.18167×10^6
$K_0 (M_\odot \text{ Kpc}^{-3} (\text{km/s})^2)$	6879.64
ml_{disk}	0.9264
ml_{bulge}	0.1394
$\alpha (\text{Kpc})$	21.0254
χ^2_{red}	2.55634

39. The Galaxy NGC3521, Non-viable, Extended Viable

For this galaxy, the optimization method we used, ensures maximum compatibility of the analytic SIDM model of Eq. (3) with the SPARC data, if we choose $\rho_0 = 6.40035 \times 10^8 M_\odot/\text{Kpc}^3$ and $K_0 = 24191.9 M_\odot \text{ Kpc}^{-3} (\text{km/s})^2$, in which case the reduced χ^2_{red} value is $\chi^2_{red} = 17.4628$. Also the parameter α in this case is $\alpha = 3.548 \text{ Kpc}$.

In Table LXXXIII we present the optimized values of K_0 and ρ_0 for the analytic SIDM model of Eq. (3) for which the maximum compatibility with the SPARC data is achieved. In Figs. 133, 134 we present

TABLE LXXXIII: SIDM Optimization Values for the galaxy NGC3521

Parameter	Optimization Values
$\rho_0 (M_\odot/\text{Kpc}^3)$	6.40035×10^8
$K_0 (M_\odot \text{ Kpc}^{-3} (\text{km/s})^2)$	24191.9

the density of the analytic SIDM model, the predicted rotation curves for the SIDM model (3), versus the SPARC observational data and the sound speed, as a function of the radius respectively. As it can be seen, for this galaxy, the SIDM model produces non-viable rotation curves which are incompatible with the SPARC data.

Now we shall include contributions to the rotation velocity from the other components of the galaxy, namely the disk, the gas, and the bulge if present. In Fig. 135 we present the combined rotation curves including all the components of the galaxy along with the SIDM. As it can be seen, the extended

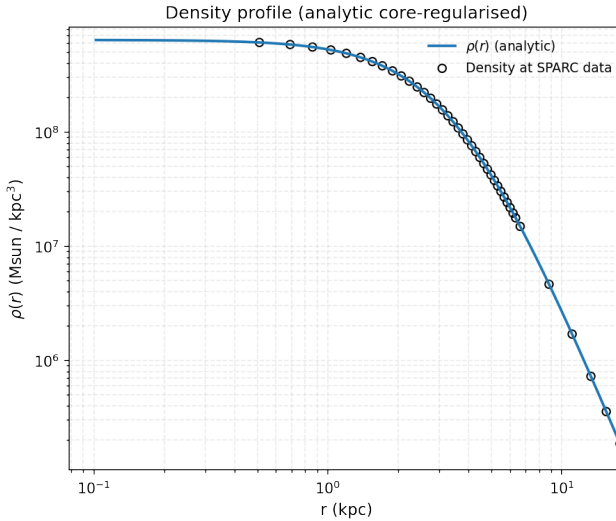


FIG. 133: The density of the SIDM model of Eq. (3) for the galaxy NGC3521, versus the radius.

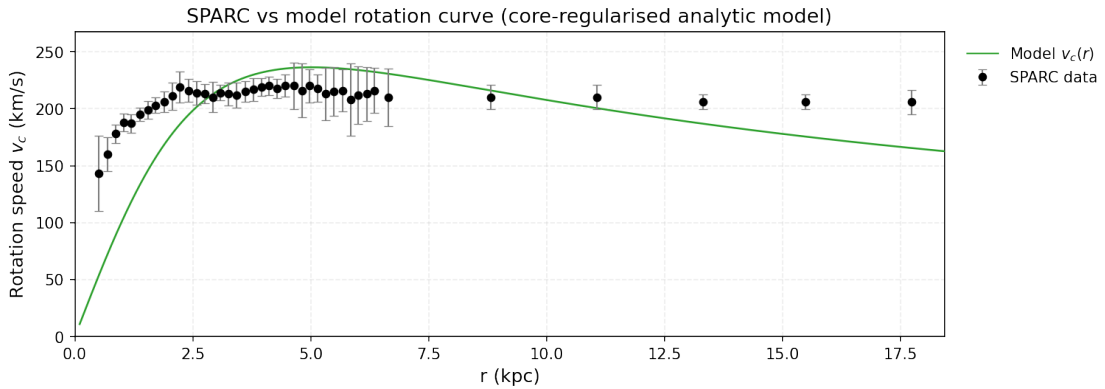


FIG. 134: The predicted rotation curves for the optimized SIDM model of Eq. (3), versus the SPARC observational data for the galaxy NGC3521.

collisional DM model is viable. Also in Table LXXXIV we present the optimized values of the free

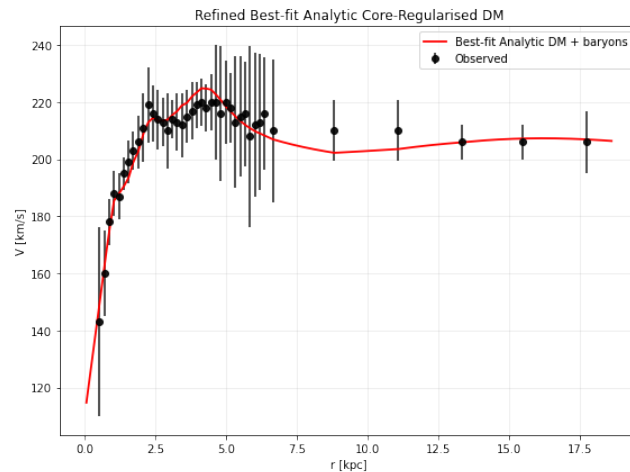


FIG. 135: The predicted rotation curves after using an optimization for the SIDM model (3), and the extended SPARC data for the galaxy NGC3521. We included the rotation curves of the gas, the disk velocities, the bulge (where present) along with the SIDM model.

parameters of the SIDM model for which we achieve the maximum compatibility with the SPARC data, for the galaxy NGC3521, and also the resulting reduced χ^2_{red} value.

TABLE LXXXIV: Optimized Parameter Values of the Extended SIDM model for the Galaxy NGC3521.

Parameter	Value
$\rho_0 (M_\odot/\text{Kpc}^3)$	1.3977×10^7
$K_0 (M_\odot \text{ Kpc}^{-3} (\text{km/s})^2)$	13466.1
m_{disk}	0.7622
m_{bulge}	0.3710
$\alpha (\text{Kpc})$	17.9106
χ^2_{red}	0.166192

40. The Galaxy NGC3726, Non-viable

For this galaxy, the optimization method we used, ensures maximum compatibility of the analytic SIDM model of Eq. (3) with the SPARC data, if we choose $\rho_0 = 4.00421 \times 10^7 M_\odot/\text{Kpc}^3$ and $K_0 = 13094.3 M_\odot \text{ Kpc}^{-3} (\text{km/s})^2$, in which case the reduced χ^2_{red} value is $\chi^2_{red} = 6.94506$. Also the parameter α in this case is $\alpha = 10.436 \text{ Kpc}$.

In Table LXXXV we present the optimized values of K_0 and ρ_0 for the analytic SIDM model of Eq. (3) for which the maximum compatibility with the SPARC data is achieved. In Figs. 136, 137 we present

TABLE LXXXV: SIDM Optimization Values for the galaxy NGC3726

Parameter	Optimization Values
$\rho_0 (M_\odot/\text{Kpc}^3)$	4.00421×10^7
$K_0 (M_\odot \text{ Kpc}^{-3} (\text{km/s})^2)$	13094.3

the density of the analytic SIDM model, the predicted rotation curves for the SIDM model (3), versus the SPARC observational data and the sound speed, as a function of the radius respectively. As it can be seen, for this galaxy, the SIDM model produces non-viable rotation curves which are incompatible with the SPARC data.

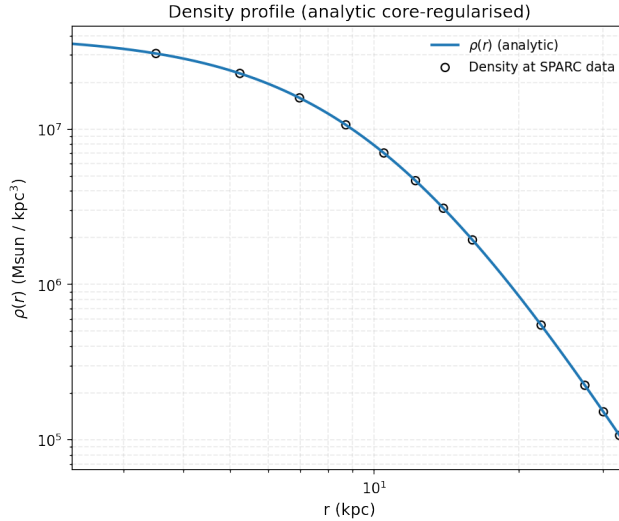


FIG. 136: The density of the SIDM model of Eq. (3) for the galaxy NGC3726, versus the radius.

Now we shall include contributions to the rotation velocity from the other components of the galaxy, namely the disk, the gas, and the bulge if present. In Fig. 138 we present the combined rotation curves including all the components of the galaxy along with the SIDM. As it can be seen, the extended collisional DM model is non-viable. Also in Table LXXXVI we present the optimized values of the free

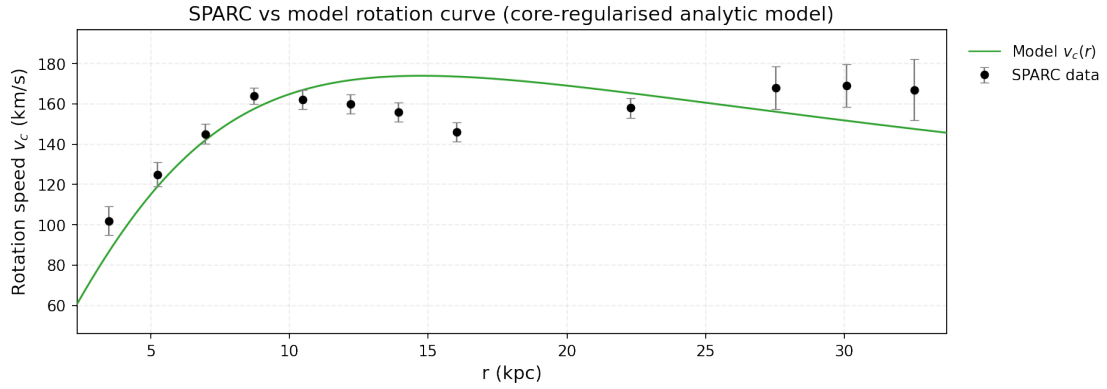


FIG. 137: The predicted rotation curves for the optimized SIDM model of Eq. (3), versus the SPARC observational data for the galaxy NGC3726.

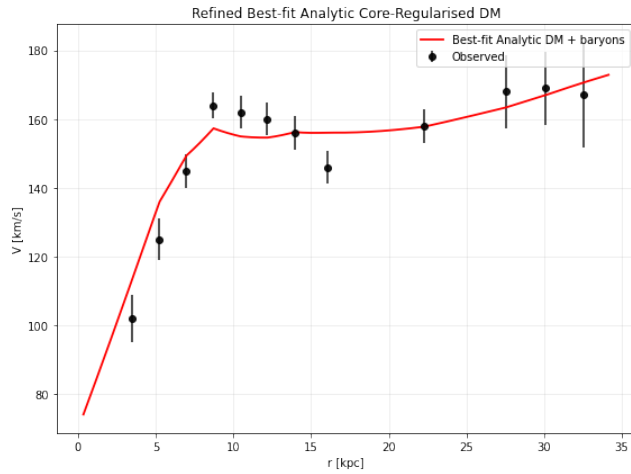


FIG. 138: The predicted rotation curves after using an optimization for the SIDM model (3), and the extended SPARC data for the galaxy NGC3726. We included the rotation curves of the gas, the disk velocities, the bulge (where present) along with the SIDM model.

parameters of the SIDM model for which we achieve the maximum compatibility with the SPARC data, for the galaxy NGC3726, and also the resulting reduced χ^2_{red} value.

TABLE LXXXVI: Optimized Parameter Values of the Extended SIDM model for the Galaxy NGC3726.

Parameter	Value
ρ_0 (M_\odot/Kpc^3)	1.7684×10^6
K_0 ($M_\odot \text{ Kpc}^{-3} (\text{km/s})^2$)	15334.2
ml_{disk}	0.8091
ml_{bulge}	0.6023
α (Kpc)	53.7324
χ^2_{red}	2.20829

41. The Galaxy NGC3741, Non-viable, Extended Viable

For this galaxy, the optimization method we used, ensures maximum compatibility of the analytic SIDM model of Eq. (3) with the SPARC data, if we choose $\rho_0 = 2.14808 \times 10^7 M_\odot/\text{Kpc}^3$ and $K_0 = 995.075 M_\odot \text{ Kpc}^{-3} (\text{km/s})^2$, in which case the reduced χ^2_{red} value is $\chi^2_{red} = 4.39585$. Also the parameter α in this case is $\alpha = 3.92784 \text{ Kpc}$.

In Table LXXXVII we present the optimized values of K_0 and ρ_0 for the analytic SIDM model of Eq. (3) for which the maximum compatibility with the SPARC data is achieved. In Figs. 139, 140 we present

TABLE LXXXVII: SIDM Optimization Values for the galaxy NGC3741

Parameter	Optimization Values
$\rho_0 (M_\odot/\text{Kpc}^3)$	2.14808×10^7
$K_0 (M_\odot \text{ Kpc}^{-3} (\text{km/s})^2)$	995.075

the density of the analytic SIDM model, the predicted rotation curves for the SIDM model (3), versus the SPARC observational data and the sound speed, as a function of the radius respectively. As it can be seen, for this galaxy, the SIDM model produces non-viable rotation curves which are incompatible with the SPARC data.

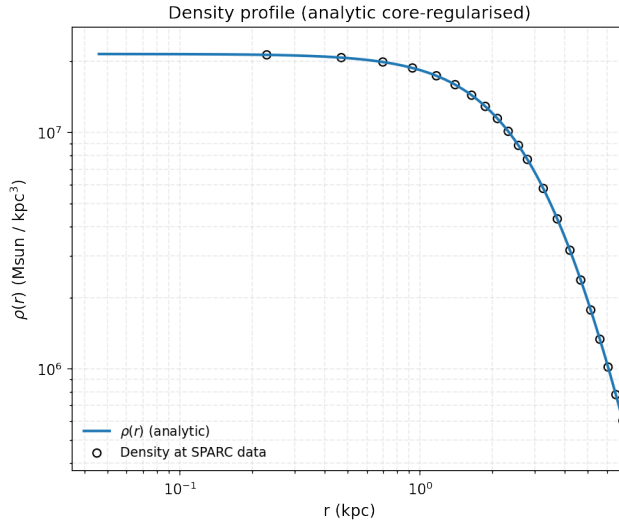


FIG. 139: The density of the SIDM model of Eq. (3) for the galaxy NGC3741, versus the radius.

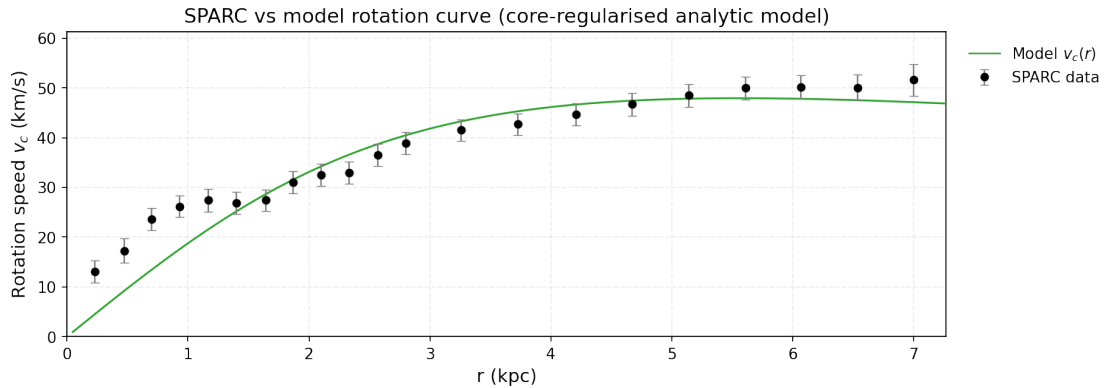


FIG. 140: The predicted rotation curves for the optimized SIDM model of Eq. (3), versus the SPARC observational data for the galaxy NGC3741.

Now we shall include contributions to the rotation velocity from the other components of the galaxy, namely the disk, the gas, and the bulge if present. In Fig. 141 we present the combined rotation curves including all the components of the galaxy along with the SIDM. As it can be seen, the extended collisional DM model is non-viable. Also in Table LXXXVIII we present the optimized values of the free parameters of the SIDM model for which we achieve the maximum compatibility with the SPARC data, for the galaxy NGC3741, and also the resulting reduced χ^2_{red} value.

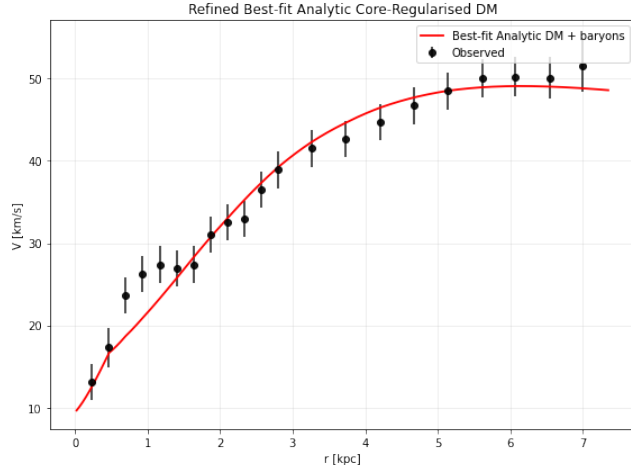


FIG. 141: The predicted rotation curves after using an optimization for the SIDM model (3), and the extended SPARC data for the galaxy NGC3741. We included the rotation curves of the gas, the disk velocities, the bulge (where present) along with the SIDM model.

TABLE LXXXVIII: Optimized Parameter Values of the Extended SIDM model for the Galaxy NGC3741.

Parameter	Value
$\rho_0 (M_\odot/\text{Kpc}^3)$	1.58989×10^7
$K_0 (M_\odot \text{ Kpc}^{-3} (\text{km/s})^2)$	953.988
ml_{disk}	1.0000
ml_{bulge}	0.46
$\alpha (\text{Kpc})$	4.46975
χ^2_{red}	1.11831

42. The Galaxy NGC3769, Non-viable, Extended Viable

For this galaxy, the optimization method we used, ensures maximum compatibility of the analytic SIDM model of Eq. (3) with the SPARC data, if we choose $\rho_0 = 4.54798 \times 10^7 M_\odot/\text{Kpc}^3$ and $K_0 = 7542.73 M_\odot \text{ Kpc}^{-3} (\text{km/s})^2$, in which case the reduced χ^2_{red} value is $\chi^2_{\text{red}} = 5.69727$. Also the parameter α in this case is $\alpha = 7.432 \text{ Kpc}$.

In Table LXXXIX we present the optimized values of K_0 and ρ_0 for the analytic SIDM model of Eq. (3) for which the maximum compatibility with the SPARC data is achieved. In Figs. 142, 143 we present

TABLE LXXXIX: SIDM Optimization Values for the galaxy NGC3769

Parameter	Optimization Values
$\rho_0 (M_\odot/\text{Kpc}^3)$	4.54798×10^7
$K_0 (M_\odot \text{ Kpc}^{-3} (\text{km/s})^2)$	7542.73

the density of the analytic SIDM model, the predicted rotation curves for the SIDM model (3), versus the SPARC observational data and the sound speed, as a function of the radius respectively. As it can be seen, for this galaxy, the SIDM model produces non-viable rotation curves which are incompatible with the SPARC data.

Now we shall include contributions to the rotation velocity from the other components of the galaxy, namely the disk, the gas, and the bulge if present. In Fig. 144 we present the combined rotation curves including all the components of the galaxy along with the SIDM. As it can be seen, the extended collisional DM model is viable. Also in Table XC we present the optimized values of the free parameters of the SIDM model for which we achieve the maximum compatibility with the SPARC data, for the galaxy NGC3769, and also the resulting reduced χ^2_{red} value.

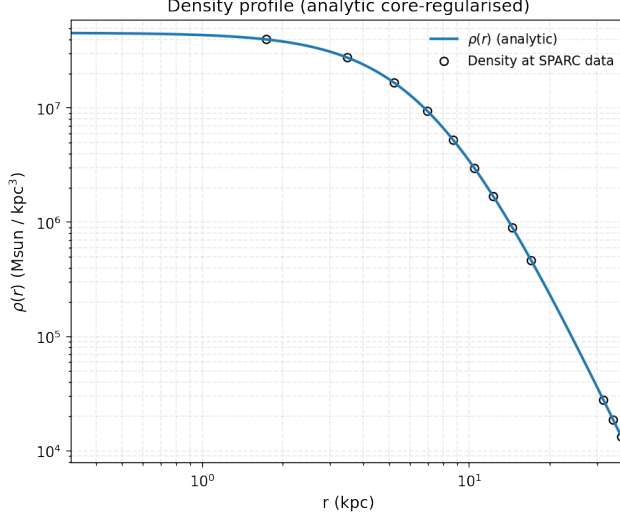


FIG. 142: The density of the SIDM model of Eq. (3) for the galaxy NGC3769, versus the radius.

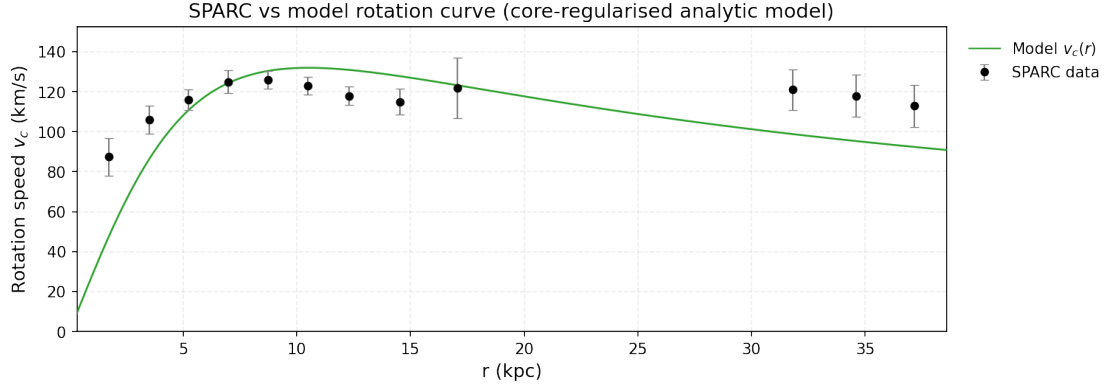


FIG. 143: The predicted rotation curves for the optimized SIDM model of Eq. (3), versus the SPARC observational data for the galaxy NGC3769.

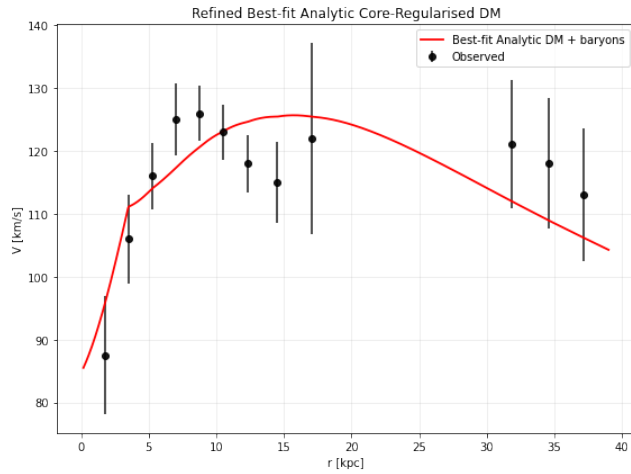


FIG. 144: The predicted rotation curves after using an optimization for the SIDM model (3), and the extended SPARC data for the galaxy NGC3769. We included the rotation curves of the gas, the disk velocities, the bulge (where present) along with the SIDM model.

TABLE XC: Optimized Parameter Values of the Extended SIDM model for the Galaxy NGC3769.

Parameter	Value
$\rho_0 (M_\odot/\text{Kpc}^3)$	1.02105×10^7
$K_0 (M_\odot \text{ Kpc}^{-3} (\text{km/s})^2)$	5173.24
ml_{disk}	0.7280
ml_{bulge}	0.42
$\alpha (\text{Kpc})$	12.9884
χ^2_{red}	1.44246

43. The Galaxy NGC3877

For this galaxy, the optimization method we used, ensures maximum compatibility of the analytic SIDM model of Eq. (3) with the SPARC data, if we choose $\rho_0 = 1.42995 \times 10^8 M_\odot/\text{Kpc}^3$ and $K_0 = 12511.1 M_\odot \text{ Kpc}^{-3} (\text{km/s})^2$, in which case the reduced χ^2_{red} value is $\chi^2_{\text{red}} = 0.523333$. Also the parameter α in this case is $\alpha = 5.39806 \text{ Kpc}$.

In Table XCI we present the optimized values of K_0 and ρ_0 for the analytic SIDM model of Eq. (3) for which the maximum compatibility with the SPARC data is achieved. In Figs. 145, 146 we present

TABLE XCI: SIDM Optimization Values for the galaxy NGC3877

Parameter	Optimization Values
$\rho_0 (M_\odot/\text{Kpc}^3)$	1.42995×10^7
$K_0 (M_\odot \text{ Kpc}^{-3} (\text{km/s})^2)$	12511.1

the density of the analytic SIDM model, the predicted rotation curves for the SIDM model (3), versus the SPARC observational data and the sound speed, as a function of the radius respectively. As it can be seen, for this galaxy, the SIDM model produces viable rotation curves which are compatible with the SPARC data.

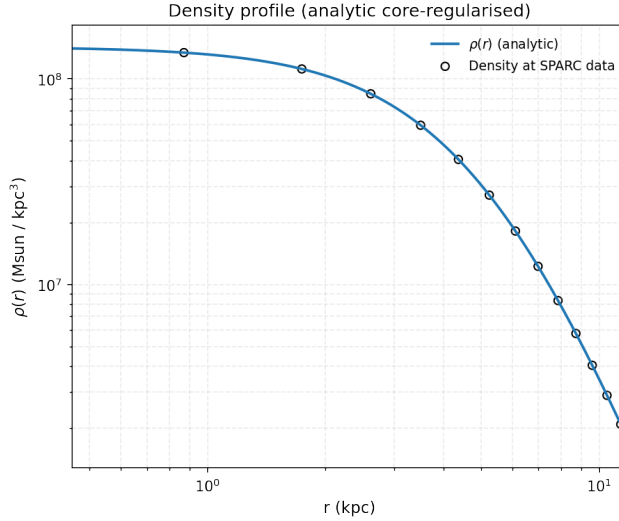


FIG. 145: The density of the SIDM model of Eq. (3) for the galaxy NGC3877, versus the radius.

44. The Galaxy NGC3893, Non-viable, Extended Viable

For this galaxy, the optimization method we used, ensures maximum compatibility of the analytic SIDM model of Eq. (3) with the SPARC data, if we choose $\rho_0 = 2.88976 \times 10^8 M_\odot/\text{Kpc}^3$ and $K_0 = 17896.5 M_\odot \text{ Kpc}^{-3} (\text{km/s})^2$, in which case the reduced χ^2_{red} value is $\chi^2_{\text{red}} = 4.67278$. Also the parameter α in this case is $\alpha = 4.54155 \text{ Kpc}$.

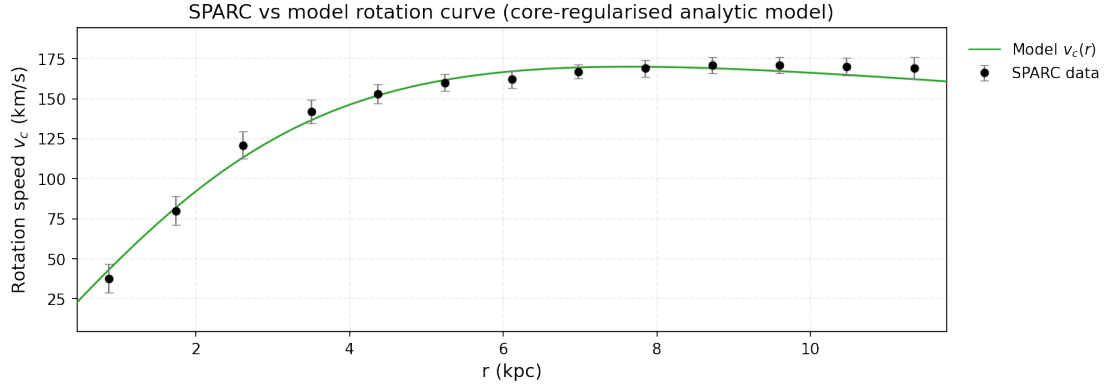


FIG. 146: The predicted rotation curves for the optimized SIDM model of Eq. (3), versus the SPARC observational data for the galaxy NGC3877.

In Table XCII we present the optimized values of K_0 and ρ_0 for the analytic SIDM model of Eq. (3) for which the maximum compatibility with the SPARC data is achieved. In Figs. 147, 148 we present

TABLE XCII: SIDM Optimization Values for the galaxy NGC3893

Parameter	Optimization Values
ρ_0 (M_\odot/Kpc^3)	2.88976×10^8
K_0 ($M_\odot \text{ Kpc}^{-3} (\text{km/s})^2$)	17896.5

the density of the analytic SIDM model, the predicted rotation curves for the SIDM model (3), versus the SPARC observational data and the sound speed, as a function of the radius respectively. As it can be seen, for this galaxy, the SIDM model produces non-viable rotation curves which are incompatible with the SPARC data.

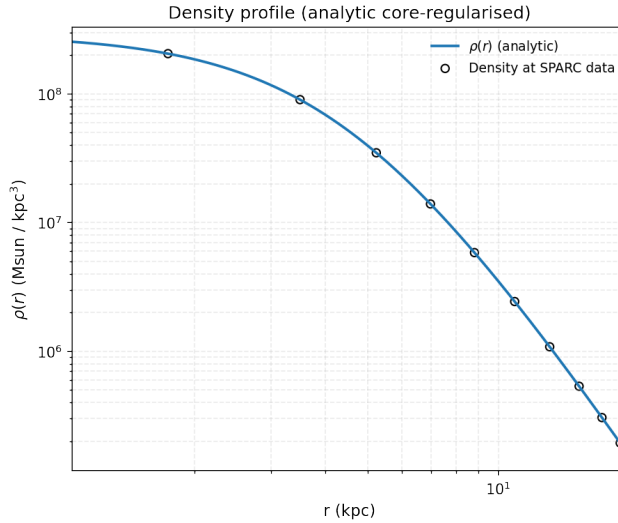


FIG. 147: The density of the SIDM model of Eq. (3) for the galaxy NGC3893, versus the radius.

Now we shall include contributions to the rotation velocity from the other components of the galaxy, namely the disk, the gas, and the bulge if present. In Fig. 149 we present the combined rotation curves including all the components of the galaxy along with the SIDM. As it can be seen, the extended collisional DM model is non-viable. Also in Table XCIII we present the optimized values of the free parameters of the SIDM model for which we achieve the maximum compatibility with the SPARC data, for the galaxy NGC3893, and also the resulting reduced χ^2_{red} value.

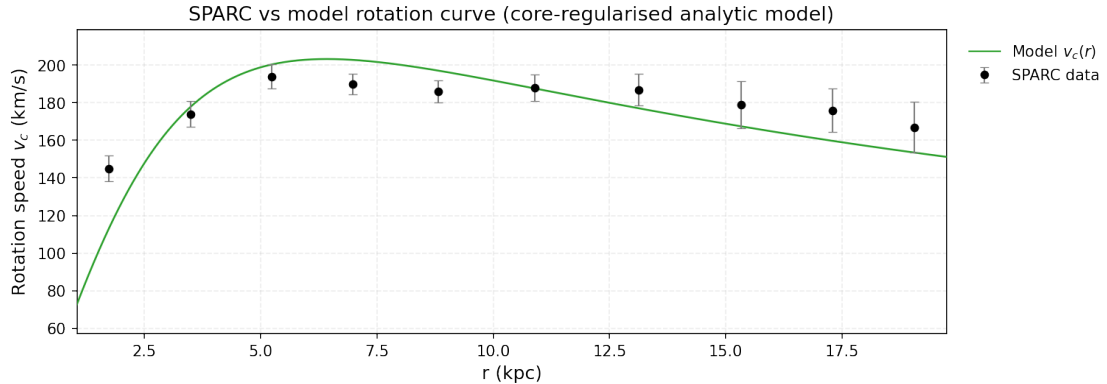


FIG. 148: The predicted rotation curves for the optimized SIDM model of Eq. (3), versus the SPARC observational data for the galaxy NGC3893.

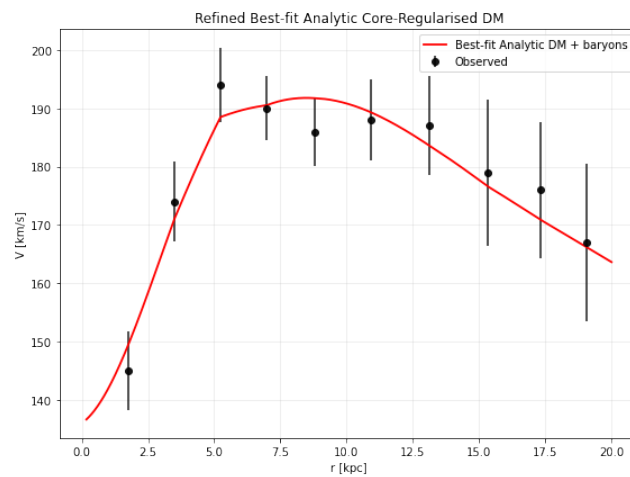


FIG. 149: The predicted rotation curves after using an optimization for the SIDM model (3), and the extended SPARC data for the galaxy NGC3893. We included the rotation curves of the gas, the disk velocities, the bulge (where present) along with the SIDM model.

TABLE XCIII: Optimized Parameter Values of the Extended SIDM model for the Galaxy NGC3893.

Parameter	Value
$\rho_0 (M_\odot/\text{Kpc}^3)$	4.35752×10^7
$K_0 (M_\odot \text{ Kpc}^{-3} (\text{km/s})^2)$	9258.6
ml_{disk}	0.6949
ml_{bulge}	0.4635
$\alpha (\text{Kpc})$	8.41103
χ^2_{red}	0.454429

45. The Galaxy NGC3917

For this galaxy, the optimization method we used, ensures maximum compatibility of the analytic SIDM model of Eq. (3) with the SPARC data, if we choose $\rho_0 = 5.60942 \times 10^7 M_\odot/\text{Kpc}^3$ and $K_0 = 8230.72 M_\odot \text{ Kpc}^{-3} (\text{km/s})^2$, in which case the reduced χ^2_{red} value is $\chi^2_{\text{red}} = 0.617376$. Also the parameter α in this case is $\alpha = 6.99054 \text{ Kpc}$.

In Table XCIV we present the optimized values of K_0 and ρ_0 for the analytic SIDM model of Eq. (3) for which the maximum compatibility with the SPARC data is achieved. In Figs. 150, 151 we present the density of the analytic SIDM model, the predicted rotation curves for the SIDM model (3), versus the SPARC observational data and the sound speed, as a function of the radius respectively. As it can be seen, for this galaxy, the SIDM model produces viable rotation curves which are compatible with the SPARC data.

TABLE XCIV: SIDM Optimization Values for the galaxy NGC3917

Parameter	Optimization Values
$\rho_0 (M_\odot/\text{Kpc}^3)$	5.60942×10^7
$K_0 (M_\odot \text{ Kpc}^{-3} (\text{km/s})^2)$	8230.72

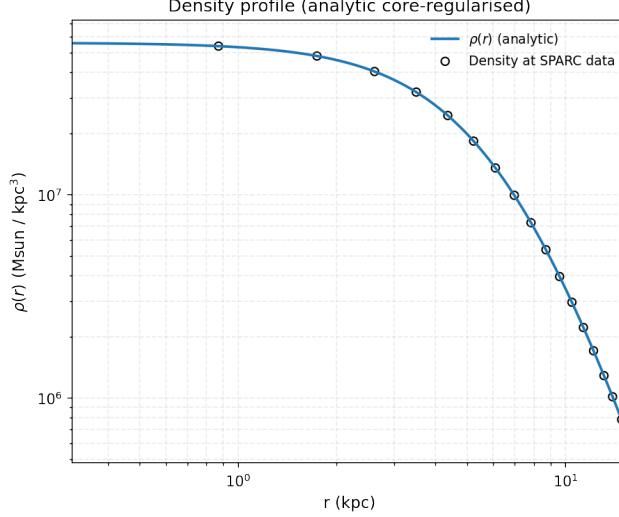


FIG. 150: The density of the SIDM model of Eq. (3) for the galaxy NGC3917, versus the radius.

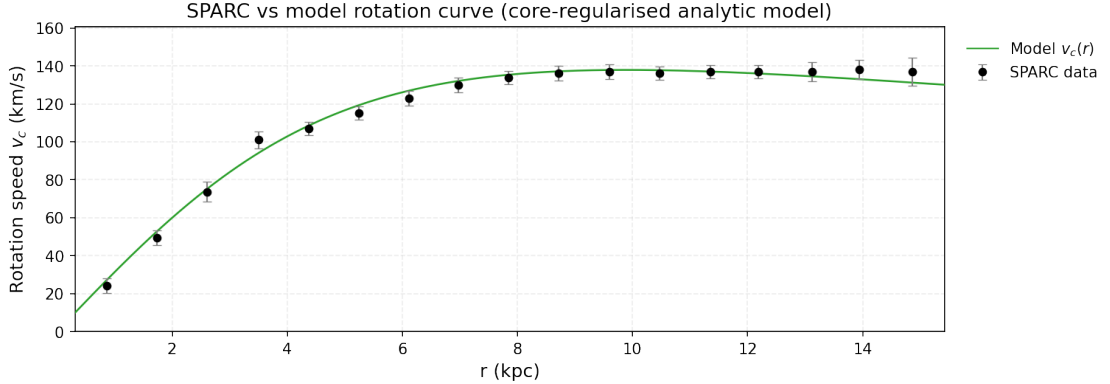


FIG. 151: The predicted rotation curves for the optimized SIDM model of Eq. (3), versus the SPARC observational data for the galaxy NGC3917.

46. The Galaxy NGC3949

For this galaxy, the optimization method we used, ensures maximum compatibility of the analytic SIDM model of Eq. (3) with the SPARC data, if we choose $\rho_0 = 3.85388 \times 10^8 M_\odot/\text{Kpc}^3$ and $K_0 = 10995.9 M_\odot \text{ Kpc}^{-3} (\text{km/s})^2$, in which case the reduced χ^2_{red} value is $\chi^2_{\text{red}} = 0.667849$. Also the parameter α in this case is $\alpha = 3.0826 \text{ Kpc}$.

In Table XCV we present the optimized values of K_0 and ρ_0 for the analytic SIDM model of Eq. (3) for which the maximum compatibility with the SPARC data is achieved. In Figs. 152, 153 we present

TABLE XCV: SIDM Optimization Values for the galaxy NGC3949

Parameter	Optimization Values
$\rho_0 (M_\odot/\text{Kpc}^3)$	3.85388×10^8
$K_0 (M_\odot \text{ Kpc}^{-3} (\text{km/s})^2)$	10995.9

the density of the analytic SIDM model, the predicted rotation curves for the SIDM model (3), versus the SPARC observational data and the sound speed, as a function of the radius respectively. As it can be seen, for this galaxy, the SIDM model produces viable rotation curves which are compatible with the SPARC data.

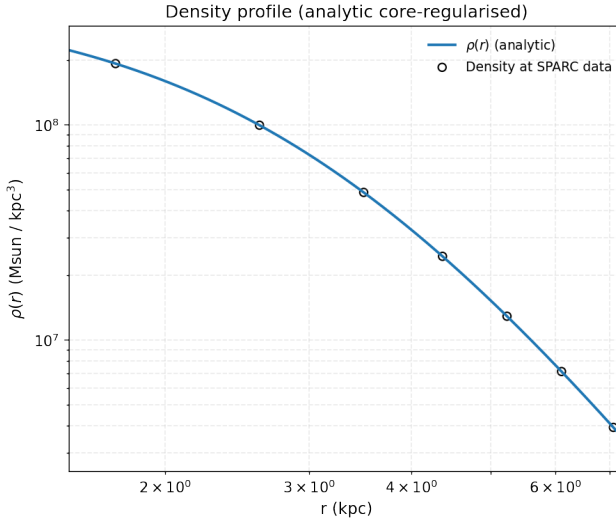


FIG. 152: The density of the SIDM model of Eq. (3) for the galaxy NGC3949, versus the radius.

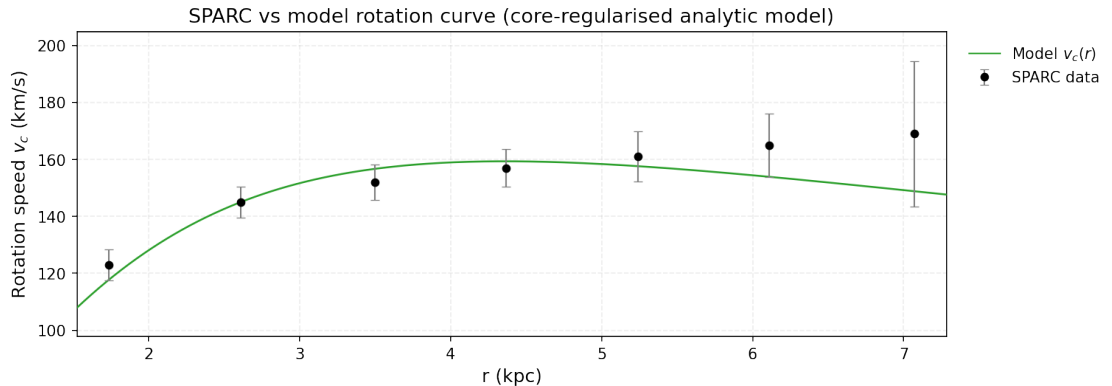


FIG. 153: The predicted rotation curves for the optimized SIDM model of Eq. (3), versus the SPARC observational data for the galaxy NGC3949.

47. The Galaxy NGC3953, Non-viable

For this galaxy, the optimization method we used, ensures maximum compatibility of the analytic SIDM model of Eq. (3) with the SPARC data, if we choose $\rho_0 = 2.03016 \times 10^8 M_\odot/\text{Kpc}^3$ and $K_0 = 22728.9 M_\odot \text{Kpc}^{-3} (\text{km/s})^2$, in which case the reduced χ^2_{red} value is $\chi^2_{red} = 1.68893$. Also the parameter α in this case is $\alpha = 6.10626 \text{Kpc}$.

In Table XCVI we present the optimized values of K_0 and ρ_0 for the analytic SIDM model of Eq. (3) for which the maximum compatibility with the SPARC data is achieved. In Figs. 154, 155 we present

TABLE XCVI: SIDM Optimization Values for the galaxy NGC3953

Parameter	Optimization Values
$\rho_0 (M_\odot/\text{Kpc}^3)$	2.03016×10^8
$K_0 (M_\odot \text{Kpc}^{-3} (\text{km/s})^2)$	22728.9

the density of the analytic SIDM model, the predicted rotation curves for the SIDM model (3), versus the SPARC observational data and the sound speed, as a function of the radius respectively. As it can be seen, for this galaxy, the SIDM model produces non-viable rotation curves which are incompatible with the SPARC data.

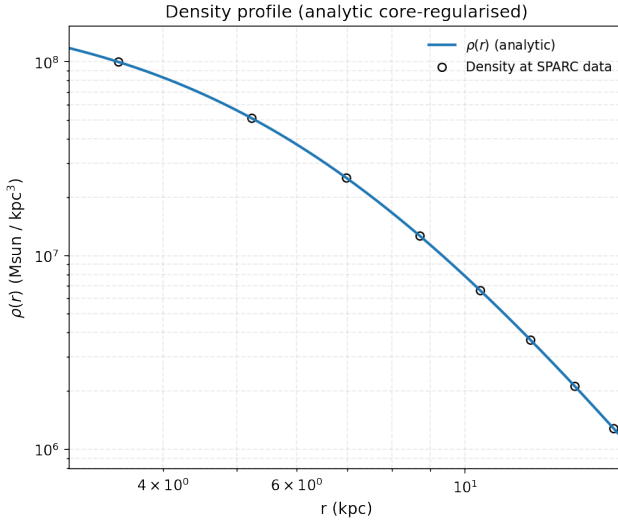


FIG. 154: The density of the SIDM model of Eq. (3) for the galaxy NGC3953, versus the radius.

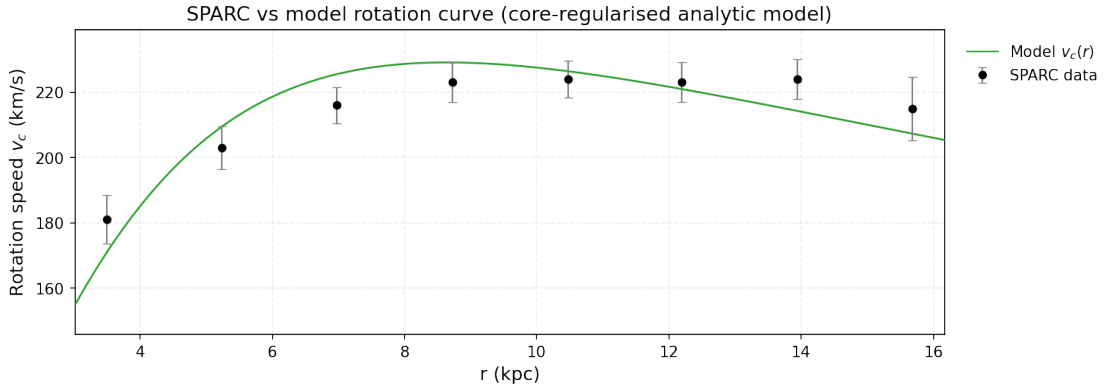


FIG. 155: The predicted rotation curves for the optimized SIDM model of Eq. (3), versus the SPARC observational data for the galaxy NGC3953.

48. The Galaxy NGC3972

For this galaxy, the optimization method we used, ensures maximum compatibility of the analytic SIDM model of Eq. (3) with the SPARC data, if we choose $\rho_0 = 7.82466 \times 10^7 M_\odot/\text{Kpc}^3$ and $K_0 = 7267.09 M_\odot \text{Kpc}^{-3} (\text{km/s})^2$, in which case the reduced χ^2_{red} value is $\chi^2_{red} = 1.70186$. Also the parameter α in this case is $\alpha = 5.56158 \text{Kpc}$.

In Table XCVII we present the optimized values of K_0 and ρ_0 for the analytic SIDM model of Eq. (3) for which the maximum compatibility with the SPARC data is achieved. In Figs. 156, 157 we present

TABLE XCVII: SIDM Optimization Values for the galaxy NGC3972

Parameter	Optimization Values
$\rho_0 (M_\odot/\text{Kpc}^3)$	7.82466×10^7
$K_0 (M_\odot \text{Kpc}^{-3} (\text{km/s})^2)$	7267.09

the density of the analytic SIDM model, the predicted rotation curves for the SIDM model (3), versus the SPARC observational data and the sound speed, as a function of the radius respectively. As it can be seen, for this galaxy, the SIDM model produces non-viable rotation curves which are incompatible with the SPARC data.

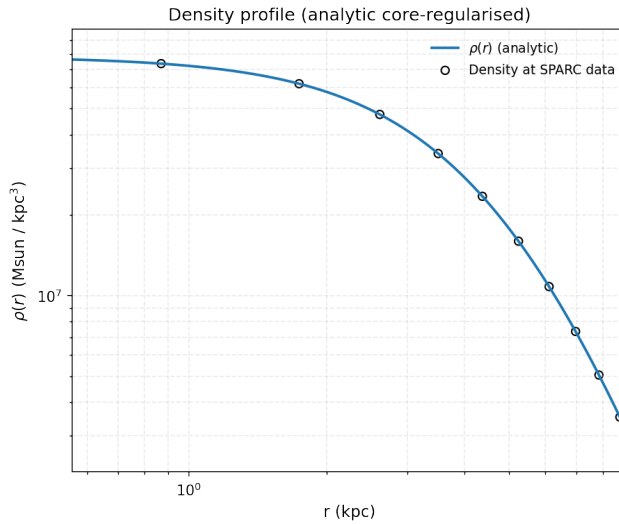


FIG. 156: The density of the SIDM model of Eq. (3) for the galaxy NGC3972, versus the radius.

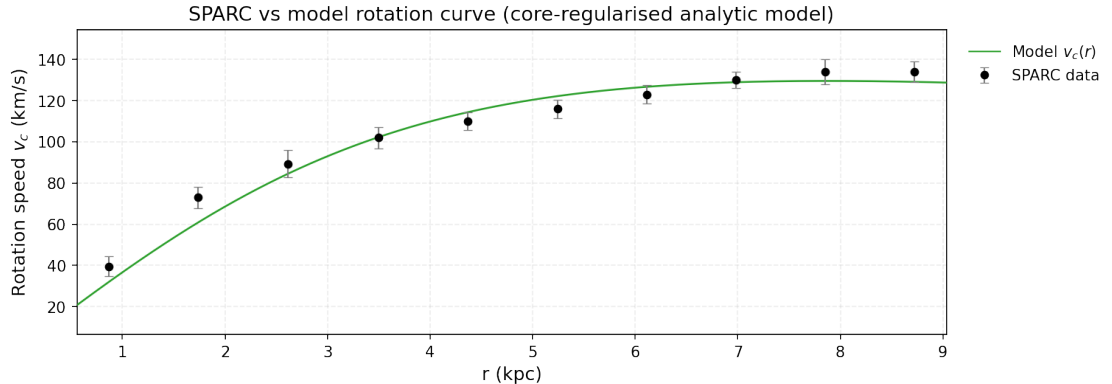


FIG. 157: The predicted rotation curves for the optimized SIDM model of Eq. (3), versus the SPARC observational data for the galaxy NGC3972.

Now we shall include contributions to the rotation velocity from the other components of the galaxy, namely the disk, the gas, and the bulge if present. In Fig. 158 we present the combined rotation curves including all the components of the galaxy along with the SIDM. As it can be seen, the extended collisional DM model is non-viable. Also in Table XCVIII we present the optimized values of the free parameters of the SIDM model for which we achieve the maximum compatibility with the SPARC data, for the galaxy NGC3972, and also the resulting reduced χ^2_{red} value.

TABLE XCVIII: Optimized Parameter Values of the Extended SIDM model for the Galaxy NGC3972.

Parameter	Value
$\rho_0 (M_\odot / \text{Kpc}^3)$	5.40336×10^7
$K_0 (M_\odot \text{ Kpc}^{-3} (\text{km/s})^2)$	5279.85
ml_{disk}	0.6178
ml_{bulge}	0.0361
$\alpha (\text{Kpc})$	5.70394
χ^2_{red}	1.60993

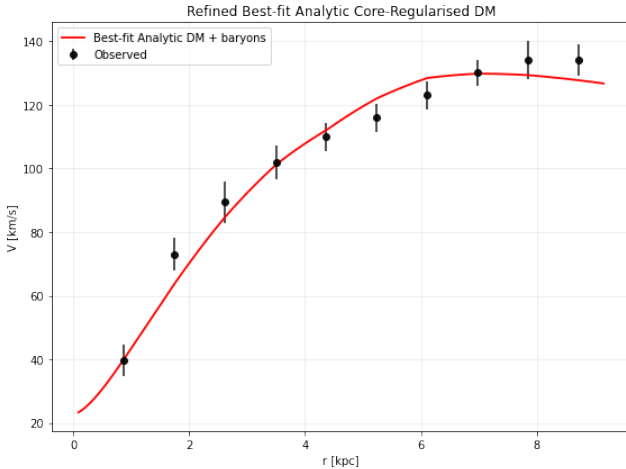


FIG. 158: The predicted rotation curves after using an optimization for the SIDM model (3), and the extended SPARC data for the galaxy NGC3972. We included the rotation curves of the gas, the disk velocities, the bulge (where present) along with the SIDM model.

49. The Galaxy NGC3992, Marginally

For this galaxy, the optimization method we used, ensures maximum compatibility of the analytic SIDM model of Eq. (3) with the SPARC data, if we choose $\rho_0 = 6.59039 \times 10^7 M_\odot/\text{Kpc}^3$ and $K_0 = 33644.4 M_\odot \text{Kpc}^{-3} (\text{km/s})^2$, in which case the reduced χ^2_{red} value is $\chi^2_{\text{red}} = 1.84261$. Also the parameter α in this case is $\alpha = 13.0392 \text{Kpc}$.

In Table XCIX we present the optimized values of K_0 and ρ_0 for the analytic SIDM model of Eq. (3) for which the maximum compatibility with the SPARC data is achieved. In Figs. 159, 160 we present

TABLE XCIX: SIDM Optimization Values for the galaxy NGC3992

Parameter	Optimization Values
$\rho_0 (M_\odot/\text{Kpc}^3)$	6.59039×10^7
$K_0 (M_\odot \text{Kpc}^{-3} (\text{km/s})^2)$	33644.4

the density of the analytic SIDM model, the predicted rotation curves for the SIDM model (3), versus the SPARC observational data and the sound speed, as a function of the radius respectively. As it can be seen, for this galaxy, the SIDM model produces marginally viable rotation curves which are incompatible with the SPARC data.

Now we shall include contributions to the rotation velocity from the other components of the galaxy, namely the disk, the gas, and the bulge if present. In Fig. 161 we present the combined rotation curves including all the components of the galaxy along with the SIDM. As it can be seen, the extended collisional DM model is marginally viable. Also in Table C we present the optimized values of the free parameters of the SIDM model for which we achieve the maximum compatibility with the SPARC data, for the galaxy NGC3992, and also the resulting reduced χ^2_{red} value.

TABLE C: Optimized Parameter Values of the Extended SIDM model for the Galaxy NGC3992.

Parameter	Value
$\rho_0 (M_\odot/\text{Kpc}^3)$	3.41415×10^6
$K_0 (M_\odot \text{Kpc}^{-3} (\text{km/s})^2)$	12823.2
ml_{disk}	1
ml_{bulge}	0.8274
$\alpha (\text{Kpc})$	35.3632
χ^2_{red}	2.03714

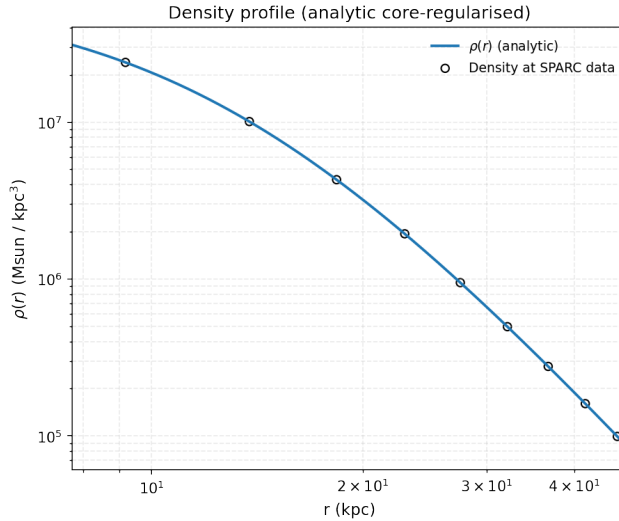


FIG. 159: The density of the SIDM model of Eq. (3) for the galaxy NGC3992, versus the radius.

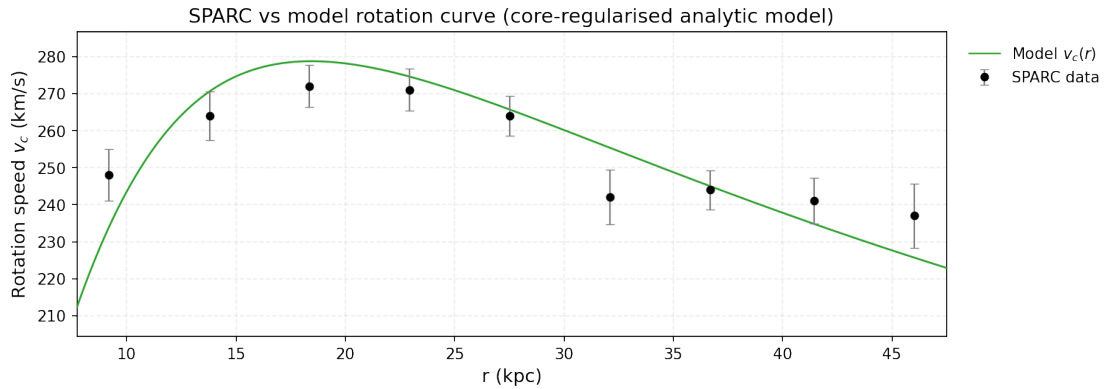


FIG. 160: The predicted rotation curves for the optimized SIDM model of Eq. (3), versus the SPARC observational data for the galaxy NGC3992.

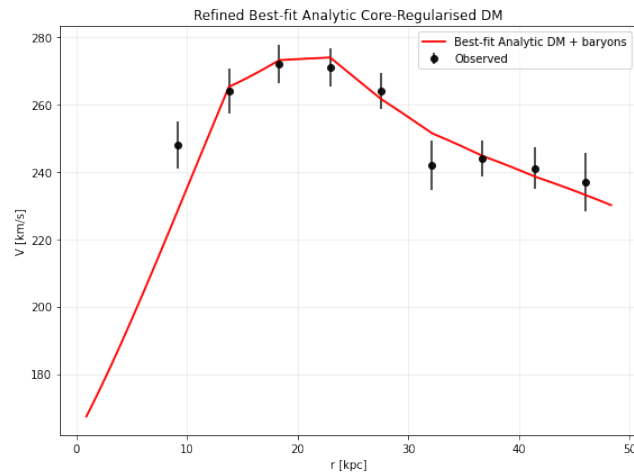


FIG. 161: The predicted rotation curves after using an optimization for the SIDM model (3), and the extended SPARC data for the galaxy NGC3992. We included the rotation curves of the gas, the disk velocities, the bulge (where present) along with the SIDM model.

50. The Galaxy NGC4010

For this galaxy, the optimization method we used, ensures maximum compatibility of the analytic SIDM model of Eq. (3) with the SPARC data, if we choose $\rho_0 = 4.92231 \times 10^7 M_\odot/\text{Kpc}^3$ and $K_0 = 6892.94 M_\odot \text{Kpc}^{-3} (\text{km/s})^2$, in which case the reduced χ^2_{red} value is $\chi^2_{red} = 1.17299$. Also the parameter α in this case is $\alpha = 6.82918 \text{Kpc}$.

In Table CI we present the optimized values of K_0 and ρ_0 for the analytic SIDM model of Eq. (3) for which the maximum compatibility with the SPARC data is achieved. In Figs. 162, 163 we present

TABLE CI: SIDM Optimization Values for the galaxy NGC4010

Parameter	Optimization Values
$\rho_0 (M_\odot/\text{Kpc}^3)$	4.92231×10^7
$K_0 (M_\odot \text{Kpc}^{-3} (\text{km/s})^2)$	6892.94

the density of the analytic SIDM model, the predicted rotation curves for the SIDM model (3), versus the SPARC observational data and the sound speed, as a function of the radius respectively. As it can be seen, for this galaxy, the SIDM model produces viable rotation curves which are compatible with the SPARC data.

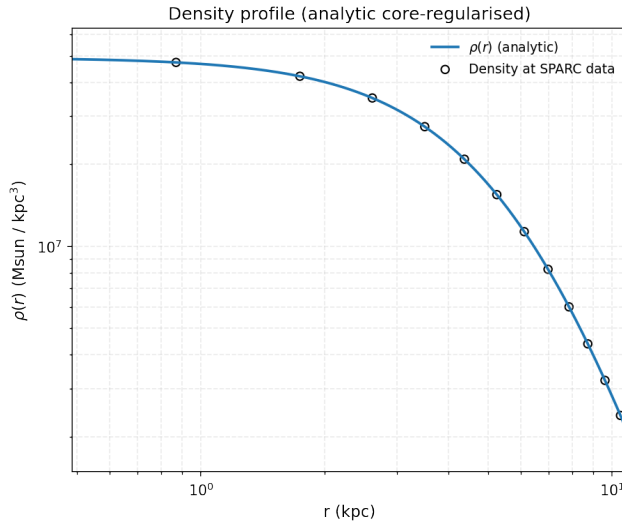


FIG. 162: The density of the SIDM model of Eq. (3) for the galaxy NGC4010, versus the radius.

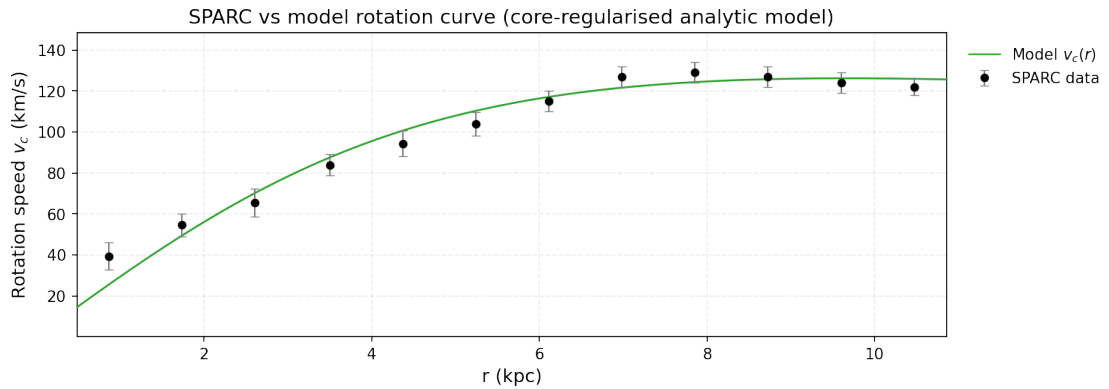


FIG. 163: The predicted rotation curves for the optimized SIDM model of Eq. (3), versus the SPARC observational data for the galaxy NGC4010.

51. The Galaxy NGC4013, Non-viable, Extended Viable

For this galaxy, the optimization method we used, ensures maximum compatibility of the analytic SIDM model of Eq. (3) with the SPARC data, if we choose $\rho_0 = 1.10219 \times 10^8 M_\odot/\text{Kpc}^3$ and $K_0 = 16800.3 M_\odot \text{Kpc}^{-3} (\text{km/s})^2$, in which case the reduced χ^2_{red} value is $\chi^2_{red} = 8.57117$. Also the parameter α in this case is $\alpha = 7.12495 \text{Kpc}$.

In Table CII we present the optimized values of K_0 and ρ_0 for the analytic SIDM model of Eq. (3) for which the maximum compatibility with the SPARC data is achieved. In Figs. 164, 165 we present the

TABLE CII: SIDM Optimization Values for the galaxy NGC4013

Parameter	Optimization Values
$\rho_0 (M_\odot/\text{Kpc}^3)$	1.10219×10^8
$K_0 (M_\odot \text{Kpc}^{-3} (\text{km/s})^2)$	16800.3

density of the analytic SIDM model, the predicted rotation curves for the SIDM model (3), versus the SPARC observational data and the sound speed, as a function of the radius respectively. As it can be seen, for this galaxy, the SIDM model produces non-viable rotation curves which are incompatible with the SPARC data.

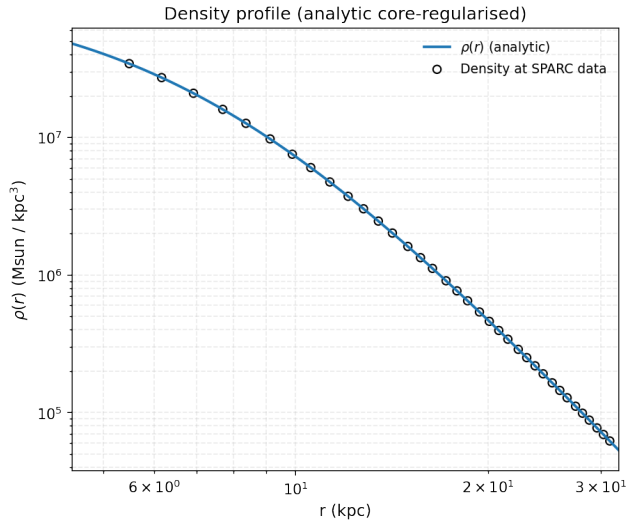


FIG. 164: The density of the SIDM model of Eq. (3) for the galaxy NGC4013, versus the radius.

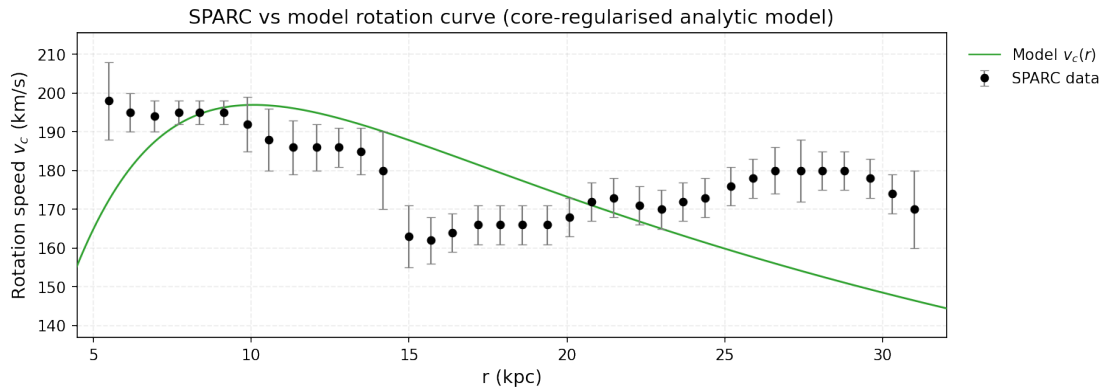


FIG. 165: The predicted rotation curves for the optimized SIDM model of Eq. (3), versus the SPARC observational data for the galaxy NGC4013.

Now we shall include contributions to the rotation velocity from the other components of the galaxy, namely the disk, the gas, and the bulge if present. In Fig. 166 we present the combined rotation

curves including all the components of the galaxy along with the SIDM. As it can be seen, the extended collisional DM model is non-viable. Also in Table CIII we present the optimized values of the free

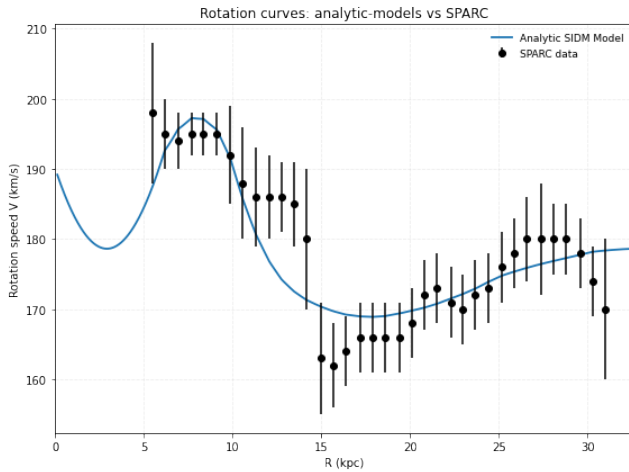


FIG. 166: The predicted rotation curves after using an optimization for the SIDM model (3), and the extended SPARC data for the galaxy NGC4013. We included the rotation curves of the gas, the disk velocities, the bulge (where present) along with the SIDM model.

parameters of the SIDM model for which we achieve the maximum compatibility with the SPARC data, for the galaxy NGC4013, and also the resulting reduced χ^2_{red} value.

TABLE CIII: Optimized Parameter Values of the Extended SIDM model for the Galaxy NGC4013.

Parameter	Value
ρ_0 (M_\odot/Kpc^3)	3.47372×10^6
K_0 ($M_\odot \text{ Kpc}^{-3} (\text{km/s})^2$)	11416.9
ml_{disk}	0.7877
ml_{bulge}	1.0000
α (Kpc)	33.0805
χ^2_{red}	0.787128

52. The Galaxy NGC4051, Non-viable, Extended Viable

For this galaxy, the optimization method we used, ensures maximum compatibility of the analytic SIDM model of Eq. (3) with the SPARC data, if we choose $\rho_0 = 1.14949 \times 10^8 M_\odot/\text{Kpc}^3$ and $K_0 = 10589.6 M_\odot \text{ Kpc}^{-3} (\text{km/s})^2$, in which case the reduced χ^2_{red} value is $\chi^2_{red} = 2.83023$. Also the parameter α in this case is $\alpha = 5.5391 \text{ Kpc}$.

In Table CIV we present the optimized values of K_0 and ρ_0 for the analytic SIDM model of Eq. (3) for which the maximum compatibility with the SPARC data is achieved. In Figs. 167, 168 we present

TABLE CIV: SIDM Optimization Values for the galaxy NGC4051

Parameter	Optimization Values
ρ_0 (M_\odot/Kpc^3)	1.14949×10^8
K_0 ($M_\odot \text{ Kpc}^{-3} (\text{km/s})^2$)	10589.6

the density of the analytic SIDM model, the predicted rotation curves for the SIDM model (3), versus the SPARC observational data and the sound speed, as a function of the radius respectively. As it can be seen, for this galaxy, the SIDM model produces non-viable rotation curves which are incompatible with the SPARC data.

Now we shall include contributions to the rotation velocity from the other components of the galaxy, namely the disk, the gas, and the bulge if present. In Fig. 169 we present the combined rotation curves including all the components of the galaxy along with the SIDM. As it can be seen, the extended collisional

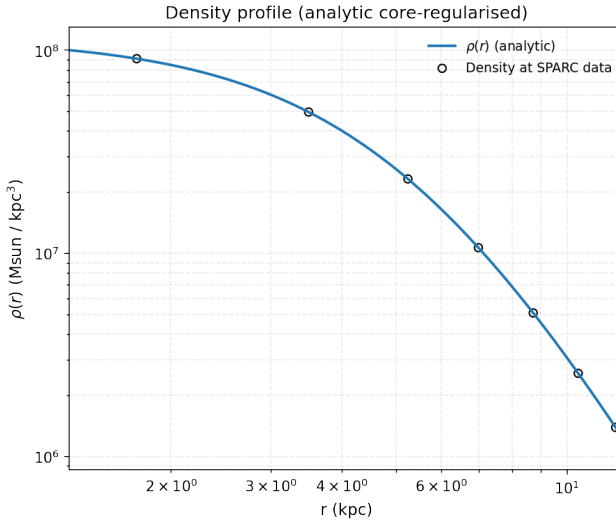


FIG. 167: The density of the SIDM model of Eq. (3) for the galaxy NGC4051, versus the radius.

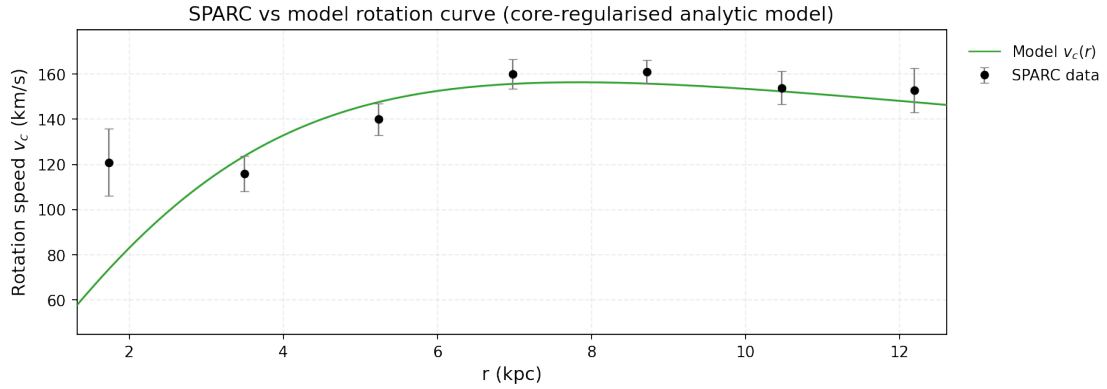


FIG. 168: The predicted rotation curves for the optimized SIDM model of Eq. (3), versus the SPARC observational data for the galaxy NGC4051.

DM model is non-viable. Also in Table CV we present the optimized values of the free parameters of

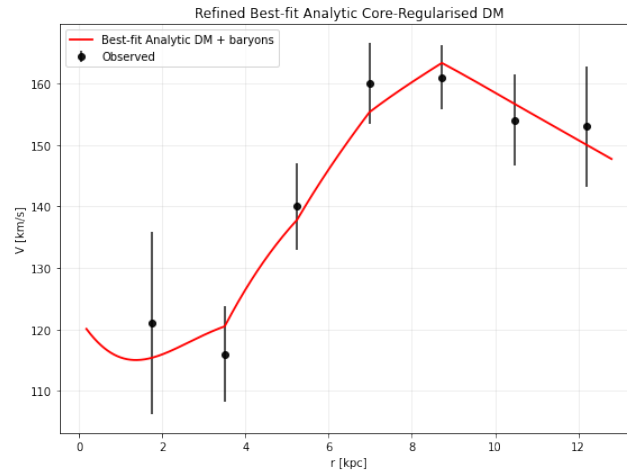


FIG. 169: The predicted rotation curves after using an optimization for the SIDM model (3), and the extended SPARC data for the galaxy NGC4051. We included the rotation curves of the gas, the disk velocities, the bulge (where present) along with the SIDM model.

the SIDM model for which we achieve the maximum compatibility with the SPARC data, for the galaxy NGC4051, and also the resulting reduced χ^2_{red} value.

TABLE CV: Optimized Parameter Values of the Extended SIDM model for the Galaxy NGC4051.

Parameter	Value
$\rho_0 (M_\odot/\text{Kpc}^3)$	5.50877×10^7
$K_0 (M_\odot \text{ Kpc}^{-3} (\text{km/s})^2)$	5011.09
ml_{disk}	0.6124
ml_{bulge}	0.2543
$\alpha (\text{Kpc})$	5.50345
χ^2_{red}	0.497737

53. The Galaxy NGC4068

For this galaxy, the optimization method we used, ensures maximum compatibility of the analytic SIDM model of Eq. (3) with the SPARC data, if we choose $\rho_0 = 3.13381 \times 10^7 M_\odot/\text{Kpc}^3$ and $K_0 = 915.044 M_\odot \text{ Kpc}^{-3} (\text{km/s})^2$, in which case the reduced χ^2_{red} value is $\chi^2_{red} = 0.637966$. Also the parameter α in this case is $\alpha = 3.11843 \text{ Kpc}$.

In Table CVI we present the optimized values of K_0 and ρ_0 for the analytic SIDM model of Eq. (3) for which the maximum compatibility with the SPARC data is achieved. In Figs. 170, 171 we present

TABLE CVI: SIDM Optimization Values for the galaxy NGC4068

Parameter	Optimization Values
$\rho_0 (M_\odot/\text{Kpc}^3)$	3.13381×10^7
$K_0 (M_\odot \text{ Kpc}^{-3} (\text{km/s})^2)$	915.044

the density of the analytic SIDM model, the predicted rotation curves for the SIDM model (3), versus the SPARC observational data and the sound speed, as a function of the radius respectively. As it can be seen, for this galaxy, the SIDM model produces viable rotation curves which are compatible with the SPARC data.

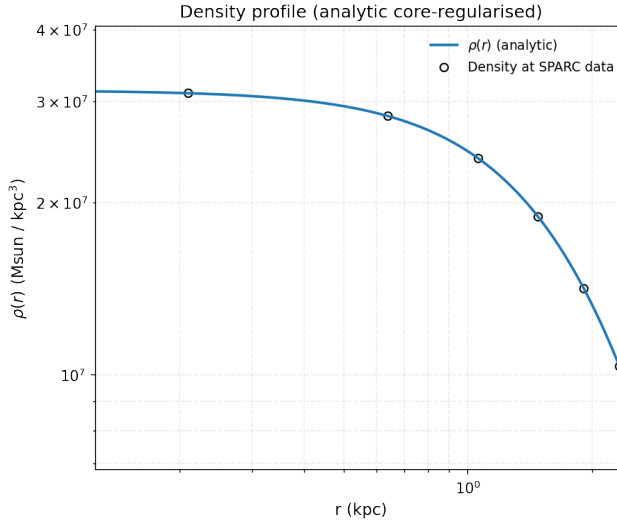


FIG. 170: The density of the SIDM model of Eq. (3) for the galaxy NGC4068, versus the radius.

54. The Galaxy NGC4085

For this galaxy, the optimization method we used, ensures maximum compatibility of the analytic SIDM model of Eq. (3) with the SPARC data, if we choose $\rho_0 = 1.49325 \times 10^8 M_\odot/\text{Kpc}^3$ and $K_0 =$

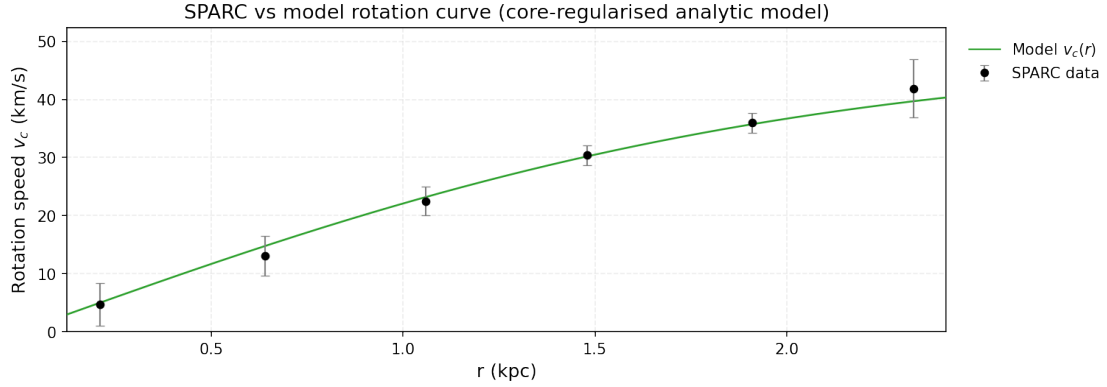


FIG. 171: The predicted rotation curves for the optimized SIDM model of Eq. (3), versus the SPARC observational data for the galaxy NGC4068.

$7851.63 M_{\odot} \text{Kpc}^{-3} (\text{km/s})^2$, in which case the reduced χ^2_{red} value is $\chi^2_{red} = 0.24862$. Also the parameter α in this case is $\alpha = 4.1847 \text{Kpc}$.

In Table CVII we present the optimized values of K_0 and ρ_0 for the analytic SIDM model of Eq. (3) for which the maximum compatibility with the SPARC data is achieved. In Figs. 172, 173 we present

TABLE CVII: SIDM Optimization Values for the galaxy NGC4085

Parameter	Optimization Values
$\rho_0 (M_{\odot}/\text{Kpc}^3)$	1.49325×10^8
$K_0 (M_{\odot} \text{Kpc}^{-3} (\text{km/s})^2)$	7851.63

the density of the analytic SIDM model, the predicted rotation curves for the SIDM model (3), versus the SPARC observational data and the sound speed, as a function of the radius respectively. As it can be seen, for this galaxy, the SIDM model produces viable rotation curves which are compatible with the SPARC data.

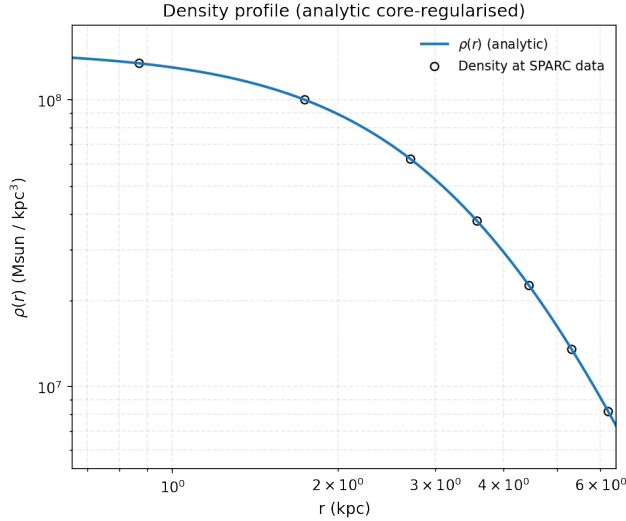


FIG. 172: The density of the SIDM model of Eq. (3) for the galaxy NGC4085, versus the radius.

55. The Galaxy NGC4088, Viable

For this galaxy, the optimization method we used, ensures maximum compatibility of the analytic SIDM model of Eq. (3) with the SPARC data, if we choose $\rho_0 = 1.09358 \times 10^8 M_{\odot}/\text{Kpc}^3$ and $K_0 =$

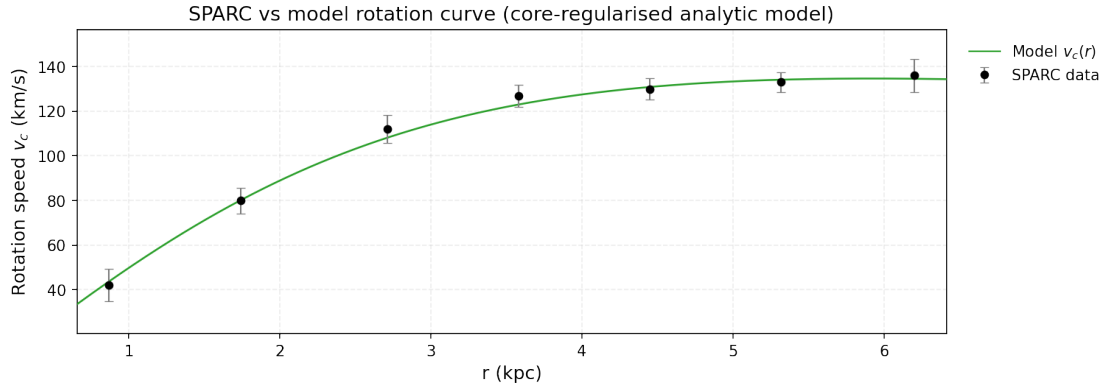


FIG. 173: The predicted rotation curves for the optimized SIDM model of Eq. (3), versus the SPARC observational data for the galaxy NGC4085.

$14986 M_{\odot} \text{Kpc}^{-3} (\text{km/s})^2$, in which case the reduced χ^2_{red} value is $\chi^2_{red} = 1.26962$. Also the parameter α in this case is $\alpha = 6.75568 \text{Kpc}$.

In Table CVIII we present the optimized values of K_0 and ρ_0 for the analytic SIDM model of Eq. (3) for which the maximum compatibility with the SPARC data is achieved. In Figs. 174, 175 we present

TABLE CVIII: SIDM Optimization Values for the galaxy NGC4088

Parameter	Optimization Values
$\rho_0 (M_{\odot}/\text{Kpc}^3)$	1.09358×10^8
$K_0 (M_{\odot} \text{Kpc}^{-3} (\text{km/s})^2)$	14986

the density of the analytic SIDM model, the predicted rotation curves for the SIDM model (3), versus the SPARC observational data and the sound speed, as a function of the radius respectively. As it can be seen, for this galaxy, the SIDM model produces marginally viable rotation curves which are marginally compatible with the SPARC data.

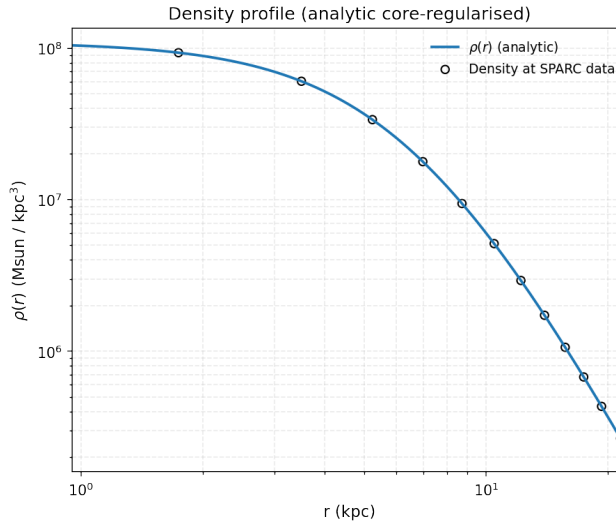


FIG. 174: The density of the SIDM model of Eq. (3) for the galaxy NGC4088, versus the radius.

56. The Galaxy NGC4100

For this galaxy, the optimization method we used, ensures maximum compatibility of the analytic SIDM model of Eq. (3) with the SPARC data, if we choose $\rho_0 = 1.4466 \times 10^8 M_{\odot}/\text{Kpc}^3$ and $K_0 =$

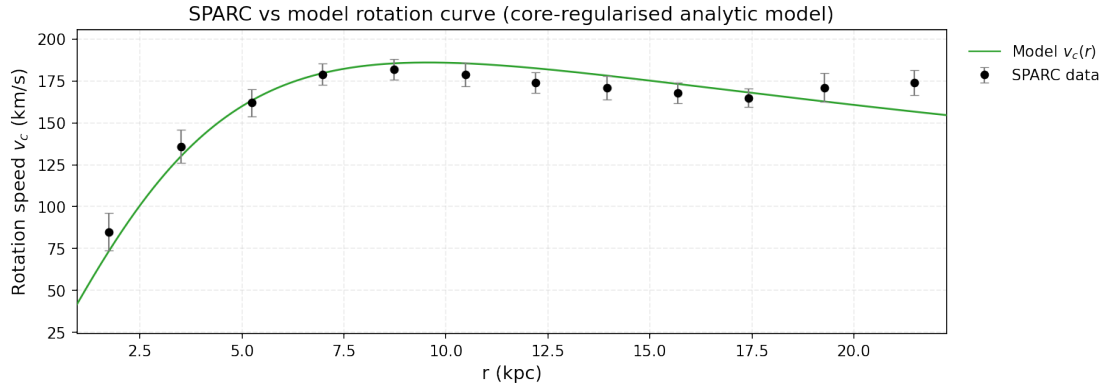


FIG. 175: The predicted rotation curves for the optimized SIDM model of Eq. (3), versus the SPARC observational data for the galaxy NGC4088.

$16706.4 M_{\odot} \text{Kpc}^{-3} (\text{km/s})^2$, in which case the reduced χ^2_{red} value is $\chi^2_{red} = 0.322466$. Also the parameter α in this case is $\alpha = 6.2018 \text{Kpc}$.

In Table CIX we present the optimized values of K_0 and ρ_0 for the analytic SIDM model of Eq. (3) for which the maximum compatibility with the SPARC data is achieved. In Figs. 176, 177 we present

TABLE CIX: SIDM Optimization Values for the galaxy NGC4100

Parameter	Optimization Values
$\rho_0 (M_{\odot}/\text{Kpc}^3)$	1.4466×10^8
$K_0 (M_{\odot} \text{Kpc}^{-3} (\text{km/s})^2)$	16706.4

the density of the analytic SIDM model, the predicted rotation curves for the SIDM model (3), versus the SPARC observational data and the sound speed, as a function of the radius respectively. As it can be seen, for this galaxy, the SIDM model produces viable rotation curves which are compatible with the SPARC data.

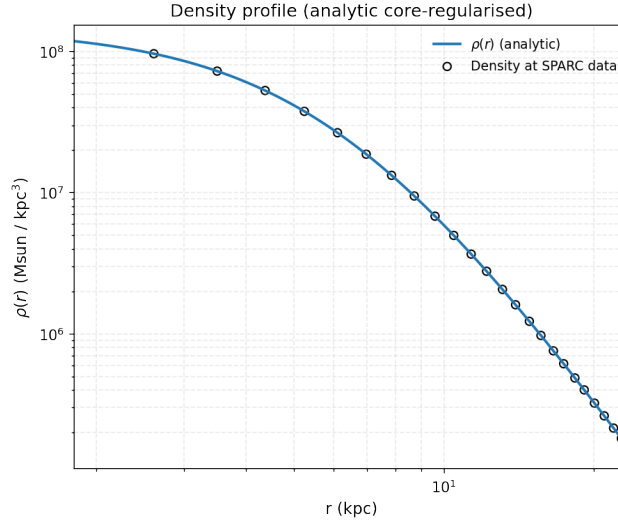


FIG. 176: The density of the SIDM model of Eq. (3) for the galaxy NGC4100, versus the radius.

57. The Galaxy NGC4138

For this galaxy, the optimization method we used, ensures maximum compatibility of the analytic SIDM model of Eq. (3) with the SPARC data, if we choose $\rho_0 = 5.01961 \times 10^8 M_{\odot}/\text{Kpc}^3$ and $K_0 =$

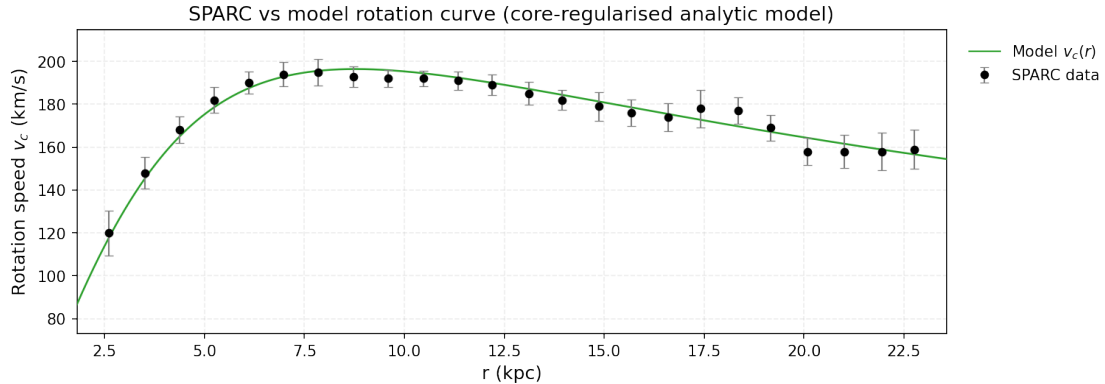


FIG. 177: The predicted rotation curves for the optimized SIDM model of Eq. (3), versus the SPARC observational data for the galaxy NGC4100.

$17200.2 M_{\odot} \text{Kpc}^{-3} (\text{km/s})^2$, in which case the reduced χ^2_{red} value is $\chi^2_{red} = 0.43578$. Also the parameter α in this case is $\alpha = 3.32603 \text{Kpc}$.

In Table CX we present the optimized values of K_0 and ρ_0 for the analytic SIDM model of Eq. (3) for which the maximum compatibility with the SPARC data is achieved. In Figs. 178, 179 we present

TABLE CX: SIDM Optimization Values for the galaxy NGC4138

Parameter	Optimization Values
$\rho_0 (M_{\odot}/\text{Kpc}^3)$	5.01961×10^8
$K_0 (M_{\odot} \text{Kpc}^{-3} (\text{km/s})^2)$	17200.2

the density of the analytic SIDM model, the predicted rotation curves for the SIDM model (3), versus the SPARC observational data and the sound speed, as a function of the radius respectively. As it can be seen, for this galaxy, the SIDM model produces viable rotation curves which are compatible with the SPARC data.

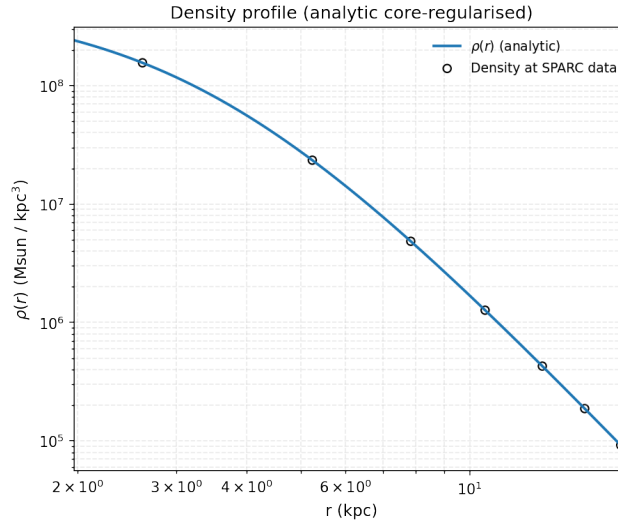


FIG. 178: The density of the SIDM model of Eq. (3) for the galaxy NGC4138, versus the radius.

58. The Galaxy NGC4157, Non-viable, Extended Viable

For this galaxy, the optimization method we used, ensures maximum compatibility of the analytic SIDM model of Eq. (3) with the SPARC data, if we choose $\rho_0 = 1.37718 \times 10^8 M_{\odot}/\text{Kpc}^3$ and $K_0 =$

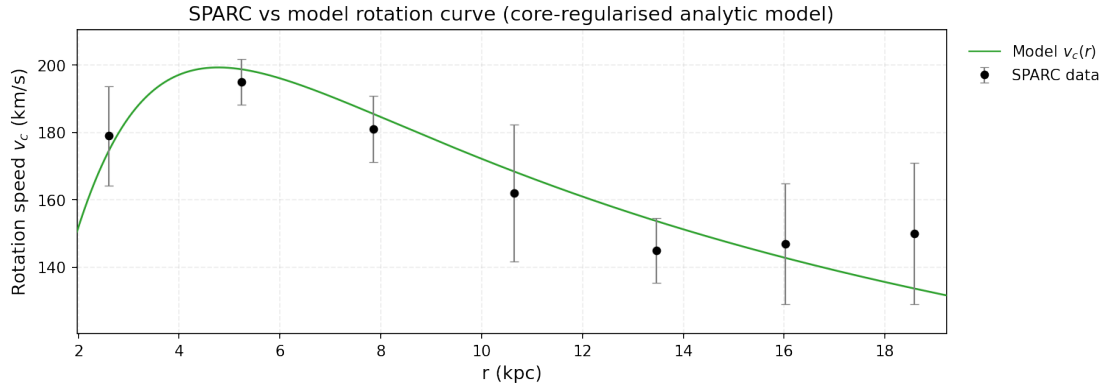


FIG. 179: The predicted rotation curves for the optimized SIDM model of Eq. (3), versus the SPARC observational data for the galaxy NGC4138.

$18971.8 M_{\odot} \text{Kpc}^{-3} (\text{km/s})^2$, in which case the reduced χ^2_{red} value is $\chi^2_{red} = 3.04141$. Also the parameter α in this case is $\alpha = 6.77345 \text{Kpc}$.

In Table CXI we present the optimized values of K_0 and ρ_0 for the analytic SIDM model of Eq. (3) for which the maximum compatibility with the SPARC data is achieved. In Figs. 180, 181 we present

TABLE CXI: SIDM Optimization Values for the galaxy NGC4157

Parameter	Optimization Values
$\rho_0 (M_{\odot}/\text{Kpc}^3)$	1.37718×10^8
$K_0 (M_{\odot} \text{Kpc}^{-3} (\text{km/s})^2)$	18971.8

the density of the analytic SIDM model, the predicted rotation curves for the SIDM model (3), versus the SPARC observational data and the sound speed, as a function of the radius respectively. As it can be seen, for this galaxy, the SIDM model produces non-viable rotation curves which are incompatible with the SPARC data.

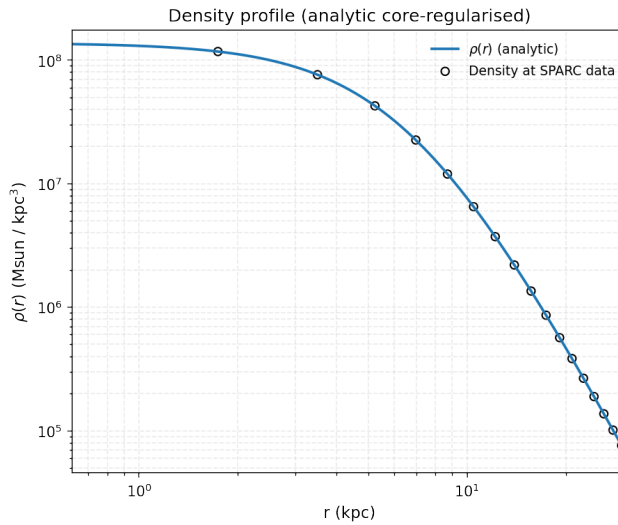


FIG. 180: The density of the SIDM model of Eq. (3) for the galaxy NGC4157, versus the radius.

Now we shall include contributions to the rotation velocity from the other components of the galaxy, namely the disk, the gas, and the bulge if present. In Fig. 182 we present the combined rotation curves including all the components of the galaxy along with the SIDM. As it can be seen, the extended collisional DM model is non-viable. Also in Table CXII we present the optimized values of the free parameters of the SIDM model for which we achieve the maximum compatibility with the SPARC data, for the galaxy NGC4157, and also the resulting reduced χ^2_{red} value.

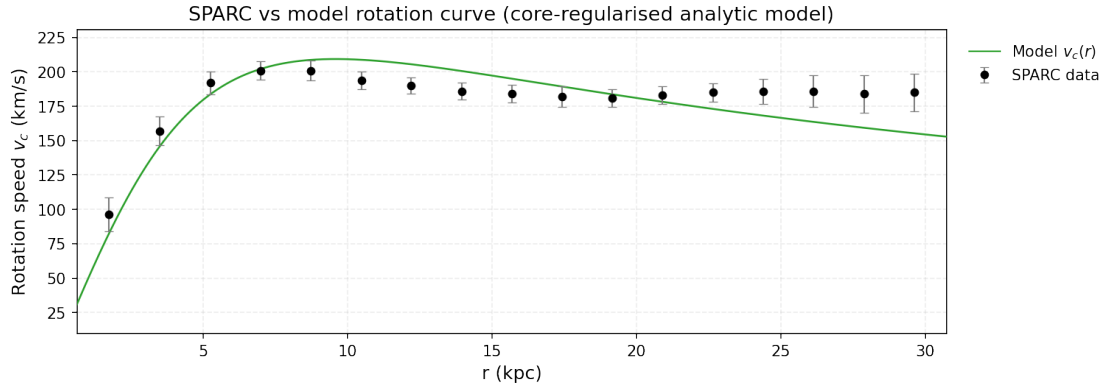


FIG. 181: The predicted rotation curves for the optimized SIDM model of Eq. (3), versus the SPARC observational data for the galaxy NGC4157.

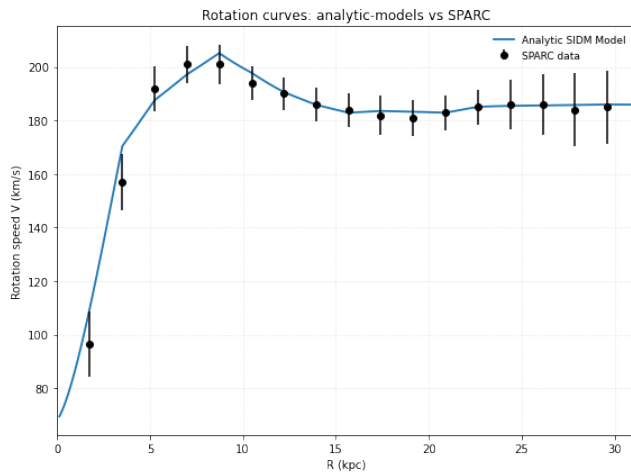


FIG. 182: The predicted rotation curves after using an optimization for the SIDM model (3), and the extended SPARC data for the galaxy NGC4157. We included the rotation curves of the gas, the disk velocities, the bulge (where present) along with the SIDM model.

TABLE CXII: Optimized Parameter Values of the Extended SIDM model for the Galaxy NGC4157.

Parameter	Value
$\rho_0 (M_\odot/\text{Kpc}^3)$	4.02447×10^6
$K_0 (M_\odot \text{ Kpc}^{-3} (\text{km/s})^2)$	11427.5
ml_{disk}	0.7542
ml_{bulge}	0.653
$\alpha (\text{Kpc})$	30.748
χ^2_{red}	0.329047

59. The Galaxy NGC4183, Non-viable

For this galaxy, the optimization method we used, ensures maximum compatibility of the analytic SIDM model of Eq. (3) with the SPARC data, if we choose $\rho_0 = 4.15754 \times 10^7 M_\odot/\text{Kpc}^3$ and $K_0 = 5923.15 M_\odot \text{ Kpc}^{-3} (\text{km/s})^2$, in which case the reduced χ^2_{red} value is $\chi^2_{\text{red}} = 1.72865$. Also the parameter α in this case is $\alpha = 6.88825 \text{ Kpc}$.

In Table CXIII we present the optimized values of K_0 and ρ_0 for the analytic SIDM model of Eq. (3) for which the maximum compatibility with the SPARC data is achieved. In Figs. 183, 184 we present the density of the analytic SIDM model, the predicted rotation curves for the SIDM model (3), versus the SPARC observational data and the sound speed, as a function of the radius respectively. As it can be seen, for this galaxy, the SIDM model produces non-viable rotation curves which are incompatible with the SPARC data.

TABLE CXIII: SIDM Optimization Values for the galaxy NGC4183

Parameter	Optimization Values
$\rho_0 (M_\odot/\text{Kpc}^3)$	4.15754×10^7
$K_0 (M_\odot \text{ Kpc}^{-3} (\text{km/s})^2)$	5923.15

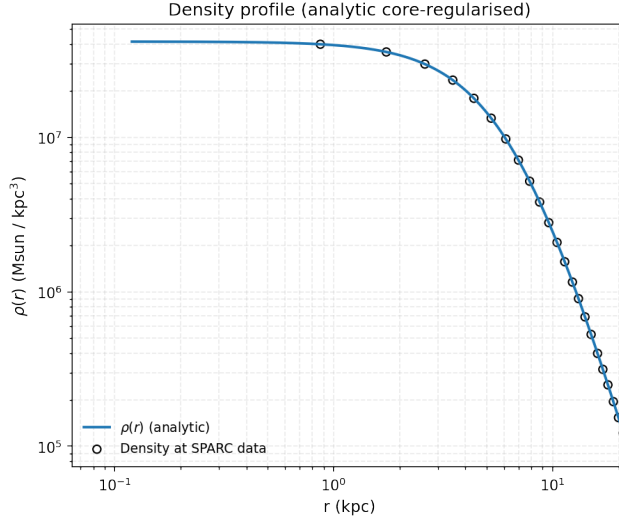


FIG. 183: The density of the SIDM model of Eq. (3) for the galaxy NGC4183, versus the radius.

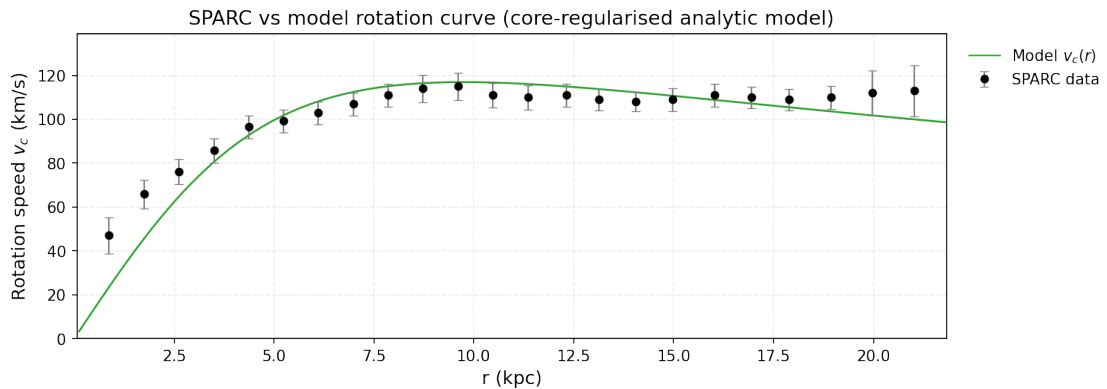


FIG. 184: The predicted rotation curves for the optimized SIDM model of Eq. (3), versus the SPARC observational data for the galaxy NGC4183.

Now we shall include contributions to the rotation velocity from the other components of the galaxy, namely the disk, the gas, and the bulge if present. In Fig. 185 we present the combined rotation curves including all the components of the galaxy along with the SIDM. As it can be seen, the extended collisional DM model is non-viable. Also in Table CXIV we present the optimized values of the free parameters of the SIDM model for which we achieve the maximum compatibility with the SPARC data, for the galaxy NGC4183, and also the resulting reduced χ^2_{red} value.

TABLE CXIV: Optimized Parameter Values of the Extended SIDM model for the Galaxy NGC4183.

Parameter	Value
$\rho_0 (M_\odot/\text{Kpc}^3)$	1.32016×10^7
$K_0 (M_\odot \text{ Kpc}^{-3} (\text{km/s})^2)$	3076.59
ml_{disk}	1
ml_{bulge}	0.0720
$\alpha (\text{Kpc})$	8.80883
χ^2_{red}	1.20285

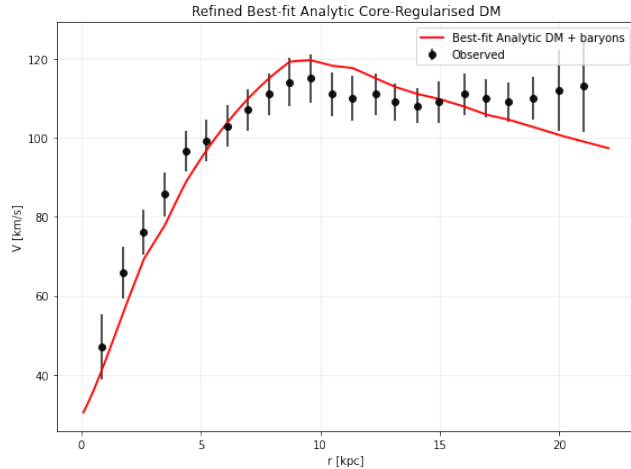


FIG. 185: The predicted rotation curves after using an optimization for the SIDM model (3), and the extended SPARC data for the galaxy NGC4183. We included the rotation curves of the gas, the disk velocities, the bulge (where present) along with the SIDM model.

60. The Galaxy NGC4217

For this galaxy, the optimization method we used, ensures maximum compatibility of the analytic SIDM model of Eq. (3) with the SPARC data, if we choose $\rho_0 = 1.84193 \times 10^8 M_\odot/\text{Kpc}^3$ and $K_0 = 16273.8 M_\odot \text{Kpc}^{-3} (\text{km/s})^2$, in which case the reduced χ^2_{red} value is $\chi^2_{red} = 1.04953$. Also the parameter α in this case is $\alpha = 5.42449 \text{Kpc}$.

In Table CXV we present the optimized values of K_0 and ρ_0 for the analytic SIDM model of Eq. (3) for which the maximum compatibility with the SPARC data is achieved. In Figs. 186, 187 we present

TABLE CXV: SIDM Optimization Values for the galaxy NGC4217

Parameter	Optimization Values
$\rho_0 (M_\odot/\text{Kpc}^3)$	5×10^7
$K_0 (M_\odot \text{Kpc}^{-3} (\text{km/s})^2)$	1250

the density of the analytic SIDM model, the predicted rotation curves for the SIDM model (3), versus the SPARC observational data and the sound speed, as a function of the radius respectively. As it can be seen, for this galaxy, the SIDM model produces marginally viable rotation curves which are marginally compatible with the SPARC data.

61. The Galaxy NGC4559, Non-viable, Extended Viable

For this galaxy, the optimization method we used, ensures maximum compatibility of the analytic SIDM model of Eq. (3) with the SPARC data, if we choose $\rho_0 = 4.10065 \times 10^7 M_\odot/\text{Kpc}^3$ and $K_0 = 6819.38 M_\odot \text{Kpc}^{-3} (\text{km/s})^2$, in which case the reduced χ^2_{red} value is $\chi^2_{red} = 2.81172$. Also the parameter α in this case is $\alpha = 7.44212 \text{Kpc}$.

In Table CXVI we present the optimized values of K_0 and ρ_0 for the analytic SIDM model of Eq. (3) for which the maximum compatibility with the SPARC data is achieved. In Figs. 188, 189 we present

TABLE CXVI: SIDM Optimization Values for the galaxy NGC4559

Parameter	Optimization Values
$\rho_0 (M_\odot/\text{Kpc}^3)$	4.10065×10^7
$K_0 (M_\odot \text{Kpc}^{-3} (\text{km/s})^2)$	6819.38

the density of the analytic SIDM model, the predicted rotation curves for the SIDM model (3), versus the SPARC observational data and the sound speed, as a function of the radius respectively. As it can

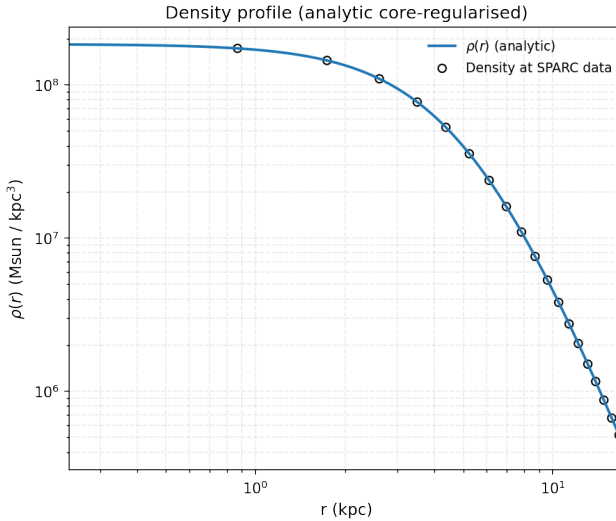


FIG. 186: The density of the SIDM model of Eq. (3) for the galaxy NGC4217, versus the radius.

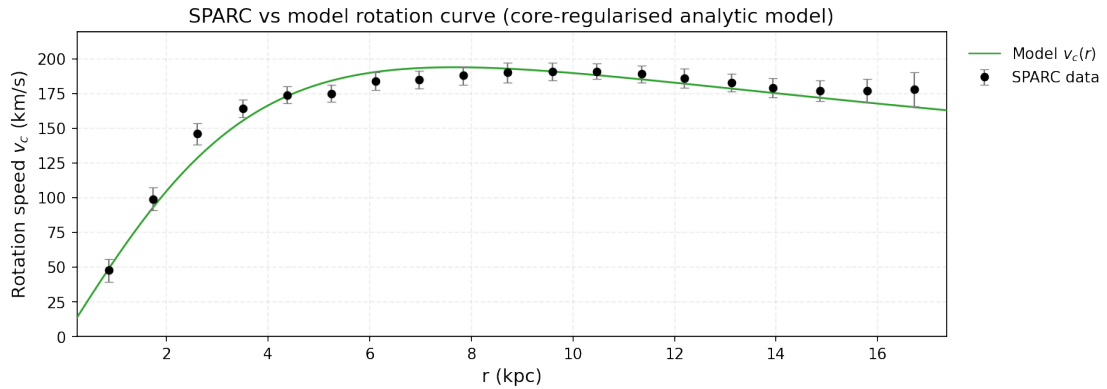


FIG. 187: The predicted rotation curves for the optimized SIDM model of Eq. (3), versus the SPARC observational data for the galaxy NGC4217.

be seen, for this galaxy, the SIDM model produces non-viable rotation curves which are incompatible with the SPARC data.

Now we shall include contributions to the rotation velocity from the other components of the galaxy, namely the disk, the gas, and the bulge if present. In Fig. 190 we present the combined rotation curves including all the components of the galaxy along with the SIDM. As it can be seen, the extended collisional DM model is non-viable. Also in Table CXVII we present the optimized values of the free parameters of the SIDM model for which we achieve the maximum compatibility with the SPARC data, for the galaxy NGC4559, and also the resulting reduced χ^2_{red} value.

TABLE CXVII: Optimized Parameter Values of the Extended SIDM model for the Galaxy NGC4559.

Parameter	Value
ρ_0 (M_\odot/Kpc^3)	7.1517×10^6
K_0 ($M_\odot \text{ Kpc}^{-3} (\text{km/s})^2$)	4169.72
ml_{disk}	0.7826
ml_{bulge}	0.1341
α (Kpc)	13.933
χ^2_{red}	0.15606

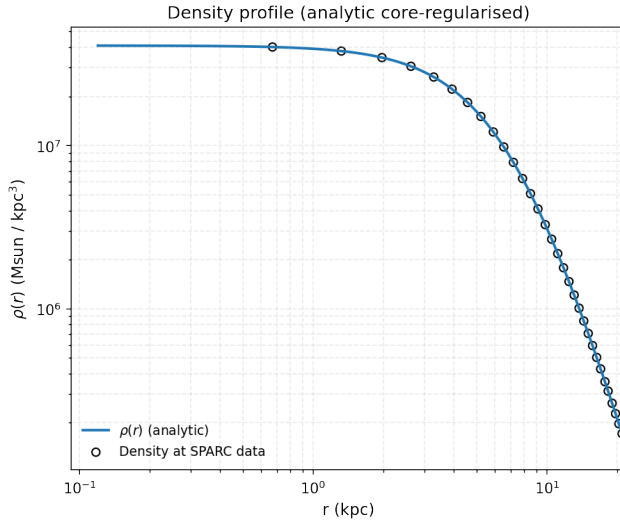


FIG. 188: The density of the SIDM model of Eq. (3) for the galaxy NGC4559, versus the radius.

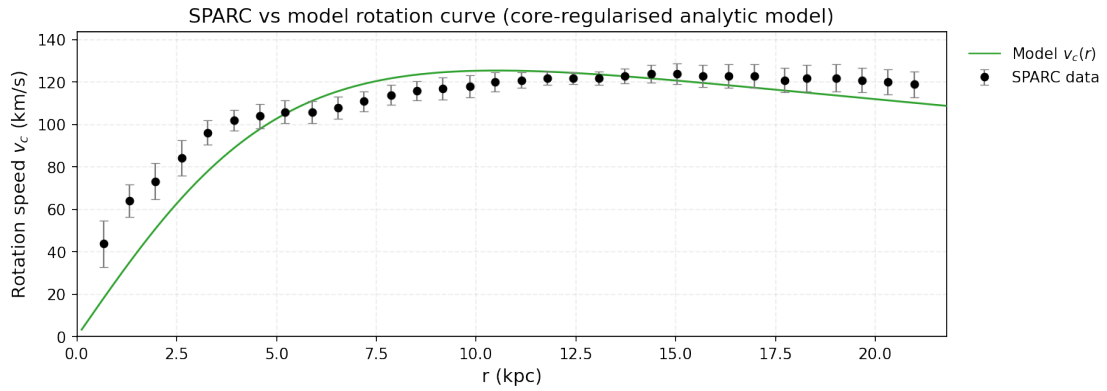


FIG. 189: The predicted rotation curves for the optimized SIDM model of Eq. (3), versus the SPARC observational data for the galaxy NGC4559.

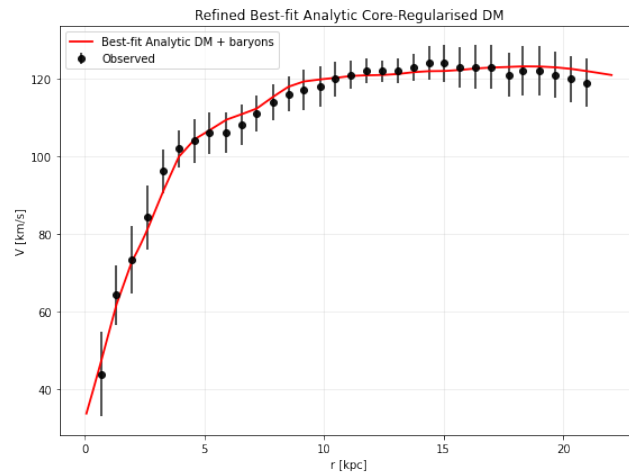


FIG. 190: The predicted rotation curves after using an optimization for the SIDM model (3), and the extended SPARC data for the galaxy NGC4559. We included the rotation curves of the gas, the disk velocities, the bulge (where present) along with the SIDM model.

62. The Galaxy NGC5005, Non-viable, Extended Viable

For this galaxy, the optimization method we used, ensures maximum compatibility of the analytic SIDM model of Eq. (3) with the SPARC data, if we choose $\rho_0 = 1.1626 \times 10^9 M_\odot/\text{Kpc}^3$ and $K_0 = 35101.4 M_\odot \text{Kpc}^{-3} (\text{km/s})^2$, in which case the reduced χ^2_{red} value is $\chi^2_{red} = 4.28754$. Also the parameter α in this case is $\alpha = 3.17101 \text{Kpc}$.

In Table CXVIII we present the optimized values of K_0 and ρ_0 for the analytic SIDM model of Eq. (3) for which the maximum compatibility with the SPARC data is achieved. In Figs. 191, 192 we present

TABLE CXVIII: SIDM Optimization Values for the galaxy NGC5005

Parameter	Optimization Values
$\rho_0 (M_\odot/\text{Kpc}^3)$	1.1626×10^9
$K_0 (M_\odot \text{Kpc}^{-3} (\text{km/s})^2)$	35101.4

the density of the analytic SIDM model, the predicted rotation curves for the SIDM model (3), versus the SPARC observational data and the sound speed, as a function of the radius respectively. As it can be seen, for this galaxy, the SIDM model produces non-viable rotation curves which are incompatible with the SPARC data.

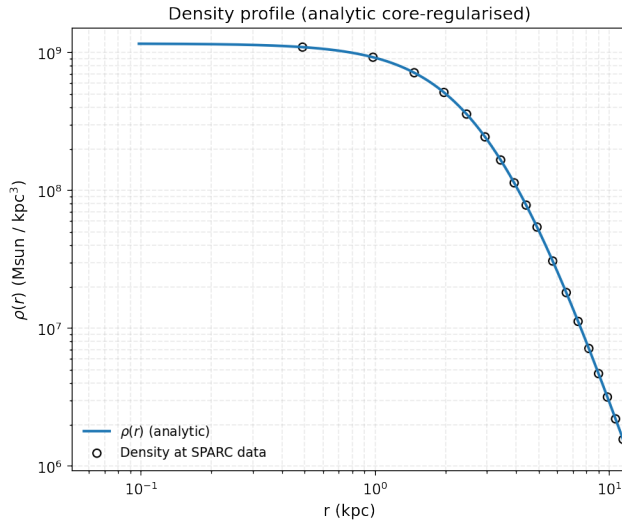


FIG. 191: The density of the SIDM model of Eq. (3) for the galaxy NGC5005, versus the radius.

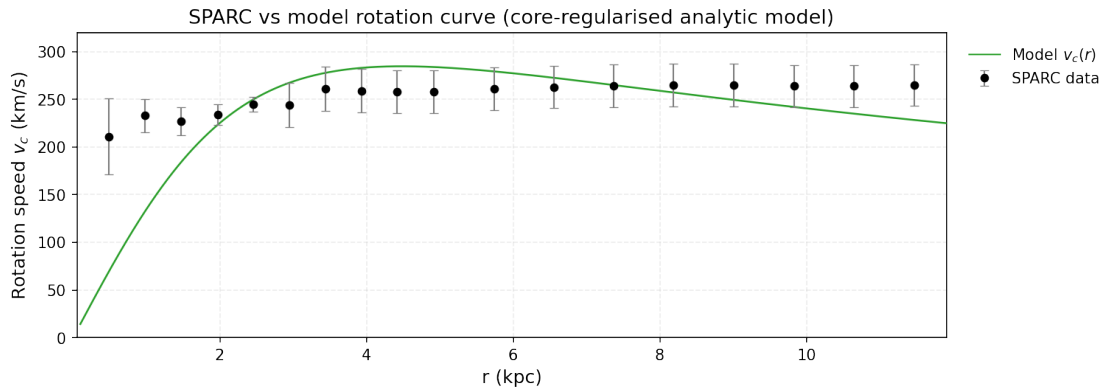


FIG. 192: The predicted rotation curves for the optimized SIDM model of Eq. (3), versus the SPARC observational data for the galaxy NGC5005.

Now we shall include contributions to the rotation velocity from the other components of the galaxy, namely the disk, the gas, and the bulge if present. In Fig. 193 we present the combined rotation curves

including all the components of the galaxy along with the SIDM. As it can be seen, the extended collisional DM model is viable. Also in Table CXIX we present the optimized values of the free parameters of the

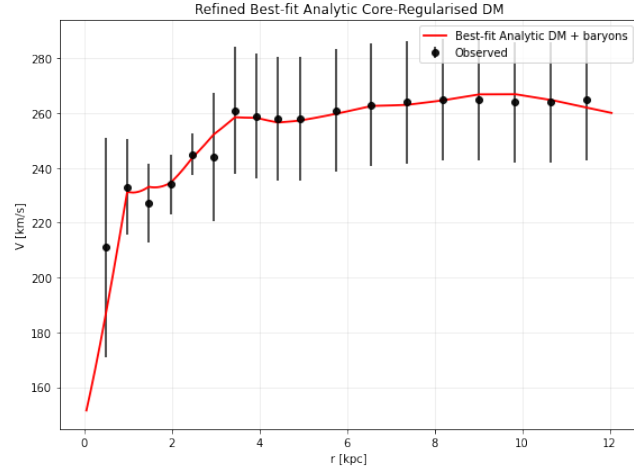


FIG. 193: The predicted rotation curves after using an optimization for the SIDM model (3), and the extended SPARC data for the galaxy NGC5005. We included the rotation curves of the gas, the disk velocities, the bulge (where present) along with the SIDM model.

SIDM model for which we achieve the maximum compatibility with the SPARC data, for the galaxy NGC5005, and also the resulting reduced χ^2_{red} value.

TABLE CXIX: Optimized Parameter Values of the Extended SIDM model for the Galaxy NGC5005.

Parameter	Value
$\rho_0 (M_\odot/\text{Kpc}^3)$	1.51217×10^7
$K_0 (M_\odot \text{ Kpc}^{-3} (\text{km/s})^2)$	17393.3
ml_{disk}	0.7760
ml_{bulge}	0.348
$\alpha (\text{Kpc})$	19.5698
χ^2_{red}	0.0565593

63. The Galaxy NGC5033, Non-viable

For this galaxy, the optimization method we used, ensures maximum compatibility of the analytic SIDM model of Eq. (3) with the SPARC data, if we choose $\rho_0 = 1.1056 \times 10^8 M_\odot/\text{Kpc}^3$ and $K_0 = 26887.6 M_\odot \text{ Kpc}^{-3} (\text{km/s})^2$, in which case the reduced χ^2_{red} value is $\chi^2_{red} = 59.3191$. Also the parameter α in this case is $\alpha = 8.99971 \text{ Kpc}$.

In Table CXX we present the optimized values of K_0 and ρ_0 for the analytic SIDM model of Eq. (3) for which the maximum compatibility with the SPARC data is achieved. In Figs. 194, 195 we present

TABLE CXX: SIDM Optimization Values for the galaxy NGC5033

Parameter	Optimization Values
$\rho_0 (M_\odot/\text{Kpc}^3)$	1.1056×10^8
$K_0 (M_\odot \text{ Kpc}^{-3} (\text{km/s})^2)$	26887.6

the density of the analytic SIDM model, the predicted rotation curves for the SIDM model (3), versus the SPARC observational data and the sound speed, as a function of the radius respectively. As it can be seen, for this galaxy, the SIDM model produces non-viable rotation curves which are incompatible with the SPARC data.

Now we shall include contributions to the rotation velocity from the other components of the galaxy, namely the disk, the gas, and the bulge if present. In Fig. 196 we present the combined rotation curves including all the components of the galaxy along with the SIDM. As it can be seen, the extended

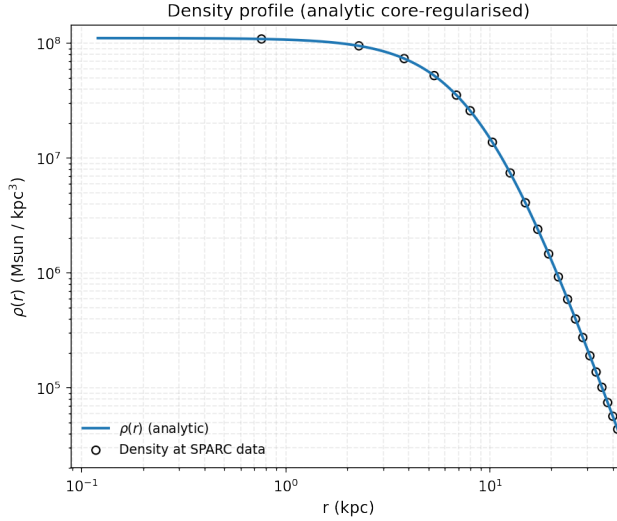


FIG. 194: The density of the SIDM model of Eq. (3) for the galaxy NGC5033, versus the radius.

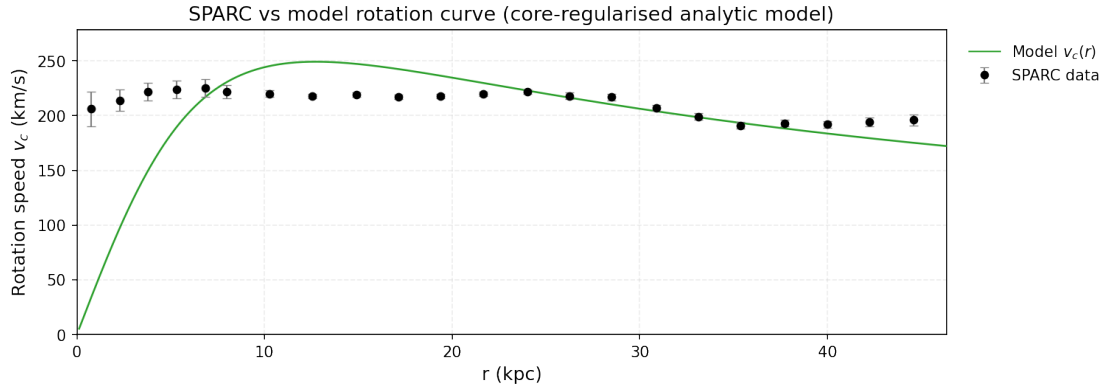


FIG. 195: The predicted rotation curves for the optimized SIDM model of Eq. (3), versus the SPARC observational data for the galaxy NGC5033.

collisional DM model is non-viable. Also in Table CXXI we present the optimized values of the free

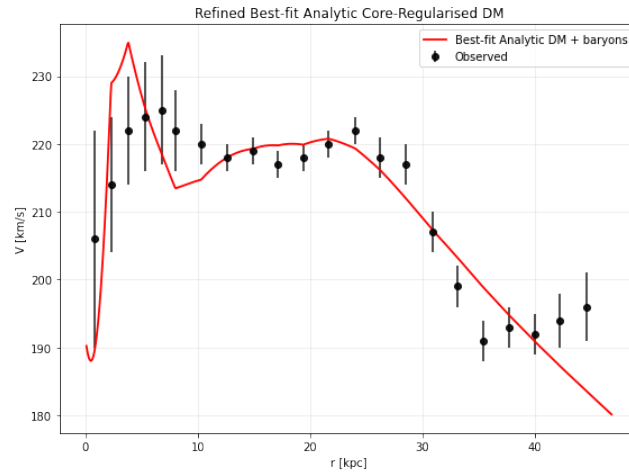


FIG. 196: The predicted rotation curves after using an optimization for the SIDM model (3), and the extended SPARC data for the galaxy NGC5033. We included the rotation curves of the gas, the disk velocities, the bulge (where present) along with the SIDM model.

parameters of the SIDM model for which we achieve the maximum compatibility with the SPARC data, for the galaxy NGC5033, and also the resulting reduced χ^2_{red} value.

TABLE CXXI: Optimized Parameter Values of the Extended SIDM model for the Galaxy NGC5033.

Parameter	Value
$\rho_0 (M_\odot/\text{Kpc}^3)$	1.57462×10^7
$K_0 (M_\odot \text{ Kpc}^{-3} (\text{km/s})^2)$	13356.2
ml_{disk}	0.8484
ml_{bulge}	0.6147
$\alpha (\text{Kpc})$	16.8055
χ^2_{red}	2.12808

64. The Galaxy NGC5055, Non-viable

For this galaxy, the optimization method we used, ensures maximum compatibility of the analytic SIDM model of Eq. (3) with the SPARC data, if we choose $\rho_0 = 6.4709 \times 10^7 M_\odot/\text{Kpc}^3$ and $K_0 = 23160.6 M_\odot \text{ Kpc}^{-3} (\text{km/s})^2$, in which case the reduced χ^2_{red} value is $\chi^2_{red} = 900.8$. Also the parameter α in this case is $\alpha = 10.918 \text{ Kpc}$.

In Table CXXII we present the optimized values of K_0 and ρ_0 for the analytic SIDM model of Eq. (3) for which the maximum compatibility with the SPARC data is achieved. In Figs. 197, 198 we present

TABLE CXXII: SIDM Optimization Values for the galaxy NGC5055

Parameter	Optimization Values
$\rho_0 (M_\odot/\text{Kpc}^3)$	6.4709×10^7
$K_0 (M_\odot \text{ Kpc}^{-3} (\text{km/s})^2)$	23160.6

the density of the analytic SIDM model, the predicted rotation curves for the SIDM model (3), versus the SPARC observational data and the sound speed, as a function of the radius respectively. As it can be seen, for this galaxy, the SIDM model produces non-viable rotation curves which are incompatible with the SPARC data.

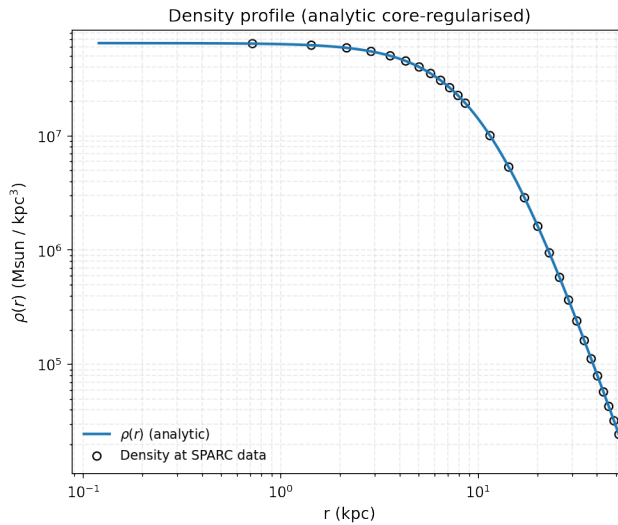


FIG. 197: The density of the SIDM model of Eq. (3) for the galaxy NGC5055, versus the radius.

Now we shall include contributions to the rotation velocity from the other components of the galaxy, namely the disk, the gas, and the bulge if present. In Fig. 199 we present the combined rotation curves including all the components of the galaxy along with the SIDM. As it can be seen, the extended collisional DM model is non-viable. Also in Table CXXIII we present the optimized values of the free

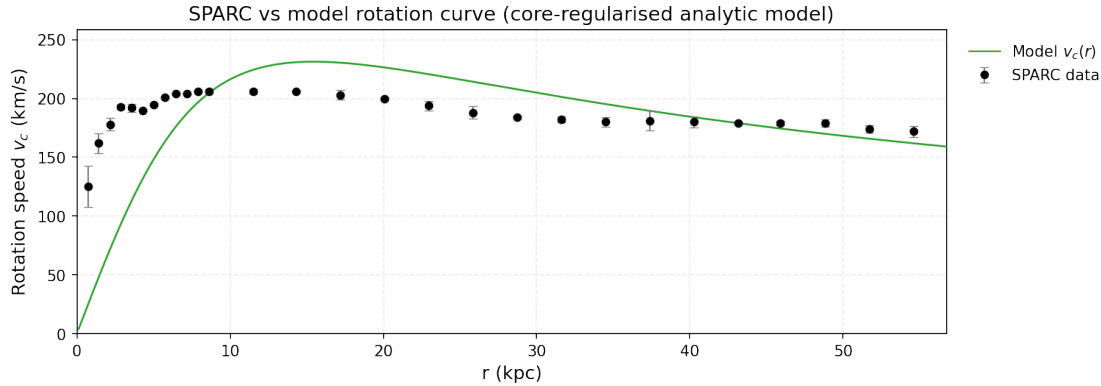


FIG. 198: The predicted rotation curves for the optimized SIDM model of Eq. (3), versus the SPARC observational data for the galaxy NGC5055.

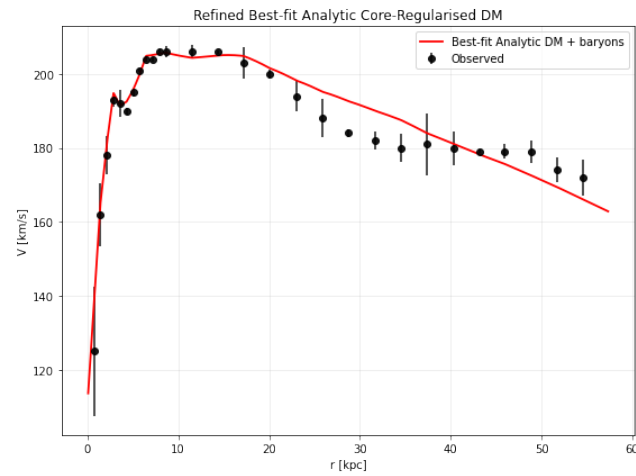


FIG. 199: The predicted rotation curves after using an optimization for the SIDM model (3), and the extended SPARC data for the galaxy NGC5055. We included the rotation curves of the gas, the disk velocities, the bulge (where present) along with the SIDM model.

parameters of the SIDM model for which we achieve the maximum compatibility with the SPARC data, for the galaxy NGC5055, and also the resulting reduced χ^2_{red} value.

TABLE CXXIII: Optimized Parameter Values of the Extended SIDM model for the Galaxy NGC5055.

Parameter	Value
ρ_0 (M_\odot/Kpc^3)	7.63898×10^6
K_0 ($M_\odot \text{ Kpc}^{-3} (\text{km/s})^2$)	10626.9
ml_{disk}	0.6838
ml_{bulge}	0.1214
α (Kpc)	21.5219
χ^2_{red}	4.79553

65. The Galaxy NGC5371, Non-viable

For this galaxy, the optimization method we used, ensures maximum compatibility of the analytic SIDM model of Eq. (3) with the SPARC data, if we choose $\rho_0 = 9.64957 \times 10^7 M_\odot/\text{Kpc}^3$ and $K_0 = 28585.2 M_\odot \text{ Kpc}^{-3} (\text{km/s})^2$, in which case the reduced χ^2_{red} value is $\chi^2_{red} = 47.002$. Also the parameter α in this case is $\alpha = 9.9327 \text{ Kpc}$.

In Table CXXIV we present the optimized values of K_0 and ρ_0 for the analytic SIDM model of Eq. (3) for which the maximum compatibility with the SPARC data is achieved. In Figs. 200, 201 we present

TABLE CXXIV: SIDM Optimization Values for the galaxy NGC5371

Parameter	Optimization Values
$\rho_0 (M_\odot/\text{Kpc}^3)$	9.64957×10^7
$K_0 (M_\odot \text{ Kpc}^{-3} (\text{km/s})^2)$	28585.2

the density of the analytic SIDM model, the predicted rotation curves for the SIDM model (3), versus the SPARC observational data and the sound speed, as a function of the radius respectively. As it can be seen, for this galaxy, the SIDM model produces non-viable rotation curves which are incompatible with the SPARC data.

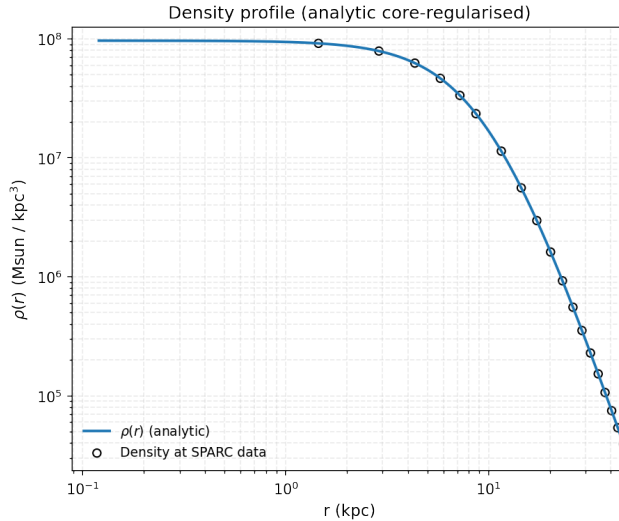


FIG. 200: The density of the SIDM model of Eq. (3) for the galaxy NGC5371, versus the radius.

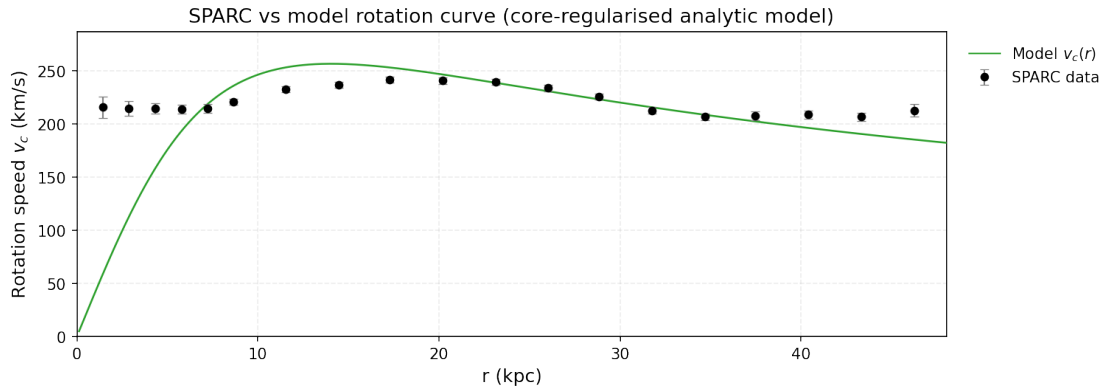


FIG. 201: The predicted rotation curves for the optimized SIDM model of Eq. (3), versus the SPARC observational data for the galaxy NGC5371.

Now we shall include contributions to the rotation velocity from the other components of the galaxy, namely the disk, the gas, and the bulge if present. In Fig. 202 we present the combined rotation curves including all the components of the galaxy along with the SIDM. As it can be seen, the extended collisional DM model is non-viable. Also in Table CXXV we present the optimized values of the free parameters of the SIDM model for which we achieve the maximum compatibility with the SPARC data, for the galaxy NGC5371, and also the resulting reduced χ^2_{red} value.

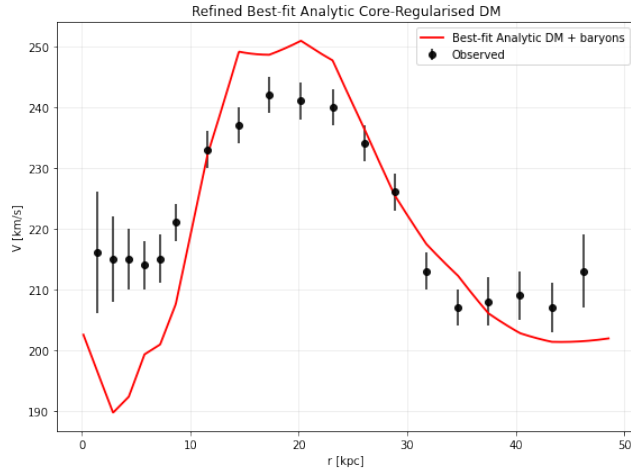


FIG. 202: The predicted rotation curves after using an optimization for the SIDM model (3), and the extended SPARC data for the galaxy NGC5371. We included the rotation curves of the gas, the disk velocities, the bulge (where present) along with the SIDM model.

TABLE CXXV: Optimized Parameter Values of the Extended SIDM model for the Galaxy NGC5371.

Parameter	Value
ρ_0 (M_\odot/Kpc^3)	4.3558×10^7
K_0 ($M_\odot \text{ Kpc}^{-3} (\text{km/s})^2$)	40678
m_{disk}	0.8149
m_{bulge}	0.567
α (Kpc)	58.3994
χ^2_{red}	9.09415

66. The Galaxy NGC5585, Non-viable

For this galaxy, the optimization method we used, ensures maximum compatibility of the analytic SIDM model of Eq. (3) with the SPARC data, if we choose $\rho_0 = 4.78164 \times 10^7 M_\odot/\text{Kpc}^3$ and $K_0 = 3635.48 M_\odot \text{ Kpc}^{-3} (\text{km/s})^2$, in which case the reduced χ^2_{red} value is $\chi^2_{\text{red}} = 51.6287$. Also the parameter α in this case is $\alpha = 5.03203 \text{ Kpc}$.

In Table CXXVI we present the optimized values of K_0 and ρ_0 for the analytic SIDM model of Eq. (3) for which the maximum compatibility with the SPARC data is achieved. In Figs. 203, 204 we present

TABLE CXXVI: SIDM Optimization Values for the galaxy NGC5585

Parameter	Optimization Values
ρ_0 (M_\odot/Kpc^3)	4.78164×10^7
K_0 ($M_\odot \text{ Kpc}^{-3} (\text{km/s})^2$)	3635.48

the density of the analytic SIDM model, the predicted rotation curves for the SIDM model (3), versus the SPARC observational data and the sound speed, as a function of the radius respectively. As it can be seen, for this galaxy, the SIDM model produces non-viable rotation curves which are incompatible with the SPARC data.

Now we shall include contributions to the rotation velocity from the other components of the galaxy, namely the disk, the gas, and the bulge if present. In Fig. 205 we present the combined rotation curves including all the components of the galaxy along with the SIDM. As it can be seen, the extended collisional DM model is non-viable. Also in Table CXXVII we present the optimized values of the free parameters of the SIDM model for which we achieve the maximum compatibility with the SPARC data, for the galaxy NGC5585, and also the resulting reduced χ^2_{red} value.

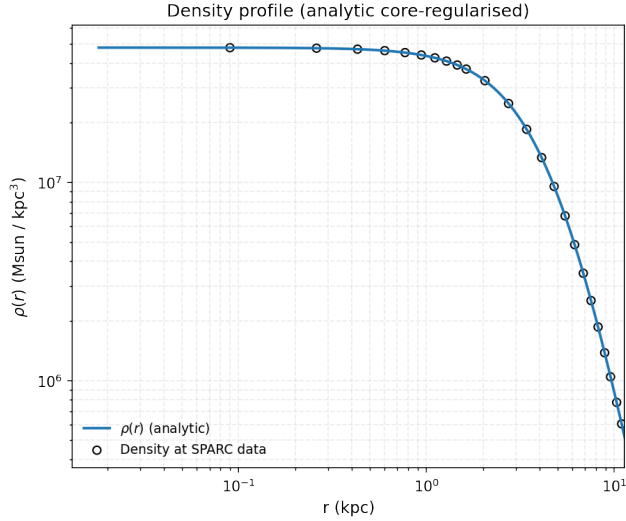


FIG. 203: The density of the SIDM model of Eq. (3) for the galaxy NGC5585, versus the radius.

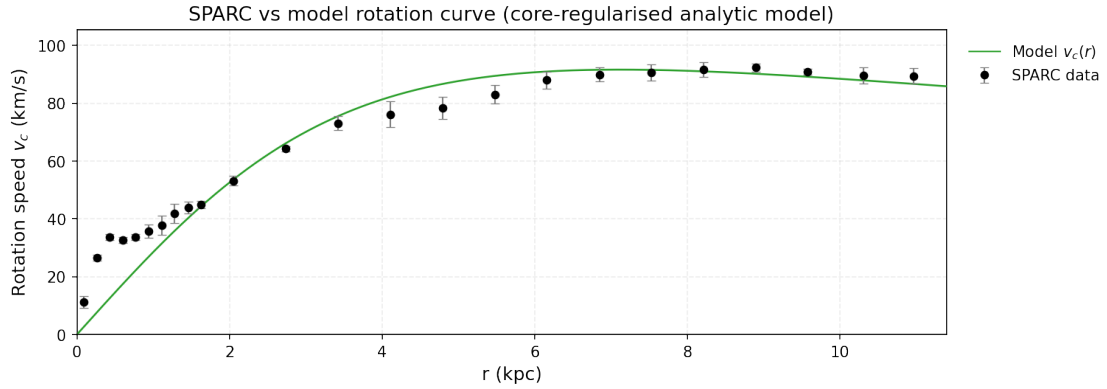


FIG. 204: The predicted rotation curves for the optimized SIDM model of Eq. (3), versus the SPARC observational data for the galaxy NGC5585.

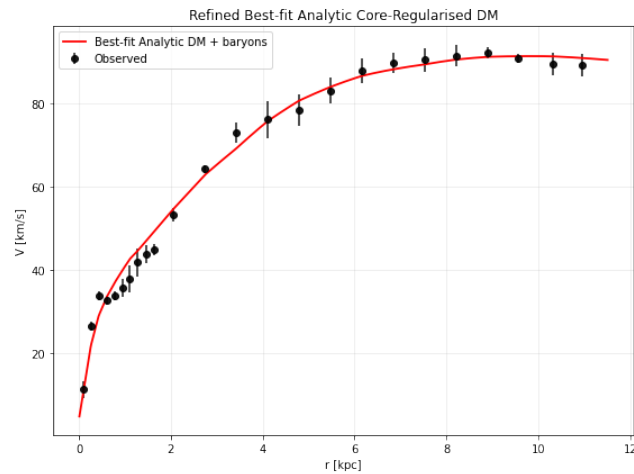


FIG. 205: The predicted rotation curves after using an optimization for the SIDM model (3), and the extended SPARC data for the galaxy NGC5585. We included the rotation curves of the gas, the disk velocities, the bulge (where present) along with the SIDM model.

TABLE CXXVII: Optimized Parameter Values of the Extended SIDM model for the Galaxy NGC5585.

Parameter	Value
$\rho_0 (M_\odot/\text{Kpc}^3)$	1.65374×10^7
$K_0 (M_\odot \text{ Kpc}^{-3} (\text{km/s})^2)$	2801.69
ml_{disk}	0.7915
ml_{bulge}	0.2957
$\alpha (\text{Kpc})$	7.51057
χ^2_{red}	4.01573

67. The Galaxy NGC5907, Non-viable

For this galaxy, the optimization method we used, ensures maximum compatibility of the analytic SIDM model of Eq. (3) with the SPARC data, if we choose $\rho_0 = 7.04918 \times 10^7 M_\odot/\text{Kpc}^3$ and $K_0 = 26855.6 M_\odot \text{ Kpc}^{-3} (\text{km/s})^2$, in which case the reduced χ^2_{red} value is $\chi^2_{\text{red}} = 34.0134$. Also the parameter α in this case is $\alpha = 11.2642 \text{ Kpc}$.

In Table CXXVIII we present the optimized values of K_0 and ρ_0 for the analytic SIDM model of Eq. (3) for which the maximum compatibility with the SPARC data is achieved. In Figs. 206, 207 we present

TABLE CXXVIII: SIDM Optimization Values for the galaxy NGC5907

Parameter	Optimization Values
$\rho_0 (M_\odot/\text{Kpc}^3)$	7.04918×10^7
$K_0 (M_\odot \text{ Kpc}^{-3} (\text{km/s})^2)$	26855.6

the density of the analytic SIDM model, the predicted rotation curves for the SIDM model (3), versus the SPARC observational data and the sound speed, as a function of the radius respectively. As it can be seen, for this galaxy, the SIDM model produces non-viable rotation curves which are incompatible with the SPARC data.

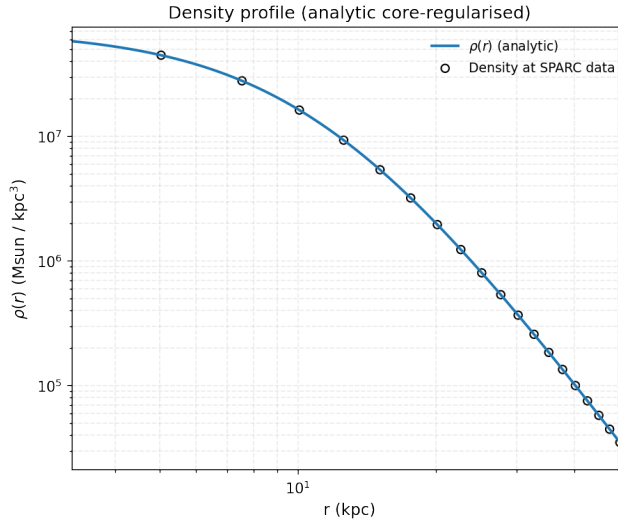


FIG. 206: The density of the SIDM model of Eq. (3) for the galaxy NGC5907, versus the radius.

Now we shall include contributions to the rotation velocity from the other components of the galaxy, namely the disk, the gas, and the bulge if present. In Fig. 208 we present the combined rotation curves including all the components of the galaxy along with the SIDM. As it can be seen, the extended collisional DM model is non-viable. Also in Table CXXIX we present the optimized values of the free parameters of the SIDM model for which we achieve the maximum compatibility with the SPARC data, for the galaxy NGC5907, and also the resulting reduced χ^2_{red} value.

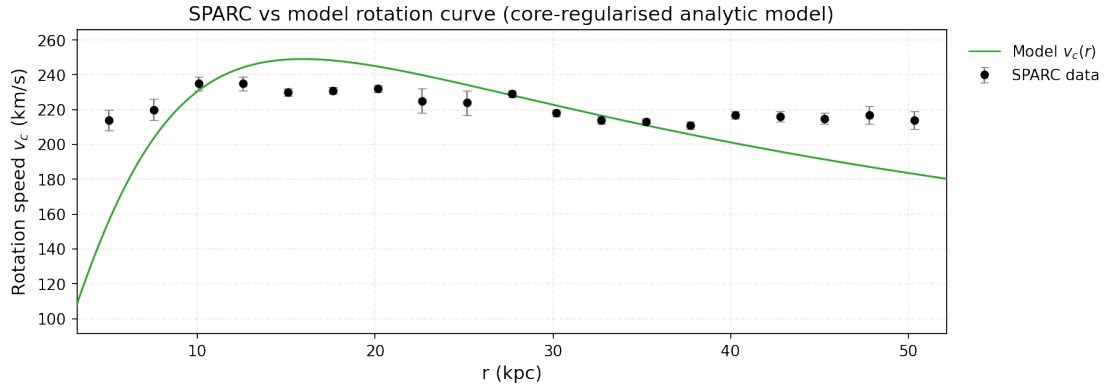


FIG. 207: The predicted rotation curves for the optimized SIDM model of Eq. (3), versus the SPARC observational data for the galaxy NGC5907.

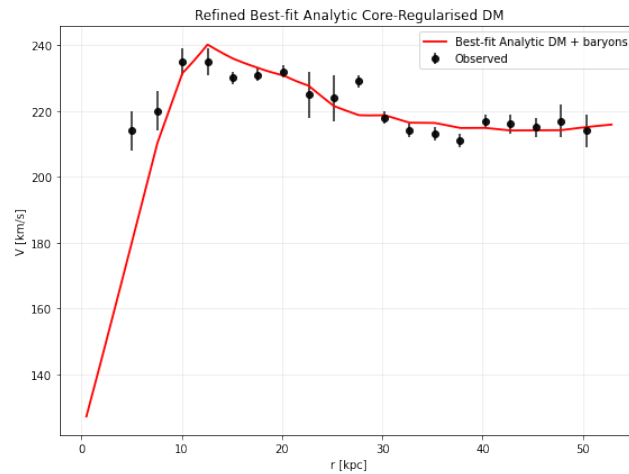


FIG. 208: The predicted rotation curves after using an optimization for the SIDM model (3), and the extended SPARC data for the galaxy NGC5907. We included the rotation curves of the gas, the disk velocities, the bulge (where present) along with the SIDM model.

TABLE CXXIX: Optimized Parameter Values of the Extended SIDM model for the Galaxy NGC5907.

Parameter	Value
$\rho_0 (M_\odot/\text{Kpc}^3)$	1.29681×10^6
$K_0 (M_\odot \text{ Kpc}^{-3} (\text{km/s})^2)$	13880.2
ml_{disk}	0.9975
ml_{bulge}	0.6240
$\alpha (\text{Kpc})$	59.6974
χ^2_{red}	5.62445

68. The Galaxy NGC5985, Non-viable

For this galaxy, the optimization method we used, ensures maximum compatibility of the analytic SIDM model of Eq. (3) with the SPARC data, if we choose $\rho_0 = 1.73176 \times 10^8 M_\odot/\text{Kpc}^3$ and $K_0 = 42340 M_\odot \text{ Kpc}^{-3} (\text{km/s})^2$, in which case the reduced χ^2_{red} value is $\chi^2_{\text{red}} = 14.2938$. Also the parameter α in this case is $\alpha = 9.02365 \text{ Kpc}$.

In Table CXXX we present the optimized values of K_0 and ρ_0 for the analytic SIDM model of Eq. (3) for which the maximum compatibility with the SPARC data is achieved. In Figs. 209, 210 we present the density of the analytic SIDM model, the predicted rotation curves for the SIDM model (3), versus the SPARC observational data and the sound speed, as a function of the radius respectively. As it can be seen, for this galaxy, the SIDM model produces non-viable rotation curves which are incompatible with the SPARC data.

TABLE CXXX: SIDM Optimization Values for the galaxy NGC5985

Parameter	Optimization Values
$\rho_0 (M_\odot/\text{Kpc}^3)$	1.73176×10^8
$K_0 (M_\odot \text{ Kpc}^{-3} (\text{km/s})^2)$	42340

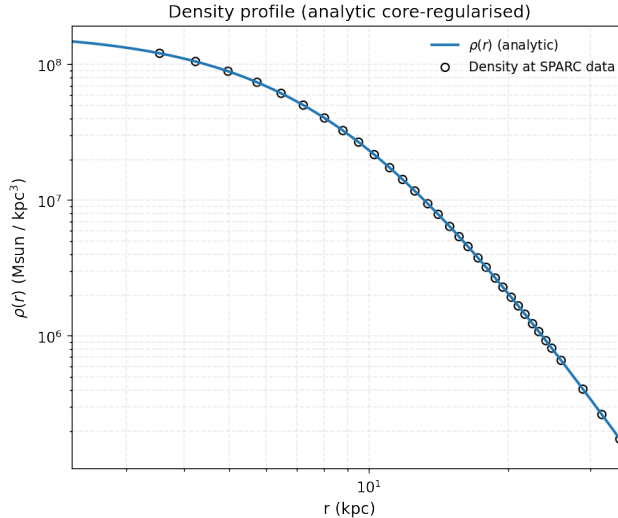


FIG. 209: The density of the SIDM model of Eq. (3) for the galaxy NGC5985, versus the radius.

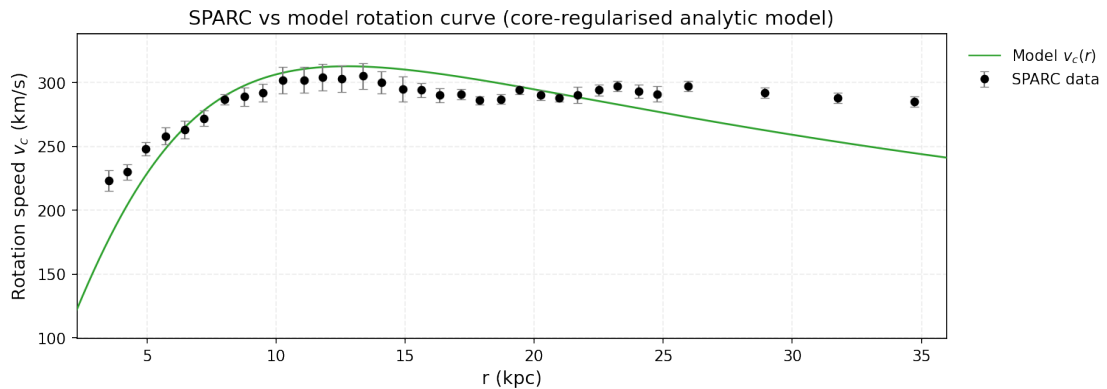


FIG. 210: The predicted rotation curves for the optimized SIDM model of Eq. (3), versus the SPARC observational data for the galaxy NGC5985.

Now we shall include contributions to the rotation velocity from the other components of the galaxy, namely the disk, the gas, and the bulge if present. In Fig. 211 we present the combined rotation curves including all the components of the galaxy along with the SIDM. As it can be seen, the extended collisional DM model is non-viable. Also in Table CXXXI we present the optimized values of the free parameters of the SIDM model for which we achieve the maximum compatibility with the SPARC data, for the galaxy NGC5985, and also the resulting reduced χ^2_{red} value.

TABLE CXXXI: Optimized Parameter Values of the Extended SIDM model for the Galaxy NGC5985.

Parameter	Value
$\rho_0 (M_\odot/\text{Kpc}^3)$	1.35395×10^8
$K_0 (M_\odot \text{ Kpc}^{-3} (\text{km/s})^2)$	40097.1
ml_{disk}	1
ml_{bulge}	1
$\alpha (\text{Kpc})$	9.9300
χ^2_{red}	10.2045

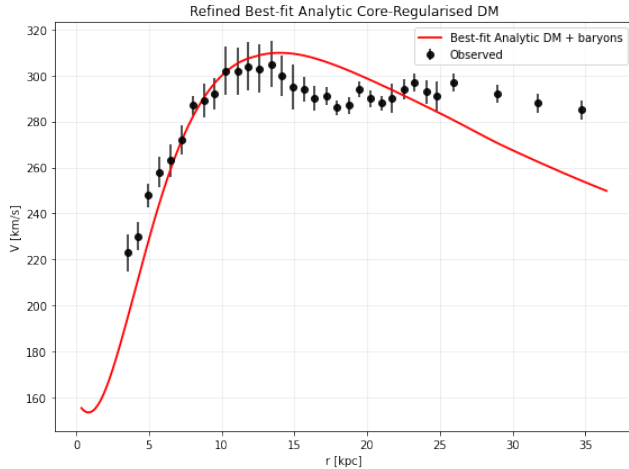


FIG. 211: The predicted rotation curves after using an optimization for the SIDM model (3), and the extended SPARC data for the galaxy NGC5985. We included the rotation curves of the gas, the disk velocities, the bulge (where present) along with the SIDM model.

69. The Galaxy NGC6015, Non-viable

For this galaxy, the optimization method we used, ensures maximum compatibility of the analytic SIDM model of Eq. (3) with the SPARC data, if we choose $\rho_0 = 1.38858 \times 10^8 M_\odot/\text{Kpc}^3$ and $K_0 = 15142 M_\odot \text{Kpc}^{-3} (\text{km/s})^2$, in which case the reduced χ^2_{red} value is $\chi^2_{\text{red}} = 59.7361$. Also the parameter α in this case is $\alpha = 6.0264 \text{Kpc}$.

In Table CXXXII we present the optimized values of K_0 and ρ_0 for the analytic SIDM model of Eq. (3) for which the maximum compatibility with the SPARC data is achieved. In Figs. 212, 213 we present

TABLE CXXXII: SIDM Optimization Values for the galaxy NGC6015

Parameter	Optimization Values
$\rho_0 (M_\odot/\text{Kpc}^3)$	1.38858×10^8
$K_0 (M_\odot \text{Kpc}^{-3} (\text{km/s})^2)$	15142

the density of the analytic SIDM model, the predicted rotation curves for the SIDM model (3), versus the SPARC observational data and the sound speed, as a function of the radius respectively. As it can be seen, for this galaxy, the SIDM model produces non-viable rotation curves which are incompatible with the SPARC data.

Now we shall include contributions to the rotation velocity from the other components of the galaxy, namely the disk, the gas, and the bulge if present. In Fig. 214 we present the combined rotation curves including all the components of the galaxy along with the SIDM. As it can be seen, the extended collisional DM model is non-viable. Also in Table CXXXIII we present the optimized values of the free parameters of the SIDM model for which we achieve the maximum compatibility with the SPARC data, for the galaxy NGC6015, and also the resulting reduced χ^2_{red} value.

TABLE CXXXIII: Optimized Parameter Values of the Extended SIDM model for the Galaxy NGC6015.

Parameter	Value
$\rho_0 (M_\odot/\text{Kpc}^3)$	5.11985×10^8
$K_0 (M_\odot \text{Kpc}^{-3} (\text{km/s})^2)$	7447.45
ml_{disk}	1
ml_{bulge}	0.6368
$\alpha (\text{Kpc})$	22.0075
χ^2_{red}	10.2067

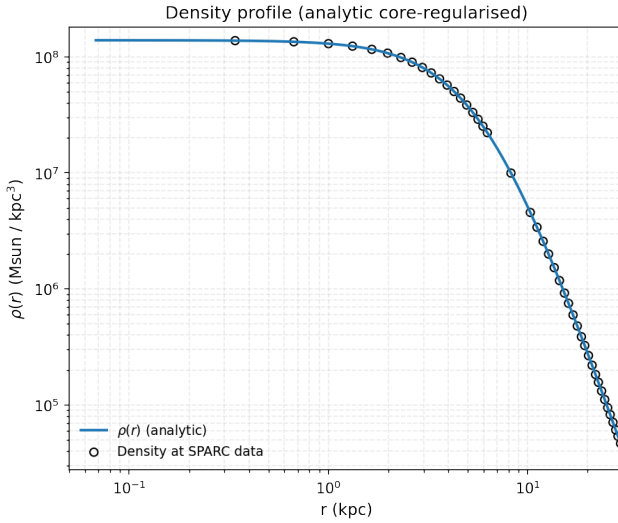


FIG. 212: The density of the SIDM model of Eq. (3) for the galaxy NGC6015, versus the radius.

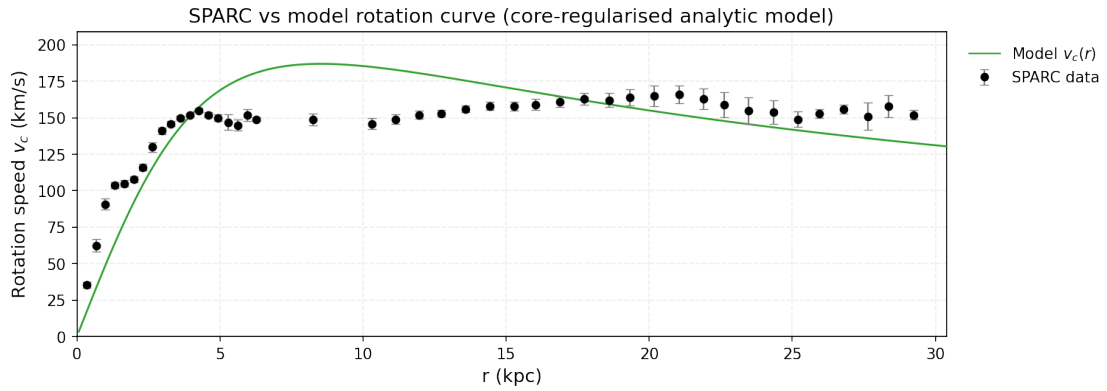


FIG. 213: The predicted rotation curves for the optimized SIDM model of Eq. (3), versus the SPARC observational data for the galaxy NGC6015.

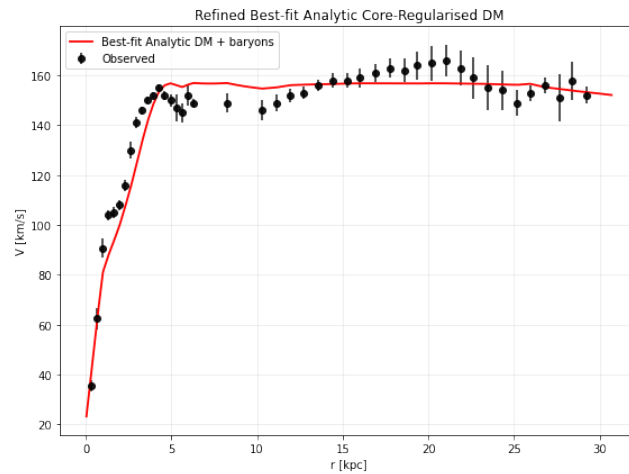


FIG. 214: The predicted rotation curves after using an optimization for the SIDM model (3), and the extended SPARC data for the galaxy NGC6015. We included the rotation curves of the gas, the disk velocities, the bulge (where present) along with the SIDM model.

70. The Galaxy NGC6195, Non-viable, Extended Viable

For this galaxy, the optimization method we used, ensures maximum compatibility of the analytic SIDM model of Eq. (3) with the SPARC data, if we choose $\rho_0 = 1.66739 \times 10^8 M_\odot/\text{Kpc}^3$ and $K_0 = 30314 M_\odot \text{Kpc}^{-3} (\text{km/s})^2$, in which case the reduced χ^2_{red} value is $\chi^2_{red} = 102.22$. Also the parameter α in this case is $\alpha = 7.78133 \text{Kpc}$.

In Table CXXXIV we present the optimized values of K_0 and ρ_0 for the analytic SIDM model of Eq. (3) for which the maximum compatibility with the SPARC data is achieved. In Figs. 215, 216 we present

TABLE CXXXIV: SIDM Optimization Values for the galaxy NGC6195

Parameter	Optimization Values
$\rho_0 (M_\odot/\text{Kpc}^3)$	1.66739×10^8
$K_0 (M_\odot \text{Kpc}^{-3} (\text{km/s})^2)$	30314

the density of the analytic SIDM model, the predicted rotation curves for the SIDM model (3), versus the SPARC observational data and the sound speed, as a function of the radius respectively. As it can be seen, for this galaxy, the SIDM model produces non-viable rotation curves which are incompatible with the SPARC data.

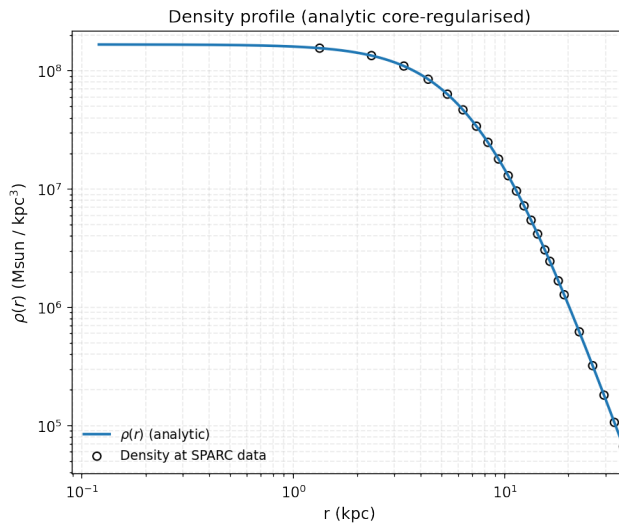


FIG. 215: The density of the SIDM model of Eq. (3) for the galaxy NGC6195, versus the radius.

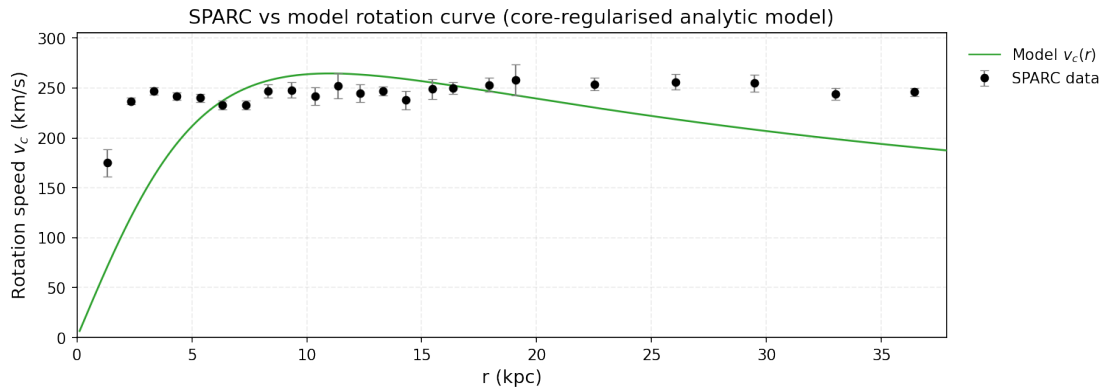


FIG. 216: The predicted rotation curves for the optimized SIDM model of Eq. (3), versus the SPARC observational data for the galaxy NGC6195.

Now we shall include contributions to the rotation velocity from the other components of the galaxy, namely the disk, the gas, and the bulge if present. In Fig. 217 we present the combined rotation

curves including all the components of the galaxy along with the SIDM. As it can be seen, the extended collisional DM model is non-viable. Also in Table CXXXV we present the optimized values of the free

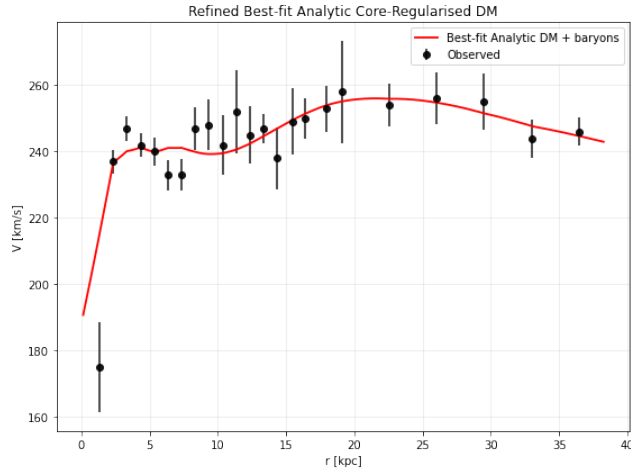


FIG. 217: The predicted rotation curves after using an optimization for the SIDM model (3), and the extended SPARC data for the galaxy NGC6195. We included the rotation curves of the gas, the disk velocities, the bulge (where present) along with the SIDM model.

parameters of the SIDM model for which we achieve the maximum compatibility with the SPARC data, for the galaxy NGC6195, and also the resulting reduced χ^2_{red} value.

TABLE CXXXV: Optimized Parameter Values of the Extended SIDM model for the Galaxy NGC6195.

Parameter	Value
$\rho_0 (M_\odot/\text{Kpc}^3)$	1.56515×10^7
$K_0 (M_\odot \text{ Kpc}^{-3} (\text{km/s})^2)$	20264.7
ml_{disk}	0.8
ml_{bulge}	0.9037
$\alpha (\text{Kpc})$	20.7629
χ^2_{red}	1.25343

71. The Galaxy NGC6503, Non-viable

For this galaxy, the optimization method we used, ensures maximum compatibility of the analytic SIDM model of Eq. (3) with the SPARC data, if we choose $\rho_0 = 6.71565 \times 10^7 M_\odot/\text{Kpc}^3$ and $K_0 = 7133.48 M_\odot \text{ Kpc}^{-3} (\text{km/s})^2$, in which case the reduced χ^2_{red} value is $\chi^2_{red} = 59.6713$. Also the parameter α in this case is $\alpha = 5.94781 \text{ Kpc}$.

In Table CXXXVI we present the optimized values of K_0 and ρ_0 for the analytic SIDM model of Eq. (3) for which the maximum compatibility with the SPARC data is achieved. In Figs. 218, 219 we present

TABLE CXXXVI: SIDM Optimization Values for the galaxy NGC6503

Parameter	Optimization Values
$\rho_0 (M_\odot/\text{Kpc}^3)$	6.71565×10^7
$K_0 (M_\odot \text{ Kpc}^{-3} (\text{km/s})^2)$	7133.48

the density of the analytic SIDM model, the predicted rotation curves for the SIDM model (3), versus the SPARC observational data and the sound speed, as a function of the radius respectively. As it can be seen, for this galaxy, the SIDM model produces non-viable rotation curves which are incompatible with the SPARC data.

Now we shall include contributions to the rotation velocity from the other components of the galaxy, namely the disk, the gas, and the bulge if present. In Fig. 220 we present the combined rotation curves including all the components of the galaxy along with the SIDM. As it can be seen, the extended

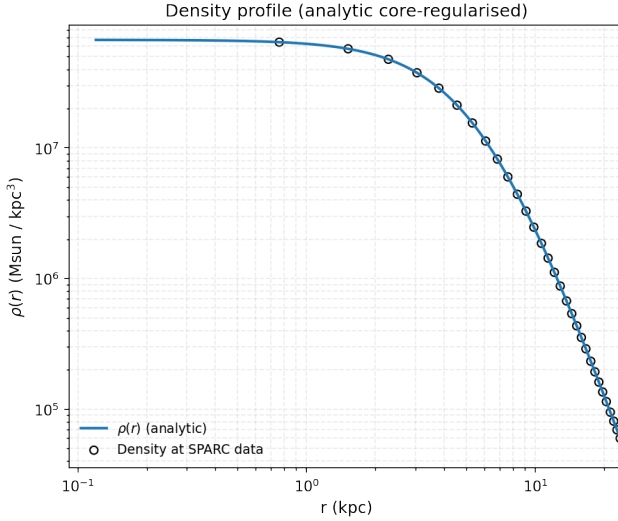


FIG. 218: The density of the SIDM model of Eq. (3) for the galaxy NGC6503, versus the radius.

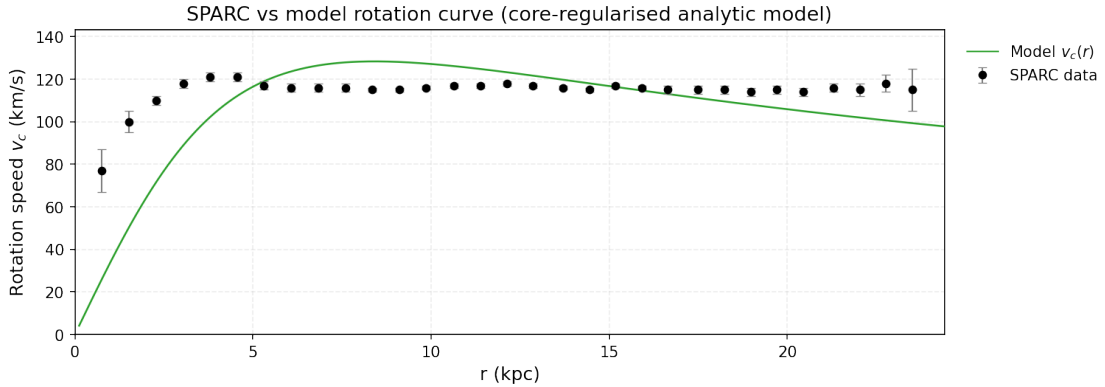


FIG. 219: The predicted rotation curves for the optimized SIDM model of Eq. (3), versus the SPARC observational data for the galaxy NGC6503.

collisional DM model is non-viable. Also in Table CXXXVII we present the optimized values of the free

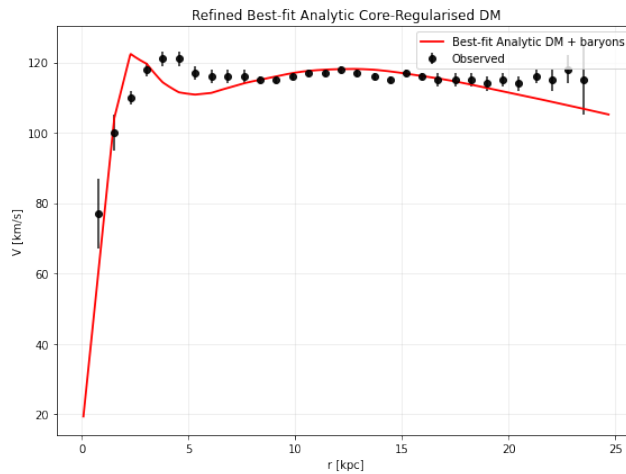


FIG. 220: The predicted rotation curves after using an optimization for the SIDM model (3), and the extended SPARC data for the galaxy NGC6503. We included the rotation curves of the gas, the disk velocities, the bulge (where present) along with the SIDM model.

parameters of the SIDM model for which we achieve the maximum compatibility with the SPARC data, for the galaxy NGC6503, and also the resulting reduced χ^2_{red} value.

TABLE CXXXVII: Optimized Parameter Values of the Extended SIDM model for the Galaxy NGC6503.

Parameter	Value
$\rho_0 (M_\odot/\text{Kpc}^3)$	1.31402×10^7
$K_0 (M_\odot \text{ Kpc}^{-3} (\text{km/s})^2)$	4458.35
ml_{disk}	0.8219
ml_{bulge}	0.5576
$\alpha (\text{Kpc})$	10.6288
χ^2_{red}	5.05801

72. The Galaxy NGC6674

For this galaxy, the optimization method we used, ensures maximum compatibility of the analytic SIDM model of Eq. (3) with the SPARC data, if we choose $\rho_0 = 5.4478 \times 10^7 M_\odot/\text{Kpc}^3$ and $K_0 = 34306.5 M_\odot \text{ Kpc}^{-3} (\text{km/s})^2$, in which case the reduced χ^2_{red} value is $\chi^2_{red} = 79.118$. Also the parameter α in this case is $\alpha = 14.482 \text{ Kpc}$.

In Table CXXXVIII we present the optimized values of K_0 and ρ_0 for the analytic SIDM model of Eq. (3) for which the maximum compatibility with the SPARC data is achieved. In Figs. 221, 222 we present

TABLE CXXXVIII: SIDM Optimization Values for the galaxy NGC6674

Parameter	Optimization Values
$\rho_0 (M_\odot/\text{Kpc}^3)$	5.4478×10^7
$K_0 (M_\odot \text{ Kpc}^{-3} (\text{km/s})^2)$	34306.5

the density of the analytic SIDM model, the predicted rotation curves for the SIDM model (3), versus the SPARC observational data and the sound speed, as a function of the radius respectively. As it can be seen, for this galaxy, the SIDM model produces non-viable rotation curves which are incompatible with the SPARC data.

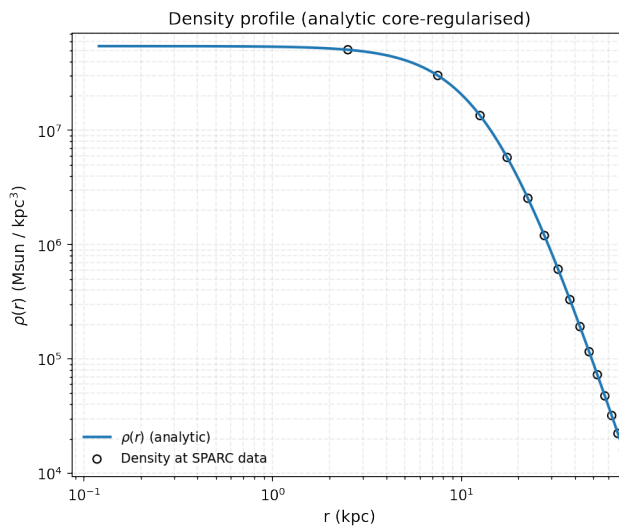


FIG. 221: The density of the SIDM model of Eq. (3) for the galaxy NGC6674, versus the radius.

Now we shall include contributions to the rotation velocity from the other components of the galaxy, namely the disk, the gas, and the bulge if present. In Fig. 223 we present the combined rotation curves including all the components of the galaxy along with the SIDM. As it can be seen, the extended collisional DM model is non-viable. Also in Table CXXXIX we present the optimized values of the free

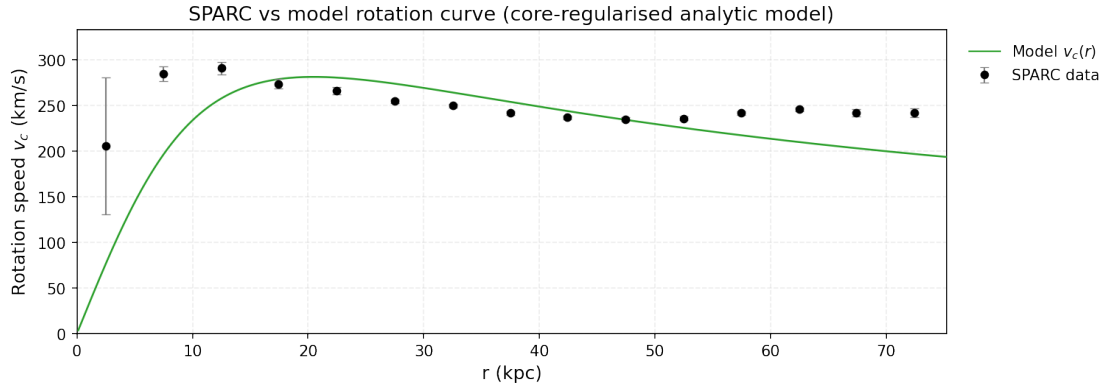


FIG. 222: The predicted rotation curves for the optimized SIDM model of Eq. (3), versus the SPARC observational data for the galaxy NGC6674.

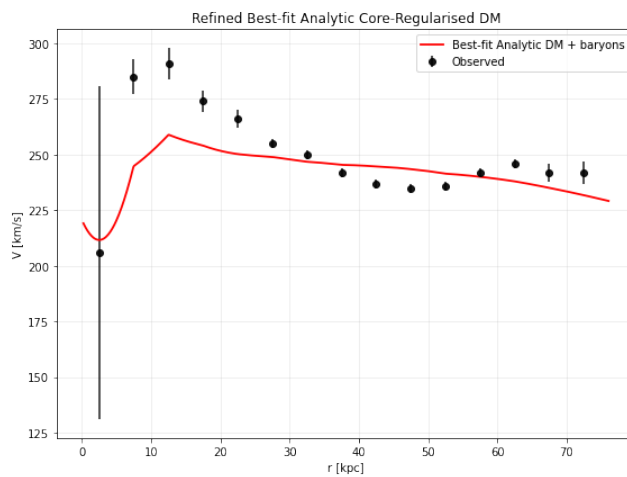


FIG. 223: The predicted rotation curves after using an optimization for the SIDM model (3), and the extended SPARC data for the galaxy NGC6674. We included the rotation curves of the gas, the disk velocities, the bulge (where present) along with the SIDM model.

parameters of the SIDM model for which we achieve the maximum compatibility with the SPARC data, for the galaxy NGC6674, and also the resulting reduced χ^2_{red} value.

TABLE CXXXIX: Optimized Parameter Values of the Extended SIDM model for the Galaxy NGC6674.

Parameter	Value
$\rho_0 (M_\odot/\text{Kpc}^3)$	2.47914×10^6
$K_0 (M_\odot \text{ Kpc}^{-3} (\text{km/s})^2)$	16756
ml_{disk}	1
ml_{bulge}	1
$\alpha (\text{Kpc})$	47.4385
χ^2_{red}	14.223

73. The Galaxy NGC6789

For this galaxy, the optimization method we used, ensures maximum compatibility of the analytic SIDM model of Eq. (3) with the SPARC data, if we choose $\rho_0 = 6.72725 \times 10^8 M_\odot/\text{Kpc}^3$ and $K_0 = 1573.45 M_\odot \text{ Kpc}^{-3} (\text{km/s})^2$, in which case the reduced χ^2_{red} value is $\chi^2_{red} = 0.626789$. Also the parameter α in this case is $\alpha = 0.882589 \text{ Kpc}$.

In Table CXL we present the optimized values of K_0 and ρ_0 for the analytic SIDM model of Eq. (3) for which the maximum compatibility with the SPARC data is achieved. In Figs. 224, 225 we present

TABLE CXL: SIDM Optimization Values for the galaxy NGC6789

Parameter	Optimization Values
$\rho_0 (M_\odot/\text{Kpc}^3)$	6.72725×10^8
$K_0 (M_\odot \text{ Kpc}^{-3} (\text{km/s})^2)$	1573.45

the density of the analytic SIDM model, the predicted rotation curves for the SIDM model (3), versus the SPARC observational data and the sound speed, as a function of the radius respectively. As it can be seen, for this galaxy, the SIDM model produces viable rotation curves which are compatible with the SPARC data.

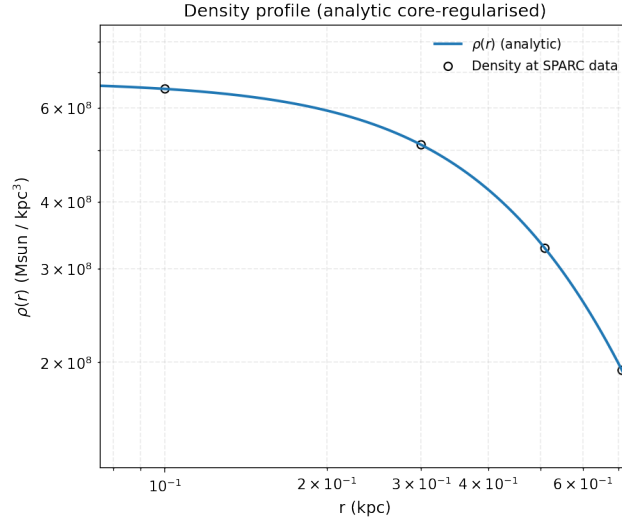


FIG. 224: The density of the SIDM model of Eq. (3) for the galaxy NGC6789, versus the radius.

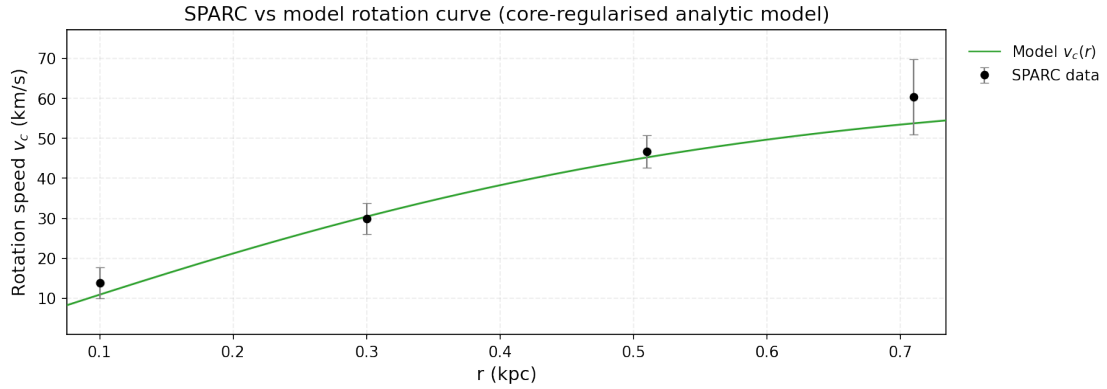


FIG. 225: The predicted rotation curves for the optimized SIDM model of Eq. (3), versus the SPARC observational data for the galaxy NGC6789.

74. The Galaxy NGC7331, Non-viable

For this galaxy, the optimization method we used, ensures maximum compatibility of the analytic SIDM model of Eq. (3) with the SPARC data, if we choose $\rho_0 = 2.20061 \times 10^8 M_\odot/\text{Kpc}^3$ and $K_0 = 34846.1 M_\odot \text{ Kpc}^{-3} (\text{km/s})^2$, in which case the reduced χ^2_{red} value is $\chi^2_{red} = 35.4787$. Also the parameter α in this case is $\alpha = 7.262 \text{ Kpc}$.

In Table CXLI we present the optimized values of K_0 and ρ_0 for the analytic SIDM model of Eq. (3) for which the maximum compatibility with the SPARC data is achieved. In Figs. 226, 227 we present

TABLE CXLI: SIDM Optimization Values for the galaxy NGC7331

Parameter	Optimization Values
$\rho_0 (M_\odot/\text{Kpc}^3)$	2.20061×10^8
$K_0 (M_\odot \text{ Kpc}^{-3} (\text{km/s})^2)$	34846.1

the density of the analytic SIDM model, the predicted rotation curves for the SIDM model (3), versus the SPARC observational data and the sound speed, as a function of the radius respectively. As it can be seen, for this galaxy, the SIDM model produces non-viable rotation curves which are incompatible with the SPARC data.

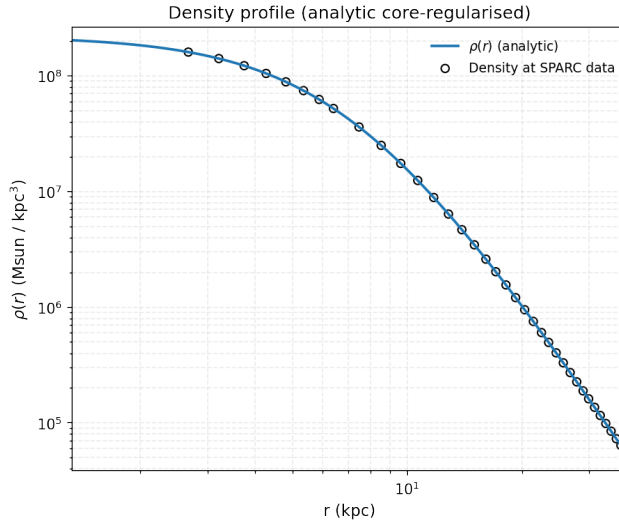


FIG. 226: The density of the SIDM model of Eq. (3) for the galaxy NGC7331, versus the radius.

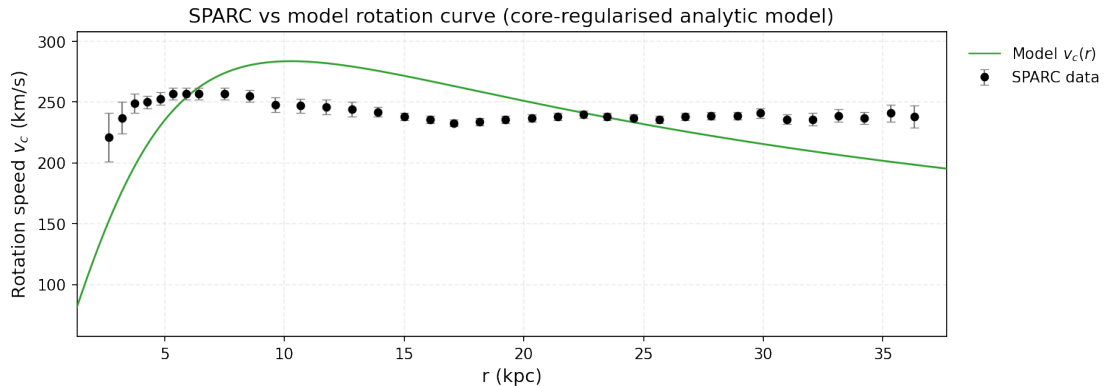


FIG. 227: The predicted rotation curves for the optimized SIDM model of Eq. (3), versus the SPARC observational data for the galaxy NGC7331.

Now we shall include contributions to the rotation velocity from the other components of the galaxy, namely the disk, the gas, and the bulge if present. In Fig. 228 we present the combined rotation curves including all the components of the galaxy along with the SIDM. As it can be seen, the extended collisional DM model is non-viable. Also in Table CXLI we present the optimized values of the free parameters of the SIDM model for which we achieve the maximum compatibility with the SPARC data, for the galaxy NGC7331, and also the resulting reduced χ^2_{red} value.

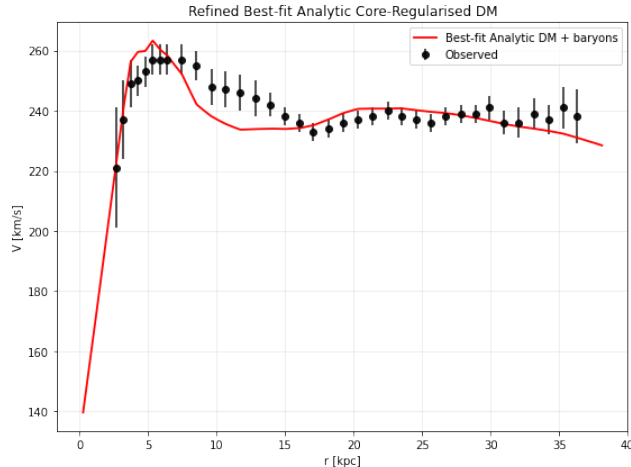


FIG. 228: The predicted rotation curves after using an optimization for the SIDM model (3), and the extended SPARC data for the galaxy NGC7331. We included the rotation curves of the gas, the disk velocities, the bulge (where present) along with the SIDM model.

TABLE CXLII: Optimized Parameter Values of the Extended SIDM model for the Galaxy NGC7331.

Parameter	Value
$\rho_0 (M_\odot/\text{Kpc}^3)$	7.12149×10^6
$K_0 (M_\odot \text{ Kpc}^{-3} (\text{km/s})^2)$	15912.5
ml_{disk}	0.6909
ml_{bulge}	0.5
$\alpha (\text{Kpc})$	27.2759
χ^2_{red}	1.5433

75. The Galaxy NGC7793, Non-viable, Extended Viable

For this galaxy, the optimization method we used, ensures maximum compatibility of the analytic SIDM model of Eq. (3) with the SPARC data, if we choose $\rho_0 = 3.09584 \times 10^8 M_\odot/\text{Kpc}^3$ and $K_0 = 4953.05 M_\odot \text{ Kpc}^{-3} (\text{km/s})^2$, in which case the reduced χ^2_{red} value is $\chi^2_{\text{red}} = 3.75772$. Also the parameter α in this case is $\alpha = 2.30833 \text{ Kpc}$.

In Table CXLIII we present the optimized values of K_0 and ρ_0 for the analytic SIDM model of Eq. (3) for which the maximum compatibility with the SPARC data is achieved. In Figs. 229, 230 we present

TABLE CXLIII: SIDM Optimization Values for the galaxy NGC7793

Parameter	Optimization Values
$\rho_0 (M_\odot/\text{Kpc}^3)$	3.09584×10^8
$K_0 (M_\odot \text{ Kpc}^{-3} (\text{km/s})^2)$	4953.05

the density of the analytic SIDM model, the predicted rotation curves for the SIDM model (3), versus the SPARC observational data and the sound speed, as a function of the radius respectively. As it can be seen, for this galaxy, the SIDM model produces non-viable rotation curves which are incompatible with the SPARC data.

Now we shall include contributions to the rotation velocity from the other components of the galaxy, namely the disk, the gas, and the bulge if present. In Fig. 231 we present the combined rotation curves including all the components of the galaxy along with the SIDM. As it can be seen, the extended collisional DM model is deemed viable. Also in Table CXLIV we present the optimized values of the free parameters of the SIDM model for which we achieve the maximum compatibility with the SPARC data, for the galaxy NGC7793, and also the resulting reduced χ^2_{red} value.

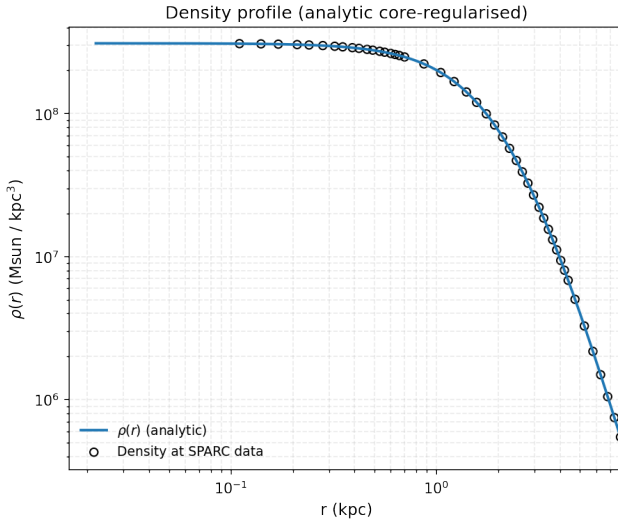


FIG. 229: The density of the SIDM model of Eq. (3) for the galaxy NGC7793, versus the radius.

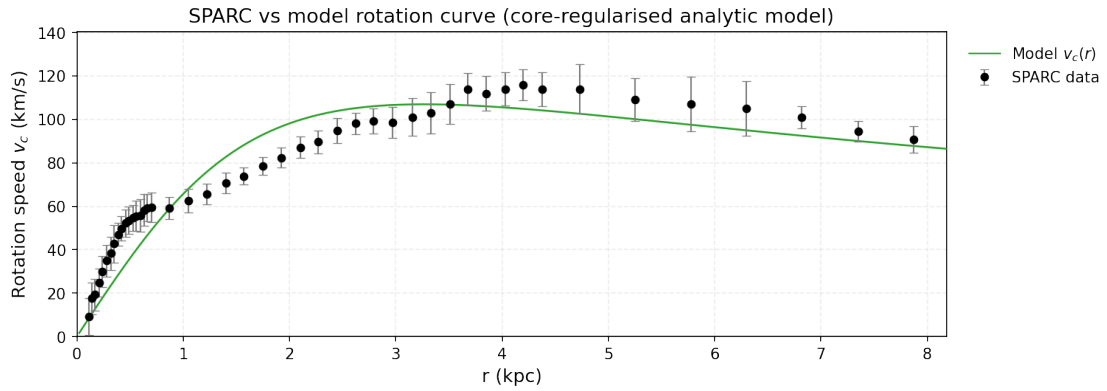


FIG. 230: The predicted rotation curves for the optimized SIDM model of Eq. (3), versus the SPARC observational data for the galaxy NGC7793.

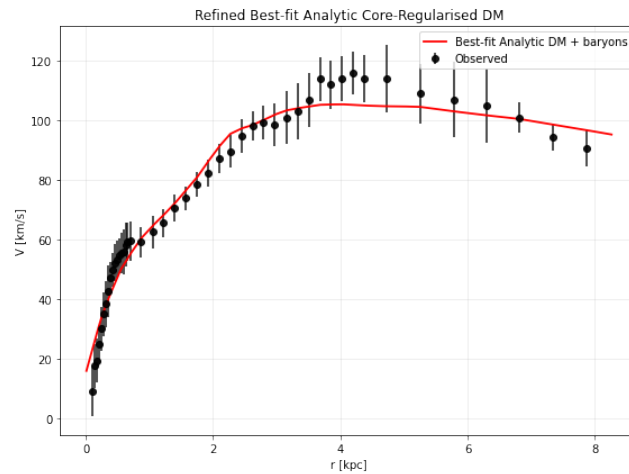


FIG. 231: The predicted rotation curves after using an optimization for the SIDM model (3), and the extended SPARC data for the galaxy NGC7793. We included the rotation curves of the gas, the disk velocities, the bulge (where present) along with the SIDM model.

TABLE CXLIV: Optimized Parameter Values of the Extended SIDM model for the Galaxy NGC7793.

Parameter	Value
ρ_0 (M_\odot/Kpc^3)	2.86207×10^7
K_0 ($M_\odot \text{ Kpc}^{-3} (\text{km/s})^2$)	2200.74
ml_{disk}	0.8641
ml_{bulge}	0.2
α (Kpc)	5.05989
χ^2_{red}	0.699734

76. The Galaxy NGC7814, Non-viable, Extended Viable

For this galaxy, the optimization method we used, ensures maximum compatibility of the analytic SIDM model of Eq. (3) with the SPARC data, if we choose $\rho_0 = 5.34343 \times 10^8 M_\odot/\text{Kpc}^3$ and $K_0 = 27059.5 M_\odot \text{ Kpc}^{-3} (\text{km/s})^2$, in which case the reduced χ^2_{red} value is $\chi^2_{\text{red}} = 30.4685$. Also the parameter α in this case is $\alpha = 4.10677 \text{ Kpc}$.

In Table CXLV we present the optimized values of K_0 and ρ_0 for the analytic SIDM model of Eq. (3) for which the maximum compatibility with the SPARC data is achieved. In Figs. 232, 233 we present

TABLE CXLV: SIDM Optimization Values for the galaxy NGC7814

Parameter	Optimization Values
ρ_0 (M_\odot/Kpc^3)	5.34343×10^8
K_0 ($M_\odot \text{ Kpc}^{-3} (\text{km/s})^2$)	27059.5

the density of the analytic SIDM model, the predicted rotation curves for the SIDM model (3), versus the SPARC observational data and the sound speed, as a function of the radius respectively. As it can be seen, for this galaxy, the SIDM model produces non-viable rotation curves which are incompatible with the SPARC data.

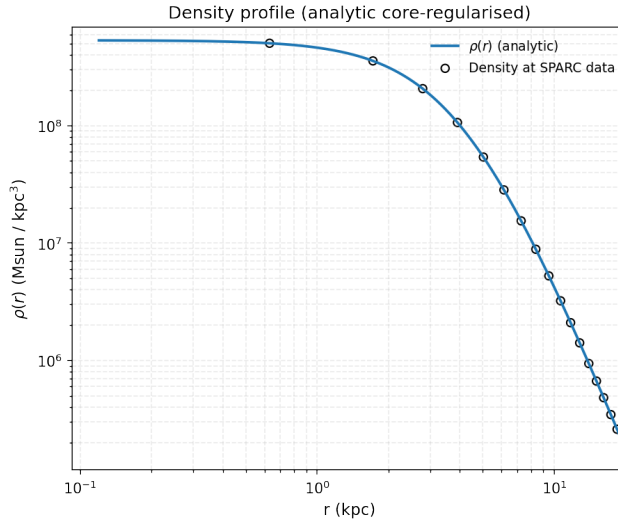


FIG. 232: The density of the SIDM model of Eq. (3) for the galaxy NGC7814, versus the radius.

Now we shall include contributions to the rotation velocity from the other components of the galaxy, namely the disk, the gas, and the bulge if present. In Fig. 234 we present the combined rotation curves including all the components of the galaxy along with the SIDM. As it can be seen, the extended collisional DM model is non-viable. Also in Table CXLVI we present the optimized values of the free parameters of the SIDM model for which we achieve the maximum compatibility with the SPARC data, for the galaxy NGC7814, and also the resulting reduced χ^2_{red} value.

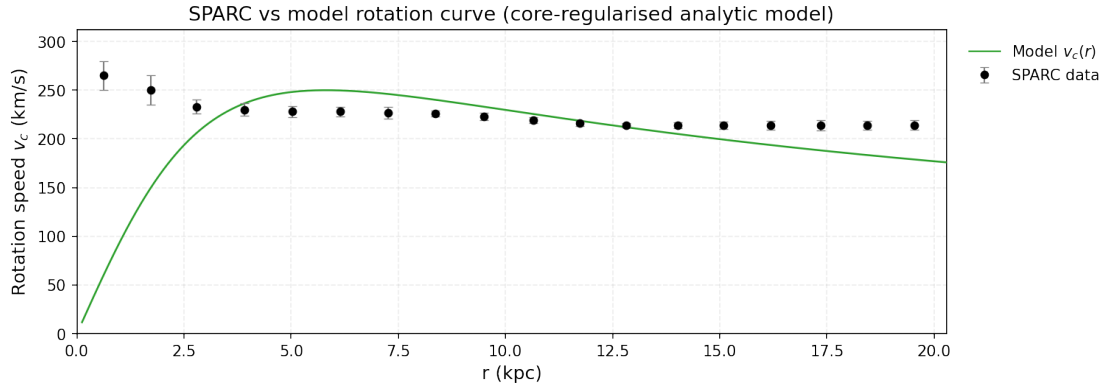


FIG. 233: The predicted rotation curves for the optimized SIDM model of Eq. (3), versus the SPARC observational data for the galaxy NGC7814.

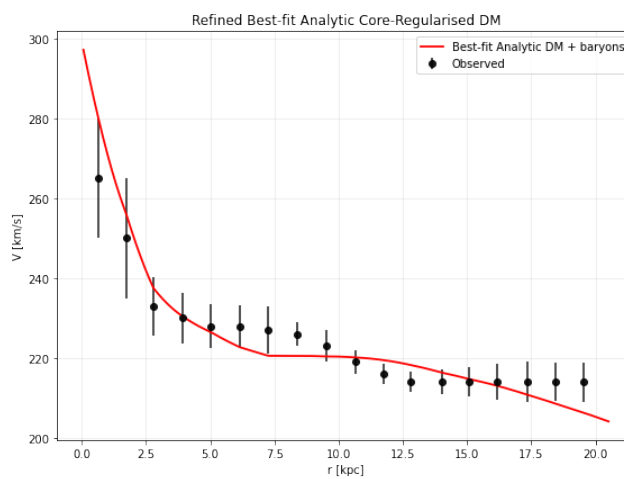


FIG. 234: The predicted rotation curves after using an optimization for the SIDM model (3), and the extended SPARC data for the galaxy NGC7814. We included the rotation curves of the gas, the disk velocities, the bulge (where present) along with the SIDM model.

TABLE CXLVI: Optimized Parameter Values of the Extended SIDM model for the Galaxy NGC7814.

Parameter	Value
$\rho_0 (M_\odot/\text{Kpc}^3)$	2.58268×10^7
$K_0 (M_\odot \text{ Kpc}^{-3} (\text{km/s})^2)$	12568.5
ml_{disk}	1
ml_{bulge}	0.8033
$\alpha (\text{Kpc})$	12.7293
χ^2_{red}	1.23637

77. The Galaxy UGC00891

For this galaxy, the optimization method we used, ensures maximum compatibility of the analytic SIDM model of Eq. (3) with the SPARC data, if we choose $\rho_0 = 1.53512 \times 10^7 M_\odot/\text{Kpc}^3$ and $K_0 = 1741.03 M_\odot \text{ Kpc}^{-3} (\text{km/s})^2$, in which case the reduced χ^2_{red} value is $\chi^2_{\text{red}} = 0.681321$. Also the parameter α in this case is $\alpha = 6.14586 \text{ Kpc}$.

In Table CXLVII we present the optimized values of K_0 and ρ_0 for the analytic SIDM model of Eq. (3) for which the maximum compatibility with the SPARC data is achieved. In Figs. 235, 236 we present the density of the analytic SIDM model, the predicted rotation curves for the SIDM model (3), versus the SPARC observational data and the sound speed, as a function of the radius respectively. As it can be seen, for this galaxy, the SIDM model produces viable rotation curves which are compatible with the SPARC data.

TABLE CXLVII: SIDM Optimization Values for the galaxy UGC00891

Parameter	Optimization Values
$\rho_0 (M_\odot/\text{Kpc}^3)$	1.53512×10^7
$K_0 (M_\odot \text{ Kpc}^{-3} (\text{km/s})^2)$	1741.03

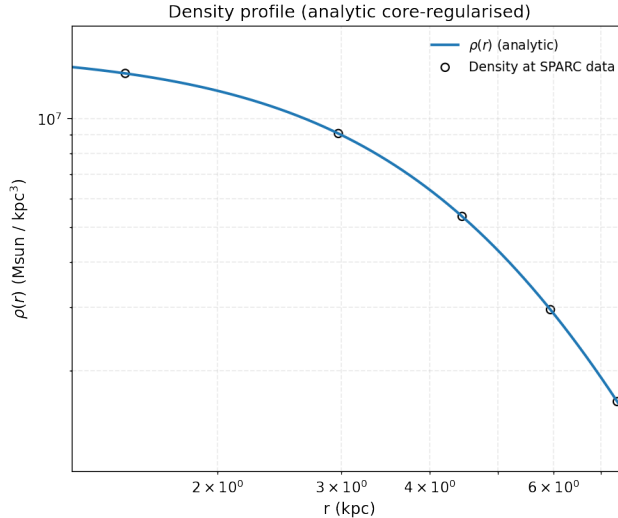


FIG. 235: The density of the SIDM model of Eq. (3) for the galaxy UGC00891, versus the radius.

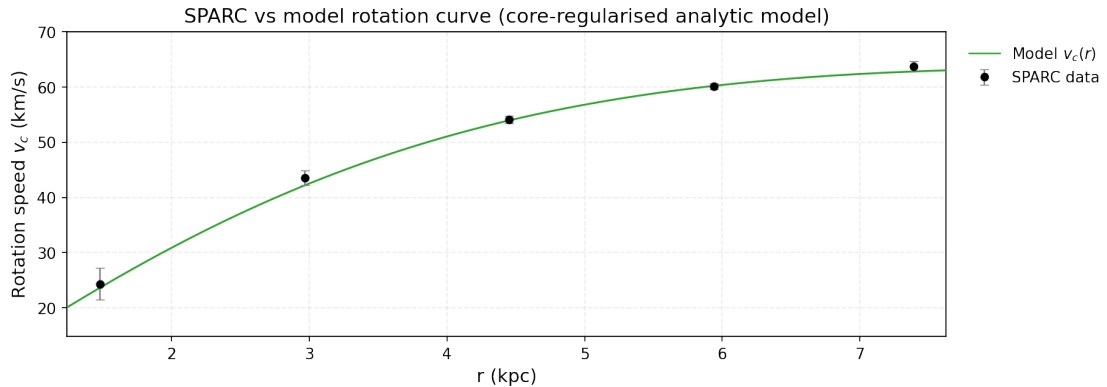


FIG. 236: The predicted rotation curves for the optimized SIDM model of Eq. (3), versus the SPARC observational data for the galaxy UGC00891.

78. The Galaxy UGC01281

For this galaxy, the optimization method we used, ensures maximum compatibility of the analytic SIDM model of Eq. (3) with the SPARC data, if we choose $\rho_0 = 2.85574 \times 10^7 M_\odot/\text{Kpc}^3$ and $K_0 = 1350.75 M_\odot \text{ Kpc}^{-3} (\text{km/s})^2$, in which case the reduced χ^2_{red} value is $\chi^2_{\text{red}} = 0.138773$. Also the parameter α in this case is $\alpha = 4.27865 \text{ Kpc}$.

In Table CXLVIII we present the optimized values of K_0 and ρ_0 for the analytic SIDM model of Eq. (3) for which the maximum compatibility with the SPARC data is achieved. In Figs. 237, 238 we present

TABLE CXLVIII: SIDM Optimization Values for the galaxy UGC01281

Parameter	Optimization Values
$\rho_0 (M_\odot/\text{Kpc}^3)$	2.85574×10^7
$K_0 (M_\odot \text{ Kpc}^{-3} (\text{km/s})^2)$	1350.75

the density of the analytic SIDM model, the predicted rotation curves for the SIDM model (3), versus the SPARC observational data and the sound speed, as a function of the radius respectively. As it can be seen, for this galaxy, the SIDM model produces viable rotation curves which are compatible with the SPARC data.

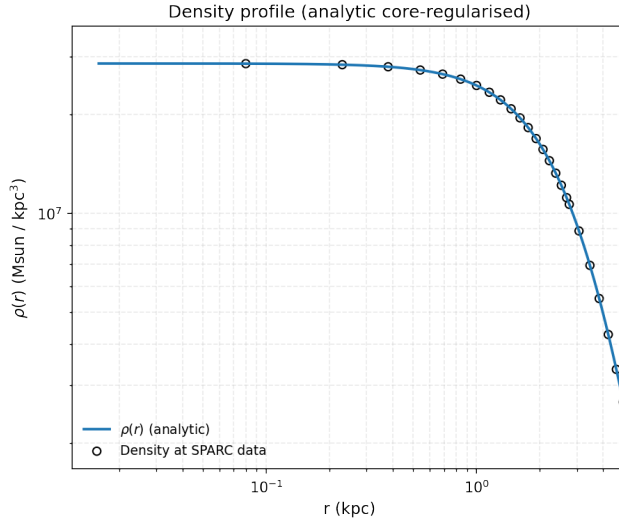


FIG. 237: The density of the SIDM model of Eq. (3) for the galaxy UGC01281, versus the radius.

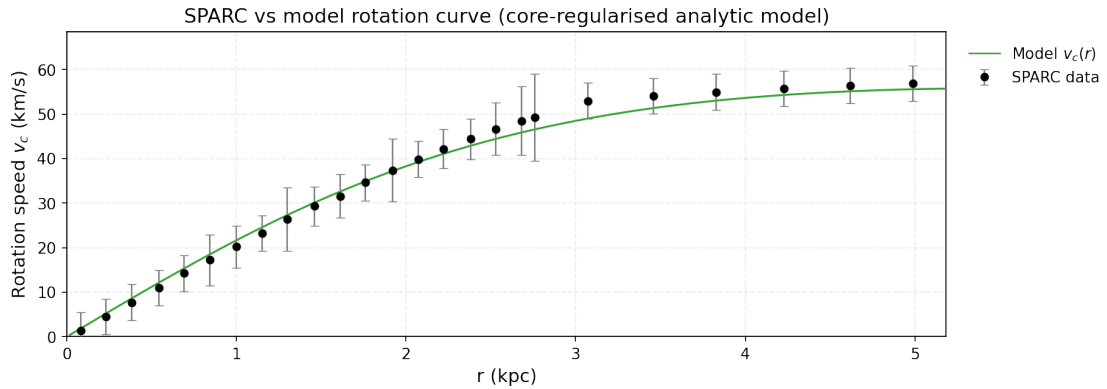


FIG. 238: The predicted rotation curves for the optimized SIDM model of Eq. (3), versus the SPARC observational data for the galaxy UGC01281.

79. The Galaxy UGC02259, Non-viable

For this galaxy, the optimization method we used, ensures maximum compatibility of the analytic SIDM model of Eq. (3) with the SPARC data, if we choose $\rho_0 = 9.76276 \times 10^7 M_\odot / \text{Kpc}^3$ and $K_0 = 3430.77 M_\odot \text{ Kpc}^{-3} (\text{km/s})^2$, in which case the reduced χ^2_{red} value is $\chi^2_{\text{red}} = 9.77349$. Also the parameter α in this case is $\alpha = 3.42105 \text{ Kpc}$.

In Table CXLIX we present the optimized values of K_0 and ρ_0 for the analytic SIDM model of Eq. (3) for which the maximum compatibility with the SPARC data is achieved. In Figs. 239, 240 we present

TABLE CXLIX: SIDM Optimization Values for the galaxy UGC02259

Parameter	Optimization Values
$\rho_0 (M_\odot / \text{Kpc}^3)$	9.76276×10^7
$K_0 (M_\odot \text{ Kpc}^{-3} (\text{km/s})^2)$	3430.771250

the density of the analytic SIDM model, the predicted rotation curves for the SIDM model (3), versus the SPARC observational data and the sound speed, as a function of the radius respectively. As it can be seen, for this galaxy, the SIDM model produces non-viable rotation curves which are incompatible with the SPARC data.

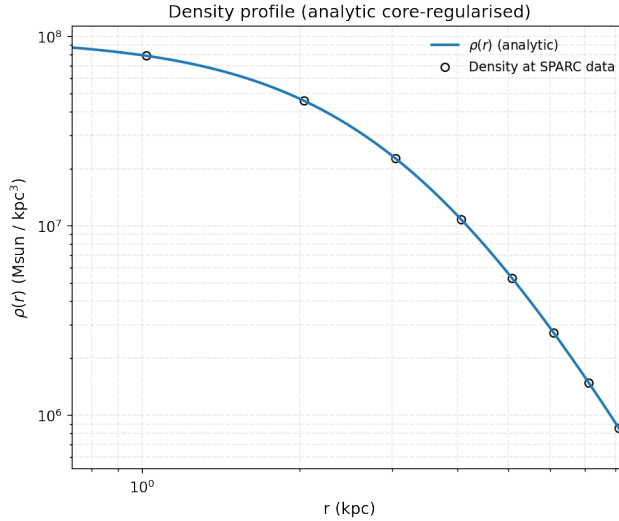


FIG. 239: The density of the SIDM model of Eq. (3) for the galaxy UGC02259, versus the radius.

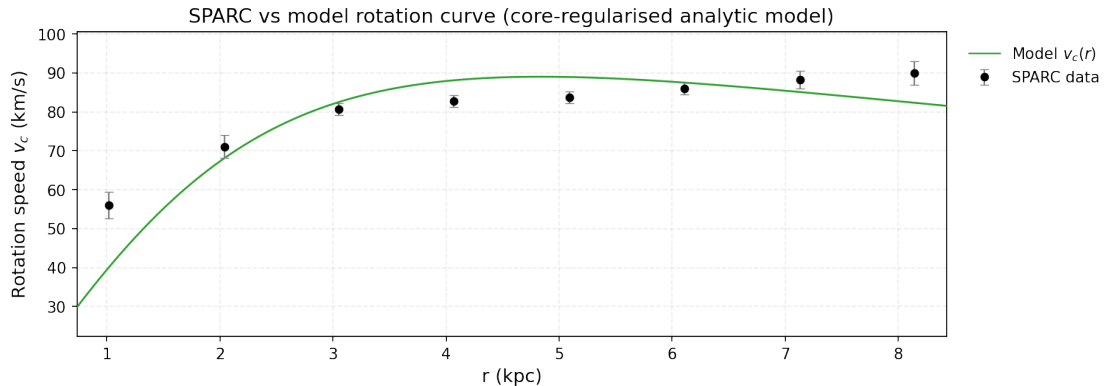


FIG. 240: The predicted rotation curves for the optimized SIDM model of Eq. (3), versus the SPARC observational data for the galaxy UGC02259.

Now we shall include contributions to the rotation velocity from the other components of the galaxy, namely the disk, the gas, and the bulge if present. In Fig. 241 we present the combined rotation curves including all the components of the galaxy along with the SIDM. As it can be seen, the extended collisional DM model is non-viable. Also in Table CL we present the optimized values of the free parameters of the SIDM model for which we achieve the maximum compatibility with the SPARC data, for the galaxy UGC02259, and also the resulting reduced χ^2_{red} value.

TABLE CL: Optimized Parameter Values of the Extended SIDM model for the Galaxy UGC02259.

Parameter	Value
ρ_0 (M_\odot/Kpc^3)	6.71904×10^7
K_0 ($M_\odot \text{ Kpc}^{-3} (\text{km/s})^2$)	2361.61
ml_{disk}	1
ml_{bulge}	0.4079
α (Kpc)	3.42095
χ^2_{red}	10.9448

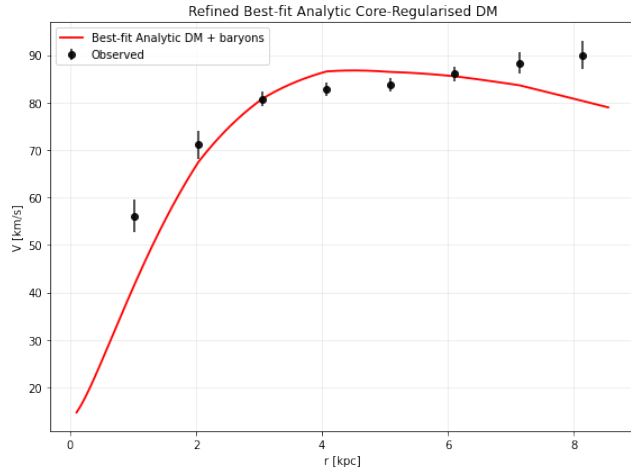


FIG. 241: The predicted rotation curves after using an optimization for the SIDM model (3), and the extended SPARC data for the galaxy UGC02259. We included the rotation curves of the gas, the disk velocities, the bulge (where present) along with the SIDM model.

80. The Galaxy UGC02487, Non-viable

For this galaxy, the optimization method we used, ensures maximum compatibility of the analytic SIDM model of Eq. (3) with the SPARC data, if we choose $\rho_0 = 9.07148 \times 10^7 M_\odot/\text{Kpc}^3$ and $K_0 = 70393.6 M_\odot \text{Kpc}^{-3} (\text{km/s})^2$, in which case the reduced χ^2_{red} value is $\chi^2_{red} = 24.7828$. Also the parameter α in this case is $\alpha = 16.076 \text{Kpc}$.

In Table CLI we present the optimized values of K_0 and ρ_0 for the analytic SIDM model of Eq. (3) for which the maximum compatibility with the SPARC data is achieved. In Figs. 242, 243 we present

TABLE CLI: SIDM Optimization Values for the galaxy UGC02487

Parameter	Optimization Values
$\rho_0 (M_\odot/\text{Kpc}^3)$	9.07148×10^7
$K_0 (M_\odot \text{Kpc}^{-3} (\text{km/s})^2)$	70393.6

the density of the analytic SIDM model, the predicted rotation curves for the SIDM model (3), versus the SPARC observational data and the sound speed, as a function of the radius respectively. As it can be seen, for this galaxy, the SIDM model produces non-viable rotation curves which are incompatible with the SPARC data.

Now we shall include contributions to the rotation velocity from the other components of the galaxy, namely the disk, the gas, and the bulge if present. In Fig. 244 we present the combined rotation curves including all the components of the galaxy along with the SIDM. As it can be seen, the extended collisional DM model is non-viable. Also in Table CLII we present the optimized values of the free parameters of the SIDM model for which we achieve the maximum compatibility with the SPARC data, for the galaxy UGC02487, and also the resulting reduced χ^2_{red} value.

TABLE CLII: Optimized Parameter Values of the Extended SIDM model for the Galaxy UGC02487.

Parameter	Value
$\rho_0 (M_\odot/\text{Kpc}^3)$	9.62207×10^6
$K_0 (M_\odot \text{Kpc}^{-3} (\text{km/s})^2)$	31456.4
ml_{disk}	1
ml_{bulge}	1
$\alpha (\text{Kpc})$	32.9926
χ^2_{red}	5.98761

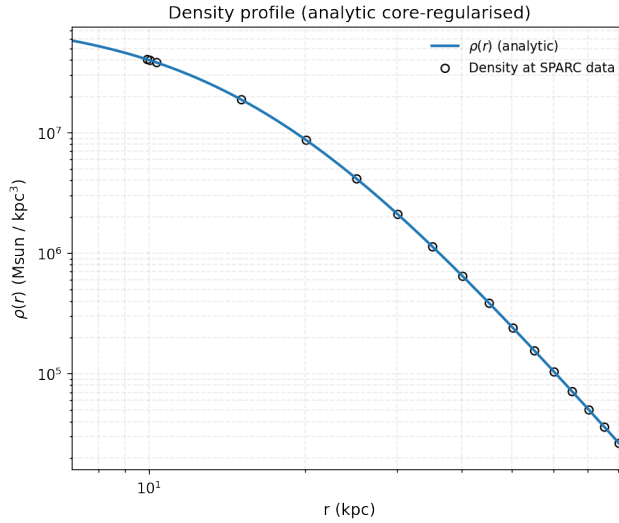


FIG. 242: The density of the SIDM model of Eq. (3) for the galaxy UGC02487, versus the radius.

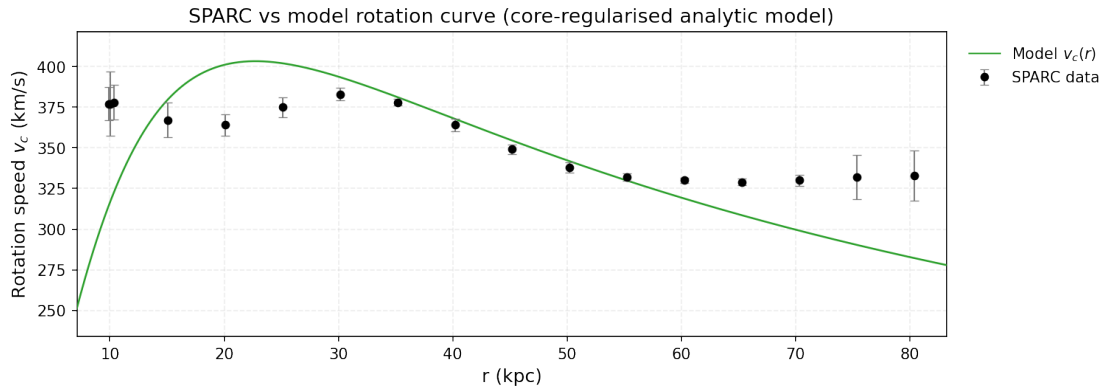


FIG. 243: The predicted rotation curves for the optimized SIDM model of Eq. (3), versus the SPARC observational data for the galaxy UGC02487.

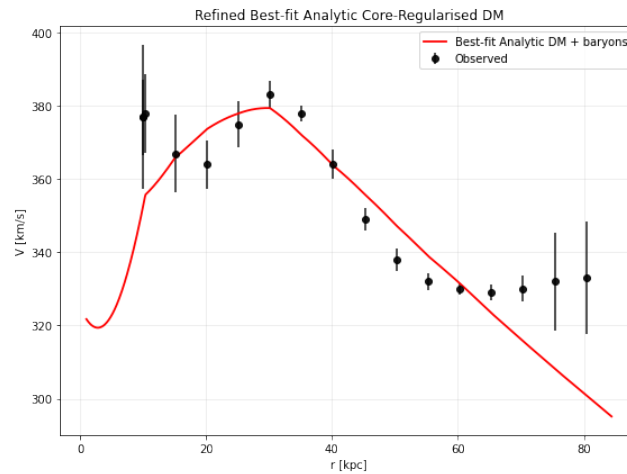


FIG. 244: The predicted rotation curves after using an optimization for the SIDM model (3), and the extended SPARC data for the galaxy UGC02487. We included the rotation curves of the gas, the disk velocities, the bulge (where present) along with the SIDM model.

81. The Galaxy UGC02885, Non-viable, Extended Viable

For this galaxy, the optimization method we used, ensures maximum compatibility of the analytic SIDM model of Eq. (3) with the SPARC data, if we choose $\rho_0 = 2.19424 \times 10^7 M_\odot/\text{Kpc}^3$ and $K_0 = 41500.7 M_\odot \text{Kpc}^{-3} (\text{km/s})^2$, in which case the reduced χ^2_{red} value is $\chi^2_{red} = 79.0084$. Also the parameter α in this case is $\alpha = 25.0979 \text{Kpc}$.

In Table CLIII we present the optimized values of K_0 and ρ_0 for the analytic SIDM model of Eq. (3) for which the maximum compatibility with the SPARC data is achieved. In Figs. 245, 246 we present

TABLE CLIII: SIDM Optimization Values for the galaxy UGC02885

Parameter	Optimization Values
$\rho_0 (M_\odot/\text{Kpc}^3)$	2.19424×10^7
$K_0 (M_\odot \text{Kpc}^{-3} (\text{km/s})^2)$	41500.7

the density of the analytic SIDM model, the predicted rotation curves for the SIDM model (3), versus the SPARC observational data and the sound speed, as a function of the radius respectively. As it can be seen, for this galaxy, the SIDM model produces non-viable rotation curves which are incompatible with the SPARC data.

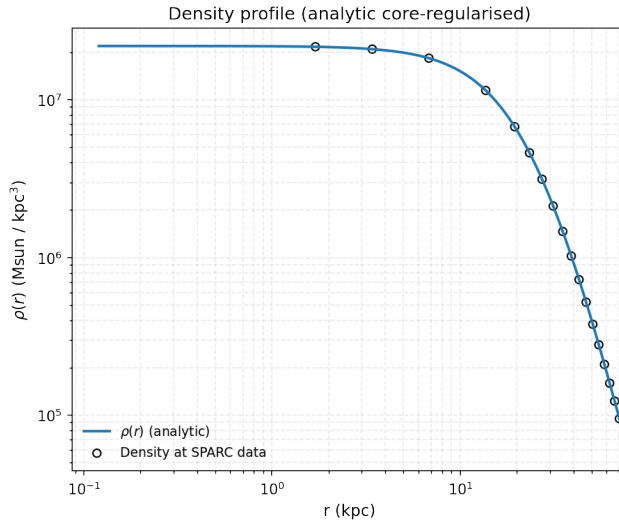


FIG. 245: The density of the SIDM model of Eq. (3) for the galaxy UGC02885, versus the radius.

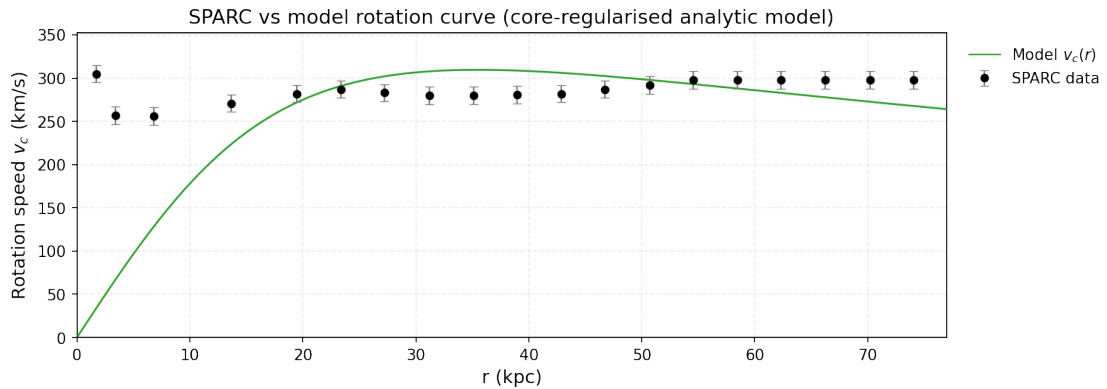


FIG. 246: The predicted rotation curves for the optimized SIDM model of Eq. (3), versus the SPARC observational data for the galaxy UGC02885.

Now we shall include contributions to the rotation velocity from the other components of the galaxy, namely the disk, the gas, and the bulge if present. In Fig. 247 we present the combined rotation curves

including all the components of the galaxy along with the SIDM. As it can be seen, the extended collisional DM model is viable. Also in Table CLIV we present the optimized values of the free parameters of the

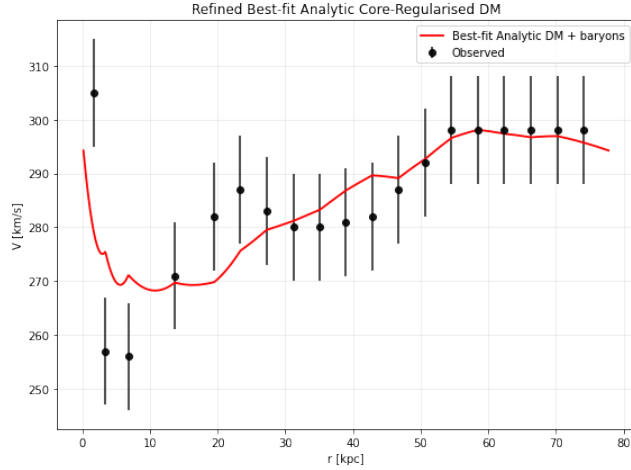


FIG. 247: The predicted rotation curves after using an optimization for the SIDM model (3), and the extended SPARC data for the galaxy UGC02885. We included the rotation curves of the gas, the disk velocities, the bulge (where present) along with the SIDM model.

SIDM model for which we achieve the maximum compatibility with the SPARC data, for the galaxy UGC02885, and also the resulting reduced χ^2_{red} value.

TABLE CLIV: Optimized Parameter Values of the Extended SIDM model for the Galaxy UGC02885.

Parameter	Value
ρ_0 (M_\odot/Kpc^3)	2.30924×10^6
K_0 ($M_\odot \text{ Kpc}^{-3} (\text{km/s})^2$)	25290.3
ml_{disk}	0.9148
ml_{bulge}	1
α (Kpc)	60.3863
χ^2_{red}	1.10113

82. The Galaxy UGC02916, Non-viable

For this galaxy, the optimization method we used, ensures maximum compatibility of the analytic SIDM model of Eq. (3) with the SPARC data, if we choose $\rho_0 = 1.32108 \times 10^8 M_\odot/\text{Kpc}^3$ and $K_0 = 22911.6 M_\odot \text{ Kpc}^{-3} (\text{km/s})^2$, in which case the reduced χ^2_{red} value is $\chi^2_{red} = 434.539$. Also the parameter α in this case is $\alpha = 7.60001 \text{ Kpc}$.

In Table CLV we present the optimized values of K_0 and ρ_0 for the analytic SIDM model of Eq. (3) for which the maximum compatibility with the SPARC data is achieved. In Figs. 248, 249 we present

TABLE CLV: SIDM Optimization Values for the galaxy UGC02916

Parameter	Optimization Values
ρ_0 (M_\odot/Kpc^3)	1.32108×10^8
K_0 ($M_\odot \text{ Kpc}^{-3} (\text{km/s})^2$)	22911.6

the density of the analytic SIDM model, the predicted rotation curves for the SIDM model (3), versus the SPARC observational data and the sound speed, as a function of the radius respectively. As it can be seen, for this galaxy, the SIDM model produces non-viable rotation curves which are incompatible with the SPARC data.

Now we shall include contributions to the rotation velocity from the other components of the galaxy, namely the disk, the gas, and the bulge if present. In Fig. 250 we present the combined rotation curves including all the components of the galaxy along with the SIDM. As it can be seen, the extended

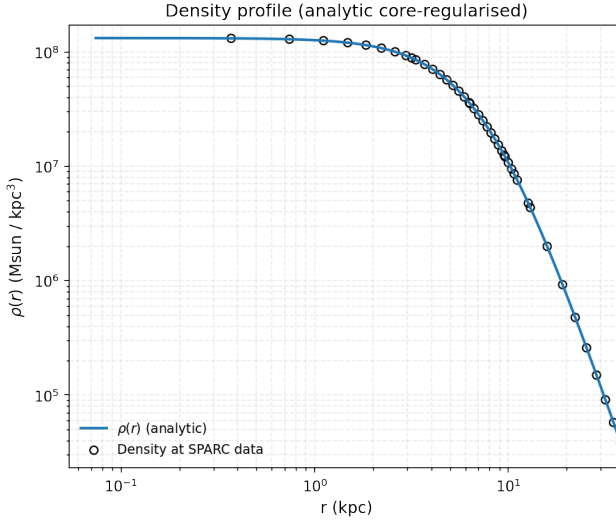


FIG. 248: The density of the SIDM model of Eq. (3) for the galaxy UGC02916, versus the radius.

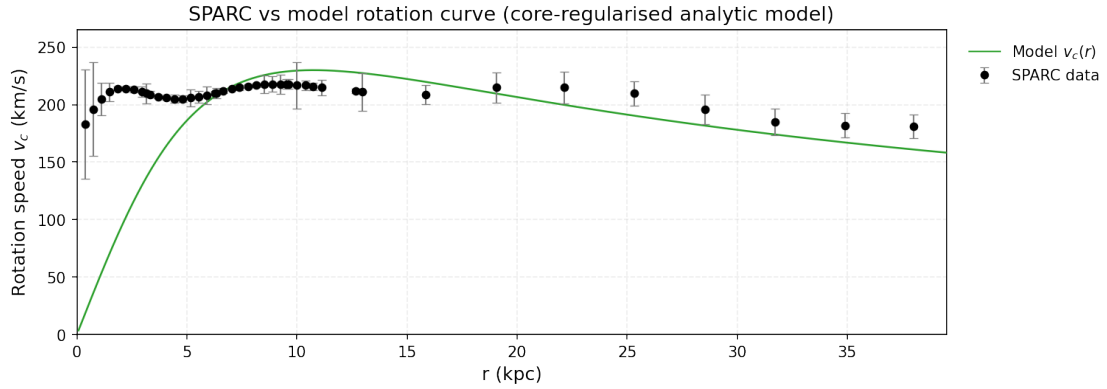


FIG. 249: The predicted rotation curves for the optimized SIDM model of Eq. (3), versus the SPARC observational data for the galaxy UGC02916.

collisional DM model is non-viable. Also in Table CLVI we present the optimized values of the free

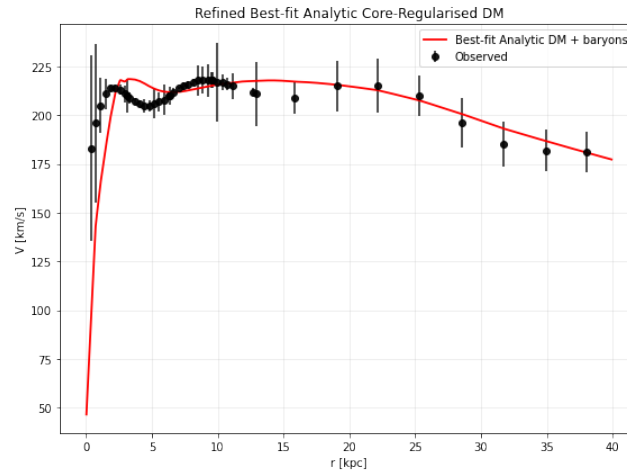


FIG. 250: The predicted rotation curves after using an optimization for the SIDM model (3), and the extended SPARC data for the galaxy UGC02916. We included the rotation curves of the gas, the disk velocities, the bulge (where present) along with the SIDM model.

parameters of the SIDM model for which we achieve the maximum compatibility with the SPARC data, for the galaxy UGC02916, and also the resulting reduced χ^2_{red} value.

TABLE CLVI: Optimized Parameter Values of the Extended SIDM model for the Galaxy UGC02916.

Parameter	Value
$\rho_0 (M_\odot/\text{Kpc}^3)$	3.66857×10^7
$K_0 (M_\odot \text{ Kpc}^{-3} (\text{km/s})^2)$	14588.2
ml_{disk}	1
ml_{bulge}	0.7
$\alpha (\text{Kpc})$	11.5067
χ^2_{red}	8.16682

83. The Galaxy UGC02953, Non-viable

For this galaxy, the optimization method we used, ensures maximum compatibility of the analytic SIDM model of Eq. (3) with the SPARC data, if we choose $\rho_0 = 1.21853 \times 10^8 M_\odot/\text{Kpc}^3$ and $K_0 = 56967.3 M_\odot \text{ Kpc}^{-3} (\text{km/s})^2$, in which case the reduced χ^2_{red} value is $\chi^2_{red} = 934.878$. Also the parameter α in this case is $\alpha = 12.478 \text{ Kpc}$.

In Table CLVII we present the optimized values of K_0 and ρ_0 for the analytic SIDM model of Eq. (3) for which the maximum compatibility with the SPARC data is achieved. In Figs. 251, 252 we present

TABLE CLVII: SIDM Optimization Values for the galaxy UGC02953

Parameter	Optimization Values
$\rho_0 (M_\odot/\text{Kpc}^3)$	1.21853×10^8
$K_0 (M_\odot \text{ Kpc}^{-3} (\text{km/s})^2)$	56967.3

the density of the analytic SIDM model, the predicted rotation curves for the SIDM model (3), versus the SPARC observational data and the sound speed, as a function of the radius respectively. As it can be seen, for this galaxy, the SIDM model produces non-viable rotation curves which are incompatible with the SPARC data.

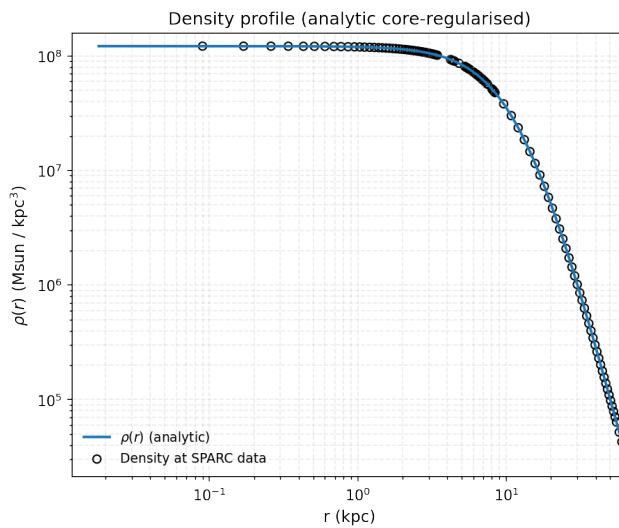


FIG. 251: The density of the SIDM model of Eq. (3) for the galaxy UGC02953, versus the radius.

Now we shall include contributions to the rotation velocity from the other components of the galaxy, namely the disk, the gas, and the bulge if present. In Fig. 253 we present the combined rotation curves including all the components of the galaxy along with the SIDM. As it can be seen, the extended collisional DM model is non-viable. Also in Table CLVIII we present the optimized values of the free

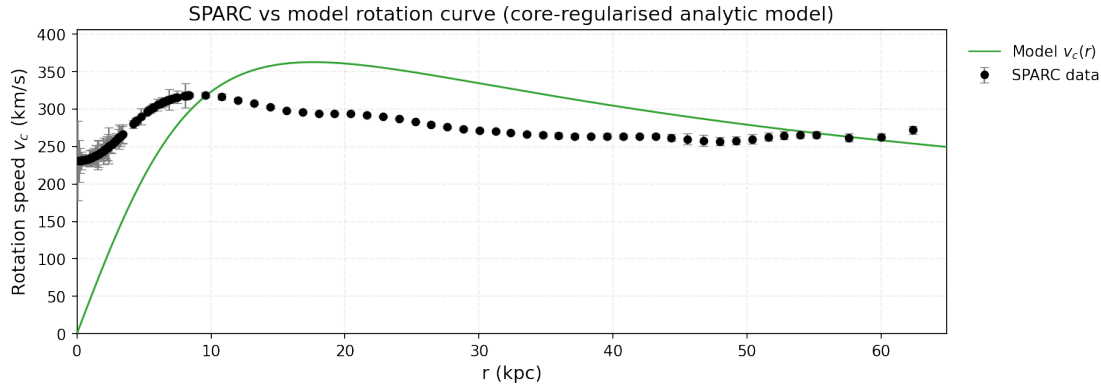


FIG. 252: The predicted rotation curves for the optimized SIDM model of Eq. (3), versus the SPARC observational data for the galaxy UGC02953.

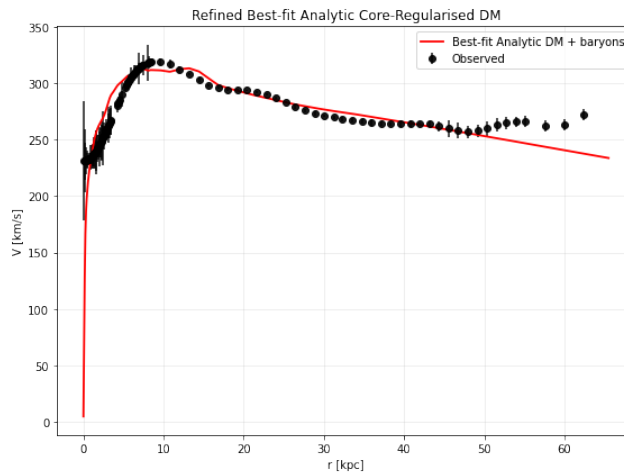


FIG. 253: The predicted rotation curves after using an optimization for the SIDM model (3), and the extended SPARC data for the galaxy UGC02953. We included the rotation curves of the gas, the disk velocities, the bulge (where present) along with the SIDM model.

parameters of the SIDM model for which we achieve the maximum compatibility with the SPARC data, for the galaxy UGC02953, and also the resulting reduced χ^2_{red} value.

TABLE CLVIII: Optimized Parameter Values of the Extended SIDM model for the Galaxy UGC02953.

Parameter	Value
ρ_0 (M_\odot/Kpc^3)	8.2663×10^6
K_0 ($M_\odot \text{ Kpc}^{-3} (\text{km/s})^2$)	19898.9
ml_{disk}	0.9064
ml_{bulge}	0.8139
α (Kpc)	28.311
χ^2_{red}	7.09491

84. The Galaxy UGC03205, Non-viable

For this galaxy, the optimization method we used, ensures maximum compatibility of the analytic SIDM model of Eq. (3) with the SPARC data, if we choose $\rho_0 = 1.3911 \times 10^8 M_\odot/\text{Kpc}^3$ and $K_0 = 26786 M_\odot \text{ Kpc}^{-3} (\text{km/s})^2$, in which case the reduced χ^2_{red} value is $\chi^2_{red} = 34.3376$. Also the parameter α in this case is $\alpha = 8.008 \text{ Kpc}$.

In Table CLIX we present the optimized values of K_0 and ρ_0 for the analytic SIDM model of Eq. (3) for which the maximum compatibility with the SPARC data is achieved. In Figs. 254, 255 we present

TABLE CLIX: SIDM Optimization Values for the galaxy UGC03205

Parameter	Optimization Values
$\rho_0 (M_\odot/\text{Kpc}^3)$	1.3911×10^8
$K_0 (M_\odot \text{ Kpc}^{-3} (\text{km/s})^2)$	26786

the density of the analytic SIDM model, the predicted rotation curves for the SIDM model (3), versus the SPARC observational data and the sound speed, as a function of the radius respectively. As it can be seen, for this galaxy, the SIDM model produces non-viable rotation curves which are incompatible with the SPARC data.

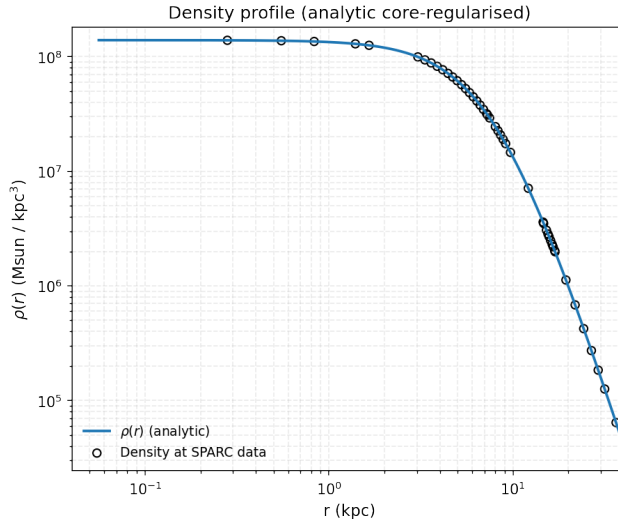


FIG. 254: The density of the SIDM model of Eq. (3) for the galaxy UGC03205, versus the radius.

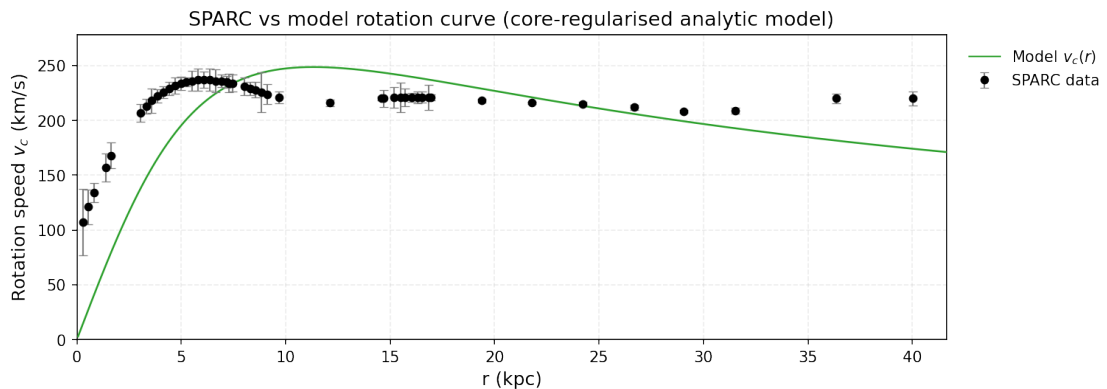


FIG. 255: The predicted rotation curves for the optimized SIDM model of Eq. (3), versus the SPARC observational data for the galaxy UGC03205.

Now we shall include contributions to the rotation velocity from the other components of the galaxy, namely the disk, the gas, and the bulge if present. In Fig. 256 we present the combined rotation curves including all the components of the galaxy along with the SIDM. As it can be seen, the extended collisional DM model is non-viable. Also in Table CLX we present the optimized values of the free parameters of the SIDM model for which we achieve the maximum compatibility with the SPARC data, for the galaxy UGC03205, and also the resulting reduced χ^2_{red} value.

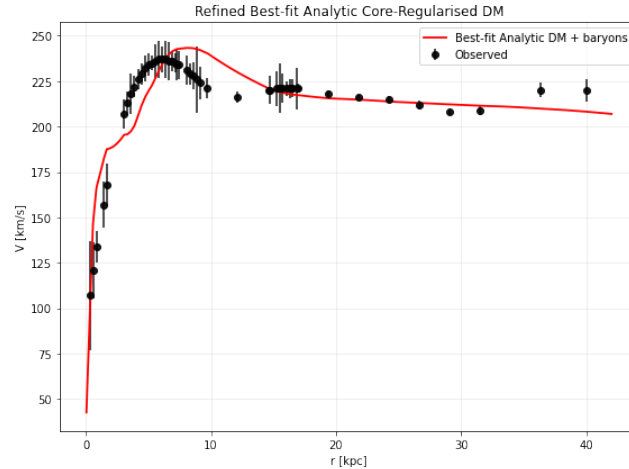


FIG. 256: The predicted rotation curves after using an optimization for the SIDM model (3), and the extended SPARC data for the galaxy UGC03205. We included the rotation curves of the gas, the disk velocities, the bulge (where present) along with the SIDM model.

TABLE CLX: Optimized Parameter Values of the Extended SIDM model for the Galaxy UGC03205.

Parameter	Value
$\rho_0 (M_\odot/\text{Kpc}^3)$	3.45378×10^6
$K_0 (M_\odot \text{ Kpc}^{-3} (\text{km/s})^2)$	13033.5
ml_{disk}	0.9924
ml_{bulge}	1
$\alpha (\text{Kpc})$	35.4469
χ^2_{red}	3.95292

85. The Galaxy UGC03546, Non-viable, Extended Viable

For this galaxy, the optimization method we used, ensures maximum compatibility of the analytic SIDM model of Eq. (3) with the SPARC data, if we choose $\rho_0 = 2.26423 \times 10^8 M_\odot/\text{Kpc}^3$ and $K_0 = 23234.7 M_\odot \text{ Kpc}^{-3} (\text{km/s})^2$, in which case the reduced χ^2_{red} value is $\chi^2_{\text{red}} = 98.132$. Also the parameter α in this case is $\alpha = 5.846 \text{ Kpc}$.

In Table CLXI we present the optimized values of K_0 and ρ_0 for the analytic SIDM model of Eq. (3) for which the maximum compatibility with the SPARC data is achieved. In Figs. 257, 258 we present

TABLE CLXI: SIDM Optimization Values for the galaxy UGC03546

Parameter	Optimization Values
$\rho_0 (M_\odot/\text{Kpc}^3)$	2.26423×10^8
$K_0 (M_\odot \text{ Kpc}^{-3} (\text{km/s})^2)$	23234.7

the density of the analytic SIDM model, the predicted rotation curves for the SIDM model (3), versus the SPARC observational data and the sound speed, as a function of the radius respectively. As it can be seen, for this galaxy, the SIDM model produces non-viable rotation curves which are incompatible with the SPARC data.

Now we shall include contributions to the rotation velocity from the other components of the galaxy, namely the disk, the gas, and the bulge if present. In Fig. 259 we present the combined rotation curves including all the components of the galaxy along with the SIDM. As it can be seen, the extended collisional DM model is viable. Also in Table CLXII we present the optimized values of the free parameters of the SIDM model for which we achieve the maximum compatibility with the SPARC data, for the galaxy UGC03546, and also the resulting reduced χ^2_{red} value.

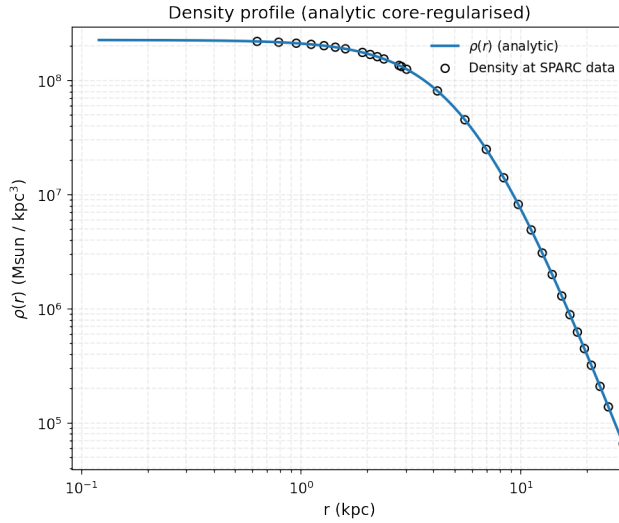


FIG. 257: The density of the SIDM model of Eq. (3) for the galaxy UGC03546, versus the radius.

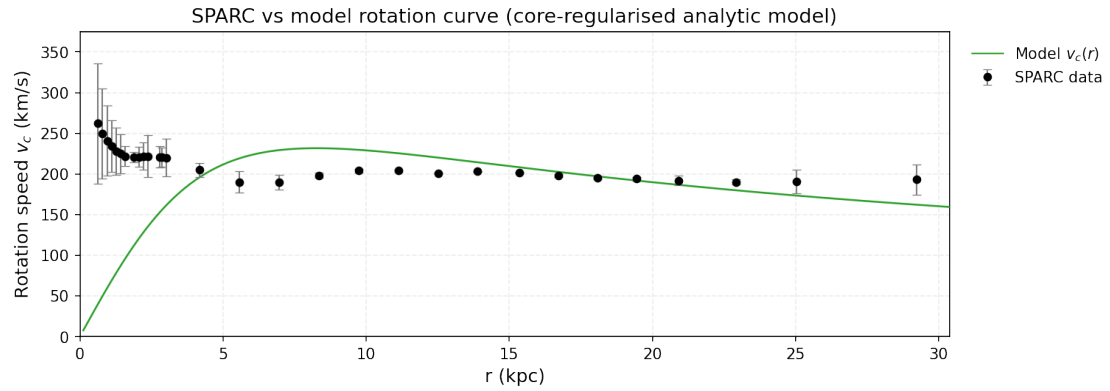


FIG. 258: The predicted rotation curves for the optimized SIDM model of Eq. (3), versus the SPARC observational data for the galaxy UGC03546.

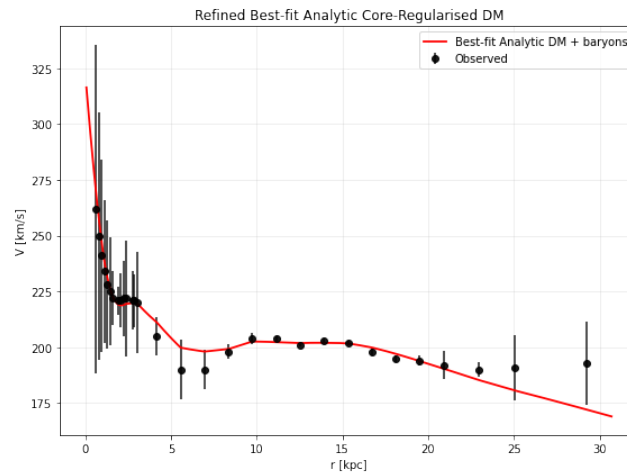


FIG. 259: The predicted rotation curves after using an optimization for the SIDM model (3), and the extended SPARC data for the galaxy UGC03546. We included the rotation curves of the gas, the disk velocities, the bulge (where present) along with the SIDM model.

TABLE CLXII: Optimized Parameter Values of the Extended SIDM model for the Galaxy UGC03546.

Parameter	Value
$\rho_0 (M_\odot/\text{Kpc}^3)$	1.62481×10^7
$K_0 (M_\odot \text{ Kpc}^{-3} (\text{km/s})^2)$	9543.66
ml_{disk}	0.7826
ml_{bulge}	0.6702
$\alpha (\text{Kpc})$	13.9847
χ^2_{red}	0.638214

86. The Galaxy UGC03580, Non-viable

For this galaxy, the optimization method we used, ensures maximum compatibility of the analytic SIDM model of Eq. (3) with the SPARC data, if we choose $\rho_0 = 8.61957 \times 10^7 M_\odot/\text{Kpc}^3$ and $K_0 = 7580.54 M_\odot \text{ Kpc}^{-3} (\text{km/s})^2$, in which case the reduced χ^2_{red} value is $\chi^2_{\text{red}} = 75.2683$. Also the parameter α in this case is $\alpha = 5.412 \text{ Kpc}$.

In Table CLXIII we present the optimized values of K_0 and ρ_0 for the analytic SIDM model of Eq. (3) for which the maximum compatibility with the SPARC data is achieved. In Figs. 260, 261 we present

TABLE CLXIII: SIDM Optimization Values for the galaxy UGC03580

Parameter	Optimization Values
$\rho_0 (M_\odot/\text{Kpc}^3)$	8.61957×10^7
$K_0 (M_\odot \text{ Kpc}^{-3} (\text{km/s})^2)$	7580.54

the density of the analytic SIDM model, the predicted rotation curves for the SIDM model (3), versus the SPARC observational data and the sound speed, as a function of the radius respectively. As it can be seen, for this galaxy, the SIDM model produces non-viable rotation curves which are incompatible with the SPARC data.

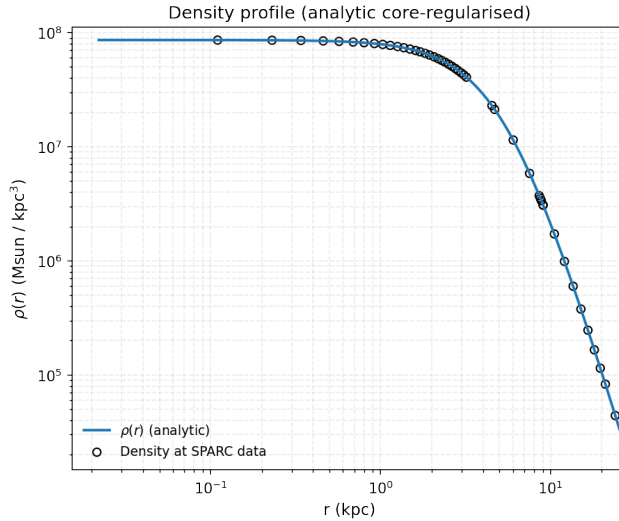


FIG. 260: The density of the SIDM model of Eq. (3) for the galaxy UGC03580, versus the radius.

Now we shall include contributions to the rotation velocity from the other components of the galaxy, namely the disk, the gas, and the bulge if present. In Fig. 262 we present the combined rotation curves including all the components of the galaxy along with the SIDM. As it can be seen, the extended collisional DM model is non-viable. Also in Table CLXIV we present the optimized values of the free parameters of the SIDM model for which we achieve the maximum compatibility with the SPARC data, for the galaxy UGC03580, and also the resulting reduced χ^2_{red} value.

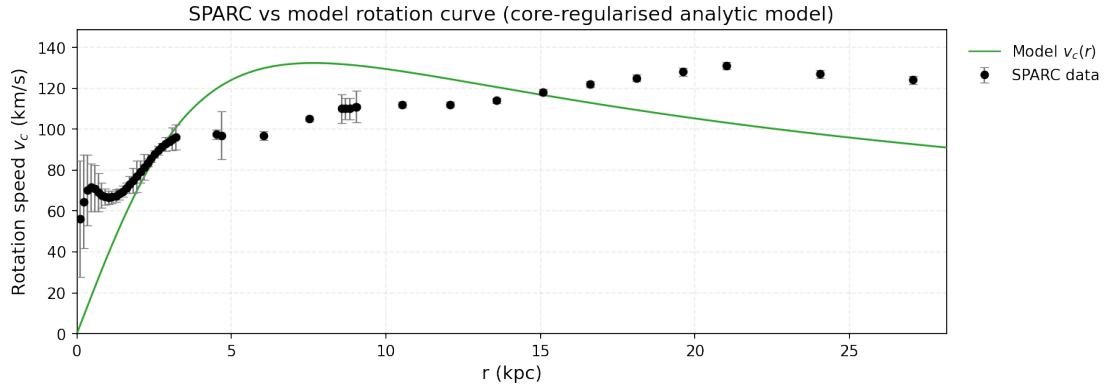


FIG. 261: The predicted rotation curves for the optimized SIDM model of Eq. (3), versus the SPARC observational data for the galaxy UGC03580.

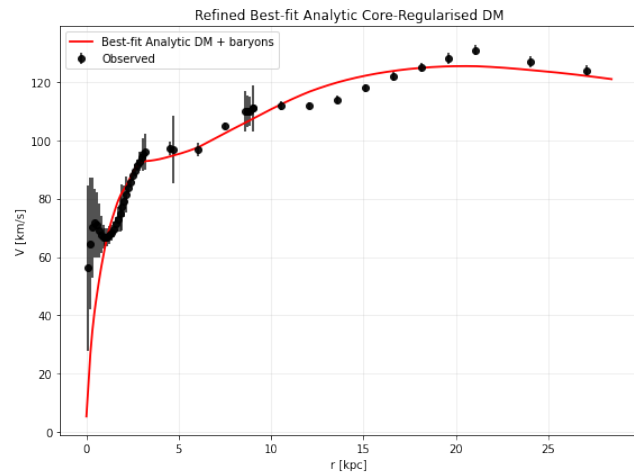


FIG. 262: The predicted rotation curves after using an optimization for the SIDM model (3), and the extended SPARC data for the galaxy UGC03580. We included the rotation curves of the gas, the disk velocities, the bulge (where present) along with the SIDM model.

TABLE CLXIV: Optimized Parameter Values of the Extended SIDM model for the Galaxy UGC03580.

Parameter	Value
$\rho_0 (M_\odot/\text{Kpc}^3)$	6.43606×10^6
$K_0 (M_\odot \text{ Kpc}^{-3} (\text{km/s})^2)$	5409
ml_{disk}	0.8941
ml_{bulge}	0.2673
$\alpha (\text{Kpc})$	16.728
χ^2_{red}	3.22713

87. The Galaxy UGC04278, Non-viable, Extended Viable

For this galaxy, the optimization method we used, ensures maximum compatibility of the analytic SIDM model of Eq. (3) with the SPARC data, if we choose $\rho_0 = 2.39591 \times 10^7 M_\odot/\text{Kpc}^3$ and $K_0 = 3846.21 M_\odot \text{ Kpc}^{-3} (\text{km/s})^2$, in which case the reduced χ^2_{red} value is $\chi^2_{\text{red}} = 1.79109$. Also the parameter α in this case is $\alpha = 7.31193 \text{ Kpc}$.

In Table CLXV we present the optimized values of K_0 and ρ_0 for the analytic SIDM model of Eq. (3) for which the maximum compatibility with the SPARC data is achieved. In Figs. 263, 264 we present the density of the analytic SIDM model, the predicted rotation curves for the SIDM model (3), versus the SPARC observational data and the sound speed, as a function of the radius respectively. As it can be seen, for this galaxy, the SIDM model produces non-viable rotation curves which are incompatible with the SPARC data.

TABLE CLXV: SIDM Optimization Values for the galaxy UGC04278

Parameter	Optimization Values
$\rho_0 (M_\odot/\text{Kpc}^3)$	2.39591×10^7
$K_0 (M_\odot \text{ Kpc}^{-3} (\text{km/s})^2)$	3846.21

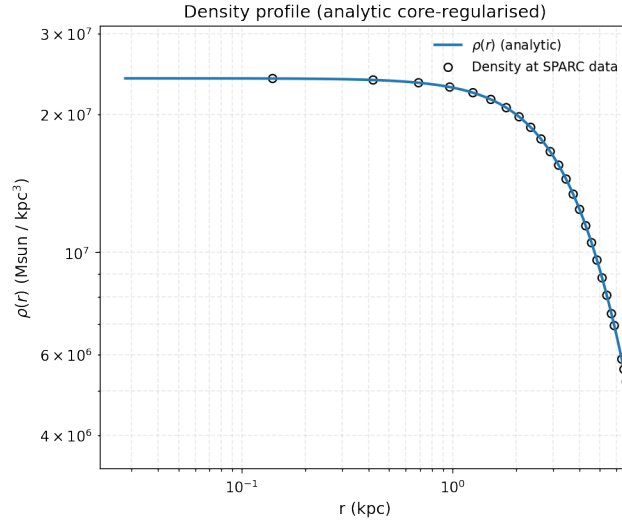


FIG. 263: The density of the SIDM model of Eq. (3) for the galaxy UGC04278, versus the radius.

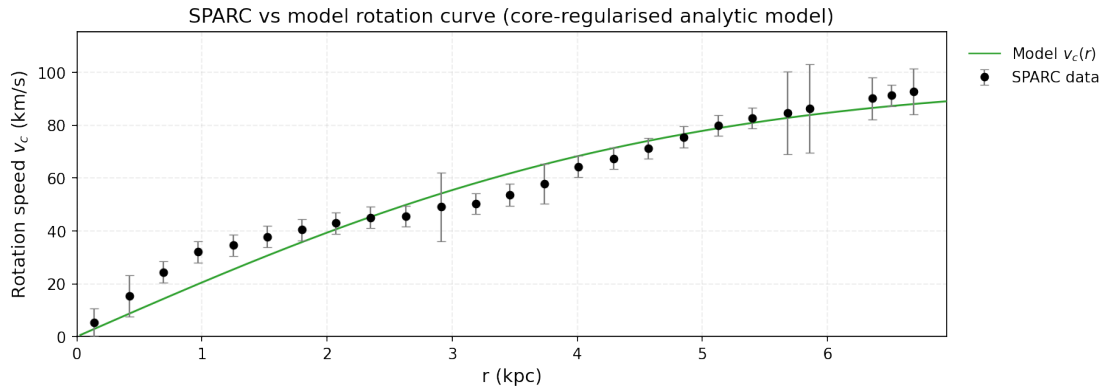


FIG. 264: The predicted rotation curves for the optimized SIDM model of Eq. (3), versus the SPARC observational data for the galaxy UGC04278.

Now we shall include contributions to the rotation velocity from the other components of the galaxy, namely the disk, the gas, and the bulge if present. In Fig. 265 we present the combined rotation curves including all the components of the galaxy along with the SIDM. As it can be seen, the extended collisional DM model is non-viable. Also in Table CLXVI we present the optimized values of the free parameters of the SIDM model for which we achieve the maximum compatibility with the SPARC data, for the galaxy UGC04278, and also the resulting reduced χ^2_{red} value.

TABLE CLXVI: Optimized Parameter Values of the Extended SIDM model for the Galaxy UGC04278.

Parameter	Value
$\rho_0 (M_\odot/\text{Kpc}^3)$	1.11917×10^7
$K_0 (M_\odot \text{ Kpc}^{-3} (\text{km/s})^2)$	6514.27
ml_{disk}	1
ml_{bulge}	0.5354
$\alpha (\text{Kpc})$	13.9214
χ^2_{red}	0.45359

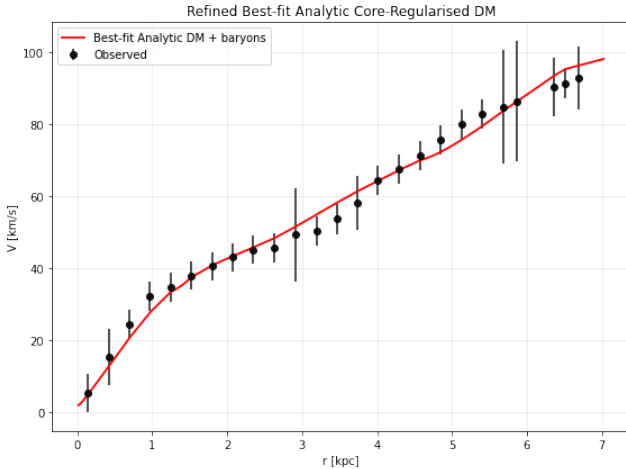


FIG. 265: The predicted rotation curves after using an optimization for the SIDM model (3), and the extended SPARC data for the galaxy UGC04278. We included the rotation curves of the gas, the disk velocities, the bulge (where present) along with the SIDM model.

88. The Galaxy UGC04325

For this galaxy, the optimization method we used, ensures maximum compatibility of the analytic SIDM model of Eq. (3) with the SPARC data, if we choose $\rho_0 = 1.8532 \times 10^8 M_\odot/\text{Kpc}^3$ and $K_0 = 3763.46 M_\odot \text{Kpc}^{-3} (\text{km/s})^2$, in which case the reduced χ^2_{red} value is $\chi^2_{\text{red}} = 0.706892$. Also the parameter α in this case is $\alpha = 2.60065 \text{Kpc}$.

In Table CLXVII we present the optimized values of K_0 and ρ_0 for the analytic SIDM model of Eq. (3) for which the maximum compatibility with the SPARC data is achieved. In Figs. 266, 267 we present

TABLE CLXVII: SIDM Optimization Values for the galaxy UGC04325

Parameter	Optimization Values
$\rho_0 (M_\odot/\text{Kpc}^3)$	1.8532×10^8
$K_0 (M_\odot \text{Kpc}^{-3} (\text{km/s})^2)$	3763.46

the density of the analytic SIDM model, the predicted rotation curves for the SIDM model (3), versus the SPARC observational data and the sound speed, as a function of the radius respectively. As it can be seen, for this galaxy, the SIDM model produces viable rotation curves which are compatible with the SPARC data.

89. The Galaxy UGC04483

For this galaxy, the optimization method we used, ensures maximum compatibility of the analytic SIDM model of Eq. (3) with the SPARC data, if we choose $\rho_0 = 1.20775 \times 10^8 M_\odot/\text{Kpc}^3$ and $K_0 = 253.812 M_\odot \text{Kpc}^{-3} (\text{km/s})^2$, in which case the reduced χ^2_{red} value is $\chi^2_{\text{red}} = 0.395683$. Also the parameter α in this case is $\alpha = 0.836599 \text{Kpc}$.

In Table CLXVIII we present the optimized values of K_0 and ρ_0 for the analytic SIDM model of Eq. (3) for which the maximum compatibility with the SPARC data is achieved. In Figs. 268, 269 we present

TABLE CLXVIII: SIDM Optimization Values for the galaxy UGC04483

Parameter	Optimization Values
$\rho_0 (M_\odot/\text{Kpc}^3)$	1.20775×10^8
$K_0 (M_\odot \text{Kpc}^{-3} (\text{km/s})^2)$	253.812

the density of the analytic SIDM model, the predicted rotation curves for the SIDM model (3), versus the SPARC observational data and the sound speed, as a function of the radius respectively. As it can

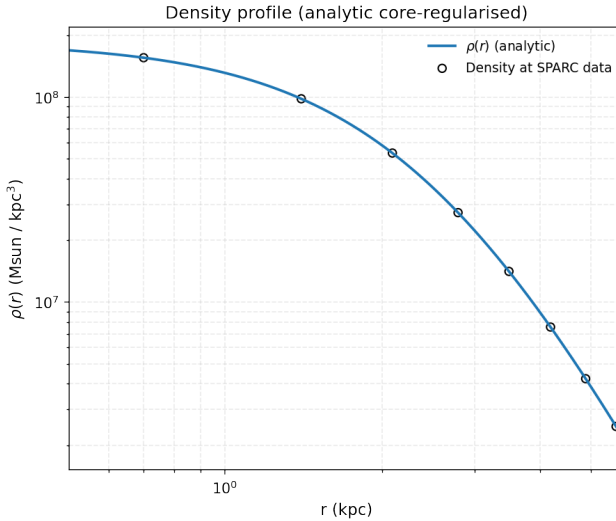


FIG. 266: The density of the SIDM model of Eq. (3) for the galaxy UGC04325, versus the radius.

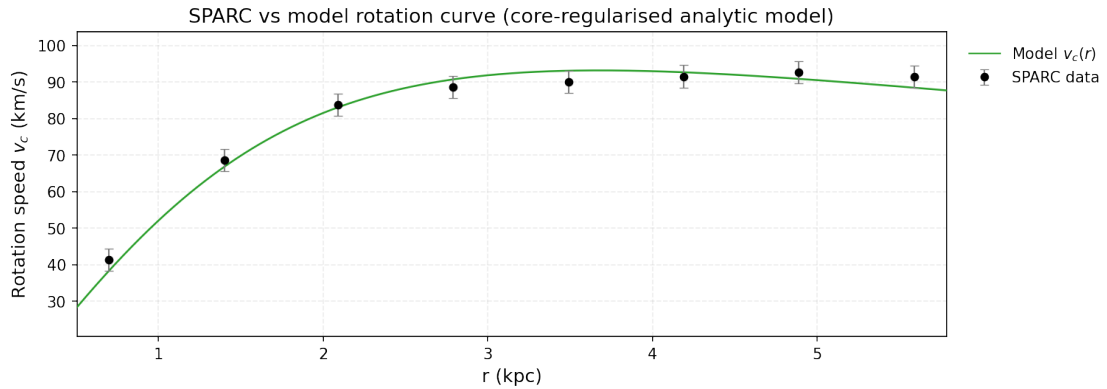


FIG. 267: The predicted rotation curves for the optimized SIDM model of Eq. (3), versus the SPARC observational data for the galaxy UGC04325.

be seen, for this galaxy, the SIDM model produces viable rotation curves which are compatible with the SPARC data.

90. The Galaxy UGC04499

For this galaxy, the optimization method we used, ensures maximum compatibility of the analytic SIDM model of Eq. (3) with the SPARC data, if we choose $\rho_0 = 3.70754 \times 10^7 M_\odot / \text{Kpc}^3$ and $K_0 = 2303.64 M_\odot \text{ Kpc}^{-3} (\text{km/s})^2$, in which case the reduced χ^2_{red} value is $\chi^2_{\text{red}} = 0.756822$. Also the parameter α in this case is $\alpha = 4.549 \text{ Kpc}$.

In Table CLXIX we present the optimized values of K_0 and ρ_0 for the analytic SIDM model of Eq. (3) for which the maximum compatibility with the SPARC data is achieved. In Figs. 270, 271 we present

TABLE CLXIX: SIDM Optimization Values for the galaxy UGC04499

Parameter	Optimization Values
$\rho_0 (M_\odot / \text{Kpc}^3)$	3.70754×10^7
$K_0 (M_\odot \text{ Kpc}^{-3} (\text{km/s})^2)$	2303.64

the density of the analytic SIDM model, the predicted rotation curves for the SIDM model (3), versus the SPARC observational data and the sound speed, as a function of the radius respectively. As it can

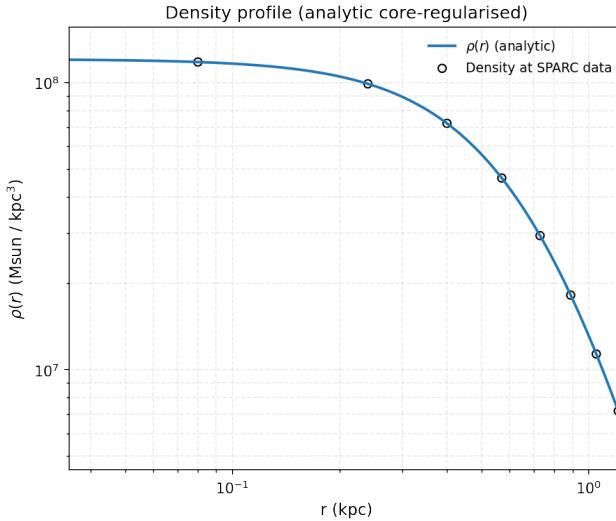


FIG. 268: The density of the SIDM model of Eq. (3) for the galaxy UGC04483, versus the radius.

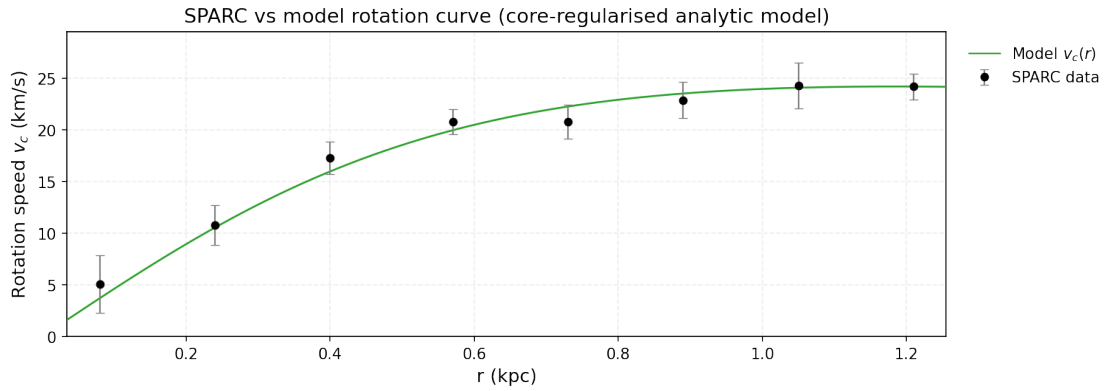


FIG. 269: The predicted rotation curves for the optimized SIDM model of Eq. (3), versus the SPARC observational data for the galaxy UGC04483.

be seen, for this galaxy, the SIDM model produces viable rotation curves which are compatible with the SPARC data.

91. The Galaxy UGC05005

For this galaxy, the optimization method we used, ensures maximum compatibility of the analytic SIDM model of Eq. (3) with the SPARC data, if we choose $\rho_0 = 6.43428 \times 10^6 M_\odot / \text{Kpc}^3$ and $K_0 = 4016.81 M_\odot \text{ Kpc}^{-3} (\text{km/s})^2$, in which case the reduced χ^2_{red} value is $\chi^2_{\text{red}} = 0.285774$. Also the parameter α in this case is $\alpha = 14.4192 \text{ Kpc}$.

In Table CLXX we present the optimized values of K_0 and ρ_0 for the analytic SIDM model of Eq. (3) for which the maximum compatibility with the SPARC data is achieved. In Figs. 272, 273 we present

TABLE CLXX: SIDM Optimization Values for the galaxy UGC05005

Parameter	Optimization Values
$\rho_0 (M_\odot / \text{Kpc}^3)$	6.43428×10^6
$K_0 (M_\odot \text{ Kpc}^{-3} (\text{km/s})^2)$	4016.81

the density of the analytic SIDM model, the predicted rotation curves for the SIDM model (3), versus the SPARC observational data and the sound speed, as a function of the radius respectively. As it can

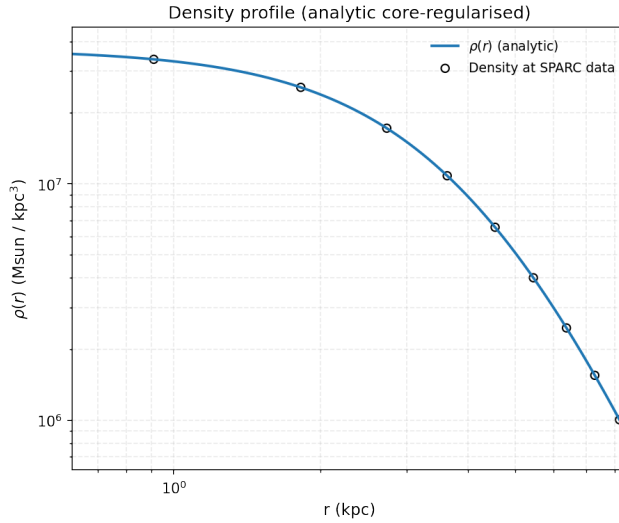


FIG. 270: The density of the SIDM model of Eq. (3) for the galaxy UGC04499, versus the radius.

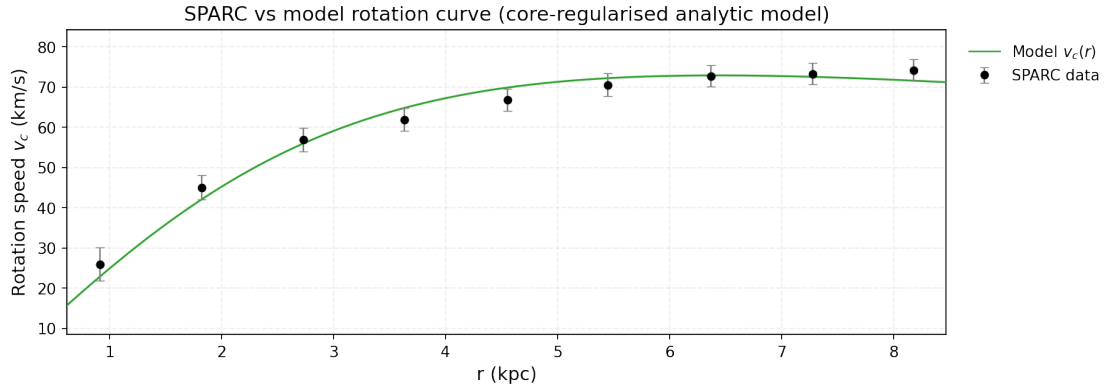


FIG. 271: The predicted rotation curves for the optimized SIDM model of Eq. (3), versus the SPARC observational data for the galaxy UGC04499.

be seen, for this galaxy, the SIDM model produces viable rotation curves which are compatible with the SPARC data.

92. The Galaxy UGC05253, Non-viable, Extended Viable

For this galaxy, the optimization method we used, ensures maximum compatibility of the analytic SIDM model of Eq. (3) with the SPARC data, if we choose $\rho_0 = 1.23585 \times 10^8 M_\odot / \text{Kpc}^3$ and $K_0 = 42151.6 M_\odot \text{ Kpc}^{-3} (\text{km/s})^2$, in which case the reduced χ^2_{red} value is $\chi^2_{\text{red}} = 1141.15$. Also the parameter α in this case is $\alpha = 10.658 \text{ Kpc}$.

In Table CLXXI we present the optimized values of K_0 and ρ_0 for the analytic SIDM model of Eq. (3) for which the maximum compatibility with the SPARC data is achieved. In Figs. 274, 275 we present

TABLE CLXXI: SIDM Optimization Values for the galaxy UGC05253

Parameter	Optimization Values
$\rho_0 (M_\odot / \text{Kpc}^3)$	1.23585×10^8
$K_0 (M_\odot \text{ Kpc}^{-3} (\text{km/s})^2)$	42151.6

the density of the analytic SIDM model, the predicted rotation curves for the SIDM model (3), versus the SPARC observational data and the sound speed, as a function of the radius respectively. As it can

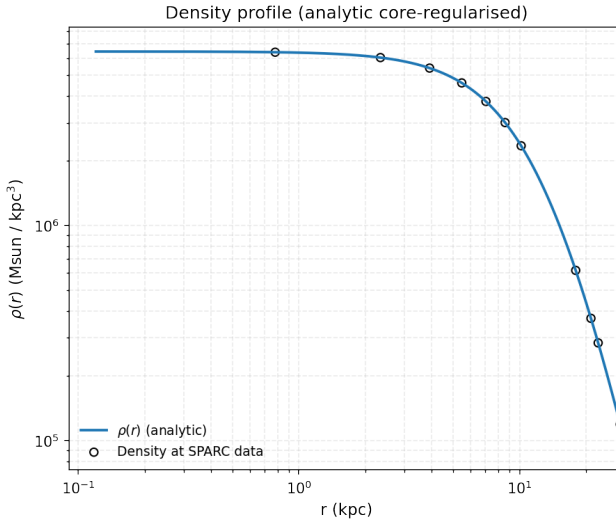


FIG. 272: The density of the SIDM model of Eq. (3) for the galaxy UGC05005, versus the radius.

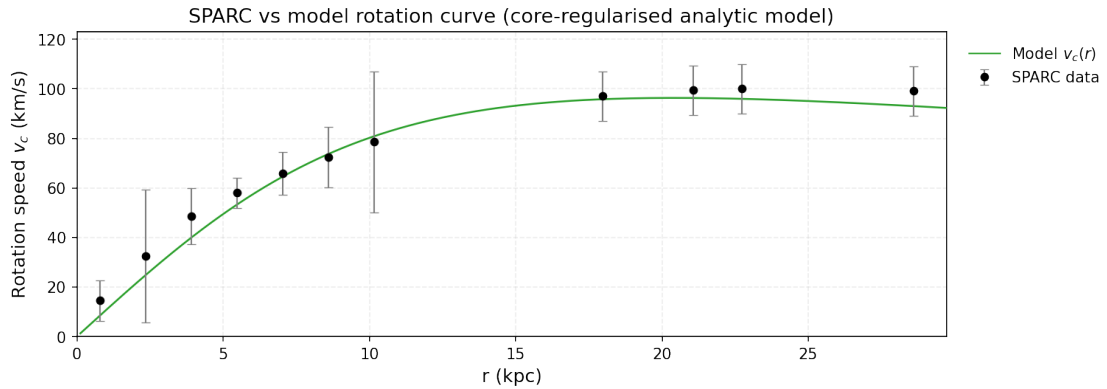


FIG. 273: The predicted rotation curves for the optimized SIDM model of Eq. (3), versus the SPARC observational data for the galaxy UGC05005.

be seen, for this galaxy, the SIDM model produces non-viable rotation curves which are incompatible with the SPARC data.

Now we shall include contributions to the rotation velocity from the other components of the galaxy, namely the disk, the gas, and the bulge if present. In Fig. 276 we present the combined rotation curves including all the components of the galaxy along with the SIDM. As it can be seen, the extended collisional DM model is viable. Also in Table CLXXII we present the optimized values of the free parameters of the SIDM model for which we achieve the maximum compatibility with the SPARC data, for the galaxy UGC05253, and also the resulting reduced χ^2_{red} value.

TABLE CLXXII: Optimized Parameter Values of the Extended SIDM model for the Galaxy UGC05253.

Parameter	Value
$\rho_0 (M_\odot / \text{Kpc}^3)$	1.35094×10^7
$K_0 (M_\odot \text{ Kpc}^{-3} (\text{km/s})^2)$	15849.8
ml_{disk}	0.8062
ml_{bulge}	0.8488
$\alpha (\text{Kpc})$	19.7647
χ^2_{red}	0.799952

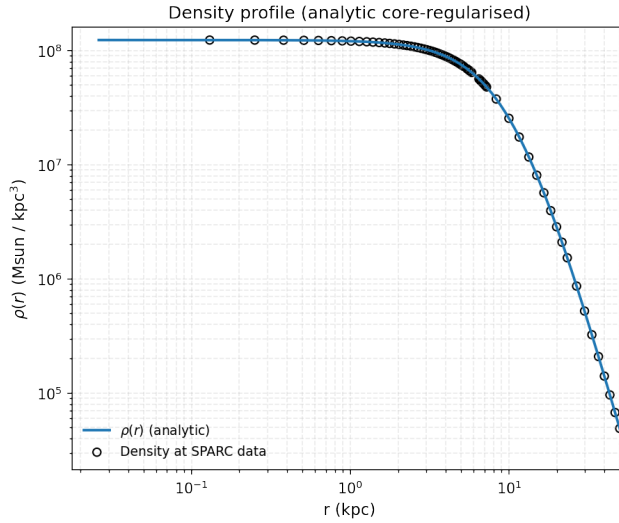


FIG. 274: The density of the SIDM model of Eq. (3) for the galaxy UGC05253, versus the radius.

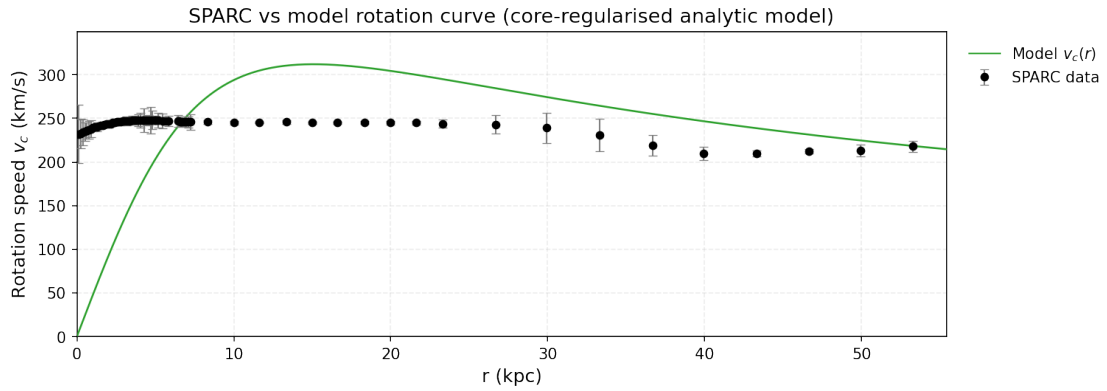


FIG. 275: The predicted rotation curves for the optimized SIDM model of Eq. (3), versus the SPARC observational data for the galaxy UGC05253.

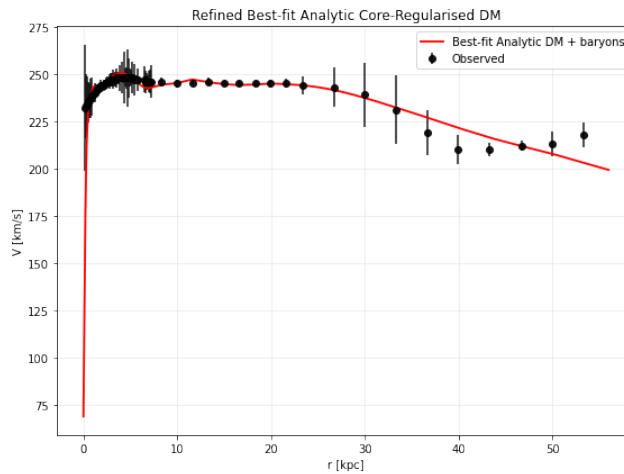


FIG. 276: The predicted rotation curves after using an optimization for the SIDM model (3), and the extended SPARC data for the galaxy UGC05253. We included the rotation curves of the gas, the disk velocities, the bulge (where present) along with the SIDM model.

93. The Galaxy UGC05414

For this galaxy, the optimization method we used, ensures maximum compatibility of the analytic SIDM model of Eq. (3) with the SPARC data, if we choose $\rho_0 = 4.14699 \times 10^7 M_\odot/\text{Kpc}^3$ and $K_0 = 1615.04 M_\odot \text{Kpc}^{-3} (\text{km/s})^2$, in which case the reduced χ^2_{red} value is $\chi^2_{red} = 0.458671$. Also the parameter α in this case is $\alpha = 3.60143 \text{Kpc}$.

In Table CLXXIII we present the optimized values of K_0 and ρ_0 for the analytic SIDM model of Eq. (3) for which the maximum compatibility with the SPARC data is achieved. In Figs. 277, 278 we present

TABLE CLXXIII: SIDM Optimization Values for the galaxy UGC05414

Parameter	Optimization Values
$\rho_0 (M_\odot/\text{Kpc}^3)$	4.14699×10^7
$K_0 (M_\odot \text{Kpc}^{-3} (\text{km/s})^2)$	1615.04

the density of the analytic SIDM model, the predicted rotation curves for the SIDM model (3), versus the SPARC observational data and the sound speed, as a function of the radius respectively. As it can be seen, for this galaxy, the SIDM model produces viable rotation curves which are compatible with the SPARC data.

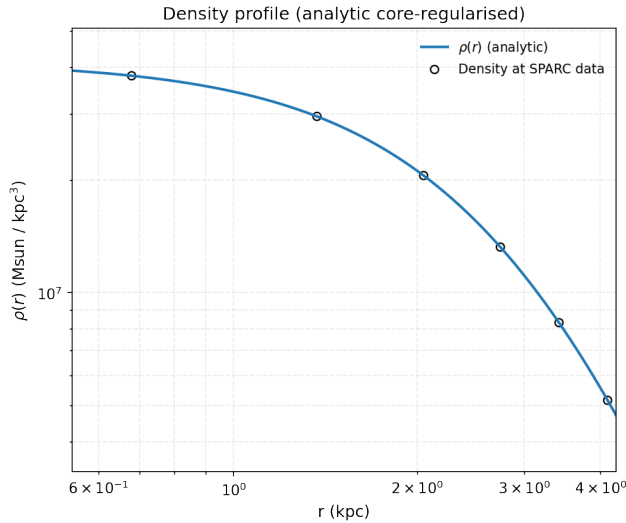


FIG. 277: The density of the SIDM model of Eq. (3) for the galaxy UGC05414, versus the radius.

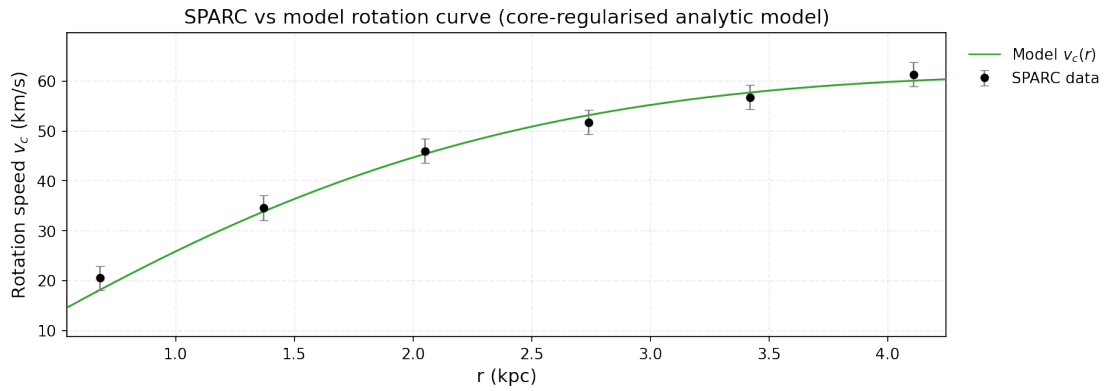


FIG. 278: The predicted rotation curves for the optimized SIDM model of Eq. (3), versus the SPARC observational data for the galaxy UGC05414.

94. The Galaxy UGC05716, Non-viable

For this galaxy, the optimization method we used, ensures maximum compatibility of the analytic SIDM model of Eq. (3) with the SPARC data, if we choose $\rho_0 = 2.00932 \times 10^7 M_\odot/\text{Kpc}^3$ and $K_0 = 2336.07 M_\odot \text{Kpc}^{-3} (\text{km/s})^2$, in which case the reduced χ^2_{red} value is $\chi^2_{red} = 20.0144$. Also the parameter α in this case is $\alpha = 6.22257 \text{Kpc}$.

In Table CLXXIV we present the optimized values of K_0 and ρ_0 for the analytic SIDM model of Eq. (3) for which the maximum compatibility with the SPARC data is achieved. In Figs. 279, 280 we present

TABLE CLXXIV: SIDM Optimization Values for the galaxy UGC05716

Parameter	Optimization Values
$\rho_0 (M_\odot/\text{Kpc}^3)$	2.00932×10^7
$K_0 (M_\odot \text{Kpc}^{-3} (\text{km/s})^2)$	2336.07

the density of the analytic SIDM model, the predicted rotation curves for the SIDM model (3), versus the SPARC observational data and the sound speed, as a function of the radius respectively. As it can be seen, for this galaxy, the SIDM model produces non-viable rotation curves which are incompatible with the SPARC data.

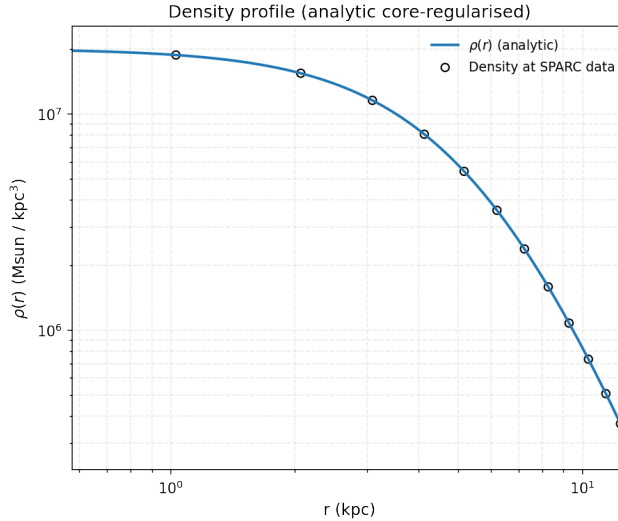


FIG. 279: The density of the SIDM model of Eq. (3) for the galaxy UGC05716, versus the radius.

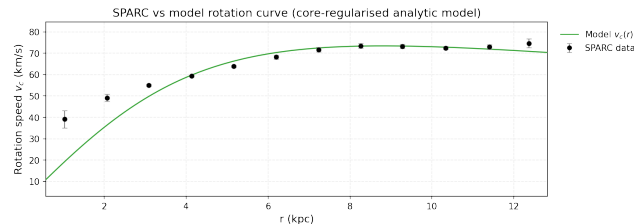


FIG. 280: The predicted rotation curves for the optimized SIDM model of Eq. (3), versus the SPARC observational data for the galaxy UGC05716.

Now we shall include contributions to the rotation velocity from the other components of the galaxy, namely the disk, the gas, and the bulge if present. In Fig. 281 we present the combined rotation curves including all the components of the galaxy along with the SIDM. As it can be seen, the extended collisional DM model is non-viable. Also in Table CLXXV we present the optimized values of the free parameters of the SIDM model for which we achieve the maximum compatibility with the SPARC data, for the galaxy UGC05716, and also the resulting reduced χ^2_{red} value.

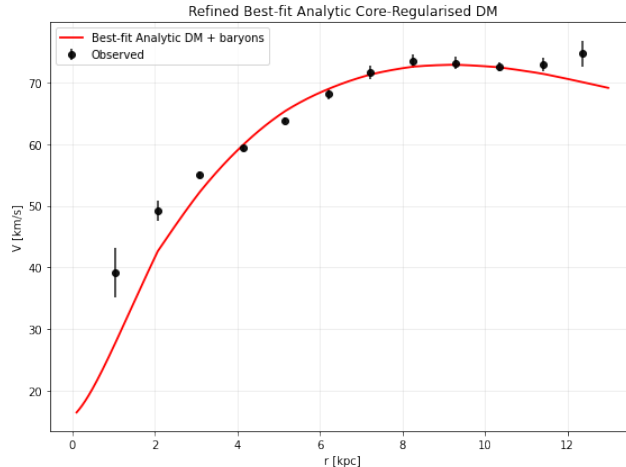


FIG. 281: The predicted rotation curves after using an optimization for the SIDM model (3), and the extended SPARC data for the galaxy UGC05716. We included the rotation curves of the gas, the disk velocities, the bulge (where present) along with the SIDM model.

TABLE CLXXV: Optimized Parameter Values of the Extended SIDM model for the Galaxy UGC05716.

Parameter	Value
$\rho_0 (M_\odot/\text{Kpc}^3)$	1.50901×10^7
$K_0 (M_\odot \text{ Kpc}^{-3} (\text{km/s})^2)$	1811.55
ml_{disk}	1
ml_{bulge}	0.3007
$\alpha (\text{Kpc})$	6.32229
χ^2_{red}	8.33583

95. The Galaxy UGC05721, Non-viable, Extended Viable

For this galaxy, the optimization method we used, ensures maximum compatibility of the analytic SIDM model of Eq. (3) with the SPARC data, if we choose $\rho_0 = 3.62066 \times 10^8 M_\odot/\text{Kpc}^3$ and $K_0 = 3269.08 M_\odot \text{ Kpc}^{-3} (\text{km/s})^2$, in which case the reduced χ^2_{red} value is $\chi^2_{\text{red}} = 2.11638$. Also the parameter α in this case is $\alpha = 1.73408 \text{ Kpc}$.

In Table CLXXVI we present the optimized values of K_0 and ρ_0 for the analytic SIDM model of Eq. (3) for which the maximum compatibility with the SPARC data is achieved. In Figs. 282, 283 we present

TABLE CLXXVI: SIDM Optimization Values for the galaxy UGC05721

Parameter	Optimization Values
$\rho_0 (M_\odot/\text{Kpc}^3)$	3.62066×10^8
$K_0 (M_\odot \text{ Kpc}^{-3} (\text{km/s})^2)$	3269.08

the density of the analytic SIDM model, the predicted rotation curves for the SIDM model (3), versus the SPARC observational data and the sound speed, as a function of the radius respectively. As it can be seen, for this galaxy, the SIDM model produces non-viable rotation curves which are incompatible with the SPARC data.

Now we shall include contributions to the rotation velocity from the other components of the galaxy, namely the disk, the gas, and the bulge if present. In Fig. 284 we present the combined rotation curves including all the components of the galaxy along with the SIDM. As it can be seen, the extended collisional DM model is non-viable. Also in Table CLXXVII we present the optimized values of the free parameters of the SIDM model for which we achieve the maximum compatibility with the SPARC data, for the galaxy UGC05721, and also the resulting reduced χ^2_{red} value.

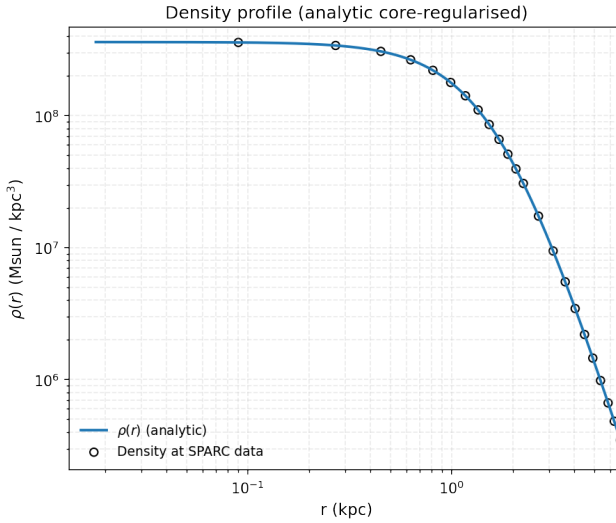


FIG. 282: The density of the SIDM model of Eq. (3) for the galaxy UGC05721, versus the radius.

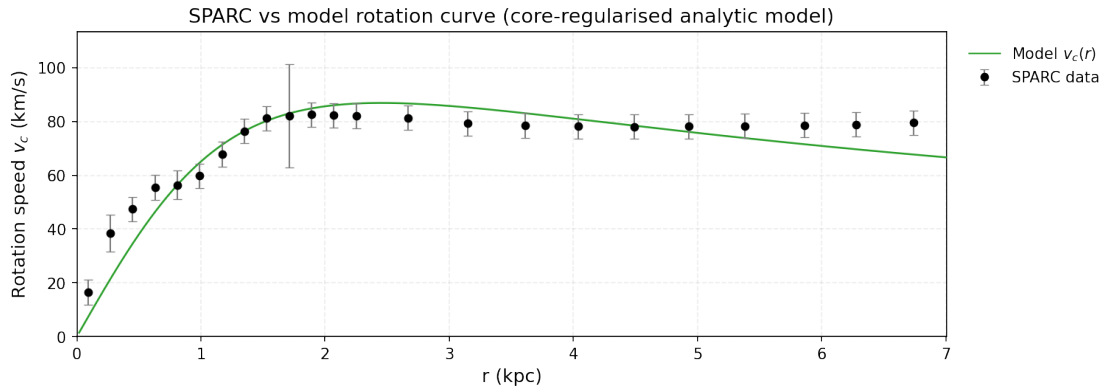


FIG. 283: The predicted rotation curves for the optimized SIDM model of Eq. (3), versus the SPARC observational data for the galaxy UGC05721.

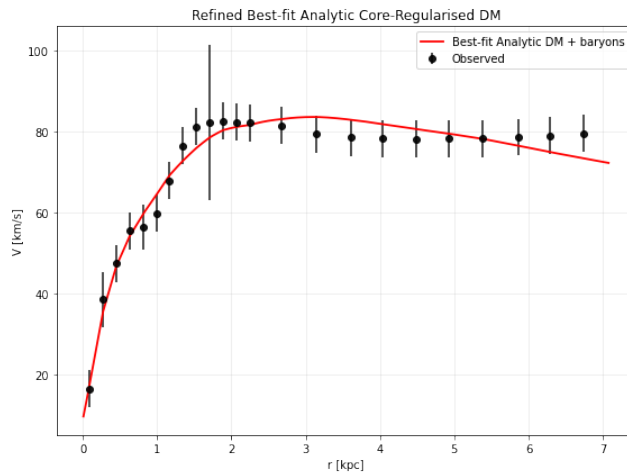


FIG. 284: The predicted rotation curves after using an optimization for the SIDM model (3), and the extended SPARC data for the galaxy UGC05721. We included the rotation curves of the gas, the disk velocities, the bulge (where present) along with the SIDM model.

TABLE CLXXVII: Optimized Parameter Values of the Extended SIDM model for the Galaxy UGC05721.

Parameter	Value
$\rho_0 (M_\odot/\text{Kpc}^3)$	1.50375×10^8
$K_0 (M_\odot \text{ Kpc}^{-3} (\text{km/s})^2)$	2511.14
ml_{disk}	1
ml_{bulge}	0.4923
$\alpha (\text{Kpc})$	2.358
χ^2_{red}	0.512261

96. The Galaxy UGC05750

For this galaxy, the optimization method we used, ensures maximum compatibility of the analytic SIDM model of Eq. (3) with the SPARC data, if we choose $\rho_0 = 1 \times 10^7 M_\odot/\text{Kpc}^3$ and $K_0 = 2398.38 M_\odot \text{ Kpc}^{-3} (\text{km/s})^2$, in which case the reduced χ^2_{red} value is $\chi^2_{\text{red}} = 0.38913$. Also the parameter α in this case is $\alpha = 11.3881 \text{ Kpc}$.

In Table CLXXVIII we present the optimized values of K_0 and ρ_0 for the analytic SIDM model of Eq. (3) for which the maximum compatibility with the SPARC data is achieved. In Figs. 285, 286 we

TABLE CLXXVIII: SIDM Optimization Values for the galaxy UGC05750

Parameter	Optimization Values
$\rho_0 (M_\odot/\text{Kpc}^3)$	1×10^7
$K_0 (M_\odot \text{ Kpc}^{-3} (\text{km/s})^2)$	2398.38

present the density of the analytic SIDM model, the predicted rotation curves for the SIDM model (3), versus the SPARC observational data and the sound speed, as a function of the radius respectively. As it can be seen, for this galaxy, the SIDM model produces viable rotation curves which are compatible with the SPARC data.

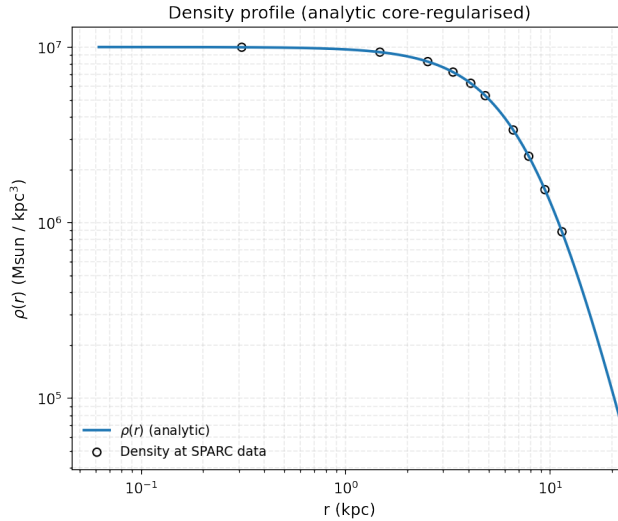


FIG. 285: The density of the SIDM model of Eq. (3) for the galaxy UGC05750, versus the radius.

97. The Galaxy UGC05764, Marginally Viable

For this galaxy, the optimization method we used, ensures maximum compatibility of the analytic SIDM model of Eq. (3) with the SPARC data, if we choose $\rho_0 = 1.36328 \times 10^8 M_\odot/\text{Kpc}^3$ and $K_0 = 1273.63 M_\odot \text{ Kpc}^{-3} (\text{km/s})^2$, in which case the reduced χ^2_{red} value is $\chi^2_{\text{red}} = 4.29775$. Also the parameter α in this case is $\alpha = 1.76392 \text{ Kpc}$.

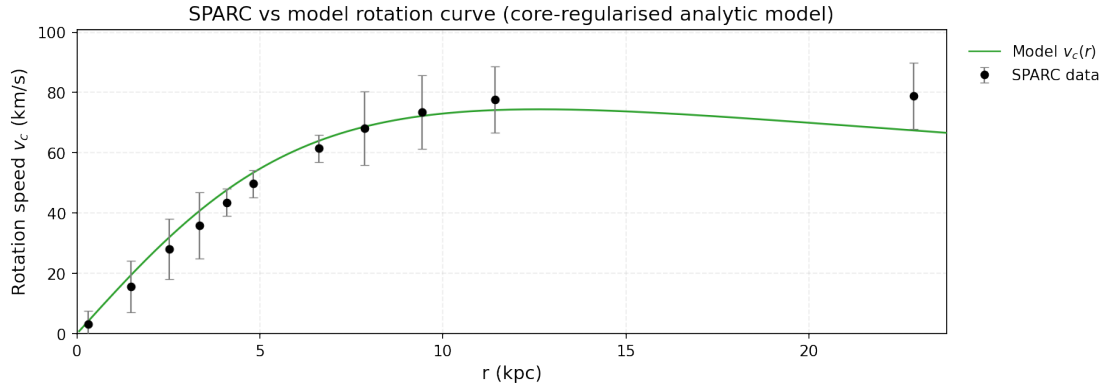


FIG. 286: The predicted rotation curves for the optimized SIDM model of Eq. (3), versus the SPARC observational data for the galaxy UGC05750.

In Table CLXXIX we present the optimized values of K_0 and ρ_0 for the analytic SIDM model of Eq. (3) for which the maximum compatibility with the SPARC data is achieved. In Figs. 287, 288 we present

TABLE CLXXIX: SIDM Optimization Values for the galaxy UGC05764

Parameter	Optimization Values
$\rho_0 (M_\odot / \text{Kpc}^3)$	1.36328×10^8
$K_0 (M_\odot \text{ Kpc}^{-3} (\text{km/s})^2)$	1273.63

the density of the analytic SIDM model, the predicted rotation curves for the SIDM model (3), versus the SPARC observational data and the sound speed, as a function of the radius respectively. As it can be seen, for this galaxy, the SIDM model produces marginally viable rotation curves which are marginally compatible with the SPARC data.

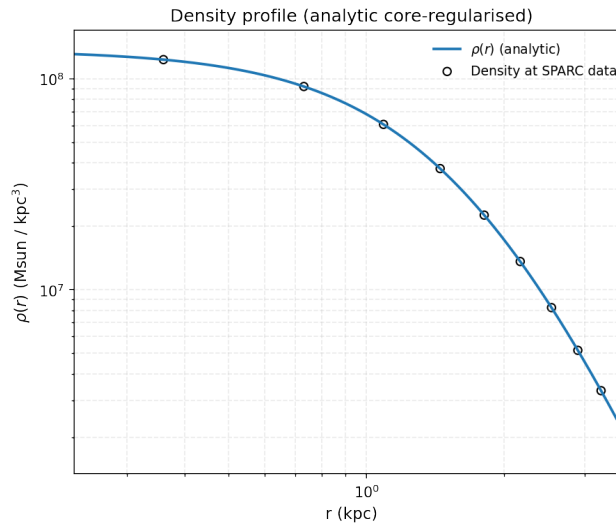


FIG. 287: The density of the SIDM model of Eq. (3) for the galaxy UGC05764, versus the radius.

Now we shall include contributions to the rotation velocity from the other components of the galaxy, namely the disk, the gas, and the bulge if present. In Fig. 289 we present the combined rotation curves including all the components of the galaxy along with the SIDM. As it can be seen, the extended collisional DM model is marginally viable. Also in Table CLXXX we present the optimized values of the free parameters of the SIDM model for which we achieve the maximum compatibility with the SPARC data, for the galaxy UGC05764, and also the resulting reduced χ^2_{red} value.

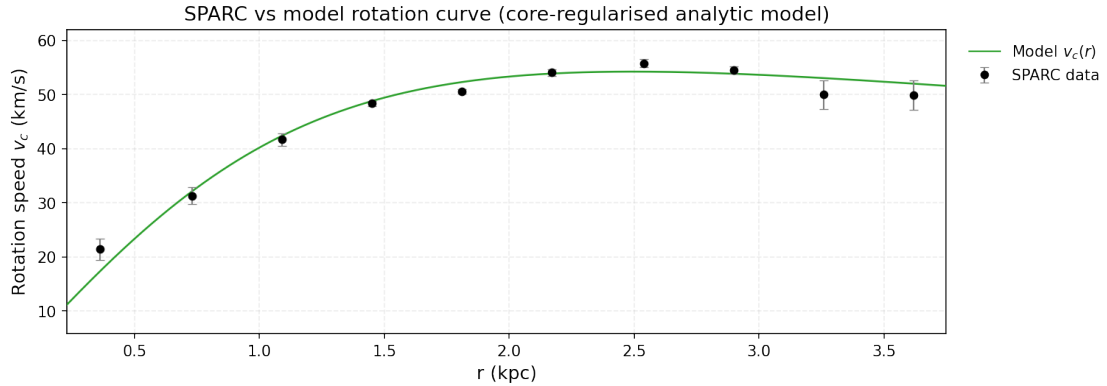


FIG. 288: The predicted rotation curves for the optimized SIDM model of Eq. (3), versus the SPARC observational data for the galaxy UGC05764.

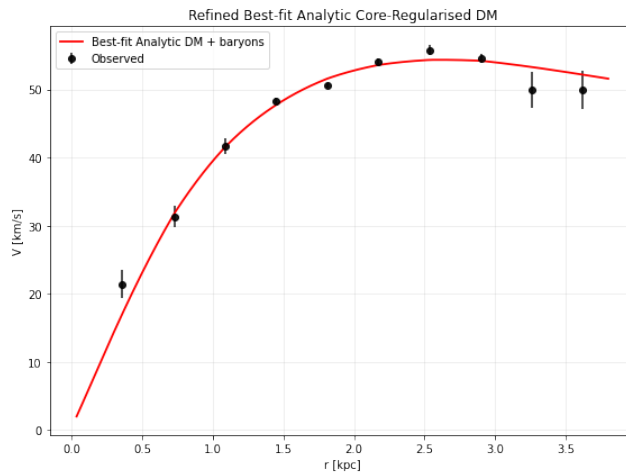


FIG. 289: The predicted rotation curves after using an optimization for the SIDM model (3), and the extended SPARC data for the galaxy UGC05764. We included the rotation curves of the gas, the disk velocities, the bulge (where present) along with the SIDM model.

TABLE CLXXX: Optimized Parameter Values of the Extended SIDM model for the Galaxy UGC05764.

Parameter	Value
$\rho_0 (M_\odot/\text{Kpc}^3)$	1.16291×10^8
$K_0 (M_\odot \text{ Kpc}^{-3} (\text{km/s})^2)$	1049.6
ml_{disk}	1
ml_{bulge}	0.3790
$\alpha (\text{Kpc})$	1.73355
χ^2_{red}	3.44125

98. The Galaxy UGC05829

For this galaxy, the optimization method we used, ensures maximum compatibility of the analytic SIDM model of Eq. (3) with the SPARC data, if we choose $\rho_0 = 1.89055 \times 10^7 M_\odot/\text{Kpc}^3$ and $K_0 = 1787.68 M_\odot \text{ Kpc}^{-3} (\text{km/s})^2$, in which case the reduced χ^2_{red} value is $\chi^2_{\text{red}} = 0.608563$. Also the parameter α in this case is $\alpha = 5.6118 \text{ Kpc}$.

In Table CLXXXI we present the optimized values of K_0 and ρ_0 for the analytic SIDM model of Eq. (3) for which the maximum compatibility with the SPARC data is achieved. In Figs. 290, 291 we present the density of the analytic SIDM model, the predicted rotation curves for the SIDM model (3), versus the SPARC observational data and the sound speed, as a function of the radius respectively. As it can be seen, for this galaxy, the SIDM model produces viable rotation curves which are compatible with the SPARC data.

TABLE CLXXXI: SIDM Optimization Values for the galaxy UGC05829

Parameter	Optimization Values
$\rho_0 (M_\odot/\text{Kpc}^3)$	1.89055×10^7
$K_0 (M_\odot \text{ Kpc}^{-3} (\text{km/s})^2)$	1787.68

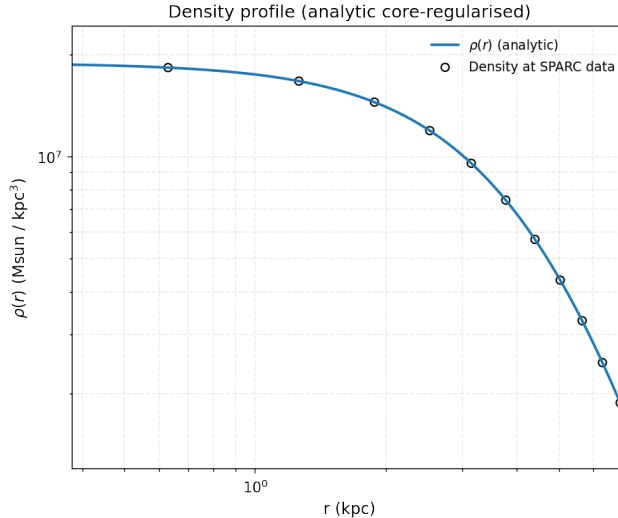


FIG. 290: The density of the SIDM model of Eq. (3) for the galaxy UGC05829, versus the radius.

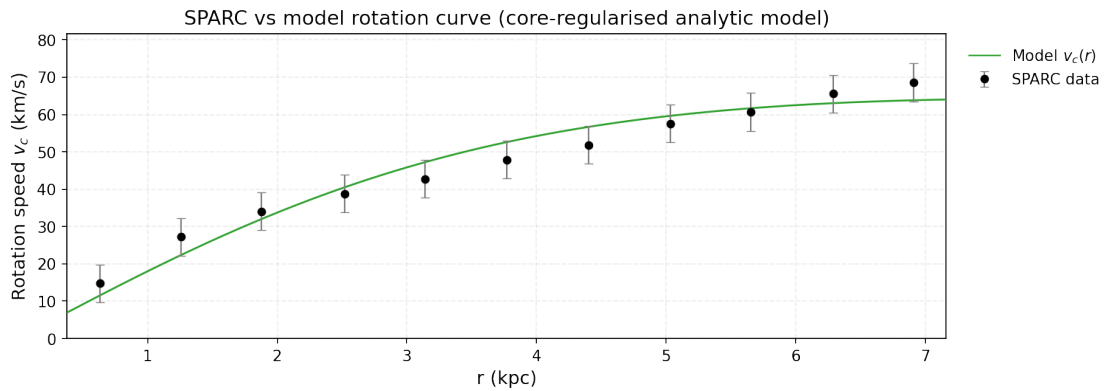


FIG. 291: The predicted rotation curves for the optimized SIDM model of Eq. (3), versus the SPARC observational data for the galaxy UGC05829.

99. The Galaxy UGC05918

For this galaxy, the optimization method we used, ensures maximum compatibility of the analytic SIDM model of Eq. (3) with the SPARC data, if we choose $\rho_0 = 3.4607 \times 10^7 M_\odot/\text{Kpc}^3$ and $K_0 = 869.36 M_\odot \text{ Kpc}^{-3} (\text{km/s})^2$, in which case the reduced χ^2_{red} value is $\chi^2_{\text{red}} = 0.494426$. Also the parameter α in this case is $\alpha = 2.89247 \text{ Kpc}$.

In Table CLXXXII we present the optimized values of K_0 and ρ_0 for the analytic SIDM model of Eq. (3) for which the maximum compatibility with the SPARC data is achieved. In Figs. 292, 293 we present

TABLE CLXXXII: SIDM Optimization Values for the galaxy UGC05918

Parameter	Optimization Values
$\rho_0 (M_\odot/\text{Kpc}^3)$	3.4607×10^7
$K_0 (M_\odot \text{ Kpc}^{-3} (\text{km/s})^2)$	869.36

the density of the analytic SIDM model, the predicted rotation curves for the SIDM model (3), versus the SPARC observational data and the sound speed, as a function of the radius respectively. As it can be seen, for this galaxy, the SIDM model produces viable rotation curves which are compatible with the SPARC data.

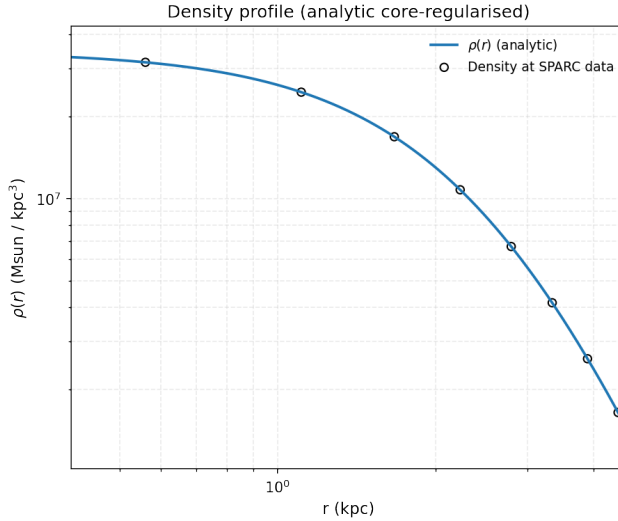


FIG. 292: The density of the SIDM model of Eq. (3) for the galaxy UGC05918, versus the radius.

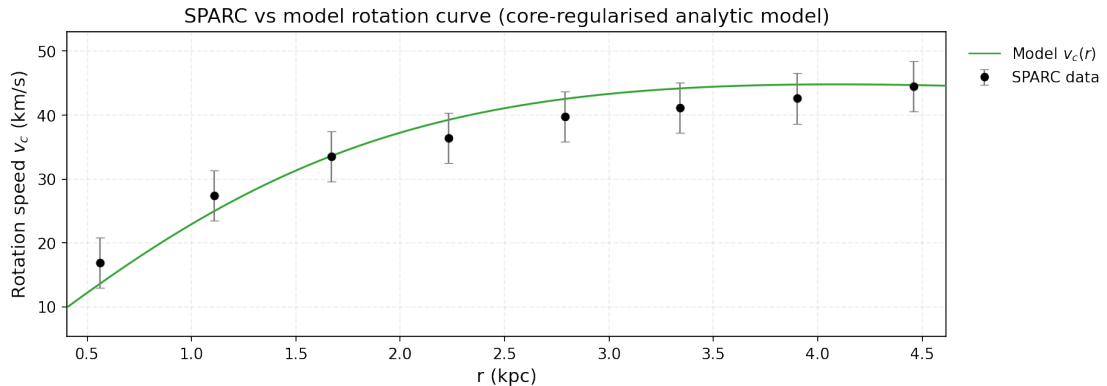


FIG. 293: The predicted rotation curves for the optimized SIDM model of Eq. (3), versus the SPARC observational data for the galaxy UGC05918.

100. The Galaxy UGC05986

For this galaxy, the optimization method we used, ensures maximum compatibility of the analytic SIDM model of Eq. (3) with the SPARC data, if we choose $\rho_0 = 1.01159 \times 10^8 M_\odot/\text{Kpc}^3$ and $K_0 = 5654.85 M_\odot \text{Kpc}^{-3} (\text{km/s})^2$, in which case the reduced χ^2_{red} value is $\chi^2_{red} = 0.564247$. Also the parameter α in this case is $\alpha = 4.31479 \text{Kpc}$.

In Table CLXXXIII we present the optimized values of K_0 and ρ_0 for the analytic SIDM model of Eq. (3) for which the maximum compatibility with the SPARC data is achieved. In Figs. 294, 295 we

TABLE CLXXXIII: SIDM Optimization Values for the galaxy UGC05986

Parameter	Optimization Values
$\rho_0 (M_\odot/\text{Kpc}^3)$	1.01159×10^8
$K_0 (M_\odot \text{Kpc}^{-3} (\text{km/s})^2)$	5654.85

present the density of the analytic SIDM model, the predicted rotation curves for the SIDM model (3), versus the SPARC observational data and the sound speed, as a function of the radius respectively. As it can be seen, for this galaxy, the SIDM model produces viable rotation curves which are compatible with the SPARC data.

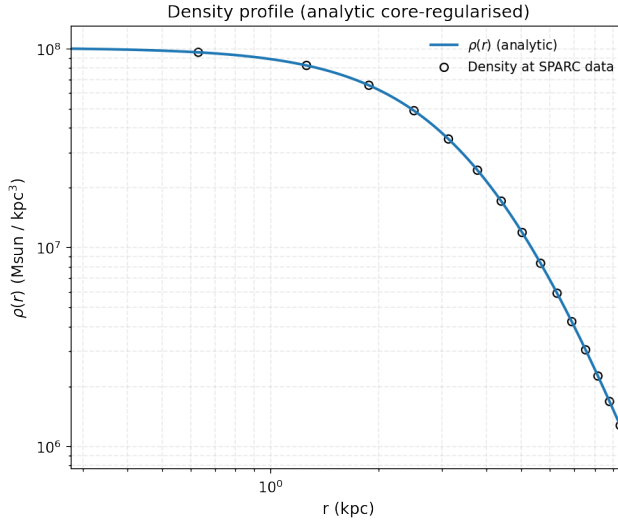


FIG. 294: The density of the SIDM model of Eq. (3) for the galaxy UGC05986, versus the radius.

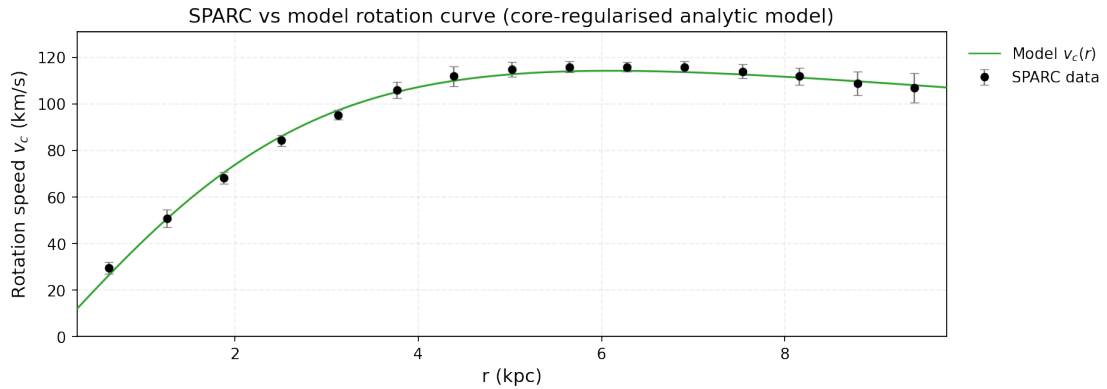


FIG. 295: The predicted rotation curves for the optimized SIDM model of Eq. (3), versus the SPARC observational data for the galaxy UGC05986.

101. The Galaxy UGC06399

For this galaxy, the optimization method we used, ensures maximum compatibility of the analytic SIDM model of Eq. (3) with the SPARC data, if we choose $\rho_0 = 3.97388 \times 10^7 M_\odot/\text{Kpc}^3$ and $K_0 = 3557.78 M_\odot \text{ Kpc}^{-3} (\text{km/s})^2$, in which case the reduced χ^2_{red} value is $\chi^2_{red} = 0.619603$. Also the parameter α in this case is $\alpha = 5.46051 \text{ Kpc}$.

In Table CLXXXIV we present the optimized values of K_0 and ρ_0 for the analytic SIDM model of Eq. (3) for which the maximum compatibility with the SPARC data is achieved. In Figs. 296, 297 we

TABLE CLXXXIV: SIDM Optimization Values for the galaxy UGC06399

Parameter	Optimization Values
$\rho_0 (M_\odot/\text{Kpc}^3)$	3.97388×10^7
$K_0 (M_\odot \text{ Kpc}^{-3} (\text{km/s})^2)$	3557.78

present the density of the analytic SIDM model, the predicted rotation curves for the SIDM model (3), versus the SPARC observational data and the sound speed, as a function of the radius respectively. As it can be seen, for this galaxy, the SIDM model produces viable rotation curves which are compatible with the SPARC data.

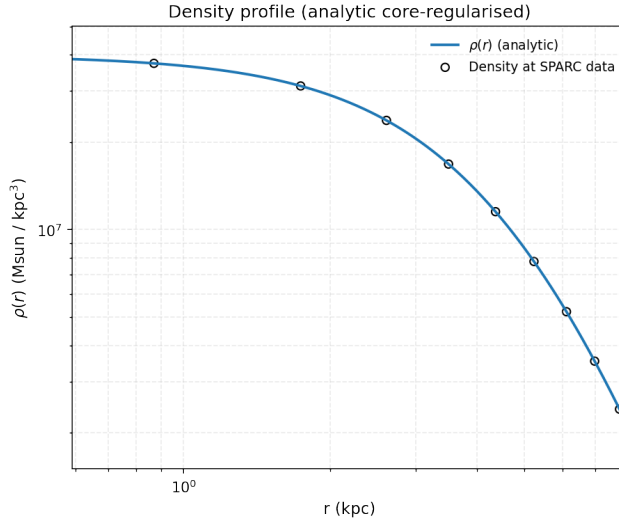


FIG. 296: The density of the SIDM model of Eq. (3) for the galaxy UGC06399, versus the radius.

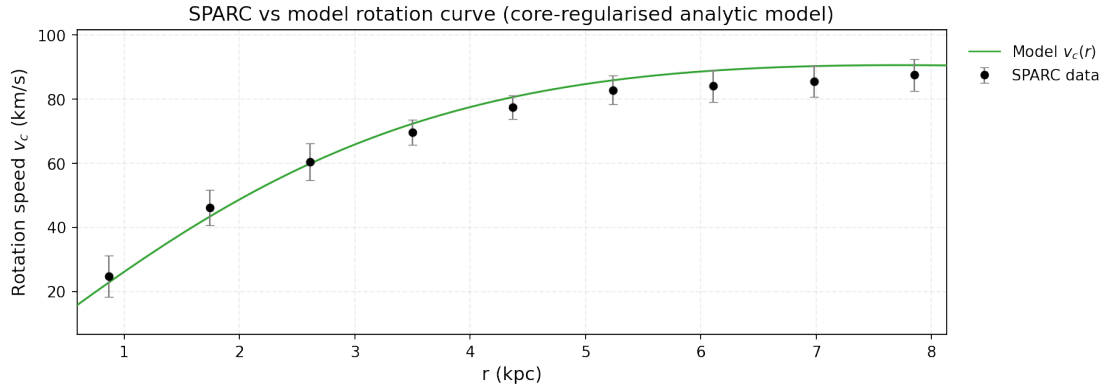


FIG. 297: The predicted rotation curves for the optimized SIDM model of Eq. (3), versus the SPARC observational data for the galaxy UGC06399.

102. The Galaxy UGC06446, Non-viable, Extended Viable

For this galaxy, the optimization method we used, ensures maximum compatibility of the analytic SIDM model of Eq. (3) with the SPARC data, if we choose $\rho_0 = 6.37837 \times 10^7 M_\odot/\text{Kpc}^3$ and $K_0 = 2994.32 M_\odot \text{Kpc}^{-3} (\text{km/s})^2$, in which case the reduced χ^2_{red} value is $\chi^2_{\text{red}} = 2.09777$. Also the parameter α in this case is $\alpha = 3.95408 \text{Kpc}$.

In Table CLXXXV we present the optimized values of K_0 and ρ_0 for the analytic SIDM model of Eq. (3) for which the maximum compatibility with the SPARC data is achieved. In Figs. 298, 299 we present

TABLE CLXXXV: SIDM Optimization Values for the galaxy UGC06446

Parameter	Optimization Values
$\rho_0 (M_\odot/\text{Kpc}^3)$	6.37837×10^7
$K_0 (M_\odot \text{Kpc}^{-3} (\text{km/s})^2)$	2994.32

the density of the analytic SIDM model, the predicted rotation curves for the SIDM model (3), versus the SPARC observational data and the sound speed, as a function of the radius respectively. As it can be seen, for this galaxy, the SIDM model produces non-viable rotation curves which are incompatible with the SPARC data.

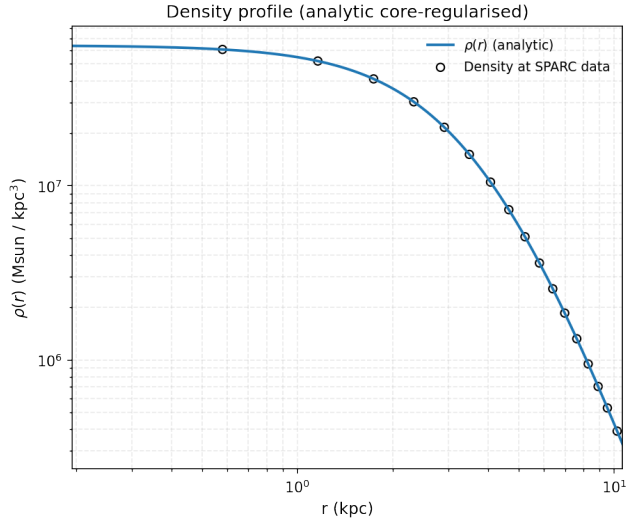


FIG. 298: The density of the SIDM model of Eq. (3) for the galaxy UGC06446, versus the radius.

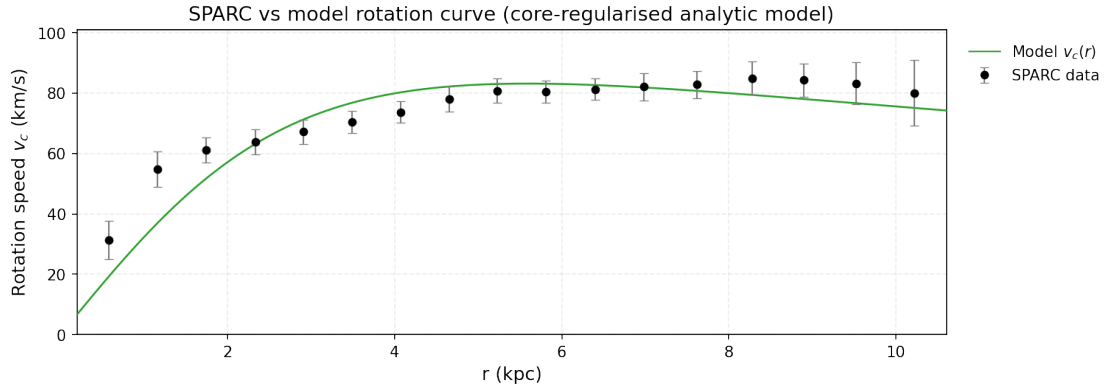


FIG. 299: The predicted rotation curves for the optimized SIDM model of Eq. (3), versus the SPARC observational data for the galaxy UGC06446.

Now we shall include contributions to the rotation velocity from the other components of the galaxy, namely the disk, the gas, and the bulge if present. In Fig. 300 we present the combined rotation curves including all the components of the galaxy along with the SIDM. As it can be seen, the extended collisional DM model is viable. Also in Table CLXXXVI we present the optimized values of the free parameters of the SIDM model for which we achieve the maximum compatibility with the SPARC data, for the galaxy UGC06446, and also the resulting reduced χ^2_{red} value.

TABLE CLXXXVI: Optimized Parameter Values of the Extended SIDM model for the Galaxy UGC06446.

Parameter	Value
ρ_0 (M_\odot/Kpc^3)	4.41183×10^7
K_0 ($M_\odot \text{ Kpc}^{-3} (\text{km/s})^2$)	2230.52
ml_{disk}	1
ml_{bulge}	0.2324
α (Kpc)	4.10289
χ^2_{red}	1.0631

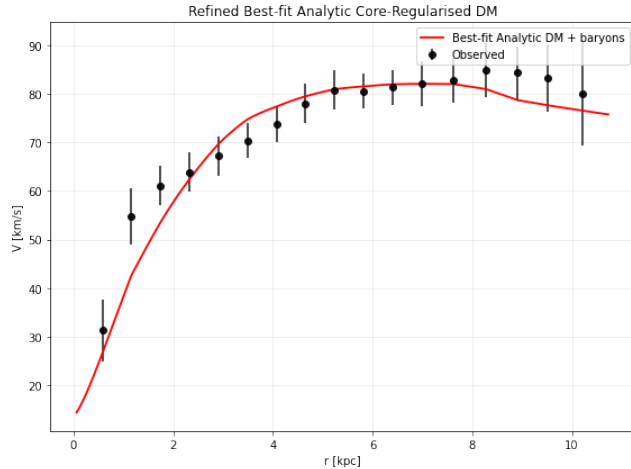


FIG. 300: The predicted rotation curves after using an optimization for the SIDM model (3), and the extended SPARC data for the galaxy UGC06446. We included the rotation curves of the gas, the disk velocities, the bulge (where present) along with the SIDM model.

103. The Galaxy UGC06614, Non-viable, Extended Viable

For this galaxy, the optimization method we used, ensures maximum compatibility of the analytic SIDM model of Eq. (3) with the SPARC data, if we choose $\rho_0 = 1.9692 \times 10^7 M_\odot/\text{Kpc}^3$ and $K_0 = 19839.8 M_\odot \text{Kpc}^{-3} (\text{km/s})^2$, in which case the reduced χ^2_{red} value is $\chi^2_{red} = 7.7828$. Also the parameter α in this case is $\alpha = 18.3179 \text{Kpc}$.

In Table CLXXXVII we present the optimized values of K_0 and ρ_0 for the analytic SIDM model of Eq. (3) for which the maximum compatibility with the SPARC data is achieved. In Figs. 301, 302 we

TABLE CLXXXVII: SIDM Optimization Values for the galaxy UGC06614

Parameter	Optimization Values
$\rho_0 (M_\odot/\text{Kpc}^3)$	1.9692×10^7
$K_0 (M_\odot \text{Kpc}^{-3} (\text{km/s})^2)$	19839.8

present the density of the analytic SIDM model, the predicted rotation curves for the SIDM model (3), versus the SPARC observational data and the sound speed, as a function of the radius respectively. As it can be seen, for this galaxy, the SIDM model produces non-viable rotation curves which are incompatible with the SPARC data.

Now we shall include contributions to the rotation velocity from the other components of the galaxy, namely the disk, the gas, and the bulge if present. In Fig. 303 we present the combined rotation curves including all the components of the galaxy along with the SIDM. As it can be seen, the extended collisional DM model is viable. Also in Table CLXXXVIII we present the optimized values of the free parameters of the SIDM model for which we achieve the maximum compatibility with the SPARC data, for the galaxy UGC06614, and also the resulting reduced χ^2_{red} value.

TABLE CLXXXVIII: Optimized Parameter Values of the Extended SIDM model for the Galaxy UGC06614.

Parameter	Value
$\rho_0 (M_\odot/\text{Kpc}^3)$	3.82792×10^6
$K_0 (M_\odot \text{Kpc}^{-3} (\text{km/s})^2)$	14400.6
ml_{disk}	0.6687
ml_{bulge}	0.8008
$\alpha (\text{Kpc})$	35.3919
χ^2_{red}	0.760491

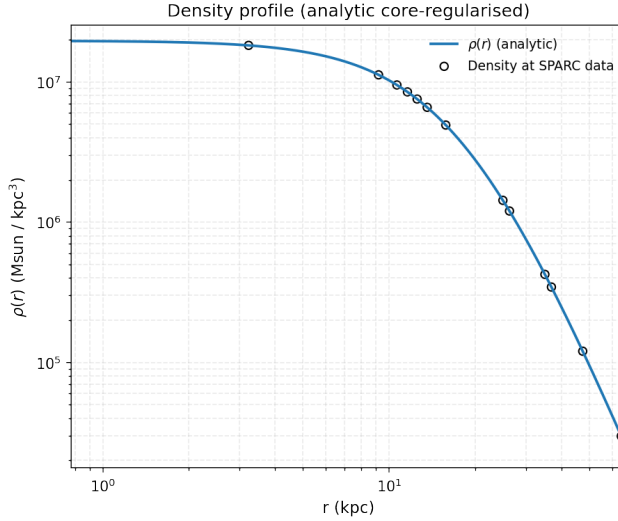


FIG. 301: The density of the SIDM model of Eq. (3) for the galaxy UGC06614, versus the radius.

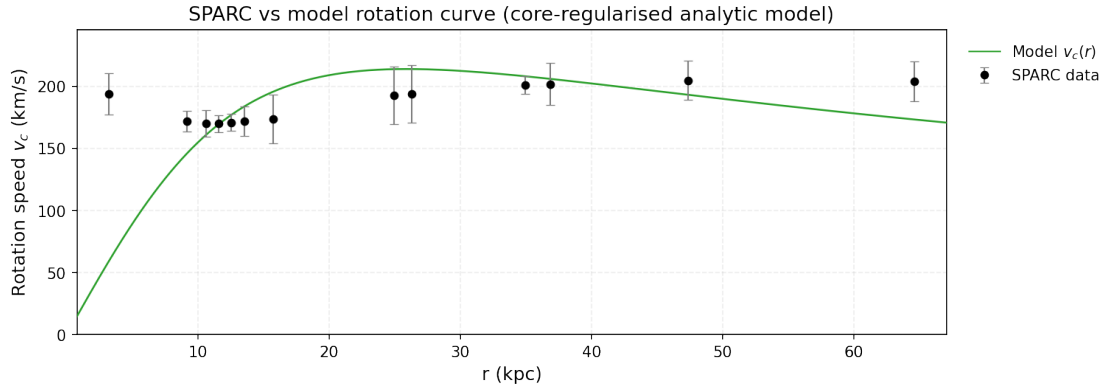


FIG. 302: The predicted rotation curves for the optimized SIDM model of Eq. (3), versus the SPARC observational data for the galaxy UGC06614.

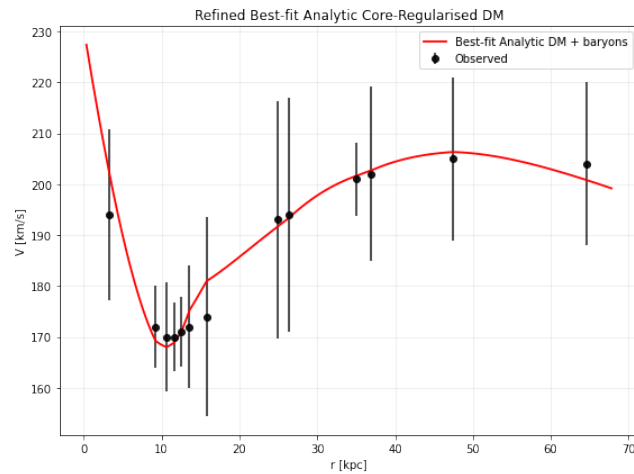


FIG. 303: The predicted rotation curves after using an optimization for the SIDM model (3), and the extended SPARC data for the galaxy UGC06614. We included the rotation curves of the gas, the disk velocities, the bulge (where present) along with the SIDM model.

104. The Galaxy UGC06667

For this galaxy, the optimization method we used, ensures maximum compatibility of the analytic SIDM model of Eq. (3) with the SPARC data, if we choose $\rho_0 = 4.63803 \times 10^7 M_\odot/\text{Kpc}^3$ and $K_0 = 3075.79 M_\odot \text{Kpc}^{-3} (\text{km/s})^2$, in which case the reduced χ^2_{red} value is $\chi^2_{red} = 0.566936$. Also the parameter α in this case is $\alpha = 5.03668 \text{Kpc}$.

In Table CLXXXIX we present the optimized values of K_0 and ρ_0 for the analytic SIDM model of Eq. (3) for which the maximum compatibility with the SPARC data is achieved. In Figs. 304, 305 we

TABLE CLXXXIX: SIDM Optimization Values for the galaxy UGC06667

Parameter	Optimization Values
$\rho_0 (M_\odot/\text{Kpc}^3)$	4.63803×10^7
$K_0 (M_\odot \text{Kpc}^{-3} (\text{km/s})^2)$	3075.79

present the density of the analytic SIDM model, the predicted rotation curves for the SIDM model (3), versus the SPARC observational data and the sound speed, as a function of the radius respectively. As it can be seen, for this galaxy, the SIDM model produces viable rotation curves which are compatible with the SPARC data.

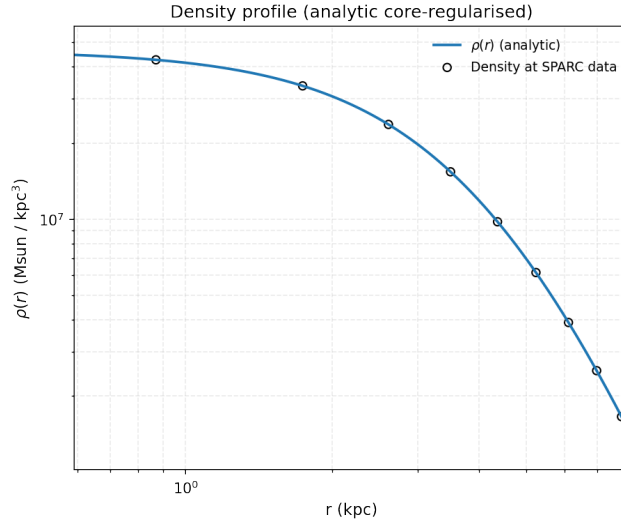


FIG. 304: The density of the SIDM model of Eq. (3) for the galaxy UGC06667, versus the radius.

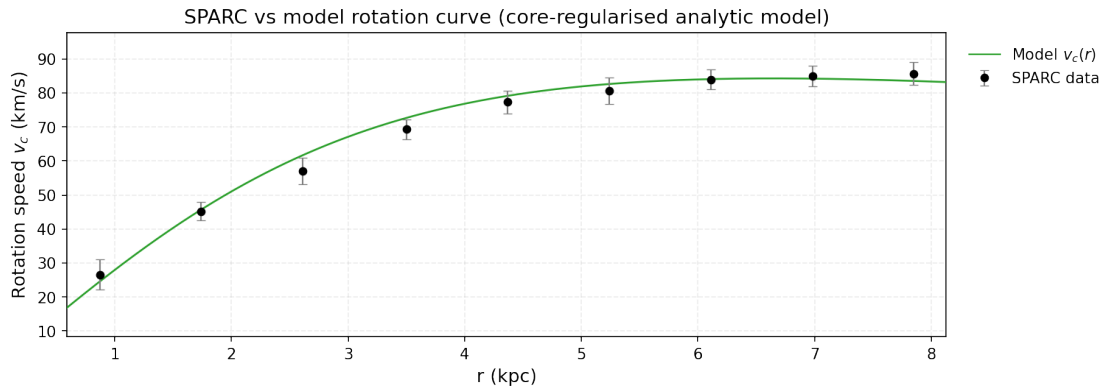


FIG. 305: The predicted rotation curves for the optimized SIDM model of Eq. (3), versus the SPARC observational data for the galaxy UGC06667.

105. The Galaxy UGC06786, Non-viable

For this galaxy, the optimization method we used, ensures maximum compatibility of the analytic SIDM model of Eq. (3) with the SPARC data, if we choose $\rho_0 = 1.90042 \times 10^8 M_\odot/\text{Kpc}^3$ and $K_0 = 26463.3 M_\odot \text{Kpc}^{-3} (\text{km/s})^2$, in which case the reduced χ^2_{red} value is $\chi^2_{red} = 52.6091$. Also the parameter α in this case is $\alpha = 6.81 \text{Kpc}$.

In Table CXC we present the optimized values of K_0 and ρ_0 for the analytic SIDM model of Eq. (3) for which the maximum compatibility with the SPARC data is achieved. In Figs. 306, 307 we present

TABLE CXC: SIDM Optimization Values for the galaxy UGC06786

Parameter	Optimization Values
$\rho_0 (M_\odot/\text{Kpc}^3)$	1.90042×10^8
$K_0 (M_\odot \text{Kpc}^{-3} (\text{km/s})^2)$	26463.3

the density of the analytic SIDM model, the predicted rotation curves for the SIDM model (3), versus the SPARC observational data and the sound speed, as a function of the radius respectively. As it can be seen, for this galaxy, the SIDM model produces non-viable rotation curves which are incompatible with the SPARC data.

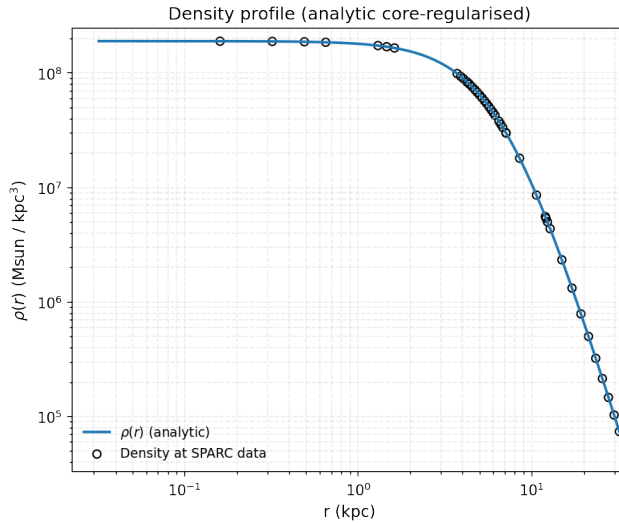


FIG. 306: The density of the SIDM model of Eq. (3) for the galaxy UGC06786, versus the radius.

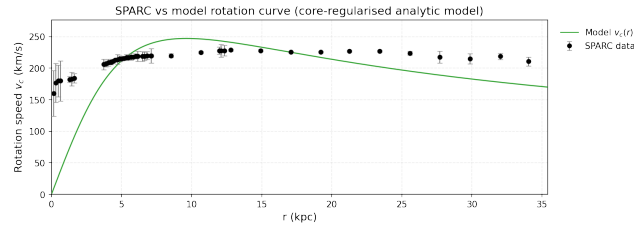


FIG. 307: The predicted rotation curves for the optimized SIDM model of Eq. (3), versus the SPARC observational data for the galaxy UGC06786.

Now we shall include contributions to the rotation velocity from the other components of the galaxy, namely the disk, the gas, and the bulge if present. In Fig. 308 we present the combined rotation curves including all the components of the galaxy along with the SIDM. As it can be seen, the extended collisional DM model is non-viable. Also in Table CXCI we present the optimized values of the free parameters of the SIDM model for which we achieve the maximum compatibility with the SPARC data, for the galaxy UGC06786, and also the resulting reduced χ^2_{red} value.

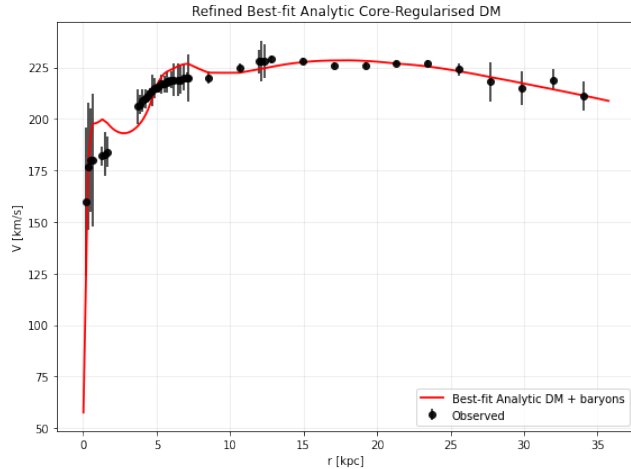


FIG. 308: The predicted rotation curves after using an optimization for the SIDM model (3), and the extended SPARC data for the galaxy UGC06786. We included the rotation curves of the gas, the disk velocities, the bulge (where present) along with the SIDM model.

TABLE CXCI: Optimized Parameter Values of the Extended SIDM model for the Galaxy UGC06786.

Parameter	Value
$\rho_0 (M_\odot/\text{Kpc}^3)$	1.45289×10^7
$K_0 (M_\odot \text{ Kpc}^{-3} (\text{km/s})^2)$	15487.9
ml_{disk}	1
ml_{bulge}	0.9395
$\alpha (\text{Kpc})$	18.8398
χ^2_{red}	2.38481

106. The Galaxy UGC06787, Non-viable

For this galaxy, the optimization method we used, ensures maximum compatibility of the analytic SIDM model of Eq. (3) with the SPARC data, if we choose $\rho_0 = 1.86717 \times 10^8 M_\odot/\text{Kpc}^3$ and $K_0 = 31016.7 M_\odot \text{ Kpc}^{-3} (\text{km/s})^2$, in which case the reduced χ^2_{red} value is $\chi^2_{\text{red}} = 177.21$. Also the parameter α in this case is $\alpha = 7.438 \text{ Kpc}$.

In Table CXCII we present the optimized values of K_0 and ρ_0 for the analytic SIDM model of Eq. (3) for which the maximum compatibility with the SPARC data is achieved. In Figs. 309, 310 we present

TABLE CXCII: SIDM Optimization Values for the galaxy UGC06787

Parameter	Optimization Values
$\rho_0 (M_\odot/\text{Kpc}^3)$	1.86717×10^8
$K_0 (M_\odot \text{ Kpc}^{-3} (\text{km/s})^2)$	31016.7

the density of the analytic SIDM model, the predicted rotation curves for the SIDM model (3), versus the SPARC observational data and the sound speed, as a function of the radius respectively. As it can be seen, for this galaxy, the SIDM model produces non-viable rotation curves which are incompatible with the SPARC data.

Now we shall include contributions to the rotation velocity from the other components of the galaxy, namely the disk, the gas, and the bulge if present. In Fig. 311 we present the combined rotation curves including all the components of the galaxy along with the SIDM. As it can be seen, the extended collisional DM model is non-viable. Also in Table CXCIII we present the optimized values of the free parameters of the SIDM model for which we achieve the maximum compatibility with the SPARC data, for the galaxy UGC06787, and also the resulting reduced χ^2_{red} value.

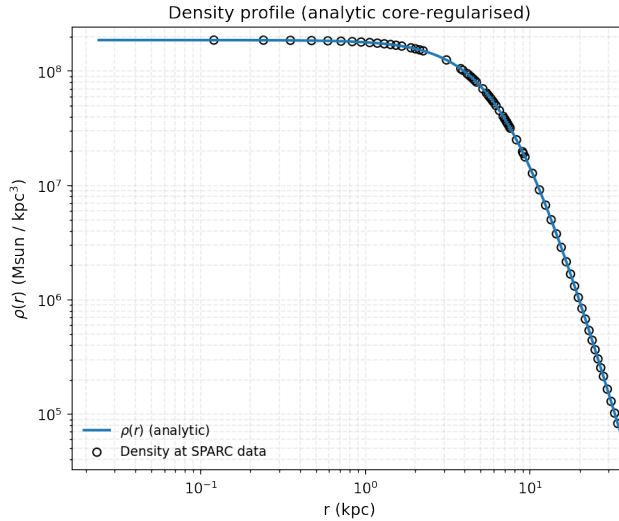


FIG. 309: The density of the SIDM model of Eq. (3) for the galaxy UGC06787, versus the radius.

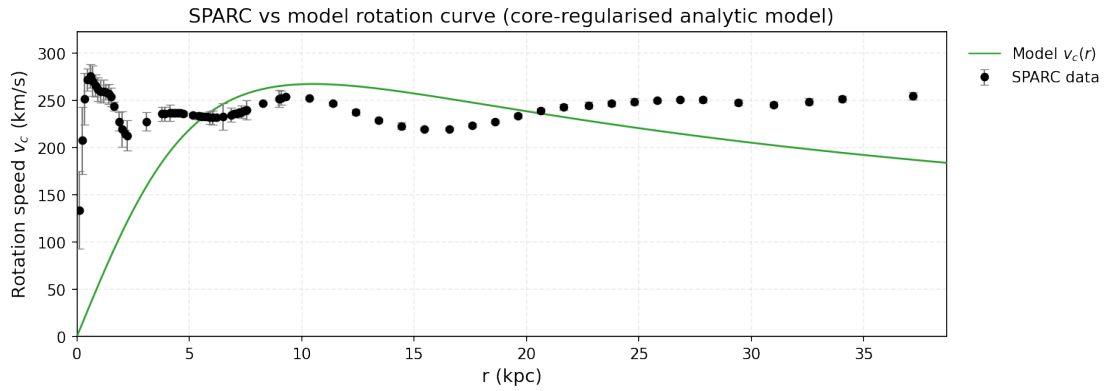


FIG. 310: The predicted rotation curves for the optimized SIDM model of Eq. (3), versus the SPARC observational data for the galaxy UGC06787.

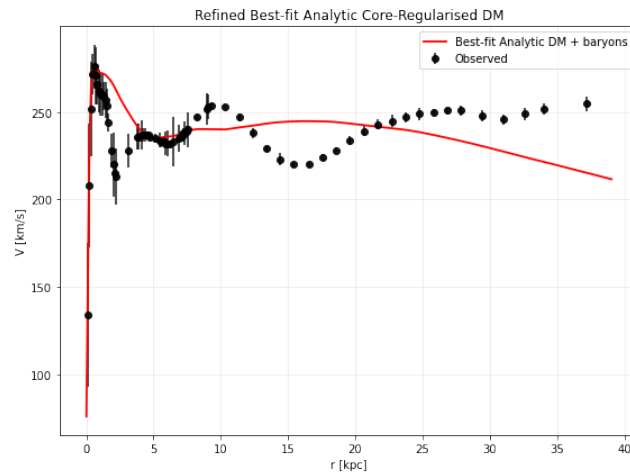


FIG. 311: The predicted rotation curves after using an optimization for the SIDM model (3), and the extended SPARC data for the galaxy UGC06787. We included the rotation curves of the gas, the disk velocities, the bulge (where present) along with the SIDM model.

TABLE CXCIII: Optimized Parameter Values of the Extended SIDM model for the Galaxy UGC06787.

Parameter	Value
$\rho_0 (M_\odot/\text{Kpc}^3)$	2.1286×10^7
$K_0 (M_\odot \text{ Kpc}^{-3} (\text{km/s})^2)$	17225.7
ml_{disk}	1
ml_{bulge}	0.8451
$\alpha (\text{Kpc})$	16.4149
χ^2_{red}	38.8218

107. The Galaxy UGC06818

For this galaxy, the optimization method we used, ensures maximum compatibility of the analytic SIDM model of Eq. (3) with the SPARC data, if we choose $\rho_0 = 1.63491 \times 10^7 M_\odot/\text{Kpc}^3$ and $K_0 = 2632.02 M_\odot \text{ Kpc}^{-3} (\text{km/s})^2$, in which case the reduced χ^2_{red} value is $\chi^2_{\text{red}} = 1.00372$. Also the parameter α in this case is $\alpha = 7.32232 \text{ Kpc}$.

In Table CXCIV we present the optimized values of K_0 and ρ_0 for the analytic SIDM model of Eq. (3) for which the maximum compatibility with the SPARC data is achieved. In Figs. 312, 313 we present

TABLE CXCIV: SIDM Optimization Values for the galaxy UGC06818

Parameter	Optimization Values
$\rho_0 (M_\odot/\text{Kpc}^3)$	1.63491×10^7
$K_0 (M_\odot \text{ Kpc}^{-3} (\text{km/s})^2)$	2632.02

the density of the analytic SIDM model, the predicted rotation curves for the SIDM model (3), versus the SPARC observational data and the sound speed, as a function of the radius respectively. As it can be seen, for this galaxy, the SIDM model produces viable rotation curves which are compatible with the SPARC data.

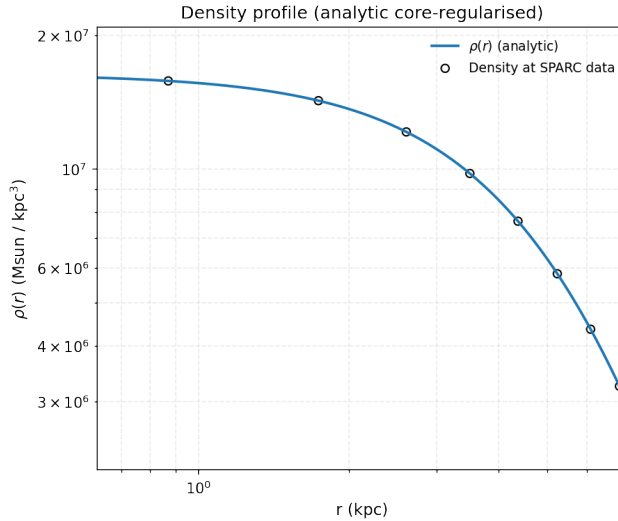


FIG. 312: The density of the SIDM model of Eq. (3) for the galaxy UGC06818, versus the radius.

Now we shall include contributions to the rotation velocity from the other components of the galaxy, namely the disk, the gas, and the bulge if present. In Fig. 314 we present the combined rotation curves including all the components of the galaxy along with the SIDM. As it can be seen, the extended collisional DM model is viable. Also in Table CXCV we present the optimized values of the free parameters of the SIDM model for which we achieve the maximum compatibility with the SPARC data, for the galaxy UGC06818, and also the resulting reduced χ^2_{red} value.

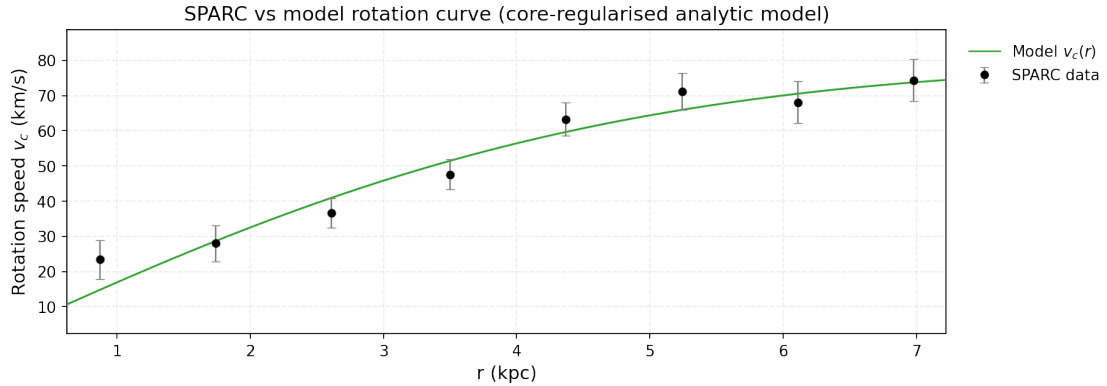


FIG. 313: The predicted rotation curves for the optimized SIDM model of Eq. (3), versus the SPARC observational data for the galaxy UGC06818.

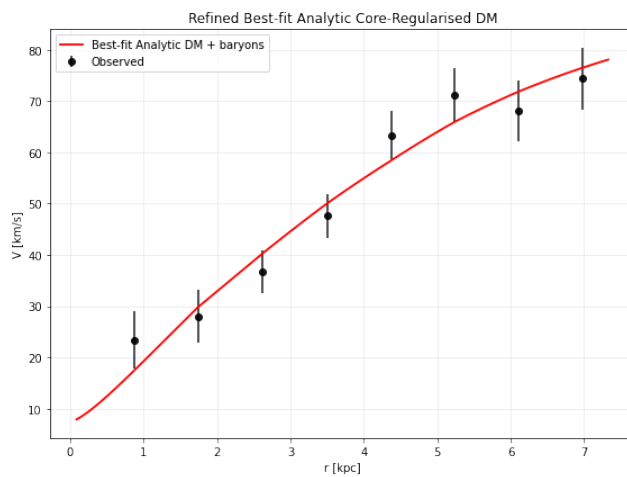


FIG. 314: The predicted rotation curves after using an optimization for the SIDM model (3), and the extended SPARC data for the galaxy UGC06818. We included the rotation curves of the gas, the disk velocities, the bulge (where present) along with the SIDM model.

TABLE CXCV: Optimized Parameter Values of the Extended SIDM model for the Galaxy UGC06818.

Parameter	Value
$\rho_0 (M_\odot/\text{Kpc}^3)$	1.14068×10^7
$K_0 (M_\odot \text{ Kpc}^{-3} (\text{km/s})^2)$	3036.28
ml_{disk}	0.4313
ml_{bulge}	0.3118
$\alpha (\text{Kpc})$	9.41424
χ^2_{red}	1.2134

108. The Galaxy UGC06917, Non-viable, Extended Viable

For this galaxy, the optimization method we used, ensures maximum compatibility of the analytic SIDM model of Eq. (3) with the SPARC data, if we choose $\rho_0 = 5.06612 \times 10^7 M_\odot/\text{Kpc}^3$ and $K_0 = 4883.69 M_\odot \text{ Kpc}^{-3} (\text{km/s})^2$, in which case the reduced χ^2_{red} value is $\chi^2_{\text{red}} = 1.65275$. Also the parameter α in this case is $\alpha = 5.66614 \text{ Kpc}$.

In Table CXCVI we present the optimized values of K_0 and ρ_0 for the analytic SIDM model of Eq. (3) for which the maximum compatibility with the SPARC data is achieved. In Figs. 315, 316 we present the density of the analytic SIDM model, the predicted rotation curves for the SIDM model (3), versus the SPARC observational data and the sound speed, as a function of the radius respectively. As it can be seen, for this galaxy, the SIDM model produces non-viable rotation curves which are incompatible with the SPARC data.

TABLE CXCVI: SIDM Optimization Values for the galaxy UGC06917

Parameter	Optimization Values
$\rho_0 (M_\odot/\text{Kpc}^3)$	5.06612×10^7
$K_0 (M_\odot \text{ Kpc}^{-3} (\text{km/s})^2)$	4883.69

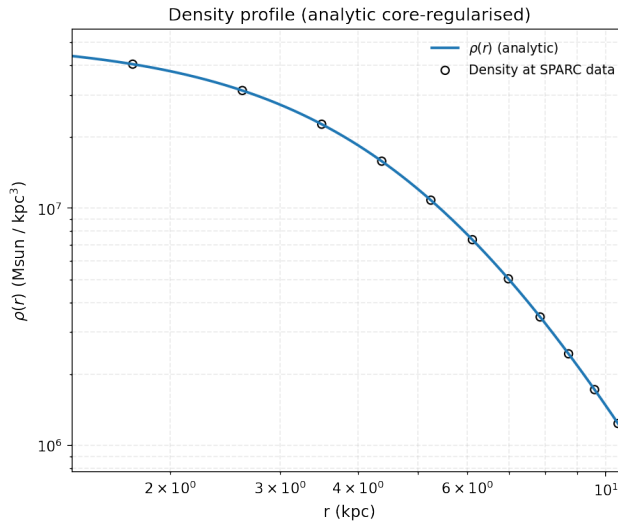


FIG. 315: The density of the SIDM model of Eq. (3) for the galaxy UGC06917, versus the radius.

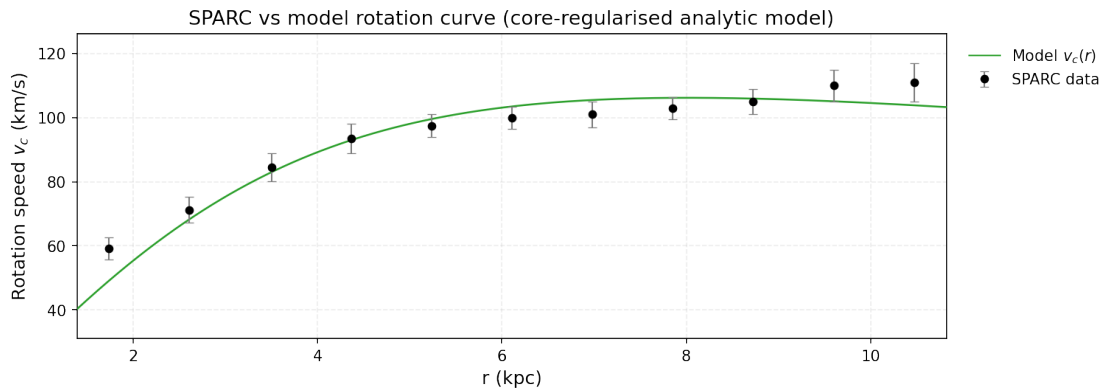


FIG. 316: The predicted rotation curves for the optimized SIDM model of Eq. (3), versus the SPARC observational data for the galaxy UGC06917.

Now we shall include contributions to the rotation velocity from the other components of the galaxy, namely the disk, the gas, and the bulge if present. In Fig. 317 we present the combined rotation curves including all the components of the galaxy along with the SIDM. As it can be seen, the extended collisional DM model is non-viable. Also in Table CXCVII we present the optimized values of the free parameters of the SIDM model for which we achieve the maximum compatibility with the SPARC data, for the galaxy UGC06917, and also the resulting reduced χ^2_{red} value.

TABLE CXCVII: Optimized Parameter Values of the Extended SIDM model for the Galaxy UGC06917.

Parameter	Value
$\rho_0 (M_\odot/\text{Kpc}^3)$	2.73664×10^7
$K_0 (M_\odot \text{ Kpc}^{-3} (\text{km/s})^2)$	3283.4
ml_{disk}	0.8401
ml_{bulge}	0.1058
$\alpha (\text{Kpc})$	6.32046
χ^2_{red}	0.39102

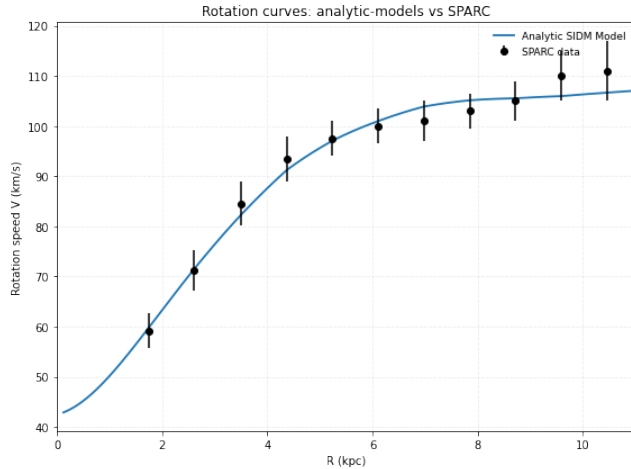


FIG. 317: The predicted rotation curves after using an optimization for the SIDM model (3), and the extended SPARC data for the galaxy UGC06917. We included the rotation curves of the gas, the disk velocities, the bulge (where present) along with the SIDM model.

109. The Galaxy UGC06923

For this galaxy, the optimization method we used, ensures maximum compatibility of the analytic SIDM model of Eq. (3) with the SPARC data, if we choose $\rho_0 = 8.29599 \times 10^7 M_\odot/\text{Kpc}^3$ and $K_0 = 2622.3 M_\odot \text{Kpc}^{-3} (\text{km/s})^2$, in which case the reduced χ^2_{red} value is $\chi^2_{\text{red}} = 0.649073$. Also the parameter α in this case is $\alpha = 3.24458 \text{Kpc}$.

In Table CXCVIII we present the optimized values of K_0 and ρ_0 for the analytic SIDM model of Eq. (3) for which the maximum compatibility with the SPARC data is achieved. In Figs. 318, 319 we present

TABLE CXCVIII: SIDM Optimization Values for the galaxy UGC06923

Parameter	Optimization Values
$\rho_0 (M_\odot/\text{Kpc}^3)$	8.29599×10^7
$K_0 (M_\odot \text{Kpc}^{-3} (\text{km/s})^2)$	2622.3

the density of the analytic SIDM model, the predicted rotation curves for the SIDM model (3), versus the SPARC observational data and the sound speed, as a function of the radius respectively. As it can be seen, for this galaxy, the SIDM model produces viable rotation curves which are compatible with the SPARC data.

110. The Galaxy UGC06930, Marginally Viable, Extended Viable

For this galaxy, the optimization method we used, ensures maximum compatibility of the analytic SIDM model of Eq. (3) with the SPARC data, if we choose $\rho_0 = 4.08457 \times 10^7 M_\odot/\text{Kpc}^3$ and $K_0 = 5165.97 M_\odot \text{Kpc}^{-3} (\text{km/s})^2$, in which case the reduced χ^2_{red} value is $\chi^2_{\text{red}} = 1.19127$. Also the parameter α in this case is $\alpha = 6.49013 \text{Kpc}$.

In Table CXCIX we present the optimized values of K_0 and ρ_0 for the analytic SIDM model of Eq. (3) for which the maximum compatibility with the SPARC data is achieved. In Figs. 320, 321 we present

TABLE CXCIX: SIDM Optimization Values for the galaxy UGC06930

Parameter	Optimization Values
$\rho_0 (M_\odot/\text{Kpc}^3)$	4.08457×10^7
$K_0 (M_\odot \text{Kpc}^{-3} (\text{km/s})^2)$	5165.97

the density of the analytic SIDM model, the predicted rotation curves for the SIDM model (3), versus the SPARC observational data and the sound speed, as a function of the radius respectively. As it can be

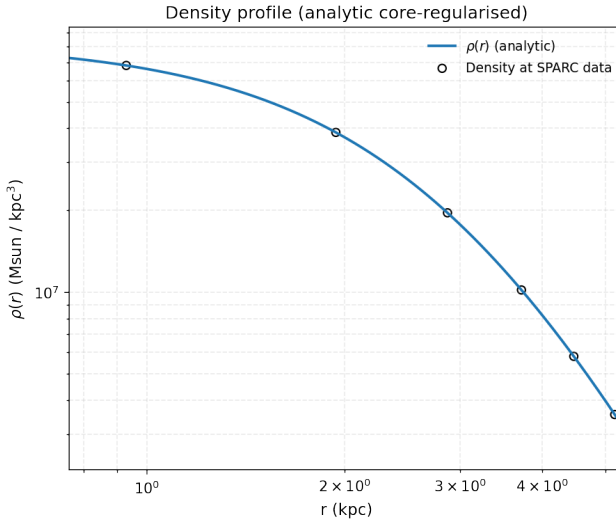


FIG. 318: The density of the SIDM model of Eq. (3) for the galaxy UGC06923, versus the radius.

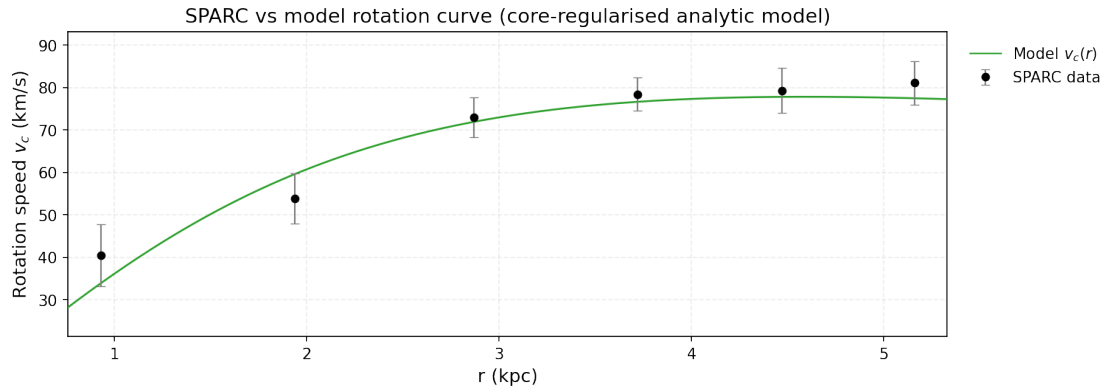


FIG. 319: The predicted rotation curves for the optimized SIDM model of Eq. (3), versus the SPARC observational data for the galaxy UGC06923.

seen, for this galaxy, the SIDM model produces marginally viable rotation curves which are marginally compatible with the SPARC data.

Now we shall include contributions to the rotation velocity from the other components of the galaxy, namely the disk, the gas, and the bulge if present. In Fig. 322 we present the combined rotation curves including all the components of the galaxy along with the SIDM. As it can be seen, the extended collisional DM model is viable. Also in Table CC we present the optimized values of the free parameters of the SIDM model for which we achieve the maximum compatibility with the SPARC data, for the galaxy UGC06930, and also the resulting reduced χ^2_{red} value.

TABLE CC: Optimized Parameter Values of the Extended SIDM model for the Galaxy UGC06930.

Parameter	Value
$\rho_0 (M_\odot / \text{Kpc}^3)$	1.28708×10^7
$K_0 (M_\odot \text{ Kpc}^{-3} (\text{km/s})^2)$	2789.07
ml_{disk}	1
ml_{bulge}	0.1717
$\alpha (\text{Kpc})$	8.4942
χ^2_{red}	0.695298

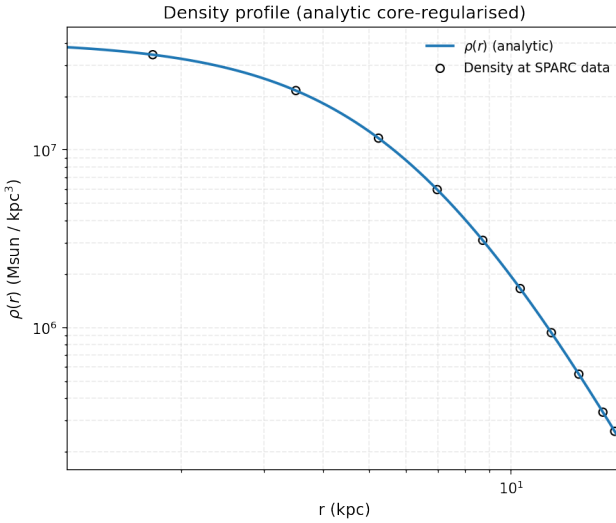


FIG. 320: The density of the SIDM model of Eq. (3) for the galaxy UGC06930, versus the radius.

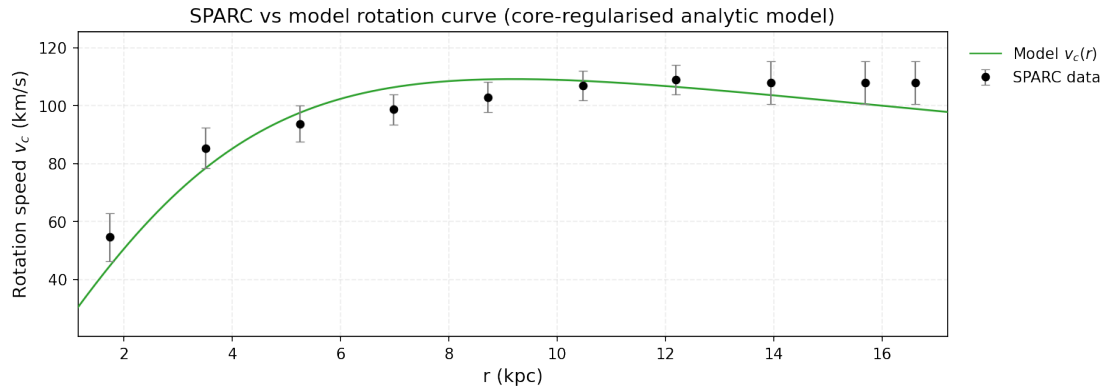


FIG. 321: The predicted rotation curves for the optimized SIDM model of Eq. (3), versus the SPARC observational data for the galaxy UGC06930.

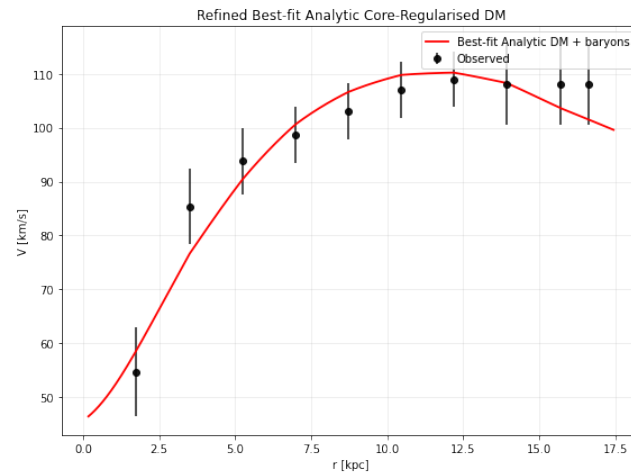


FIG. 322: The predicted rotation curves after using an optimization for the SIDM model (3), and the extended SPARC data for the galaxy UGC06930. We included the rotation curves of the gas, the disk velocities, the bulge (where present) along with the SIDM model.

111. The Galaxy UGC06983, Non-viable, Extended Viable

For this galaxy, the optimization method we used, ensures maximum compatibility of the analytic SIDM model of Eq. (3) with the SPARC data, if we choose $\rho_0 = 5.54619 \times 10^7 M_\odot/\text{Kpc}^3$ and $K_0 = 5224.15 M_\odot \text{Kpc}^{-3} (\text{km/s})^2$, in which case the reduced χ^2_{red} value is $\chi^2_{red} = 1.92876$. Also the parameter α in this case is $\alpha = 5.60094 \text{Kpc}$.

In Table CCI we present the optimized values of K_0 and ρ_0 for the analytic SIDM model of Eq. (3) for which the maximum compatibility with the SPARC data is achieved. In Figs. 323, 324 we present

TABLE CCI: SIDM Optimization Values for the galaxy UGC06983

Parameter	Optimization Values
$\rho_0 (M_\odot/\text{Kpc}^3)$	5.54619×10^7
$K_0 (M_\odot \text{Kpc}^{-3} (\text{km/s})^2)$	5224.15

the density of the analytic SIDM model, the predicted rotation curves for the SIDM model (3), versus the SPARC observational data and the sound speed, as a function of the radius respectively. As it can be seen, for this galaxy, the SIDM model produces non-viable rotation curves which are incompatible with the SPARC data.

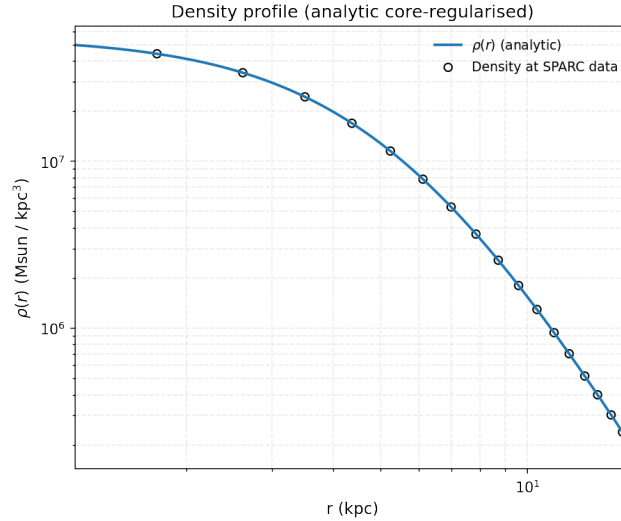


FIG. 323: The density of the SIDM model of Eq. (3) for the galaxy UGC06983, versus the radius.

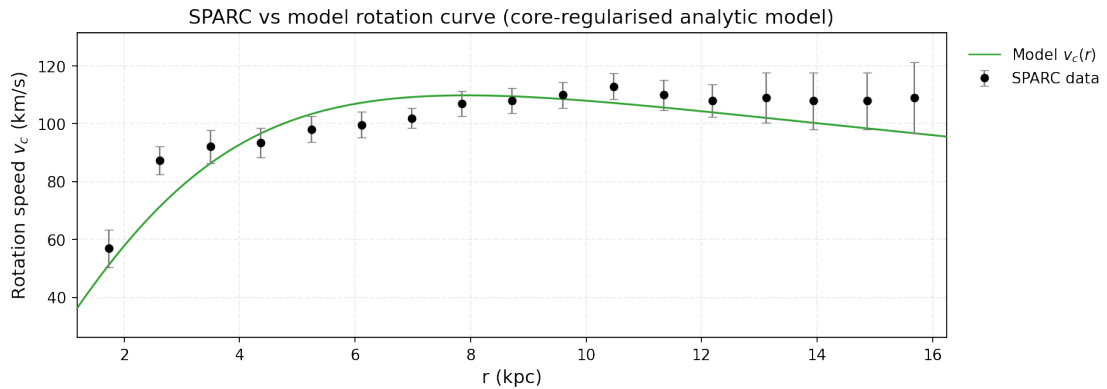


FIG. 324: The predicted rotation curves for the optimized SIDM model of Eq. (3), versus the SPARC observational data for the galaxy UGC06983.

Now we shall include contributions to the rotation velocity from the other components of the galaxy, namely the disk, the gas, and the bulge if present. In Fig. 325 we present the combined rotation curves

including all the components of the galaxy along with the SIDM. As it can be seen, the extended collisional DM model is viable. Also in Table CCII we present the optimized values of the free parameters of the

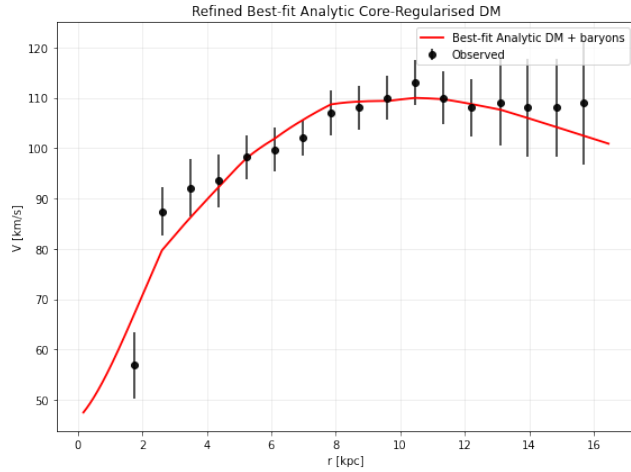


FIG. 325: The predicted rotation curves after using an optimization for the SIDM model (3), and the extended SPARC data for the galaxy UGC06983. We included the rotation curves of the gas, the disk velocities, the bulge (where present) along with the SIDM model.

SIDM model for which we achieve the maximum compatibility with the SPARC data, for the galaxy UGC06983, and also the resulting reduced χ^2_{red} value.

TABLE CCII: Optimized Parameter Values of the Extended SIDM model for the Galaxy UGC06983.

Parameter	Value
ρ_0 (M_\odot/Kpc^3)	2.32153×10^7
K_0 ($M_\odot \text{ Kpc}^{-3} (\text{km/s})^2$)	3544.87
ml_{disk}	1
ml_{bulge}	0.0396
α (Kpc)	7.13032
χ^2_{red}	0.653901

112. The Galaxy UGC07089

For this galaxy, the optimization method we used, ensures maximum compatibility of the analytic SIDM model of Eq. (3) with the SPARC data, if we choose $\rho_0 = 2.26195 \times 10^7 M_\odot/\text{Kpc}^3$ and $K_0 = 2262.44 M_\odot \text{ Kpc}^{-3} (\text{km/s})^2$, in which case the reduced χ^2_{red} value is $\chi^2_{red} = 0.608198$. Also the parameter α in this case is $\alpha = 5.77161 \text{ Kpc}$.

In Table CCIII we present the optimized values of K_0 and ρ_0 for the analytic SIDM model of Eq. (3) for which the maximum compatibility with the SPARC data is achieved. In Figs. 326, 327 we present

TABLE CCIII: SIDM Optimization Values for the galaxy UGC07089

Parameter	Optimization Values
ρ_0 (M_\odot/Kpc^3)	2.26195×10^7
K_0 ($M_\odot \text{ Kpc}^{-3} (\text{km/s})^2$)	2262.44

the density of the analytic SIDM model, the predicted rotation curves for the SIDM model (3), versus the SPARC observational data and the sound speed, as a function of the radius respectively. As it can be seen, for this galaxy, the SIDM model produces viable rotation curves which are compatible with the SPARC data.

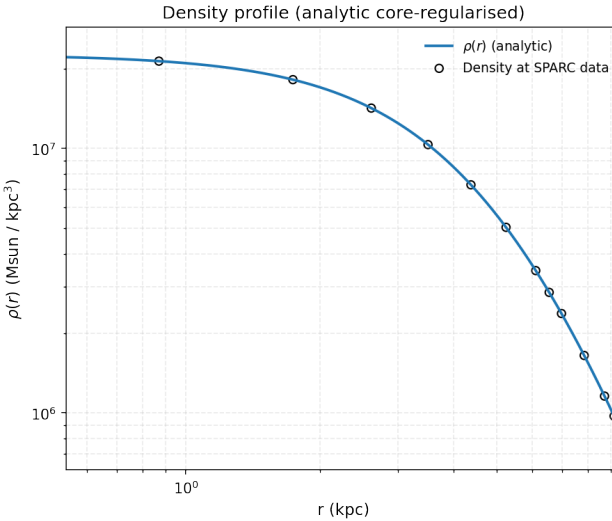


FIG. 326: The density of the SIDM model of Eq. (3) for the galaxy UGC07089, versus the radius.

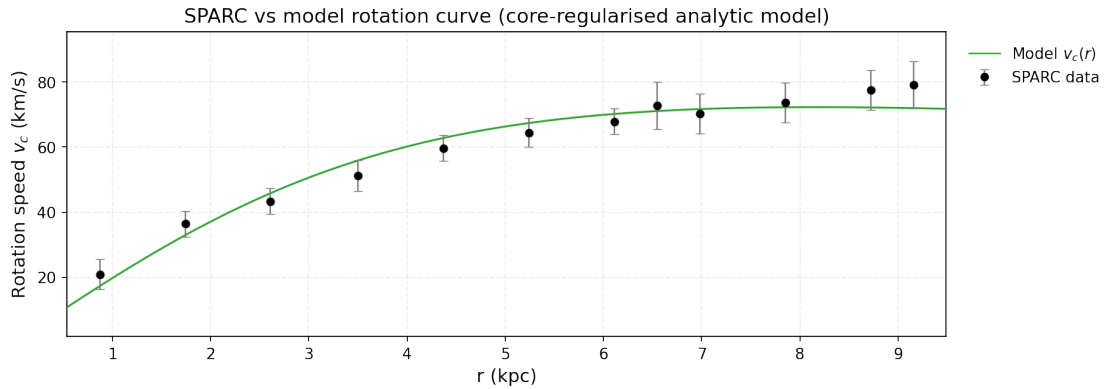


FIG. 327: The predicted rotation curves for the optimized SIDM model of Eq. (3), versus the SPARC observational data for the galaxy UGC07089.

113. The Galaxy UGC07125, Non-viable, Extended Viable

For this galaxy, the optimization method we used, ensures maximum compatibility of the analytic SIDM model of Eq. (3) with the SPARC data, if we choose $\rho_0 = 9.09695 \times 10^6 M_\odot / \text{Kpc}^3$ and $K_0 = 1825.39 M_\odot \text{ Kpc}^{-3} (\text{km/s})^2$, in which case the reduced χ^2_{red} value is $\chi^2_{\text{red}} = 2.54759$. Also the parameter α in this case is $\alpha = 8.17486 \text{ Kpc}$.

In Table CCIV we present the optimized values of K_0 and ρ_0 for the analytic SIDM model of Eq. (3) for which the maximum compatibility with the SPARC data is achieved. In Figs. 328, 329 we present

TABLE CCIV: SIDM Optimization Values for the galaxy UGC07125

Parameter	Optimization Values
$\rho_0 (M_\odot / \text{Kpc}^3)$	9.09695×10^6
$K_0 (M_\odot \text{ Kpc}^{-3} (\text{km/s})^2)$	1825.39

the density of the analytic SIDM model, the predicted rotation curves for the SIDM model (3), versus the SPARC observational data and the sound speed, as a function of the radius respectively. As it can be seen, for this galaxy, the SIDM model produces non-viable rotation curves which are incompatible with the SPARC data.

Now we shall include contributions to the rotation velocity from the other components of the galaxy, namely the disk, the gas, and the bulge if present. In Fig. 330 we present the combined rotation curves

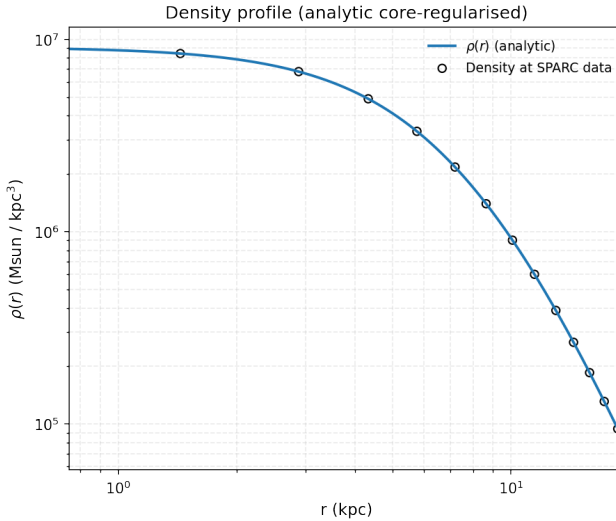


FIG. 328: The density of the SIDM model of Eq. (3) for the galaxy UGC07125, versus the radius.

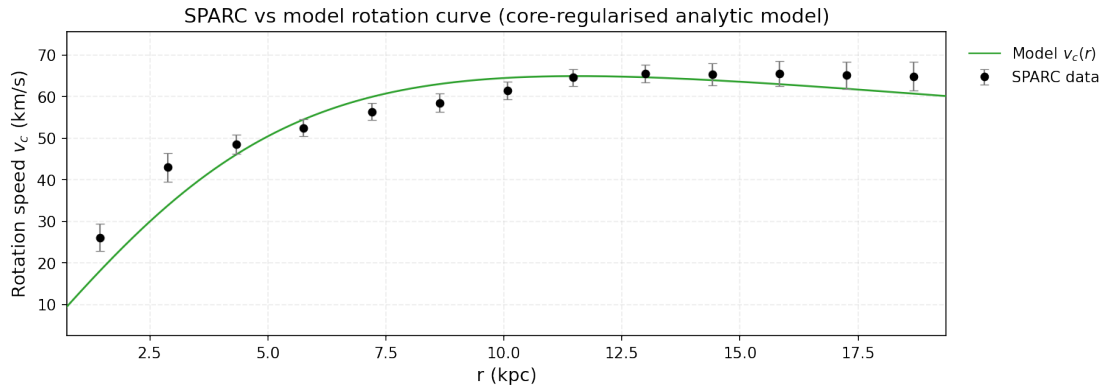


FIG. 329: The predicted rotation curves for the optimized SIDM model of Eq. (3), versus the SPARC observational data for the galaxy UGC07125.

including all the components of the galaxy along with the SIDM. As it can be seen, the extended collisional DM model is viable. Also in Table CCV we present the optimized values of the free parameters of the SIDM model for which we achieve the maximum compatibility with the SPARC data, for the galaxy UGC07125, and also the resulting reduced χ^2_{red} value.

TABLE CCV: Optimized Parameter Values of the Extended SIDM model for the Galaxy UGC07125.

Parameter	Value
ρ_0 (M_\odot/Kpc^3)	4.01917×10^6
K_0 ($M_\odot \text{ Kpc}^{-3} (\text{km/s})^2$)	1013.34
ml_{disk}	0.8239
ml_{bulge}	0.129
α (Kpc)	9.16234
χ^2_{red}	0.296445

114. The Galaxy UGC07151, Non-viable, Extended Viable

For this galaxy, the optimization method we used, ensures maximum compatibility of the analytic SIDM model of Eq. (3) with the SPARC data, if we choose $\rho_0 = 1.05704 \times 10^8 M_\odot/\text{Kpc}^3$ and $K_0 = 2266.67 M_\odot \text{ Kpc}^{-3} (\text{km/s})^2$, in which case the reduced χ^2_{red} value is $\chi^2_{red} = 2.42944$. Also the parameter α in this case is $\alpha = 2.67239 \text{ Kpc}$.

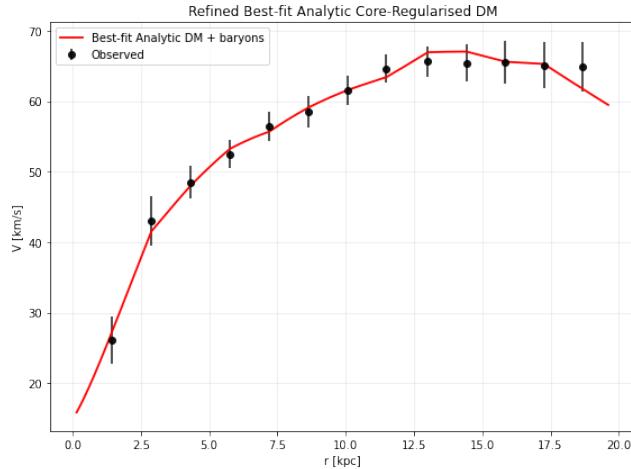


FIG. 330: The predicted rotation curves after using an optimization for the SIDM model (3), and the extended SPARC data for the galaxy UGC07125. We included the rotation curves of the gas, the disk velocities, the bulge (where present) along with the SIDM model.

In Table CCVI we present the optimized values of K_0 and ρ_0 for the analytic SIDM model of Eq. (3) for which the maximum compatibility with the SPARC data is achieved. In Figs. 331, 332 we present

TABLE CCVI: SIDM Optimization Values for the galaxy UGC07151

Parameter	Optimization Values
ρ_0 (M_\odot/Kpc^3)	1.05704×10^8
K_0 ($M_\odot \text{ Kpc}^{-3} (\text{km/s})^2$)	2266.67

the density of the analytic SIDM model, the predicted rotation curves for the SIDM model (3), versus the SPARC observational data and the sound speed, as a function of the radius respectively. As it can be seen, for this galaxy, the SIDM model produces non-viable rotation curves which are incompatible with the SPARC data.

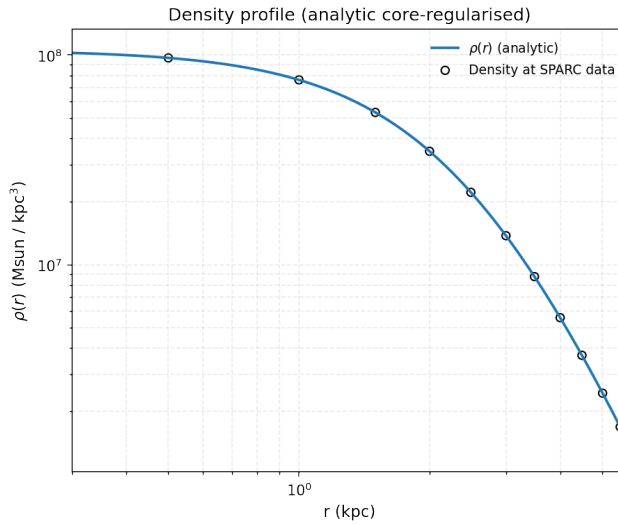


FIG. 331: The density of the SIDM model of Eq. (3) for the galaxy UGC07151, versus the radius.

Now we shall include contributions to the rotation velocity from the other components of the galaxy, namely the disk, the gas, and the bulge if present. In Fig. 333 we present the combined rotation curves including all the components of the galaxy along with the SIDM. As it can be seen, the extended collisional DM model is non-viable. Also in Table CCVII we present the optimized values of the free

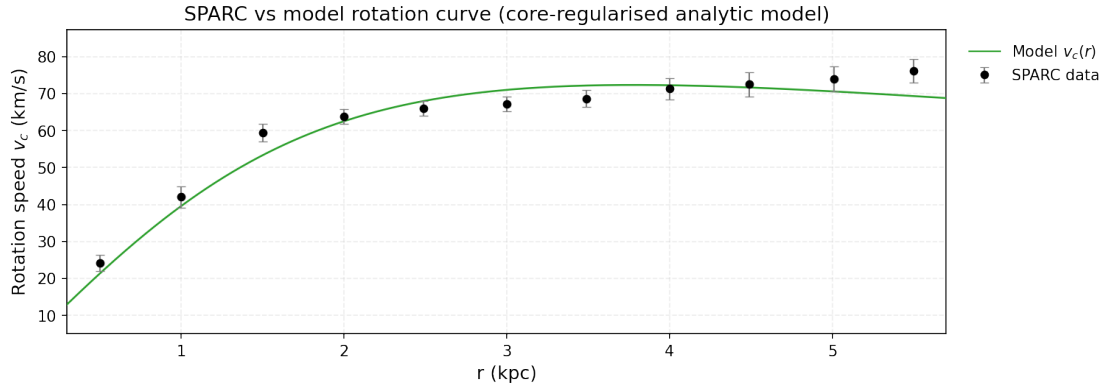


FIG. 332: The predicted rotation curves for the optimized SIDM model of Eq. (3), versus the SPARC observational data for the galaxy UGC07151.

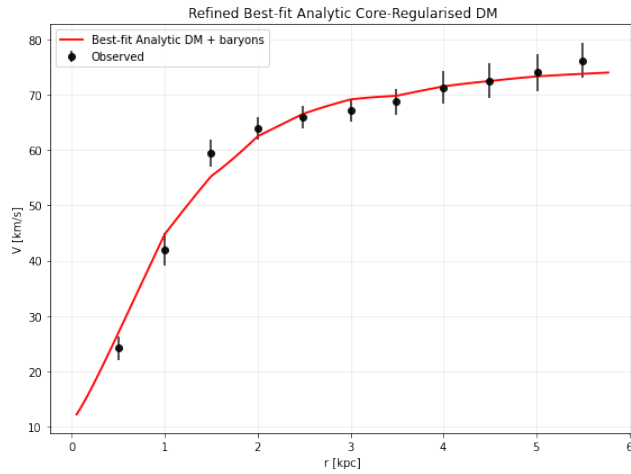


FIG. 333: The predicted rotation curves after using an optimization for the SIDM model (3), and the extended SPARC data for the galaxy UGC07151. We included the rotation curves of the gas, the disk velocities, the bulge (where present) along with the SIDM model.

parameters of the SIDM model for which we achieve the maximum compatibility with the SPARC data, for the galaxy UGC07151, and also the resulting reduced χ^2_{red} value.

TABLE CCVII: Optimized Parameter Values of the Extended SIDM model for the Galaxy UGC07151.

Parameter	Value
ρ_0 (M_\odot/Kpc^3)	3.46961×10^7
K_0 ($M_\odot \text{ Kpc}^{-3} (\text{km/s})^2$)	1104.72
ml_{disk}	0.9669
ml_{bulge}	0.3661
α (Kpc)	3.25598
χ^2_{red}	1.10662

115. The Galaxy UGC07232

For this galaxy, the optimization method we used, ensures maximum compatibility of the analytic SIDM model of Eq. (3) with the SPARC data, if we choose $\rho_0 = 3.17341 \times 10^8 M_\odot/\text{Kpc}^3$ and $K_0 = 862.3 M_\odot \text{ Kpc}^{-3} (\text{km/s})^2$, in which case the reduced χ^2_{red} value is $\chi^2_{red} = 0.582015$. Also the parameter α in this case is $\alpha = 0.951298 \text{ Kpc}$.

In Table CCVIII we present the optimized values of K_0 and ρ_0 for the analytic SIDM model of Eq. (3) for which the maximum compatibility with the SPARC data is achieved. In Figs. 334, 335 we present

TABLE CCVIII: SIDM Optimization Values for the galaxy UGC07232

Parameter	Optimization Values
$\rho_0 (M_\odot/\text{Kpc}^3)$	3.17341×10^8
$K_0 (M_\odot \text{ Kpc}^{-3} (\text{km/s})^2)$	862.3

the density of the analytic SIDM model, the predicted rotation curves for the SIDM model (3), versus the SPARC observational data and the sound speed, as a function of the radius respectively. As it can be seen, for this galaxy, the SIDM model produces viable rotation curves which are compatible with the SPARC data.

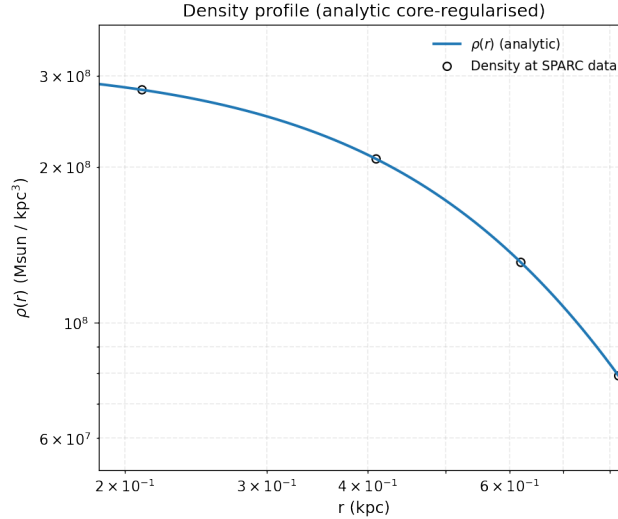


FIG. 334: The density of the SIDM model of Eq. (3) for the galaxy UGC07232, versus the radius.

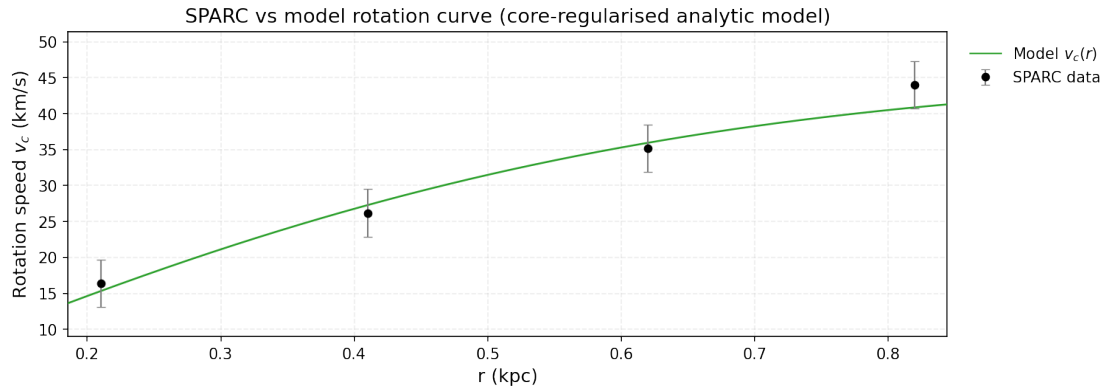


FIG. 335: The predicted rotation curves for the optimized SIDM model of Eq. (3), versus the SPARC observational data for the galaxy UGC07232.

116. The Galaxy UGC07261, Marginally Viable, Extended Viable

For this galaxy, the optimization method we used, ensures maximum compatibility of the analytic SIDM model of Eq. (3) with the SPARC data, if we choose $\rho_0 = 1.03253 \times 10^8 M_\odot/\text{Kpc}^3$ and $K_0 = 2455.77 M_\odot \text{ Kpc}^{-3} (\text{km/s})^2$, in which case the reduced χ^2_{red} value is $\chi^2_{red} = 1.2108$. Also the parameter α in this case is $\alpha = 2.81444 \text{ Kpc}$.

In Table CCIX we present the optimized values of K_0 and ρ_0 for the analytic SIDM model of Eq. (3) for which the maximum compatibility with the SPARC data is achieved. In Figs. 336, 337 we present

TABLE CCIX: SIDM Optimization Values for the galaxy UGC07261

Parameter	Optimization Values
$\rho_0 (M_\odot/\text{Kpc}^3)$	1.03253×10^8
$K_0 (M_\odot \text{ Kpc}^{-3} (\text{km/s})^2)$	2455.77

the density of the analytic SIDM model, the predicted rotation curves for the SIDM model (3), versus the SPARC observational data and the sound speed, as a function of the radius respectively. As it can be seen, for this galaxy, the SIDM model produces marginally viable rotation curves which are marginally compatible with the SPARC data.

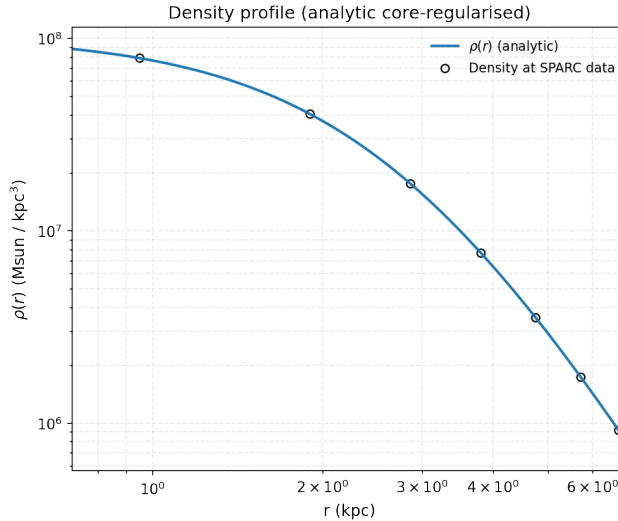


FIG. 336: The density of the SIDM model of Eq. (3) for the galaxy UGC07261, versus the radius.

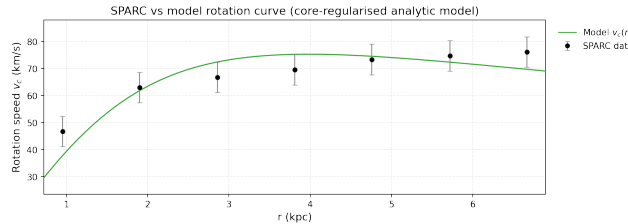


FIG. 337: The predicted rotation curves for the optimized SIDM model of Eq. (3), versus the SPARC observational data for the galaxy UGC07261.

Now we shall include contributions to the rotation velocity from the other components of the galaxy, namely the disk, the gas, and the bulge if present. In Fig. 338 we present the combined rotation curves including all the components of the galaxy along with the SIDM. As it can be seen, the extended collisional DM model is marginally viable. Also in Table CCX we present the optimized values of the free parameters of the SIDM model for which we achieve the maximum compatibility with the SPARC data, for the galaxy UGC07261, and also the resulting reduced χ^2_{red} value.

117. The Galaxy UGC07323, Marginally Viable, Extended Viable

For this galaxy, the optimization method we used, ensures maximum compatibility of the analytic SIDM model of Eq. (3) with the SPARC data, if we choose $\rho_0 = 4.19782 \times 10^7 M_\odot/\text{Kpc}^3$ and $K_0 = 2944.37 M_\odot \text{ Kpc}^{-3} (\text{km/s})^2$, in which case the reduced χ^2_{red} value is $\chi^2_{red} = 1.31901$. Also the parameter α in this case is $\alpha = 4.8332 \text{ Kpc}$.

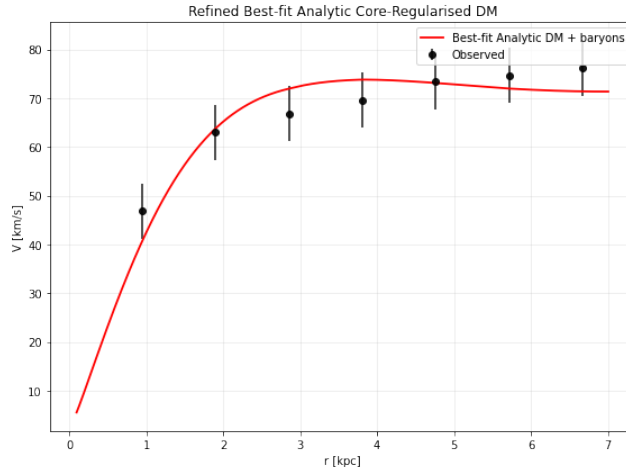


FIG. 338: The predicted rotation curves after using an optimization for the SIDM model (3), and the extended SPARC data for the galaxy UGC07261. We included the rotation curves of the gas, the disk velocities, the bulge (where present) along with the SIDM model.

TABLE CCX: Optimized Parameter Values of the Extended SIDM model for the Galaxy UGC07261.

Parameter	Value
$\rho_0 (M_\odot/\text{Kpc}^3)$	1.24235×10^8
$K_0 (M_\odot \text{ Kpc}^{-3} (\text{km/s})^2)$	2298.32
ml_{disk}	1
ml_{bulge}	0.2
$\alpha (\text{Kpc})$	2.48188
χ^2_{red}	1.15754

In Table CCXI we present the optimized values of K_0 and ρ_0 for the analytic SIDM model of Eq. (3) for which the maximum compatibility with the SPARC data is achieved. In Figs. 339, 340 we present

TABLE CCXI: SIDM Optimization Values for the galaxy UGC07323

Parameter	Optimization Values
$\rho_0 (M_\odot/\text{Kpc}^3)$	4.19782×10^7
$K_0 (M_\odot \text{ Kpc}^{-3} (\text{km/s})^2)$	2944.37

the density of the analytic SIDM model, the predicted rotation curves for the SIDM model (3), versus the SPARC observational data and the sound speed, as a function of the radius respectively. As it can be seen, for this galaxy, the SIDM model produces marginally viable rotation curves which are marginally compatible with the SPARC data.

Now we shall include contributions to the rotation velocity from the other components of the galaxy, namely the disk, the gas, and the bulge if present. In Fig. 341 we present the combined rotation curves including all the components of the galaxy along with the SIDM. As it can be seen, the extended collisional DM model is marginally viable. Also in Table CCXII we present the optimized values of the free parameters of the SIDM model for which we achieve the maximum compatibility with the SPARC data, for the galaxy UGC07323, and also the resulting reduced χ^2_{red} value.

TABLE CCXII: Optimized Parameter Values of the Extended SIDM model for the Galaxy UGC07323.

Parameter	Value
$\rho_0 (M_\odot/\text{Kpc}^3)$	9.54047×10^6
$K_0 (M_\odot \text{ Kpc}^{-3} (\text{km/s})^2)$	2693.68
ml_{disk}	0.8887
ml_{bulge}	0.4027
$\alpha (\text{Kpc})$	9.69581
χ^2_{red}	0.263756

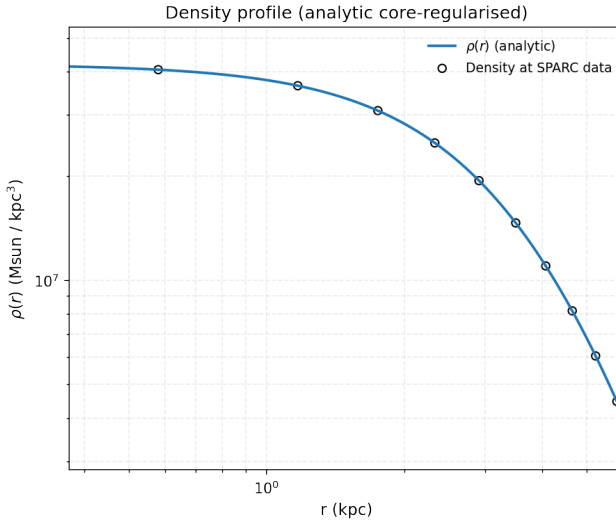


FIG. 339: The density of the SIDM model of Eq. (3) for the galaxy UGC07323, versus the radius.

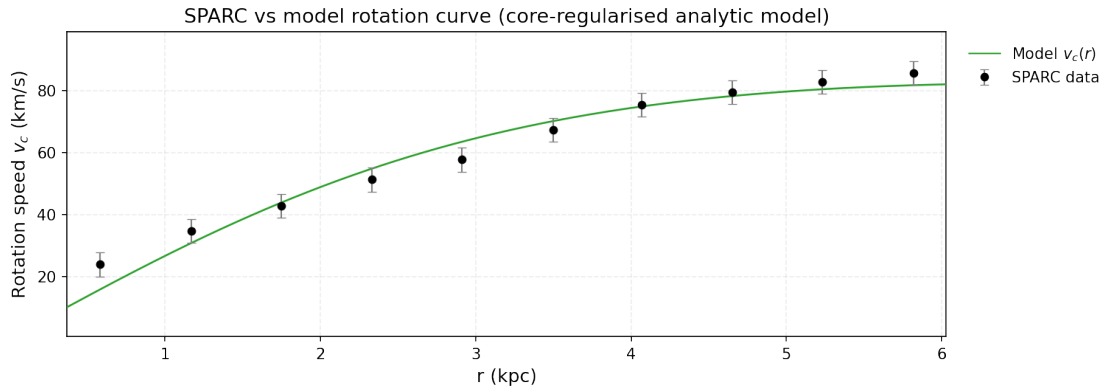


FIG. 340: The predicted rotation curves for the optimized SIDM model of Eq. (3), versus the SPARC observational data for the galaxy UGC07323.

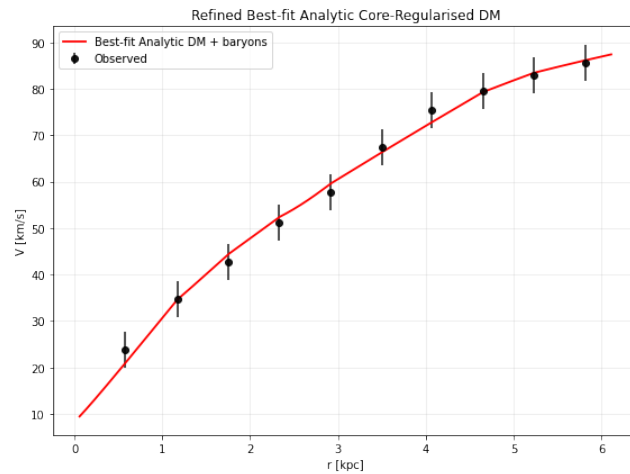


FIG. 341: The predicted rotation curves after using an optimization for the SIDM model (3), and the extended SPARC data for the galaxy UGC07323. We included the rotation curves of the gas, the disk velocities, the bulge (where present) along with the SIDM model.

118. The Galaxy UGC07399, Non-viable

For this galaxy, the optimization method we used, ensures maximum compatibility of the analytic SIDM model of Eq. (3) with the SPARC data, if we choose $\rho_0 = 1.84111 \times 10^8 M_\odot/\text{Kpc}^3$ and $K_0 = 4391.78 M_\odot \text{Kpc}^{-3} (\text{km/s})^2$, in which case the reduced χ^2_{red} value is $\chi^2_{red} = 6.30798$. Also the parameter α in this case is $\alpha = 2.81859 \text{Kpc}$.

In Table CCXIII we present the optimized values of K_0 and ρ_0 for the analytic SIDM model of Eq. (3) for which the maximum compatibility with the SPARC data is achieved. In Figs. 342, 343 we present

TABLE CCXIII: SIDM Optimization Values for the galaxy UGC07399

Parameter	Optimization Values
$\rho_0 (M_\odot/\text{Kpc}^3)$	1.84111×10^8
$K_0 (M_\odot \text{Kpc}^{-3} (\text{km/s})^2)$	4391.78

the density of the analytic SIDM model, the predicted rotation curves for the SIDM model (3), versus the SPARC observational data and the sound speed, as a function of the radius respectively. As it can be seen, for this galaxy, the SIDM model produces non-viable rotation curves which are incompatible with the SPARC data.

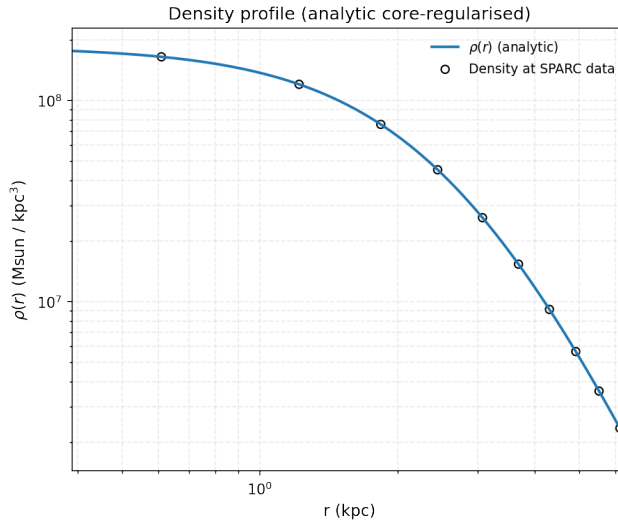


FIG. 342: The density of the SIDM model of Eq. (3) for the galaxy UGC07399, versus the radius.

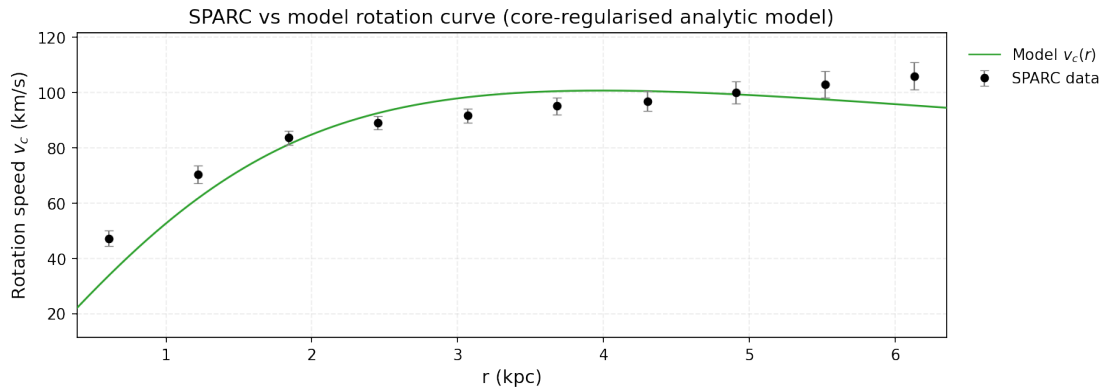


FIG. 343: The predicted rotation curves for the optimized SIDM model of Eq. (3), versus the SPARC observational data for the galaxy UGC07399.

Now we shall include contributions to the rotation velocity from the other components of the galaxy, namely the disk, the gas, and the bulge if present. In Fig. 344 we present the combined rotation

curves including all the components of the galaxy along with the SIDM. As it can be seen, the extended collisional DM model is non-viable. Also in Table CCXIV we present the optimized values of the free

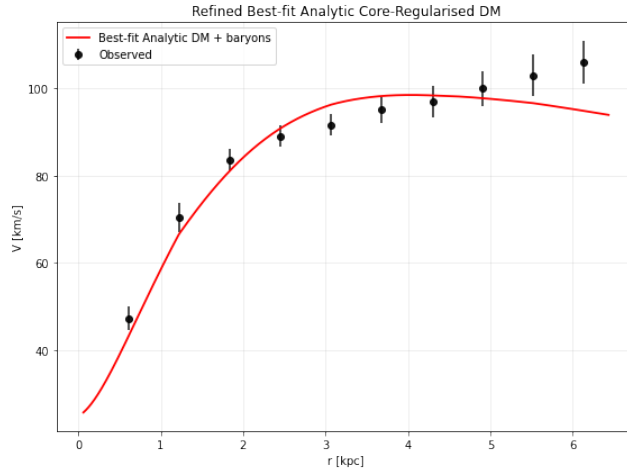


FIG. 344: The predicted rotation curves after using an optimization for the SIDM model (3), and the extended SPARC data for the galaxy UGC07399. We included the rotation curves of the gas, the disk velocities, the bulge (where present) along with the SIDM model.

parameters of the SIDM model for which we achieve the maximum compatibility with the SPARC data, for the galaxy UGC07399, and also the resulting reduced χ^2_{red} value.

TABLE CCXIV: Optimized Parameter Values of the Extended SIDM model for the Galaxy UGC07399.

Parameter	Value
$\rho_0 (M_\odot/\text{Kpc}^3)$	1.34382×10^8
$K_0 (M_\odot \text{ Kpc}^{-3} (\text{km/s})^2)$	3501.73
ml_{disk}	1
ml_{bulge}	0.9901
$\alpha (\text{Kpc})$	2.94555
χ^2_{red}	2.80419

119. The Galaxy UGC07524, Marginally Viable, Extended Viable

For this galaxy, the optimization method we used, ensures maximum compatibility of the analytic SIDM model of Eq. (3) with the SPARC data, if we choose $\rho_0 = 2.48844 \times 10^7 M_\odot/\text{Kpc}^3$ and $K_0 = 2726.02 M_\odot \text{ Kpc}^{-3} (\text{km/s})^2$, in which case the reduced χ^2_{red} value is $\chi^2_{red} = 1.23716$. Also the parameter α in this case is $\alpha = 6.0402 \text{ Kpc}$.

In Table CCXV we present the optimized values of K_0 and ρ_0 for the analytic SIDM model of Eq. (3) for which the maximum compatibility with the SPARC data is achieved. In Figs. 345, 346 we present

TABLE CCXV: SIDM Optimization Values for the galaxy UGC07524

Parameter	Optimization Values
$\rho_0 (M_\odot/\text{Kpc}^3)$	2.48844×10^7
$K_0 (M_\odot \text{ Kpc}^{-3} (\text{km/s})^2)$	2726.02

the density of the analytic SIDM model, the predicted rotation curves for the SIDM model (3), versus the SPARC observational data and the sound speed, as a function of the radius respectively. As it can be seen, for this galaxy, the SIDM model produces marginally viable rotation curves which are marginally compatible with the SPARC data.

Now we shall include contributions to the rotation velocity from the other components of the galaxy, namely the disk, the gas, and the bulge if present. In Fig. 347 we present the combined rotation curves including all the components of the galaxy along with the SIDM. As it can be seen, the extended collisional

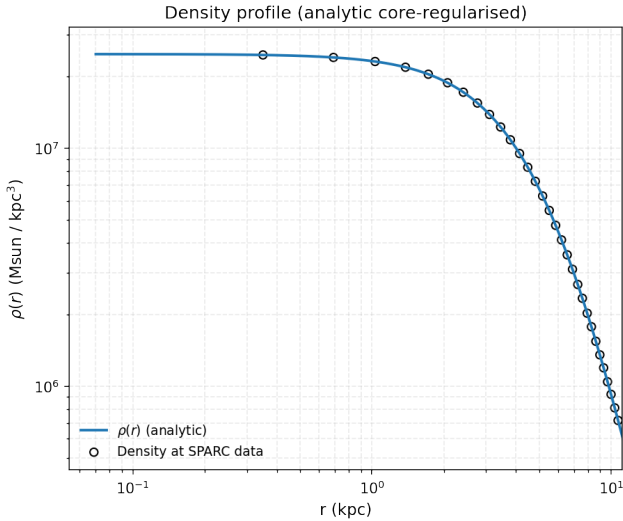


FIG. 345: The density of the SIDM model of Eq. (3) for the galaxy UGC07524, versus the radius.

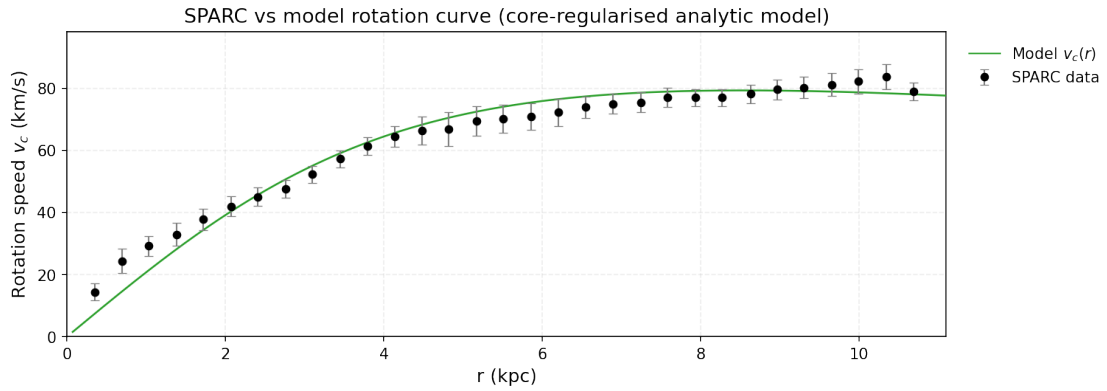


FIG. 346: The predicted rotation curves for the optimized SIDM model of Eq. (3), versus the SPARC observational data for the galaxy UGC07524.

DM model is viable. Also in Table CCXVI we present the optimized values of the free parameters of

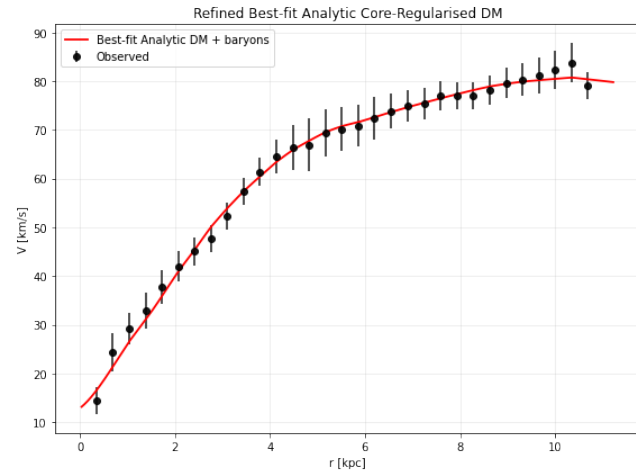


FIG. 347: The predicted rotation curves after using an optimization for the SIDM model (3), and the extended SPARC data for the galaxy UGC07524. We included the rotation curves of the gas, the disk velocities, the bulge (where present) along with the SIDM model.

the SIDM model for which we achieve the maximum compatibility with the SPARC data, for the galaxy UGC07524, and also the resulting reduced χ^2_{red} value.

TABLE CCXVI: Optimized Parameter Values of the Extended SIDM model for the Galaxy UGC07524.

Parameter	Value
$\rho_0 (M_\odot/\text{Kpc}^3)$	1.57695×10^7
$K_0 (M_\odot \text{ Kpc}^{-3} (\text{km/s})^2)$	1703.08
ml_{disk}	1
ml_{bulge}	0.1308
$\alpha (\text{Kpc})$	5.99659
χ^2_{red}	0.201786

120. The Galaxy UGC07559

For this galaxy, the optimization method we used, ensures maximum compatibility of the analytic SIDM model of Eq. (3) with the SPARC data, if we choose $\rho_0 = 3.81394 \times 10^7 M_\odot/\text{Kpc}^3$ and $K_0 = 379.708 M_\odot \text{ Kpc}^{-3} (\text{km/s})^2$, in which case the reduced χ^2_{red} value is $\chi^2_{red} = 0.265754$. Also the parameter α in this case is $\alpha = 1.82091 \text{ Kpc}$.

In Table CCXVII we present the optimized values of K_0 and ρ_0 for the analytic SIDM model of Eq. (3) for which the maximum compatibility with the SPARC data is achieved. In Figs. 348, 349 we present

TABLE CCXVII: SIDM Optimization Values for the galaxy UGC07559

Parameter	Optimization Values
$\rho_0 (M_\odot/\text{Kpc}^3)$	3.81394×10^7
$K_0 (M_\odot \text{ Kpc}^{-3} (\text{km/s})^2)$	379.708

the density of the analytic SIDM model, the predicted rotation curves for the SIDM model (3), versus the SPARC observational data and the sound speed, as a function of the radius respectively. As it can be seen, for this galaxy, the SIDM model produces viable rotation curves which are compatible with the SPARC data.

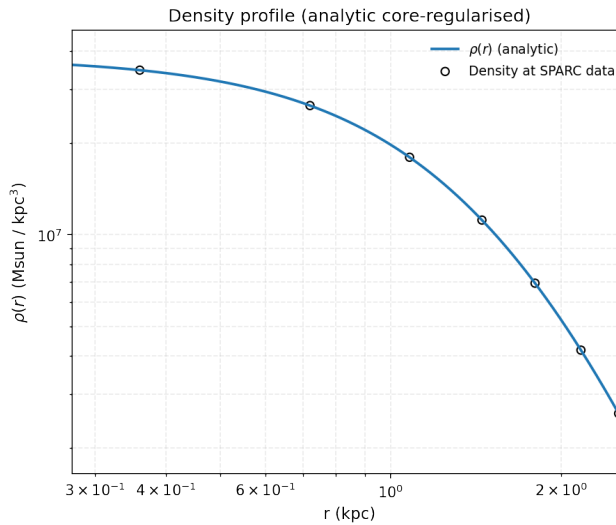


FIG. 348: The density of the SIDM model of Eq. (3) for the galaxy UGC07559, versus the radius.

121. The Galaxy UGC07577

For this galaxy, the optimization method we used, ensures maximum compatibility of the analytic SIDM model of Eq. (3) with the SPARC data, if we choose $\rho_0 = 1.82893 \times 10^7 M_\odot/\text{Kpc}^3$ and $K_0 =$

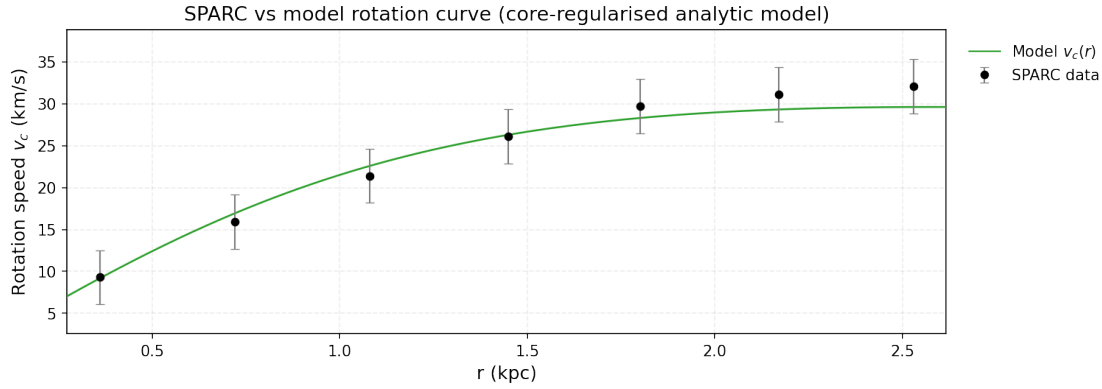


FIG. 349: The predicted rotation curves for the optimized SIDM model of Eq. (3), versus the SPARC observational data for the galaxy UGC07559.

$119.082 M_{\odot} \text{Kpc}^{-3} (\text{km/s})^2$, in which case the reduced χ^2_{red} value is $\chi^2_{red} = 0.38068$. Also the parameter α in this case is $\alpha = 1.47257 \text{Kpc}$.

In Table CCXVIII we present the optimized values of K_0 and ρ_0 for the analytic SIDM model of Eq. (3) for which the maximum compatibility with the SPARC data is achieved. In Figs. 350, 351 we present

TABLE CCXVIII: SIDM Optimization Values for the galaxy UGC07577

Parameter	Optimization Values
$\rho_0 (M_{\odot}/\text{Kpc}^3)$	1.82893×10^7
$K_0 (M_{\odot} \text{Kpc}^{-3} (\text{km/s})^2)$	119.082

the density of the analytic SIDM model, the predicted rotation curves for the SIDM model (3), versus the SPARC observational data and the sound speed, as a function of the radius respectively. As it can be seen, for this galaxy, the SIDM model produces viable rotation curves which are compatible with the SPARC data.

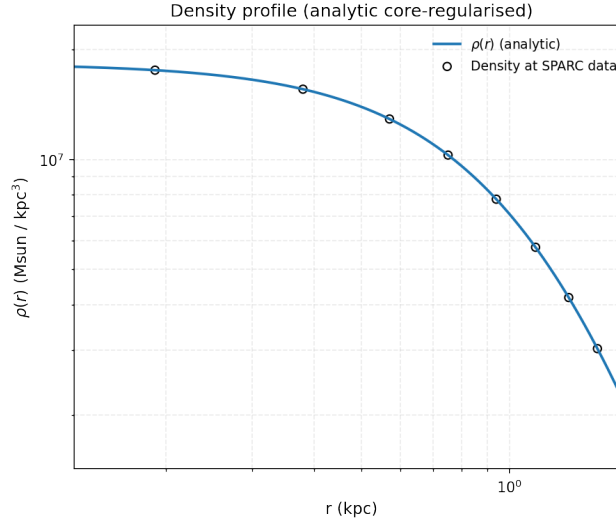


FIG. 350: The density of the SIDM model of Eq. (3) for the galaxy UGC07577, versus the radius.

122. The Galaxy UGC07603

For this galaxy, the optimization method we used, ensures maximum compatibility of the analytic SIDM model of Eq. (3) with the SPARC data, if we choose $\rho_0 = 1.39702 \times 10^8 M_{\odot}/\text{Kpc}^3$ and $K_0 =$

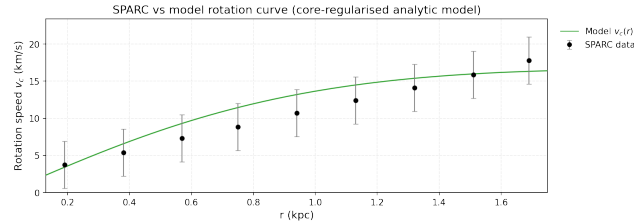


FIG. 351: The predicted rotation curves for the optimized SIDM model of Eq. (3), versus the SPARC observational data for the galaxy UGC07577.

$1744.97 M_{\odot} \text{ Kpc}^{-3} (\text{km/s})^2$, in which case the reduced χ^2_{red} value is $\chi^2_{red} = 0.537465$. Also the parameter α in this case is $\alpha = 2.03959 \text{ Kpc}$.

In Table CCXIX we present the optimized values of K_0 and ρ_0 for the analytic SIDM model of Eq. (3) for which the maximum compatibility with the SPARC data is achieved. In Figs. 352, 353 we present

TABLE CCXIX: SIDM Optimization Values for the galaxy UGC07603

Parameter	Optimization Values
$\rho_0 (M_{\odot}/\text{Kpc}^3)$	1.39702×10^8
$K_0 (M_{\odot} \text{ Kpc}^{-3} (\text{km/s})^2)$	1744.97

the density of the analytic SIDM model, the predicted rotation curves for the SIDM model (3), versus the SPARC observational data and the sound speed, as a function of the radius respectively. As it can be seen, for this galaxy, the SIDM model produces viable rotation curves which are compatible with the SPARC data.

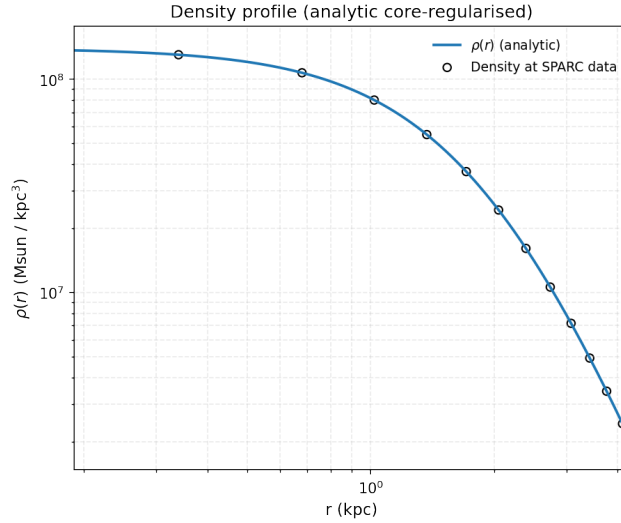


FIG. 352: The density of the SIDM model of Eq. (3) for the galaxy UGC07603, versus the radius.

Now we shall include contributions to the rotation velocity from the other components of the galaxy, namely the disk, the gas, and the bulge if present. In Fig. 354 we present the combined rotation curves including all the components of the galaxy along with the SIDM. As it can be seen, the extended collisional DM model is viable. Also in Table CCXX we present the optimized values of the free parameters of the SIDM model for which we achieve the maximum compatibility with the SPARC data, for the galaxy UGC07603, and also the resulting reduced χ^2_{red} value.

123. The Galaxy UGC07690

For this galaxy, the optimization method we used, ensures maximum compatibility of the analytic SIDM model of Eq. (3) with the SPARC data, if we choose $\rho_0 = 4.34713 \times 10^8 M_{\odot}/\text{Kpc}^3$ and $K_0 =$

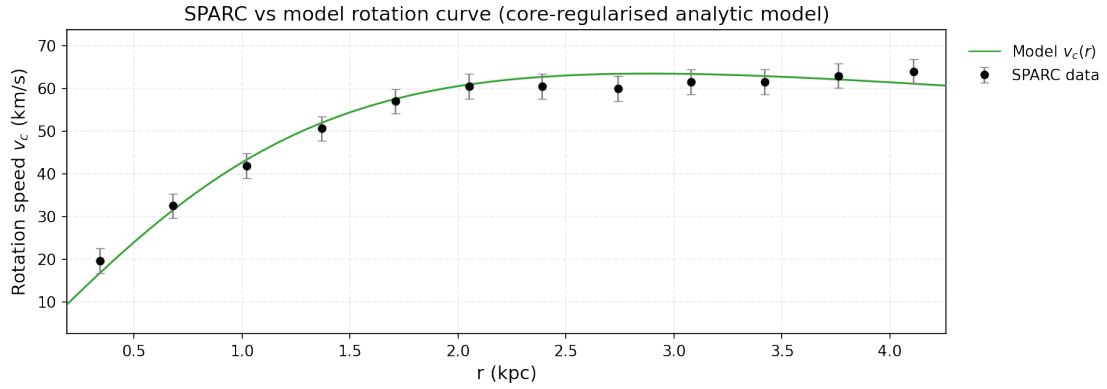


FIG. 353: The predicted rotation curves for the optimized SIDM model of Eq. (3), versus the SPARC observational data for the galaxy UGC07603.

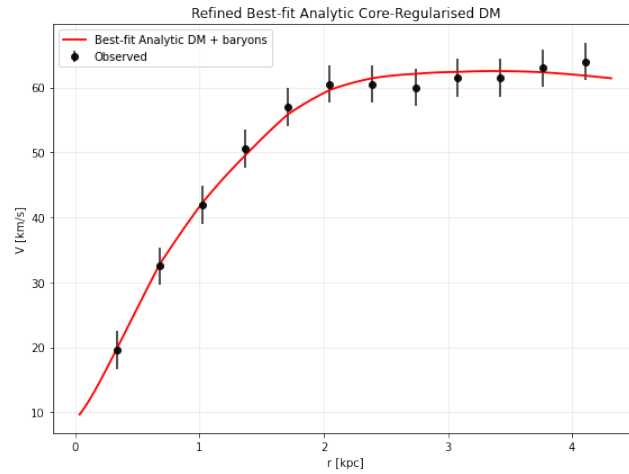


FIG. 354: The predicted rotation curves after using an optimization for the SIDM model (3), and the extended SPARC data for the galaxy UGC07603. We included the rotation curves of the gas, the disk velocities, the bulge (where present) along with the SIDM model.

TABLE CCXX: Optimized Parameter Values of the Extended SIDM model for the Galaxy UGC07603.

Parameter	Value
$\rho_0 (M_\odot/\text{Kpc}^3)$	8.03207×10^7
$K_0 (M_\odot \text{ Kpc}^{-3} (\text{km/s})^2)$	1447.94
ml_{disk}	0.7492
ml_{bulge}	0.2680
$\alpha (\text{Kpc})$	2.44995
χ^2_{red}	0.235451

$1786.83 M_\odot \text{ Kpc}^{-3} (\text{km/s})^2$, in which case the reduced χ^2_{red} value is $\chi^2_{\text{red}} = 0.48353$. Also the parameter α in this case is $\alpha = 1.17001 \text{ Kpc}$.

In Table CCXXI we present the optimized values of K_0 and ρ_0 for the analytic SIDM model of Eq. (3) for which the maximum compatibility with the SPARC data is achieved. In Figs. 355, 356 we present

TABLE CCXXI: SIDM Optimization Values for the galaxy UGC07690

Parameter	Optimization Values
$\rho_0 (M_\odot/\text{Kpc}^3)$	4.34713×10^8
$K_0 (M_\odot \text{ Kpc}^{-3} (\text{km/s})^2)$	1786.83

the density of the analytic SIDM model, the predicted rotation curves for the SIDM model (3), versus

the SPARC observational data and the sound speed, as a function of the radius respectively. As it can be seen, for this galaxy, the SIDM model produces viable rotation curves which are compatible with the SPARC data.

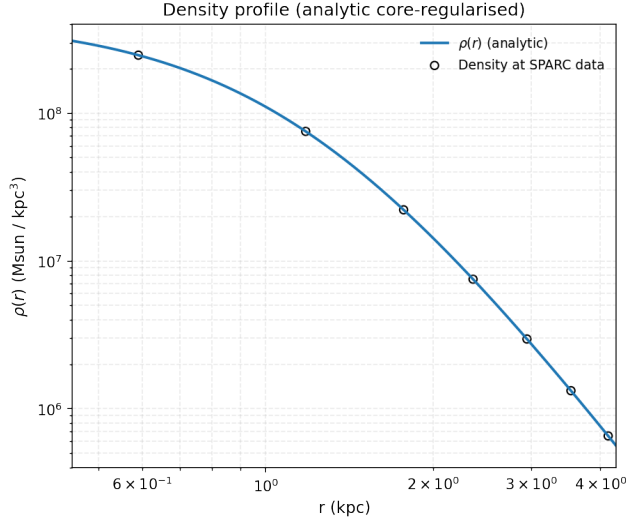


FIG. 355: The density of the SIDM model of Eq. (3) for the galaxy UGC07690, versus the radius.

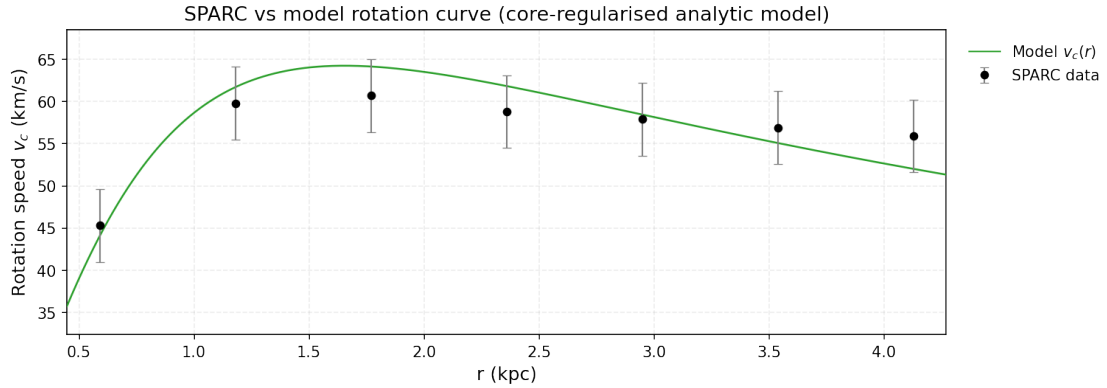


FIG. 356: The predicted rotation curves for the optimized SIDM model of Eq. (3), versus the SPARC observational data for the galaxy UGC07690.

124. The Galaxy UGC07866

For this galaxy, the optimization method we used, ensures maximum compatibility of the analytic SIDM model of Eq. (3) with the SPARC data, if we choose $\rho_0 = 4.19666 \times 10^7 M_\odot / \text{Kpc}^3$ and $K_0 = 522.148 M_\odot \text{ Kpc}^{-3} (\text{km/s})^2$, in which case the reduced χ^2_{red} value is $\chi^2_{\text{red}} = 0.463844$. Also the parameter α in this case is $\alpha = 2.03562 \text{ Kpc}$.

In Table CCXXII we present the optimized values of K_0 and ρ_0 for the analytic SIDM model of Eq. (3) for which the maximum compatibility with the SPARC data is achieved. In Figs. 357, 358 we present

TABLE CCXXII: SIDM Optimization Values for the galaxy UGC07866

Parameter	Optimization Values
$\rho_0 (M_\odot / \text{Kpc}^3)$	4.19666×10^7
$K_0 (M_\odot \text{ Kpc}^{-3} (\text{km/s})^2)$	522.148

the density of the analytic SIDM model, the predicted rotation curves for the SIDM model (3), versus

the SPARC observational data and the sound speed, as a function of the radius respectively. As it can be seen, for this galaxy, the SIDM model produces viable rotation curves which are compatible with the SPARC data.

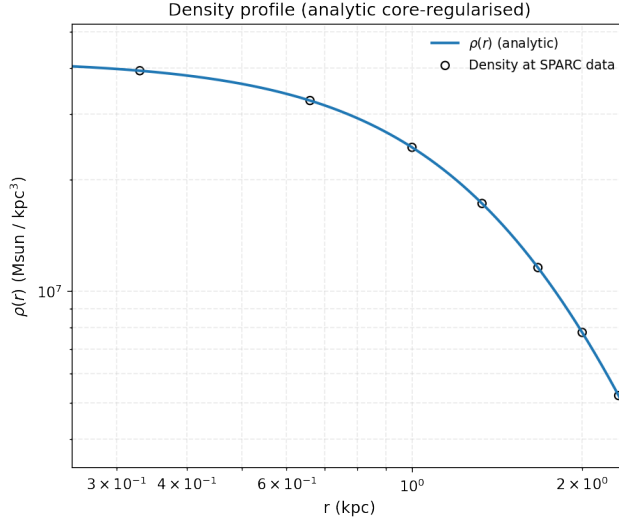


FIG. 357: The density of the SIDM model of Eq. (3) for the galaxy UGC07866, versus the radius.

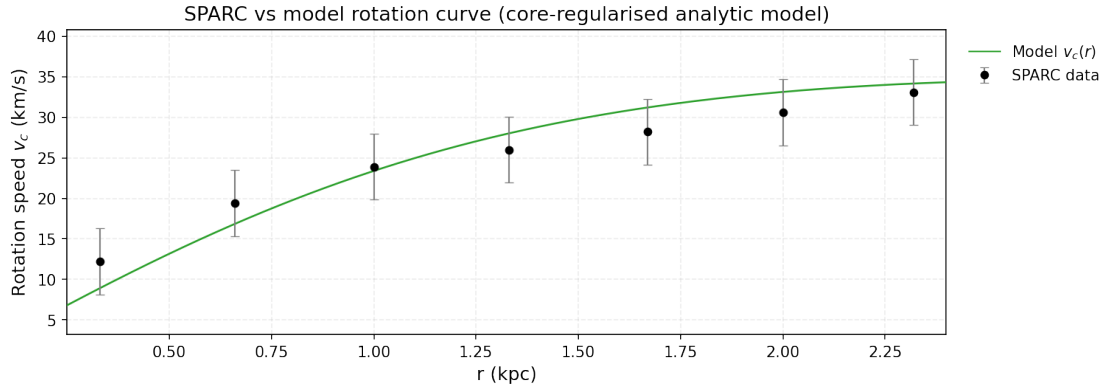


FIG. 358: The predicted rotation curves for the optimized SIDM model of Eq. (3), versus the SPARC observational data for the galaxy UGC07866.

125. The Galaxy UGC08286, Non-viable

For this galaxy, the optimization method we used, ensures maximum compatibility of the analytic SIDM model of Eq. (3) with the SPARC data, if we choose $\rho_0 = 8.99622 \times 10^7 M_\odot / \text{Kpc}^3$ and $K_0 = 3052.87 M_\odot \text{ Kpc}^{-3} (\text{km/s})^2$, in which case the reduced χ^2_{red} value is $\chi^2_{red} = 4.76634$. Also the parameter α in this case is $\alpha = 3.36182 \text{ Kpc}$.

In Table CCXXIII we present the optimized values of K_0 and ρ_0 for the analytic SIDM model of Eq. (3) for which the maximum compatibility with the SPARC data is achieved. In Figs. 359, 360 we present

TABLE CCXXIII: SIDM Optimization Values for the galaxy UGC08286

Parameter	Optimization Values
$\rho_0 (M_\odot / \text{Kpc}^3)$	8.99622×10^7
$K_0 (M_\odot \text{ Kpc}^{-3} (\text{km/s})^2)$	$= 3052.87$

the density of the analytic SIDM model, the predicted rotation curves for the SIDM model (3), versus

the SPARC observational data and the sound speed, as a function of the radius respectively. As it can be seen, for this galaxy, the SIDM model produces non-viable rotation curves which are incompatible with the SPARC data.

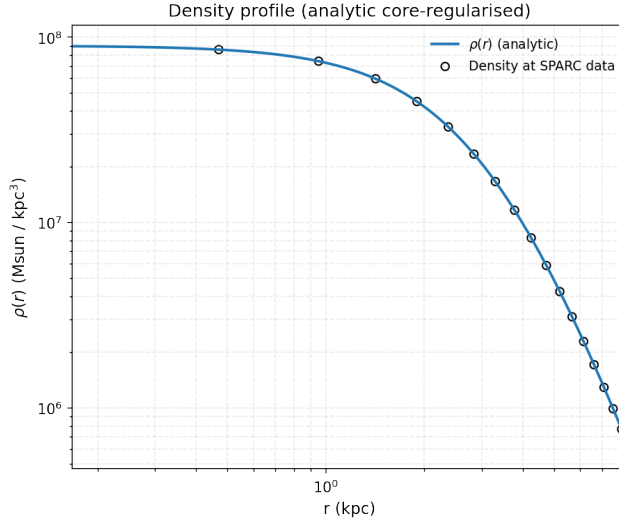


FIG. 359: The density of the SIDM model of Eq. (3) for the galaxy UGC08286, versus the radius.

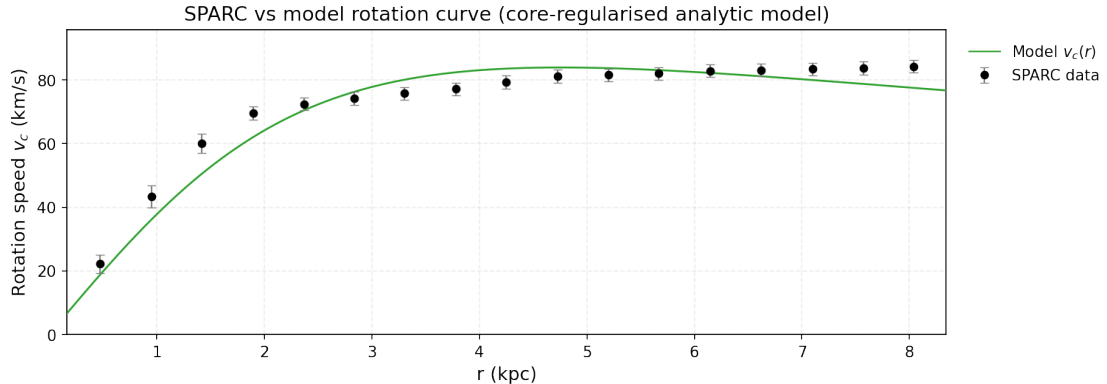


FIG. 360: The predicted rotation curves for the optimized SIDM model of Eq. (3), versus the SPARC observational data for the galaxy UGC08286.

Now we shall include contributions to the rotation velocity from the other components of the galaxy, namely the disk, the gas, and the bulge if present. In Fig. 361 we present the combined rotation curves including all the components of the galaxy along with the SIDM. As it can be seen, the extended collisional DM model is non-viable. Also in Table CCXXIV we present the optimized values of the free parameters of the SIDM model for which we achieve the maximum compatibility with the SPARC data, for the galaxy UGC08286, and also the resulting reduced χ^2_{red} value.

TABLE CCXXIV: Optimized Parameter Values of the Extended SIDM model for the Galaxy UGC08286.

Parameter	Value
$\rho_0 (M_\odot / \text{Kpc}^3)$	9.81387×10^7
$K_0 (M_\odot \text{ Kpc}^{-3} (\text{km/s})^2)$	2886.24
ml_{disk}	0.77
ml_{bulge}	0.2364
$\alpha (\text{Kpc})$	3.12927
χ^2_{red}	4.54762

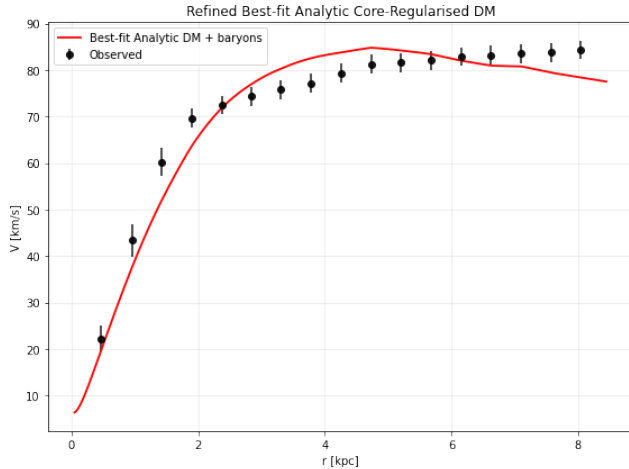


FIG. 361: The predicted rotation curves after using an optimization for the SIDM model (3), and the extended SPARC data for the galaxy UGC08286. We included the rotation curves of the gas, the disk velocities, the bulge (where present) along with the SIDM model.

126. The Galaxy UGC08490, Non-viable

For this galaxy, the optimization method we used, ensures maximum compatibility of the analytic SIDM model of Eq. (3) with the SPARC data, if we choose $\rho_0 = 1.24736 \times 10^8 M_\odot/\text{Kpc}^3$ and $K_0 = 3195.87 M_\odot \text{Kpc}^{-3} (\text{km/s})^2$, in which case the reduced χ^2_{red} value is $\chi^2_{red} = 4.99288$. Also the parameter α in this case is $\alpha = 2.92112 \text{Kpc}$.

In Table CCXXV we present the optimized values of K_0 and ρ_0 for the analytic SIDM model of Eq. (3) for which the maximum compatibility with the SPARC data is achieved. In Figs. 362, 363 we present

TABLE CCXXV: SIDM Optimization Values for the galaxy UGC08490

Parameter	Optimization Values
$\rho_0 (M_\odot/\text{Kpc}^3)$	1.24736×10^8
$K_0 (M_\odot \text{Kpc}^{-3} (\text{km/s})^2)$	3195.87

the density of the analytic SIDM model, the predicted rotation curves for the SIDM model (3), versus the SPARC observational data and the sound speed, as a function of the radius respectively. As it can be seen, for this galaxy, the SIDM model produces non-viable rotation curves which are incompatible with the SPARC data.

Now we shall include contributions to the rotation velocity from the other components of the galaxy, namely the disk, the gas, and the bulge if present. In Fig. 364 we present the combined rotation curves including all the components of the galaxy along with the SIDM. As it can be seen, the extended collisional DM model is non-viable. Also in Table CCXXVI we present the optimized values of the free parameters of the SIDM model for which we achieve the maximum compatibility with the SPARC data, for the galaxy UGC08490, and also the resulting reduced χ^2_{red} value.

TABLE CCXXVI: Optimized Parameter Values of the Extended SIDM model for the Galaxy UGC08490.

Parameter	Value
$\rho_0 (M_\odot/\text{Kpc}^3)$	5.38884×10^7
$K_0 (M_\odot \text{Kpc}^{-3} (\text{km/s})^2)$	2344.78
ml_{disk}	1
ml_{bulge}	0.4631
$\alpha (\text{Kpc})$	3.80627
χ^2_{red}	1.254

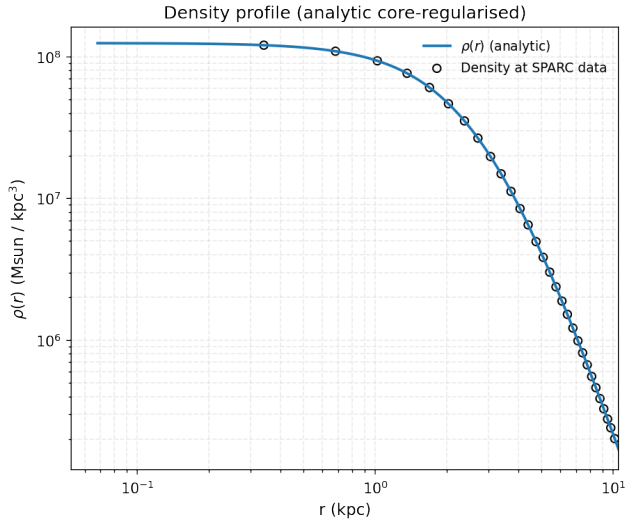


FIG. 362: The density of the SIDM model of Eq. (3) for the galaxy UGC08490, versus the radius.

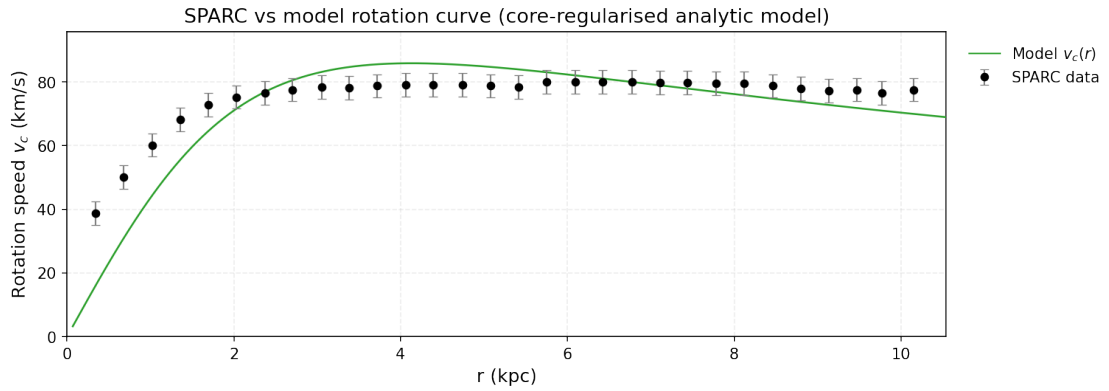


FIG. 363: The predicted rotation curves for the optimized SIDM model of Eq. (3), versus the SPARC observational data for the galaxy UGC08490.

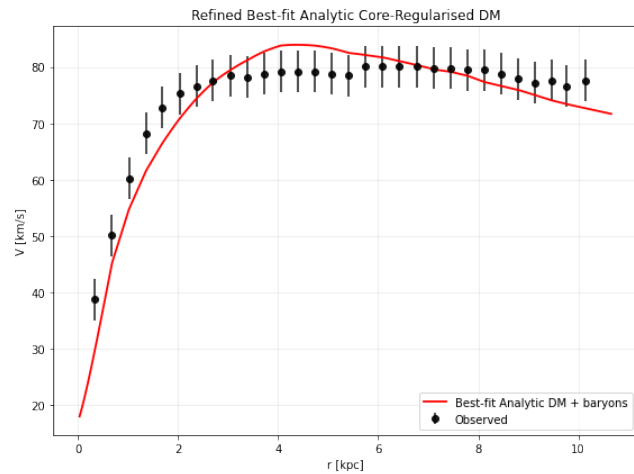


FIG. 364: The predicted rotation curves after using an optimization for the SIDM model (3), and the extended SPARC data for the galaxy UGC08490. We included the rotation curves of the gas, the disk velocities, the bulge (where present) along with the SIDM model.

127. The Galaxy UGC08550, Non-viable

For this galaxy, the optimization method we used, ensures maximum compatibility of the analytic SIDM model of Eq. (3) with the SPARC data, if we choose $\rho_0 = 9.10509 \times 10^7 M_\odot/\text{Kpc}^3$ and $K_0 = 1417.93 M_\odot \text{Kpc}^{-3} (\text{km/s})^2$, in which case the reduced χ^2_{red} value is $\chi^2_{red} = 5.10517$. Also the parameter α in this case is $\alpha = 2.27738 \text{Kpc}$.

In Table CCXXVII we present the optimized values of K_0 and ρ_0 for the analytic SIDM model of Eq. (3) for which the maximum compatibility with the SPARC data is achieved. In Figs. 365, 366 we present

TABLE CCXXVII: SIDM Optimization Values for the galaxy UGC08550

Parameter	Optimization Values
$\rho_0 (M_\odot/\text{Kpc}^3)$	9.10509×10^7
$K_0 (M_\odot \text{Kpc}^{-3} (\text{km/s})^2)$	1417.93

the density of the analytic SIDM model, the predicted rotation curves for the SIDM model (3), versus the SPARC observational data and the sound speed, as a function of the radius respectively. As it can be seen, for this galaxy, the SIDM model produces non-viable rotation curves which are incompatible with the SPARC data.

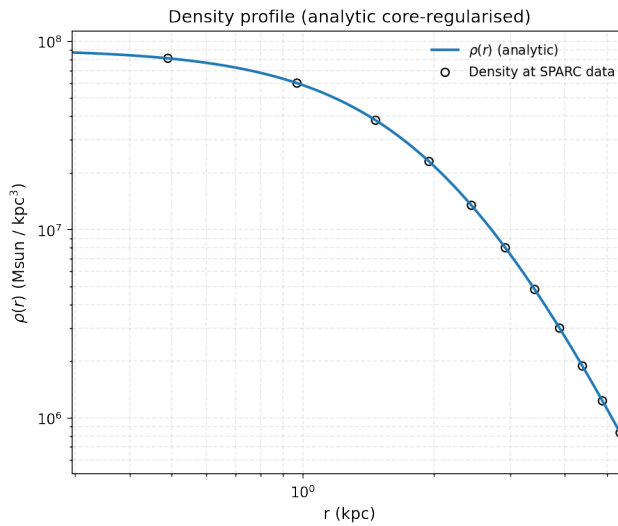


FIG. 365: The density of the SIDM model of Eq. (3) for the galaxy UGC08550, versus the radius.

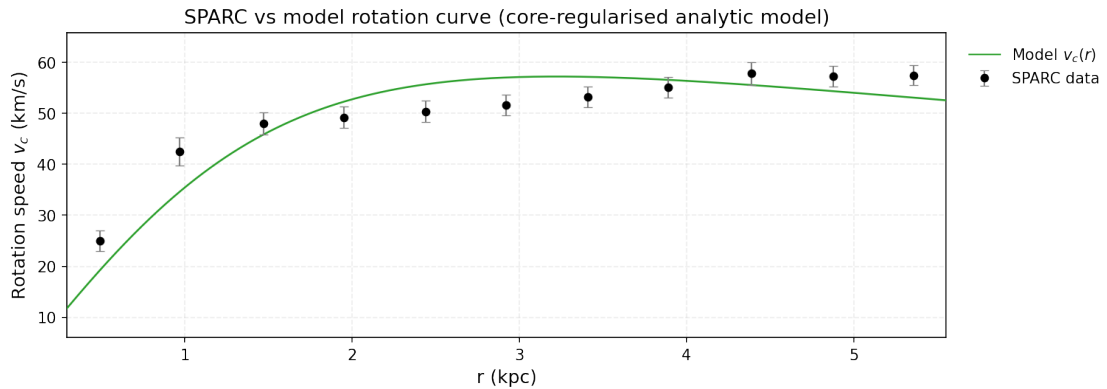


FIG. 366: The predicted rotation curves for the optimized SIDM model of Eq. (3), versus the SPARC observational data for the galaxy UGC08550.

Now we shall include contributions to the rotation velocity from the other components of the galaxy, namely the disk, the gas, and the bulge if present. In Fig. 367 we present the combined rotation

curves including all the components of the galaxy along with the SIDM. As it can be seen, the extended collisional DM model is non-viable. Also in Table CCXXVIII we present the optimized values of the free

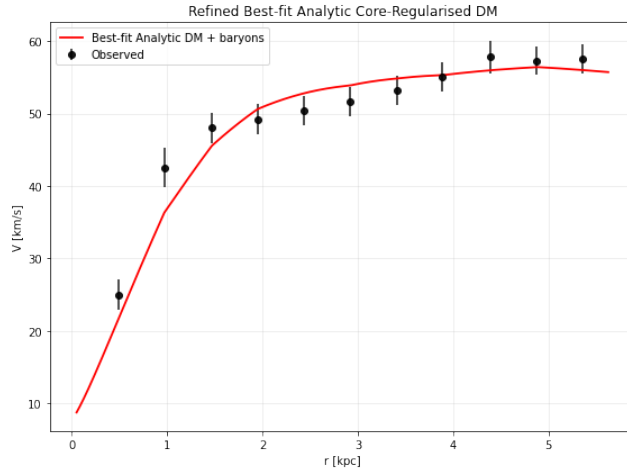


FIG. 367: The predicted rotation curves after using an optimization for the SIDM model (3), and the extended SPARC data for the galaxy UGC08550. We included the rotation curves of the gas, the disk velocities, the bulge (where present) along with the SIDM model.

parameters of the SIDM model for which we achieve the maximum compatibility with the SPARC data, for the galaxy UGC08550, and also the resulting reduced χ^2_{red} value.

TABLE CCXXVIII: Optimized Parameter Values of the Extended SIDM model for the Galaxy UGC08550.

Parameter	Value
$\rho_0 (M_\odot/\text{Kpc}^3)$	4.04304×10^7
$K_0 (M_\odot \text{ Kpc}^{-3} (\text{km/s})^2)$	1080.68
ml_{disk}	1
ml_{bulge}	0.3544
$\alpha (\text{Kpc})$	2.98326
χ^2_{red}	2.04733

128. The Galaxy UGC08699, Non-viable

For this galaxy, the optimization method we used, ensures maximum compatibility of the analytic SIDM model of Eq. (3) with the SPARC data, if we choose $\rho_0 = 2.06633 \times 10^8 M_\odot/\text{Kpc}^3$ and $K_0 = 16391.8 M_\odot \text{ Kpc}^{-3} (\text{km/s})^2$, in which case the reduced χ^2_{red} value is $\chi^2_{red} = 155.888$. Also the parameter α in this case is $\alpha = 5.14 \text{ Kpc}$.

In Table CCXXIX we present the optimized values of K_0 and ρ_0 for the analytic SIDM model of Eq. (3) for which the maximum compatibility with the SPARC data is achieved. In Figs. 368, 369 we present

TABLE CCXXIX: SIDM Optimization Values for the galaxy UGC08699

Parameter	Optimization Values
$\rho_0 (M_\odot/\text{Kpc}^3)$	2.06633×10^8
$K_0 (M_\odot \text{ Kpc}^{-3} (\text{km/s})^2)$	16391.8

the density of the analytic SIDM model, the predicted rotation curves for the SIDM model (3), versus the SPARC observational data and the sound speed, as a function of the radius respectively. As it can be seen, for this galaxy, the SIDM model produces non-viable rotation curves which are incompatible with the SPARC data.

Now we shall include contributions to the rotation velocity from the other components of the galaxy, namely the disk, the gas, and the bulge if present. In Fig. 370 we present the combined rotation curves including all the components of the galaxy along with the SIDM. As it can be seen, the extended

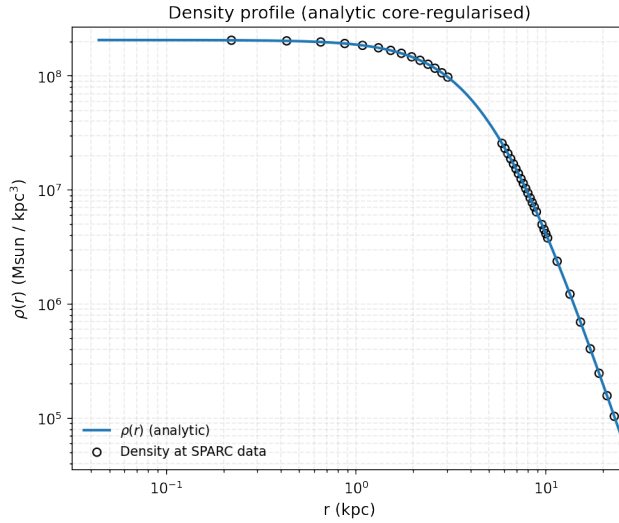


FIG. 368: The density of the SIDM model of Eq. (3) for the galaxy UGC08699, versus the radius.

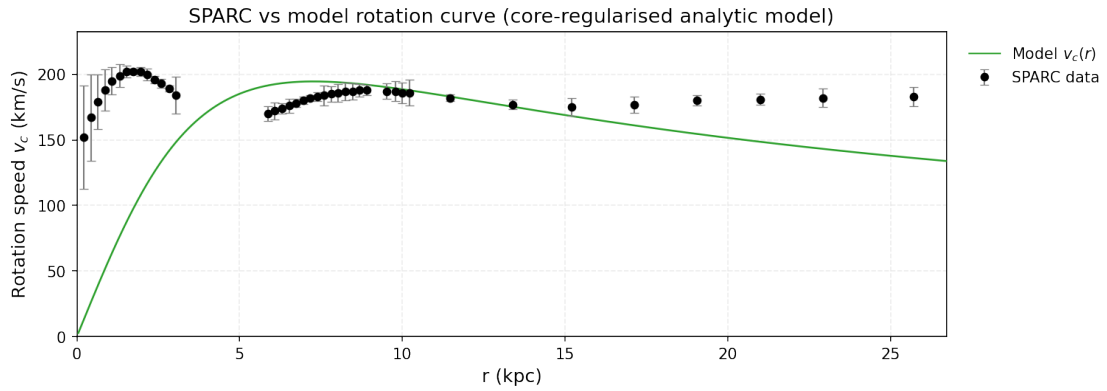


FIG. 369: The predicted rotation curves for the optimized SIDM model of Eq. (3), versus the SPARC observational data for the galaxy UGC08699.

collisional DM model is non-viable. Also in Table CCXXX we present the optimized values of the free

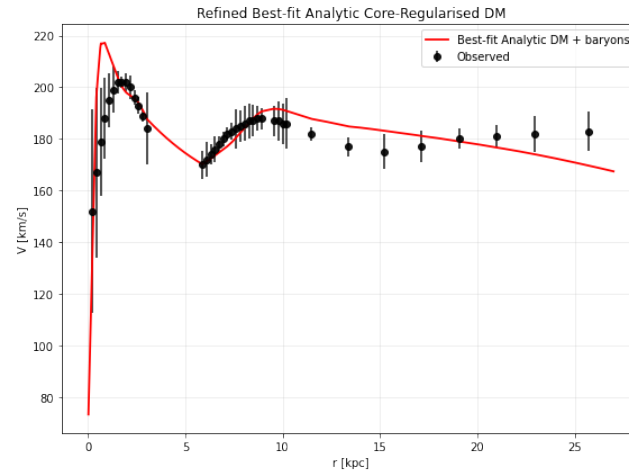


FIG. 370: The predicted rotation curves after using an optimization for the SIDM model (3), and the extended SPARC data for the galaxy UGC08699. We included the rotation curves of the gas, the disk velocities, the bulge (where present) along with the SIDM model.

parameters of the SIDM model for which we achieve the maximum compatibility with the SPARC data, for the galaxy UGC08699, and also the resulting reduced χ^2_{red} value.

TABLE CCXXX: Optimized Parameter Values of the Extended SIDM model for the Galaxy UGC08699.

Parameter	Value
ρ_0 (M_\odot/Kpc^3)	1.15203×10^7
K_0 ($M_\odot \text{ Kpc}^{-3} (\text{km/s})^2$)	8544.33
ml_{disk}	1.0000
ml_{bulge}	0.8248
α (Kpc)	15.7146
χ^2_{red}	1.21621

129. The Galaxy UGC08837

For this galaxy, the optimization method we used, ensures maximum compatibility of the analytic SIDM model of Eq. (3) with the SPARC data, if we choose $\rho_0 = 1.25744 \times 10^7 M_\odot/\text{Kpc}^3$ and $K_0 = 1886.63 M_\odot \text{ Kpc}^{-3} (\text{km/s})^2$, in which case the reduced χ^2_{red} value is $\chi^2_{red} = 0.408737$. Also the parameter α in this case is $\alpha = 7.06888 \text{ Kpc}$.

In Table CCXXXI we present the optimized values of K_0 and ρ_0 for the analytic SIDM model of Eq. (3) for which the maximum compatibility with the SPARC data is achieved. In Figs. 371, 372 we present

TABLE CCXXXI: SIDM Optimization Values for the galaxy UGC08837

Parameter	Optimization Values
ρ_0 (M_\odot/Kpc^3)	1.25744×10^7
K_0 ($M_\odot \text{ Kpc}^{-3} (\text{km/s})^2$)	1886.63

the density of the analytic SIDM model, the predicted rotation curves for the SIDM model (3), versus the SPARC observational data and the sound speed, as a function of the radius respectively. As it can be seen, for this galaxy, the SIDM model produces viable rotation curves which are compatible with the SPARC data.

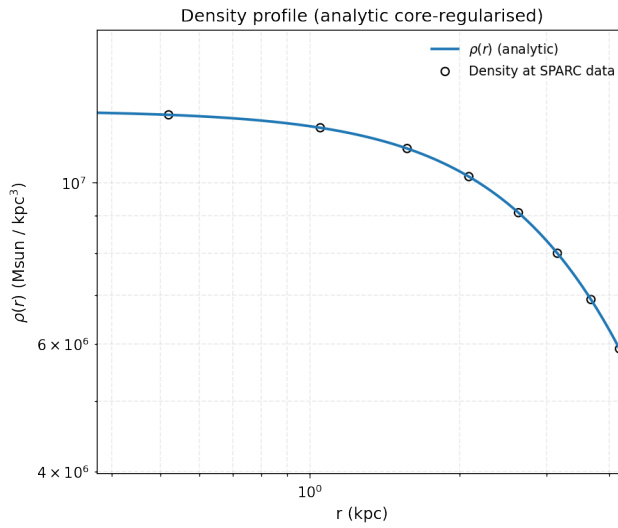


FIG. 371: The density of the SIDM model of Eq. (3) for the galaxy UGC08837, versus the radius.

130. The Galaxy UGC09037, Non-viable, Extended Viable

For this galaxy, the optimization method we used, ensures maximum compatibility of the analytic SIDM model of Eq. (3) with the SPARC data, if we choose $\rho_0 = 2.58578 \times 10^7 M_\odot/\text{Kpc}^3$ and $K_0 =$

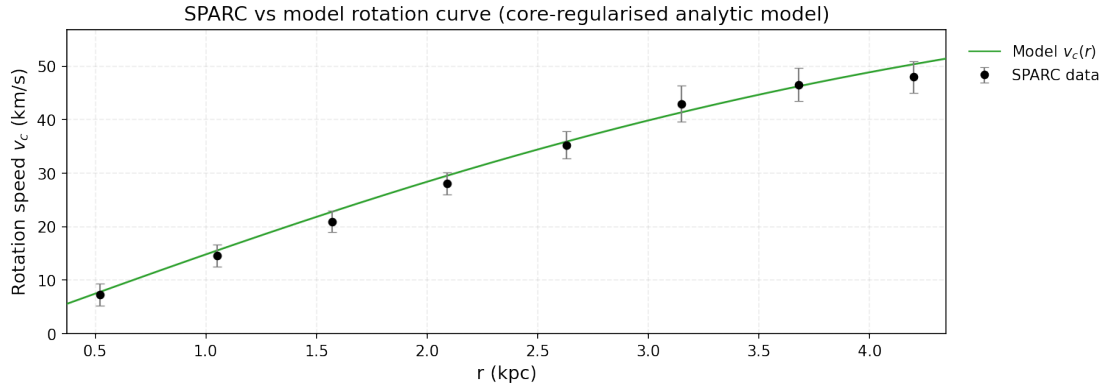


FIG. 372: The predicted rotation curves for the optimized SIDM model of Eq. (3), versus the SPARC observational data for the galaxy UGC08837.

$10243.5 M_{\odot} \text{Kpc}^{-3} (\text{km/s})^2$, in which case the reduced χ^2_{red} value is $\chi^2_{red} = 2.59911$. Also the parameter α in this case is $\alpha = 11.4863 \text{Kpc}$.

In Table CCXXXII we present the optimized values of K_0 and ρ_0 for the analytic SIDM model of Eq. (3) for which the maximum compatibility with the SPARC data is achieved. In Figs. 373, 374 we present

TABLE CCXXXII: SIDM Optimization Values for the galaxy UGC09037

Parameter	Optimization Values
$\rho_0 (M_{\odot}/\text{Kpc}^3)$	2.58578×10^7
$K_0 (M_{\odot} \text{Kpc}^{-3} (\text{km/s})^2)$	10243.5

the density of the analytic SIDM model, the predicted rotation curves for the SIDM model (3), versus the SPARC observational data and the sound speed, as a function of the radius respectively. As it can be seen, for this galaxy, the SIDM model produces non-viable rotation curves which are incompatible with the SPARC data.

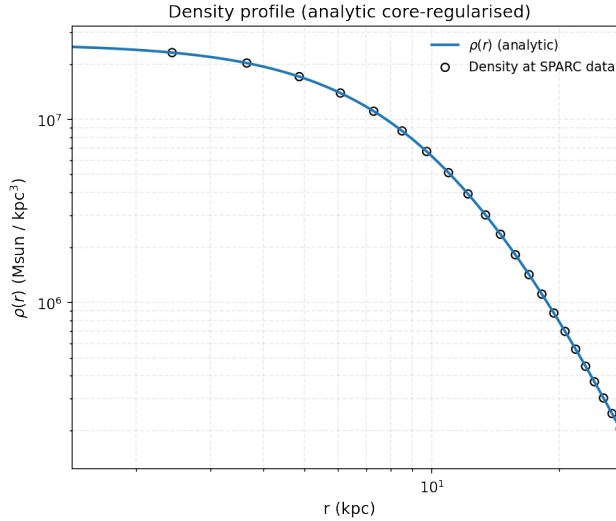


FIG. 373: The density of the SIDM model of Eq. (3) for the galaxy UGC09037, versus the radius.

Now we shall include contributions to the rotation velocity from the other components of the galaxy, namely the disk, the gas, and the bulge if present. In Fig. 375 we present the combined rotation curves including all the components of the galaxy along with the SIDM. As it can be seen, the extended collisional DM model is viable. Also in Table CCXXXIII we present the optimized values of the free parameters of the SIDM model for which we achieve the maximum compatibility with the SPARC data, for the galaxy UGC09037, and also the resulting reduced χ^2_{red} value.

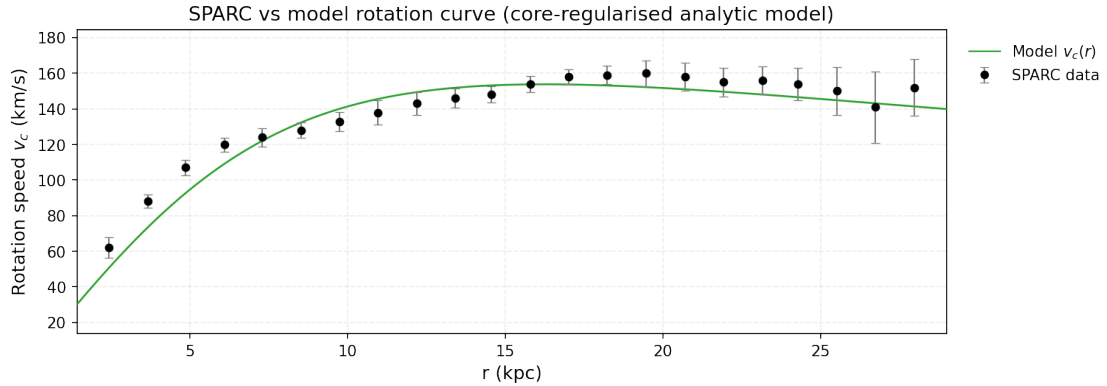


FIG. 374: The predicted rotation curves for the optimized SIDM model of Eq. (3), versus the SPARC observational data for the galaxy UGC09037.

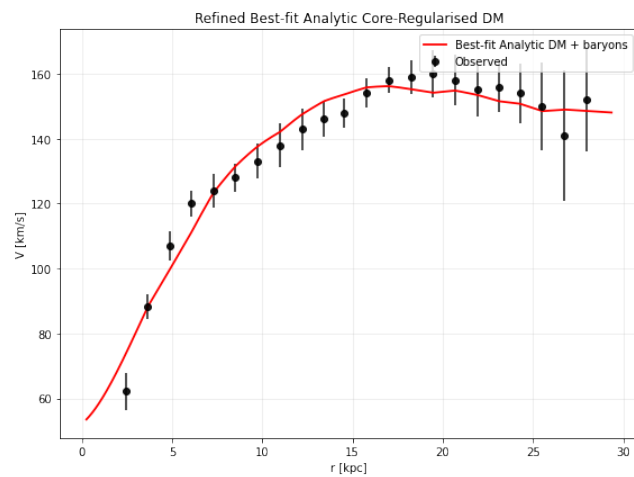


FIG. 375: The predicted rotation curves after using an optimization for the SIDM model (3), and the extended SPARC data for the galaxy UGC09037. We included the rotation curves of the gas, the disk velocities, the bulge (where present) along with the SIDM model.

TABLE CCXXXIII: Optimized Parameter Values of the Extended SIDM model for the Galaxy UGC09037.

Parameter	Value
$\rho_0 (M_\odot/\text{Kpc}^3)$	1.37733×10^7
$K_0 (M_\odot \text{ Kpc}^{-3} (\text{km/s})^2)$	7327.13
ml_{disk}	0.4595
ml_{bulge}	0.5412
$\alpha (\text{Kpc})$	13.309
χ^2_{red}	1.05996

131. The Galaxy UGC09133, Non-viable

For this galaxy, the optimization method we used, ensures maximum compatibility of the analytic SIDM model of Eq. (3) with the SPARC data, if we choose $\rho_0 = 2.56523 \times 10^7 M_\odot/\text{Kpc}^3$ and $K_0 = 36142.8 M_\odot \text{ Kpc}^{-3} (\text{km/s})^2$, in which case the reduced χ^2_{red} value is $\chi^2_{\text{red}} = 829.59$. Also the parameter α in this case is $\alpha = 21.662 \text{ Kpc}$.

In Table CCXXXIV we present the optimized values of K_0 and ρ_0 for the analytic SIDM model of Eq. (3) for which the maximum compatibility with the SPARC data is achieved. In Figs. 376, 377 we present the density of the analytic SIDM model, the predicted rotation curves for the SIDM model (3), versus the SPARC observational data and the sound speed, as a function of the radius respectively. As it can be seen, for this galaxy, the SIDM model produces non-viable rotation curves which are incompatible with the SPARC data.

TABLE CCXXXIV: SIDM Optimization Values for the galaxy UGC09133

Parameter	Optimization Values
$\rho_0 (M_\odot/\text{Kpc}^3)$	2.56523×10^7
$K_0 (M_\odot \text{ Kpc}^{-3} (\text{km/s})^2)$	36142.8

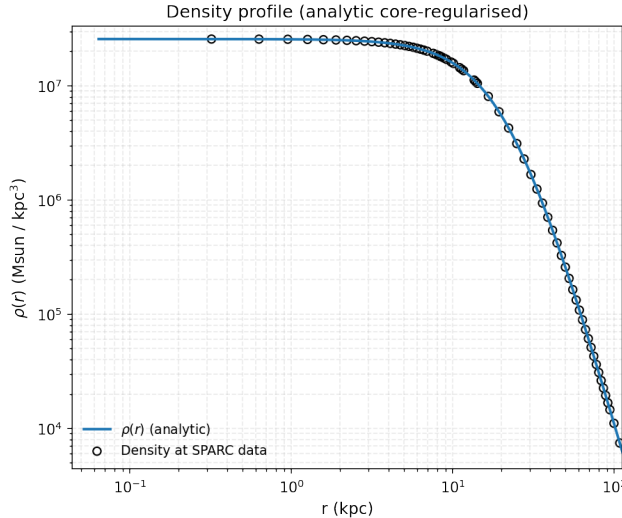


FIG. 376: The density of the SIDM model of Eq. (3) for the galaxy UGC09133, versus the radius.

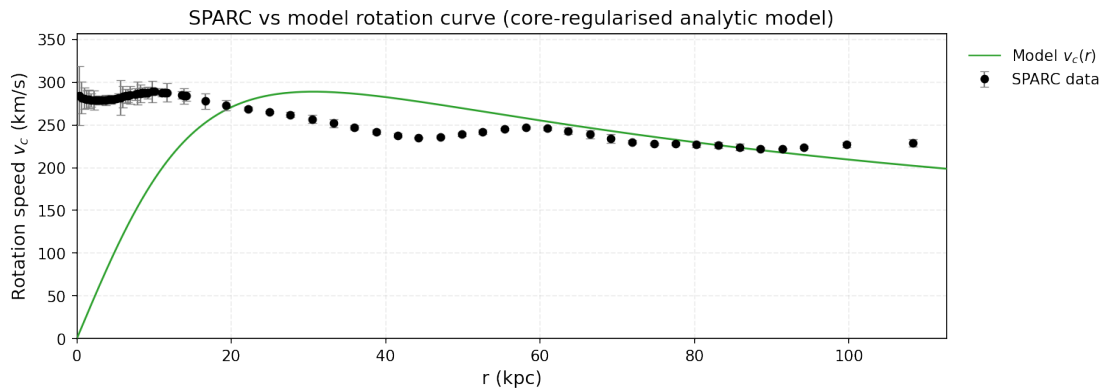


FIG. 377: The predicted rotation curves for the optimized SIDM model of Eq. (3), versus the SPARC observational data for the galaxy UGC09133.

Now we shall include contributions to the rotation velocity from the other components of the galaxy, namely the disk, the gas, and the bulge if present. In Fig. 378 we present the combined rotation curves including all the components of the galaxy along with the SIDM. As it can be seen, the extended collisional DM model is non-viable. Also in Table CCXXXV we present the optimized values of the free parameters of the SIDM model for which we achieve the maximum compatibility with the SPARC data, for the galaxy UGC09133, and also the resulting reduced χ^2_{red} value.

TABLE CCXXXV: Optimized Parameter Values of the Extended SIDM model for the Galaxy UGC09133.

Parameter	Value
$\rho_0 (M_\odot/\text{Kpc}^3)$	1.90461×10^6
$K_0 (M_\odot \text{ Kpc}^{-3} (\text{km/s})^2)$	15594.2
ml_{disk}	1
ml_{bulge}	0.7274
$\alpha (\text{Kpc})$	52.2126
χ^2_{red}	9.34344

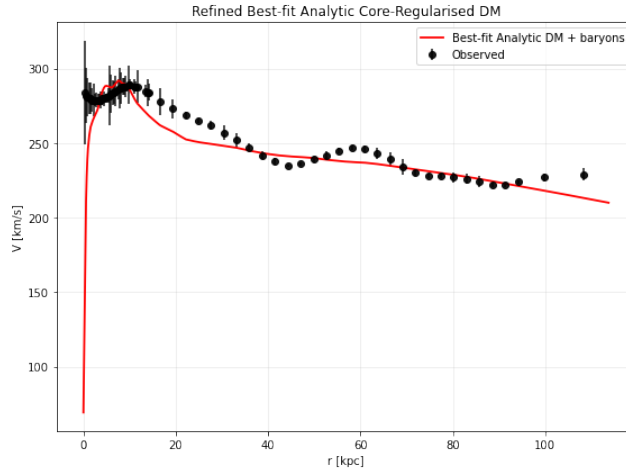


FIG. 378: The predicted rotation curves after using an optimization for the SIDM model (3), and the extended SPARC data for the galaxy UGC09133. We included the rotation curves of the gas, the disk velocities, the bulge (where present) along with the SIDM model.

132. The Galaxy UGC09992

For this galaxy, the optimization method we used, ensures maximum compatibility of the analytic SIDM model of Eq. (3) with the SPARC data, if we choose $\rho_0 = 1.31564 \times 10^8 M_\odot/\text{Kpc}^3$ and $K_0 = 575.789 M_\odot \text{Kpc}^{-3} (\text{km/s})^2$, in which case the reduced χ^2_{red} value is $\chi^2_{\text{red}} = 0.484757$. Also the parameter α in this case is $\alpha = 1.2073 \text{Kpc}$.

In Table CCXXXVI we present the optimized values of K_0 and ρ_0 for the analytic SIDM model of Eq. (3) for which the maximum compatibility with the SPARC data is achieved. In Figs. 379, 380 we

TABLE CCXXXVI: SIDM Optimization Values for the galaxy UGC09992

Parameter	Optimization Values
$\rho_0 (M_\odot/\text{Kpc}^3)$	1.31564×10^8
$K_0 (M_\odot \text{Kpc}^{-3} (\text{km/s})^2)$	575.789

present the density of the analytic SIDM model, the predicted rotation curves for the SIDM model (3), versus the SPARC observational data and the sound speed, as a function of the radius respectively. As it can be seen, for this galaxy, the SIDM model produces viable rotation curves which are compatible with the SPARC data.

133. The Galaxy UGC10310

For this galaxy, the optimization method we used, ensures maximum compatibility of the analytic SIDM model of Eq. (3) with the SPARC data, if we choose $\rho_0 = 5.77999 \times 10^7 M_\odot/\text{Kpc}^3$ and $K_0 = 2353.19 M_\odot \text{Kpc}^{-3} (\text{km/s})^2$, in which case the reduced χ^2_{red} value is $\chi^2_{\text{red}} = 0.33138$. Also the parameter α in this case is $\alpha = 3.6822 \text{Kpc}$.

In Table CCXXXVII we present the optimized values of K_0 and ρ_0 for the analytic SIDM model of Eq. (3) for which the maximum compatibility with the SPARC data is achieved. In Figs. 381, 382 we

TABLE CCXXXVII: SIDM Optimization Values for the galaxy UGC10310

Parameter	Optimization Values
$\rho_0 (M_\odot/\text{Kpc}^3)$	5.77999×10^7
$K_0 (M_\odot \text{Kpc}^{-3} (\text{km/s})^2)$	2353.19

present the density of the analytic SIDM model, the predicted rotation curves for the SIDM model (3), versus the SPARC observational data and the sound speed, as a function of the radius respectively. As

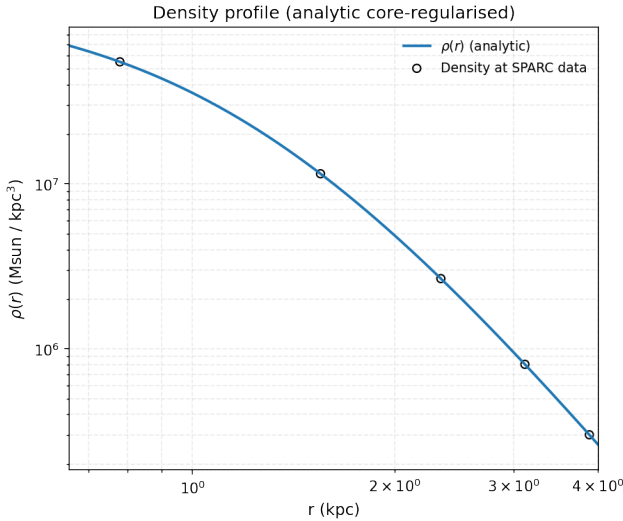


FIG. 379: The density of the SIDM model of Eq. (3) for the galaxy UGC09992, versus the radius.

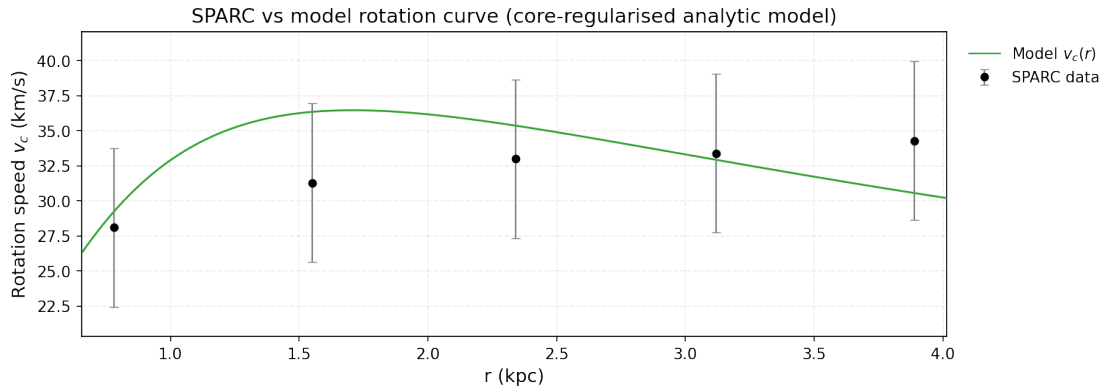


FIG. 380: The predicted rotation curves for the optimized SIDM model of Eq. (3), versus the SPARC observational data for the galaxy UGC09992.

it can be seen, for this galaxy, the SIDM model produces viable rotation curves which are compatible with the SPARC data.

134. The Galaxy UGC11455, Non-viable

For this galaxy, the optimization method we used, ensures maximum compatibility of the analytic SIDM model of Eq. (3) with the SPARC data, if we choose $\rho_0 = 7.79297 \times 10^7 M_\odot / \text{Kpc}^3$ and $K_0 = 37694.7 M_\odot \text{ Kpc}^{-3} (\text{km/s})^2$, in which case the reduced χ^2_{red} value is $\chi^2_{\text{red}} = 3.84583$. Also the parameter α in this case is $\alpha = 12.6923 \text{ Kpc}$.

In Table CCXXXVIII we present the optimized values of K_0 and ρ_0 for the analytic SIDM model of Eq. (3) for which the maximum compatibility with the SPARC data is achieved. In Figs. 383, 384 we

TABLE CCXXXVIII: SIDM Optimization Values for the galaxy UGC11455

Parameter	Optimization Values
$\rho_0 (M_\odot / \text{Kpc}^3)$	7.79297×10^7
$K_0 (M_\odot \text{ Kpc}^{-3} (\text{km/s})^2)$	37694.7

present the density of the analytic SIDM model, the predicted rotation curves for the SIDM model (3), versus the SPARC observational data and the sound speed, as a function of the radius respectively. As it

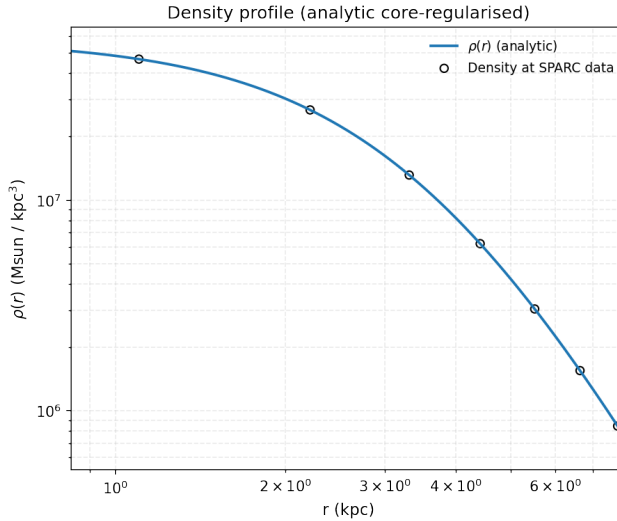


FIG. 381: The density of the SIDM model of Eq. (3) for the galaxy UGC10310, versus the radius.

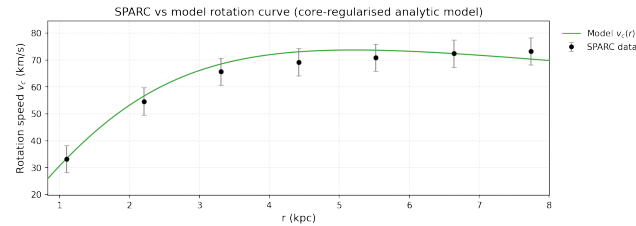


FIG. 382: The predicted rotation curves for the optimized SIDM model of Eq. (3), versus the SPARC observational data for the galaxy UGC10310.

can be seen, for this galaxy, the SIDM model produces non-viable rotation curves which are incompatible with the SPARC data.

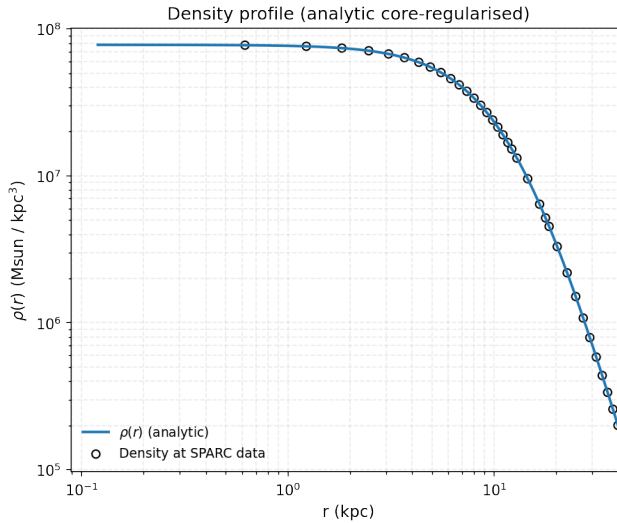


FIG. 383: The density of the SIDM model of Eq. (3) for the galaxy UGC11455, versus the radius.

Now we shall include contributions to the rotation velocity from the other components of the galaxy, namely the disk, the gas, and the bulge if present. In Fig. 385 we present the combined rotation curves including all the components of the galaxy along with the SIDM. As it can be seen, the extended collisional DM model is non-viable. Also in Table CCXXXIX we present the optimized values of the free

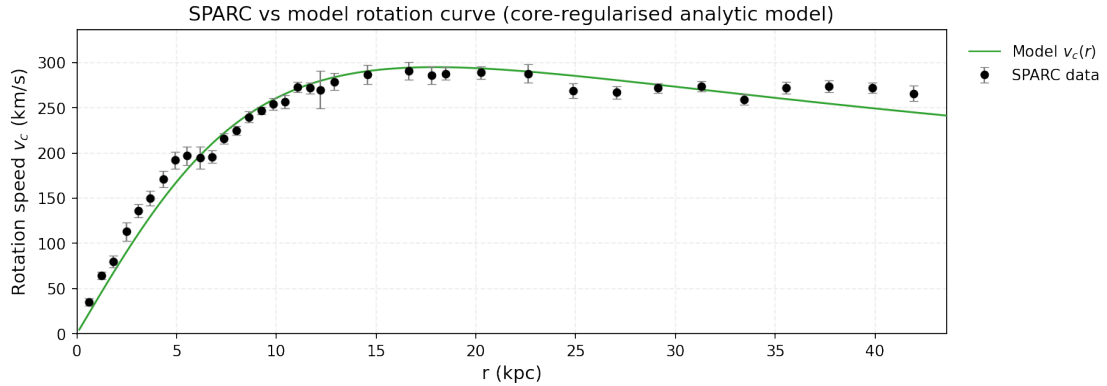


FIG. 384: The predicted rotation curves for the optimized SIDM model of Eq. (3), versus the SPARC observational data for the galaxy UGC11455.

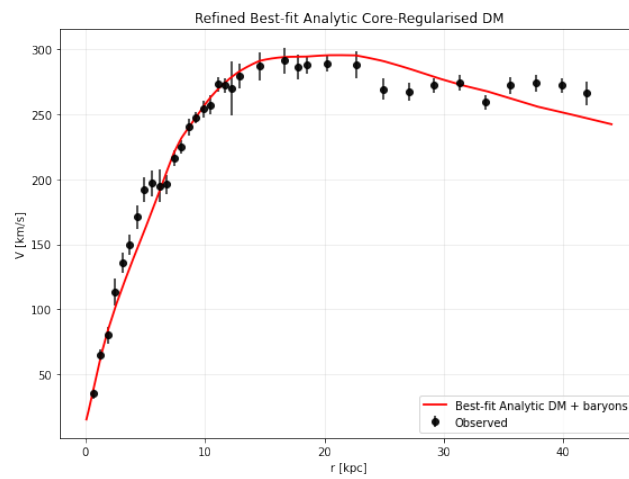


FIG. 385: The predicted rotation curves after using an optimization for the SIDM model (3), and the extended SPARC data for the galaxy UGC11455. We included the rotation curves of the gas, the disk velocities, the bulge (where present) along with the SIDM model.

parameters of the SIDM model for which we achieve the maximum compatibility with the SPARC data, for the galaxy UGC11455, and also the resulting reduced χ^2_{red} value.

TABLE CCXXXIX: Optimized Parameter Values of the Extended SIDM model for the Galaxy UGC11455.

Parameter	Value
ρ_0 (M_\odot/Kpc^3)	4.73819×10^7
K_0 ($M_\odot \text{ Kpc}^{-3} (\text{km/s})^2$)	28755
ml_{disk}	0.4580
ml_{bulge}	0.5154
α (Kpc)	14.215
χ^2_{red}	2.87458

135. The Galaxy UGC11557

For this galaxy, the optimization method we used, ensures maximum compatibility of the analytic SIDM model of Eq. (3) with the SPARC data, if we choose $\rho_0 = 2.88776 \times 10^7 M_\odot/\text{Kpc}^3$ and $K_0 = 3089.47 M_\odot \text{ Kpc}^{-3} (\text{km/s})^2$, in which case the reduced χ^2_{red} value is $\chi^2_{red} = 0.423089$. Also the parameter α in this case is $\alpha = 6.85794 \text{ Kpc}$.

In Table CCXL we present the optimized values of K_0 and ρ_0 for the analytic SIDM model of Eq. (3) for which the maximum compatibility with the SPARC data is achieved. In Figs. 386, 387 we present

TABLE CCXL: SIDM Optimization Values for the galaxy UGC11557

Parameter	Optimization Values
$\rho_0 (M_\odot/\text{Kpc}^3)$	2.88776×10^7
$K_0 (M_\odot \text{ Kpc}^{-3} (\text{km/s})^2)$	3089.47

the density of the analytic SIDM model, the predicted rotation curves for the SIDM model (3), versus the SPARC observational data and the sound speed, as a function of the radius respectively. As it can be seen, for this galaxy, the SIDM model produces viable rotation curves which are compatible with the SPARC data.

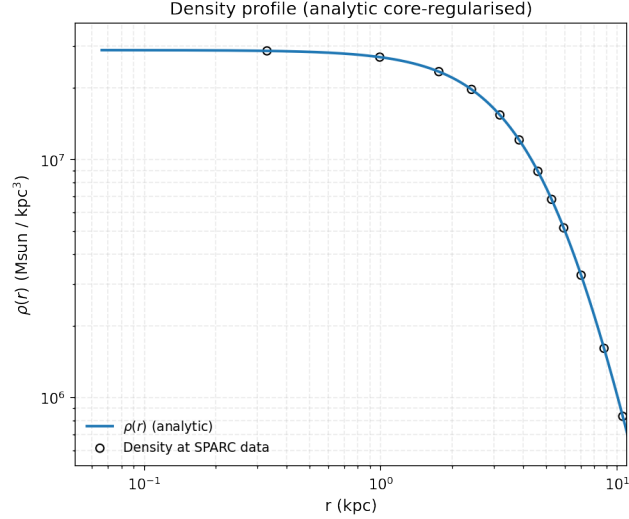


FIG. 386: The density of the SIDM model of Eq. (3) for the galaxy UGC11557, versus the radius.

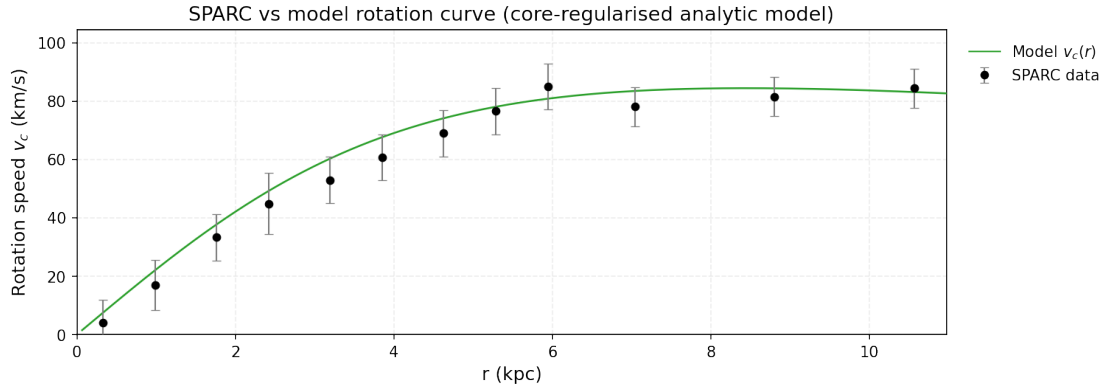


FIG. 387: The predicted rotation curves for the optimized SIDM model of Eq. (3), versus the SPARC observational data for the galaxy UGC11557.

136. The Galaxy UGC11820, Non-viable

For this galaxy, the optimization method we used, ensures maximum compatibility of the analytic SIDM model of Eq. (3) with the SPARC data, if we choose $\rho_0 = 9.84877 \times 10^7 M_\odot/\text{Kpc}^3$ and $K_0 = 3474.48 M_\odot \text{ Kpc}^{-3} (\text{km/s})^2$, in which case the reduced χ^2_{red} value is $\chi^2_{red} = 188.997$. Also the parameter α in this case is $\alpha = 3.42772 \text{ Kpc}$.

In Table CCXLI we present the optimized values of K_0 and ρ_0 for the analytic SIDM model of Eq. (3) for which the maximum compatibility with the SPARC data is achieved. In Figs. 388, 389 we present

TABLE CCXLI: SIDM Optimization Values for the galaxy UGC11820

Parameter	Optimization Values
$\rho_0 (M_\odot/\text{Kpc}^3)$	5×10^7
$K_0 (M_\odot \text{ Kpc}^{-3} (\text{km/s})^2)$	1250

the density of the analytic SIDM model, the predicted rotation curves for the SIDM model (3), versus the SPARC observational data and the sound speed, as a function of the radius respectively. As it can be seen, for this galaxy, the SIDM model produces non-viable rotation curves which are incompatible with the SPARC data.

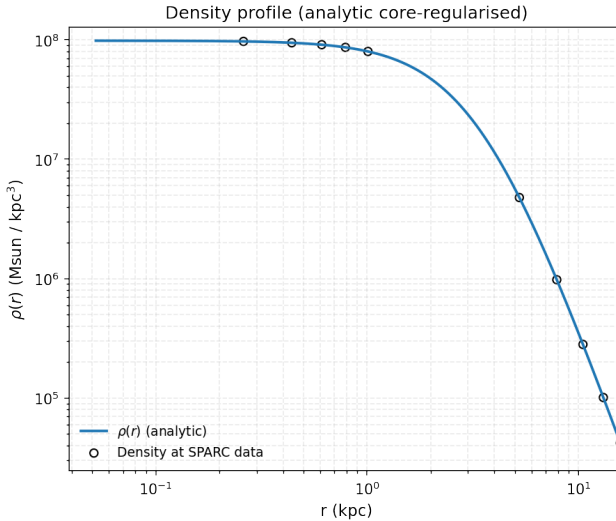


FIG. 388: The density of the SIDM model of Eq. (3) for the galaxy UGC11820, versus the radius.

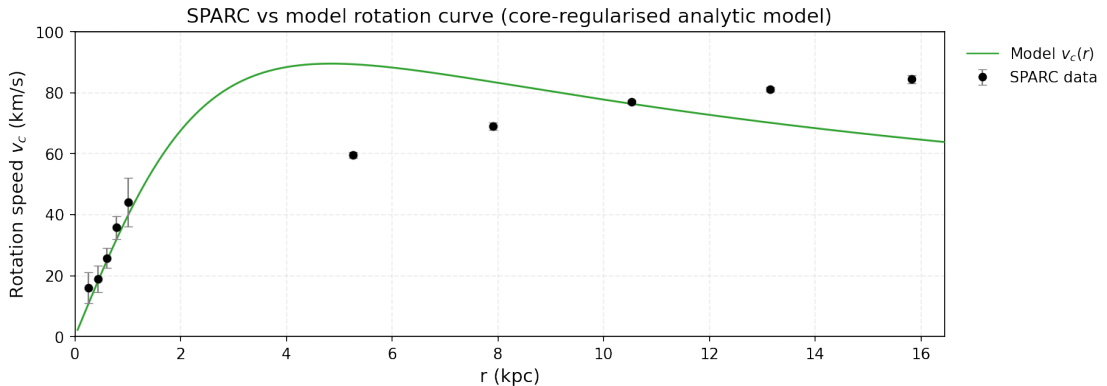


FIG. 389: The predicted rotation curves for the optimized SIDM model of Eq. (3), versus the SPARC observational data for the galaxy UGC11820.

Now we shall include contributions to the rotation velocity from the other components of the galaxy, namely the disk, the gas, and the bulge if present. In Fig. 390 we present the combined rotation curves including all the components of the galaxy along with the SIDM. As it can be seen, the extended collisional DM model is non-viable. Also in Table CCXLII we present the optimized values of the free parameters of the SIDM model for which we achieve the maximum compatibility with the SPARC data, for the galaxy UGC11820, and also the resulting reduced χ^2_{red} value.

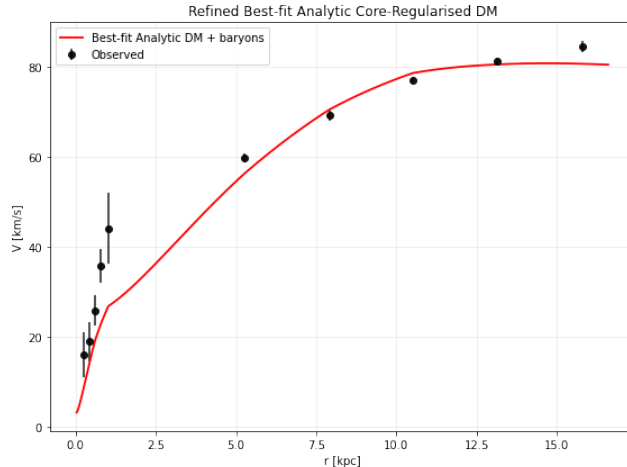


FIG. 390: The predicted rotation curves after using an optimization for the SIDM model (3), and the extended SPARC data for the galaxy UGC11820. We included the rotation curves of the gas, the disk velocities, the bulge (where present) along with the SIDM model.

TABLE CCXLII: Optimized Parameter Values of the Extended SIDM model for the Galaxy UGC11820.

Parameter	Value
$\rho_0 (M_\odot/\text{Kpc}^3)$	5.88535×10^6
$K_0 (M_\odot \text{ Kpc}^{-3} (\text{km/s})^2)$	2149.24
ml_{disk}	1
ml_{bulge}	0.2255
$\alpha (\text{Kpc})$	11.0269
χ^2_{red}	9.15937

137. The Galaxy UGC11914, Non-viable

For this galaxy, the optimization method we used, ensures maximum compatibility of the analytic SIDM model of Eq. (3) with the SPARC data, if we choose $\rho_0 = 3.80519 \times 10^9 M_\odot/\text{Kpc}^3$ and $K_0 = 44161.3 M_\odot \text{ Kpc}^{-3} (\text{km/s})^2$, in which case the reduced χ^2_{red} value is $\chi^2_{\text{red}} = 54.7408$. Also the parameter α in this case is $\alpha = 1.966 \text{ Kpc}$.

In Table CCXLIII we present the optimized values of K_0 and ρ_0 for the analytic SIDM model of Eq. (3) for which the maximum compatibility with the SPARC data is achieved. In Figs. 391, 392 we present

TABLE CCXLIII: SIDM Optimization Values for the galaxy UGC11914

Parameter	Optimization Values
$\rho_0 (M_\odot/\text{Kpc}^3)$	3.80519×10^9
$K_0 (M_\odot \text{ Kpc}^{-3} (\text{km/s})^2)$	44161.3

the density of the analytic SIDM model, the predicted rotation curves for the SIDM model (3), versus the SPARC observational data and the sound speed, as a function of the radius respectively. As it can be seen, for this galaxy, the SIDM model produces non-viable rotation curves which are incompatible with the SPARC data.

Now we shall include contributions to the rotation velocity from the other components of the galaxy, namely the disk, the gas, and the bulge if present. In Fig. 393 we present the combined rotation curves including all the components of the galaxy along with the SIDM. As it can be seen, the extended collisional DM model is non-viable. Also in Table CCXLIV we present the optimized values of the free parameters of the SIDM model for which we achieve the maximum compatibility with the SPARC data, for the galaxy UGC11914, and also the resulting reduced χ^2_{red} value.

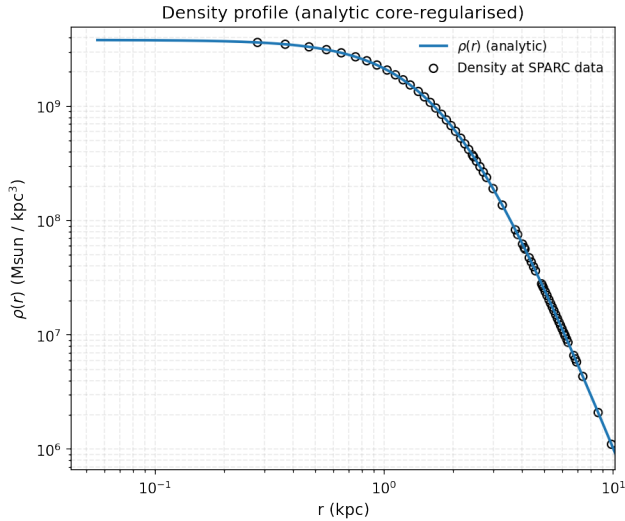


FIG. 391: The density of the SIDM model of Eq. (3) for the galaxy UGC11914, versus the radius.

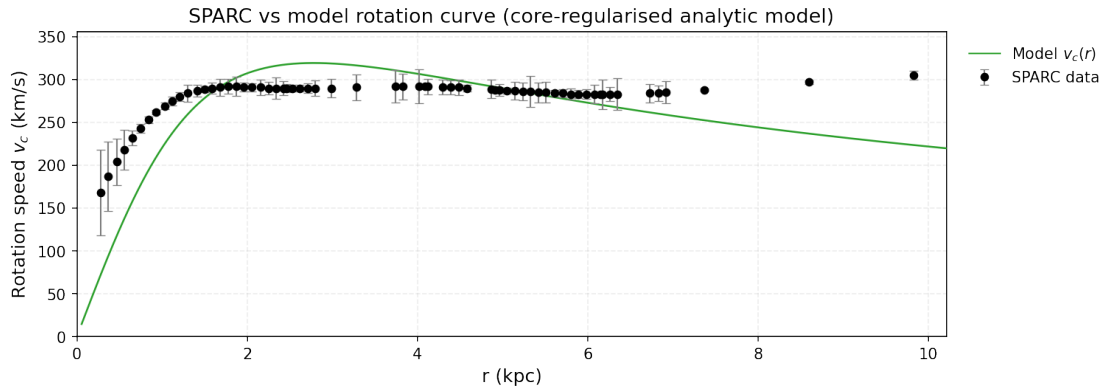


FIG. 392: The predicted rotation curves for the optimized SIDM model of Eq. (3), versus the SPARC observational data for the galaxy UGC11914.

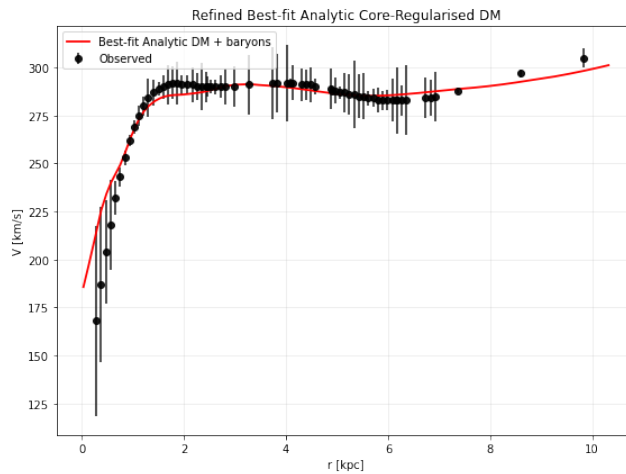


FIG. 393: The predicted rotation curves after using an optimization for the SIDM model (3), and the extended SPARC data for the galaxy UGC11914. We included the rotation curves of the gas, the disk velocities, the bulge (where present) along with the SIDM model.

TABLE CCXLIV: Optimized Parameter Values of the Extended SIDM model for the Galaxy UGC11914.

Parameter	Value
$\rho_0 (M_\odot/\text{Kpc}^3)$	2.37289×10^7
$K_0 (M_\odot \text{ Kpc}^{-3} (\text{km/s})^2)$	125459
ml_{disk}	0.7914
ml_{bulge}	1
$\alpha (\text{Kpc})$	118.456
χ^2_{red}	0.527133

138. The Galaxy UGC12506, Non-viable

For this galaxy, the optimization method we used, ensures maximum compatibility of the analytic SIDM model of Eq. (3) with the SPARC data, if we choose $\rho_0 = 6.11517 \times 10^7 M_\odot/\text{Kpc}^3$ and $K_0 = 30315.4 M_\odot \text{ Kpc}^{-3} (\text{km/s})^2$, in which case the reduced χ^2_{red} value is $\chi^2_{\text{red}} = 2.65417$. Also the parameter α in this case is $\alpha = 12.8492 \text{ Kpc}$.

In Table CCXLV we present the optimized values of K_0 and ρ_0 for the analytic SIDM model of Eq. (3) for which the maximum compatibility with the SPARC data is achieved. In Figs. 394, 395 we present

TABLE CCXLV: SIDM Optimization Values for the galaxy UGC12506

Parameter	Optimization Values
$\rho_0 (M_\odot/\text{Kpc}^3)$	6.11517×10^7
$K_0 (M_\odot \text{ Kpc}^{-3} (\text{km/s})^2)$	30315.4

the density of the analytic SIDM model, the predicted rotation curves for the SIDM model (3), versus the SPARC observational data and the sound speed, as a function of the radius respectively. As it can be seen, for this galaxy, the SIDM model produces non-viable rotation curves which are incompatible with the SPARC data.

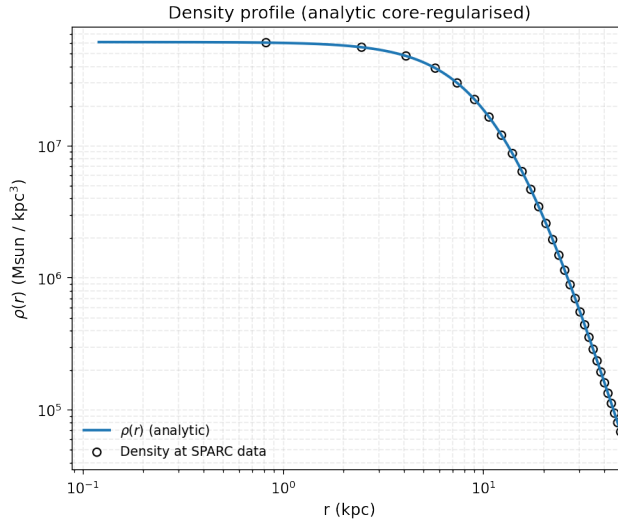


FIG. 394: The density of the SIDM model of Eq. (3) for the galaxy UGC12506, versus the radius.

Now we shall include contributions to the rotation velocity from the other components of the galaxy, namely the disk, the gas, and the bulge if present. In Fig. 396 we present the combined rotation curves including all the components of the galaxy along with the SIDM. As it can be seen, the extended collisional DM model is non-viable. Also in Table CCXLVI we present the optimized values of the free parameters of the SIDM model for which we achieve the maximum compatibility with the SPARC data, for the galaxy UGC12506, and also the resulting reduced χ^2_{red} value.

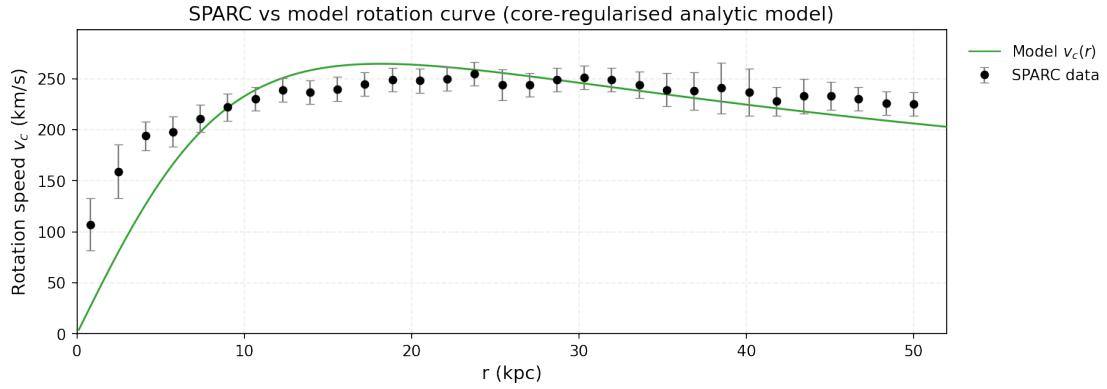


FIG. 395: The predicted rotation curves for the optimized SIDM model of Eq. (3), versus the SPARC observational data for the galaxy UGC12506.

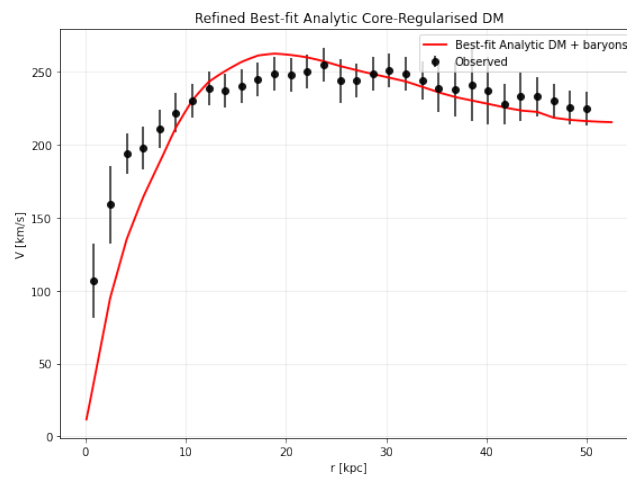


FIG. 396: The predicted rotation curves after using an optimization for the SIDM model (3), and the extended SPARC data for the galaxy UGC12506. We included the rotation curves of the gas, the disk velocities, the bulge (where present) along with the SIDM model.

TABLE CCXLVI: Optimized Parameter Values of the Extended SIDM model for the Galaxy UGC12506.

Parameter	Value
$\rho_0 (M_\odot/\text{Kpc}^3)$	2.08225×10^7
$K_0 (M_\odot \text{ Kpc}^{-3} (\text{km/s})^2)$	15949.2
ml_{disk}	1
ml_{bulge}	1
$\alpha (\text{Kpc})$	15.9698
χ^2_{red}	2.0016

139. The Galaxy UGC12632

For this galaxy, the optimization method we used, ensures maximum compatibility of the analytic SIDM model of Eq. (3) with the SPARC data, if we choose $\rho_0 = 2.59734 \times 10^7 M_\odot/\text{Kpc}^3$ and $K_0 = 2234.72 M_\odot \text{ Kpc}^{-3} (\text{km/s})^2$, in which case the reduced χ^2_{red} value is $\chi^2_{\text{red}} = 0.984724$. Also the parameter α in this case is $\alpha = 5.35301 \text{ Kpc}$.

In Table CCXLVII we present the optimized values of K_0 and ρ_0 for the analytic SIDM model of Eq. (3) for which the maximum compatibility with the SPARC data is achieved. In Figs. 397, 398 we present the density of the analytic SIDM model, the predicted rotation curves for the SIDM model (3), versus the SPARC observational data and the sound speed, as a function of the radius respectively. As it can be seen, for this galaxy, the SIDM model produces viable rotation curves which are compatible with the SPARC data.

TABLE CCXLVII: SIDM Optimization Values for the galaxy UGC12632

Parameter	Optimization Values
$\rho_0 (M_\odot/\text{Kpc}^3)$	2.59734×10^7
$K_0 (M_\odot \text{ Kpc}^{-3} (\text{km/s})^2)$	2234.72

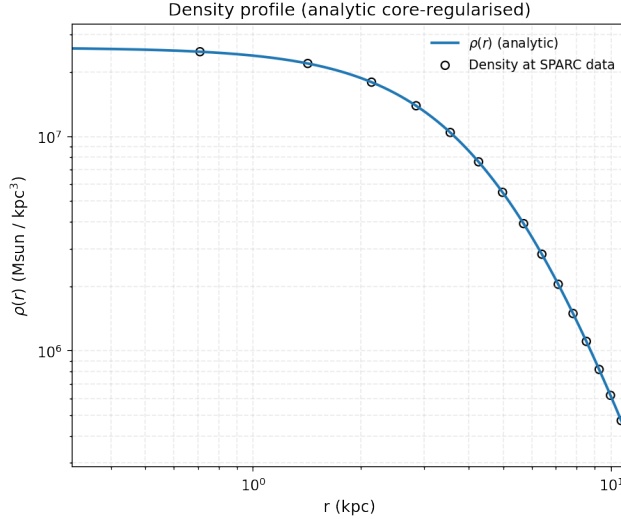


FIG. 397: The density of the SIDM model of Eq. (3) for the galaxy UGC12632, versus the radius.

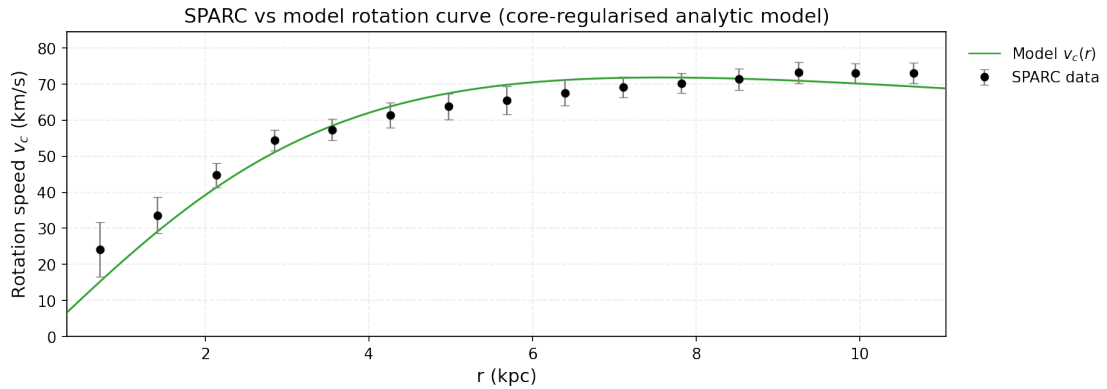


FIG. 398: The predicted rotation curves for the optimized SIDM model of Eq. (3), versus the SPARC observational data for the galaxy UGC12632.

140. The Galaxy UGC12732, Non-viable

For this galaxy, the optimization method we used, ensures maximum compatibility of the analytic SIDM model of Eq. (3) with the SPARC data, if we choose $\rho_0 = 1.98779 \times 10^7 M_\odot/\text{Kpc}^3$ and $K_0 = 3344.88 M_\odot \text{ Kpc}^{-3} (\text{km/s})^2$, in which case the reduced χ^2_{red} value is $\chi^2_{\text{red}} = 6.14551$. Also the parameter α in this case is $\alpha = 7.48609 \text{ Kpc}$.

In Table CCXLVIII we present the optimized values of K_0 and ρ_0 for the analytic SIDM model of Eq. (3) for which the maximum compatibility with the SPARC data is achieved. In Figs. 399, 400 we present

TABLE CCXLVIII: SIDM Optimization Values for the galaxy UGC12732

Parameter	Optimization Values
$\rho_0 (M_\odot/\text{Kpc}^3)$	1.98779×10^7
$K_0 (M_\odot \text{ Kpc}^{-3} (\text{km/s})^2)$	3344.88

the density of the analytic SIDM model, the predicted rotation curves for the SIDM model (3), versus the SPARC observational data and the sound speed, as a function of the radius respectively. As it can be seen, for this galaxy, the SIDM model produces non-viable rotation curves which are incompatible with the SPARC data.

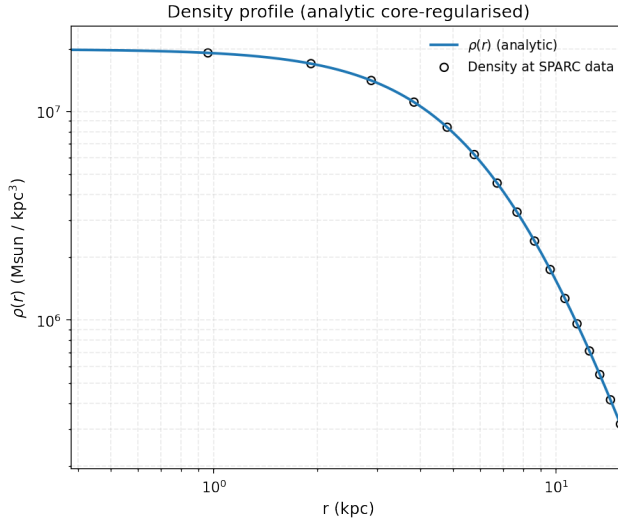


FIG. 399: The density of the SIDM model of Eq. (3) for the galaxy UGC12732, versus the radius.

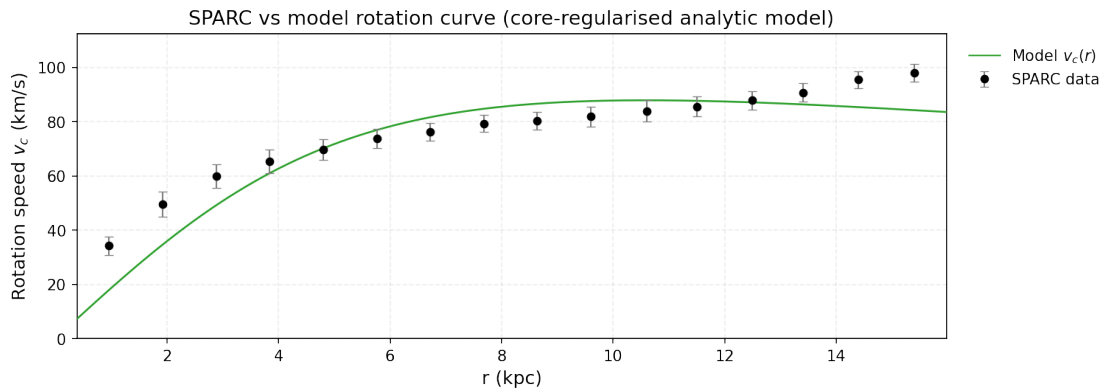


FIG. 400: The predicted rotation curves for the optimized SIDM model of Eq. (3), versus the SPARC observational data for the galaxy UGC12732.

Now we shall include contributions to the rotation velocity from the other components of the galaxy, namely the disk, the gas, and the bulge if present. In Fig. 401 we present the combined rotation curves including all the components of the galaxy along with the SIDM. As it can be seen, the extended collisional DM model is non-viable. Also in Table CCXLIX we present the optimized values of the free parameters of the SIDM model for which we achieve the maximum compatibility with the SPARC data, for the galaxy UGC12732, and also the resulting reduced χ^2_{red} value.

TABLE CCXLIX: Optimized Parameter Values of the Extended SIDM model for the Galaxy UGC12732.

Parameter	Value
ρ_0 (M_\odot / Kpc^3)	1.18726×10^7
K_0 ($M_\odot \text{ Kpc}^{-3} (\text{km/s})^2$)	2646.01
ml_{disk}	1
ml_{bulge}	0.5865
α (Kpc)	8.61428
χ^2_{red}	2.38378

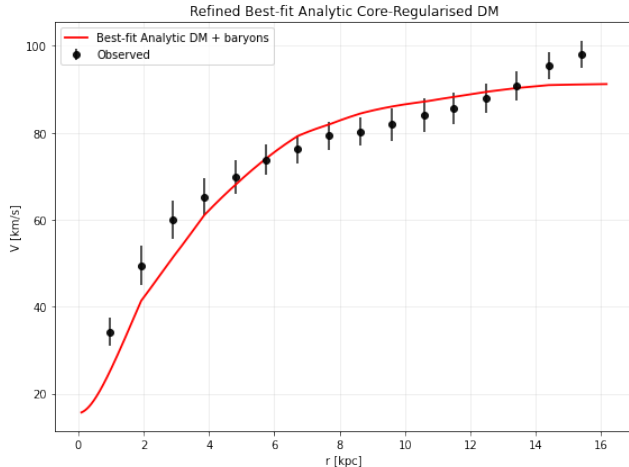


FIG. 401: The predicted rotation curves after using an optimization for the SIDM model (3), and the extended SPARC data for the galaxy UGC12732. We included the rotation curves of the gas, the disk velocities, the bulge (where present) along with the SIDM model.

141. The Galaxy UGCA442

For this galaxy, the optimization method we used, ensures maximum compatibility of the analytic SIDM model of Eq. (3) with the SPARC data, if we choose $\rho_0 = 3.53164 \times 10^7 M_\odot/\text{Kpc}^3$ and $K_0 = 1389.69 M_\odot \text{Kpc}^{-3} (\text{km/s})^2$, in which case the reduced χ^2_{red} value is $\chi^2_{red} = 1.16858$. Also the parameter α in this case is $\alpha = 3.6201 \text{Kpc}$.

In Table CCL we present the optimized values of K_0 and ρ_0 for the analytic SIDM model of Eq. (3) for which the maximum compatibility with the SPARC data is achieved. In Figs. 402, 403 we present

TABLE CCL: SIDM Optimization Values for the galaxy UGCA442

Parameter	Optimization Values
$\rho_0 (M_\odot/\text{Kpc}^3)$	3.53164×10^7
$K_0 (M_\odot \text{Kpc}^{-3} (\text{km/s})^2)$	1389.69

the density of the analytic SIDM model, the predicted rotation curves for the SIDM model (3), versus the SPARC observational data and the sound speed, as a function of the radius respectively. As it can be seen, for this galaxy, the SIDM model produces viable rotation curves which are compatible with the SPARC data.

142. The Galaxy UGCA444

For this galaxy, the optimization method we used, ensures maximum compatibility of the analytic SIDM model of Eq. (3) with the SPARC data, if we choose $\rho_0 = 5.91282 \times 10^7 M_\odot/\text{Kpc}^3$ and $K_0 = 446.298 M_\odot \text{Kpc}^{-3} (\text{km/s})^2$, in which case the reduced χ^2_{red} value is $\chi^2_{red} = 0.35789$. Also the parameter α in this case is $\alpha = 1.5855 \text{Kpc}$.

In Table CCLI we present the optimized values of K_0 and ρ_0 for the analytic SIDM model of Eq. (3) for which the maximum compatibility with the SPARC data is achieved. In Figs. 404, 405 we present

TABLE CCLI: SIDM Optimization Values for the galaxy UGCA444

Parameter	Optimization Values
$\rho_0 (M_\odot/\text{Kpc}^3)$	5.91282×10^7
$K_0 (M_\odot \text{Kpc}^{-3} (\text{km/s})^2)$	446.298

the density of the analytic SIDM model, the predicted rotation curves for the SIDM model (3), versus the SPARC observational data and the sound speed, as a function of the radius respectively. As it can

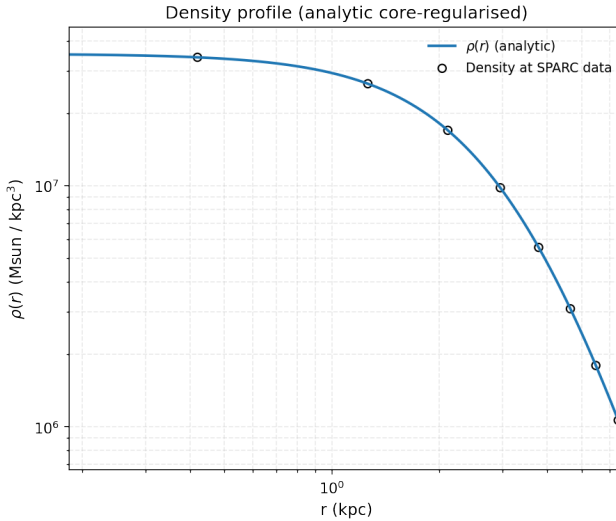


FIG. 402: The density of the SIDM model of Eq. (3) for the galaxy UGCA442, versus the radius.

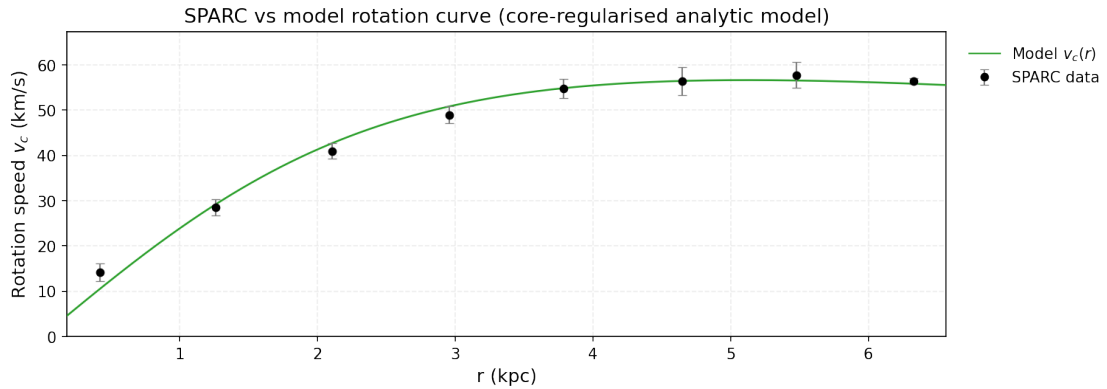


FIG. 403: The predicted rotation curves for the optimized SIDM model of Eq. (3), versus the SPARC observational data for the galaxy UGCA442.

be seen, for this galaxy, the SIDM model produces viable rotation curves which are compatible with the SPARC data.

143. The Galaxy F561-1

For this galaxy, the optimization method we used, ensures maximum compatibility of the analytic SIDM model of Eq. (3) with the SPARC data, if we choose $\rho_0 = 1.19454 \times 10^7 M_\odot / \text{Kpc}^3$ and $K_0 = 943.258 M_\odot \text{ Kpc}^{-3} (\text{km/s})^2$, in which case the reduced χ^2_{red} value is $\chi^2_{\text{red}} = 0.631898$. Also the parameter α in this case is $\alpha = 5.12822 \text{ Kpc}$.

In Table CCLII we present the optimized values of K_0 and ρ_0 for the analytic SIDM model of Eq. (3) for which the maximum compatibility with the SPARC data is achieved. In Figs. 406, 407 we present

TABLE CCLII: SIDM Optimization Values for the galaxy F561-1

Parameter	Optimization Values
$\rho_0 (M_\odot / \text{Kpc}^3)$	1.19454×10^7
$K_0 (M_\odot \text{ Kpc}^{-3} (\text{km/s})^2)$	943.258

the density of the analytic SIDM model, the predicted rotation curves for the SIDM model (3), versus the SPARC observational data and the sound speed, as a function of the radius respectively. As it can

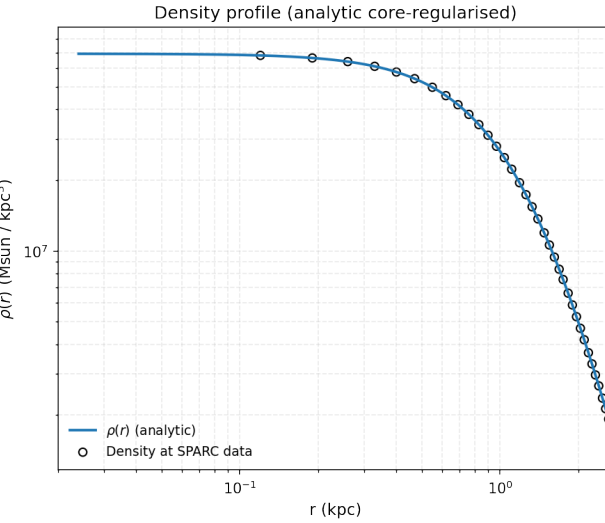


FIG. 404: The density of the SIDM model of Eq. (3) for the galaxy UGCA444, versus the radius.

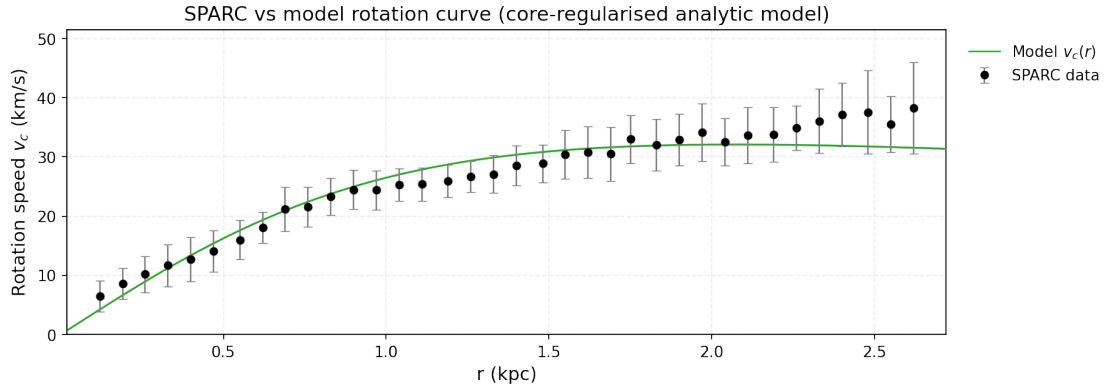


FIG. 405: The predicted rotation curves for the optimized SIDM model of Eq. (3), versus the SPARC observational data for the galaxy UGCA444.

be seen, for this galaxy, the SIDM model produces viable rotation curves which are compatible with the SPARC data.

144. The Galaxy F563-1

For this galaxy, the optimization method we used, ensures maximum compatibility of the analytic SIDM model of Eq. (3) with the SPARC data, if we choose $\rho_0 = 3.47649 \times 10^7 M_\odot / \text{Kpc}^3$ and $K_0 = 5149.08 M_\odot \text{ Kpc}^{-3} (\text{km/s})^2$, in which case the reduced χ^2_{red} value is $\chi^2_{\text{red}} = 1.05607$. Also the parameter α in this case is $\alpha = 7.02337 \text{ Kpc}$.

In Table CCLIII we present the optimized values of K_0 and ρ_0 for the analytic SIDM model of Eq. (3) for which the maximum compatibility with the SPARC data is achieved. In Figs. 408, 409 we present

TABLE CCLIII: SIDM Optimization Values for the galaxy F563-1

Parameter	Optimization Values
$\rho_0 (M_\odot / \text{Kpc}^3)$	3.47649×10^7
$K_0 (M_\odot \text{ Kpc}^{-3} (\text{km/s})^2)$	5149.08

the density of the analytic SIDM model, the predicted rotation curves for the SIDM model (3), versus the SPARC observational data and the sound speed, as a function of the radius respectively. As it can

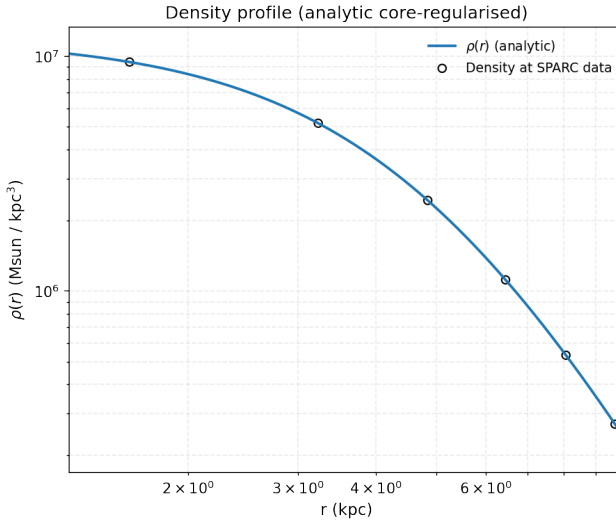


FIG. 406: The density of the SIDM model of Eq. (3) for the galaxy F561-1, versus the radius.

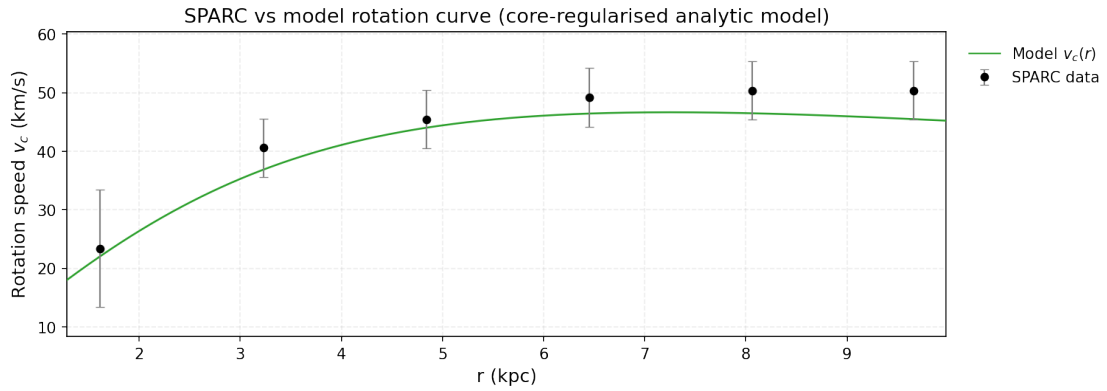


FIG. 407: The predicted rotation curves for the optimized SIDM model of Eq. (3), versus the SPARC observational data for the galaxy F561-1.

be seen, for this galaxy, the SIDM model produces viable rotation curves which are incompatible with the SPARC data.

145. The Galaxy F563-V1

For this galaxy, the optimization method we used, ensures maximum compatibility of the analytic SIDM model of Eq. (3) with the SPARC data, if we choose $\rho_0 = 5.23175 \times 10^6 M_\odot / \text{Kpc}^3$ and $K_0 = 421.941 M_\odot \text{ Kpc}^{-3} (\text{km/s})^2$, in which case the reduced χ^2_{red} value is $\chi^2_{\text{red}} = 0.235344$. Also the parameter α in this case is $\alpha = 5.18267 \text{ Kpc}$.

In Table CCLIV we present the optimized values of K_0 and ρ_0 for the analytic SIDM model of Eq. (3) for which the maximum compatibility with the SPARC data is achieved. In Figs. 410, 411 we present

TABLE CCLIV: SIDM Optimization Values for the galaxy F563-V1

Parameter	Optimization Values
$\rho_0 (M_\odot / \text{Kpc}^3)$	5.23175×10^6
$K_0 (M_\odot \text{ Kpc}^{-3} (\text{km/s})^2)$	421.941

the density of the analytic SIDM model, the predicted rotation curves for the SIDM model (3), versus the SPARC observational data and the sound speed, as a function of the radius respectively. As it can

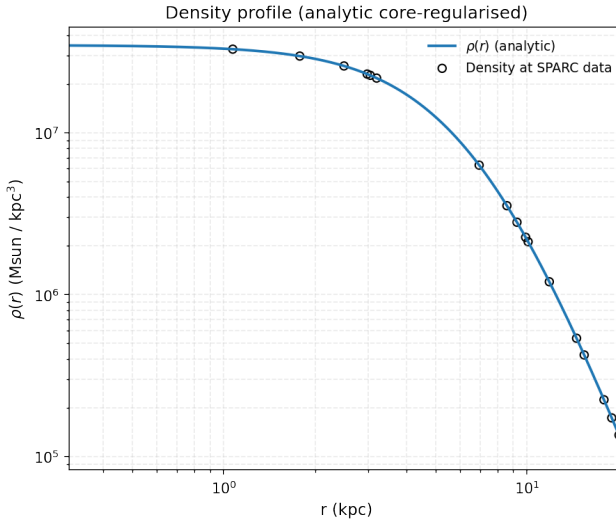


FIG. 408: The density of the SIDM model of Eq. (3) for the galaxy F563-1, versus the radius.

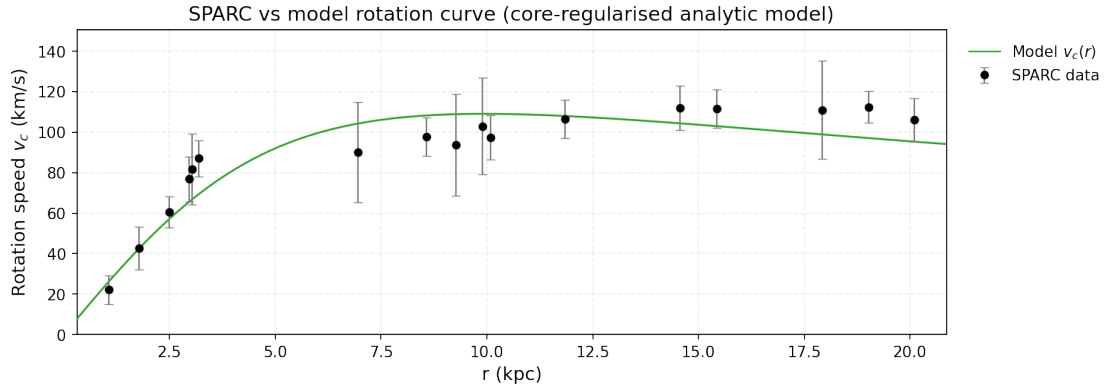


FIG. 409: The predicted rotation curves for the optimized SIDM model of Eq. (3), versus the SPARC observational data for the galaxy F563-1.

be seen, for this galaxy, the SIDM model produces viable rotation curves which are compatible with the SPARC data.

146. The Galaxy F563-V2

For this galaxy, the optimization method we used, ensures maximum compatibility of the analytic SIDM model of Eq. (3) with the SPARC data, if we choose $\rho_0 = 7.91462 \times 10^7 M_\odot / \text{Kpc}^3$ and $K_0 = 5793.97 M_\odot \text{ Kpc}^{-3} (\text{km/s})^2$, in which case the reduced χ^2_{red} value is $\chi^2_{\text{red}} = 0.336871$. Also the parameter α in this case is $\alpha = 4.93769 \text{ Kpc}$.

In Table CCLV we present the optimized values of K_0 and ρ_0 for the analytic SIDM model of Eq. (3) for which the maximum compatibility with the SPARC data is achieved. In Figs. 412, 413 we present

TABLE CCLV: SIDM Optimization Values for the galaxy F563-V2

Parameter	Optimization Values
$\rho_0 (M_\odot / \text{Kpc}^3)$	7.91462×10^7
$K_0 (M_\odot \text{ Kpc}^{-3} (\text{km/s})^2)$	5793.97

the density of the analytic SIDM model, the predicted rotation curves for the SIDM model (3), versus the SPARC observational data and the sound speed, as a function of the radius respectively. As it can

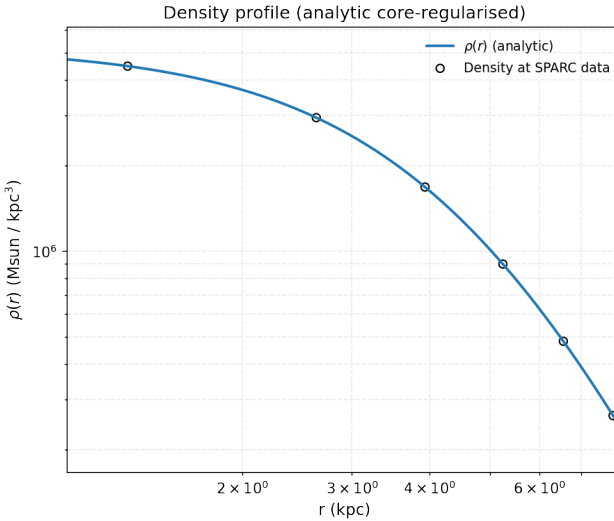


FIG. 410: The density of the SIDM model of Eq. (3) for the galaxy F563-V1, versus the radius.

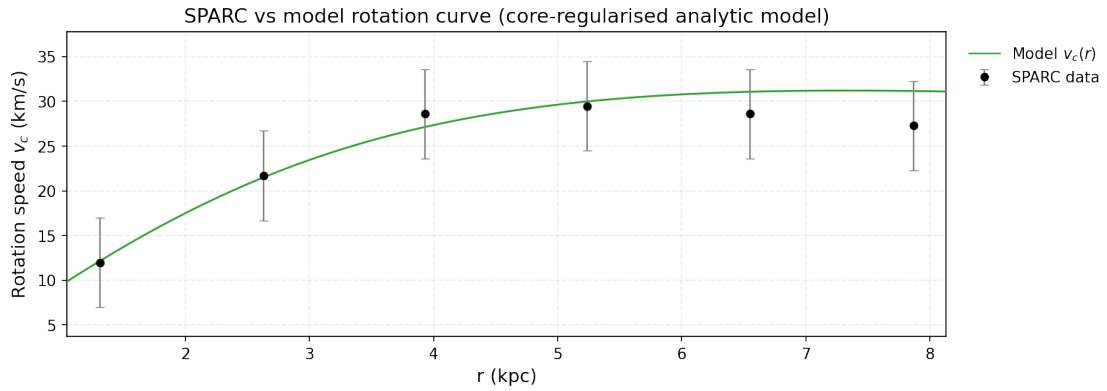


FIG. 411: The predicted rotation curves for the optimized SIDM model of Eq. (3), versus the SPARC observational data for the galaxy F563-V1.

be seen, for this galaxy, the SIDM model produces viable rotation curves which are compatible with the SPARC data.

147. The Galaxy F567-2

For this galaxy, the optimization method we used, ensures maximum compatibility of the analytic SIDM model of Eq. (3) with the SPARC data, if we choose $\rho_0 = 1.4789 \times 10^7 M_\odot / \text{Kpc}^3$ and $K_0 = 1151.54 M_\odot \text{ Kpc}^{-3} (\text{km/s})^2$, in which case the reduced χ^2_{red} value is $\chi^2_{\text{red}} = 0.27007$. Also the parameter α in this case is $\alpha = 5.09239 \text{ Kpc}$.

In Table CCLVI we present the optimized values of K_0 and ρ_0 for the analytic SIDM model of Eq. (3) for which the maximum compatibility with the SPARC data is achieved. In Figs. 414, 415 we present

TABLE CCLVI: SIDM Optimization Values for the galaxy F567-2

Parameter	Optimization Values
$\rho_0 (M_\odot / \text{Kpc}^3)$	1.4789×10^7
$K_0 (M_\odot \text{ Kpc}^{-3} (\text{km/s})^2)$	1151.54

the density of the analytic SIDM model, the predicted rotation curves for the SIDM model (3), versus the SPARC observational data and the sound speed, as a function of the radius respectively. As it can

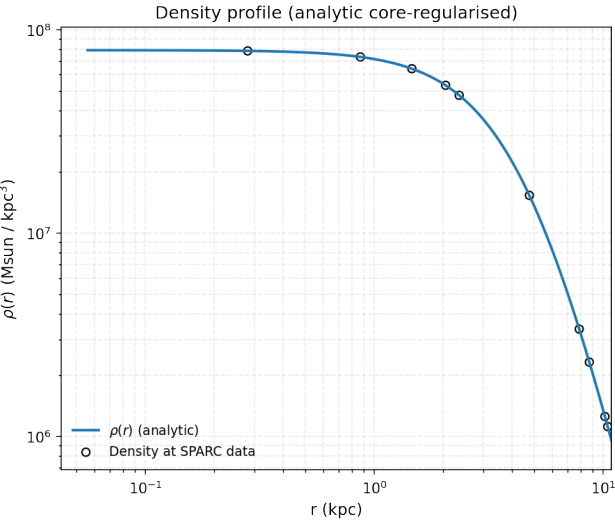


FIG. 412: The density of the SIDM model of Eq. (3) for the galaxy F563-V2, versus the radius.

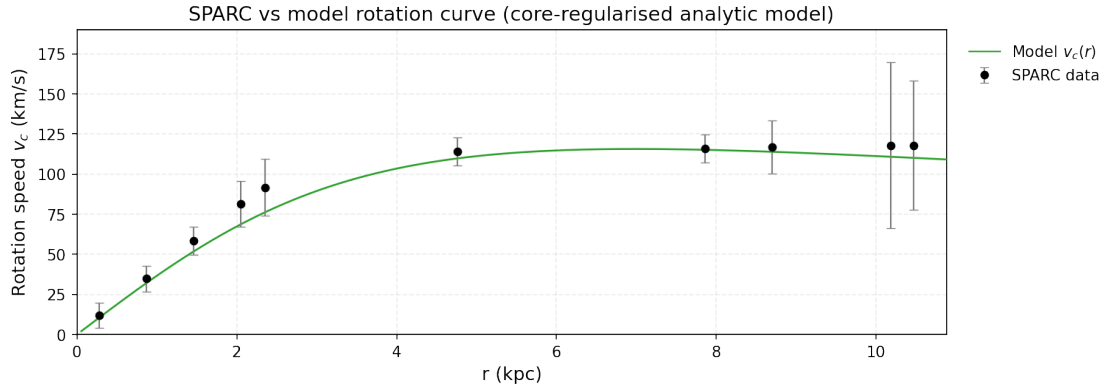


FIG. 413: The predicted rotation curves for the optimized SIDM model of Eq. (3), versus the SPARC observational data for the galaxy F563-V2.

be seen, for this galaxy, the SIDM model produces viable rotation curves which are compatible with the SPARC data.

148. The Galaxy F568-1

For this galaxy, the optimization method we used, ensures maximum compatibility of the analytic SIDM model of Eq. (3) with the SPARC data, if we choose $\rho_0 = 5.59467 \times 10^7 M_\odot / \text{Kpc}^3$ and $K_0 = 7857.31 M_\odot \text{ Kpc}^{-3} (\text{km/s})^2$, in which case the reduced χ^2_{red} value is $\chi^2_{\text{red}} = 0.256689$. Also the parameter α in this case is $\alpha = 6.83913 \text{ Kpc}$.

In Table CCLVII we present the optimized values of K_0 and ρ_0 for the analytic SIDM model of Eq. (3) for which the maximum compatibility with the SPARC data is achieved. In Figs. 416, 417 we present

TABLE CCLVII: SIDM Optimization Values for the galaxy F568-1

Parameter	Optimization Values
$\rho_0 (M_\odot / \text{Kpc}^3)$	5.59467×10^7
$K_0 (M_\odot \text{ Kpc}^{-3} (\text{km/s})^2)$	7857.31

the density of the analytic SIDM model, the predicted rotation curves for the SIDM model (3), versus the SPARC observational data and the sound speed, as a function of the radius respectively. As it can

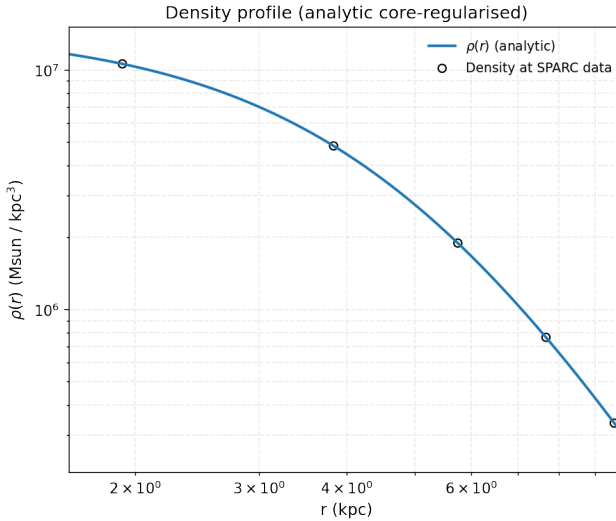


FIG. 414: The density of the SIDM model of Eq. (3) for the galaxy F567-2, versus the radius.

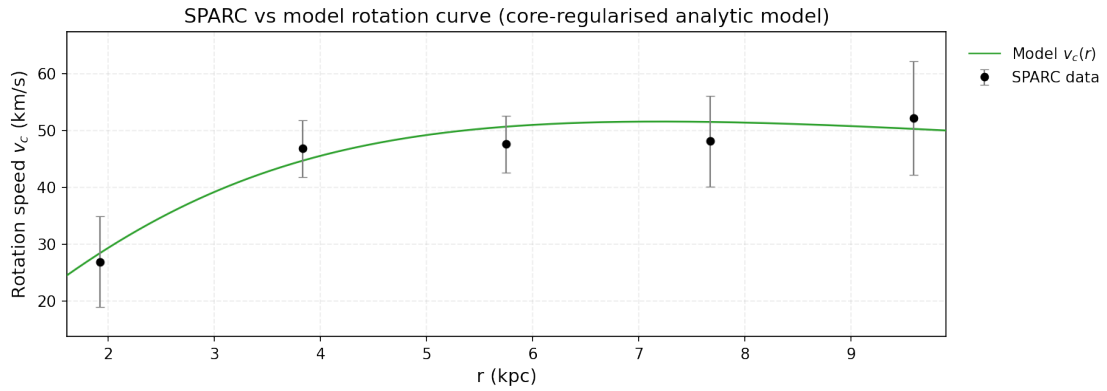


FIG. 415: The predicted rotation curves for the optimized SIDM model of Eq. (3), versus the SPARC observational data for the galaxy F567-2.

be seen, for this galaxy, the SIDM model produces viable rotation curves which are compatible with the SPARC data.

149. The Galaxy F574-2

For this galaxy, the optimization method we used, ensures maximum compatibility of the analytic SIDM model of Eq. (3) with the SPARC data, if we choose $\rho_0 = 2.36801 \times 10^6 M_\odot / \text{Kpc}^3$ and $K_0 = 1131.68 M_\odot \text{ Kpc}^{-3} (\text{km/s})^2$, in which case the reduced χ^2_{red} value is $\chi^2_{\text{red}} = 0.640246$. Also the parameter α in this case is $\alpha = 12.616 \text{ Kpc}$.

In Table CCLVIII we present the optimized values of K_0 and ρ_0 for the analytic SIDM model of Eq. (3) for which the maximum compatibility with the SPARC data is achieved. In Figs. 418, 419 we present

TABLE CCLVIII: SIDM Optimization Values for the galaxy F574-2

Parameter	Optimization Values
$\rho_0 (M_\odot / \text{Kpc}^3)$	2.36801×10^6
$K_0 (M_\odot \text{ Kpc}^{-3} (\text{km/s})^2)$	1131.68

the density of the analytic SIDM model, the predicted rotation curves for the SIDM model (3), versus the SPARC observational data and the sound speed, as a function of the radius respectively. As it can

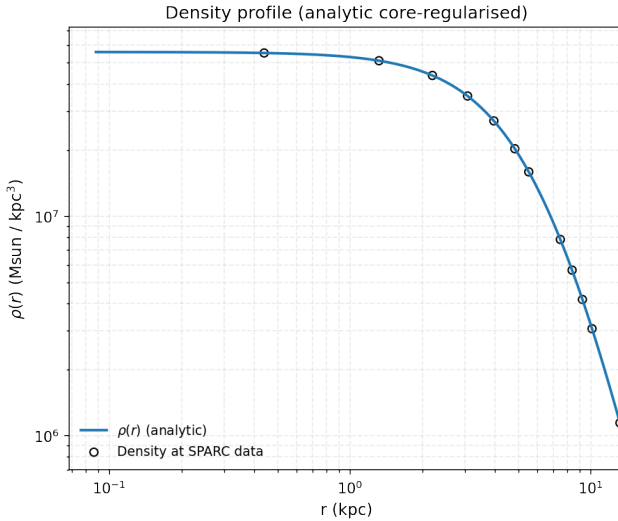


FIG. 416: The density of the SIDM model of Eq. (3) for the galaxy F568-1, versus the radius.

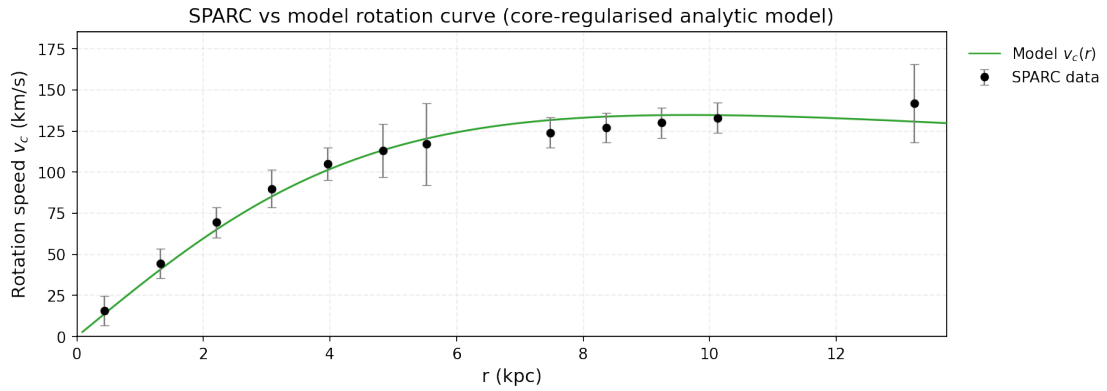


FIG. 417: The predicted rotation curves for the optimized SIDM model of Eq. (3), versus the SPARC observational data for the galaxy F568-1.

be seen, for this galaxy, the SIDM model produces viable rotation curves which are compatible with the SPARC data.

150. The Galaxy F579-V1, Non-viable, Extended Viable

For this galaxy, the optimization method we used, ensures maximum compatibility of the analytic SIDM model of Eq. (3) with the SPARC data, if we choose $\rho_0 = 1.25165 \times 10^8 M_\odot / \text{Kpc}^3$ and $K_0 = 6219.26 M_\odot \text{ Kpc}^{-3} (\text{km/s})^2$, in which case the reduced χ^2_{red} value is $\chi^2_{red} = 1.62409$. Also the parameter α in this case is $\alpha = 4.06798 \text{ Kpc}$.

In Table CCLIX we present the optimized values of K_0 and ρ_0 for the analytic SIDM model of Eq. (3) for which the maximum compatibility with the SPARC data is achieved. In Figs. 420, 421 we present

TABLE CCLIX: SIDM Optimization Values for the galaxy F579-V1

Parameter	Optimization Values
$\rho_0 (M_\odot / \text{Kpc}^3)$	1.25165×10^8
$K_0 (M_\odot \text{ Kpc}^{-3} (\text{km/s})^2)$	6219.26

the density of the analytic SIDM model, the predicted rotation curves for the SIDM model (3), versus the SPARC observational data and the sound speed, as a function of the radius respectively. As it can

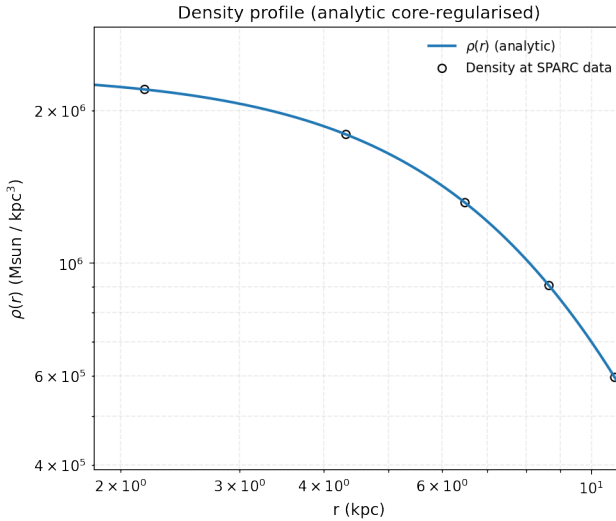


FIG. 418: The density of the SIDM model of Eq. (3) for the galaxy F574-2, versus the radius.

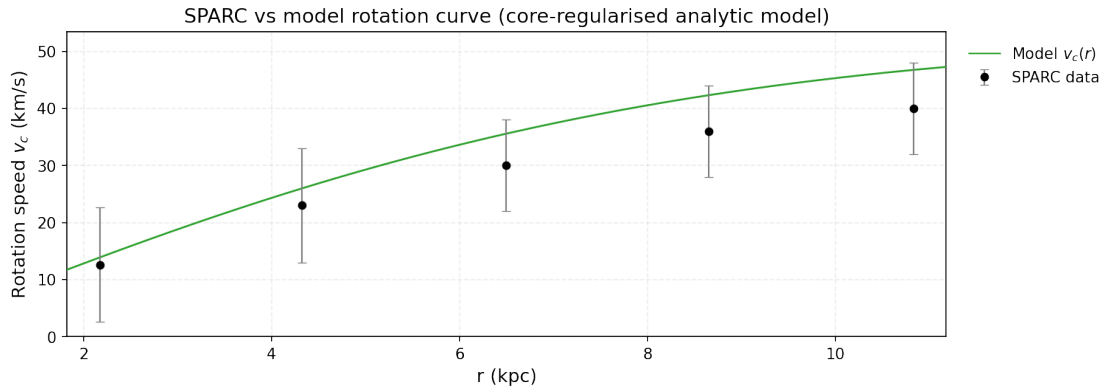


FIG. 419: The predicted rotation curves for the optimized SIDM model of Eq. (3), versus the SPARC observational data for the galaxy F574-2.

be seen, for this galaxy, the SIDM model produces non-viable rotation curves which are incompatible with the SPARC data.

Now we shall include contributions to the rotation velocity from the other components of the galaxy, namely the disk, the gas, and the bulge if present. In Fig. 422 we present the combined rotation curves including all the components of the galaxy along with the SIDM. As it can be seen, the extended collisional DM model is viable. Also in Table CCLX we present the optimized values of the free parameters of the SIDM model for which we achieve the maximum compatibility with the SPARC data, for the galaxy F579-V1, and also the resulting reduced χ^2_{red} value.

TABLE CCLX: Optimized Parameter Values of the Extended SIDM model for the Galaxy F579-V1.

Parameter	Value
$\rho_0 (M_\odot / \text{Kpc}^3)$	1.34471×10^8
$K_0 (M_\odot \text{ Kpc}^{-3} (\text{km/s})^2)$	3756.51
ml_{disk}	1
ml_{bulge}	0.4708
$\alpha (\text{Kpc})$	3.04982
χ^2_{red}	0.870182

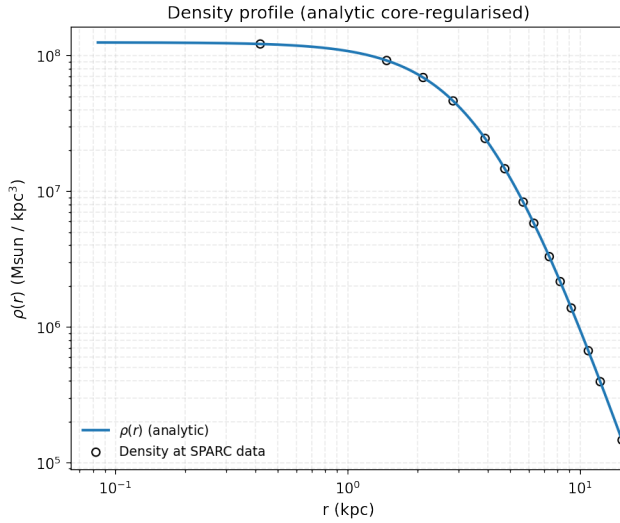


FIG. 420: The density of the SIDM model of Eq. (3) for the galaxy F579-V1, versus the radius.

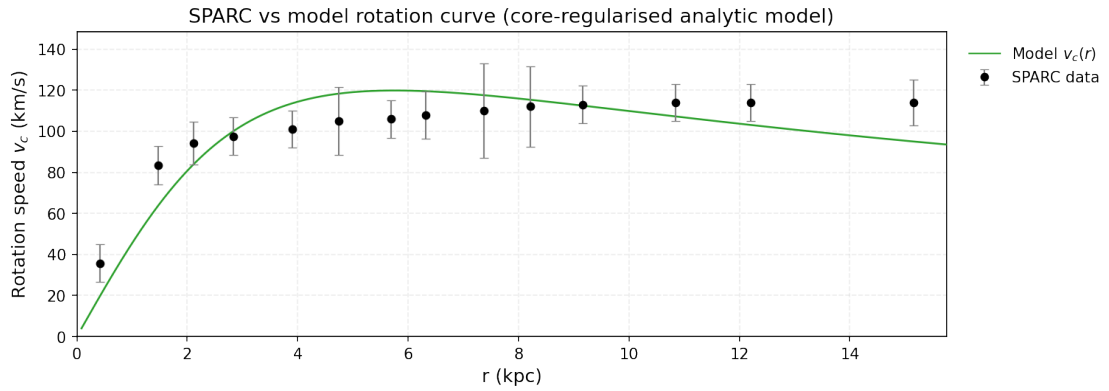


FIG. 421: The predicted rotation curves for the optimized SIDM model of Eq. (3), versus the SPARC observational data for the galaxy F579-V1.

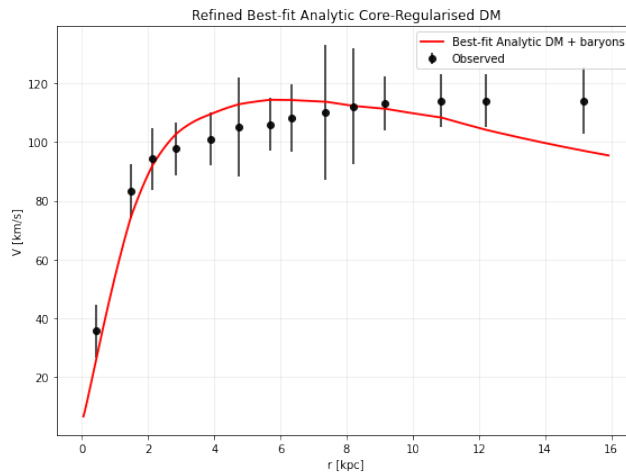


FIG. 422: The predicted rotation curves after using an optimization for the SIDM model (3), and the extended SPARC data for the galaxy F579-V1. We included the rotation curves of the gas, the disk velocities, the bulge (where present) along with the SIDM model.

151. The Galaxy NGC1705, Non-viable, Extended Viable

For this galaxy, the optimization method we used, ensures maximum compatibility of the analytic SIDM model of Eq. (3) with the SPARC data, if we choose $\rho_0 = 4.15243 \times 10^8 M_\odot/\text{Kpc}^3$ and $K_0 = 2692.68 M_\odot \text{Kpc}^{-3} (\text{km/s})^2$, in which case the reduced χ^2_{red} value is $\chi^2_{red} = 3.00796$. Also the parameter α in this case is $\alpha = 1.46957 \text{Kpc}$.

In Table CCLXI we present the optimized values of K_0 and ρ_0 for the analytic SIDM model of Eq. (3) for which the maximum compatibility with the SPARC data is achieved. In Figs. 423, 424 we present

TABLE CCLXI: SIDM Optimization Values for the galaxy NGC1705

Parameter	Optimization Values
$\rho_0 (M_\odot/\text{Kpc}^3)$	4.15243×10^8
$K_0 (M_\odot \text{Kpc}^{-3} (\text{km/s})^2)$	2692.68

the density of the analytic SIDM model, the predicted rotation curves for the SIDM model (3), versus the SPARC observational data and the sound speed, as a function of the radius respectively. As it can be seen, for this galaxy, the SIDM model produces non-viable rotation curves which are incompatible with the SPARC data.

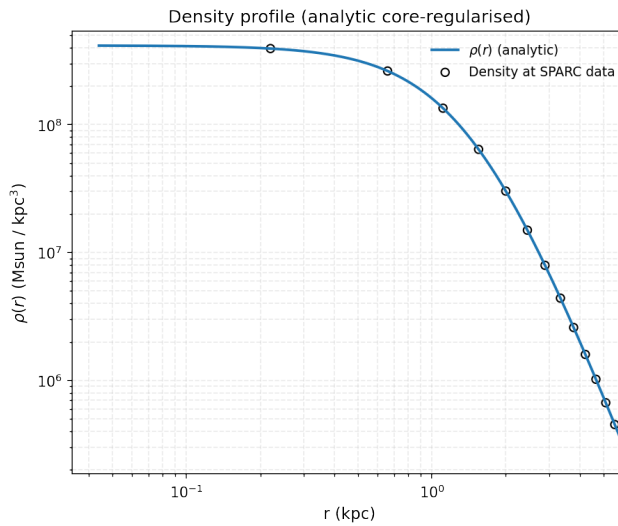


FIG. 423: The density of the SIDM model of Eq. (3) for the galaxy NGC1705, versus the radius.

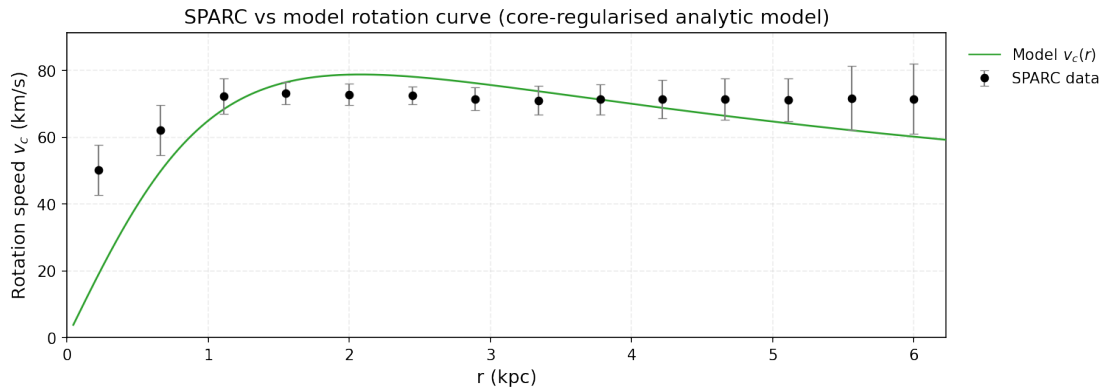


FIG. 424: The predicted rotation curves for the optimized SIDM model of Eq. (3), versus the SPARC observational data for the galaxy NGC1705.

Now we shall include contributions to the rotation velocity from the other components of the galaxy, namely the disk, the gas, and the bulge if present. In Fig. 425 we present the combined rotation

curves including all the components of the galaxy along with the SIDM. As it can be seen, the extended collisional DM model is viable. Also in Table CCLXII we present the optimized values of the free

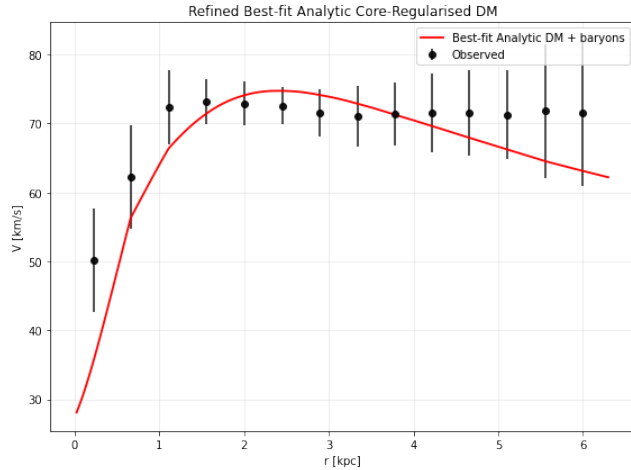


FIG. 425: The predicted rotation curves after using an optimization for the SIDM model (3), and the extended SPARC data for the galaxy NGC1705. We included the rotation curves of the gas, the disk velocities, the bulge (where present) along with the SIDM model.

parameters of the SIDM model for which we achieve the maximum compatibility with the SPARC data, for the galaxy NGC1705, and also the resulting reduced χ^2_{red} value.

TABLE CCLXII: Optimized Parameter Values of the Extended SIDM model for the Galaxy NGC1705.

Parameter	Value
$\rho_0 (M_\odot/\text{Kpc}^3)$	1.42866×10^8
$K_0 (M_\odot \text{ Kpc}^{-3} (\text{km/s})^2)$	1918.09
ml_{disk}	1
ml_{bulge}	0.34
$\alpha (\text{Kpc})$	2.1143
χ^2_{red}	0.980005

152. The Galaxy NGC2366

For this galaxy, the optimization method we used, ensures maximum compatibility of the analytic SIDM model of Eq. (3) with the SPARC data, if we choose $\rho_0 = 3.31738 \times 10^7 M_\odot/\text{Kpc}^3$ and $K_0 = 1175.78 M_\odot \text{ Kpc}^{-3} (\text{km/s})^2$, in which case the reduced χ^2_{red} value is $\chi^2_{red} = 0.260425$. Also the parameter α in this case is $\alpha = 3.43571 \text{ Kpc}$.

In Table CCLXIII we present the optimized values of K_0 and ρ_0 for the analytic SIDM model of Eq. (3) for which the maximum compatibility with the SPARC data is achieved. In Figs. 426, 427 we present

TABLE CCLXIII: SIDM Optimization Values for the galaxy NGC2366

Parameter	Optimization Values
$\rho_0 (M_\odot/\text{Kpc}^3)$	3.31738×10^7
$K_0 (M_\odot \text{ Kpc}^{-3} (\text{km/s})^2)$	1175.78

the density of the analytic SIDM model, the predicted rotation curves for the SIDM model (3), versus the SPARC observational data and the sound speed, as a function of the radius respectively. As it can be seen, for this galaxy, the SIDM model produces viable rotation curves which are compatible with the SPARC data.

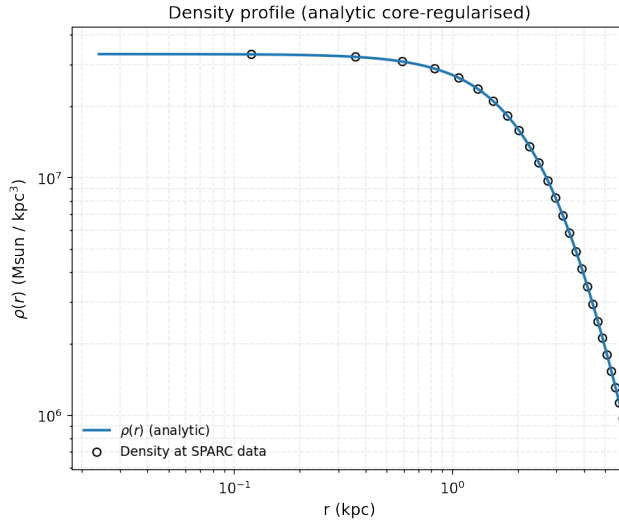


FIG. 426: The density of the SIDM model of Eq. (3) for the galaxy NGC2366, versus the radius.

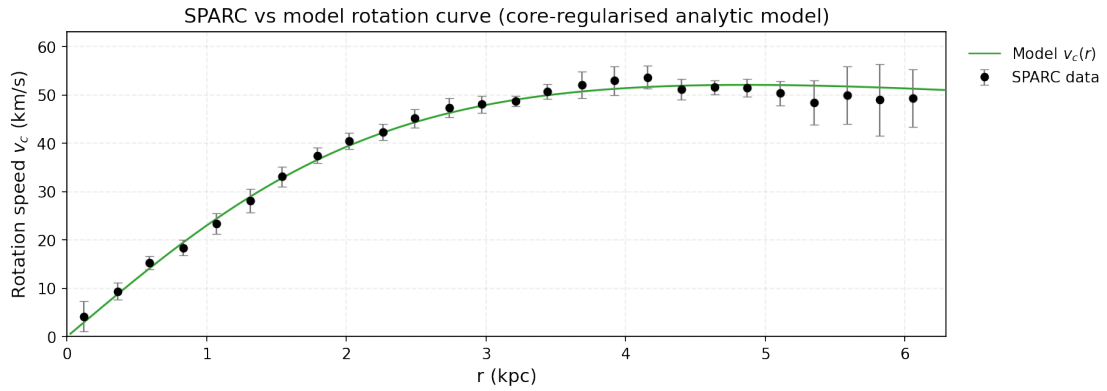


FIG. 427: The predicted rotation curves for the optimized SIDM model of Eq. (3), versus the SPARC observational data for the galaxy NGC2366.

153. The Galaxy NGC4214, Non-viable, Extended Viable

For this galaxy, the optimization method we used, ensures maximum compatibility of the analytic SIDM model of Eq. (3) with the SPARC data, if we choose $\rho_0 = 3.18236 \times 10^8 M_\odot / \text{Kpc}^3$ and $K_0 = 3022.45 M_\odot \text{ Kpc}^{-3} (\text{km/s})^2$, in which case the reduced χ^2_{red} value is $\chi^2_{\text{red}} = 4.23692$. Also the parameter α in this case is $\alpha = 1.77851 \text{ Kpc}$.

In Table CCLXIV we present the optimized values of K_0 and ρ_0 for the analytic SIDM model of Eq. (3) for which the maximum compatibility with the SPARC data is achieved. In Figs. 428, 429 we present

TABLE CCLXIV: SIDM Optimization Values for the galaxy NGC4214

Parameter	Optimization Values
$\rho_0 (M_\odot / \text{Kpc}^3)$	3.18236×10^8
$K_0 (M_\odot \text{ Kpc}^{-3} (\text{km/s})^2)$	3022.45

the density of the analytic SIDM model, the predicted rotation curves for the SIDM model (3), versus the SPARC observational data and the sound speed, as a function of the radius respectively. As it can be seen, for this galaxy, the SIDM model produces non-viable rotation curves which are incompatible with the SPARC data.

Now we shall include contributions to the rotation velocity from the other components of the galaxy, namely the disk, the gas, and the bulge if present. In Fig. 430 we present the combined rotation

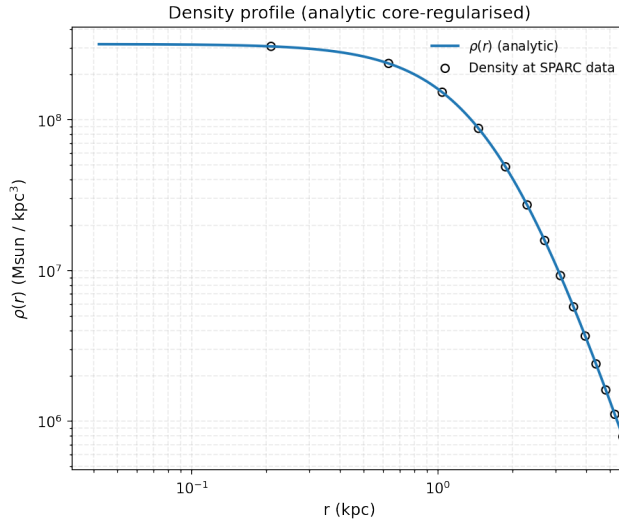


FIG. 428: The density of the SIDM model of Eq. (3) for the galaxy NGC4214, versus the radius.

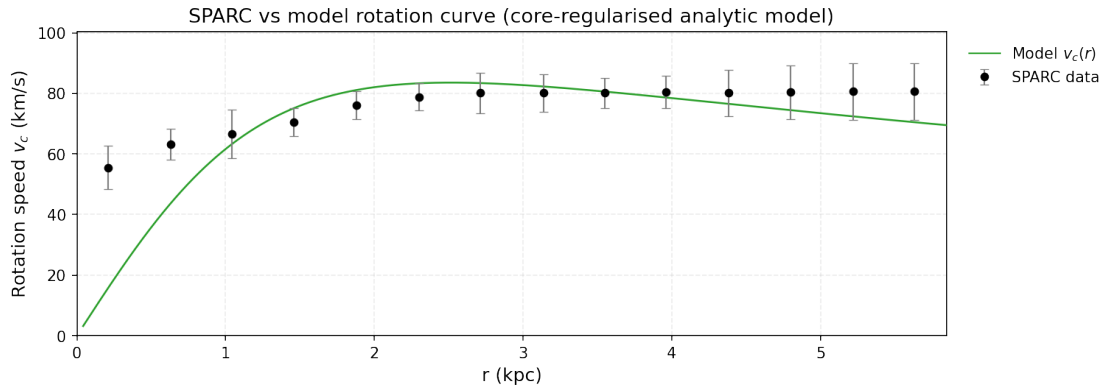


FIG. 429: The predicted rotation curves for the optimized SIDM model of Eq. (3), versus the SPARC observational data for the galaxy NGC4214.

curves including all the components of the galaxy along with the SIDM. As it can be seen, the extended collisional DM model is viable. Also in Table CCLXV we present the optimized values of the free parameters of the SIDM model for which we achieve the maximum compatibility with the SPARC data, for the galaxy NGC4214, and also the resulting reduced χ^2_{red} value.

TABLE CCLXV: Optimized Parameter Values of the Extended SIDM model for the Galaxy NGC4214.

Parameter	Value
ρ_0 (M_\odot/Kpc^3)	6.0791×10^7
K_0 ($M_\odot \text{ Kpc}^{-3} (\text{km/s})^2$)	2251.03
m_{disk}	1
m_{bulge}	0.2552
α (Kpc)	3.5113
χ^2_{red}	1.09386

154. The Galaxy NGC4389

For this galaxy, the optimization method we used, ensures maximum compatibility of the analytic SIDM model of Eq. (3) with the SPARC data, if we choose $\rho_0 = 4.85533 \times 10^7 M_\odot/\text{Kpc}^3$ and $K_0 = 6639.95 M_\odot \text{ Kpc}^{-3} (\text{km/s})^2$, in which case the reduced χ^2_{red} value is $\chi^2_{red} = 0.381669$. Also the parameter α in this case is $\alpha = 6.74875 \text{ Kpc}$.

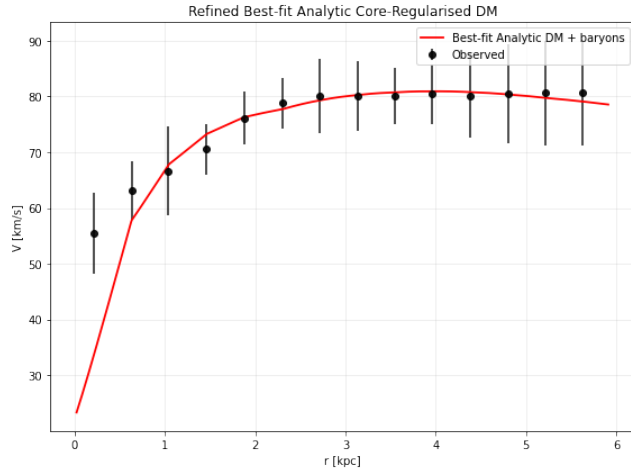


FIG. 430: The predicted rotation curves after using an optimization for the SIDM model (3), and the extended SPARC data for the galaxy NGC4214. We included the rotation curves of the gas, the disk velocities, the bulge (where present) along with the SIDM model.

In Table CCLXVI we present the optimized values of K_0 and ρ_0 for the analytic SIDM model of Eq. (3) for which the maximum compatibility with the SPARC data is achieved. In Figs. 431, 432 we present

TABLE CCLXVI: SIDM Optimization Values for the galaxy NGC4389

Parameter	Optimization Values
ρ_0 (M_\odot/Kpc^3)	4.85533×10^7
K_0 ($M_\odot \text{ Kpc}^{-3} (\text{km/s})^2$)	6639.95

the density of the analytic SIDM model, the predicted rotation curves for the SIDM model (3), versus the SPARC observational data and the sound speed, as a function of the radius respectively. As it can be seen, for this galaxy, the SIDM model produces viable rotation curves which are compatible with the SPARC data.

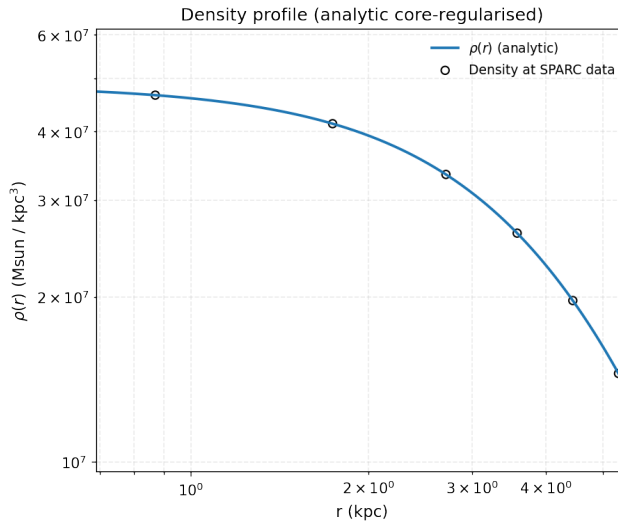


FIG. 431: The density of the SIDM model of Eq. (3) for the galaxy NGC4389, versus the radius.

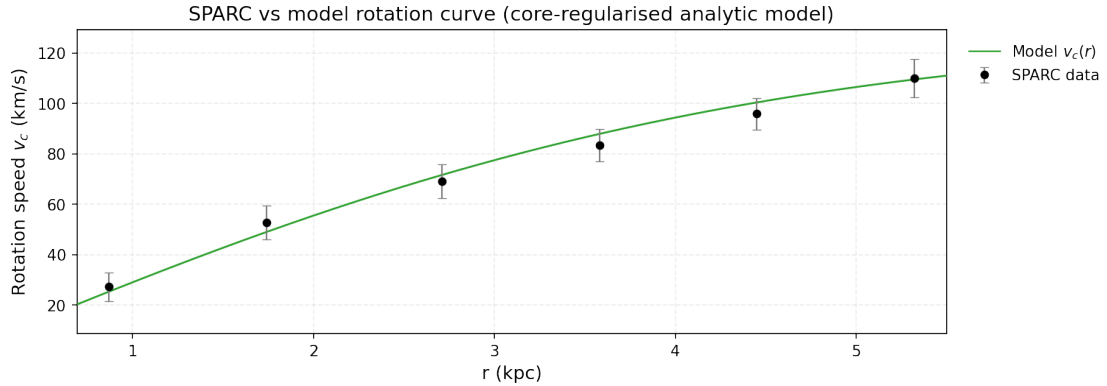


FIG. 432: The predicted rotation curves for the optimized SIDM model of Eq. (3), versus the SPARC observational data for the galaxy NGC4389.

155. The Galaxy NGC6946, Non-viable

For this galaxy, the optimization method we used, ensures maximum compatibility of the analytic SIDM model of Eq. (3) with the SPARC data, if we choose $\rho_0 = 1.91358 \times 10^8 M_\odot/\text{Kpc}^3$ and $K_0 = 14582.9 M_\odot \text{Kpc}^{-3} (\text{km/s})^2$, in which case the reduced χ^2_{red} value is $\chi^2_{red} = 31.94$. Also the parameter α in this case is $\alpha = 5.0379 \text{Kpc}$.

In Table CCLXVII we present the optimized values of K_0 and ρ_0 for the analytic SIDM model of Eq. (3) for which the maximum compatibility with the SPARC data is achieved. In Figs. 433, 434 we present

TABLE CCLXVII: SIDM Optimization Values for the galaxy NGC6946

Parameter	Optimization Values
$\rho_0 (M_\odot/\text{Kpc}^3)$	5×10^7
$K_0 (M_\odot \text{Kpc}^{-3} (\text{km/s})^2)$	1250

the density of the analytic SIDM model, the predicted rotation curves for the SIDM model (3), versus the SPARC observational data and the sound speed, as a function of the radius respectively. As it can be seen, for this galaxy, the SIDM model produces non-viable rotation curves which are incompatible with the SPARC data.

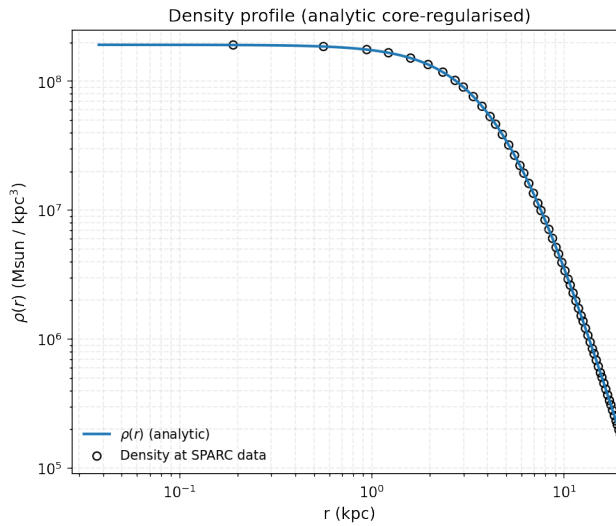


FIG. 433: The density of the SIDM model of Eq. (3) for the galaxy NGC6946, versus the radius.

Now we shall include contributions to the rotation velocity from the other components of the galaxy, namely the disk, the gas, and the bulge if present. In Fig. 435 we present the combined rotation

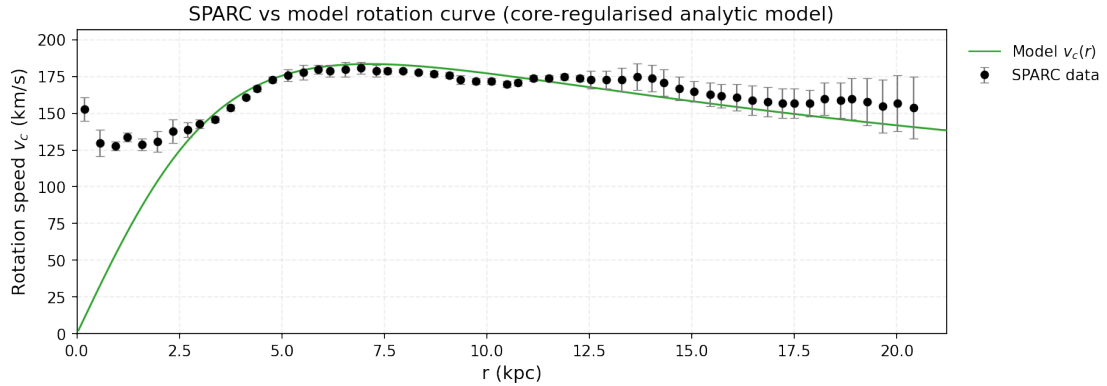


FIG. 434: The predicted rotation curves for the optimized SIDM model of Eq. (3), versus the SPARC observational data for the galaxy NGC6946.

curves including all the components of the galaxy along with the SIDM. As it can be seen, the extended collisional DM model is non-viable. Also in Table CCLXVIII we present the optimized values of the free

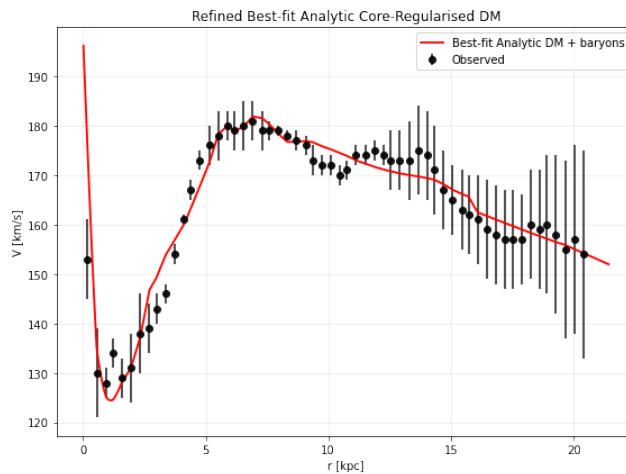


FIG. 435: The predicted rotation curves after using an optimization for the SIDM model (3), and the extended SPARC data for the galaxy NGC6946. We included the rotation curves of the gas, the disk velocities, the bulge (where present) along with the SIDM model.

parameters of the SIDM model for which we achieve the maximum compatibility with the SPARC data, for the galaxy NGC6946, and also the resulting reduced χ^2_{red} value.

TABLE CCLXVIII: Optimized Parameter Values of the Extended SIDM model for the Galaxy NGC6946.

Parameter	Value
ρ_0 (M_\odot/Kpc^3)	1.06206×10^7
K_0 ($M_\odot \text{ Kpc}^{-3} (\text{km/s})^2$)	5917.91
ml_{disk}	0.7724
ml_{bulge}	0.7454
α (Kpc)	13.6209
χ^2_{red}	1.48679

156. The Galaxy PGC51017, Non-viable, Extended Viable

For this galaxy, the optimization method we used, ensures maximum compatibility of the analytic SIDM model of Eq. (3) with the SPARC data, if we choose $\rho_0 = 1.37511 \times 10^8 M_\odot/\text{Kpc}^3$ and $K_0 =$

$217.625 M_{\odot} \text{ Kpc}^{-3} (\text{km/s})^2$, in which case the reduced χ^2_{red} value is $\chi^2_{red} = 1.72797$. Also the parameter α in this case is $\alpha = 0.726 \text{ Kpc}$.

In Table CCLXIX we present the optimized values of K_0 and ρ_0 for the analytic SIDM model of Eq. (3) for which the maximum compatibility with the SPARC data is achieved. In Figs. 436, 437 we present

TABLE CCLXIX: SIDM Optimization Values for the galaxy PGC51017

Parameter	Optimization Values
$\rho_0 (M_{\odot}/\text{Kpc}^3)$	1.37511×10^8
$K_0 (M_{\odot} \text{ Kpc}^{-3} (\text{km/s})^2)$	217.625

the density of the analytic SIDM model, the predicted rotation curves for the SIDM model (3), versus the SPARC observational data and the sound speed, as a function of the radius respectively. As it can be seen, for this galaxy, the SIDM model produces non-viable rotation curves which are incompatible with the SPARC data.

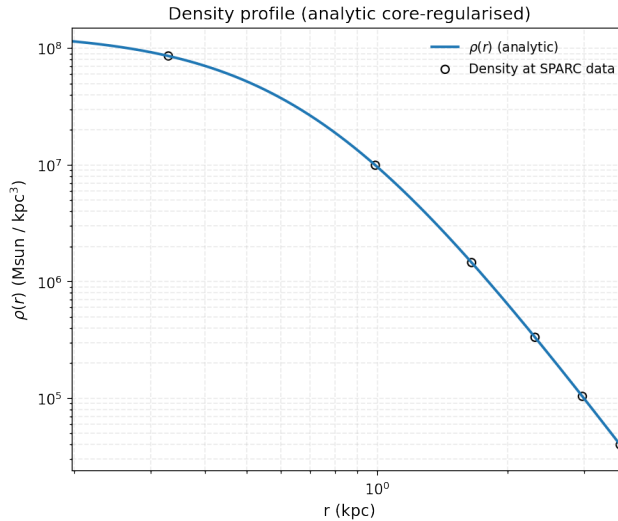


FIG. 436: The density of the SIDM model of Eq. (3) for the galaxy PGC51017, versus the radius.

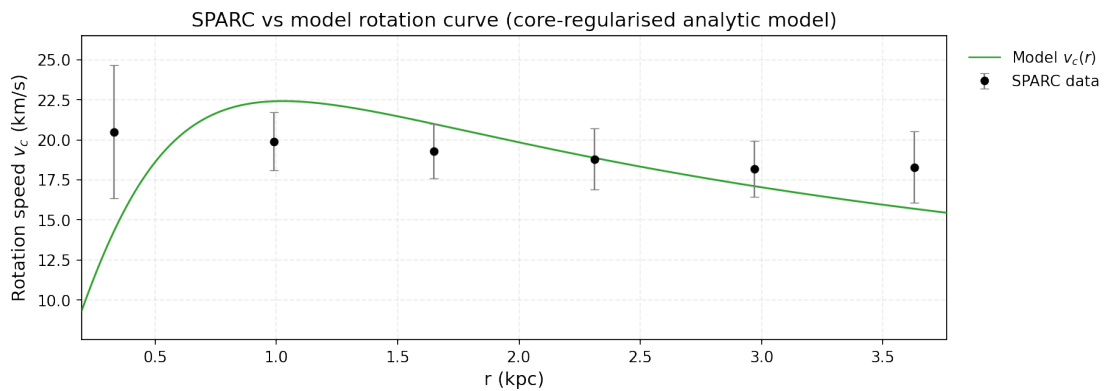


FIG. 437: The predicted rotation curves for the optimized SIDM model of Eq. (3), versus the SPARC observational data for the galaxy PGC51017.

Now we shall include contributions to the rotation velocity from the other components of the galaxy, namely the disk, the gas, and the bulge if present. In Fig. 438 we present the combined rotation curves including all the components of the galaxy along with the SIDM. As it can be seen, the extended collisional DM model is non-viable. Also in Table CCLXX we present the optimized values of the free parameters of the SIDM model for which we achieve the maximum compatibility with the SPARC data, for the galaxy PGC51017, and also the resulting reduced χ^2_{red} value.

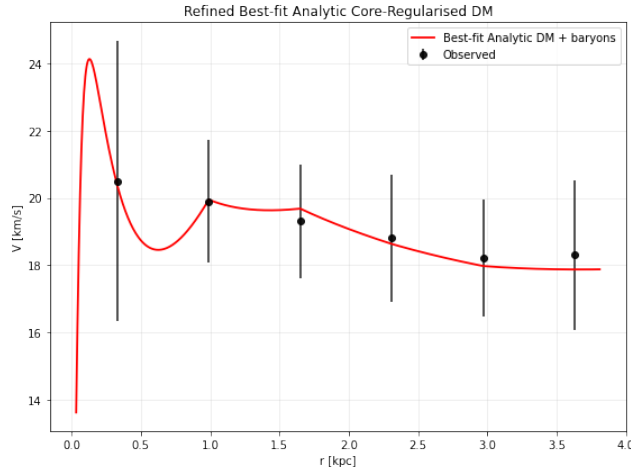


FIG. 438: The predicted rotation curves after using an optimization for the SIDM model (3), and the extended SPARC data for the galaxy PGC51017. We included the rotation curves of the gas, the disk velocities, the bulge (where present) along with the SIDM model.

TABLE CCLXX: Optimized Parameter Values of the Extended SIDM model for the Galaxy PGC51017.

Parameter	Value
$\rho_0 (M_\odot/\text{Kpc}^3)$	1×10^9
$K_0 (M_\odot \text{ Kpc}^{-3} (\text{km/s})^2)$	106.461
ml_{disk}	0.6284
ml_{bulge}	0.0628
$\alpha (\text{Kpc})$	2.67
χ^2_{red}	0.303901

157. The Galaxy UGC01230 Marginally Viable, Extended Viable

For this galaxy, the optimization method we used, ensures maximum compatibility of the analytic SIDM model of Eq. (3) with the SPARC data, if we choose $\rho_0 = 2.89655 \times 10^7 M_\odot/\text{Kpc}^3$ and $K_0 = 6578.29 M_\odot \text{ Kpc}^{-3} (\text{km/s})^2$, in which case the reduced χ^2_{red} value is $\chi^2_{\text{red}} = 0.686649$. Also the parameter α in this case is $\alpha = 8.69695 \text{ Kpc}$.

In Table CCLXXI we present the optimized values of K_0 and ρ_0 for the analytic SIDM model of Eq. (3) for which the maximum compatibility with the SPARC data is achieved. In Figs. 439, 440 we present

TABLE CCLXXI: SIDM Optimization Values for the galaxy UGC01230

Parameter	Optimization Values
$\rho_0 (M_\odot/\text{Kpc}^3)$	2.89655×10^7
$K_0 (M_\odot \text{ Kpc}^{-3} (\text{km/s})^2)$	6578.29

the density of the analytic SIDM model, the predicted rotation curves for the SIDM model (3), versus the SPARC observational data and the sound speed, as a function of the radius respectively. As it can be seen, for this galaxy, the SIDM model produces marginally viable rotation curves which are marginally compatible with the SPARC data.

Now we shall include contributions to the rotation velocity from the other components of the galaxy, namely the disk, the gas, and the bulge if present. In Fig. 441 we present the combined rotation curves including all the components of the galaxy along with the SIDM. As it can be seen, the extended collisional DM model is viable. Also in Table CCLXXII we present the optimized values of the free parameters of the SIDM model for which we achieve the maximum compatibility with the SPARC data, for the galaxy UGC01230, and also the resulting reduced χ^2_{red} value.

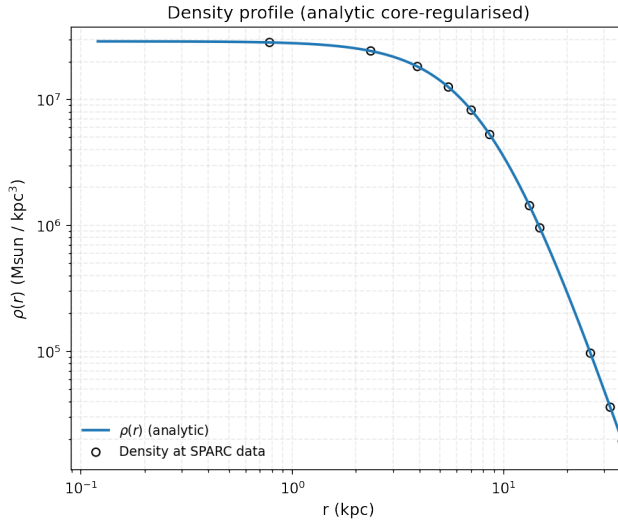


FIG. 439: The density of the SIDM model of Eq. (3) for the galaxy UGC01230, versus the radius.

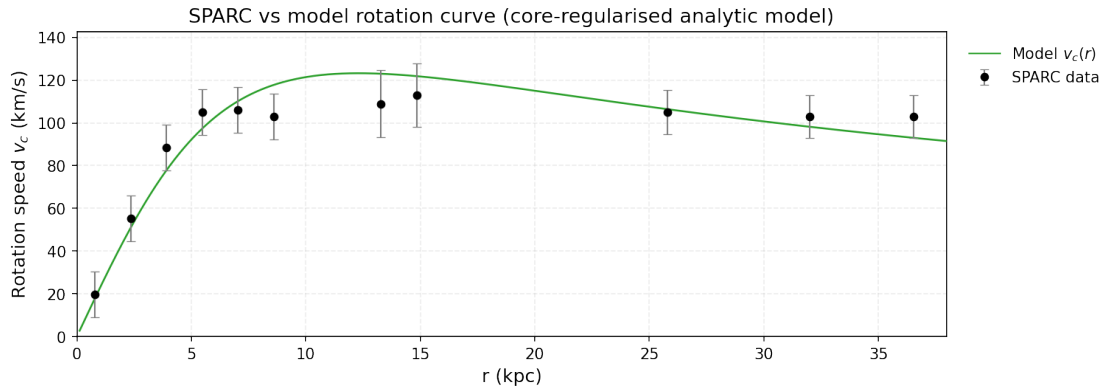


FIG. 440: The predicted rotation curves for the optimized SIDM model of Eq. (3), versus the SPARC observational data for the galaxy UGC01230.

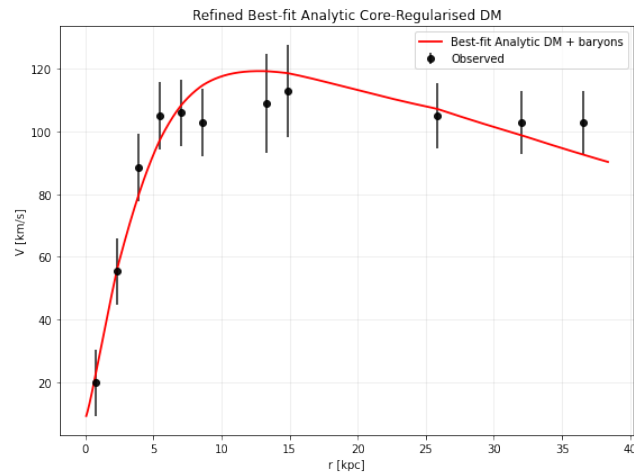


FIG. 441: The predicted rotation curves after using an optimization for the SIDM model (3), and the extended SPARC data for the galaxy UGC01230. We included the rotation curves of the gas, the disk velocities, the bulge (where present) along with the SIDM model.

TABLE CCLXXII: Optimized Parameter Values of the Extended SIDM model for the Galaxy UGC01230.

Parameter	Value
$\rho_0 (M_\odot/\text{Kpc}^3)$	2.4609×10^7
$K_0 (M_\odot \text{ Kpc}^{-3} (\text{km/s})^2)$	5118.51
ml_{disk}	0.7409
ml_{bulge}	0.2610
$\alpha (\text{Kpc})$	8.32188
χ^2_{red}	0.62717

158. The Galaxy UGC02023

For this galaxy, the optimization method we used, ensures maximum compatibility of the analytic SIDM model of Eq. (3) with the SPARC data, if we choose $\rho_0 = 1.5771 \times 10^7 M_\odot/\text{Kpc}^3$ and $K_0 = 1802.32 M_\odot \text{ Kpc}^{-3} (\text{km/s})^2$, in which case the reduced χ^2_{red} value is $\chi^2_{\text{red}} = 0.536421$. Also the parameter α in this case is $\alpha = 6.16932 \text{ Kpc}$.

In Table CCLXXIII we present the optimized values of K_0 and ρ_0 for the analytic SIDM model of Eq. (3) for which the maximum compatibility with the SPARC data is achieved. In Figs. 442, 443 we

TABLE CCLXXIII: SIDM Optimization Values for the galaxy UGC02023

Parameter	Optimization Values
$\rho_0 (M_\odot/\text{Kpc}^3)$	1.5771×10^7
$K_0 (M_\odot \text{ Kpc}^{-3} (\text{km/s})^2)$	1802.32

present the density of the analytic SIDM model, the predicted rotation curves for the SIDM model (3), versus the SPARC observational data and the sound speed, as a function of the radius respectively. As it can be seen, for this galaxy, the SIDM model produces viable rotation curves which are compatible with the SPARC data.

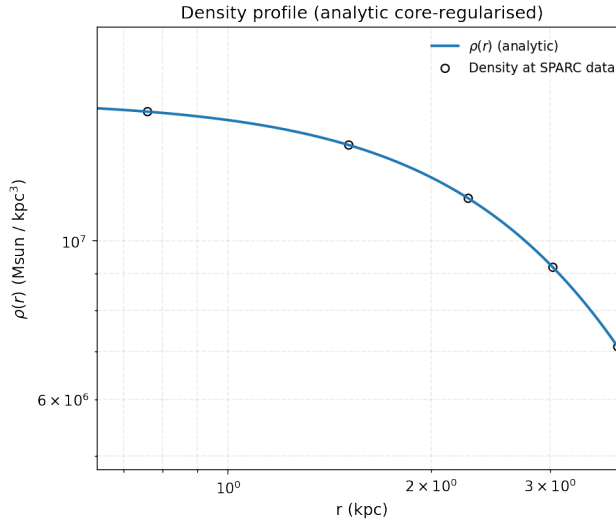


FIG. 442: The density of the SIDM model of Eq. (3) for the galaxy UGC02023, versus the radius.

159. The Galaxy UGC04305

For this galaxy, the optimization method we used, ensures maximum compatibility of the analytic SIDM model of Eq. (3) with the SPARC data, if we choose $\rho_0 = 4.51145 \times 10^7 M_\odot/\text{Kpc}^3$ and $K_0 = 537.831 M_\odot \text{ Kpc}^{-3} (\text{km/s})^2$, in which case the reduced χ^2_{red} value is $\chi^2_{\text{red}} = 0.657603$. Also the parameter α in this case is $\alpha = 1.99258 \text{ Kpc}$.

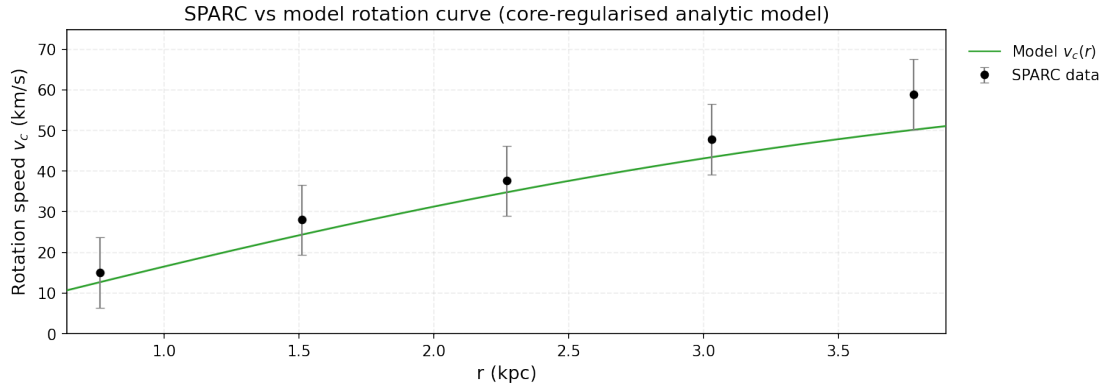


FIG. 443: The predicted rotation curves for the optimized SIDM model of Eq. (3), versus the SPARC observational data for the galaxy UGC02023.

In Table CCLXXIV we present the optimized values of K_0 and ρ_0 for the analytic SIDM model of Eq. (3) for which the maximum compatibility with the SPARC data is achieved. In Figs. 444, 445 we

TABLE CCLXXIV: SIDM Optimization Values for the galaxy UGC04305

Parameter	Optimization Values
$\rho_0 (M_\odot/\text{Kpc}^3)$	4.51145×10^7
$K_0 (M_\odot \text{ Kpc}^{-3} (\text{km/s})^2)$	537.831

present the density of the analytic SIDM model, the predicted rotation curves for the SIDM model (3), versus the SPARC observational data and the sound speed, as a function of the radius respectively. As it can be seen, for this galaxy, the SIDM model produces marginally viable rotation curves which are compatible with the SPARC data.

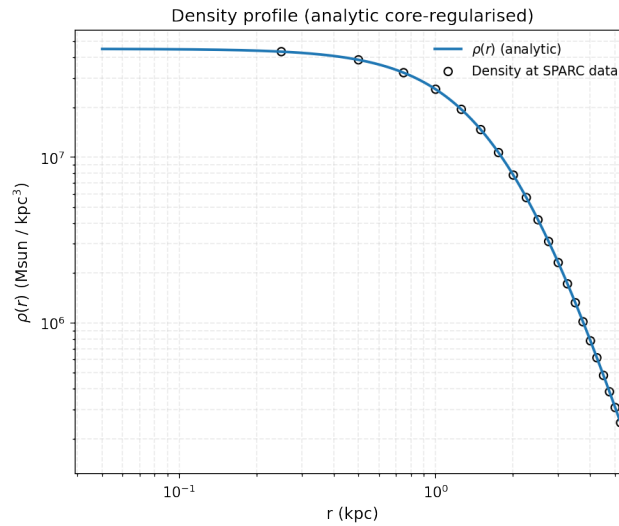


FIG. 444: The density of the SIDM model of Eq. (3) for the galaxy UGC04305, versus the radius.

160. The Galaxy UGC05999

For this galaxy, the optimization method we used, ensures maximum compatibility of the analytic SIDM model of Eq. (3) with the SPARC data, if we choose $\rho_0 = 1.1002 \times 10^7 M_\odot/\text{Kpc}^3$ and $K_0 = 4076.88 M_\odot \text{ Kpc}^{-3} (\text{km/s})^2$, in which case the reduced χ^2_{red} value is $\chi^2_{red} = 0.448089$. Also the parameter α in this case is $\alpha = 11.1091 \text{ Kpc}$.

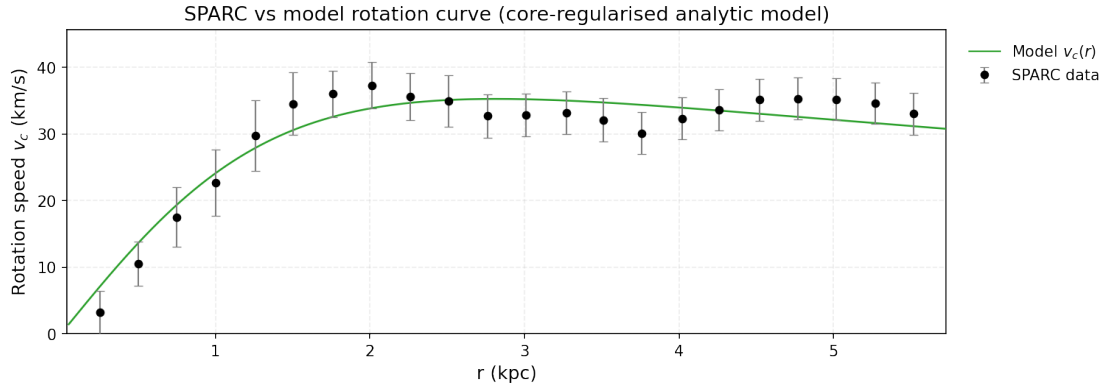


FIG. 445: The predicted rotation curves for the optimized SIDM model of Eq. (3), versus the SPARC observational data for the galaxy UGC04305.

In Table CCLXXV we present the optimized values of K_0 and ρ_0 for the analytic SIDM model of Eq. (3) for which the maximum compatibility with the SPARC data is achieved. In Figs. 446, 447 we present

TABLE CCLXXV: SIDM Optimization Values for the galaxy UGC05999

Parameter	Optimization Values
$\rho_0 (M_\odot/\text{Kpc}^3)$	1.1002×10^7
$K_0 (M_\odot \text{ Kpc}^{-3} (\text{km/s})^2)$	4076.88

the density of the analytic SIDM model, the predicted rotation curves for the SIDM model (3), versus the SPARC observational data and the sound speed, as a function of the radius respectively. As it can be seen, for this galaxy, the SIDM model produces viable rotation curves which are compatible with the SPARC data.

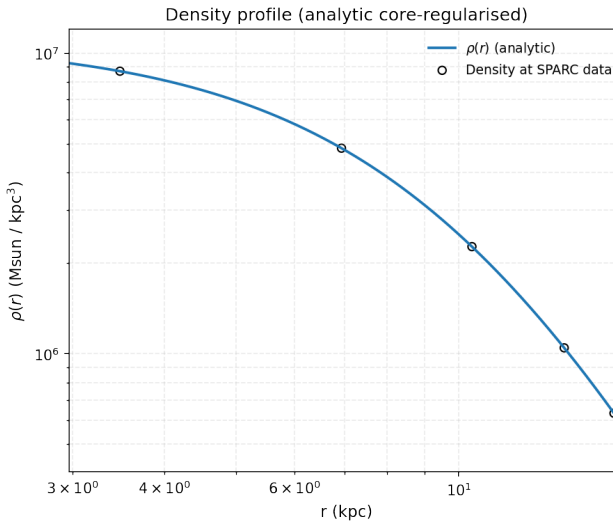


FIG. 446: The density of the SIDM model of Eq. (3) for the galaxy UGC05999, versus the radius.

161. The Galaxy UGC06628

For this galaxy, the optimization method we used, ensures maximum compatibility of the analytic SIDM model of Eq. (3) with the SPARC data, if we choose $\rho_0 = 2.14819 \times 10^7 M_\odot/\text{Kpc}^3$ and $K_0 = 1032.319 M_\odot \text{ Kpc}^{-3} (\text{km/s})^2$, in which case the reduced χ^2_{red} value is $\chi^2_{red} = 0.603718$. Also the parameter α in this case is $\alpha = 3.23535 \text{ Kpc}$.

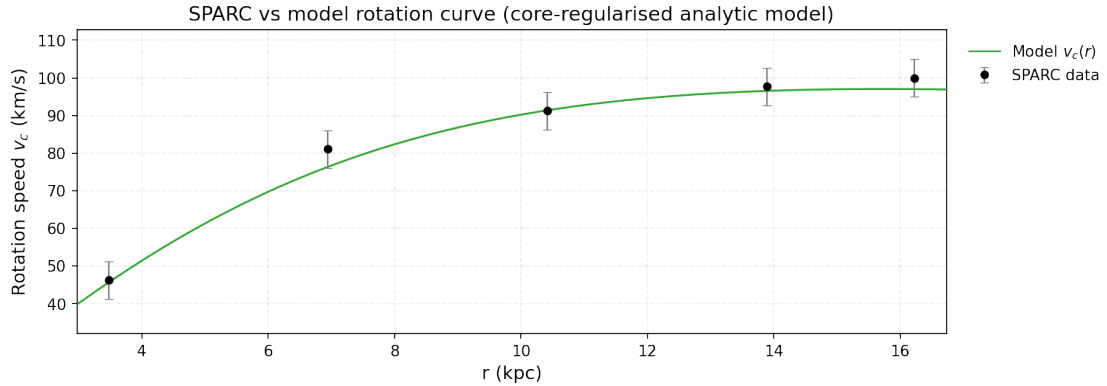


FIG. 447: The predicted rotation curves for the optimized SIDM model of Eq. (3), versus the SPARC observational data for the galaxy UGC05999.

In Table CCLXXVI we present the optimized values of K_0 and ρ_0 for the analytic SIDM model of Eq. (3) for which the maximum compatibility with the SPARC data is achieved. In Figs. 448, 449 we

TABLE CCLXXVI: SIDM Optimization Values for the galaxy UGC06628

Parameter	Optimization Values
$\rho_0 (M_\odot/\text{Kpc}^3)$	2.14819×10^7
$K_0 (M_\odot \text{ Kpc}^{-3} (\text{km/s})^2)$	1032.319

present the density of the analytic SIDM model, the predicted rotation curves for the SIDM model (3), versus the SPARC observational data and the sound speed, as a function of the radius respectively. As it can be seen, for this galaxy, the SIDM model produces viable rotation curves which are compatible with the SPARC data.

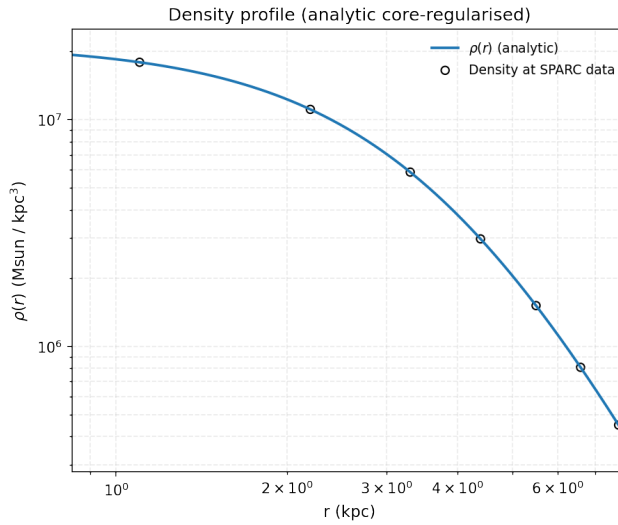


FIG. 448: The density of the SIDM model of Eq. (3) for the galaxy UGC06628, versus the radius.

162. The Galaxy UGC06973, Non-viable

For this galaxy, the optimization method we used, ensures maximum compatibility of the analytic SIDM model of Eq. (3) with the SPARC data, if we choose $\rho_0 = 5.93142 \times 10^8 M_\odot/\text{Kpc}^3$ and $K_0 = 14203.9 M_\odot \text{ Kpc}^{-3} (\text{km/s})^2$, in which case the reduced χ^2_{red} value is $\chi^2_{red} = 9.32271$. Also the parameter α in this case is $\alpha = 2.82407 \text{ Kpc}$.

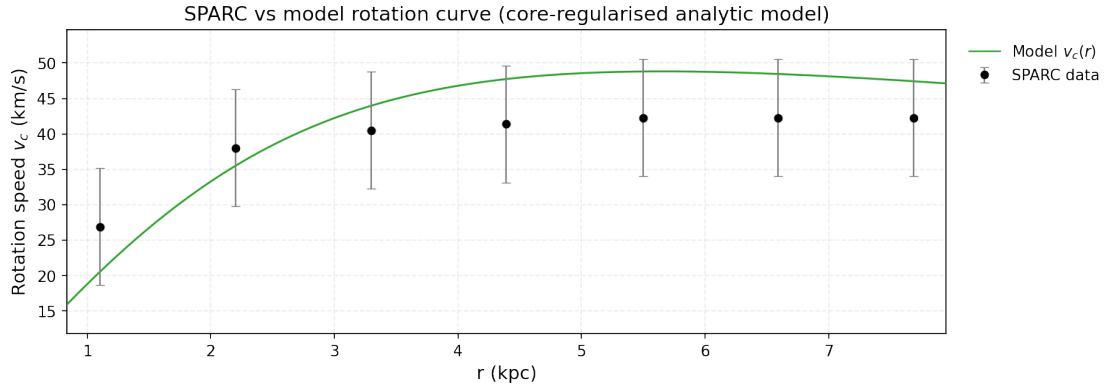


FIG. 449: The predicted rotation curves for the optimized SIDM model of Eq. (3), versus the SPARC observational data for the galaxy UGC06628.

In Table CCLXXVII we present the optimized values of K_0 and ρ_0 for the analytic SIDM model of Eq. (3) for which the maximum compatibility with the SPARC data is achieved. In Figs. 450, 451 we

TABLE CCLXXVII: SIDM Optimization Values for the galaxy UGC06973

Parameter	Optimization Values
$\rho_0 (M_\odot / \text{Kpc}^3)$	5.93142×10^7
$K_0 (M_\odot \text{ Kpc}^{-3} (\text{km/s})^2)$	14203.9

present the density of the analytic SIDM model, the predicted rotation curves for the SIDM model (3), versus the SPARC observational data and the sound speed, as a function of the radius respectively. As it can be seen, for this galaxy, the SIDM model produces non-viable rotation curves which are incompatible with the SPARC data.

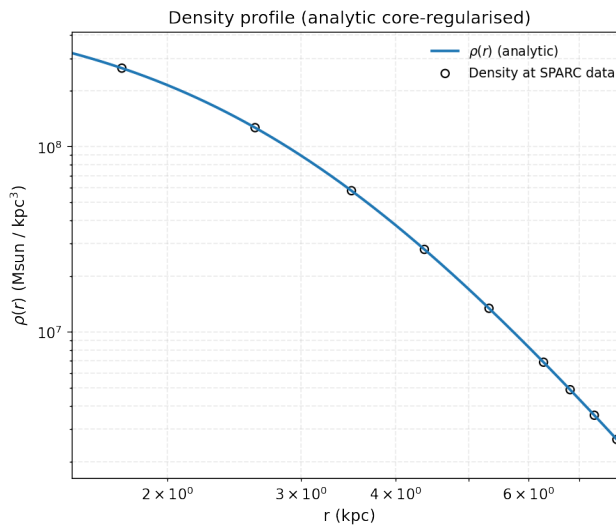


FIG. 450: The density of the SIDM model of Eq. (3) for the galaxy UGC06973, versus the radius.

Now we shall include contributions to the rotation velocity from the other components of the galaxy, namely the disk, the gas, and the bulge if present. In Fig. 452 we present the combined rotation curves including all the components of the galaxy along with the SIDM. As it can be seen, the extended collisional DM model is non-viable. Also in Table CCLXXVIII we present the optimized values of the free parameters of the SIDM model for which we achieve the maximum compatibility with the SPARC data, for the galaxy UGC06973, and also the resulting reduced χ^2_{red} value.

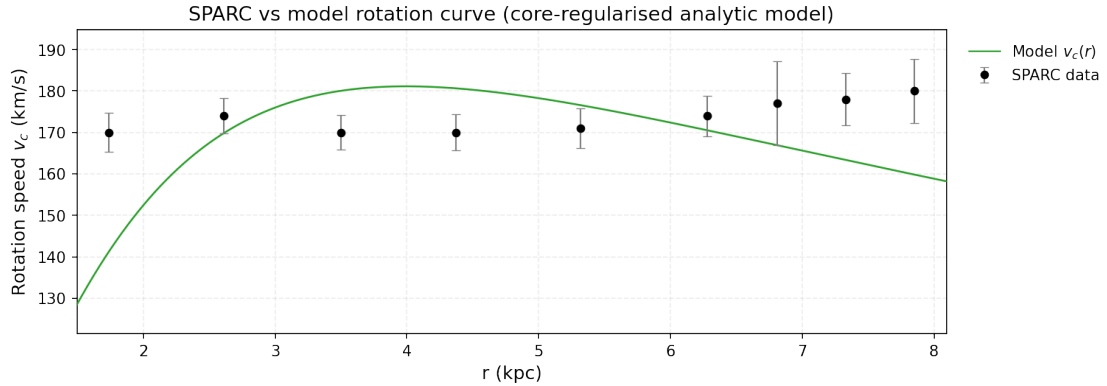


FIG. 451: The predicted rotation curves for the optimized SIDM model of Eq. (3), versus the SPARC observational data for the galaxy UGC06973.

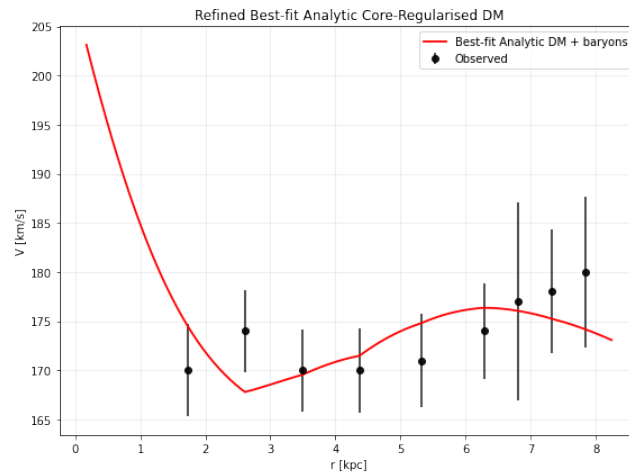


FIG. 452: The predicted rotation curves after using an optimization for the SIDM model (3), and the extended SPARC data for the galaxy UGC06973. We included the rotation curves of the gas, the disk velocities, the bulge (where present) along with the SIDM model.

TABLE CCLXXVIII: Optimized Parameter Values of the Extended SIDM model for the Galaxy UGC06973.

Parameter	Value
$\rho_0 (M_\odot/\text{Kpc}^3)$	9.611×10^7
$K_0 (M_\odot \text{ Kpc}^{-3} (\text{km/s})^2)$	9991.29
ml_{disk}	0.4852
ml_{bulge}	0
$\alpha (\text{Kpc})$	5.88332
χ^2_{red}	0.965879

163. The Galaxy UGC07608

For this galaxy, the optimization method we used, ensures maximum compatibility of the analytic SIDM model of Eq. (3) with the SPARC data, if we choose $\rho_0 = 7.199838 \times 10^7 M_\odot/\text{Kpc}^3$ and $K_0 = 1752.32 M_\odot \text{ Kpc}^{-3} (\text{km/s})^2$, in which case the reduced χ^2_{red} value is $\chi^2_{\text{red}} = 0.916443$. Also the parameter α in this case is $\alpha = 3.92396 \text{ Kpc}$.

In Table CCLXXIX we present the optimized values of K_0 and ρ_0 for the analytic SIDM model of Eq. (3) for which the maximum compatibility with the SPARC data is achieved. In Figs. 453, 454 we present the density of the analytic SIDM model, the predicted rotation curves for the SIDM model (3), versus the SPARC observational data and the sound speed, as a function of the radius respectively. As it can be seen, for this galaxy, the SIDM model produces viable rotation curves which are compatible with the SPARC data.

TABLE CCLXXIX: SIDM Optimization Values for the galaxy UGC07608

Parameter	Optimization Values
$\rho_0 (M_\odot/\text{Kpc}^3)$	7.199838×10^7
$K_0 (M_\odot \text{ Kpc}^{-3} (\text{km/s})^2)$	1752.32

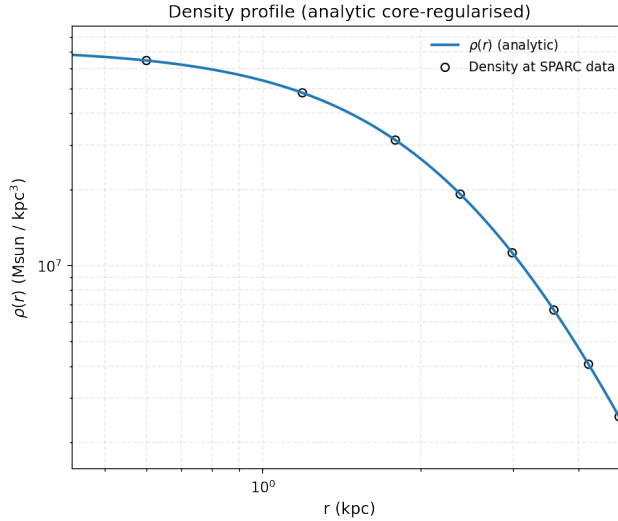


FIG. 453: The density of the SIDM model of Eq. (3) for the galaxy UGC07608, versus the radius.

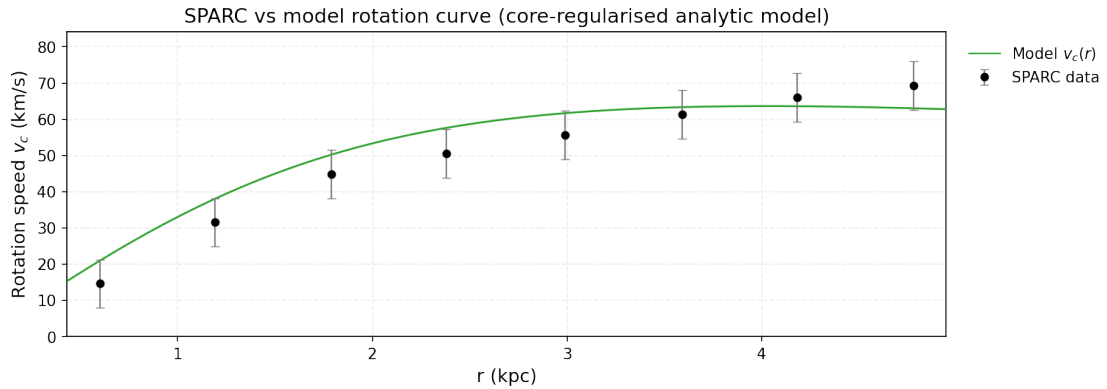


FIG. 454: The predicted rotation curves for the optimized SIDM model of Eq. (3), versus the SPARC observational data for the galaxy UGC07608.

164. The Galaxy UGCA281

For this galaxy, the optimization method we used, ensures maximum compatibility of the analytic SIDM model of Eq. (3) with the SPARC data, if we choose $\rho_0 = 2.12792 \times 10^8 M_\odot/\text{Kpc}^3$ and $K_0 = 379.708 M_\odot \text{ Kpc}^{-3} (\text{km/s})^2$, in which case the reduced χ^2_{red} value is $\chi^2_{red} = 0.75153$. Also the parameter α in this case is $\alpha = 0.7709 \text{ Kpc}$.

In Table CCLXXX we present the optimized values of K_0 and ρ_0 for the analytic SIDM model of Eq. (3) for which the maximum compatibility with the SPARC data is achieved. In Figs. 455, 456 we present

TABLE CCLXXX: SIDM Optimization Values for the galaxy UGCA281

Parameter	Optimization Values
$\rho_0 (M_\odot/\text{Kpc}^3)$	2.12792×10^8
$K_0 (M_\odot \text{ Kpc}^{-3} (\text{km/s})^2)$	379.708

the density of the analytic SIDM model, the predicted rotation curves for the SIDM model (3), versus the SPARC observational data and the sound speed, as a function of the radius respectively. As it can be seen, for this galaxy, the SIDM model produces viable rotation curves which are compatible with the SPARC data.

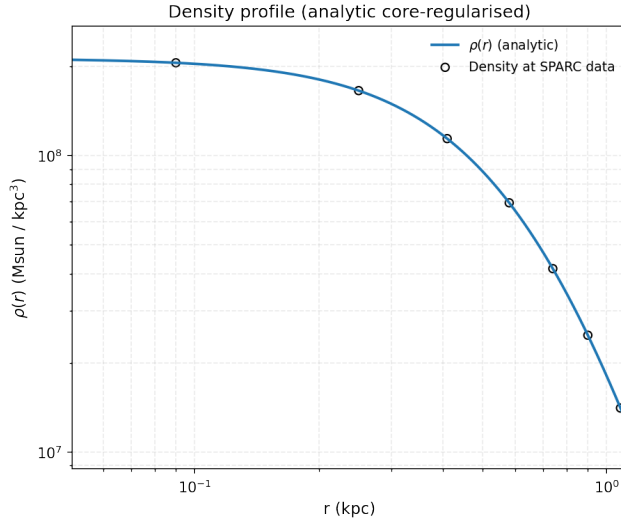


FIG. 455: The density of the SIDM model of Eq. (3) for the galaxy UGCA281, versus the radius.

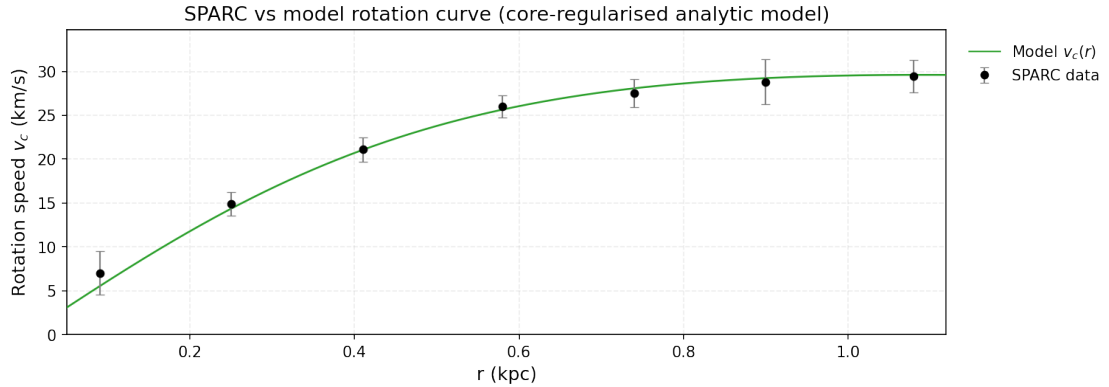


FIG. 456: The predicted rotation curves for the optimized SIDM model of Eq. (3), versus the SPARC observational data for the galaxy UGCA281.

[1] S. Tulin and H. B. Yu, Phys. Rept. **730** (2018), 1-57 doi:10.1016/j.physrep.2017.11.004 [arXiv:1705.02358 [hep-ph]].

[2] V. K. Oikonomou, [arXiv:2511.13929 [astro-ph.CO]].

[3] Z. Slepian and J. Goodman, Mon. Not. Roy. Astron. Soc. **427** (2012), 839 doi:10.1111/j.1365-2966.2012.21901.x [arXiv:1109.3844 [astro-ph.CO]].

[4] C. J. Saxton, R. Soria and K. Wu, Mon. Not. Roy. Astron. Soc. **445** (2014) no.4, 3415-3434 doi:10.1093/mnras/stu1984 [arXiv:1409.6725 [astro-ph.GA]].

[5] G. Alonso-Álvarez, J. M. Cline and C. Dewar, Phys. Rev. Lett. **133** (2024) no.2, 021401 doi:10.1103/PhysRevLett.133.021401 [arXiv:2401.14450 [astro-ph.CO]].

[6] M. Kaplinghat, S. Tulin and H. B. Yu, Phys. Rev. Lett. **116** (2016) no.4, 041302 doi:10.1103/PhysRevLett.116.041302 [arXiv:1508.03339 [astro-ph.CO]].

[7] K. J. Ahn and P. R. Shapiro, Mon. Not. Roy. Astron. Soc. **363** (2005), 1092-1124 doi:10.1111/j.1365-2966.2005.09492.x [arXiv:astro-ph/0412169 [astro-ph]].

[8] C. J. Saxton, Mon. Not. Roy. Astron. Soc. **430** (2013), 1578 doi:10.1093/mnras/sts689 [arXiv:1212.5294 [astro-ph.CO]].

[9] C. J. Saxton and I. Ferreras, Mon. Not. Roy. Astron. Soc. **405** (2010), 77 doi:10.1111/j.1365-2966.2010.16448.x [arXiv:1002.0845 [astro-ph.CO]].

[10] C. J. Saxton, Z. Younsi and K. Wu, Mon. Not. Roy. Astron. Soc. **461** (2016) no.4, 4295-4316 doi:10.1093/mnras/stw1626 [arXiv:1606.07066 [astro-ph.GA]].

[11] A. Arbey, J. Lesgourgues and P. Salati, Phys. Rev. D **68** (2003), 023511 doi:10.1103/PhysRevD.68.023511 [arXiv:astro-ph/0301533 [astro-ph]].

[12] M. Heikinheimo, M. Raidal, C. Spethmann and H. Veermäe, Phys. Lett. B **749** (2015), 236-241 doi:10.1016/j.physletb.2015.08.012 [arXiv:1504.04371 [hep-ph]].

[13] B. D. Wandelt, R. Dave, G. R. Farrar, P. C. McGuire, D. N. Spergel and P. J. Steinhardt, [arXiv:astro-ph/0006344 [astro-ph]].

[14] D. N. Spergel and P. J. Steinhardt, Phys. Rev. Lett. **84** (2000), 3760-3763 doi:10.1103/PhysRevLett.84.3760 [arXiv:astro-ph/9909386 [astro-ph]].

[15] A. Loeb and N. Weiner, Phys. Rev. Lett. **106** (2011), 171302 doi:10.1103/PhysRevLett.106.171302 [arXiv:1011.6374 [astro-ph.CO]].

[16] L. Ackerman, M. R. Buckley, S. M. Carroll and M. Kamionkowski, Phys. Rev. D **79** (2009), 023519 doi:10.1103/PhysRevD.79.023519 [arXiv:0810.5126 [hep-ph]].

[17] J. Goodman, New Astron. **5** (2000), 103 doi:10.1016/S1384-1076(00)00015-4 [arXiv:astro-ph/0003018 [astro-ph]].

[18] A. Arbey, Phys. Rev. D **74** (2006), 043516 doi:10.1103/PhysRevD.74.043516 [arXiv:astro-ph/0601274 [astro-ph]].

[19] W. Yang, S. Pan, E. Di Valentino, O. Mena, D. F. Mota and S. Chakraborty, Phys. Rev. D **111** (2025) no.10, 103509 doi:10.1103/PhysRevD.111.103509 [arXiv:2504.11973 [astro-ph.CO]].

[20] M. Abedin, L. A. Escamilla, S. Pan, E. Di Valentino and W. Yang, [arXiv:2505.09470 [astro-ph.CO]].

[21] I. Y. Kobzarev, L. B. Okun and I. Y. Pomeranchuk, Sov. J. Nucl. Phys. **3** (1966) no.6, 837-841

[22] H. M. Hodges, Phys. Rev. D **47** (1993), 456-459 doi:10.1103/PhysRevD.47.456

[23] R. Foot, Int. J. Mod. Phys. D **13** (2004), 2161-2192 doi:10.1142/S0218271804006449 [arXiv:astro-ph/0407623 [astro-ph]].

[24] Z. Berezhiani, P. Ciarcelluti, D. Comelli and F. L. Villante, Int. J. Mod. Phys. D **14** (2005), 107-120 doi:10.1142/S0218271805005165 [arXiv:astro-ph/0312605 [astro-ph]].

[25] Z. K. Silagadze, ICFAI U. J. Phys. **2** (2009), 143-154 [arXiv:0808.2595 [astro-ph]].

[26] R. Foot, H. Lew and R. R. Volkas, JHEP **07** (2000), 032 doi:10.1088/1126-6708/2000/07/032 [arXiv:hep-ph/0006027 [hep-ph]].

[27] Z. Chacko, H. S. Goh and R. Harnik, Phys. Rev. Lett. **96** (2006), 231802 doi:10.1103/PhysRevLett.96.231802 [arXiv:hep-ph/0506256 [hep-ph]].

[28] Z. Berezhiani, D. Comelli and F. L. Villante, Phys. Lett. B **503** (2001), 362-375 doi:10.1016/S0370-2693(01)00217-9 [arXiv:hep-ph/0008105 [hep-ph]].

[29] S. I. Blinnikov, Phys. Atom. Nucl. **73** (2010), 593-603 doi:10.1134/S1063778810040034 [arXiv:0904.3609 [astro-ph.CO]].

[30] S. Tulin and H. B. Yu, Phys. Rept. **730** (2018), 1-57 doi:10.1016/j.physrep.2017.11.004 [arXiv:1705.02358 [hep-ph]].

[31] R. N. Mohapatra, S. Nussinov and V. L. Teplitz, Phys. Rev. D **66** (2002), 063002 doi:10.1103/PhysRevD.66.063002 [arXiv:hep-ph/0111381 [hep-ph]].

[32] S. I. Blinnikov and M. Y. Khlopov, Sov. J. Nucl. Phys. **36** (1982), 472 ITEP-11-1982.

[33] S. I. Blinnikov and M. Khlopov, Sov. Astron. **27** (1983), 371-375

[34] R. Foot and S. Vagnozzi, JCAP **07** (2016), 013 doi:10.1088/1475-7516/2016/07/013 [arXiv:1602.02467 [astro-ph.CO]].

[35] R. Foot and S. Vagnozzi, Phys. Lett. B **748** (2015), 61-66 doi:10.1016/j.physletb.2015.06.063 [arXiv:1412.0762 [hep-ph]].

[36] R. Foot and S. Vagnozzi, Phys. Rev. D **91** (2015), 023512 doi:10.1103/PhysRevD.91.023512 [arXiv:1409.7174 [hep-ph]].

[37] R. Foot and R. R. Volkas, Phys. Rev. D **69** (2004), 123510 doi:10.1103/PhysRevD.69.123510 [arXiv:hep-ph/0402267 [hep-ph]].

[38] R. Foot, Phys. Lett. B **505** (2001), 1-5 doi:10.1016/S0370-2693(01)00361-6 [arXiv:astro-ph/0101055 [astro-ph]].

[39] R. Foot, Acta Phys. Polon. B **35** (2004), 2473-2478 [arXiv:astro-ph/0406257 [astro-ph]].

[40] R. Foot, Phys. Lett. B **452** (1999), 83-86 doi:10.1016/S0370-2693(99)00230-0 [arXiv:astro-ph/9902065 [astro-ph]].

[41] R. Foot and R. R. Volkas, Phys. Lett. B **517** (2001), 13-17 doi:10.1016/S0370-2693(01)01011-5 [arXiv:hep-ph/0108051 [hep-ph]].

[42] R. Foot and Z. K. Silagadze, Acta Phys. Polon. B **32** (2001), 2271-2278 [arXiv:astro-ph/0104251 [astro-ph]].

[43] R. Foot, A. Y. Ignatiev and R. R. Volkas, Astropart. Phys. **17** (2002), 195-198 doi:10.1016/S0927-6505(01)00149-9 [arXiv:astro-ph/0010502 [astro-ph]].

[44] M. Pavsic, Int. J. Theor. Phys. **9** (1974), 229-244 doi:10.1007/BF01810695 [arXiv:hep-ph/0105344 [hep-ph]].

[45] R. Foot, Mod. Phys. Lett. A **9** (1994), 169-180 doi:10.1142/S0217732394000186 [arXiv:hep-ph/9402241 [hep-ph]].

[46] A. Y. Ignatiev and R. R. Volkas, Phys. Lett. B **487** (2000), 294-298 doi:10.1016/S0370-2693(00)00836-4 [arXiv:hep-ph/0005238 [hep-ph]].

[47] A. Y. Ignatiev and R. R. Volkas, Phys. Rev. D **68** (2003), 023518 doi:10.1103/PhysRevD.68.023518 [arXiv:hep-ph/0304260 [hep-ph]].

[48] P. Ciarcelluti, Int. J. Mod. Phys. D **14** (2005), 187-222 doi:10.1142/S0218271805006213 [arXiv:astro-ph/0409630 [astro-ph]].

[49] P. Ciarcelluti, Int. J. Mod. Phys. D **14** (2005), 223-256 doi:10.1142/S0218271805006225 [arXiv:astro-ph/0409633 [astro-ph]].

[50] P. Ciarcelluti, Int. J. Mod. Phys. D **19** (2010), 2151-2230 doi:10.1142/S0218271810018438 [arXiv:1102.5530 [astro-ph.CO]].

[51] G. Dvali, I. Sawicki and A. Vikman, JCAP **08** (2009), 009 doi:10.1088/1475-7516/2009/08/009 [arXiv:0903.0660 [hep-th]].

[52] R. Foot, Phys. Lett. B **728** (2014), 45-50 doi:10.1016/j.physletb.2013.11.019 [arXiv:1305.4316 [astro-ph.CO]].

[53] R. Foot, Phys. Rev. D **88** (2013) no.2, 023520 doi:10.1103/PhysRevD.88.023520 [arXiv:1304.4717 [astro-ph.CO]].

[54] J. W. Cui, H. J. He, L. C. Lu and F. R. Yin, Phys. Rev. D **85** (2012), 096003 doi:10.1103/PhysRevD.85.096003 [arXiv:1110.6893 [hep-ph]].

[55] R. Foot, JCAP **07** (2016), 011 doi:10.1088/1475-7516/2016/07/011 [arXiv:1506.01451 [astro-ph.GA]].

[56] R. Foot, Int. J. Mod. Phys. A **29** (2014), 1430013 doi:10.1142/S0217751X14300130 [arXiv:1401.3965 [astro-ph.CO]].

[57] J. M. Cline, Z. Liu, G. D. Moore and W. Xue, Phys. Rev. D **90** (2014) no.1, 015023 doi:10.1103/PhysRevD.90.015023 [arXiv:1312.3325 [hep-ph]].

[58] M. Ibe, A. Kamada, S. Kobayashi, T. Kuwahara and W. Nakano, Phys. Rev. D **100** (2019) no.7, 075022 doi:10.1103/PhysRevD.100.075022 [arXiv:1907.03404 [hep-ph]].

[59] R. Foot, Phys. Rev. D **97** (2018) no.10, 103006 doi:10.1103/PhysRevD.97.103006 [arXiv:1801.09359 [astro-ph.GA]].

[60] A. Howe, J. Setford, D. Curtin and C. D. Matzner, JHEP **07** (2022), 059 doi:10.1007/JHEP07(2022)059 [arXiv:2112.05766 [hep-ph]].

[61] F. Y. Cyr-Racine, F. Ge and L. Knox, Phys. Rev. Lett. **128** (2022) no.20, 201301 doi:10.1103/PhysRevLett.128.201301 [arXiv:2107.13000 [astro-ph.CO]].

[62] I. Armstrong, B. Gurbuz, D. Curtin and C. D. Matzner, Astrophys. J. **965** (2024) no.1, 42 doi:10.3847/1538-4357/ad283c [arXiv:2311.18086 [astro-ph.HE]].

[63] A. C. Ritter and R. R. Volkas, Phys. Rev. D **110** (2024) no.1, 015032 doi:10.1103/PhysRevD.110.015032 [arXiv:2404.05999 [hep-ph]].

[64] R. N. Mohapatra and V. L. Teplitz, Astrophys. J. **478** (1997), 29-38 doi:10.1086/303762 [arXiv:astro-ph/9603049 [astro-ph]].

[65] R. N. Mohapatra and V. L. Teplitz, Phys. Rev. D **62** (2000), 063506 doi:10.1103/PhysRevD.62.063506 [arXiv:astro-ph/0001362 [astro-ph]].

[66] I. Goldman, R. N. Mohapatra, S. Nussinov, D. Rosenbaum and V. Teplitz, Phys. Lett. B **725** (2013), 200-207 doi:10.1016/j.physletb.2013.07.017 [arXiv:1305.6908 [astro-ph.CO]].

[67] Z. G. Berezhiani, A. D. Dolgov and R. N. Mohapatra, Phys. Lett. B **375** (1996), 26-36 doi:10.1016/0370-2693(96)00219-5 [arXiv:hep-ph/9511221 [hep-ph]].

[68] V. K. Oikonomou, Phys. Rev. D **110** (2024) no.12, 123509 doi:10.1103/PhysRevD.110.123509 [arXiv:2409.16095 [gr-qc]].

[69] F. Lelli, S. S. McGaugh and J. M. Schombert, Astron. J. **152** (2016), 157 doi:10.3847/0004-6256/152/6/157 [arXiv:1606.09251 [astro-ph.GA]].

[70] J. Fan, A. Katz, L. Randall and M. Reece, Phys. Dark Univ. **2** (2013), 139-156 doi:10.1016/j.dark.2013.07.001 [arXiv:1303.1521 [astro-ph.CO]].

[71] M. McCullough and L. Randall, JCAP **10** (2013), 058 doi:10.1088/1475-7516/2013/10/058 [arXiv:1307.4095

[hep-ph]].

[72] G. S. Anand, A. Benítez-Llambay, R. Beaton, A. J. Fox, J. F. Navarro and E. D’Onghia, *Astrophys. J. Lett.* **993** (2025) no.2, L55 doi:10.3847/2041-8213/ae1584 [arXiv:2508.20157 [astro-ph.GA]].

[73] A. Benítez-Llambay, R. Dutta, M. Fumagalli and J. F. Navarro, [arXiv:2406.18643 [astro-ph.GA]].

[74] A. Benítez-Llambay and J. F. Navarro, *Astrophys. J.* **956** (2023) no.1, 1 doi:10.3847/1538-4357/acf767 [arXiv:2309.03253 [astro-ph.GA]].